Methods in Molecular Biology™

VOLUME 247

Drosophila Cytogenetics Protocols

Edited by

Daryl S. Henderson

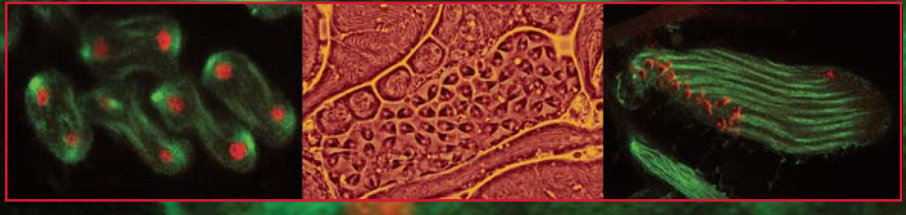

HUMANA PRESS

1

The Chromosomes of *Drosophila melanogaster*

Daryl S. Henderson

1. Introduction

Drosophila have two basic forms of chromosomes—mitotic and polytene—that have vastly different morphologies and cellular roles. Polytene chromosomes are found in interphase nuclei of differentiated cells, being especially prominent in certain tissues of the larva and adult ovary. They are produced by repeated rounds of chromosome replication unhitched from nuclear division in a process termed "endoreplication." Among the largest and most familiar of polytene chromosomes are those of the larval salivary gland, which can consist of >2000 sister chromatids tightly aligned in register. Such scaled-up chromosomes permit production of large quantities of gene products in a narrow developmental window. The highly compact mitotic chromosomes, found in proliferating tissues (e.g., the larval central nervous system [CNS], imaginal discs, ovaries, and testes), are genome-packaging vehicles that, in association with the spindle apparatus, function to transmit complete copies of the genome between mother and daughter nuclei. Meiotic chromosomes also can be categorized as mitotic chromosomes, and some of their unique properties are touched on in Chapters 2–5 (for recent reviews, *see* **refs. *1–3***).

Just as mitotic and polytene chromosomes serve different functions in the fly, they are exploited by drosophilists for different purposes. The large size and distinctive banding patterns of salivary gland polytene chromosomes—Darlington likened them to "contorted earthworms" ***(4)***—make them an excellent material on which to locate genes and gene products *in situ* (*see* Chapters 13–15) or to finely map the breakpoints of chromosomal aberrations (*see* Chapters 12–13). The rise of *Drosophila melanogaster* to preeminence as an experimental organism owes much to these giant chromosomes. Mitotic chromosomes are useful for investigating basic questions of mitotic and meiotic cell biology

From: *Methods in Molecular Biology, vol. 247:* Drosophila *Cytogenetics Protocols*
Edited by: D. S. Henderson © Humana Press Inc., Totowa, NJ

(*see* Chapters 2–5, 17, and 18), including cytological studies of heterochromatin (*see* **Subheading 3.** and Chapters 16, 18, and 19).

This chapter provides an introduction to the chromosomes of *D. melanogaster*, in both their mitotic and polytene forms. It begins with an outline of some of the pioneering work in the field of *Drosophila* cytogenetics, focusing mainly on achievements from the first half of the 20th century. More recent discoveries, flowing from advances in molecular biology, microscopy, probe technology, and electronic imaging, are referred to later in the chapter and throughout this volume.

2. *Drosophila* Cytogenetics: Early Milestones

Sutton's 1903 landmark paper, "The Chromosomes in Heredity" (***5***; *see also* **ref.** ***6***), in which he pointed out that the behavior of chromosomes in meiosis parallels the observed patterns of inheritance of Mendelian traits, is considered to mark the beginning of the field of cytogenetics (the actual term would be coined years later). Before then, cytology with its focus on animals specimens, and genetics, which consisted of breeding experiments involving mainly plants, had been separate areas of inquiry ***(6)***. In the practical melding of cytology and genetics that soon followed, *D. melanogaster* would be unrivaled in its fundamental contributions to the new field of cytogenetics, many of which are listed in **Table 1**.

Ahead of her time and seldom acknowledged since, Nettie Stevens of Bryn Mawr College, Pennsylvania ***(34,35)***, was the first person to study chromosomes of *Drosophila*, beginning in the autumn of 1906 ***(7)***. Stevens, a codiscoverer of chromosomal sex determination, was already an accomplished cytologist when she worked the preceding summer at Cold Spring Harbor, NY, examining chromosomes of cucumber beetles (*Diabrotica* spp.; *see* **ref.** ***36***). It is then and there that she likely obtained her first *Drosophila* specimens from entomologist Frank Lutz. It was Lutz also, according to Kohler ***(37)***, who probably introduced Morgan to *Drosophila* that same year. Attempts in Morgan's laboratory to identify *Drosophila* mutations did not begin in earnest until either the fall of 1907 or 1908, and it was not until 1910 that the first unequivocal mutants were actually found ***(8,37)***. Thus, Stevens' cytological studies of *D. melanogaster* (then called *D. ampelophila*) predate the first use of *Drosophila* for genetic analysis.

Stevens' research was important because it helped substantiate Sutton's chromosome theory of heredity ***(5)***. Indeed, she was far ahead of Morgan in recognizing the significance of chromosomes ***(34,35)***. For example, Stevens discovered that the karyotypes of male and female *Drosophila* (and other insects) differ at a single chromosome pair, from which she inferred a role for such heteromorphic chromosomes in determining sex ***(7,38)***, following

Table 1
Some Notable Achievements in Studies of *Drosophila* Chromosomes

1906	N. M. Stevens begins first ever study of *Drosophila* chromosomes; observes heterochromosomes (X and Y) in males; observes somatic pairing of homologous chromosomes (***7***; see text).
1910	T. H. Morgan discovers sex-linked inheritance; first assignment of a specific gene (*white*) to a specific chromosome (the X) ***(8)***.
1913	A. H. Sturtevant constructs the first genetic map (involving X-linked genes) ***(9)***.
1914, 1916	C. W. Metz builds on Stevens' work; examines chromosomes in approx 80 species of Diptera, in gonads of both sexes, and in somatic tissues of embryos, larvae and pupae ***(10,11)***.
1916	C. B. Bridges proves chromosome theory of heredity through observations of nondisjunction ***(12)***.
1916	H. J. Muller discovers crossover suppressors, later shown to be chromosome inversions, from which the concept of "balancer" chromosome is derived ***(13)***.
1917, 1919	C. B. Bridges describes the first chromosome deficiency, first chromosome duplication (inferred from genetic analysis) ***(14,15)***.
1930	H. J. Muller discovers variegating mutations ("eversporting displacements," e.g., white-mottleds) resulting from chromosome rearrangements ***(16)***.
1930s	E. Heitz investigates *Drosophila* heterochromatin ***(17–19)***.
1931	T. S. Painter discovers giant chromosomes in larval salivary glands and demonstrates their usefulness for mapping ***(20–25)***.
1934	B. P. Kaufmann publishes survey of chromosomes from various tissues of *Drosophila*; reports that cells of the larval brain are most useful for observing mitoses; presents extensive morphological description of same ***(26)***.
1935	C. B. Bridges devises map coordinate system for polytene chromosomes ***(27)***.
1938	H. J. Muller and colleagues coin the term "telomere" to describe the specialized ends of chromosomes ***(28)***.
1940s	T. O. Caspersson undertakes first cytochemical studies using microscopy ***(29)***.
1959	K. W. Cooper undertakes extensive cytological investigation of heterochromatin, including morphological descriptions of the X and Y heterochromatic elements ***(30)***.
1969	M.-L. Pardue and J. G. Gall develop in situ hybridization method for polytene chromosomes ***(31)***.
1972	D. L. Lindsley et al. systematically analyze the genome using synthetic duplications and deficiencies created in crosses of Y-autosome translocation stocks ***(32)***.
1977	G. T. Rudkin and B. D. Stollar demonstrate first FISH experiment ***(33)***.

Note: Some of these advances may be considered purely "genetic" rather than "cytogenetic," but they are included as historical reference points.

McClung ***(39)***. [**N.B.**: It was later established by Bridges that sex in *Drosophila* is determined by the ratio of X chromosomes to sets of autosomes ***(40)***, and not by the presence or absence of a Y chromosome, as in humans, for example. The Y chromosome of *Drosophila* is essential for male fertility but not for male*ness*.] Stevens was also the first to note the tendency of homologous chromosomes of Diptera to pair in diploid somatic cells (i.e., outside of meiosis; *see* **ref. *7***).

The methods Stevens used to study insect chromosomes are not so different from the basic techniques we use today. She dissected testes and ovaries of adult flies in physiological salt solution, transferred the tissues to a drop of stain (acetocarmine) on a microscope slide, pressed the cover slip down to break and spread the cells, and removed the excess stain by wicking with filter paper. Of the nine dipteran species she studied, Stevens found the tissues of *Drosophila* to be the most difficult to work with, requiring her to examine an inordinate number of specimens. She wrote,

> While in Sarcophaga all the stages necessary for a description of the behavior of the heterochromosomes of both sexes were found in the course of a few hours' work on perhaps ten or twelve preparations, satisfactory results in the case of Drosophila have been obtained only after prolonged study extending over more than a year and involving dissection of some two thousand individuals. ***(7)***

(See Chapters 2–5, and reduce the number of your *Drosophila* dissections to Sarcophagan levels!) Despite such inauspicious beginnings, Stevens' camera lucida drawings of *Drosophila* prophase figures clearly show a complement of eight chromosomes, with males having a heteromorphic pair (later designated X and Y). Stevens concluded, "The general results of the nine species of flies are the same; i.e., an unequal pair of heterochromosomes in the male leading to dimorphism of the spermatozoa, and a corresponding equal pair in the female, each equivalent to the larger heterochromosome of the male. . ." ***(7)***. Unfortunately, Stevens' promising work on flies was abruptly stopped by the breast cancer that claimed her life in 1912. It was left to Charles Metz ***(10,11)*** and many others to build on Stevens' discoveries (*see* **Table 1**).

3. Mitotic Chromosomes

Diploid nuclei of wild-type *D. melanogaster* contain eight chromosomes ($2n$=8) that can be seen most easily in squash preparations of the third instar larval CNS (*see* **Fig. 1**). The autosomal complement consists of two pairs of large metacentric chromosomes, designated 2 and 3, and a pair of tiny, spherical fourth chromosomes. Chromosomes 2 and 3 appear morphologically very similar after aceto-orcein or Giemsa staining, but sometimes they can be distinguished: Chromosome 3 is slightly larger, and chromosome 2 may display a

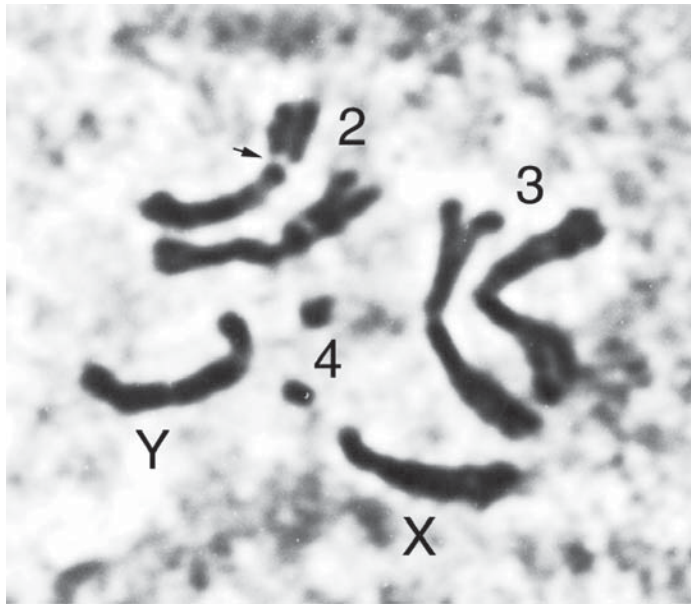

Fig. 1. Mitotic chromosomes from a male third instar larval brain stained with aceto-orcein. This metaphase spread was prepared as described in **ref.** ***41*** without colchicine or hypotonic treatment. The secondary constriction of chromosome 2 is marked with an arrow. Note the homologous associations first observed by Stevens ***(7)***. A helpful guide to mitotic chromosome morphology and landmarks (e.g., primary and secondary constrictions) is Kaufmann's 1934 article "Somatic mitoses of *Drosophila melanogaster*" ***(26)***. *See also* Cooper's 1959 study of the X and Y chromosomes ***(30)***.

prominent secondary constriction in its left arm (*see* **Fig. 1** and **ref.** ***26***). Unambiguous identification can be achieved by using the DNA stains Hoechst 33258, quinacrine, or 4',6-diamidino-2-phenylindole (DAPI), which produce fluorescence banding patterns characteristic for each chromosome arm (*see* Chapter 16 and **refs.** ***42***,***43***).

Female *Drosophila* have two X chromosomes and males have one X and one Y. The X chromosome (also sometimes referred to as the first chromosome) is slightly larger than a single arm of chromosome 2 or 3 and very nearly acrocentric. The heterochromatic Y chromosome is divided into short (Y^S) and long (Y^L) arms. Y^S and the proximal part of the X both possess a nucleolus organizer region (NOR) of 18S and 28S ribosomal-DNA tandem repeats. Spacer regions between rDNA repeat units mediate X-Y pairing to achieve normal disjunction in male meiosis ***(1,44,45)***. Otherwise, the X and Y chromosomes are nonhomologous, except where they share simple satellite and certain other repetitive DNAs (e.g., **refs.** ***46,47***).

Two simple treatments can improve mitotic chromosome cytology (*see* Chapter 16). First, incubating the larval brain in 1 m*M* colchicine prior to squashing increases the proportion of cells in mitosis (i.e., the mitotic index). Colchicine, an alkaloid derived from certain plants of the lily family (e.g., *Colchicum autumnale*), interferes with spindle assembly and thereby prevents cells from entering anaphase. The chromosomes in colchicine-treated cells show both increased condensation and repulsion of sister chromatid arms, a phenotype referred to as a "C-metaphase" (or "C-mitosis"). Colchicine treatment can sometimes cause even the centromeric regions of sister chromatids to come apart, generating a configuration of closely aligned sisters termed a "ski anaphase" (e.g., **ref.** ***48***). A similar phenotype of chromatid separation can be seen in brains of mutants defective in a spindle checkpoint function, even in the absence of colchicine ***(49)***. Incubation in sodium citrate solution typically follows colchicine treatment. Hypotonic sodium citrate causes nuclear swelling and spreads the chromosomes apart. The combination of colchicine treatment and hypotonic shock is useful in karyotyping or when investigating the possibility of chromosome breakage because it results in large numbers of mitotic figures and makes individual chromosomes and any fragments of chromosomes (and chromatids) easier to observe (e.g., **refs.** ***50,51***). Hypotonic shock alone is also routinely applied in studies of mitotic figures (*see* Chapters 16 and 17), but it can disrupt chromatin organization in interphase nuclei (e.g., **ref.** ***48***).

3.1. Euchromatin and Heterochromatin Topography

Mitotic chromosomes are differentiated longitudinally into regions of euchromatin and heterochromatin. Euchromatin is the gene-rich portion of the genome that decondenses after mitosis. Heterochromatin exists in a relatively condensed state throughout the mitotic cell cycle ***(17–19,52)***, generally replicates late in the S-phase after euchromatin ***(53)***, contains few genes (e.g., **refs.** ***54–57***), and consists of mainly satellite DNAs and transposable elements (e.g., **refs.** ***46,48,58–67***). In *D. melanogaster*, approximately one-third of the male and approximately one-fourth of the female genomes are heterochromatic ***(68)***, including the entire Y chromosome, the proximal approximately one-third of the X chromosome, the middle 20% (i.e., the pericentric regions) of chromosomes 2 and 3, and roughly three-quarters of chromosome 4. In addition, the telomeric regions of all chromosomes are heterochromatic ***(69)***.

At the molecular level, heterochromatin domains are associated with histone H3 methylated at conserved residue lysine 9, a modification catalyzed by SU(VAR)3-9 methyltransferase in *Drosophila* and by its homologs in other multicellular eukaryotes (e.g., **refs.** ***70,71***). This modification creates a binding site on histone H3 for heterochromatin protein 1 [HP1; encoded by

Su(var)2-5], which in turn may recruit other heterochromatin-associated proteins to form higher-order chromatin complexes.

In polytene chromosomes, heterochromatin-associated DNAs usually show reduced polyteny compared to euchromatic sequences, and they coalesce into a nuclear structure termed a chromocenter (*see* **Subheading 4.3.**). Another type of chromatin, "intercalary heterochromatin," is associated with polytene chromosomes and is discussed in **Subheading 4.4.**

3.2. Satellite DNAs and Associated Proteins

Highly repetitive DNAs, often simple reiterations of AT-rich sequences, make up approx 20% of the *D. melanogaster* genome and therefore the bulk of heterochromatin ***(72)***. These can be separated by centrifugation through cesium gradients into four major satellite bands having buoyant densities distinct from main-band DNA (*see* **Table 2**). Satellite classes I, II, and IV each contain a predominant simple repeat sequence together with less abundant repeats distributed in large blocks on one or more chromosome arms ***(46)***. As examples, the AATAT repeat is especially abundant on the Y (approx 5.8 Mb, visible as four discrete blocks) and fourth (approx 2.7 Mb) chromosomes, is moderately represented on the X (approx 600 kb) and third (approx 630 kb) chromosomes, and is practically absent from chromosome 2 ***(46,61)***. The AAGAG repeat is present on all chromosomes in different amounts: It is abundant on both the Y (approx 7.2 Mb) and chromosome 2 (approx 5.5 Mb, in mainly its right arm); it is present in smaller amounts on both the X (approx 1.2 Mb) and third (approx 1.1 Mb) chromosomes; and it represents a substantial portion of chromosome 4 (170 kb).

The class III satellite consists mostly of a 359-bp AT-rich repeat ***(73)*** located almost entirely on the X chromosome (approx 11 Mb; ***46***). Dimers and trimers of this satellite behave as efficient scaffold-associated/attached regions (SARs) (***79***; for a review, *see* **ref. *80***), defined as DNA restriction fragments that bind strongly to histone-depleted "chromosomal scaffolds" extracted from nuclei. SARs (also referred to as matrix-associated regions [MARs]) are typically AT-rich sequences of several hundred basepairs and are cooperatively bound by DNA topoisomerase II ***(79)***. SARs have been found flanking a number of *Drosophila* genes, in some cases comapping with transcription enhancerlike sequences ***(81)***, and are postulated to define the sites where chromatin loops attach to an underlying scaffold or nuclear matrix ***(80)***. The observed cleavage of a 359-bp satellite by topoisomerase II may be important for satellite III condensation ***(79)***.

The chromatin-associated protein D1, identified more than 20 yr ago ***(82)***, is an AT-hook protein likely to be important in organizing the structure of heterochromatin. The AT-hook motif ***(83)*** occurs in a wide variety of eukaryotic

Table 2
Satellite DNAs of *Drosophila melanogaster*

Satellite band, buoyant density class (g/cm^3)	Major constituent repeat	Comments	Minor constituent repeats	Ref.
I, 1.672	AATAT (85%)	~3% of haploid genome; maps to multiple heterochromatic sites, major sites on fourth and Y chromosomes	AATAG, AATAC, AATAAAC, AATAGAC	***(46,61)***
II, 1.686	AATAACATAG (73%)	~2.1% of the genome	AAGAC, ~2.4% of the genome; also bands at 1.689 and 1.701 g/cm^3	***(46,73)***
III, 1.688	359-bp Repeat	Maps to proximal X; 2 sites in proximal 3L in pseudo-nurse cell (PNC) polytene chromosomes		***(46,74)***
IV, 1.705	AAGAG (or circularly permuted as GAGAA)	Very abundant; ~5.6% of haploid genome; maps to multiple discrete sites on Y and pericentric heterochromatin of all other chromosomes; a translocated block of this repeat is associated with the bw^D mutation	AAGAGAG ~ 1.5% of the genome	***(46,75)***
Dodeca-satellite	CCCGTACTCGGT	Maps to proximal 3R		***(48,76)***

Note: Satellite classifications are after Endow et al. ***(77)***. The buoyant density of main-band DNA is 1.701 (at peak). Information about the density, chromosome distribution, and genome percentage for the AT-rich satellites can be found in (**refs. *46*,*61*,*72***). Without exception, each specific satellite repeat listed maps to one or more heterochromatic sites ***(46,61)***. Repeat units 63–81% identical to the 359-bp satellite and usually in clusters of two to four have been mapped to multiple euchromatic sites of the X chromosome (e.g., *see* **ref. *78***).

DNA-binding proteins in single or multiple copies ***(84)***. AT-Hooks consist of approx nine amino acids centered around a highly conserved Gly-Arg-Pro core flanked by mostly basic residues that bind to AT-rich sequences through DNA minor groove contacts ***(83)***. D1 has 10 or 11 AT-hooks and must therefore have considerable affinity for AT-rich DNA. Indeed, immunostaining of mitotic chromosomes with anti-D1 antibodies shows a pattern that reflects the overall distribution of AT-rich satellites: The Y chromosome, the proximal part of the X, and chromosome 4 are all heavily stained; faint staining is observed on one arm of chromosome 3; and there is no detectable staining of chromosome 2 ***(85)***. Loss of zygotic D1 results in early lethality that is remarkable because the embryos appear to complete development normally but are unable to escape the eggshell.

The proliferation disrupter (Prod) protein is concentrated at the pericentric regions of mitotic chromosomes 2 and 3 ***(86,87)***, mirroring the distribution of AATAACATAG satellite to which it can bind cooperatively ***(88)***. Prod is also found at much lower levels along all mitotic chromosome arms, and on polytene chromosomes it localizes to >400 euchromatic sites ***(86)***. Null *prod* mutants (obtained from heterozygous parents) are slow-growing late larval lethals whose brain cells show defects in both chromosome condensation and chromatid separation ***(86)***. The condensation problem can affect all chromosomes but is especially pronounced near the centromeres of the major autosomes, the same regions that in wild type show heavy accumulation of Prod.

The transcription factor and chromatin protein GAGA factor (GAF) binds to the very abundant AAGAG satellite (as well as to other GA repeat-rich sequences; e.g., **ref. *89***) and shows heavy accumulation at known GA-rich sites in mitotic heterochromatin ***(87,90)***. In polytene nuclei, GAF binds hundreds of sites in euchromatin but is not detectable at the chromocenter ***(90)***, a pattern it shares with Prod ***(87)***. Assuming that the chromosomal distributions of GAF and Prod seen in polytene nuclei are magnified views of their distributions in diploid interphase nuclei (this is by no means certain), these observations suggest that during the mitotic cell cycle, there is a massive relocalization of GAF and Prod from heterochromatic to euchromatic sites and then back again ***(87)***. It is not known how such protein redistribution occurs or whether it is a cause or consequence of mitotic chromosome condensation. A self-assembly mechanism involving differences in affinities of protein-binding sites in euchromatin versus heterochromatin has been proposed by Platero and colleagues ***(87)*** to explain the apparent cyclical movements of these proteins.

Cryptic satellites are highly repetitive DNAs with buoyant densities the same as main-band DNA. An example is the GC-rich dodeca satellite ***(48,76)***, which was cloned from a partial genomic library enriched for pericentric DNA fragments ***(76)***. Dodeca satellite-binding protein (DDP1) binds oligo-repeats of the

pyrimidine-rich strand of dodeca satellite ***(91,92)***. The purine-rich strand of dodeca satellite is able to form very stable hairpin structures in vitro ***(93,94)***, which suggests how its pyrimidine-rich strand is made accessible to DDP1 in vivo. DDP1 also has significant binding affinity for the pyrimidine strand of the AAGAG repeat, the purine strand of which can also form foldback structures in vitro ***(92)***. The ability of DDP1 to bind at least two satellite repeats apparently explains why the protein distributes over a much wider region of the polytene chromocenter than is occupied by dodeca satellite alone ***(91)***. DDP1 also binds at several sites in polytene euchromatin bound by HP1 ***(91)***, although the functional significance of that colocalization is not known.

DNA-binding compounds having particular affinity for the minor groove of AT-rich sequences have been known for many years (e.g., the fluorescent dye Hoechst 33258, the antibiotic distamycin). New compounds composed of multiple imidazole, pyrrole, and hydroxypyrrole units, called hairpin polyamides and based on the structure of distamycin, show not only high affinity for the minor groove but also high DNA sequence specificity (reviewed in **ref. *95***; also *see* **ref. *96***). Pairing rules for minor groove recognition by hairpin polyamides have been worked out by Dervan and collaborators and offer the potential that specific polyamides may be synthesized to target almost any DNA sequence of interest. Importantly for in vivo applications, small-molecule polyamides are soluble in aqueous solution, are not manifestly toxic, and can be tagged with fluorescent dyes.

Laemmli and colleagues synthesized polyamides designed to target specific *Drosophila* satellite repeats, either the AT tracts of satellites I and III or the GAGAA repeats of satellite IV (***97***; note, these authors have adopted a nomenclature that defines GAGAA as belonging to satellite class V). Nuclei stained with fluorophore-tagged versions of these compounds show fluorescence patterns consistent with known locations and amounts of the target repeats, demonstrating their targeting capability in vivo ***(97)***,

The most interesting properties of these polyamide compounds were observed after feeding them to developing flies of certain genotypes ***(98)***. The polyamide P9 that is specific for AT tracts was found to partially restore expression to the epigenetically silenced *white* eye-color gene when fed to the strain *In(1)*w^{m4}. In this strain, an inversion of the X chromosome has moved the wild-type *white* gene (w^+; necessary for eye pigment deposition) from its normal euchromatic location into heterochromatin. There, the condensed heterochromatin prevents w^+ from being expressed in some (or sometimes all) ommatidial clones, resulting in patches of white against a wild-type red background. The general phenomenon is referred to as position-effect variegation (PEV). Janssen et al. ***(98)*** proposed that suppression of PEV by P9 results from its binding to AT tracts in X heterochromatin (and especially to the 359-bp repeat

of satellite III), which, in turn, appears to stimulate chromatin unfolding and derepression of w^+. A similar mechanism of suppression of w^{m4} variegation is proposed to be at work in the case of an artificial protein containing 20 AT-hook motifs, MATH20 (multi-AT-hook). MATH20 appears to outcompete and displace D1 from its binding sites in the 359-bp satellite repeat, causing condensed chromatin to open and w^+ expression to occur ***(99)***.

A more dramatic effect of polyamide treatment was observed when *brown-dominant* (bw^D) flies were fed polyamide P31 that is specific for GAGAA repeats. These flies, but not wild type, showed developmental delay, high levels of lethality, and homeotic transformations similar to those seen in Trl^{13C} mutants (the *Trithorax-like* gene encodes GAF). The basis of these deleterious effects lies in the peculiar nature of the bw^D mutation, which is caused by insertion of approx 1.5 Mb of GAGAA repeat at the *bw* locus near the tip of the right arm of chromosome 2 ***(87)***. P31 binds to the bw^D GAGAA satellite, apparently causing it to open and accept large quantities of GAF [bw^D GAGAA does not normally bind GAF ***(87)***]. Massive titration of GAF away from euchromatic sites to bw^D is postulated to disrupt GAF-dependent gene expression on a large scale, leading to homeotic transformations and lethality.

These polyamide feeding experiments recall studies by Pimpinelli and colleagues done some 25 yr earlier, in which larval brains in short-term culture were exposed to the minor groove-binder Hoechst 33258 ***(100)***. Although it lacks the sequence specificity (and apparent nontoxicity to wild type) of the polyamides used by Janssen and colleagues ***(98)***, Hoechst 33258 treatment was observed to cause striking region-specific decondensation of heterochromatin at locations of AT-rich satellites.

3.3. Transposable Elements

FlyBase ***(101)*** lists >80 transposable elements (TEs), which largely constitute the middle repetitive DNAs of *D. melanogaster*. These fall into two main classes: elements that transpose via DNA intermediates (e.g., *P*, *hobo*, *FB*, *Bari-1*) and elements that transpose via RNA intermediates (i.e., retrotransposons; e.g., *copia*, *Doc*, *gypsy*, *jockey, hoppel*). TEs are found in both euchromatin and heterochromatin, and although they are "transposable" in name, many are incomplete and probably do not transpose to any appreciable extent. TEs in heterochromatin can exist both in very large clusters detectable cytologically on mitotic chromosomes (e.g., by fluorescence *in situ* hybridization [FISH] ***(63,65)***, and as dispersed single elements detectable by DNA cloning and sequencing (e.g., **ref.** ***67***). Most TEs are probably stable structural components of heterochromatin ***(63,65)***, and some may also help regulate expression of heterochromatic genes (reviewed in **refs.** ***102,103***). The retrotransposons *TART*

and *HeT-A* are essential components of *D. melanogaster* telomeres (*see* **Subheading 3.4.**).

P transposable elements only very recently (in the last 100 yr) took up residence in *D. melanogaster*, having found their way into the genome by horizontal transfer from an external source (e.g., *see* **refs. *104,105***). Although the *P* element is not a significant TE in the evolutionary history of *D. melanogaster*, in the last 20 yr it has been of incalculable value as a tool in molecular genetics, having revolutionized approaches to mutagenesis and methods for analyzing gene function.

3.4. Telomeres

The telomeric DNAs of most eukaryotes consist of tandem arrays of a short sequence motif (e.g., $[TTAGGG]_n$ in vertebrates) synthesized by a reverse transcriptase, telomerase. The telomeres of *Drosophila*, and apparently of Diptera in general, are exceptions (*see* **refs. *106–109***). *D. melanogaster* telomeres not only lack such short canonical repeats, but the fly genome does not encode a telomerase. Instead, the ends of *D. melanogaster* chromosomes consist of head-to-tail arrays of two telomere-specific retrotransposons, *TART* and *HeT-A*, produced by rounds of transposition events that counter chromosome-end erosion. (*Drosophila* telomeres lose an average of 2 bp per DNA strand per replication cycle, approx 70–75 bp per fly generation; *see* **refs. *109–111***).

Both *TART* ("telomere-associated retrotransposon") and *HeT-A* belong to the non-LTR (long terminal repeat) family of retrotransposons ***(112–114)***. Full-length *TART* elements are approx 12 kb and have four sequence domains, including open reading frames (ORFs) encoding a reverse transcriptase and retroviral gag-like protein. There are approx 5–10 *TART* elements per haploid genome, scarcely enough for each and every chromosome tip. Indeed, in some nuclei there may be telomeres without a *TART* element, and in a population of flies, both the number and order of *HeT-A* and *TART* elements may vary for any given chromosome end ***(115)***.

There are approx 30–50 *HeT-A* elements per haploid genome. Full-length *HeT-A* elements are approx 6 kb and show very little overall nucleotide sequence identity to *TART* elements (there is some similarity between the *gag*-like ORFs). Remarkably, *HeT-A* elements do not encode a reverse transcriptase and its source is unknown. It may be encoded by another retrotransposon, including possibly *TART*, or by a host a gene. The finding of both *HeT-A* and *TART* elements at the telomeres of another *Drosophila* species, *D. yakuba*, estimated to have diverged from *D. melanogaster* some 5–15 million years ago, supports the idea that the two telomeric retrotransposons are interdependent ***(116)***. A tandem array of *HeT-A*- and *TART*-related sequences has been identified in the centromeric region of the Y

chromosome of *D. melanogaster*, suggesting a possible telomeric origin for the Y centromere ***(117)***.

Short (<1 kb) repetitive DNAs called telomere-associated sequences (TASs) occupy a transition zone between the distal *HeT-A/TART* elements and the proximal, gene-encoding part of each chromosome arm ***(69,115,118–120)***; chromosome 4 may be an exception, with its transition zones possibly consisting of transposons instead. Genetically marked transgenes integrated into TAS arrays show PEV, indicating that these regions are in a heterochromatic state ***(69,119,121,122)***. Indeed, HP1 is found at all chromosome ends and its presence there helps prevent telomere–telomere fusions ***(123)***.

The mechanism by which *TART* and *HeT-A* elements are specifically targeted to receding chromosome ends and its regulation are not known, but almost certainly involve telomere–telomere associations (e.g., **refs. *119,121***). Golubovsky et al. ***(121)*** suggest that pairing of homologous telomeres would allow each telomere to "assess" the condition of the other and stimulate *HeT-A* promoter activity and transposition if end elongation was required. *HeT-A* transcript, synthesized by RNA polymerase II, is present in both the nucleus and cytoplasm at high levels in both the male and female germ lines, at lower levels in proliferating larval cells, and is not detected in polytene cells of larval salivary glands (*see* **refs. *119,124***). Transcription of *TART* is more complex ***(124)***. An intriguing dominant mutation, *Telomere elongation* (*Tel*), causes unusually long telomeres to be formed on all chromosome ends ***(125)***, identifying the Tel^+ gene product as a likely candidate for a trans regulator of telomere length. *Tel* elongated telomeres are highly enriched for *HeT-A* elements, and *TART* elements are also enriched but to a smaller degree. In both polytene and mitotic nuclei, the mutant chromosomes show a striking propensity to associate end to end. Such interactions are transient in mitotic cells because those seen at metaphase are dissolved at anaphase ***(125)***.

3.5. Centromeres

Drosophila centromeres are embedded deep in heterochromatin, amid large blocks of satellite DNAs and islands of transposable elements ***(64,66)***. A *Drosophila* centromere "signature" sequence, like the short modular *CEN* DNAs of budding yeast, has eluded detection despite impressive efforts to find one ***(64,66)***. Recent thinking has shifted to the idea that *Drosophila* centromeres (as well as those of most other animals) are defined by a specific and heritable localized chromatin modification, rather than by a DNA sequence *per se* (e.g., **ref. *126***). Indeed, the primary constriction of a metaphase chromosome, which defines the centromere cytologically, is an obvious manifestation of altered chromatin structure. Furthermore, observations in humans, *Drosophila,* and other organisms of noncentromeric DNAs being able to acquire

stable centromere function, so-called "neocentromeres," supports epigenetic models of centromere identity and function (e.g., **refs.** ***127,128***).

Centromere identifier (Cid) in *Drosophila* ***(129)*** and CENP-A in vertebrates are histone H3-like proteins that mark DNA as "centromeric" when they are incorporated into nucleosomes in place of histone H3, independent of the normal replication-coupled nucleosome assembly mechanism (*see* **ref.** ***130***). On stretched centromeric chromatin fibers, blocks of Cid-containing nucleosomes can be seen interspersed with blocks of H3-containing nucleosomes ***(131,132)***. Although the mechanism of Cid deposition is not yet known, the DNA associated with Cid nucleosomes appears to be replicated earlier than that associated with the interspersed H3 nucleosomes ***(132)***, which suggests that origins of replication are somehow involved.

Models for how the linear arrangement of alternating Cid and H3 subdomains might form a functional centromere in three dimensions are nicely illustrated in ***(131)***. One possibility is that Cid and H3 nucleosomes are assembled into a solenoid, with Cid nucleosomes grouped on one side of the structure and H3 nucleosomes on the opposite side, analogous to the way hydrophobic and hydrophilic amino acids are distributed to opposite sides of an amphipathic helix. On such a centromere at metaphase, kinetochore proteins could attach to the Cid side, where they would capture spindle microtubules, and on the H3 side, cohesins could bind and tie together sister chromatids ***(131)***. Possible explanations for why centromeres are embedded in large blocks of repetitive DNAs can be found in **refs.** ***131,132***.

3.6. Of Autosomes and Sex Chromosomes

Theories of sex chromosome evolution generally suppose that the X and Y chromosomes evolved from a homologous pair, with a proto-Y having "degenerated" into its present-day heterochromatic form (e.g., **ref.** ***133***). The *D. melanogaster* Y chromosome carries male-fertility factors but has no essential genes apart from the NOR (or *bobbed* locus), which is duplicated on the X. This explains why X/0 males are viable but sterile. Brosseau in 1960 ***(134)*** described seven Y-linked fertility factors. However, that number was reduced to six in 1981 when the existence of one of Brosseau's genes could not be confirmed ***(135–137)***; they are *kl-1*, *kl-2*, *kl-3* and *kl-5* on Y^L, and *ks-1* and *ks-2* on Y^S, where *k* refers to a male-fertility *complex* ***(138)***. At least three of these genes are extremely large, approx 1.3–4.3 Mb. *kl-3*, *kl-5* and *ks-1* are associated with megabase-size lampbrushlike loops visible in primary spermatocyte nuclei ***(139)***, and *kl-5* contains a "mega-intron" composed of repetitive DNAs ***(140)***. Such large introns may be a normal structural feature of single-copy genes in heterochromatin because both the *rolled* gene in chromosome 2 heterochromatin ***(141)*** and

the *Parp* gene in chromosome 3 heterochromatin ***(67)*** are known to have large introns composed of repetitive DNAs.

Using a new approach to scrutinize unmapped sequences in the *Drosophila* genome databases, Carvalho and colleagues recently discovered four, and possibly six, additional Y-linked genes ***(142,143)***. Moreover, they speculate that as many as 10 more genes may yet be found. *kl-2*, *kl-3* and *kl-5* all encode previously identified sperm axonemal dynein components ***(144,145)***, and *ks-1* and *ks-2* may correspond to the newly discovered genes *ORY* and *CCY*, respectively, both of which encode proteins with coiled-coil motifs. Three other new genes encode protein phosphatases of unknown function, and the *PRY* product may be involved in sperm–egg recognition ***(143)***. A sequence corresponding to *kl-1* still awaits identification. As pointed out by Carvalho et al. ***(143)***, a striking feature of nearly all of these genes is that their closest homologs are autosomal rather than X linked. This suggests that the ancestral Y genes originated on the autosomes and were translocated somehow to the proto-Y. Models of Y evolution certainly allow for such gene transposition, but the apparent large contribution of genes from the autosomes (as opposed to the X) is curious. For a discussion of these and other interesting aspects of Y chromosome evolution, *see* **ref. *143***.

Chromosome 4 is an unusual autosome in many respects (e.g., *see* **refs. *146,147***). At only approx 5 Mb, it is obviously much smaller than chromosome 2 or 3 (*see* **Fig. 1**), and its "pericentric" region covers approximately three-quarters of its length and consists of mostly simple satellite repeats. Its "euchromatic" portion contains single-copy genes interspersed between blocks of repetitive DNAs that in the two major autosomes are largely confined to heterochromatin ***(59,148)***. In addition to its diminutive size, or perhaps because of it, chromosome 4 has a heterochromatic quality. HP1 associates with much of chromosome 4 ***(149)***, and reporter genes carried on transposable elements inserted into chromosome 4 often show variegated expression (i.e., PEV ***(69,148)***. Furthermore, chromosome 4 does not normally undergo crossing over in female meiosis, a property it shares with pericentric heterochromatic regions.

In a number of ways, chromosome 4 shows closer affinity with the X chromosome than it does with the autosomes (*see* **ref. *147***). A recent and fascinating example of this is the putative RNA-binding protein Painting of fourth (POF), which specifically "paints" chromosome 4 (in polytene nuclei) by spreading over the chromosome in much the same way that the complex of male-specific lethal proteins and *roX* RNAs coats the hypertranscribed X chromosome in dosage-compensated males ***(150,151)***. In *D. busckii*, where the counterpart to *D. melanogaster* chromosome 4 is inserted at the base of the X, anti-POF antibodies paint the entire X chromosome but only in males. In *D. melanogaster*, POF paints the fourth chromosomes of both males and females,

although inexplicably the *Pof* gene (on chromosome 2 at 60E) is expressed at far higher levels in males compared to females. Assuming the *D. busckii* constitution to be ancestral, Larsson et al. ***(147)*** supposed that *D. busckii* POF may function in X chromosome dosage compensation and that *D. melanogaster* may have adapted that function to help regulate expression of chromosome 4 genes in their heterochromatic environment.

4. Salivary Gland Polytene Chromosomes

For a comprehensive treatment (through 1998) of both structure and function of polytene chromosomes, consult Igor Zhimulev's excellent review occupying three entire volumes of *Advances in Genetics* ***(152–154)***. His monographs cover *D. melanogaster* and other *Drosophila* species as well as other insect and noninsect organisms. Daneholt ***(155)*** has reviewed the packaging and trafficking of a transcript between nucleus and cytoplasm of a salivary gland cell of the midge *Chironomus tentans*, and similar mechanisms are likely to be operating in *Drosophila*. Edgar and Orr-Weaver have reviewed factors controlling the transition from mitotic to endomitotic cycles as well as regulation of endoreplication itself ***(156)***.

The salivary gland polytene chromosome complement of *D. melanogaster* consists of five large arms of similar size and a nubbin (*see* Chapters 11–15). The large arms correspond to the euchromatic portions of the X chromosome and the left and right arms of chromosomes 2 and 3. The nubbin is polytene chromosome 4, and the heterochromatic Y chromosome is not evident. Both homologs of a chromosome contribute to the polytene arm; consequently, there are half as many chromosome arms in a polytene nucleus as in a 2*n* (mitotic) nucleus. Each arm has a characteristic and reproducible pattern of alternating dark and light regions, termed bands (or chromomeres) and interbands, respectively.[1] The banded pattern is a fundamental morphological feature of the chromosome that can be seen in nonstained squashes by phase-contrast microscopy, and in non-fixed, DAPI-stained whole mounts by fluorescence microscopy (*see* **refs.** ***158,159***). The pericentric heterochromatic regions of these chromosomes and the entire Y chromosome, if present, coalesce into a "chromocenter" from which the X and autosomal arms extend. In squash preparations, the single X chromosome of the male appears somewhat thinner and stains less intensely than the two X's of the female. The chromocenter consists of compact α-heterchromatin, which appears as a single dense body in the middle of the chromocenter, surrounded

[1]Phase dark regions of polytene chromosomes are bands; phase light regions are interbands. This terminology differs from the cytogenetic nomenclature adopted for banded human metaphase chromosomes, where by definition there are no interbands, only dark bands and light bands depending on the staining technique ***(157)***.

by diffuse, netlike β-heterochromatin ***(17,18,158)***. However, α-heterchromatin of *D. melanogaster* is normally difficult to see with conventional staining (in constrast to *D. virilis*). This is remedied by a simple "differential" staining method developed by Belyaeva for phase-contrast microscopy ***(160)***.

4.1. Organization of Polytene Chromosomes in the Nucleus

Elegant light microscopic studies by Sedat and colleagues have provided close-up views of polytene chromosome organization in the nucleus (*see*, e.g., **refs.** ***158***, ***159,161***). A detailed review of those studies is beyond the scope of this chapter; however, the "rules" for salivary gland polytene chromosome organization in three dimensions can be summarized as follows:

1. The chromocenter is always closely associated with the nuclear envelope.
2. The telomeres of the X chromosome and major autosomes are positioned away from the chromocenter toward the opposite side of the nucleus, as in a Rabl orientation.
3. Each chromosome arm is confined to its own compact axial domain and there is no intertwining of arms, which explains why individual arms can be well separated in squash preparations.
4. Both arms of a particular metacentric chromosome (i.e., chromosome 2 or 3) are usually folded next to one another, and each can fold in a wide variety of configurations.
5. All arms show right-handed coiling.
6. Points of frequent contact between a chromosome and the nuclear envelope are almost exclusively at sites of intercalary heterochromatin (*see* **Subheading 4.4.**).

These characteristics of salivary gland chromosomes apply also to polytene chromosomes of the larval prothoracic gland (approx 256C; *see* **ref.** ***159***). However, the smaller chromosomes of both the midgut and hindgut show many striking departures. For example, chromosomes of larval midgut cells are rarely arranged in a polarized manner and their centromeres and telomeres can be scattered throughout the nucleus. This anomalous "organization" may stem from disruptions to nuclear structure caused by peristaltic contractions of the gut ***(159)***.

4.2. Chromatid Measurements

Soon after Painter's discovery of giant chromosomes in salivary glands of *D. melanogaster* ***(20–25)***, Koltzoff was among the first to propose they were multistranded and that chromosome enlargement occurred by multiplication of chromatids (he called them "genonemes") without mitosis ***(162)***. Three decades later, Beermann and Pelling ***(163)*** provided autoradiographic evidence that the DNA strands of *Chironomus* polytenes are unit chromatids, apparently extending the entire length of the polytene structure.

Table 3
Polytene Levels in Tissues of *Drosophila melanogaster*

Tissue/developmental stage	Level of polyteny Range or maximum (modal)	Method of quantification	Ref.
Salivary Glands			
First and second instar larvae	~25–200 "chromatids"	Direct count of interband fibers by electron microscopy (EM)	***(164)***
Late second instar female larvae	32–64C	Feulgen cytophotometry	***(165)***
Third instar female larvae	128–512C		
Prepupae	128–512C		
Newly hatched to early third instar female larvae	~4C–415C[a]	Feulgen cytophotometry	***(166)***
Third instar larvae	256–512C	Feulgen cytophotometry	***(167)***
Prepupae	256–1024C		
Third instar larvae, prepupae	256–2048C ~45% of nuclei at 1024C ~30% at 2048C ~10% at 512C	Feulgen cytophotometry	***(168)***
	~1100 "chromatids"	Direct counting by scanning electron microscopy	***(169)***
Prepupae	256–1024C	Feulgen cytophotometry	***(167)***
Third instar larvae, largest nuclei	~1500C	Densitometry of EM negatives and extrapolation from Feulgen data	***(170)***
	2048C max.	Feulgen cytophotometry	***(171)***

Prepupa female		Feulgen cytophotometry	***(171)***
proximal 1/3	256–1024C		
middle 1/3	1024–2048C		
distal 1/3	1024C		
Ring Gland			
Third instar larvae	64C	Feulgen cytophotmetry	***(167)***
Prepupae	64C		
Midgut			
Anterior third of gut from adult male	64C (32C)	Feulgen cytophotometry	***(173)***
Malpighian Tubules			
Adult male	256C max., but few nuclei reach that level (128C)	Feulgen cytophotometry	***(173)***
Fat Body			
Cells surrounding the third instar ovary	64–256C	Feulgen cytophotometry	***(170)***
Late second instar larvae	64–256C (128C)[b]	Feulgen cytophotometry	***(171,174)***
Mid third instar larvae	32–512C (256C)[b]		
Late third instar larvae	64–512C (256C)[b]		

[a]415C would be equivalent to the 512-chromatid class when adjusted for underrepresentaion of centric heterochromatin [Rudkin ***(68)*** estimated approx 22% of the female genome is heterochromatic].

[b]Anterior–posterior ploidy gradient with posterior nuclei tending to be of higher ploidy.

Numerous studies have attempted to measure polytene levels in various tissues of *D. melanogaster*, in other Diptera, and in certain other organisms where polyteny occurs (reviewed in **ref. *152***). **Table 3** lists some of the quantitative studies done on tissues of *D. melanogaster*, most of which used Feulgen cytophotometry to measure DNA amounts (*see* Chapter 7). The maximum level of polyteny estimated for wild-type *D. melanogaster* salivary glands is 1024–2048C (i.e., the two homologs having undergone 9 or 10 rounds of replication each), and regional differences in ploidy levels can exist within a gland ***(172)***. Note, however, that even 2048C is puny in comparison to the polytene levels observed in some chironomid salivary glands, up to 16,000C ***(152,171,175)***. Polytene levels in other *D. melanogaster* tissues are typically substantially lower than those in salivary glands, with the exception of nurse cells (*see* **Table 3**; *also see* Chapters 6 and 7).

In a cross-sectional scanning electron microscopic view (22,500× magnification) of a salivary gland polytene chromosome from *D. melanogaster*, Iino and Naguro ***(169)*** counted approx 1100 fibers, 12–20 nm in diameter, that they assumed were chromatids—a number consistent with cytophotometric data.

Urata et al. ***(176)*** used wide-field optical microscopy to study DAPI-stained polytene chromosomes preserved in three dimensions. Punctate DAPI staining was observed in cross sections of bands, suggesting that chromatids are bundled. The number of such bundles in the 39 bands analyzed ranged from 25 to 53 (mean = 36 ± 7). Bundles were of varying intensities, circular or ellipsoid in shape, and approx 0.2–0.4 μm in diameter (this is close to the resolution limit of the light microscope so that bundle size may be smaller) ***(176)***. Assuming 1024 chromatids per chromosome, each bundle would contain approx 20–40 chromatids. In tracing the bundles for several microns along the chromosome axis, they appeared to be continuous and were sometimes seen to merge with and split from one another. Similar results were obtained for cross sections of interbands. For these experiments, however, antibodies against a subunit of RNA polymerase II were used to highlight interbands because, unlike bands, they are stained poorly by DAPI. [Anti-RNA pol II antibodies localize to interbands and puffs ***(177)***, and RNA pol II staining does not overlap with DAPI-bright bands ***(176)***.] These authors also observed that polytene chromosomes have a cylindrical shape (and actually toroidal at the *Notch* locus) when viewed in cross section.

Antibodies against histone H1 stain both bands and interbands (puffs are stained less intensely) ***(178)***. This suggests that the 30-nm nucleosomal filament (*see* **ref. *179***), which is H1 dependent (or facilitated), is a common structural element of both bands and interbands.

Electron micrographs of whole-mount preparations of *D. melanogaster* salivary gland polytene chromosomes at low levels of polyteny (64–128 chroma-

tids) show discrete fibers in interbands oriented parallel to the chromosome axis ***(164)*** (*see also* Chapter 15). Individual fibers separated by approx 30–50 nm were seen to have an irregular beaded appearance suggesting nucleosomes (approx 10–30 nm including Pt coating). Electron microscopic (EM) analysis of polytenes of first and second instar larvae revealed specimens with approx 25, 50, 100, and 200 fibers in interbands, close to the expected geometric progression 2^5, 2^6, 2^7, and 2^8, and that all interbands of a given chromosome have the same number of fibers. In interbands at higher levels of polyteny and in bands, it was not possible to make direct counts of fibers by EM, and the ultrastructure of bands was too complex to interpret ***(164)***.

Images of squashed *D. melanogaster* salivary gland polytene chromosomes obtained by atomic force microscopy revealed discrete classes of parallel thin fibers in interbands, roughly 11, 30, and 200–250 nm wide, sometimes associated with regularly spaced "dots" (12 ± 3 nm wide), possibly nucleosomes ***(180)***. Higher squashing forces applied to interbands caused stretching and revealed additional thin fibers, whereas banded regions were largely unaffected by squashing. Seven-hundred-nanometer-wide fibers were observed in interbands of unstretched chromosomes and apparently also in bands. De Grauw et al. ***(180)*** suggest a hierarchical structure in which 11-nm "nucleosomal" fibers aggregate into 30-nm-thick then 240-nm-thick fibers, and, finally, into 700-nm-thick fibers. The 240-nm fibers were often found to have a cablelike appearance, suggesting they are coils of thinner fibers. A 110- to 130-nm-wide fiber was also sometimes observed, but its relationship to the others is unclear. It also remains to be determined whether the 700-nm (or other size) fibers seen by de Grauw et al. ***(180)*** and the bundles observed by Urata et al. ***(176)*** are the same polytene substructure.

4.3. Some DNA Sequences Associated With Mitotic Heterochromatin Are Underrepresented in Polytene Chromosomes

The notion that the DNA of both the Y and pericentric regions of mitotic chromosomes is underrepresented in polytene chromosomes dates back to Heitz's pioneering cytological studies of heterochromatin around 1930 (*see* **ref. *19***). However, direct evidence for such underrepresentation in *D. melanogaster* was first provided by Rudkin in the 1960s ***(68,165)***. Using Feulgen–DNA cytophotometry, Rudkin found that the successive replicative classes of salivary gland polytene nuclei of young (0–72 h) larvae contained significantly less DNA than 2^n-tuples of 2C expected for complete genome replication. Moreover, the deviations he observed were greater for males than females, consistent with males having a heterochromatic Y chromosome. It should be noted that two later Feulgen cytophotometry studies yielded results at odds with Rudkin's data. Dennhofer ***(168)*** reported that the DNA levels in small

polytene nuclei (8C–128C range) of salivary glands were exact doublings of the diploid values she measured in brain nuclei, and Lamb ***(173)*** found no evidence of sequence underrepresentation in polytene nuclei of midgut and Malpighian tubule cells of adults (*see* **Table 3**). However, the balance of experiments addressing this question favor Rudkin's observations and conclusions, as discussed next.

Compelling evidence for underrepresentaion of satellite DNA in *Drosophila* polytene nuclei was first provided by Gall and colleagues ***(58)***. Using the technique of CsCl equilibrium centrifugation, they found that the 1.688 satellite band (III) present in DNA isolated from diploid tissues (imaginal discs and brains) was "almost undetectable" in salivary gland DNA. Consistent with this result, they also found that *in situ* hybridization to this satellite produced signals of nearly equivalent intensities in mitotic and polytene nuclei, suggesting that both types of chromosome contain similar amounts of 1.688 satellite despite having vastly different overall ploidies. It has since been shown that both dodeca satellite ***(48)*** and the AAGAC repeat of satellite II ***(160)*** are also underrepresented in salivary gland polytene chromosomes, and sequences corresponding to the 1.705 satellite are underrepresented in nurse cell polytenes ***(181)***.

Further evidence for underrepresentation of heterochromatic sequences of polytene chromosomes includes the following: (1) some transposable elements in heterochromatin were found not to be polytenized in salivary gland chromosomes (*see* **refs. *60*, *62,141***); and (2) a gradient of polytenization of >50-fold was detected at the euchromatin–heterochromatin (E-H) junction of a minichromosome (*Dp1187*) in salivary nuclei ***(182)***.

P element constructs inserted into mitotic heterochromatin represent unique sequence DNAs whose ploidy in polytene chromosomes can be estimated by quantitative Southern blotting. Zhang and Spradling ***(183)*** found that 15 of 15 *PZ* elements (*P*[*ry*$^+$, *lacZ*]) distributed over much of Y^L were underrepresented by at least 20-fold in salivary gland DNA compared to DNA of adult males (the latter have a mix of diploid and low-level polytene nuclei). Furthermore, 13 of those inserts were undetectable by FISH analysis on salivary gland polytene chromosomes. These results argue that much of the Y chromosome is not polytenized in salivary gland nuclei.

However, not all DNA in heterochromatin is underrepresented. For example, at least three unique-sequence genes located in β-heterochromatin—*light*, *rolled*, and *suppressor of forked*—are extensively polytenized in salivary gland chromosomes ***(141,184,185)***, and the pericentric AAGAC satellite repeat is polytenized in pseudo-nurse-cell polytene chromosomes ***(160)***.

Zhang and Spradling ***(183)*** found that 16 of 16 *PZ* inserts in pericentric heterochromatin of chromosomes 2 and 3 were fully polytenized and produced FISH signals in the chromocenter. Some FISH signals were like bands, similar to those

in euchromatin, whereas others appeared as dots or covered relatively large areas of the chromocenter while remaining intensely fluorescent. Did the *PZ* elements integrate into heterochromatin domains that normally undergo polytenization or did the very presence of the insert, euchromatic as it is, stimulate polytenization where it does not normally occur? The answer to this question remains unknown. The mere presence of a *PZ* insert in heterochromatin does not guarantee its polytenization, as shown by the Y chromosome inserts mentioned earlier. Furthermore, polytenization in the 16 autosomal lines tested was not restricted to just the *PZ* inserts because middle repetitive DNAs flanking the inserts were also fully polytenized, although, in such cases, a "coattail" effect of the *PZ* insert causing adjacent sequences to polytenize cannot be excluded.

Taken together, these results reveal a complex state of polyteny in the salivary gland chromocenter, with some heterochromatin-associated DNAs underrepresented (e.g., most satellite DNAs and much or all of the Y chromosome) and some others more or less fully represented in dispersed polytenized domains.

It is generally assumed that the nonpolytenized sequences of the chromocenter give rise to α-heterochromatin and the polytenized regions to β-heterochromatin. Looping out of DNAs from interspersed polytenized domains and ectopic contacts between them are proposed to generate the reticular morphology of β-heterochromatin (*see* **refs.** ***74,160,184,186***). Such ectopic contacts may be stimulated by DNA breaks in heterochromatin ***(187,188)***. Koryakov et al. ***(160)*** reported finding no obvious cytological differences in the α-heterochromatin between X0, XY, XYY, XX, and XXY animals, which led them to suggest that the Y chromosome does not contribute substantially to α-heterochromatin formation. Given that the Y chromosome is heavily laden with satellite DNAs, this unexpected observation would challenge current models of chromocenter organization, so that further critical studies are required to address this issue.

4.4. Architecture and Morphology of the Polytene Chromosome Where Polytenized and Underrepresented Regions Meet

A plausible and long-held model for the structure of E-H junctions supposes a branched or nested arrangement of static replication forks, sometimes referred to as an "onion-skin" DNA structure, in which the multiple chromatids of euchromatin are merged with the much fewer chromatids (minimally two) of heterochromatin (*see* **Fig. 2A**). Results of recent studies by Glaser and colleagues ***(188,189)*** suggest instead that a nonbranched chromosome structure joins regions of high and low polyteny (*see* **Fig. 2B**). They propose that underrepresentation of heterochromatin-associated DNA results from the blocking of replication fork progression from euchromatin into heterochromatin at certain preferred sites and that this generates truncated euchromatic chromatids that are amplified in subsequent S-phases by "replication runoff." By

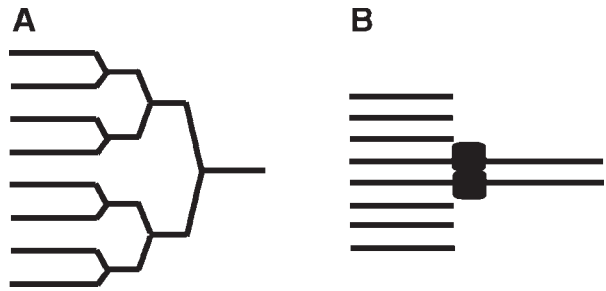

Fig. 2. Models of euchromatin-heterochromatin (E-H) junctions. **(A)** "Onion-skin" model showing branched chromatid structure as if replication forks have stalled. **(B)** Model of an E-H junction produced by a strong block to replication (filled rectangles) and subsequent "runoff replication" of truncated chromatids ***(188)***. In both **A** and **B**, the lines represent single chromatids; euchromatin is on the left and underreplicated heterochromatin on the right; for simplicity, only eight chromatids are shown in euchromatin.

subjecting genomic DNA extracted from flow-sorted follicle cell nuclei of different ploidies (*see* Chapter 8) to pulsed-field or two-dimensional gel analysis, Leach et al. ***(188)*** found that very large E-H junction-spanning DNA molecules (defined by restriction enzyme digestion) gave rise to truncated progeny molecules during the course of polytenization. For example, a 650-kb restriction fragment across the E-H junction of chromosome 3 gave rise to smaller fragments ranging in size from approx 77 kb to nearly full length. However, molecules of approx 340 kb were the most abundant, suggesting a strong stop site for replication at a position about midway along the 650-kb molecule, possibly involving satellite DNA repeats ***(188)***. They showed that the truncation process commences during the first polyploid S-phase, but that truncated duplex molecules begin to appear only after the second polyploid S-phase (8C nuclei), after the truncated strand produced in the first S-phase is able to serve as a template for replication.

In addition to E-H junctions, other regions of underrepresentation occur in euchromatic regions of polytene chromosomes, referred to as intercalary heterochromatin (IH; *see* Chapter 6). The histone gene cluster at 39DE ***(190)*** and the *Bithorax Complex* locus at 89E1-4 ***(191)*** are two prominent examples of underreplicated IH sites. IH sites replicate late compared to bulk euchromatin ***(192)***, they are often broken in squash preparations of salivary gland chromosomes (i.e., they are weak points) and they tend to form ectopic associations with nonhomologous sites and pericentric regions of chromosomes. IH sites occur frequently on the paired X chromosomes of females, but they are practically absent from the single X of males, and dosage compensation proteins

have been implicated in this sexual dimorphism (*see* **ref. *193***). No differences between sexes are observed for autosomal IH sites.

Belyaeva et al. ***(194)*** identified a fascinating mutation, *SuUR* [originally called *Su(UR)ES*], that suppresses underreplication of DNA in both pericentric and intercalary heterochromatin. Weak spots seen in $SuUR^+$ strains are absent in *SuUR* homozygotes and are replaced by one or more solid bands ***(191,194)***. Much of the β-heterochromatin becomes polytenized and shows reproducible banding. This effect is most striking for chromosome 3 pericentric heterochromatin, where a new banded segment, "Plato Atlantis," is seen that is nearly the size of chromosome 4. Ectopic associations between IH sites are greatly reduced in *SuUR* mutants, often resulting in perfectly spread polytene chromosomes. *SuUR* homozygous animals are otherwise normal in terms of morphology, viability, fertility, and meiotic recombination. *SuUR/+* heterozygotes have an intermediate suppressor phenotype.

The *SuUR* gene encodes a predicted protein of 962 amino acids that is not fully homologous to any known protein. The *N*-terminal 250 residues of SuUR show moderate similarity to sequence motifs that define the ATPase domain of members of the SWI/SNF family of proteins ***(195)***. However, the motifs in SuUR are divergent enough that a putative ATPase function is in doubt. The middle region of the protein contains an AT-hook motif, which suggests that it associates with AT-rich sequences in DNA (*see* **Subheading 3.2.**). Antibodies against SuUR stain the chromocenter very strongly, and approx 110 sites in euchromatin are also stained, all but 2 of which correspond to late-replicating IH sites ***(192)***. Some specific element shared by IH sites must direct SuUR to bind, but how this is achieved and how the protein interferes with DNA replication locally is not known ***(195)***. α-Heterochromatin and some β-heterochromatin remain underreplicated in *SuUR* mutants.

Just as the polymerase chain reaction can transform trace amounts of DNA into quantities suitable for experimental manipulation, the amplified and banded heterochromatic domains in *SuUR* mutants are providing new and valuable chromosomal material for cytology. For example, *SuUR* polytene chromosomes are being used to determine precise chromosomal locations of unassigned (heterochromatic) DNA sequences produced by the genome project ***(196)***, and to study the distribution of proteins in β-heterochromatin ***(197)***. Also, libraries of DNA fragments microdissected from *SuUR*-amplified regions have allowed polytene chromosome E-H junctions to be characterized at the molecular level ***(196)***. The *SuUR* system would also be useful in refining the positions of breakpoints of chromosomal rearrangements involving heterochromatin (*see* Chapter 12).

4.5. What Makes a Band?

To the extent that it is possible to examine banding patterns of polytene chromosomes from different tissues of a single species, they appear to be the same (*see* **ref. *198***). In *D. melanogaster*, for example, detailed comparative analysis of polytene chromosomes of ovarian nurse cells and salivary glands revealed essentially identical banding patterns in those two very different tissues (*see* Chapter 6). Furthermore, blocks of the same chromomeric patterns can be recognized across species of *Drosophila* that diverged millions of years ago ***(199)***. Models of how and where bands are formed must be able to account for such intertissue constancy and evolutionary stability.

Does the banding pattern reflect the underlying genic organization of the chromosome? The "one gene, one band" hypothesis (for an historical account, *see* **ref. *200***) began to unravel in a hurry when genomic DNA sequencing became routine (e.g., **ref. *201***) and different bands were found to contain either no, one, or multiple genes. Indeed, we now know that the *Drosophila* genome encodes approx 13,600 genes ***(202)***, which is three times the number of polytene chromosome bands. Furthermore, in comparing, for example, the mapped distribution of genes in approx 2.6 Mb of DNA sequence from the tip of the X chromosome ***(203)*** against its distinctive banded polytene structure, there is no obvious correlated pattern of genes and bands. (A banding anomaly in polytene division 2 can apparently be explained from the sequence data; it likely results from ectopic associations between two widely spaced and inverted small clusters of a repeat related to the 359-bp satellite; *see* **ref. *78***.)

In one of the first immunostaining experiments done on salivary gland polytene chromosomes, antibodies directed against a subunit of RNA polymerase II were found to stain interbands and puffs, but not bands ***(177)***. This, and earlier observations of ^{3}H-uridine labeling of interbands (*see* **ref. *204***), indicated that interband regions are transcriptionally active (this was long known to be true of puffs). A current and widely held view is that puffs reflect high levels of gene expression, interbands correspond to genes expressed at lower levels (e.g., housekeeping genes), and bands are transcriptionally silent regions. Microarray technology now permits expression levels to be measured for each and every gene along a chromosome arm, so that a transcription profile for salivary gland cells may be compared against the polytene banding pattern. Preliminary results of this kind of experiment suggest, surprisingly, that a significant portion of the genome of *Drosophila* embryos and adults is expressed in blocks of 10–30 adjacent genes, with members of each block all being expressed at a similar level irrespective of gene function. However, no obvious correlation was found between such expression domains and polytene banding patterns ***(205)***.

DuPraw and Rae in 1966 ***(206)*** proposed a "folded fiber" model of polytene chromosome structure in which unit chromatids were aligned and bands were posited to be regions of chromatid folding or coiling separated by regions of low DNA density, the interbands, in which chromatids were packaged as extended parallel fibers. A competing model, rooted in early observations of differential DNA representation (*see* **Subheading 4.3.**), was that interbands were underreplicated relative to bands (*see* **refs. *170,207,208***; for criticisms of this model at the time, *see* **ref. *190***). Spierer and Spierer ***(209)*** settled this question using quantitative Southern blot hybridization to measure DNA levels across a contiguous 315-kb stretch of polytene region 87D5-E6 containing approx 13 chromomeric units (band and adjacent interband). They found no significant variation in the levels of DNA between bands and interbands, nor within the large (>160 kb) band at 87E1,2. Lifschytz ***(190)*** reached the same conclusion using a similar method but with probes from dispersed regions of the genome. Generalizing to all chromomeric units, these results showed there is a "monotonous polyteny" along the euchromatic arms, excluding chromosomal pinch points such as IH sites.

A folded fiber model of the salivary gland polytene chromosome ***(206)*** is almost certainly correct: Chromatids are synapsed in register, bands are compact structures containing on average 10–20 times more DNA than interbands ***(176)***, and interbands are arrays of extended parallel fibers (*see* **Subheading 4.2.**). However, a detailed picture of polytene chromosome structure is still a matter for conjecture. For example, we know very little about how DNA is organized in bands or why bands form where they do. With the aim of provoking some thoughtful discussion on these topics, I propose here a possible explanation for the formation of bands that is based on the twin-domain model of transcription-induced supercoiling postulated by Liu and Wang ***(210)***. Their model asserts that as RNA polymerase transcribes a segment of duplex DNA—either a plasmid or a chromosomal loop anchored at its base—torsional strain exerted on the DNA causes positive (+) supercoils to form ahead of the polymerase complex and an equal number of negative (–) supercoils to accumulate in its wake (*see* **Fig. 3A**). The model also states that for supercoiling to occur, the translocating RNA polymerase must not rotate about the DNA helical axis—that the DNA rotates instead and its anchored ends prevent the generated twisting forces from diffusing away. There is considerable experimental support for the twin-domain model, and recent studies of transcription-induced plasmid supercoiling in *Escherichia coli* show that sequence-specific DNA-binding proteins can enhance supercoiling, apparently by forming barriers that impede diffusion and merging of adjacent (+) and (–) supercoil domains ***(211)***.

An essential requirement of the twin-domain model is that the transcribed DNA segment be topologically closed. SARs and their associated proteins ***(80,212,213)***,

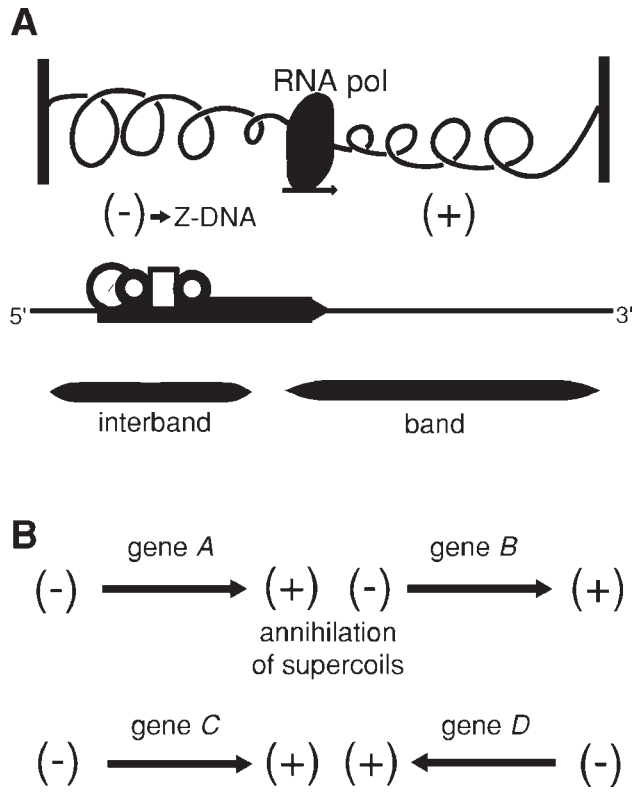

Fig. 3. Twin-domain model of polytene chromosome banding. **(A)** Schematic representation of the torsional stresses on DNA generated during transcription of a gene. (+) indicates positive supercoils ahead of the RNA polymerase complex (oblong box) and (–) indicates negative supercoils in the wake of the complex. The vertical bars flanking the chromatin loop domain represent anchoring points (e.g., SARs) on the chromatid. The hypothetical gene that has just been transcribed is indicated below the coiled DNA, and the squares and circles covering the 5' end represent transcription factors bound to enhancers and other regulatory sequences. Z-DNA can form in regions of high (–) supercoiling. The limits of the marked band and interband regions are speculative. The supercoiling aspect of this figure was redrawn and modified from ***(210)***. **(B)** Topological domains may have more than one gene. **Top:** The tandem arrangement of genes *A* and *B* transcribed at similar levels causes the (+) and (–) supercoils generated in the intergenic region to annihilate each other, but supercoils would still accumulate in the flanking regions of the domain essentially as in panel **A** (*see* **ref. *210***). **Bottom:** Convergently transcribed genes *C* and *D* will accumulate high levels of positive supercoils in the intergenic region. The model predicts a band should form in this region, assuming topoisomerase activity is low and protein complexes in the adjacent interband regions prevent diffusion and merging of (+) and (–) supercoils.

for example, might fulfill the roles of DNA loop anchors, as depicted by the vertical bars in **Fig. 3A**. Certain insulators/boundary elements might also have this capability; these are nucleoprotein complexes able to block the effects of a transcription enhancer element on a promoter when interposed between the two, which is how they are operationally defined (for reviews, *see* **refs. *212–217***). However, irrespective of whatever else a putative anchor might do, it must be able to prevent free rotation of DNA at the bases of a chromatin loop, otherwise it is not an anchor.

With this assumption of chromosome loops in place, I propose that the bands of polytene chromosomes result from torsional stresses generated as a consequence of constitutive transcription (e.g., of housekeeping genes) in each chromatin loop. In the simplest case of a chromatin loop having just a single gene, (+) supercoils would form at the 3' side of the transcribed gene and (–) supercoils would form at the 5' side (*see* **Fig. 3A**). I further propose that the (+) and (–) supercoil domains would give rise to bands and interbands, respectively, to a first approximation [(–) supercoils might also be able to form bands under certain circumstances]. Transcription factors are expected to be associated with 5' regulatory elements and to possibly constrain the (–) supercoils there, whereas the 3' end of the gene (and nongenic regions) is likely to be relatively devoid of proteins (apart from histones and possibly some other packaging proteins). At sufficient levels of (–) supercoiling, DNA in its usual B conformation can be transformed into left-handed Z-DNA ***(218,219)***. It is therefore significant that antibodies against Z-DNA specifically stain interbands of polytene chromosomes ***(220,221)***. Conversion of (–) supercoils to Z-DNA and/or transcription factor binding to regulatory sequences could result in the extended parallel chromatin fibers seen as an interband. What about the (+) supercoils? They could be constrained by proteins like mammalian DEK, which induces (+) supercoiling upon binding SV40 nucleosomal DNA ***(222)***. Moreover, DEK proteins whether on the same or on different DNA molecules can interact with each other to form multimers. At high DEK : DNA ratios, chromatin becomes compacted into an irregular structure that is not fully superhelical ***(222)***. Perhaps polytene bands also are formed in this way.

Different chromatin loops will, of course, contain different numbers and arrangements of genes, and this will have important consequences for the distribution of (+) and (–) supercoil domains in the loop. For example, for two genes in tandem and transcribed at similar levels, supercoils generated in the intergenic region will be of similar magnitude and opposite sign and therefore mutually annihilated (*see* **Fig. 3B**, top). However, the net result on supercoiling in the chromatin loop will be similar to that depicted in **Fig. 3A**. In contrast, (+) supercoils generated by convergently transcribed genes will amplify supercoiling (*see* **Fig. 3B**, bottom). With three of more genes in a chromatin

loop, more complex interactions would occur (not shown). Other factors that can affect supercoiling are gene size and level of expression. Transcription of a large gene will induce more supercoiling than will a small gene expressed at a comparable level because of the greater twisting forces generated in transcribing a large gene. Localized activities of topoisomerases, able to relax (+) and (–) supercoils, and the effects of ATP-dependent chromatin remodeling complexes (e.g., SWI/SNF) ***(223)*** will also influence the degree of supercoiling. All of these factors will combine within each chromatin loop to ultimately determine the banding pattern of the chromosome. (In the absence of such information, I will refrain here from attempting to fit to the model the interesting observations of the *Notch* gene locus in band 3C7) ***(224,225)***.

An attraction of this model is that it can explain the observed constancy of polytene chromosome banding patterns, both between different tissues of an organism and between different species of *Drosophila* where certain syntenic gene relationships have been maintained. Furthermore, because genomic context determines banding in this model, it can explain the observation that the same transgene construct inserted at different chromosomal sites can form a band, an interband, or a puff ***(226)***.

Acknowledgments

I would like to thank Taya, my muse.

References

1. McKee, B. D. (1998) Pairing sites and the role of chromosome pairing in meiosis and spermatogenesis in male *Drosophila*. *Curr. Topics Dev. Biol.* **37,** 77–115.
2. Maines, J. and Wasserman, S. (1998) Regulation and execution of meiosis in *Drosophila* males. *Curr. Topics Dev. Biol.* **37,** 301–332.
3. McKim, K. S., Jang, J. K., and Manheim, E. A. (2002) Meiotic recombination and chromosome segregation in *Drosophila* females. *Annu. Rev. Genet.* **36,** 205–232.
4. Darlington, C. D. (1937) *Recent Advances in Cytology*. Blackiston, Philadelphia.
5. Sutton, W. S. (1903) The chromosomes in heredity. *Biol. Bull.* **4,** 231–251.
6. Peters, J. A. (1959) *Classic Papers in Genetics.* Prentice-Hall, Englewood Cliffs, NJ.
7. Stevens, N. M. (1908) A study of the germ cells of certain Diptera, with reference to the heterochromosomes and the phenomenon of synapsis. *J. Exp. Zool.* **5,** 359–374.
8. Morgan, T.H. (1910) Sex limited inheritance in *Drosophila*. *Science* **32,** 120–122.
9. Sturtevant, A. H. (1913) The linear arrangement of six sex-linked factors in Drosophila, as shown by their mode of association. *J. Exp. Zool.* **14,** 43–59.
10. Metz, C. W. (1914) Chromosome studies in the Diptera. I. A preliminary survey of five different types of chromosome groups in the genus *Drosophila*. *J. Exp. Zool.* **17,** 45–49.

11. Metz, C. W. (1916) Chromosome studies on the Diptera. II. The paired association of chromosomes in the Diptera, and its significance. *J. Exp. Zool.* **21,** 213–279.
12. Bridges, C. B. (1916) Non-disjunction as proof of the chromosome theory of heredity. *Genetics* **1,** 1–52, 107–163.
13. Muller, H. J. (1962) *Studies in Genetics: The Selected Papers of H. J. Muller.* Indiana University Press, Bloomington, IN.
14. Bridges, C. B. (1917) Deficiency. *Genetics* **2,** 445–465.
15. Bridges, C. B. (1919) Vermillion-deficiency. *J. Gen. Physiol.* **1,** 645–656.
16. Muller, H. J. (1930) Types of visible variations induced by X-rays in *Drosophila*. *J. Genet.* **22,** 299–334.
17. Heitz, E. (1933) Die somatische Heteropyknose bei *Drosophila melanogaster* und ihre genetische Bedeutung. *Z. Zellforsch Mikr. Anat.* **20,** 237–287.
18. Heitz, E. (1934) Uber α und β-heterochromatin sowie Konstanz und Bau der Chromomeren bei *Drosophila*. *Biol. Zbl.* **54,** 588–609.
19. Zacharias, H. (1995) Emil Heitz (1892–1965): Chloroplasts, heterochromatin, and polytene chromosomes. *Genetics* **141,** 7–14.
20. Painter, T. S. (1931) A cytological map of the X-chromosome of *Drosophila melanogaster*. *Anat. Record* **51,** 111 (abstract).
21. Painter, T. S. (1933) A new method for the study of chromosome rearrangements and plotting chromosome maps. *Science* **78,** 585–586.
22. Painter, T. S. (1934) A new method for the study of chromosome aberrations and the plotting of chromosomes in *Drosophila melanogaster*. *Genetics* **19,** 175–188.
23. Painter, T. S. (1934) The morphology of the X-chromosomes in salivary glands of *Drosophila melanogaster* and a new type of chromosome map for this element. *Genetics* **19,** 448–469.
24. Painter, T. S. (1934) Salivary gland chromosomes and the attack on the gene. *J. Heredity* **25,** 464–476.
25. Painter, T.S. (1971) Chromosomes and genes viewed from a perspective of fifty years research. *Stadler Genet. Symp.* **1,** 33–42.
26. Kaufmann, B.P. (1934) Somatic mitoses of *Drosophila melanogaster*. *J. Morph.* **56,** 125–155.
27. Bridges, C. B. (1935) Salivary chromosome maps. *J. Heredity* **26,** 60–64.
28. Muller, H. J. (1938) The remaking of chromosomes. *Collecting Net* **8,** 182–195. [Reproduced in **ref. 13**, pp. 384–408.]
29. Caspersson, T.O. (1950) *Cell Growth and Cell Function: A Cytochemical Study.* W.W. Norton, New York.
30. Cooper, K.W. (1959) Cytogenetic analysis of major heterochromatic elements (especially Xh and Y) in *Drosophila melanogaster,* and the theory of "heterochromatin." *Chromosoma* **10,** 535–588.
31. Pardue, M.-L. and Gall, J. G. (1969) Molecular hybridization of radioactive DNA to the DNA of cytological preparations. *Proc. Natl. Acad. Sci. USA* **64,** 600–604.
32. Lindsley, D. L., Sandler, L., Baker, B. S., et al. (1972) Segmental aneuploidy and the genetic gross structure of the *Drosophila* genome. *Genetics* **71,** 157–184.

33. Rudkin, G. T. and Stollar, B. D. (1977) High resolution detection of DNA-RNA hybrids *in situ* by indirect immunofluorescence. *Nature* **265,** 472–473.
34. Ogilvie, M. B. and Choquette, C. J. (1981) Nettie Maria Stevens (1861–1912): Her life and contributions to cytogenetics. *Proc. Am. Phil. Soc.* **125,** 292–311.
35. Brush, S. G. (1978) Nettie M. Stevens and the discovery of sex determination by chromosomes. *ISIS* **69,** 163–172.
36. Stevens, N. M. (1908) The chromosomes in Diabrotica vittata, Diabrotica soror, and Diabrotica 12-punctata: a contribution to the literature on heterochromosomes and sex determination. *J. Exp. Zool.* **5,** 453–469.
37. Kohler, R. E. (1994) *Lords of the Fly:* Drosophila *Genetics and the Experimental Life,* University of Chicago Press, Chicago.
38. Stevens, N. M. (1905) Studies in spermatogenesis with especial reference to the "accessory chromosome." *Carnegie Inst. Wash. Pub.* 36.
39. McClung, C. E. (1902) The accessory chromosome—sex determinant? *Biol. Bull.* **3,** 43–84.
40. Bridges, C. B. (1925) Sex in relation to chromosomes and genes. *Am. Nat.* **59,** 127–137.
41. Gonzalez, C. and Glover, D. M. (1993) Techniques for studying mitosis in Drosophila, in *The Cell Cycle: A Practical Approach* (Fantes, P. and Brooks, R., eds.), IRL, Oxford, pp. 143–175.
42. Holmquist, G. (1975) Hoechst 33258 staining of *Drosophila* chromosomes. *Chromosoma* **49,** 333–356.
43. Gatti, M., Pimpinelli, S., and Santini, G. (1976) Characterization of *Drosophila* heterochromatin. I. Staining and decondensation with Hoechst 33258 and quinacrine. *Chromosoma* **57,** 351–375.
44. McKee, B. D. and Karpen, G. H. (1990) Drosophila ribosomal RNA genes function as an X-Y pairing site during male meiosis. *Cell* **61,** 61–72.
45. McKee, B. D., Habera, L., and Vrana, J. L. (1992) Evidence that intergenic spacer repeats of *Drosophila melanogaster* rRNA genes function as X-Y pairing sites in male meiosis, and a general model for achiasmatic pairing. *Genetics* **132,** 529–544.
46. Lohe, A. R., Hilliker, A. J., and Roberts, P. A. (1993) Mapping simple repeated DNA sequences in heterochromatin of *Drosophila melanogaster*. *Genetics* **134,** 1149–1174.
47. Kogan, G. L., Epstein, V. N., Aravin, A. A., and Gvozdev, V. A. (2000) Molecular evolution of two paralogous tandemly repeated heterochromatic gene clusters linked to the X and Y chromosomes of *Drosophila melanogaster*. *Mol. Biol. Evol.* **17,** 697–702.
48. Carmena, M., Abad, J. P., Villasante, A., and Gonzalez, C. (1993) The *Drosophila melanogaster dodecasatellite* sequence is closely linked to the centromere and can form connections between sister chromatids during mitosis. *J. Cell Sci.* **105,** 41–50.
49. Basu, J., Bousbaa, H., Logarinho, E., et al. (1999) Mutations in the essential spindle checkpoint gene *bub1* cause chromosome missegregation and fail to block apoptosis in *Drosophila*. *J. Cell Biol*. **146,** 13–28.

50. Gatti, M., Tanzarella, C., and Olivieri, G. (1974) Analysis of the chromosome aberrations induced by X-rays in somatic cells of *Drosophila melanogaster*. *Genetics* **77,** 701–719.
51. Gatti, M. (1979) Genetic control of chromosome breakage and rejoining in *Drosophila melanogaster*: spontaneous chromosome aberrations in X-linked mutants defective in DNA metabolism. *Proc. Natl. Acad. Sci. USA* **76,** 1377–1381.
52. Heitz, E. (1928) Das Heterochromatin der Moose. *Jb. Wiss. Bot.* **69,** 728–818.
53. Barigozzi, C., Dolfini, S., Fraccaro, M., Rezzonico Raimondi, G., and Tiepolo, L. (1966) In vitro study of the DNA replication patterns of somatic chromosomes of *Drosophila melanogaster*. *Exp. Cell Res.* **43,** 231–234.
54. Hilliker, A. J. (1976) Genetic analysis of the centromeric heterochromatin of chromosome 2 of *Drosophila melanogaster*: deficiency mapping of EMS-induced lethal complementation groups. *Genetics* **83,** 765–782.
55. Marchant, G. E. and Holm, D. G. (1988) Genetic analysis of the heterochromatin of chromosome *3* in *Drosophila melanogaster*. II. Vital loci identified through EMS mutagenesis. *Genetics* **120,** 519–532.
56. Schulze, S., Sinclair, D. A. R., Silva, E., et al. (2001) Essential genes in proximal *3L* heterochromatin of *Drosophila melanogaster*. *Mol. Gen. Genet.* **264,** 782–789.
57. Koryakov, D. E., Zhimulev, I. F., and Dimitri, P. (2002) Cytogenetic analysis of the third chromosome heterochromatin of *Drosophila melanogaster*. *Genetics* **160,** 509–517.
58. Gall, J. G., Cohen, E. H., and Polan, M. L. (1971) Repetitive DNA sequences in *Drosophila*. *Chromosoma* **33,** 319–344.
59. Miklos, G. L. G., Yamamoto, M. T., Davies, J., and Pirrotta, V. (1988) Microcloning reveals a high frequency of repetitive sequences characteristic of chromosome 4 and the β-heterochromatin of *Drosophila melanogaster*. *Proc. Natl. Acad. Sci. USA* **85,** 2051–2055.
60. Shevelyov, Y. Y., Balakireva, M. D., and Gvozdev, V. A. (1989) Heterochromatic regions in different *Drosophila melanogaster* stocks contain similar arrangements of moderate repeats with inserted *copia*-like elements (*MDG1*). *Chromosoma* **98,** 117–122.
61. Bonaccorsi, S. and Lohe, A. (1991) Fine mapping of satellite DNA sequences along the Y chromosome of *Drosophila melanogaster*: relationships between satellite sequences and fertility factors. *Genetics* **129,** 177–189.
62. Shevelyov, Y. Y. (1993) *Aurora*, a non-mobile retrotransposon in *Drosophila melanogaster* heterochromatin. *Mol. Gen. Genet.* **239,** 205–208.
63. Carmena, M. and González, C. (1995) Transposable elements map in a conserved pattern of distribution extending from beta-heterochromatin to centromeres in *Drosophila melanogaster*. *Chromosoma* **103,** 676–684.
64. Le, M.-H., Duricka, D., and Karpen, G. H. (1995) Islands of complex DNA are widespread in *Drosophila* centric heterochromatin. *Genetics* **141,** 283–303.
65. Pimpinelli, S., Berloco, M., Fanti, L., et al. (1995) Transposable elements are stable structural components of *Drosophila melanogaster* heterochromatin. *Proc. Natl. Acad. Sci.* **92,** 3804–3808.

66. Sun, X., Wahlstrom, J., and Karpen, G. H. (1997) Molecular structure of a functional *Drosophila* centromere. *Cell* **91,** 1007–1019.
67. Tulin, A., Steward, D., and Spradling, A. C. (2002) The *Drosophila* heterochromatic gene encoding poly(ADP-ribose) polymerase (PARP) is required to modulate chromatin structure during development. *Genes Dev.* **16,** 2108–2119.
68. Rudkin, G. T. (1965) Nonreplicating DNA in giant chromosomes. *Genetics* 52(2), 470 (abstract).
69. Cryderman, D. E., Morris, E. J., Biessmann, H., Elgin, S. C. R., and Wallrath, L. L. (1999) Silencing at *Drosophila* telomeres: nuclear organization and chromatin structure play critical roles. *EMBO J.* **18,** 3724–3735.
70. Czermin, B., Schotta, G., Hülsmann, B. B., et al. (2001) Physical and functional association of SU(VAR)3–9 and HDAC1 in *Drosophila*. *EMBO Rep.* **2,** 915–919.
71. Schotta, G., Ebert, A., Krauss, V., et al. (2002) Central role of *Drosophila* SU(VAR)3–9 in histone H3–K9 methylation and heterochromatic gene silencing. *EMBO J.* **21,** 1121–1131.
72. Peacock, W., Lohe, A. R., Gerlach, W. L., Dunsmuir, P., Dennis, E. S., and Appels, R. (1977) Fine structure and evolution of DNA in heterochromatin. *Cold Spring Harbor Symp. Quant. Biol.* **42,** 1121–1135.
73. Lohe, A. R. and Brutlag, D. L. (1986) Multiplicity of satellite DNA sequences in *Drosophila melanogaster*. *Proc. Natl. Acad. Sci. USA* **83,** 696–700.
74. Koryakov, D. E., Alekseyenko, A. A., and Zhimulev, I. F. (1999) Dynamic organization of the β-heterochromatin in the *Drosophila melanogaster* polytene *X* chromosome. *Mol. Gen. Genet.* **260,** 503–508.
75. Csink, A. K. and Henikoff, S. (1996) Genetic modification of heterochromatic association and nuclear organization in *Drosophila*. *Nature* **381,** 529–531.
76. Abad, J. P., Carmena, M., Baars, S., et al. (1992) Dodeca satellite: a conserved G+C-rich satellite from the centromeric heterochromatin of *Drosophila melanogaster*. *Proc. Natl. Acad. Sci. USA* **89,** 4663–4667.
77. Endow, S. A., Polan, M. L., and Gall, J. G. (1975) Satellite DNA sequences of *Drosophila melanogaster*. *J. Mol. Biol.* **96,** 665–692.
78. Benos, P. V., Gatt, M. K., Ashburner, M., et al. (2000) From sequence to chromosome: the tip of the X chromosome of *D. melanogaster*. *Science* **287,** 2220–2222.
79. Käs, E. and Laemmli, U. K. (1992) In vivo topoisomerase II cleavage of the *Drosophila* histone and satellite III repeats: DNA sequence and structural characteristics. *EMBO J.* **11,** 705–716.
80. Laemmli, U. K., Käs, E., Poljak, L., and Adachi, Y. (1992) Scaffold-associated regions: cis-acting determinants of chromatin structural loops and functional domains. *Curr. Opin. Gen. Dev.* **2,** 275–285.
81. Gasser, S. M. and Laemmli, U. K. (1986) Cohabitation of scaffold binding regions with upstream/enhancer elements of three developmentally regulated genes of *D. melanogaster*. *Cell* **46,** 521–530.

82. Rodriguez Alfageme, C., Rudkin, G. T., and Cohen, L. H. (1980) Isolation, properties and cellular distribution of D1, a chromosomal protein of *Drosophila*. *Chromosoma* **78,** 1–31.
83. Reeves, R. and Nissen, M. S. (1990) The AT-binding domain of mammalian high mobility group I chromosomal proteins: a novel peptide motif for recognizing DNA structure. *J. Biol. Chem.* **265,** 8573–8582.
84. Aravind, L. and Landsman, D. (1998) AT-Hook motifs identified in a wide variety of DNA-binding proteins. *Nucleic Acids Res.* **26,** 4413–4421.
85. Aulner, N., Monod, C., Mandicourt, G., et al. (2002) The AT-hook protein D1 is essential for *Drosophila melanogaster* development and is implicated in position-effect variegation. *Mol. Cell. Biol.* **22,** 1218–1232.
86. Török, T., Harvie, P. D., Buratovich, M., and Bryant, P. J. (1997) The product of *proliferation disrupter* is concentrated at centromeres and required for mitotic chromosome condensation and cell proliferation in *Drosophila*. *Genes Dev.* **11,** 213–225.
87. Platero, J. S., Csink, A. K., Quintanilla, A., and Henikoff, S. (1998) Changes in chromosomal localization of heterochromatin-binding proteins during the cell cycle in Drosophila. *J. Cell Biol.* **140,** 1297–1306.
88. Török, T., Gorjánácz, M., Bryant, P. J., and Kiss, I. (2000) Prod is a novel DNA-binding protein that binds to the 1.686 g/cm3 10 bp satellite repeat of *Drosophila melanogaster*. *Nucleic Acids Res.* **28,** 3551–3557.
89. Wilkins, R. C. and Liss, J. T. (1998) GAGA factor binding to DNA via a single trinucleotide sequence element. *Nucleic Acids Res.* **26,** 2672–2678.
90. Raff, J. W., Kellum, R., and Alberts, B. (1994) The *Drosophila* GAGA transcription factor is associated with specific regions of heterochromatin throughout the cell cycle. *EMBO J.* **13,** 5977–5983.
91. Cortés, A., Huertas, D., Fanti, L., et al. (1999) DDP1, a single-stranded nucleic acid-binding protein of *Drosophila*, associates with pericentric heterochromatin and is functionally homologous to the yeast Scp160p, which is involved in the control of cell ploidy. *EMBO J.* **18,** 3820–3833.
92. Cortés, A. and Azorín, F. (2000) DDP1, a heterochromatin-associated multi-KH-domain protein of *Drosophila melanogaster*, interacts specifically with centromeric satellite DNA sequences. *Mol. Cell. Biol.* **20,** 3860–3869.
93. Ferrer, N., Azorín, F., Villasante, A, Gutiérrez, C., and Abad, J. P. (1995) Centromeric dodeca-satellite DNA sequences form fold-back structures. *J. Mol. Biol.* **245,** 8–21.
94. Ortiz-Lombardía, M., Cortés, A., Huertas, D., Eritja, R., and Azorín, F. (1998) Tandem 5'-GA:GA-3' mismatches account for the high stability of the fold-back structures formed by the centromeric *Drosophila* dodeca-satellite. *J. Mol. Biol.* **277,** 757–762.
95. Dervan, P. B. (2001) Molecular recognition of DNA by small molecules. *Biorg. Med. Chem.* **9,** 2215–2235.
96. Henikoff, S. and Vermaak, D. (2000) Bugs on drugs go GAGAA. *Cell* **103,** 695–698.
97. Janssen, S., Durussel, T., and Laemmli, U. K. (2000) Chromatin opening of DNA satellites by targeted sequence-specific drugs. *Mol. Cell* **6,** 999–1011.

98. Janssen, S., Cuvier, O., Müller, M., and Laemmli, U. K. (2000) Specific gain- and loss-of-function phenotypes induced by satellite-specific DNA-binding drugs fed to *Drosophila melanogaster*. *Mol. Cell* **6,** 1013–1024.
99. Monod, C., Aulner, N., Cuvier, O., and Käs, E. (2002) Modification of position-effect variegation by competition for binding to *Drosophila* satellites. *EMBO Rep.* **3,** 747–752.
100. Pimpinelli, S., Gatti, M., and De Marco, A (1975) Evidence for heterogeneity in heterochromatin of *Drosophila melanogaster*. *Nature* **256,** 335–337.
101. The FlyBase Consortium (2002) The FlyBase database of the *Drosophila* genome projects and community literature. *Nucleic Acids Res.* **30,** 106–108. Available at www.flybase.bio.indiana.edu.
102. Dimitri, P. (1997) Constitutive heterochromatin and transposable elements in *Drosophila melanogaster*. *Genetica* **100,** 85–93.
103. Eissenberg, J. C. and Hilliker, A. J. (2000) Versatility of conviction: heterochromatin as both a repressor and an activator of transcription. *Genetica* **109,** 19–24.
104. Engels, W. R. (1997) Invasions of *P* elements. *Genetics* **145,** 11–15.
105. Pinkster, W., Haring, E., Hagemann, S., and Miller, W. J. (2001) The evolutionary life history of P transposons: from horizontal invaders to domesticated neogenes. *Chromosoma* **110,** 148–158.
106. Mason, J. M. and Biessmann, H. (1995) The unusual telomeres of *Drosophila*. *Trends Genet.* **11,** 58–62.
107. Biessmann, H. and Mason, J. M. (1997) Telomere maintenance without telomerase. *Chromosoma* **106,** 63–69.
108. Pardue, M.-L. and DeBaryshe, P. G. (1999) Telomeres and telomerase: more than the end of the line. *Chromosoma* **108,** 73–82.
109. Beissmann, H. and Mason, J. M. (1988) Progressive loss of DNA sequences from terminal chromosome deficiencies in *Drosophila melanogaster*. *EMBO J.* **7,** 1081–1086.
110. Levis, R. W. (1989) Viable deletions of a telomere from a Drosophila chromosome. *Cell* **58,** 791–801.
111. Beissmann, H., Carter, S. B., and Mason, J. M. (1990) Chromosome ends in *Drosophila* without telomeric DNA sequences. *Proc. Natl. Acad. Sci. USA* **87,** 1758–1761.
112. Beissmann, H., Valgeirsdottir, K., Lofsky, A., et al. (1992) HeT-A, a transposable element specifically involved in "healing" broken chromosome ends in *Drosophila melanogaster*. *Mol. Cell. Biol.* **12,** 3910–3918.
113. Levis, R. W., Ganesan, R., Houtchens, K., Tolar, L. A., and Sheen, F.-M. (1993) Transposons in place of telomere repeats at a Drosophila telomere. *Cell* **75,** 1083–1093.
114. Sheen, F.-M. and Levis, R. W. (1994) Transposition of the LINE-like retrotransposon TART to *Drosophila* chromosome termini. *Proc. Natl. Acad. Sci. USA* **91,** 12,510–12,514.
115. Walter, M. F., Jang, C., Kasravi, B., et al. (1995) DNA organization and polymorphism of a wild-type *Drosophila* telomere region. *Chromosoma* **104,** 229–241.

116. Casacuberta, E. and Pardue, M.-L. (2002) Coevolution of the telomeric retrotransposons across Drosophila species. *Genetics* **161,** 1113–1124.
117. Agudo, M., Losada, A., Abad, J. P., Pimpinelli, S., Ripoll, P., and Villasante, A. (1999) Centromeres from telomeres? The centromeric regions of the *Y* chromosome of *Drosophila melanogaster* contains a tandem array of telomeric HeT-A- and TART-related sequences. *Nucleic Acids Res.* **27,** 3318–3324.
118. Rubin, G. M. (1978) Isolation of a telomeric DNA sequence from *Drosophila melanogaster*. *Cold Spring Harbor Symp. Quant. Biol.* **42,** 1041–1046.
119. Mason, J. M., Haoudi, A., Konev, A. Y., Kurenova, E., Walter, M. F., and Biessmann, H. (2000) Control of telomere elongation and telomeric silencing in *Drosophila melanogaster*. *Genetica* **109,** 61–70.
120. Karpen, G. H. and Spradling, A. C. (1992) Analysis of subtelomeric heterochromatin in the Drosophila minichromosome *Dp1187* by single *P* element insertional mutagenesis. *Genetics* **132,** 737–753.
121. Golubovsky, M. D., Konev, A. Y., Walter, M. F., Biessmann, H., and Mason, J. M. (2001) Terminal retrotransposons activate a subtelomeric *white* transgene at the 2L telomere in Drosophila. *Genetics* **158,** 1111–1123.
122. Pardue, M.-L. and DeBaryshe, P. G. (2000) *Drosophila* telomere transposons: genetically active elements in heterochromatin. *Genetica* **109,** 45–52.
123. Fanti, L., Giovinazzo, G., Berloco, M., and Pimpinelli, S. (1998) The heterochromatin protein 1 prevents telomere fusions in *Drosophila*. *Mol. Cell* **2,** 527–538.
124. Danilevskaya, O. N., Traverse, K. L., Hogan, N. C., DeBaryshe, P. G., and Pardue, M.-L. (1999) The two *Drosophila* telomeric transposable elements have very different patterns of transcription. *Mol. Cell. Biol.* **19,** 873–881.
125. Siriaco, G. M., Cenci, G., Haoudi, A., et al. (2002) *Telomere elongation* (*Tel*), a new mutation in *Drosophila melanogaster* that produces long telomeres. *Genetics* **160,** 235–245.
126. Karpen, G. H. and Allshire, R. C. (1997) The case for epigenetic effects on centromere identity and function. *Trends Genet.* **13,** 489–496.
127. Williams, B. C., Murphy, T. D., Goldberg, M. L., and Karpen, G. H. (1998) Neocentromere activity of structurally acentric mini-chromosomes in *Drosophila*. *Nature Genet.* **18,** 30–37.
128. Maggert, K. A. and Karpen, G. H. (2001) The activation of a neocentromere in *Drosophila* requires proximity to an endogenous centromere. *Genetics* **158,** 1615–1628.
129. Henikoff, S., Ahmad, K., Platero, J. S., and van Steensel, B. (2000) Heterochromatic deposition of centromeric histone H3-like proteins. *Proc. Natl. Acad. Sci. USA* **97,** 716–721.
130. Henikoff, S., Ahmad, K., and Malik, H. S. (2001) The centromere paradox: stable inheritance with rapidly evolving DNA. *Science* **293,** 1098–1102.
131. Blower, M. D., Sullivan, B. A., and Karpen, G. H. (2002) Conserved organization of centromeric chromatin in flies and humans. *Dev. Cell* **2,** 319–330.
132. Ahmad, K. and Henikoff, S. (2002) Histone H3 variants specify modes of chromatin assembly. *Proc. Natl. Acad. Sci. USA* **99,** 16,477–16,484.

133. Steinemann, M. and Steinemann, S. (2000) Common mechanisms of Y chromosome evolution. *Genetica* **109,** 105–111.
134. Brosseau, G. E. (1960) Genetic analysis of the male fertility factors on the Y chromosome of *Drosophila melanogaster. Genetics* **45,** 257–274.
135. Kennison, J. A. (1981) The genetic and cytological organization of the *Y* chromosome of *Drosophila melanogaster*. *Genetics* **98,** 529–548.
136. Kennison, J. A. (1983) Analysis of *Y*-linked mutations to male sterility in Drosophila melanogaster. *Genetics* **103,** 219–234.
137. Lindsley, D. L. and Zimm, G. G. (1992) *The Genome of* Drosophila melanogaster, Academic, San Diego, CA.
138. Stern, C. (1929) Untersuchungen über Aberrationen des Y-Chromosoms von *Drosophila melanogaster. Z. Indukt. Abstammungs-Vererbungslehre* **51,** 253–353.
139. Bonaccorsi, S., Pisano, C., Puoti, F., and Gatti, M. (1988) Y chromosome loops in *Drosophila melanogaster*. *Genetics* **120,** 1015–1034.
140. Kurek, R., Reugels, A. M., Lammermann, U., and Bunemann, H. (2000) Molecular aspects of intron evolution in dynein encoding mega-genes on the heterochromatic Y chromosome of *Drosophila* sp. *Genetica* **109,** 113–123.
141. Berghella, L. and Dimitri, P. (1996) The heterochromatic rolled gene of *Drosophila melanogaster* is extensively polytenized and transcriptionally active in the salivary gland chromocenter. *Genetics* **144,** 117–125.
142. Carvalho, A. B., Lazzaro, B. P., and Clark, A. G. (2000) Y chromosomal fertility factors *kl-2* and *kl-3* of *Drosophila melanogaster* encode dynein heavy chain polypeptids. *Proc. Natl. Acad. Sci. USA* **97,** 13,239–13,244.
143. Carvalho, A. B., Dobo, B. A., Vibranovski, M. D., and Clark, A. G. (2001) Identification of five new genes on the Y chromosome of *Drosophila melanogaster*. *Proc. Natl. Acad. Sci. USA* **98,** 13,225–13,230.
144. Hardy, R. W., Tokuyasu, K. T., and Lindsley, D. L. (1981) Analysis of spermatogenesis in *Drosophila melanogaster* bearing deletions for Y-chromosome fertility genes. *Chromosoma* **83,** 593–617.
145. Goldstein, L. S., Hardy, R. W., Lindsley, D. L. (1982) Structural genes on the Y chromosome of *Drosophila melanogaster*. *Proc. Natl. Acad. Sci. USA* **79,** 7405–7409.
146. Locke, J., Podemski, L., Aippersbach, N., Kemp, H., and Hodgetts, R. (2000) A physical map of the polytenized region (101EF–102F) of chromosome 4 in *Drosophila melanogaster*. *Genetics* **155,** 1175–1183.
147. Larson, J., Chen, J.D., Rasheva, V., Rasmuson-Lestander, A., and Pirrota, V. (2001) Painting of fourth, a chromosome-specific protein in *Drosophila*. *Proc. Natl. Acad. Sci. USA* **98,** 6273–6278.
148. Sun, F.-L., Cuaycong, M. H., Craig, C. A., Wallrath, L. L., Locke, J., and Elgin, S. C. R. (2000) The fourth chromosome of *Drosophila melanogaster*: interspersed euchromatic and heterochromatic domains. *Proc. Natl. Acad. Sci. USA* **97,** 5350–5345.
149. Eissenberg, J. C., Morris, G. D., Reuter, G., and Hartnett, T. (1992) The heterochromatin-associated protein HP-1 is an essential protein in *Drosophila* with dosage-dependent effects on position-effect variegation. *Genetics* **131,** 345–352.

150. Stuckenholz, C., Kageyama, Y., and Kuroda, M. I. (1999) Guilt by association: non-coding RNAs, chromosome-specific proteins and dosage compensation in *Drosophila*. *Trends Genet.* **15,** 454–458.
151. Park, Y. and Kuroda, M. I. (2001) Epigenetic aspects of X-chromosome dosage compensation. *Science 293,* 1083–1085.
152. Zhimulev, I. F. (1996) Morphology and structure of polytene chromosomes. *Adv. Genet.* **34,** 1–497.
153. Zhimulev, I. F. (1998) Polytene chromosomes, heterochromatin, and position effect variegation. *Adv. Genet.* **37,** 1–566.
154. Zhimulev, I. F. (1999) Genetic organization of polytene chromosomes. *Adv. Genet.* **39,** 1–599.
155. Daneholt, B. (2001) Packing and delivery of a genetic message. *Chromosoma* **110,** 173–185.
156. Edgar, B.A. and Orr-Weaver, T.L. (2001) Endroreplication cell cycles: more for less. *Cell* **105,** 297–306.
157. ISCN (1995) *An International System for Human Cytogenetic Nomenclature* (Mitelman, F., ed.), Karger, Basel.
158. Mathog, D., Hochstrasser, M., Gruenbaum, Y., Saumweber, H., and Sedat, J. W. (1984) Characteristic folding patterns of polytene chromosomes in *Drosophila* salivary gland nuclei. *Nature* **308,** 414–421.
159. Hochstrasser, M. and Sedat, J. W. (1987) Three-dimensional organization of *Drosophila melanogaster* interphase nuclei. I. Tissue-specific aspects of polytene nuclear architecture. *J. Cell Biol.* **104,** 1455–1470.
160. Koryakov, D. E., Belyaeva, E. S., Alekseyenko, A. A., and Zhimulev, I. F. (1996) Alpha and beta heterochromatin in polytene chromosome 2 of *Drosophila melanogaster*. *Chromosoma* **105,** 310–319.
161. Hochstrasser, M., Mathog, D., Gruenbaum, Y., Saumweber, H. and Sedat, J. W. (1986) Spatial organization of chromosomes in the salivary gland nuclei of *Drosophila melanogaster*. *J. Cell Biol.* **102,** 112–123.
162. Koltzoff, N. K. (1934) The structure of the chromosomes in the salivary glands of *Drosophila*. *Science* **80,** 312.
163. Beermann, W. and Pelling, C. (1965) H3-Thymidin-Markierung einzelner Chromatinden in Riesenchromosomen. *Chromosoma* **16,** 1–21.
164. Ananiev, E. V. and Barsky, V. E. (1985) Elementary structures in polytene chromosomes of *Drosophila melanogaster*. *Chromosoma* **93,** 104–112.
165. Rodman, T. C. (1967) DNA replication in salivary gland nuclei of *Drosophila melanogaster* at successive larval and prepupal stages. *Genetics* **55,** 375–386.
166. Rudkin, G. T. (1969) Non replicating DNA in Drosophila. *Genetics* **61(Suppl.),** 227–238.
167. Welch, R. M. (1957) A developmental analysis of the lethal mutant l(2)gl of *Drosophila melanogaster* based on cytophotometric determination of nuclear desoxyribonucleic acid (DNA) content. *Genetics* **42,** 544–559.
168. Dennhofer, L. (1981) Complete replication of DNA in polytene nuclei of salivary glands of *Drosophila melanogaster*. *Wilhelm Roux' Arch. Dev. Biol.* **190,** 237–240.

169. Iino, A. and Naguro, T. (1980) Polytene chromosomes observed by scanning electron microscope. *Cytobios* **27,** 157–165.
170. Laird, C. D., Ashburner, M., and Wilkinson, L. (1980) Relationship between relative dry mass and average band width in regions of polytene chromosomes of *Drosophila*. *Chromosoma* **76,** 175–189.
171. Butterworth, F. M., Rasch, E. M., and Johnson, M. B. (1985) Is there a limit of in situ genomic replication in *Drosophila*? *J. Exp. Zool.* **234,** 325–328.
172. Rasch, E. M. (1970) DNA cytophotometry of salivary gland nuclei and other tissue systems in dipteran larvae, in *Introduction to Quantitative Cytochemistry* (Wied, G. L. and Bahr, G. F., eds.), Academic, New York, vol. 2, pp. 357–397.
173. Lamb, M. J. (1982) The DNA content of polytene nuclei in midgut and Malpighian tubule cells of adult *Drosophila melanogaster*. *Wilhelm Roux' Arch. Dev. Biol.* **191,** 381–384.
174. Butterworth, F. M. and Rasch, E. M. (1986) Adipose tissue of *Drosophila melanogaster*. VII. Distribution of nuclear DNA amounts along the anterior–posterior axis in the larval fat body. *J. Exp. Zool.* **239,** 77–85.
175. Beerman, W. and Clever, U. (1964) Chromosome puffs. *Sci. Am.* **210,** 50–58.
176. Urata, Y., Parmelee, S. J., Agard, D. A., and Sedat, J. W. (1995) A three-dimensional structural dissection of *Drosophila* polytene chromosomes. *J. Cell Biol.* **131,** 279–295.
177. Jamrich, M., Greenleaf, A.L., and Bautz, E.K.F. (1977) Localization of RNA polymerase in polytene chromosomes of *Drosophila melanogaster*. *Proc. Natl. Acad. Sci. USA* **74,** 2079–83.
178. Hill, R. J., Watt, F., Wilson, C. M., et al. (1989) Bands, interbands and puffs in native *Drosophila* polytene chromosomes are recognized by a monoclonal antibody to an epitope in the carboxy-terminal tail of histone H1. *Chromosoma* **98,** 411–421.
179. van Holde, K. and Zlatanova, J. (1996) What determines the folding of the chromatin fiber? *Proc. Natl. Acad. Sci. USA* **93,** 10,548–10,555.
180. de Grauw, C. J., Avogadro, A., van den Heuvel, D. J., et al. (1998) Chromatin structure in bands and interbands of polytene chromosomes imaged by atomic force microscopy. *Struct, J. Biol.* **121,** 2–8.
181. Hammond, M. P. and Laird, C. D. (1985) Chromosome structure and DNA replication in nurse and follicle cells of *Drosophila melanogaster*. *Chromosoma* **91,** 267–278.
182. Karpen, G. H. and Spradling, A.C. (1990) Reduced DNA polytenization of a minichromosome region undergoing position effect variegation in *Drosophila*. *Cell* **63,** 97–107.
183. Zhang, P. and Spradling, A. C. (1995) The *Drosophila* salivary gland chromocenter contains highly polytenized subdomains of mitotic heterochromatin. *Genetics* **139,** 659–670.
184. Devlin, R. H., Holm, D. G., Morin, K. R., and Honda, B. M. (1990) Identifying a single-copy DNA sequence associated with the expression of a heterochromatic gene, the *light* locus of *Drosophila melanogaster*. *Genome* **33,** 405–415.

185. Yamamoto, M., Mitchelson, A., Tudor, M., O'Hare, K., Davies, J. A., and Miklos, G, G. L. (1990) Molecular and cytogenetic analysis of the heterochromatin-euchromatin junction region of the *Drosophila melanogaster X* chromosome using cloned DNA sequences. *Genetics* **125,** 821–832.
186. Traverse, K. L. and Pardue, M.-L. (1989) Studies of He-T DNA sequences in the pericentric regions of *Drosophila* chromosomes. *Chromosoma* **97,** 261–271.
187. Kuzin, F. E., Shilova, I. E., Lezzi, M., and Gruzdev, A. D. (2002) DNA in the centromeric heterochromatin of polytene chromosomes is topologically open. *Chromosoma* **10,** 201–208.
188. Leach, T. J., Chotlowski, H. L., Wotring, M.G., Dilwith, R. L., and Glaser, R. L. (2000) Replication of heterochromatin and structure of polytene chromosomes. *Mol. Cell. Biol.* **20,** 6308–6316.
189. Glaser, R. L., Leach, T. J., and Ostrowski, S. E. (1997) The structure of heterochromatic DNA is altered in polyploid cells of *Drosophila melanogaster*. *Mol. Cell. Biol.* **17,** 1254–1263.
190. Lifschytz, E. (1983) Sequence replication and banding organization in the polytene chromosomes of *Drosophila melanogaster*. *J. Mol. Biol.* **164,** 17–34.
191. Moshkin, Y. M., Alekseyenko, A. A., Semeshin, V. F., et al. (2001) The *Bithorax Complex* of *Drosophila melanogaster*: underreplication and morphology in polytene chromosomes. *Proc. Natl. Acad. Sci. USA* **98,** 570–574.
192. Zhimulev, I. F., Semeshin, V. F., Kulichkov, V. A., and Belyaeva, E. S. (1982) Intercalary heterochromatin in *Drosophila*. I. Localization and general characteristics. *Chromosoma*. **87,** 197–228.
193. Alekseyenko, A. A., Demakova, O. V., Belyaeva, E. S., et al. (2002) Dosage compensation and intercalary heterochromatin in X chromosomes of *Drosophila melanogaster*. *Chromosoma* **111,** 106–113.
194. Belyaeva, E. S., Zhimulev, I. F., Volkova, E. I., Alekseyenko, A. A., Moshkin, Y. M., and Koryakov, D. E. (1998) *Su(UR)ES*: a gene suppressing DNA underreplication in intercalary and pericentric heterochromatin of *Drosophila melanogaster* polytene chromosomes. *Proc. Natl. Acad. Sci. USA* **95,** 7532–7537.
195. Makunin, I. V., Volkova, E. I., Belyaeva, E. S., Nabirochkina, E. N., Pirrotta, V., and Zhimulev, I. F. (2002) The Drosophila Suppressor of Underreplication protein binds late-replicating regions of polytene chromosomes. *Genetics* **160,** 1023–1034.
196. Moshkin, Y. M., Belyakin, S. N., Rubtov, N. B., et al. (2002) Microdissection and sequence analysis of pericentric heterochromatin from the *Drosophila melanogaster* mutant *Suppressor of Underreplication*. *Chromosoma* **111,** 114–125.
197. Gonzy, G., Pokholkova, G. V., Peronnet, F., et al. (2002) Isolation and characterization of novel mutations of the *Broad-Complex*, a key regulatory gene of ecdysone induction in *Drosophila melanogaster*. *Insect Biochem. Mol. Biol.* **32,** 121–132.
198. Beermann, W. (1972) Chromomeres and genes, in *Results and Problems in Cell Differentitation. Vol.4. Developmental Studies on Giant Chromosomes.* Springer-Verlag, Berlin, pp. 1–30.

199. Sturtevant, A. H. and Novitski, E. (1941) The homologues of the chromosomal elements of the genus Drosophila. *Genetics* **26,** 517–541.
200. Judd, B. H. (1998) Genes and chromomeres: a puzzle in three dimensions. *Genetics* **150,** 1–9.
201. Hall, L. M., Mason, P. J., and Spierer, P. (1983) Transcripts, genes and bands in 315,000 base-pairs of *Drosophila* DNA. *J. Mol. Biol.* **169,** 83–96.
202. Adams, M. D., Celniker, S. E., Holt, R. E., et al. (2000) The genome sequence of *Drosophila melanogaster*. *Science* **287,** 2185–2195.
203. Benos, P. V., Gatt, M. K., Murphy, L., et al. (2001) From first base: the sequence of the tip of the X chromosome of *Drosophila melanogaster*. *Genome Res.* **11,** 710–730.
204. Zhimulev, I. F. and Belyaeva, E. S. (1975) 3H-uridine labeling patterns in the Drosophila melanogaster salivary gland chromosomes X, 2R and 3L. *Chromosoma* **49,** 219–311.
205. Spellman, P. T. and Rubin, G. M. (2002) Evidence for large domains of similarly expressed genes in the *Drosophila* genome. *J. Biol.* **1,** 5.1–5.8.
206. DuPraw, E. J. and Rae, M, P. M. (1966) Polytene chromosome structure in relation to the "folded fibre" concept. *Nature* **212,** 598–600.
207. Sorsa, V. (1974) Organization of replicative units in salivary gland chromosome bands. *Hereditas* **78,** 298–302.
208. Laird, C.D. (1980) Structural paradox of polytene chromosomes. *Cell* **22,** 869–874.
209. Spierer, A. and Spierer, P. (1984) Similar levels of polyteny in bands and interbands of *Drosophila* giant chromosomes. *Nature* **307,** 176–178.
210. Liu, L. F. and Wang, J. C. (1987) Supercoiling of the DNA template during transcription. *Proc. Natl. Acad. Sci. USA* **84,** 7024–7027.
211. Leng, F. and McMacken, R. (2002) Potent stimulation of transcription-coupled DNA supercoiling by sequence-specific DNA-binding proteins. *Proc. Natl. Acad. Sci. USA* **99,** 9139–9144.
212. Geyer, P. K. (1997) The role of insulator elements in defining domains of gene expression. *Curr. Opin. Gene. Dev.* **7,** 242–248.
213. Bell, A. C. and Felsenfeld, G. (1999) Stopped at the border: boundaries and insulators. *Curr. Opin. Gene. Dev.* **9,** 191–198.
214. Udvardy, A. (1999) Dividing the empire: boundary chromatin elements delimit the territory of enhancers. *EMBO J.* **18,** 1–8.
215. Sun, F.-L. and Elgin, S. C. R. (1999) Putting boundaries on silence. *Cell* **99,** 459–462.
216. Dorsett, D. (1999) Distant liaisons: long-range enhancer-promoter interactions in *Drosophila*. *Curr. Opin. Gene. Dev.* **9,** 505–514.
217. Müller, J. (2000) Trancriptional control: the benefits of selective insulation. *Curr. Biol.* **10,** R241–R244.
218. Herbert, A. and Rich, A. (1996) The biology of left-handed Z-DNA. *J. Biol. Chem.* **271,** 11,595–11,598.
219. Oh, D.-B., Kim, Y.-G., and Rich, A. (2002) Z-DNA-binding proteins can act as potent effectors of gene expression *in vivo*. *Proc. Natl. Acad. Sci. USA* **99,** 16,666–16,671.

220. Nordheim, A., Pardue, M. L., Lafer, E. M., Moller, A., Stollar, B. D., and Rich, A. (1981) Antibodies to left-handed Z-DNA bind to interband regions of *Drosophila* polytene chromosomes. *Nature* **294,** 417–422.
221. Lancillotti, F., Lopez, M. C., Alonso, C., and Stollar, B. D. (1985) Locations of Z-DNA in polytene chromosomes. *J. Cell Biol.* **100,** 1759–1766.
222. Waldmann, T., Eckerich, C., Baack, M., and Gruss, C. (2002) The ubiquitous chromatin protein DEK alters the structure of DNA by introducing positive supercoils. *J. Biol. Chem.* **277,** 24,988–24,994.
223. Havas, K., Flaus, A., Phelan, M., et al. (2000) Generation of superhelical torsion by ATP-dependent chromatin remodeling activities. *Cell* **103,** 1133–1142.
224. Rykowski, M. C., Parmelee, S. J., Agard, D. A., and Sedat, J. W. (1988) Precise determination of the molecular limits of a polytene chromosome band: regulatory sequences for the *Notch* gene are in the interband. *Cell* **54,** 461–472.
225. Vasquez, J. and Schedl, P. (2000) Deletion of an insulator element by the mutation *facet-strawberry* in *Drosophila melanogaster*. *Genetics* **155,** 1297–1311.
226. Semeshin, V. F., Demakov, S. A., Perez Alonso, M., Belyaeva, E. S., Bonner, J. J., and Zhimulev, I. F. (1989) Electron microscopical analysis of *Drosophila* polytene chromosomes. V. Characteristics of structures formed by transposed DNA segments of mobile elements. *Chromosoma* **97,** 396–412.

2

Spermatogenesis

Analysis of Meiosis and Morphogenesis

Helen White-Cooper

1. Introduction

1.1. Cytogenetic Analysis of the Drosophila *Testis*

In this chapter, I hope to convince the reader that *Drosophila* spermatogenesis is an ideal system for the cytogeneticist. Spermatogenesis is relatively simple, dispensable for adult viability, and amenable to genetic, cell biological, and biochemical approaches. The stages of spermatogenesis are well defined, the cells are large, easily accessible, and easily identified. Because spermatogenesis initiates with a stem cell division, there is continuous production through the life of the fly. Therefore, a normal adult testis presents all of the stages of spermatogenesis as a spatio-temporal array (*see* **Fig. 1A**). Excellent and comprehensive reviews of the genetics of spermatogenesis and ultrastructure of wild-type spermatogenesis are available ***(1,2)***. In this introduction, I will review only the essential features needed to interpret the results of experiments performed according to the protocols given here.

Spermatogenesis follows a multistep differentiation program involving dramatic changes in cell cycle dynamics, gene expression, and morphogenesis. The transformation of a 15-µm-diameter round spermatid into a 1.8-mm-long mature motile sperm is a truly remarkable act of cellular remodeling. This includes changes in mitochondrial morphology that occur nowhere else in the fly; mitochondria aggregate, fuse, and wrap to give a characteristic Nebenkern mitochondrial derivative at the onion stage. The centriole is transformed into a flagellar basal body embedded in the nuclear envelope. Flagellal elongation is accompanied by elongation of the two mitochondrial derivatives. Nuclear shaping and chromatin condensation transforms a round nucleus into a bear-claw-shaped

From: *Methods in Molecular Biology, vol. 247:* Drosophila *Cytogenetics Protocols*
Edited by: D. S. Henderson © Humana Press Inc., Totowa, NJ

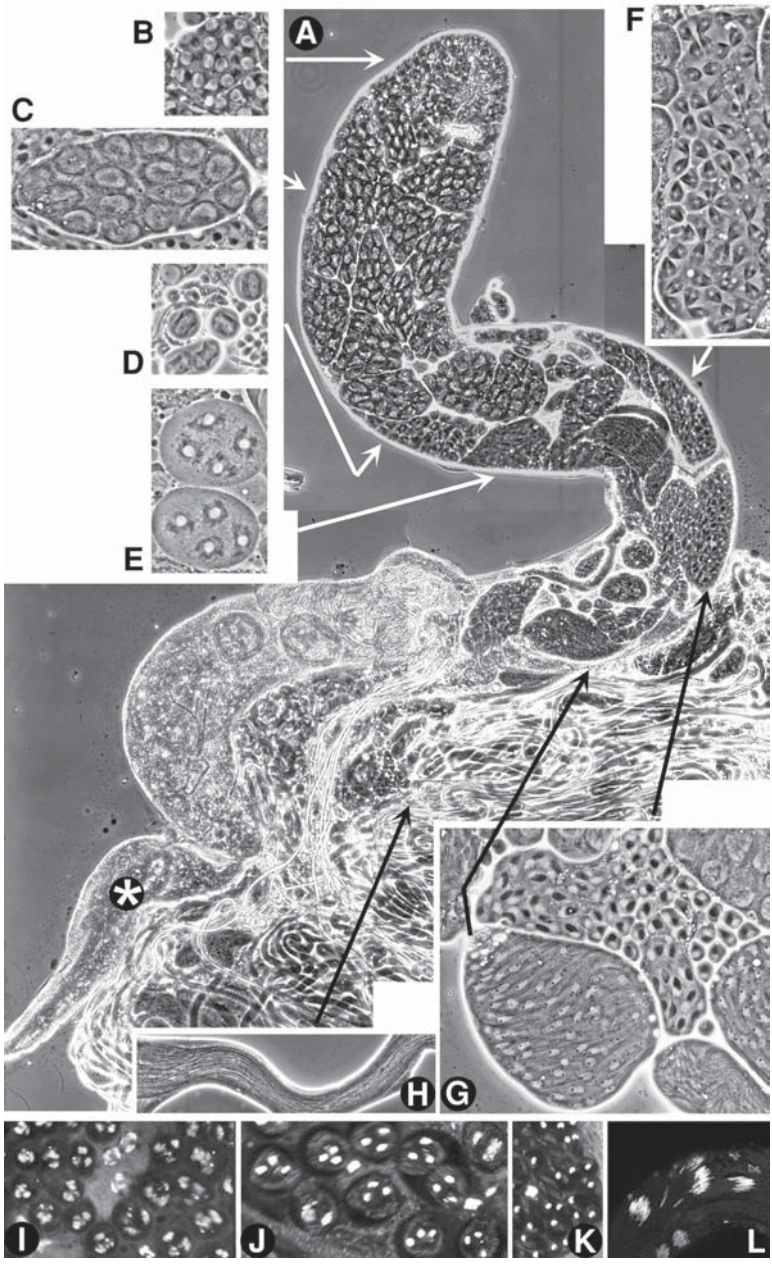

Fig. 1. Phase-contrast microscopy of wild-type testes. The stages of spermatogenesis are easily visible with phase-contrast optics in gently squashed preparations. **(A)** A whole wild-type testis, cut near the distal end, with most of the elongating spermatids spilled out through the cut. There is a temporal progression of cell types from very

highly compact structure. Some processes and gene products are shared with other tissues and developmental stages; others are spermatogenesis-specific. Male meiosis, for example, is much more similar to mitosis than to female meiosis. Many mitotic gene products are used for male meiosis and, therefore the application of a few simple techniques for studying testes can reveal much about the mechanics of cell division. For example, we have learned about the maintenance of sister chromatid cohesion through analysis of *mei-S332* and *ord*. Analysis of weak *ord* mutants suggests Ord is required for proper centromeric cohesion after arm cohesion is released at the metaphase I–anaphase I transition. Ord activity appears to promote centromeric cohesion during meiosis II. Mei-S332 protein is localized to the centromeric region in meiosis; its destruction at the metaphase II–anaphase II transition allows sister chromatid separation. A balance between the activity of Mei-S332 and Ord is required for proper regulation of meiotic cohesion ***(3–7)***. Analysis of *asp* alleles indicates a role for Asp protein in the normal meiotic and mitotic spindle structure. Immunolocalization of Asp in spermatocytes revealed that it is required for the bundling of microtubules at spindle poles, but it is not an integral centrosome component implicated in microtubule nucleation ***(8,9)***. There has been a long-standing debate over the role of asters in determining the position of the cleavage furrow of cytokinesis. Recent evidence from *Drosophila* spermatogenesis has shown that asters are not required for cytokinesis, because *asterless* mutants undergo cytokinesis ***(10)***. Instead, it appears that the cleavage furrow depends on the central spindle ***(9)***. Analysis of cell cycle regulatory genes has revealed that differentiation can continue in the absence of cell cycle progression. Mutation of the meiosis-specific Cdc2-activator *twine* blocks progression through the meiotic divisions; however, the cells continue with aspects of spermatid differentiation, including axoneme elongation and nuclear shaping ***(11–14)***.

A notable feature of the recent completion of the genome sequencing and continuation of the expressed sequence tag (EST) sequencing projects has been

---

early stages at the apical end **(top)** to nearly mature sperm at the distal end **(bottom)**, leading into the seminal vesicle (*). **(B–H)** Higher magnification of specific stages of spermatogenesis; **(B)** polar spermatocytes. **(C)** mature primary spermatocytes; **(D)** part of a cyst in metaphase–anaphase I; **(E)** part of a secondary spermatocyte cyst (meiotic interphase); **(F)** a telophase II cyst; **(G)** onion-stage spermatids (right) and comet stage of early spermatid elongation (left); **(H)** part of a cyst late in elongation before individualization. **(I–L)** Hoechst 33342 labeling of DNA in wild-type live squashes. **(I)** Primary spermatocytes with decondensed chromosomes visible as three discrete regions in each nucleus; **(J)** prophase of meiosis I, partially condensed chromosomes are visible; **(K)** leaf blade stage, DNA is compact within the nucleus, faint staining of the mitochondrial DNA is seen in the Nebenkern; **(L)** tightly clustered and fully shaped nuclei in nearly mature bundles of elongated spermatids, before individualization.

the identification of a large set of testis-specific transcripts. Andrews et al. ***(15)*** sequenced 3141 testis ESTs, representing 1560 contigs, of which 47% were not represented in the 80,000 ESTs sequenced by the Berkley Drosophila Genome Project (BDGP) from other tissues. Sixteen percent had not even been predicted as genes on the first annotation of the genome sequence, and only 11% corresponded to known named genes. This study highlights how little we know and how much more there is to learn about the genes required to carry out this most remarkable cellular process of spermatogenesis. Fortunately, a large set of new male sterile mutants, the tool we need to take a genetic approach to understanding spermatogenesis, is now available. A large-scale mutagenesis screen was undertaken in the Charles Zuker lab and yielded over 12,000 new viable mutagenized chromosomes. These were tested for male and female sterility by Barbara Wakimoto and Dan Lindsley, yielding approx 2000 male sterile lines (cited in **ref. *16***). This collection supplements our existing battery of male sterile mutants (e.g., those generated by Castrillon et al. ***[17]***). They are available to the whole community and have formed the basis of a new wave of excitement and analysis of cytogenetics in *Drosophila* spermatogenesis ***(18–20)***.

1.2. Key Phases of Cellular Differentiation During Spermatogenesis

The testis sheath is a closed tube made up of muscle and pigment cells, separated from the lumen by a basement membrane. At the apical tip (the closed end of the tube), the basement membrane is thickened adjacent to a group of approx 20 somatic cells called the hub (*see* **Fig. 2A**). About eight germ-line stem cells are found around the hub, each associated with two cyst progenitor somatic stem cells. Division of the germ-line stem cell, accompanied by division of the two cyst progenitor cells, results in a spermatogonium encapsulated by two cyst cells. These two cyst cells will never divide again, but they will grow and remain intimately associated with the germ-line cells. Division of the spermatogonium generates two spermatogonia, and three subsequent spermatogonial mitotic divisions (*see* **Fig. 3A**) followed by premeiotic S-phase results in a cyst of 16 primary spermatocytes still surrounded by two cyst cells. Cells within each cyst remain interconnected by cytoplasmic bridges called ring canals, derived from the cleavage furrow after incomplete cytokinesis. A specialized membrane-rich region of cytoplasm, the fusome, extends through these bridges to connect all of the cells in the cyst ***(21)***.

The primary spermatocyte period is primarily one of cell growth (approx 25-fold increase in cell volume **ref. *2***), with certain morphological changes indicating the early, middle, and mature primary spermatocyte. Notable is the transition to the polar spermatocyte stage (*see* **Fig. 1B**), where the phase dark mitochondria are aggregated to one side of the cell and the phase light nucleus

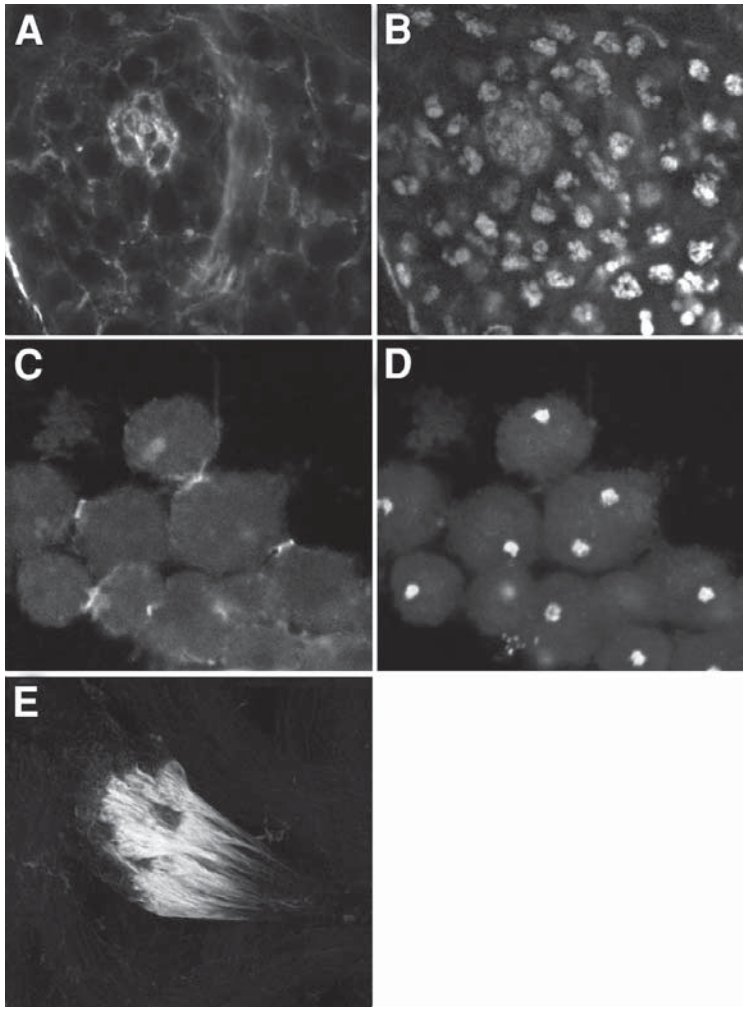

Fig. 2. FITC Phalloidin shows the hub, meiotic cleavage furrows and investment cones. Formaldehyde-fixed testis squash preparations stained with FITC phalloidin (**A,C,E**), which labels F-actin, and counterstained with propidium iodide to reveal the DNA (**B,D**). **(A,B)** The apical tip of a testis. The somatic hub structure appears as a small rosette where there is a more extensive array of F-actin. The large cells around this rosette are the germ-line stem cells. **(C,D)** Several cells at telophase of meiosis I. The F-actin is concentrated in the contractile rings of the cleavage furrows separating sister cells. **(E)** Investment cones are formed around the nuclei of elongated spermatids; they are then displaced from the nuclei as they progress along the cyst, investing each spermatid with its own plasma membrane and extruding the minor mitochondrial derivative and excess cytoplasm into a cytoplasmic waste bag. This set of investment cones has progressed part way along the spermatid tails.

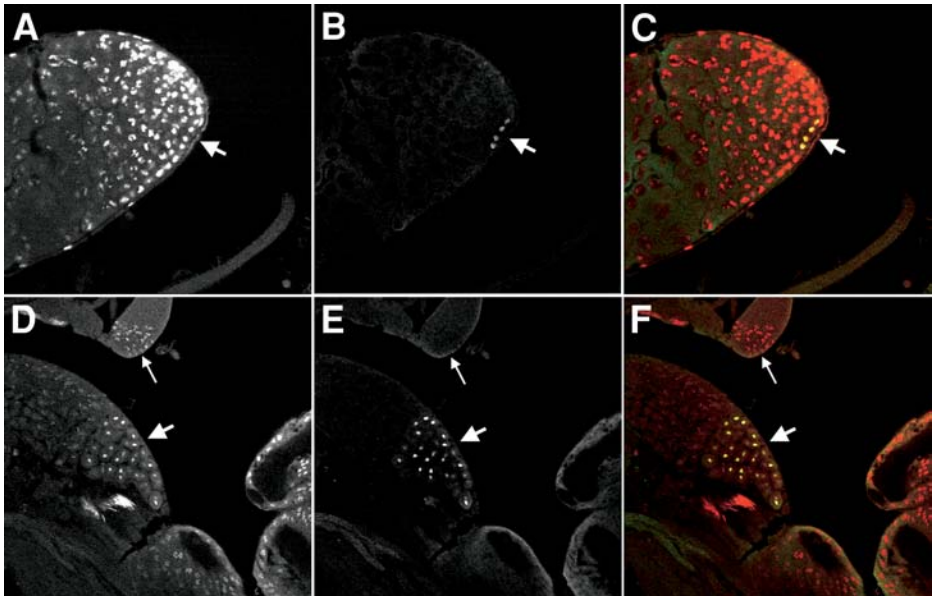

Fig. 3. Phosphorylation of histone H3 identifies mitotic and meiotic chromosomes. Methanol/acetone fixed testes stained with an antibody against phosphorylated histone H3 (**B,E** green [yellow] in **C** and **F**) and counterstained with propidium iodide (**A,D**, red in **C** and **F**). **(A–C)** A cyst of four spermatogonia (arrow) near the apical tip of the testis undergoing mitosis. Note the bright staining of spermatogonial cell DNA and the relatively weak staining of the DNA of the maturing primary spermatocytes to the left of the figure. **(D–F)** A cyst of cells completing meiosis I (large arrow) have phosphorylated histone H3. Early in elongation (small arrow), the nuclei are all clustered to one side of the cyst and histone H3 is no longer phosphorylated. (*See* color plate 1 in the insert following p. 242.)

resides in the other side. Later, the asymmetry is lost as the cells become apolar spermatocytes. Throughout the primary spermatocyte stage, the decondensed chromosomes are in three nuclear domains, corresponding to the two major autosome and the sex chromosome bivalents (*see* **Fig. 1I**). Primary spermatocytes have a very prominent phase dark nucleolus, which is associated with the sex chromosome bivalent. Bulk transcription shuts down as primary spermatocytes mature ***(22,23)***, so transcripts for genes required late in spermatogenesis need to have accumulated in the cells by this stage. They are then stored in RNP particles in the cytoplasm until translation ***(24)*** (*see* **Fig. 4B**).

As mature primary spermatocytes (*see* **Fig. 1C**) enter the meiotic divisions the nucleus becomes rounder and the chromosomes condense and move away from the nuclear envelope (*see* **Fig. 1J**). Mitochondria aligned on the meiotic spindle make this structure readily visible in phase-contrast preparations (*see*

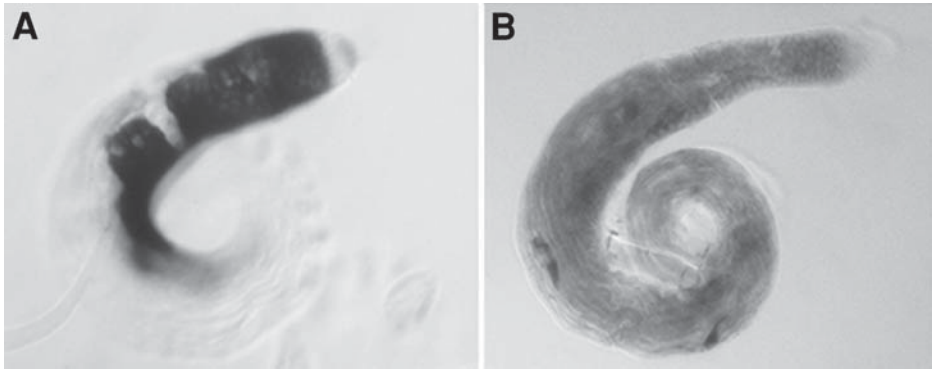

Fig. 4. *In situ* to wild type with cyclin B, Mst87F. **(A)** In situ hybridization to *cyclin B* transcript reveals a two-phase expression pattern. *cyclin B* message is expressed in the mitotic cells at the apical tip of the testis, but is absent from cells undergoing premeiotic S-phase. *cyclin B* message then reappears in early primary spermatocytes, persists until meiosis, and is degraded before the cysts progress to onion stage. **(B)** *Mst87F* encodes a protein important for the structure of the sperm heads. The transcript first accumulates in primary spermatocytes and persists through to very late stage of spermatogenesis, when it is translated.

Figs. 1D and **5**). An aster can be seen on one side of the nucleus, and this separates as the centrosomes migrate to opposite poles to set up the bipolar spindle. During meiotic telophase the cleavage furrow separating the sisters pinches the spindle to generate a "bow tie" effect (*see* **Fig. 1F**, [telophase II], **Fig. 5** [bottom left panel], and **2C**) and, finally, give a secondary spermatocyte cyst consisting of 32 cells connected by ring canals, encapsulated by 2 cyst cells. Meiosis II follows after a very short interphase (*see* **Fig. 1E**). Morphologically, meiosis II is very similar to meiosis I, although there is clearly half as much DNA, only 1 centriole per centrosome, the cells are smaller, and the final product is a cyst of 64 interconnected spermatids, still surrounded by the 2 cyst cells.

After the second meiotic division, all of the mitochondria aggregate and fuse to form two giant mitochondria. These are interleaved by the onion stage to make a Nebenkern, which, by transmission electron microscopy, resembles an onion slice ***(25)*** and, by phase contrast, is a dark sphere adjacent to the phase light nucleus (*see* **Figs. 1G,J**). The centriole inserts into the nuclear membrane and axoneme elongation initiates ***(2)***. A phase dark dot, the pseudonucleolus or protein body, appears inside the otherwise featureless phase light nucleus. During elongation, the mitochondria unfurl from each other and two distinct phase dark mitochondrial derivatives can be seen elongating alongside

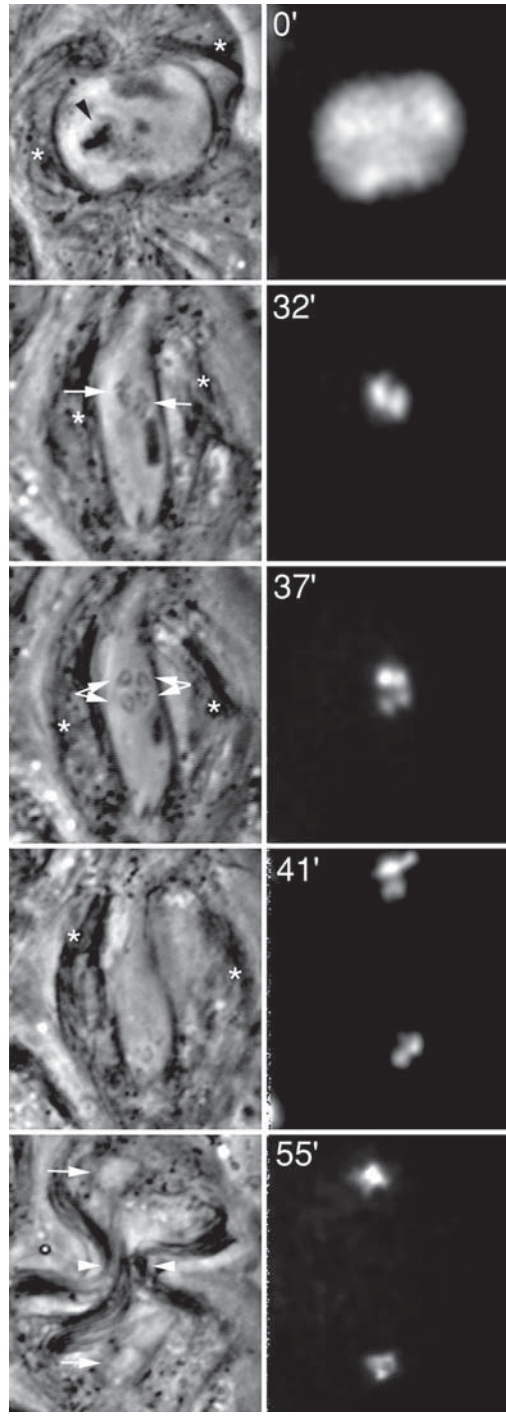
0'
32'
37'
41'
55'

the flagellar axoneme at the comet stage (*see* **Fig. 1H**). All of the spermatids in a cyst develop in synchrony; during elongation, their heads become more closely aligned. This is already visible at the comet stage where the nuclei are found at one side of the cyst, and the tails extending toward the other side (*see* **Fig. 3D**). Intercellular bridges remain at the distal end of the elongating cysts ***(26)***. During elongation, the two cyst cells behave somewhat differently, each encompassing one end of the cyst. The head end cyst cell contacts the terminal epithelium near the base of the testis, so that cysts elongate with their heads anchored and the tails pushing up the length of the testis. During elongation, the nuclei become invisible with phase contrast as they compact and are transformed from a sphere into a needle shape (*see* **Fig. 1L**).

Finally, the fully elongated spermatids individualize and coil. Individualization initiates with an actin-based structure, the investment cone, at the head end of each spermatid ***(27)***. This progresses along the length of each tail (*see* **Fig. 2E**), stripping off all excess cytoplasm and the minor mitochondrial derivative into a cytoplasmic waste bag (*see* **Fig. 6C**) that is eventually shed into the lumen of the testis. Individual sperm are coiled into the seminal vesicle ready for transfer to the female during copulation.

2. Materials

2.1. Phase-Contrast Microscopy

1. Testis buffer: 183 m*M* KCl, 47 m*M* NaCl, 10 m*M* Tris-HCl, pH 6.8 **or** TB1: 15 m*M* potassium phosphate (equimolar dibasic and monobasic), pH 6.7, 80 m*M* KCl, 16 m*M* NaCl, 5 m*M* $MgCl_2$, 1% polyethylene glycol (PEG) 6000.

Fig. 5. (*opposite page*) Meiosis I progression in wild-type spermatocytes observed by time-lapse phase-contrast and fluorescence microscopy. Meiosis was followed from early prometaphase to the end of meiosis I at a rate of 20 frames/min using a combination of phase contrast (left panels) and fluorescence (right panels) microscopy. The chromosomes were labeled with a His2-GFP fusion protein (right panels). Five significant time-points are shown in this figure, reproduced from Rebollo and Gonzalez ***(41)***: 0' corresponds to late prophase, the two centrosomes have migrated to opposite poles and organized large asters. The meiotic spindle is forming and is highlighted with phase dark mitochondria (asterisks). A nonchromosomal phase dark nuclear structure, which remains throughout meiosis, can be seen (arrowhead). At 32', the spermatocyte contains a fully formed elongated spindle. Two bivalents are stabilized at the metaphase plate in this focal plane (arrows). At 37', anaphase has just started. Two pairs of homologous chromosomes can be seen segregating from each other (double arrows). At 41', the chromosomes have reached the poles and are decondensing. Chromosome decondensation is first apparent midway through anaphase. At 55', the two daughter nuclei have formed (arrows) and the cleavage furrow begins to pinch the central spindle (white arrowheads).

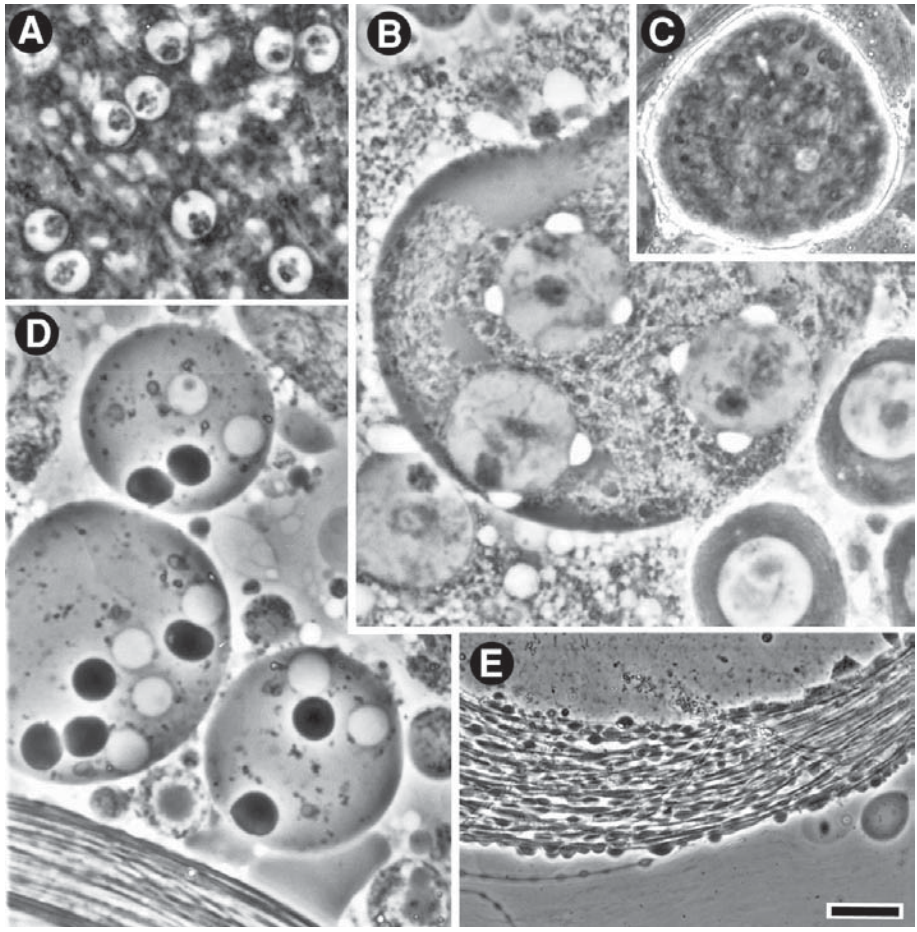

Fig. 6. Other cell types and typical artefacts that should be ignored. **(A)** Cells from the accessory gland can be confused with early primary spermatocytes. However, primary spermatocytes are in cysts, the nuclei of accessory gland cells are more uniform, and there is never a polarity to the accessory gland cytoplasm. **(B)** Oversquashed primary spermatocytes can develop vacuoles adjacent to the nucleus. These can be confused with mutant onion stages; however, the large spermatocyte nuclei are usually still apparent. **(C)** The cytoplasmic waste bag extruded upon individualization can sometimes be confused with a very disorganized early elongation cyst. **(D)** Cells can fuse under pressure from the cover slip. Fused normal onion stage cells can be confused for cytokinesis mutants. True cytokinesis mutants show two or four phase light nuclei adjacent to only one (large) Nebenkern. Here, the nuclei and Nebenkern are similar in size and equal in number. **(E)** Occasionally, when elongated cysts are disrupted just before individualization the sperm tails have a blebby rather than smooth appearance. For this to be classified as the mutant phenotype, it has to be consistently rather than rarely seen. (Scale bar is 10 μm and applies to all panels, except panel **C**.)

2. Dissecting plate; for example, a 10-cm-diameter plastic Petri dish with the sides removed.
3. Sharp forceps (the sharper the better).
4. Tungsten mounted needles (sharp!).
5. Microscope slides and cover slips, 22×22 mm^2.
6. Phase-contrast compound microscope with camera.
7. Kimwipes.
8. Hoechst 33342 (bis-benzimide; e.g., Sigma-Aldrich) (1 mg/mL stock). Store in the dark at 4°C. Dilute in dissection buffer to 2–5 µg/mL when needed.
9. 45% Acetic acid.
10. Halocarbon oil (Voltalef 10S).

2.2. Immunostaining

2.2.1. Whole Mount Immunohistochemistry

1. Testis buffer or TB1 (*see* **item 1, Subheading 2.1.**). For monoclonal antibodies directed against phosphorylated epitopes, use TBPi buffer: 10 m*M* Tris-HCl, pH 6.8, 180 m*M* KCl, 50 m*M* NaF, 1 m*M* Na_3VO_4, 10 m*M* Na β-glycerophosphate.
2. 4% Formaldehyde (from 40% stock) in phosphate-buffered saline (PBS), or make up fresh 4% paraformaldehyde in PBS or HEPES buffer: 100 m*M* HEPES, pH 6.9, 2 m*M* $MgSO_4$, 1 m*M* EGTA. HEPES buffer may be stored at –20°C, but check pH before (re)use.
3. PBS+0.1% Triton-X100 (PBSTx).
4. Fetal calf serum (FCS). Sterile, but out of date will do; it is used as a blocking agent.
5. 24-Well tissue culture plates and tissue culture inserts with 8-µm mesh (Falcon no. 3097).
6. Primary antibody.
7. Secondary antibody, biotin-conjugated (Vector Laboratories).
8. ExtrAvidin-HRP conjugate (Sigma-Aldrich), or Vectastain ABC reagents (Vector Laboratories).
9. 3,3'-Diaminobenzidine (DAB; available in tablet form from Sigma). DAB is a potent carcinogen. Wear gloves and use caution.
10. Hydrogen peroxide.
11. Microscope slides and cover slips.
12. Mounting medium: 85% Glycerol. Add 2.5% *n*-propyl-gallate if counterstaining with Hoechst.
13. Hoechst 33258 (e.g., Sigma-Aldrich) (optional; *see* **Subheading 3.2.1.**).

2.2.2. Formaldehyde Fixation for Confocal Microscopy

1. Testis buffer or TB1 (*see* **item 1**, **Subheading 2.1.**).
2. Liquid nitrogen, scalpel, safety glasses.
3. 100% Ethanol (chilled on dry ice).
4. 4% Formaldehyde in PBS.
5. PBST: PBS + 0.1% Triton X-100 or 0.1% Tween-20.

6. PBST-DOC: PBS + 0.3% Triton X-100 + 0.3% sodium deoxycholate (from 10% stock).
7. FCS (sterile, but does not have to be in date), or bovine serum albumin (BSA).
8. Poly-L-lysine-coated slides.
9. Siliconized 22 × 22-mm^2 cover slips.
10. Evostick impact adhesive or rubber cement.
11. Clear nail polish.
12. Humid chamber (e.g., sandwich box with wet tissue paper).
13. Primary antibody.
14. Fluorescently conjugated secondary antibody (Jackson ImmunoResearch Laboratories or Vector Laboratories).
15. Propidium iodide or DAPI (4,6-diamidino-2-phenylindole) if staining for DNA.
16. RNAse A, 10 mg/mL stock (store at –20°C). Required if using propidium iodide.

2.2.3. Methanol/Acetone Fixation for Confocal Microscopy

As per **Subheading 2.2.2.**, except replace **item 3** (ethanol) with methanol cooled on dry ice, **item 4** (4% formaldehyde) with acetone cooled on dry ice, and **items 5** and **6** (PBST and PBS-DOC) with PBS + 1% Triton X-100 + 0.5% acetic acid (PBS-T-AA).

2.3. X-Gal Staining

1. 1% Glutaraldehyde in PBS.
2. 20% 5-Bromo-4-chloro-3-indolyl-β-D-galactopyranoside (X-gal) in dimethylformamide (DMF). Store at –20°C.
3. X-gal buffer: 150 m*M* NaCl, 7.2 m*M* Na_2HPO_4, 2.8 m*M* NaH_2PO_4, 1 m*M* $MgCl_2$. Keep as 5X stock.
4. Staining solution: X-gal buffer containing 5 m*M* $K_4Fe(CN)_6$, 5 m*M* $K_3Fe(CN)_6$. Store 50 m*M* stock solutions in the dark.
5. 85% Glycerol.
6. Microscope slides and cover slips for mounting.

2.4. *RNA* In Situ *Hybridization*

2.4.1. Probe

1. Plasmid clone of cDNA with suitable RNA polymerase promoter sites (e.g., pBluescript, Stratagene).
2. 10X DIG RNA labeling mix (Roche): 10 m*M* ATP, 10 m*M* CTP, 10 m*M* GTP, 6.5 m*M* UTP, 3.5 m*M* DIG-UTP in Tris-HCl, pH 7.5.
3. RNA polymerase and buffer (for an antisense transcript, the one that transcribes from the 3' end of the gene) (New England Biolabs [NEB] or Roche).
4. RNAse-free water.
5. 2X Carbonate buffer: 60 m*M* Na_2CO_3, 40 m*M* $NaHCO_3$, pH 10.2.
6. 2X Neutralization buffer: 200 m*M* sodium acetate, 1% (v/v) acetic acid.

2.4.2. Hybridization

1. Fix: 4% Paraformaldehyde in 100 m*M* HEPES, pH 6.9, 2 m*M* $MgSO_4$, 1 m*M* EGTA. May be stored at –20°C. Check pH before (re)use.
2. PBS + 0.1% Tween-20 (PBST).
3. Proteinase K (Roche). Stock is 19 mg/mL. Store at –20°C.
4. 2 mg/mL Glycine in PBST. Glycine stock is 200 mg/mL (store at room temperature).
5. Hybridization buffer (HB): 50% Formamide, 5X SSC, 100 µg/mL denatured sonicated salmon sperm DNA, 50 µg/mL heparin, 0.1% Tween-20, adjust to pH 4.5 with 2 *M* citric acid (approx 100 m*M* final concentration). Store at –20°C. Preheat for 65°C washes. 20X SSC is 3 *M* NaCl, 0.3 *M* sodium citrate, pH 7.0.
6. RNA probe (*see* **Subheading 3.4.1.**).
7. High pH buffer (HP): 100 m*M* NaCl, 100 m*M* Tris-HCl, pH 9.5, 50 m*M* $MgCl_2$, 0.1% Tween-20. Make up fresh, and add $MgCl_2$ last to prevent precipitation.
8. Nitroblue tetrazolium (NBT): 18.75 mg/mL in 70% DMF stock (Roche).
9. X-Phosphate (5-bromo-4-chloro-3-indolyl-phosphate [BCIP]): stock solution is 50 mg/mL in DMF (Roche).
10. Alkaline phosphatase conjugated antidigoxygenin antibody (Roche), preadsorbed against embryos (*see* **Note 1**).
11. Gary's Magic Mountant (GMM): 1.6 g/mL Canada balsam (powder) in methyl salicylate. If only liquid Canada balsam is available, mix 4 : 1 with methyl salicylate.
12. 24-Well tissue culture plates and tissue culture inserts with 8-µm mesh (Falcon no. 3097).
13. Glass staining blocks.
14. Microscope slides and cover slips.

3. Methods

3.1. Phase Contrast Microscopy of Live Testes

This is the first technique to apply when asking the question "Why are my mutant males sterile?" Because the key stages of spermatogenesis have a very distinctive appearance in wild-type testes (*see* **Fig. 1**), it is relatively easy to look at a squash and preliminarily classify the mutant based on the morphologies observed. **Table 1** gives a key to the types of defects you may observe; these give clues as to what cytological process may be affected and, therefore, will direct your future experiments. This list is by no means exhaustive; many characterized phenotypes are not listed here. Additionally, as more mutations are characterized the number of distinct phenotypes seen will increase substantially. **Figure 7** shows examples of some mutant phenotypes seen in phase-contrast squash preparations. As with analysis of mutant phenotypes in other stages of the life cycle (e.g., embryogenesis), it is critical to identify the earliest stage at which faults are detectable. Sometimes, mutant males will show more than one defect; the challenge then becomes to

Table 1
Some Well-Characterized Testes Phenotypes

Observation	Avenues to follow	Example	Ref.
There are motile sperm in the seminal vesicle	Fertilization/paternal effect	*sneaky*	***28***
	Mating or courtship behavior	*fru*	***29***
	Nondisjunction in meiosis	*asp* (weak)	***8***
Mature sperm bundles are present, no other defect seen	Individualization	*Chc4*	***27***
	Axoneme structure	*wrl*	***30***
Classic male sterile phenotype	Nuclear shaping. Mitochondrial morphogenesis	*moz*	
Unequal nuclear and Nebenkern size at onion stage	Chromosome nondisjunction	*asp*	***8***
Too few cells at onion stage	Meiotic division failed?	*twine*	***11***
16 cells, 16 large nuclei, 16 large Nebenkern	No nuclear or cell division, nuclei are 4N	*mgr*	***31***
16 cells, 64 normal nuclei, 16 large Nebenkern	Nuclear division occurred, but cytokinesis failed	*fwd*	***32***
Nebenkern looks abnormal at onion stage and early elongation	Mitochondrial aggregation	*nmd*	***1***
	Mitochondrial fusion	*fzo*	***33***
	Mitochondrial unfurling		
Primary spermatocytes look normal, no later stages seen	Meiotic arrest	*mia*	***34***
Spermatogonial cysts contain more than 16 cells	Failure to activate spermatocyte differentiation program	*bam*	***35***
Many small cells present, not all in cysts	Stem cell overproliferation	*egfr* *raf*	***36,37***
No germ-line cells in testis	Maternal effect, pole cell formation failed	*tud*	***38***
	Stem cell maintenance		

identify whether one is primary and the other secondary, or whether the gene in question acts directly in both affected processes. For example, spermatids in males mutant for proteins required for nuclear shaping fail to individualize, because correct shaping of the nucleus is required for the normal assembly of the investment cone ***(27)***. Mutations affecting spindle structure may show defects in both chromosome segregation (uneven nuclear size at onion stage) and cytokinesis (Nebenkern larger than wild type and fewer in number) because of the relationship between spindle structure, especially the central spindle, and the cleavage furrow.

Cell division is an extremely dynamic process; however, the transient nature of standard squash preparations observed by phase contrast yields only snapshot images of meiosis. In many cases, it is desirable to observe cells undergoing the divisions using time-lapse microscopy ***(40,41)***. By observing living cells, we can characterize in much more detail the exact nature of any meiotic defect. For example, a four-wheel-drive phenotype, where karyokinesis is unaffected but cytokinesis fails (e.g., **Fig. 7D**), could be the result of one of two fundamentally different defects. There may be a failure in the contractile ring, such that there is no contraction; alternatively, the intercellular bridge that should remain after incomplete cytokinesis may not be stabilized ***(42)***. Observations of living cells can rapidly distinguish between these possibilities ***(32)***. For analysis of live specimens undergoing meiosis *see* **Subheading 3.1.3.** and Chapter 3.

1. Dissect testes from a newly eclosed male in fresh testis buffer (0–1 d old) (*see* **Note 2**).
2. Place a drop of testis buffer on a clean microscope slide, using the surface tension of the buffer transfer the testes to this drop.
3. Open up the testes (and seminal vesicles if looking for motile sperm) by cutting them open with the tungsten needles or by ripping with the forceps (*see* **Note 3**).
4. Place a clean cover slip over the testes; this will gently squash the cells. Squashing can be increased to give better phase contrast by wicking buffer out using a Kimwipe. This can be done while observing the cells under the phase-contrast microscope (*see* **Note 4**).

3.1.1. Analyzing Nuclear Morphology

Nuclear morphology can be examined in live squashes by staining the DNA with the vital dye Hoechst 33342. This is included in the testes buffer at 2–5 µg/mL during dissection.

1. Proceed as described in **Subheading 3.1.**, but allow the testes to sit in the buffer for 5 min after dissection and before adding the cover slip (*see* **Fig. 1I–L**). Alternatively, chromatin can be observed using a stock carrying a His2-GFP transgene ***(41)*** (*see* **Fig. 5**).

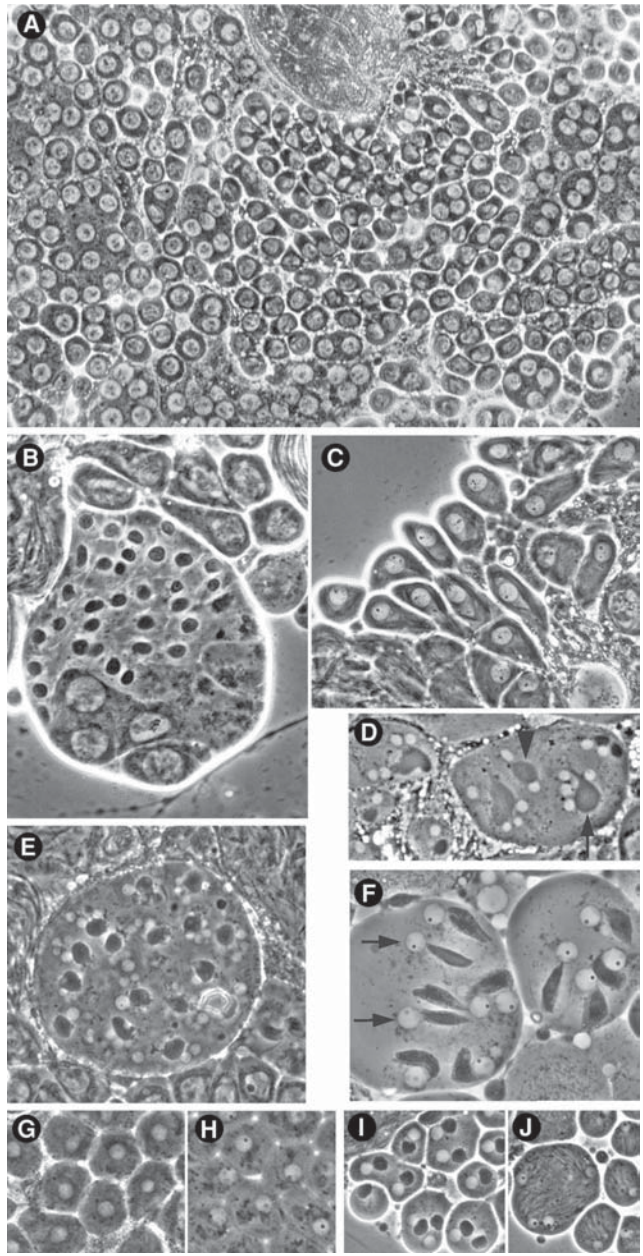

Fig. 7. Some examples of mutant phenotypes. **(A)** Meiotic arrest (e.g., *aly, can, mia, sa*): Testes mutant for meiotic arrest genes accumulate morphologically normal primary spermatocytes. No meiotic or postmeiotic cells are present. **(B)** Intracyst asynchrony (e.g., *polo*): Some alleles of cell cycle mutants can result in asynchrony within cysts. Here, half of the cyst has progressed to onion stage, four cells are attempting

3.1.2. Analyzing Meiotic Chromosome Morphology

Meiotic chromosome morphology can be assessed in acetic acid squashes. Because acid destroys much of the cellular structure, the morphology of the squashed testis will be compromised; however, condensed meiotic chromosomes and sperm heads will be visible ***(14)***.

1. Dissect testes as described in **Subheading 3.1., step 1**, then transfer to 45% acetic acid on the slide, and allow to swell for 15 s before cutting.
2. Proceed to **step 3** of **Subheading 3.1.**

3.1.3. Time-Lapse Microscopy

1. Dissect out the testes and place into a large drop of halocarbon oil on a cover slip. Remove as much nontestis material as possible from the preparation.
2. Cut the testes open and spill the contents out by pulling the sheath around the cover slip.
3. Pick up the cover slip with a slide and observe with phase-contrast optics for up to 1 h ***(32)***. The addition of extra cover slips (or pieces of cover slip) as supports alongside the testes prevents oversquashing and increases the viability of the cells to 2 h (*see* **Note 5**).

Fig. 7. (*continued*) meiosis, and four are still primary spermatocytes. **(C)** No meiotic divisions (e.g., *twine, boule, mgr,* β*2-tubulin*): Failure to form a meiotic spindle results in failure of both chromosome segregation and cell division. Onion stage cysts can be seen containing 16 rather than 64 cells, each having a large (4N) nucleus and a large (usually misshapen) Nebenkern. **(D)** Cytokinesis failure (e.g., *fwd, shank*): Normal chromosome segregation followed by failure of cytokinesis at both meiotic divisions results in an onion stage cell (arrow) containing four nuclei associated with just one very large mitochondrial derivative. If only one cytokinesis fails, two nuclei are associated with one large mitochondrial derivative (arrowhead). **(F)** Chromosome nondisjunction (e.g., *asp*, compound chromosomes): Chromosome nondisjunction results in one daughter nucleus having more DNA than its sister nucleus. Because the nuclear size at onion stage is directly proportional to DNA content, this is manifest as variable nuclear diameters in early spermatids (compare arrowed nuclei). **(E)** Cytokinesis failure and chromosome nondisjunction: Mutants that affect both cytokinesis and chromosome segregation can result in postmeiotic cysts containing 64 variable-sized nuclei associated with 16 large Nebenkern. **(G,H)** No mitochondrial derivative (e.g., *nmd*): Failure of mitochondrial aggregation and fusion results in a cloud of mitochondria in onion-stage cells **(G)**. At the leaf blade stage **(H)**, they are scattered, mostly to one side of the nucleus, but a normal Nebenkern is never formed. **(I,J)** Mitochondrial fusion (e.g., *fzo*): At onion stage, mitochondria aggregate but fail to fuse. Wrapping of pairs of mitochondria forms a Nebenkern, which at this stage (**I**) looks somewhat lumpy. By the comet stage **(J)**, many individual mitochondrial pairs are seen elongating from each nucleus. Panel **E** was provided by Cayetano Gonzalez (EMBO), and panels **G–J** were provided by Karen Hales (Davidson College).

Because in each preparation only one field can be imaged, it is wasteful to dissect more than one male per slide. Care should be taken in choosing the image field; cells near the edge of the displaced testis contents may be easier to see, but will die sooner than those that remain surrounded by other testis material in slightly more physiological conditions. Cytokinesis seems to be more sensitive to perturbation than chromosome segregation. If the aim of the experiment is to observe cytokinesis in a mutant, it is best to select cells in anaphase at the start of the recording session. Cells can easily fuse during preparation of the slide; if two cells in meiotic prophase are artificially fused, both spindle morphology and kinetochore attachment to microtubules may be disrupted. The effect will be an aberrant meiosis, and often failed cytokinesis, which could be misinterpreted as representing the true mutant phenotype.

3.2. Immunostaining

Phase-contrast observation of mutant testes can only give a broad indication of the cytological defect in any particular mutant. Immunostaining mutant testes can give information on both cell-type distributions and subcellular structures. At the subcellular level, for example, staining of the meiotic spindle with anti-tubulin antibodies and a DNA dye will reveal much about the cytological mechanism underlying a chromosome nondisjunction phenotype. Antibodies or markers can also reveal which cell types are present in the testes. This is especially important in situations where relatively few, or very small, cells are seen in phase contrast. Are these germ-line or somatic cells? Are they stem cells or spermatogonia? Is the hub present and normal? Many of these cell type-specific markers are LacZ enhancer traps, so staining can be done either with an anti-LacZ antibody (**Subheading 3.2.**) or with a β-galactosidase activity assay (*see* **Subheading 3.3.**). A selection of useful antibodies and markers for probing subcellular structure and cellular identity in the testis is given in **Tables 3** and **4**. The detailed analysis of mutant phenotypes is, of course, not the only reason for wanting to immunostain testes. Having generated an antibody to a protein expressed in testes, one will always want to know its cellular and subcellular distribution patterns.

The choice of the following protocols depends on the exact question being addressed in the experiment. If information is needed on the pattern of protein localization at a global scale, then clearly whole-mount immunohistochemistry is required. This has the advantage of maintaining the temporal pattern of cysts in the testes; however, the resolution at the subcellular level is relatively low. This can be somewhat helped by counterstaining the preparation with Hoechst 33258. Immunofluorescence of squashed preparations has greater resolution of subcellular structures, but at the cost of loss of the temporal

Table 3
Choosing Antibodies and Reagents for Labeling

Antibody/probe	Structure revealed	Suggested conc.	Supplier (ref.)
DAPI	DNA	1 µg/mL	Molecular Probes
Propidium iodide (*see* **Figs. 2** and **3**)	DNA	1 µg/mL	Sigma
Hoechst 33342 (*see* **Fig. 1**)	DNA (vital dye)	2–5 µg/mL	Sigma ***(34)***
Phospho-Histone H3 (*see* **Fig. 3**)	Mitotic/meiotic chromosomes	1:200	Upstate Biotechnology ***(36)***
Phalloidin (*see* **Fig. 2**)	F-actin Hub Fusome Cleavage furrow Investment cone Muscle of sheath	5 µg/mL	Sigma/Molecular Probes ***(27)***
Tubulin (YL1/2)	Microtubules	1:20 (tissue culture supernatant)	Serolab ***(14)***
Fasiclin III	Hub	1:50	***(43)***
Phospho-tyrosine	Ring canals	1:100	Sigma/Upstate Biotechnology ***(26)***
Spectrin mAb1b1 (adducin)	Fusome	1:50	***(44,45)***
Bam-C	Spermatogonia	1:1500	***(46)***
Anillin	Nuclei and ring canals	1:300	***(26)***
Gamma-tubulin	Centrosomes	1:400	***(47)***
MPM2	DNA spindles and centrosomes		Upstate Biotechnology ***(14)***
β-galactosidase	LacZ reporter patterns		Promega ***(18)***

Table 4
Enhancer Traps That Reveal Specific Cell Types and GFP Reporters for Substructures

Reporter line	Cell type/structure	Ref.
M34a	Germ-line stem cells and gonialblasts	***36***
LacZ600, eyes absent	Hub and cyst cells	***37,48***
Vein	Cyst cells	***36***
M5-4	Hub, germ-line stem cells and gonialblasts	***49***
Don Juan GFP	Sperm tails	***50***
His2-GFP	Meiotic chromosomes	***41***

sequence of cysts. Two different fixation protocols for immunofluorescence of squashed preparations are given here. The choice of which to use is partly personal preference and partly antibody/antigen-specific. As a general rule, if trying a new antibody, do both protocols. I find that the methanol/acetone method (**Subheading 3.2.3.**) gives better fixation of meiotic spindles. However, phalloidin staining of F-actin is significantly better with formaldehyde fixation (**Subheading 3.2.2.**).

3.2.1. Whole Mount Immunohistochemistry

1. Dissect the testes in the appropriate buffer and transfer to an Eppendorf tube (*see* **Notes 2** and **6**).
2. Fix the testes in 4% formaldehyde in PBS, for 20–30 min at room temperature.
3. Rinse once, transfer to tissue culture inserts in a 24-well tissue culture plate, then wash three times in PBSTx, 20 min each wash (*see* **Note 7**).
4. Block 30 min in PBSTx + 5% FCS (*see* **Note 8**).
5. Incubate in 1° antibody diluted in PBSTx + 5% FCS overnight at 4°C, or at room temperature for 2 h (*see* **Note 9**).
6. Rinse once, then wash three times in PBSTx, 20 min each.
7. Incubate in biotinylated 2° antibody diluted 1 : 2000 in PBSTx + 5% FCS for 1 h at room temperature.
8. Rinse once, then wash three times in PBSTx, 20 min each. (If using Vectastain ABC kit, *see* **Note 10**.)
9. Incubate for 30 min at room temperature with ExtrAvidin-HRP conjugate diluted 1 : 1000 in PBSTx.
10. Rinse once, then wash three times in PBSTx, 20 min each.
11. Stain with 0.7 mg/mL DAB, 0.001% H_2O_2 in PBS (*see* **Note 11**).
12. Stop the reaction by rinsing once, then washing several times (10 min each) in PBS.
13. Counterstain DNA with 1 µg/mL Hoechst 33258 in PBS for 15 min if required.
14. Mount on slides in mounting medium and observe with Nomarski optics (*see* **Note 12**) (*see* **Fig. 8**).

3.2.2. Formaldehyde Fixation for Confocal Microscopy

1. Dissect testes from young adults in testis buffer, four or five pairs per slide (*see* **Note 2**).
2. Transfer the testes to a drop of testis buffer on a poly-L-lysine-treated slide and cut open to spill the contents (*see* **Notes 3** and **13**).
3. Squash gently under a 22 × 22-mm^2 siliconized cover slip.
4. Freeze immediately in liquid nitrogen (wear safety glasses) and pop off the cover slip using a scalpel.
5. Immediately place in chilled (on dry ice) 100% ethanol, 10 min.
6. Place the slide flat and flood with 0.5–1 mL of 4% formaldehyde solution; incubate for 7 min.
7. Tip off the formaldehyde onto paper towels (wear gloves). If staining with phalloidin, *see* **Note 14**.
8. Permeabilize the testes by incubating twice in PBST-DOC, 15 min each.
9. Store in PBST until all the slides have been prepared.
10. Make a well on the slide with Evostick (rubber cement), block for a minimum of 30 min in PBST + 3% BSA or PBST + 5% FCS (*see* **Note 15**).
11. Incubate with primary antibody diluted in PBST + BSA (or PBST + FCS) for a minimum of 2 h at room temperature, or overnight at 4°C in a humid chamber (*see* **Notes 9** and **16**).
12. Remove the evostick. Wash 4 times, 15 min each, in PBST.
13. Incubate with secondary antibody 1 : 500–1 : 1000 (in fresh Evostick wells) for at least 1 h at room temperature, or overnight at 4°C, in a humid chamber (*see* **Note 16**).
14. Remove the Evostick. Wash four times in PBST, 15 min each.
15. Optional: Incubate 10 min in 1 µg/mL DAPI in PBST.
16. Wash once in PBS for 10 min.
17. Mount under a siliconized cover slip in 85% glycerol + 2.5% *n*-propyl gallate (containing 1 µg/mL propidium iodide if required). Seal with nail polish.
18. Image with conventional epifluorescence or confocal laser scanning microscopy.

3.2.3. Methanol/Acetone Fixation for Confocal Microscopy

1. Dissect testes from young adults in testis buffer or TB1, four or five pairs per slide (*see* **Note 2**).
2. Transfer to a drop of testis buffer on a poly-L-lysine-treated slide and cut open to spill the contents (*see* **Note 3**).
3. Squash gently under a 22 × 22-mm^2 siliconized cover slip.
4. Freeze immediately in liquid nitrogen (wear safety glasses) and pop off cover slip using a scalpel.
5. Transfer to methanol, chilled on dry ice, and incubate for 5 min.
6. Transfer to acetone, chilled on dry ice, and incubate for 5 min.
7. Incubate in PBS-T-AA for 10 min at room temperature.
8. Store in PBST until all the slides are prepared.
9. Continue from **step 10** of **Subheading 3.3.2.**

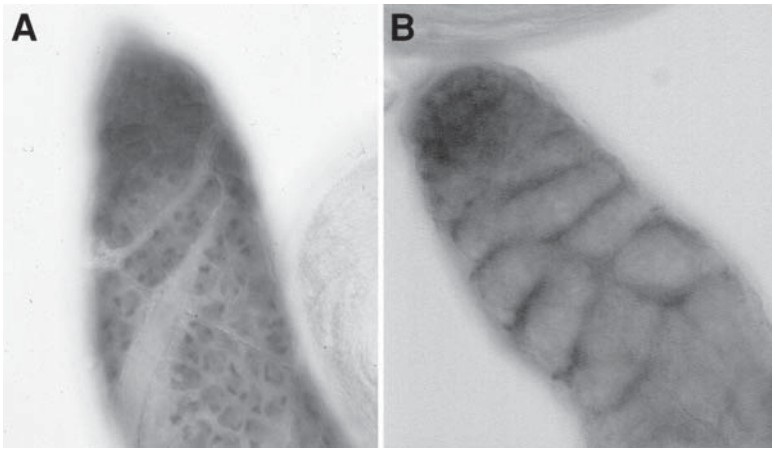

Fig. 8. Immunohistochemistry of Aly and dpERK protein localization. Immunohistochemical staining retains the spatial relationship between different stages of differentiation in the testes, and so allows temporal changes in the cellular or subcellular distribution of an antigen to be assessed. **(A)** The tip of a testis stained with an antibody against Aly protein. Aly is not expressed in the mitotic domain (out of focus in this image). When Aly is first detected, it is both cytoplasmic and nuclear in the germline cells. As the cysts mature, the localization resolves to be concentrated on chromatin in primary spermatocytes. Aly protein is not found in cyst cells; hence, the gaps seen between the areas of staining. **(B)** A monoclonal antibody specific to the activated (diphosphorylated) form of ERK/MAP kinase stains only the cyst cells near the apical tip of the testis. This staining is particularly sensitive to buffer conditions and only works when testes are dissected in TBPi buffer.

3.3. X-Gal Staining

1. Dissect testes in testis buffer or TB1 (*see* **Note 2**). Transfer to a 24-well tissue culture dish or glass staining block (*see* **Note 17**).
2. Fix in 1% glutaraldehyde (wear gloves) in PBS for 15 min (*see* **Note 18**).
3. Rinse three times in X-gal buffer. Leave in this buffer for at least 30 min.
4. Prepare 5 mL of staining solution and warm to 37°C.
5. Add 50 µL of 20% X-gal. Vortex. Keep at 37°C.
6. Incubate tissue in staining solution plus X-Gal at 37°C for 1 h to overnight. Monitor the reaction and leave until color develops.
7. Wash in X-gal buffer, counterstain (if desired) by incubating in 1 µg/mL Hoechst 33258 for 15 min, and mount in 85% glycerol.

3.4. RNA In Situ *Hybridization*

The pattern of expression of your gene can give a clue as to its function. Most testis transcripts are made in primary spermatocytes and stored until use.

A transcript that persists along the testis is more likely to encode a protein needed late in differentiation. Early degradation of a transcript suggests an earlier function (*see* **Fig 4**).

3.4.1. Preparation of Probe

Essentially follow the labeling protocol given with the Roche RNA labeling mix, outlined as follows.

1. Linearize plasmid with a suitable restriction enzyme (usually one that cuts in the polylinker at the 5' end of the gene).
2. Set up a 20–µL reaction using 1 µg of linear template and the relevant RNA polymerase. A typical reaction contains 2 µL of 10X RNA labeling mix, 2 µL of 10X RNA polymerase buffer, 1 µg of template DNA in 14 µL of RNAse-free water, and 2 µL of RNA polymerase.
3. Allow the transcription reaction to continue for 2 h at 37°C, then stop the reaction by adding 2 µL of 0.5 *M* EDTA.
4. Hydrolyze the probe by diluting with distilled water to 100 µL and adding 100 µL of 2X carbonate buffer; incubate at 60°C. Probe hydrolysis times vary according to transcript length. The aim is to generate short RNA fragments (approx 100 bp) that will penetrate the tissue more easily. I allow 15 min per 500 bp (i.e., incubate a 2-kb probe for 1 h).
5. Neutralize by adding 200 µL of 2X neutralization buffer.
6. Precipitate the RNA product by adding 3 vol of ethanol and incubating at –20°C for at least 30 min.
7. Spin in a microcentrifuge 15 min, wash with 70% ethanol, dry the pellet, and resuspend in 200 µL of RNAse-free water. Store the probe at –70°C. For hybridization, use 0.5–1 µL per 100 µL of hybridization buffer.

3.4.2. Hybridization

1. Dissect testes from young adults (0–1 d old) in testis buffer and transfer to a 1.5 mL tube (*see* **Notes 2**, **6**, and **19**).
2. Fix in 4% paraformaldehyde in HEPES buffer for 20–60 min; agitation is not required—simply leave the tube on its side.
3. Wash three times in PBST, 5 min each.
4. Incubate in 50 µg/mL of proteinase K in PBST for 5–7 min (*see* **Note 20**).
5. Remove the proteinase K solution and stop the digestion by incubating the testes in 2 mg/mL glycine in PBST for 2 min.
6. Wash twice in PBST, 5 min each.
7. Refix in 4% paraformaldehyde in HEPES buffer for 20 min.
8. Wash three times in PBST, 10 min each.
9. Incubate in 1 : 1 PBST : HB for 10 min.
10. Wash in HB for 10 min.
11. Transfer testes into tissue culture inserts in a 24-well tissue culture plate (*see* **Note 7**).

12. Prehybridize in HB at 65°C for at least 1 h (*see* **Notes 21** and **22**).
13. Dilute the RNA probe (from **Subheading 3.4.1.**) in HB, heat denature at 80°C for 10 min, and briefly chill on ice.
14. Hybridize at 65°C overnight.
15. Wash at least six times, 30 min each, in HB at 65°C (*see* **Note 23**).
16. Wash once in 4 : 1 HB : PBST for 15 min at room temperature.
17. Wash once in 3 : 2 HB : PBST for 15 min at room temperature.
18. Wash once in 2 : 3 HB : PBST for 15 min at room temperature.
19. Wash once in 1 : 4 HB : PBST for 15 min at room temperature.
20. Wash twice in PBST, 15 min each.
21. Incubate overnight at 4°C in preadsorbed (*see* **Note 1**) alkaline phosphatase-conjugated antidigoxygenin antibody diluted 1 : 2000 in PBST.
22. Wash four times in PBST, 20 min each.
23. Wash three times in freshly made buffer HP, 5 min each.
24. Make staining solution in HP buffer by adding 4.5 μL of NBT and 3.5 μL of X-phosphate per milliliter.
25. Add the color reaction solution to the testes and leave to develop in the dark. The signal typically takes 10 min to 1 h, although for some transcripts incubation for several hours may be required. The staining needs to look quite dark, and purple not pink, at this stage to get good pictures at high magnification.
26. Stop the reaction by washing three times in PBST, 5 min each.
27. Dehydrate through an ethanol series: 10 min in each of 30%, 50%, 70%, 90%, and 100% (twice) ethanol. Transfer testes into a glass staining block (*see* **Note 24**).
28. Incubate 15 min in 1 : 1 ethanol : methyl salicylate, then in 100% methyl salicylate (*see* **Note 25**).
29. Mount in GMM and observe with Nomarski optics.

4. Notes

1. To preadsorb the antibody, fix embryos using a protocol suitable for immunostaining (*see* Chapter 9). Dilute the antibody 1 : 20 in PBST and incubate with the rehydrated fixed embryos for 2 h. Remove the antibody solution from the embryos and store at 4°C.
2. Newly eclosed males are used for all of these protocols, as they show the best morphology. To dissect testes from flies, place an anesthetized male next to a drop of testis buffer on the dissecting dish. Hold near the top of the abdomen with a pair of fine forceps in your left hand (or your right hand if you are left-handed). Grasp the external genitalia with the other pair of forceps and pull into the drop of buffer. The male genital tract, including testes, should come clear of the carcass. If it does not come clear, you will have to "fish" for the testes in the abdomen. Transfer the genital tract into a fresh drop of testis buffer and dissect the coiled testes and attached seminal vesicle from the rest of the tissues. If scoring for sperm motility, it is important to note that many males have no mature sperm for about 12 h after eclosion. To be sure of the absence of motile sperm from a

mutant, keep males isolated from females for 3 d, then dissect their seminal vesicles.

3. Generally, it is best to cut halfway along the straight portion of the testis. The contents should partially spill out, and this can be encouraged by gently tapping on the slide. The diameter of the drop of buffer should be approx 7 mm to get good preparations under a 22 × 22-mm^2 cover slip. Cysts of spermatocytes or spermatids should stay intact. The seminal vesicle from males that produce normal motile sperm will normally be slightly opaque. When it is opened, the sperm spill out. Motile sperm will show a shimmering effect visible even under the dissecting microscope.
4. Take pictures first, ask questions later. Photography can be done with either a digital camera or using black-and-white film. Squash preparations are only good for approx 20 min. After that, the cells are usually too flat and dead to observe. **Figure 6** shows some typical squash artifacts.
5. Alternatively, preparations can be made for visualization with an inverted microscope by using slides with a hole cut in them, sealing a cover slip over the bottom of the hole with vaseline, and dissecting the male into halocarbon oil in the chamber thus generated. Under these conditions, the cells remain viable for at least 3 h ***(40,41)***. (*See* Chapter 3.)
6. To transfer testes, place a small drop of testis buffer in the lid, put the testes into this, add 600 µL of fix to the tube, close the lid, and mix. Testes stick to tweezers if you try to put them directly into fix.
7. Add testes and washes into inserts; remove by lifting up the insert and aspirating solution from the well (*see* **Fig. 9**). Be careful; sometimes the mesh at the bottom detaches. Check for loose testes before aspirating. Do not fix testes in these dishes, as they may stick to the mesh.
8. Blocking does not seem to be essential for whole-mount immunohistochemistry, but it may improve the staining with certain antibodies.
9. The optimal dilution for each antibody needs to be empirically determined. As a first guess try using it two to four times more concentrated than gives an acceptable signal on Western blots. Immunohistochemistry often works with the antibody more dilute than is needed for immunofluorescence. For example, if an antibody works well at 1 : 4000 on Western blots, try 1 : 2000 for whole-mount immunohistochemistry and 1 : 1000 for immunofluorescence on squashed preparations. Antibody incubations can generally be done for a few hours at room temperature or overnight at 4°C. The choice is usually governed by convenience, although some primary antibodies work better overnight at 4°C.
10. The Vectastain ABC kit gives a slightly stronger signal, which decreases the development time, and may be useful for some proteins with relatively low levels of expression. Substitute the following for **step 9** of **Subheading 3.2.1.**: Incubate testes in 0.5X ABC reagent (50 µL solution A, 50 µL solution B, 5 mL PBS mixed 30 min before use) for 30 min. Go to **step 10** of **Subheading 3.2.1.**
11. DAB is a potent carcinogen; wear gloves and inactivate DAB with bleach after use. Tablets from Sigma are 0.7 mg and should be dissolved in 1 mL of PBS.

Lowering the concentration of DAB to 0.35 mg/mL (i.e., one tablet in 2 mL) does not significantly compromise the staining.

12. To mount stained testes in 85% glycerol, first transfer to a glass staining block. Remove the PBS and replace with glycerol. Mix well with a tungsten mounted needle or tweezers. Leave the testes in glycerol for 15–30 min before transferring to a cover slip, cutting off accessory gland and picking up with a clean slide. Imaging stained tissue under Nomarski optics usually requires that the optics be somewhat compromised, because the stain rarely shows up well when the Nomarski is set up to give the most structural information. Photograph using a tungsten balanced color slide film or a daylight correction filter and normal color slide film.
13. Write the genotype on the slide with pencil or a diamond pen; marker dissolves in ethanol! Use at least two slides per genotype, per antibody combination.
14. For phalloidin staining, testes do not need to be permeabilized with DOC. Instead, wash in PBST, then block in PBST-FCS. Dry the required amount of labeled phalloidin (stored at –20°C in methanol) in a Speed Vac just before use, and resuspend in the appropriate volume of PBST. Incubate for 2 h at room temperature, wash three times in PBST for 15 min each, then counterstain and mount. If costaining with an antibody, the phalloidin can be included in the secondary antibody incubation. **Caution:** Phalloidin is extremely hazardous! Wear protective clothing and be aware of the risks and safety procedures before using this compound.
15. To make Evostick wells, dry off the surface of the slide around the testes, taking care not to let the testes dry out. Paint a ring of Evostick or rubber cement around the area containing the testes and leave to dry for about 1 min (*see* **Fig. 10**). This forms a barrier, keeping a good depth of antibody solution above the tissue. Use 100 µL of diluted antibody per slide. Some antibodies penetrate the tissue much better under these conditions. Additionally, the testes remain stuck more firmly to the slide than if they are covered with a cover slip during antibody incubations. Evostick can be removed from the slide with tweezers.
16. If propidium iodide will be used to stain DNA, then RNAse A (0.5–1 mg/mL) must be added to one of the antibody incubations to reduce background fluorescence. I generally add it to whichever antibody incubation is being carried out at room temperature.
17. Do not fix in the tissue culture inserts used for other protocols, because glutaraldehyde makes testes stick to the mesh. Testes can be transferred to the inserts during the washes after fixation, but because the whole protocol is short, little time is saved.
18. Four percent formaldehyde may be substituted for glutaraldehyde. It is less toxic, but the staining intensity will be lower, so it is only suitable for reporters that express well.
19. Prepare about 10 males per probe. If many probes are to be used, process the testes together until the transfer into tissue culture inserts step. Removal of the accessory glands and other bits of genital tract is not essential; they can provide a nice in-sample negative control. If any mutant testes being used are different enough to be easily told apart from wild-type by Nomarski optics, then an excel-

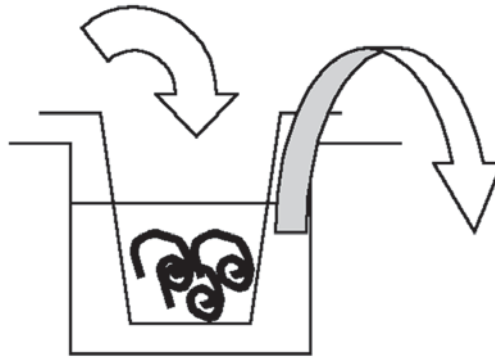

Fig. 9. Diagram of an insert and well of a tissue culture plate containing testes bathed in wash solution (*see* **Note 7**).

lent control is to mix wild type and mutant testes together after fixation. This allows a somewhat more accurate assessment of relative transcript levels, as the treatment of both genotypes will have been identical.

20. New batches of proteinase K should be checked. Overdigestion results in testes that are extra fragile and sticky, with a tendency to clump together.
21. To incubate at 65°C, the tissue culture dish can be left floating in a water bath.
22. Testes may be stored in HB at –20°C for up to 1 wk (in Eppendorf tubes).
23. The numbers of washes given here is a minimum. Increasing the number and total time of washing, especially in HB, can improve the signal-to-noise ratio.
24. To transfer stained testes, use a 200–µL pipet tip with the end cut off. Watch under the dissecting microscope to ensure complete transfer, especially of lightly stained tissue. Transfer of the testes at this stage is essential because methyl salicylate dissolves the tissue culture plastic.
25. Methyl salicylate clears the testes, but also dissolves some of the color product. Therefore, this incubation will make background staining disappear, but care must be taken to prevent the real staining from disappearing too. Canada balsam stabilizes the color, so remove the methyl salicylate and add GMM to the staining block when ready. The color should look quite intense under the dissecting microscope, in order to obtain good higher-magnification pictures. To mount the stained testes, transfer them in GMM onto a 22×22-mm^2 cover slip with a cut-off pipet tip. Methyl salicylate also makes the testes very brittle so that any dissection (e.g., separation of pairs of testes) can be done by prodding or cutting with a tungsten needle.

Acknowledgments

I would like to thank David Neville and Daimark Bennett for proofreading this manuscript. Thanks to Natasha Vereshegina and Liz Benson for testing protocols, Karen Hales for figures of mutants and Cayetano Gonzalez for pictures of mutants and for the time-lapse figure.

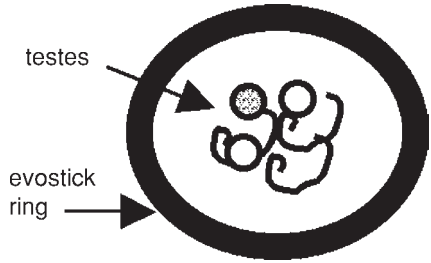

Fig. 10. Diagram of testes incubating in an Evostick well on a microscope slide (*see* **Note 15**).

References

1. Fuller, M. T. (1993) Spermatogenesis, in *The Development of Drosophila* (Bate, M. and Martinez-Arias, A., eds.), Cold Spring Harbor Laboratory Press, Cold Spring Harbor, NY, pp. 71–147.
2. Lindsley, D. and Tokuyasu, K. T. (1980) Spermatogenesis, in *Genetics and Biology of Drosophila* (Ashburner, M. and Wright, T. R. F., eds.), Academic, New York, pp. 225–294.
3. Kerrebrock, A. W., Miyazaki, W. Y., Birnby, D., and Orr-Weaver, T. L. (1992) The *Drosophila mei-S332* gene promotes sister-chromatid cohesion in meiosis following kinetochore differentiation. *Genetics* **130,** 827–841.
4. Kerrebrock, A. W., Moore, D. P., Wu, J. S., and Orr-Weaver, T. L. (1995) Mei-S332, a *Drosophila* protein required for sister-chromatid cohesion, can localize to meiotic centromere regions. *Cell* **83,** 247–256.
5. Miyazaki, W. Y. and Orr-Weaver, T. L. (1992) Sister chromatid misbehavior in *Drosophila ord* mutants. *Genetics* **132,** 1047–1061.
6. Bickel, S. E., Moore, D. P., Lai, C., and Orr-Weaver, T. L. (1998) Genetic interactions between *mei-S332* and *ord* in the control of sister-chromatid cohesion. *Genetics* **150,** 1467–1476.
7. Bickel, S. E., Wyman, D. W., and Orr-Weaver, T. L. (1997) Mutational analysis of the *Drosophila* sister-chromatid cohesion protein ORD and its role in the maintenance of centromeric cohesion. *Genetics* **146,** 1319–1331.
8. Casal, J., Gonzalez, C., Wandosell, F., Avila, J., and Ripoll, P. (1990) Abnormal meiotic spindles cause a cascade of defects during spermatogenesis in *asp* males of *Drosophila*. *Development* **108,** 251–260.
9. Wakefield, J. G., Bonaccorsi, S., and Gatti, M. (2001) The *Drosophila* protein asp is involved in microtubule organization during spindle formation and cytokinesis. *J. Cell Biol.* **153,** 637–648.
10. Bonaccorsi, S., Giansanti, M. G., and Gatti, M. (1998) Spindle self-organization and cytokinesis during male meiosis in *asterless* mutants of *Drosophila melanogaster*. *J. Cell Biol.* **142,** 751–761.

11. Alphey, L., Jimenez, J., White-Cooper, H., Dawson, I., Nurse, P., and Glover, D.M. (1992) *twine*, a *cdc25* homologue that functions in the male and female germlines of Drosophila. *Cell* **69,** 977–988.
12. Eberhart, C. G., Maines, J. Z. and Wasserman, S. A. (1996) Meiotic cell cycle requirement for a fly homologue of human Deleted in Azoospermia. *Nature* **381,** 783–785.
13. Eberhart, C. G. and Wasserman, S. A. (1995) The *pelota* locus encodes a protein required for meiotic cell division: an analysis of G2/M arrest in *Drosophila* spermatogenesis. *Development* **121,** 3477–3486.
14. White-Cooper, H., Alphey, L., and Glover, D. M. (1993) The cdc25 homologue twine is required for only some aspects of the entry into meiosis in Drosophila. *J Cell Sci* **106,** 1035–1044.
15. Andrews, J., Bouffard, G. G., Cheadle, C., Lu, J., Becker, K. G., and Oliver, B. (2000) Gene discovery using computational and microarray analysis of transcription in the *Drosophila melanogaster* testis. *Genome Res.* **10,** 2030–2043.
16. Wakimoto, B. T. (2000) Doubling the rewards: testis ESTs for *Drosophila* gene discovery and spermatogenesis expression profile analysis. *Genome Res.* **10,** 1841–1842.
17. Castrillon, D. H., Gönczy, P., Alexander, S., et al. (1993) Toward a molecular genetic analysis of spermatogenesis in *Drosophila melanogaster*: characterization of male-sterile mutants generated by single P element mutagenesis. *Genetics* **135,** 489–505.
18. Maines, J. Z. and Wasserman, S. A. (1999) Post-transcriptional regulation of the meiotic Cdc25 protein Twine by the Dazl orthologue Boule. *Nature Cell Biol.* **1,** 171–174.
19. Tomkiel, J. E., Wakimoto, B. T., and Briscoe, A. (2001) The *teflon* gene is required for maintenance of autosomal homolog pairing at meiosis I in male *Drosophila melanogaster*. *Genetics* **157,** 273–281.
20. White-Cooper, H., Leroy, D., MacQueen, A., and Fuller, M. T. (2000) Transcription of meiotic cell cycle and terminal differentiation genes depends on a conserved chromatin associated protein, whose nuclear localisation is regulated. *Development* **127,** 5463–5473.
21. McKearin, D. (1997) The *Drosophila* fusome, organelle biogenesis and germ cell differentiation: if you build it. . . . *Bioessays* **19,** 147–152.
22. Gould-Somero, M. and Holland, L. (1974) The timing of RNA synthesis for spermiogenesis in organ cultures of *Drosophila melanogaster* testes. *Wilhelm Roux. Arch.* **174,** 133–148.
23. Olivieri, G. and Olivieri, A. (1965) Autoradiographic study of nucleic acid synthesis during spermatogenesis in *Drosophila melanogaster*. *Mutat. Res.* **2,** 366–380.
24. Schafer, M., Nayernia, K., Engel, W. and Schafer, U. (1995) Translational control in spermatogenesis. *Dev. Biol.* **172,** 344–352.
25. Tates, A. D. (1971) Cytodifferentiation during spermatogenesis in *Drosophila melanogaster*: an electron microscope study. Thesis, Rijksuniversiteit, Leiden.

26. Hime, G. R., Brill, J. A., and Fuller, M. T. (1996) Assembly of ring canals in the male germ line from structural components of the contractile ring. *J. Cell Sci.* **109,** 2779–2788.
27. Fabrizio, J. J., Hime, G. R., Lemmon, S. K., and Bazinet, C. (1998) Genetic dissection of sperm individualisation in *Drosophila melanogaster*. *Development* **125,** 1833–1843.
28. Fitch, K. R. and Wakimoto, B. T. (1998) The paternal effect gene *ms(3)sneaky* is required for sperm activation and the initiation of embryogenesis in *Drosophila melanogaster*. *Dev. Biol.* **197,** 270–282.
29. Ryner, L. C., Goodwin, S. F., Castrillon, D. H., et al. (1996) Control of male sexual behavior and sexual orientation in *Drosophila* by the *fruitless* gene. *Cell* **87,** 1079–1089.
30. Green, L. L., Wolf, N., McDonald, K. L., and Fuller, M. T. (1990) Two types of genetic interaction implicate the *whirligig* gene of *Drosophila melanogaster* in microtubule organization in the flagellar axoneme. *Genetics* **126,** 961–973.
31. Gonzalez, C., Casal, J., and Ripoll, P. (1988) Functional monopolar spindles caused by mutation in *mgr*, a cell division gene of *Drosophila melanogaster*. *J. Cell Sci.* **89,** 39–47.
32. Brill, J. A., Hime, G. R., Scharer-Schuksz, M., and Fuller, M. T. (2000) A phospholipid kinase regulates actin organisation and intercellular bridge formation during germline cytokinesis. *Development* **127,** 3855–3864.
33. Hales, K. G. and Fuller, M. T. (1997) Developmentally regulated mitochondrial fusion mediated by a conserved novel predicted GTPase. *Cell* **90,** 121–129.
34. Lin, T.-Y., Viswanathan, S., Wood, C., Wilson, P. G., Wolf, N., and Fuller, M. T. (1996) Coordinate developmental control of the meiotic cell cycle and spermatid differentiation in *Drosophila* males. *Development* **122,** 1331–1341.
35. Gönczy, P., Matunis, E., and DiNardo, S. (1997) *bag-of-marbles* and *benign gonial cell neoplasm* act in the germline to restrict proliferation during *Drosophila* spermatogenesis. *Development* **124,** 4361–4371.
36. Kiger, A. A., White-Cooper, H., and Fuller, M. T. (2000) Somatic support cells restrict germline stem cell self-renewal and promote differentiation. *Nature* **407,** 750–754.
37. Tran, J., Brenner, T., and DiNardo, S. (2000) Somatic control over the germline stem cell lineage during *Drosophila* spermatogenesis. *Nature* **407,** 754–757.
38. Boswell, R. E. and Mahowald, A. P. (1985) *tudor*, a gene required for assembly of the germ plasm in *Drosophila melanogaster*. *Cell* **43,** 97–104.
39. Kiger, A. A., Gigliotti, S., and Fuller, M. T. (1999) Developmental genetics of the essential Drosophila nucleoporin *nup154*: allelic differences due to an outward-directed promoter in the P-element 3' end. *Genetics* **153,** 799–812.
40. Church, K. and Lin, H.-P. P. (1985) Kinetochore microtubules and chromosome movement during prometaphase in *Drosophila melanogaster* spermatocytes studied in life and with the electron microscope. *Chromosoma* **92,** 273–282.
41. Rebollo, E. and Gonzalez, C. (2000) Visualizing the spindle checkpoint in *Drosophila* spermatocytes. *EMBO Rep.* **1,** 65–70.

42. Giansanti, M. G., Bonaccorsi, S., Williams, B., et al. (1998) Cooperative interactions between the central spindle and the contractile ring during *Drosophila* cytokinesis. *Genes Dev.* **12,** 396–410.
43. Patel, N. H., Snow, P. M., and Goodman, C. S. (1987) Characterization and cloning of Fasciclin III: a glycoprotein expressed on a subset of neurons and axon pathways in Drosophila. *Cell* **48,** 975–988.
44. Pesacreta, T. C., Byers, T. J., Dubreuil, R., Kiehart, D. P., and Branton, D. (1989) *Drosophila* spectrin: the membrane skeleton during embryogenesis. *J. Cell Biol.* **108,** 1697–1709.
45. Zaccai, M. and Lipshitz, H. D. (1996) Differential distributions of two adducin-like protein isoforms in the *Drosophila* ovary and early embryo. *Zygote* **4,** 159–166.
46. McKearin, D. and Ohlstein, B. (1995) A role for the *Drosophila* bag-of-marbles protein in the differentiation of cystoblasts from germline stem cells. *Development* **121,** 2937–2947.
47. Callaini, G., Whitfield, W. G. F., and Riparbelli, M. G. (1997) Centriole and centrosome dynamics during the embryonic cell cycles that follow the formation of the cellular blastoderm in Drosophila. *Exp. Cell Res.* **234,** 183–190.
48. Gönczy, P., Viswanathan, S., and DiNardo, S. (1992) Probing spermatogenesis in *Drosophila* with P-element enhancer detectors. *Development* **114,** 89–98.
49. Gönczy, P., Matunis, E., and DiNardo, S. (1997) *bag-of-marbles* and *benign gonial cell neoplasm* act in the germline to restrict proliferation during *Drosophila* spermatogenesis. *Development* **124,** 4361–4371.
50. Santel, A., Blumer, N., Kampfer, M., and Renkawitz-Pohl, R. (1998) Flagellar mitochondrial association of the male-specific Don Juan protein in *Drosophila* spermatozoa. *J. Cell Sci.* **111,** 3299–3309.

3

Time-Lapse Imaging of Male Meiosis by Phase-Contrast and Fluorescence Microscopy

Elena Rebollo and Cayetano González

1. Introduction

Meiosis is one of the key stages of spermatogenesis during which two rounds of chromosome segregation follow a single doubling of the DNA, thus reducing the chromosome number to produce haploid cells. *Drosophila* spermatocytes have been used extensively to study the basic mechanisms that govern cell division and meiosis. They are well suited for this purpose because they are easily accessible, readily identifiable, and relatively large and abundant. Moreover, large collections of mutants that disrupt many aspects of cell division and green fluorescent protein (GFP)-fusion proteins that label different components of the cell division machinery, are available in *Drosophila* and can be studied in these cells ***(1–12)***.

Classically, studies in *Drosophila* male meiosis have been performed by direct observation of unfixed and unstained cysts under phase-contrast optics ***(3,8,9,13)***. Detailed analyses of chromosome behavior have required staining with aceto-orcein or Hoechst dye (reviewed in **ref. *14***). In the mid-1990s, a reliable fixation protocol was developed that allows immunofluorescence staining ***(15)***, thus providing a better basis to study the organization of the major cell structures and organelles, as well as the localization of proteins of interest. Although very informative, these methods based on either short-lived or fixed cells do not allow for the observation of meiosis progression, which is essential to follow the dynamic events that take place during cell division. The first description of a method for generating primary cultures of primary *Drosophila* spermatocytes that could be visualized by time-lapse video microscopy was published by Church and Lin ***(16)***. Using this method in combination with

From: *Methods in Molecular Biology, vol. 247:* Drosophila *Cytogenetics Protocols*
Edited by: D. S. Henderson © Humana Press Inc., Totowa, NJ

micromanipulation and electron microscopy, they provided beautiful descriptions of kinetochore and chromosome behavior during the first meiotic division in *Drosophila* testes ***(16,17)***. However, this approach has not been exploited at all. It has not been until very recently that time-lapse video microscopy of cultured *Drosophila* spermatocytes has been used again to study meiosis in *Drosophila* males ***(18–21)***.

To some extent, *Drosophila* spermatocytes are actually well suited for this technique: They remain flat, thus producing sharp phase-contrast images during cell division; they have large spindles and centrosomes beautifully delineated by phase dark spindle and aster-associated membranes; and the small number of chromosomes, only four, makes it possible to follow each of them in detail. However, the tolerance of *Drosophila* spermatocytes to culture is very limited. They can break easily if the manipulations required to set up the cultures are not carried out with extreme care, and they are very sensitive to light, thus imposing some limitation in terms of the recording conditions. We have introduced some minor, yet useful, modifications in the original protocol described by Church and Lin ***(16)*** that ameliorate these problems and allow for relatively long recording sessions, including observations of such critical steps as cytokinesis, interkinesis, and the second meiotic division, which have not been reported previously (Rebollo and González, unpublished data). We have also set up the conditions for two-channel imaging to record both phase-contrast as well as fluorescence images from the same cell, so that the localization of GFP-fusion proteins can be followed. Special attention is paid to the culturing steps. Although the technique looks unbelievably simple, it requires some practice and expertise until viable cells can be followed under the microscope.

2. Materials

2.1. Equipment for Culture Chambers

2.1.1. Cover Slips and Cleaning Materials

1. 24×24 mm^2 cover slips (we use Marienfeld, product no. 5370).
2. Porcelain staining racks for cover slips (product no. 8542-E42, Thomas Scientific, www.thomassci.com).
3. Curved forceps (A. Dumont inox No. 7).
4. Long anatomical forceps, 200 mm (Bochem 18/8).
5. Pyrex beaker, 1-L capacity.
6. Cleaning solution 7X® PF 1% in distilled water (ICN Biomedicals, Inc., cat. no. 76-671-210).
7. Standard distilled water.
8. Ultrapure water (double distilled, or Milli-Q).
9. Staining glass box with cup, $90 \times 60 \times 50$ mm^3.
10. Ethanol absolute grade (GR) for analysis (Merck, cat. no. K30598083).

2.1.2. Culture Chamber Mounting

1. 24×24-mm^2 Cover slips, treated as discussed in **Subheading 3.1.1.**
2. Aluminum slides with a 20-mm hole bored through its center, treated as discussed in **Subheading 3.1.3.** (we make them ourselves from aluminum sheets).
3. Acetone GR for analysis (Merck).
4. Tissue papers. (We use professional wipes; Kimberly-Clark, code 7102.)
5. Filter paper (Whatman 3MM, cat. no. 3030 917).
6. Bunsen burner.
7. Nail polish.
8. Slides support. We make it ourselves by attaching two foam stripes to the bottom of a box that can be closed afterward. The slides must touch the support only at the two extremes.

2.1.3. Microscope Slide Cleaning and Recycling

1. Eight staining glass boxes with cup, $90 \times 60 \times 50$ mm^3.
2. Removable staining tray for slides, 76×26 mm^2.
3. Wire clip for staining tray.
4. Aceton GR for analysis (Merck cat. no. K30688514).
5. Xylene 99+%, high-performance liquid chromatography (HPLC) grade (Sigma-Aldrich, cat. no. 31,719-5).
6. Ethanol, absolute GR for analysis (Merck, cat. no. K30598083).

2.2. Equipment for Preparing Living Spermatocytes

1. Newly eclosed *Drosophila* males, expressing the GFP-fusion protein of interest in testis.
2. Standard CO_2 source.
3. Standard dissecting microscope with a white-light source.
4. Heavy white mineral oil (Trinity Biotech GmbH, cat. no. 400-5) specific gravity (77°F): 0.875–0.885.
5. Two straight dissection forceps (A. Dumont inox No. 5).
6. Filter paper, extremely thin, cut into triangles of approx 3 cm/side (Schleicher & Schuell 595, cat. no. 10311614).
7. Sterile needles (BD Microlance™ 3, 27-gage 3/4, 0.4×19 mm, No. 20. (Becton Dickinson, cat. no. 302200).

2.3. Image Recording and Processing Equipment for Phase-Contrast Microscopy

1. Inverted microscope. We use a Leica DM IRB/E.
2. Charge coupled device (CCD) camera. We use a CCD Cohu High performance Model 4912–5100.
3. Temperature controller. We use either a temperature-controlled chamber specially built for the microscope, or a Bioptechs objective controller.
4. Objectives. We use either an oil $63\times$/1.32 PLAN APO Ph3 or an oil $100\times$/1.25 C PLAN Ph3.

5. Shutter. We use a Vincent V Uniblitz electronic.
6. Shutter driver. Uniblitz Model D122.
7. Computer for recording. We use a Power Macintosh 9600/233, with a video card compatible with the camera and the shutter driver.
8. Acquisition software: NIH-Scion Image, version 1.62. (www.rsb.info.nih.gov/nih-image).
9. Computer for image processing. Any computer having enough RAM memory and processing speed. We use a single processor 500-MHz power Macintosh G4 with 384MB RAM memory.
10. Processing software: NIH-Scion Image, version 1.62. (www.rsb.info.nih.gov/nih-image).

2.4. Multiframe Video Recording and Processing Equipment for Confocal Microscopy

1. Inverted microscope. We use a Leica DM IRB/E TCS SP2 Confocal Microscope, which allows us to record different channels simultaneously.
2. Temperature-controlled chamber for the microscope.
3. Objective 63× oil/1.32 PLAN APO Ph3.
4. Acquisition software: Leica confocal software version 2.00 (Leica Microsystems Heidelberg GmbH).
5. Computer. Any computer having enough RAM memory and processing speed. We use a single processor 500-MHz power Macintosh G4 with 384MB RAM memory.
6. Processing software: Any software that can be programmed to read and combine the confocal images. We use both NIH-Scion Image, version 1.62 and IDL (Interactive Data Language), version 5.3.1.

3. Methods

3.1. Construction of the Culture Chambers

We use culture chambers similar to those described by Nicklas and Staehly ***(22)***. Ours consist of an aluminum slide (instead of a glass slide) with a 20-mm-diameter (instead of 15-mm) hole covered on one side with a scrupulously clean (*see* **Subheading 3.1.1.**) square cover slip (24×24 mm^2) that is fixed to the slide with nail polish (instead of petroleum jelly).

3.1.1. Cleaning the Cover Slips

Cover slips may have a thin film of oil to keep them dust-free. This must be removed to reliably maintain living cells on them. Cover slips have a tendency to stack up, so care must be taken to ensure that all surfaces are exposed during the cleaning process.

1. Place the cover slips in the porcelain racks. Always use forceps to manipulate the cover slips (*see* **Note 1**).
2. Place the racks into Pyrex beakers filled with 1 L cleaning solution 7X® PF 1%. Use long forceps to manipulate the trays (*see* **Note 2**).
3. Boil everything for 10 min in a microwave oven, taking care that the soapy solution does not overflow while boiling. This step will remove the film protecting the cover slips.
4. Let the cover slips cool down at room temperature for 5 min and rinse them with abundant distilled water, being careful not to move the cover slips away from the racks.
5. Fill the Pyrex beaker again with distilled water and repeat **step 3**. This will remove the remaining soap from the glass surface. Repeat this step until the soap has completely disappeared (at least twice).
6. Cool the cover slips down for 5 min and rinse again using ultrapure water.
7. Fill the Pyrex beaker with ultrapure water and boil once more for 10 min. This step will eliminate ions coming from the standard distilled water.
8. Repeat **step 6**.
9. Place the porcelain racks carrying the cover slips on a filter paper to drain the excess of water. Use a clean tissue to absorb the water from the edge of the cover slips, without touching the surface of the glass.
10. Put the cover slips together with the racks into a glass box filled with absolute ethanol and store it closed at room temperature.

3.1.2. Mounting the Culture Chambers

1. Keep the aluminum slide in acetone for 5 min to remove any adhered particles, and let it dry.
2. Place it horizontally on the slide's support in such a way that only the two extremes of the slide make any contact.
3. Take a treated cover slip from the alcohol using curved forceps, drain the edges on a tissue, and burn the remaining alcohol in a bunsen burner.
4. Place the cover slip on the slide, covering the well, and seal the edges with nail polish.
5. Store the culture chambers inside the slide's support, keeping the open side of the hole facing down.
6. Let the culture chambers dry for at least 30 min before use.

3.1.3. Cleaning and Recycling the Slides

1. Place the used slides in a removable staining tray and immerse the tray in a staining glass box filled with acetone to remove the attached cover slip.
2. Transfer the tray with the slides through three staining glass boxes filled with xylene, keeping them for at least 4 h in each one. This will remove the oil from the slides.
3. Transfer the tray through three other glass boxes filled with alcohol, keeping the slides in each for at least 4 h. This will remove any xylene residues.

4. Put the tray inside a dry glass box and store it closed. The slides are now ready to be reused starting at **step 1** of **Subheading 3.1.2.**

3.2. Preparation of Living Spermatocytes

1. Fill the culture chamber, prepared as indicated in **Subheading 3.1.2.**, with a layer 0.5–1 mm thick of heavy mineral oil. Discard old culture chambers that might have accumulated dust.
2. Anesthetize the flies on the CO_2 source surface and sort a young *Drosophila* male under the dissection microscope (*see* **Note 4**).
3. Using clean curved forceps, place the fly inside the oil-containing well in a position close to an edge and dissect the testis directly under the oil using two No. 5 dissection forceps. This will avoid evaporation during dissection and cell preparation.
4. Remove the unwanted fly parts. Clean the testis of adhering fat using small triangles of filter paper and drag them onto an untouched area of the cover slip, pulling them from the end with the straight No. 5 forceps (*see* **Note 5**).
5. Dry all of the liquid surrounding the testis sac using the small filter paper triangles. This will allow the released spermatocytes to attach to the glass afterward.
6. Using a sterile needle, cut each testis into two pieces at a position close to the cells of interest.
7. Using the straight No. 5 forceps, drag each half gently over the surface of the cover slip to let the cysts come out and spread over the surface of the glass (*see* **Note 6**).
8. Put the preparation under the microscope. The life-span of these cells in culture is limited, so time counts. Do as specified in **Subheading 3.3.1.**

3.3. Recording Living Spermatocytes by Phase-Contrast Microscopy

In this subsection, we provide the necessary tips to acquire and process a time-lapse series of meiosis by phase-contrast microscopy using some basic image acquisition equipment. By following these steps, nice videos of *Drosophila* male meiosis can be obtained, as shown in **refs.** ***18***, ***20***, and ***21***, and Fig. 5 of Chapter 2.

3.3.1. Recording Single Section Videos by Phase Contrast Microscopy

No time must be wasted once the spermatocytes are prepared within the culture chamber, because their life-span in primary cultures is short. Therefore, before dissection, it is important to already have done **steps 1–4**.

1. Adjust the recording temperature to 25°C at least 1 h in advance.
2. Make sure that the optics for phase-contrast microscopy is properly adjusted.
3. Check the shutter and shutter-driver connections.
4. Start the Scion-Image software and set up the acquisition mode.
5. Place the testes preparation under the microscope and find the region of interest (*see* **Note 7**).

6. Select the cells that are going to be followed (*see* **Note 8**).
7. Readjust phase contrast (*see* **Note 9**).
8. Adjust the illumination conditions (*see* **Note 10**).
9. Specify the recording rate depending on the process to be followed (*see* **Note 11**).
10. Restart the timer to 0 (*see* **Note 12**).
11. Record the cells during the time required, no longer than 2 h or until the first signs of cell damage start to appear (*see* **Note 13**).
12. While recording, pay attention to the focusing and repositioning of the cells within the field (*see* **Note 14**).
13. Save the images (*see* **Note 15**).

3.3.2. Processing Single Section Time-Lapse Series by Phase-Contrast Microscopy

1. Open all of the single images within the NIH-image software and make a stack. This can be animated and visualized as a movie at the desired speed following the instructions indicated in the software.
2. Process the stack so that the cells and the processes of interest can be followed. This includes brightness and contrast adjustment, alignment of the cells, and cropping of the desired region (*see* **Note 16**).
3. Save the modified stack as a movie in a format that is compatible with other computer platforms and image processing programs. QuickTime and AVI are the most commonly used.

3.4. Recording GFP-Fusion Proteins in Living Spermatocytes by Confocal Microscopy

In this subsection, we describe a way to obtain a series of time-points each containing multiple sections observed by phase-contrast optics and fluorescence microscopy with a confocal microscope. This method is especially useful for following the behavior of cell structures such as the chromosomes or the spindle, by recording α-tubulin–GFP or Histone2–GFP (*see* **refs. *18,21***, and Fig. 5 of Chapter 2).

3.4.1. Recording a Multisection, Dual-Channel, Time-Lapse Series of a GFP-Fusion Protein

As explained in **Subheading 3.3.1.**, the recording conditions for the microscope must be set up before starting the dissection.

1. Follow **steps 1** and **2** of **Subheading 3.3.1.**
2. Switch on the lasers and initialize the software.
3. Select the objective from the software (*see* **Note 17**).
4. Set up the beam path by selecting the intensities and excitation wavelengths of the irradiated light and define the corresponding detectors used to record the image (*see* **Note 18**).
5. Choose the image resolution (we use 512 × 512) (*see* **Note 19**).

6. Specify the recording mode to be able to acquire a time lapse by scanning a stack of sections at each time point (we use the xyzt mode).
7. Follow **steps 2–4** of **Subheading 3.3.1.**
8. Set the light source and change the microscope settings to the scanning mode.
9. Acquire in a continuous mode to be able to readjust the acquisition settings for the actual preparation (laser intensity, gain, offset, pinhole) in order to minimize irradiation and optimize the quality of the image (*see* **Note 19**).
10. Select the scanning speed (*see* **Note 19**).
11. Center the region of interest and zoom in to the desired degree.
12. Set origin and end of the series to be scanned at each time-point.
13. Set the number of series to be taken at each time-point and the number of accumulated frames per image (*see* **Note 19**).
14. Set up recording rate (number of time-points per minute). This will depend on the speed of the biological process to be followed (*see* **Note 19**).
15. Start acquisition. Record the cells during the time required, no more than 2 h or until signs of cell death start to appear (*see* **Note 13**).
16. Start a new series whenever refocusing or readjustment of the field is required.
17. Save the experiment (*see* **Note 20**).

3.4.2. Processing Multisection Time-Point Series

1. Two stacks (one per channel) can be built from the individual tiff images, using the NIH-Scion Image software as specified in **Subheading 3.3.2.** Each stack will display sequentially all the sections recorded at each time-point for the whole series of time-points (*see* **Note 20**).
2. Another possibility is to build stacks in which the information of the sections has been resumed. For the gfp channel, all of the sections can be projected at each time-point. For the phase-contrast channel, the optical section containing the focal plane of interest can be selected at each time-point (*see* **Note 20**).
3. In both cases two stacks (phase contrast and gfp) of the same dimensions and number of time-points will be obtained. Both stacks can be visualized and processed at the same time using Scion Image. Processing is similar to that described in **Subheading 3.3.2.** (*see* **Note 16**).
4. Merge the two processed phase and gfp stacks in order to visualize both at the same time.
5. Save the final merged stacks as movies in a format that is compatible with other computer platforms and image processing programs (*see* **Subheading 3.3.2.**)

4. Notes

1. Twelve cover slips can be placed in a single rack. We process four racks at a time.
2. We fit two racks in each beaker and use two beakers at a time.
3. Any boiling method can be used; heating in a microwave oven is simply the most practical.
4. Newly eclosed males are the best option, because a dense layer of fat does not yet surround the testis. Larvae and pupae can also be used, but require more expertise.

5. **Steps 3** and **4** must be done fast and clean because enzymes released from the digestive tract may damage the spermatocytes.
6. Spreading of the cells is the most critical step of the protocol. Too little spreading will give rise to round spermatocytes that cannot be easily visualized, whereas too much spreading will break the cysts and produce separate spermatocytes with damaged cell surfaces. Dispersed spermatocytes become too flat and deformed, show abnormal spindles, and often fail to divide. We have substituted the traditionally used halocarbon oil Voltalef 10S by a lighter one, Trinity Biotech GmbH heavy mineral oil, which makes manipulation easier. Nevertheless, a considerable amount of practice will be required until the right degree of spreading can be achieved.
7. When cell spreading is properly done, there is a gradient of the different stages along a track that can be easily followed.
8. The following criteria facilitate identification of the best suited cells: (1) Cysts must be as intact as possible so that several cells at similar stages can be found together; (2) do not follow cells that are alone or positioned at one edge, because they are most likely damaged; (3) do not follow cells in which clear signs of cell breakage can be seen (bent spindles, missegregating chromosomes, disorganized membranes, etc.).
9. The cells are not completely flat (under optimal conditions they are approx 8 μm thick), so that phase adjustment might be required from one part to another within the same preparation.
10. Too much light will heat and damage the cells. It is important to reduce the intensity of the light source and the exposure time as much as possible in order to get longer cell survival and, hence, recording time.
11. For fast processes (chromosome movement during early prometaphase or anaphase) images must be taken frequently (at least 20 frames/min), whereas slower processes (centrosome migration during prophase, interkinesis or cytokinesis, morphological modifications, etc.) can be recorded at 2 frames/min (Rebollo and González, unpublished data).
12. NIH software can be set up so that the real time appears in each individual image. This can be reset so that the counting starts from zero.
13. The chromosomes stack up and fail to segregate, the spindles are bent, and cytokinesis fails to proceed.
14. Focusing must be controlled manually, as the cells have no fixed reference point that can be used to set up an auto-focus. Also, the stage will have to be moved to recenter cells that move slightly within the oil.
15. It is convenient to save the images as individual files, naming them with the date and time of the acquisition. In this way, they are saved right after being recorded, not at the end of the session. They can easily be converted to a stack with the Scion Image software. The images must be saved in a format that can be easily processed later. Uncompressed tiff formats are best for these purposes.
16. To process the stacks, a series of macros, some included with the software and others that can be easily programmed, will be required. These macros can be applied to one or two stacks at the same time.

17. The microscope model DM IRBE2 uses a software program to control the objective nosepiece. The program automatically rotates the selected objective into the beam path. Other microscope models require manual rotation of the objective.
18. Instructions to define the beam path are included in the Leica software. We activate the transmission light and the 488-nm wavelength light and record them simultaneously. For long recording sessions, we recommend keeping the intensity of the radiated light at the minimum level necessary to detect the GFP signal. This will allow the spermatocytes to survive longer.
19. The specifications given in this chapter are optimized for (1) long acquisition times, (2) intermediate image resolution, (3) fast scanning speed, (4) reduced number of sections (two to six) per time-point, (5) reduced number of frames (two to four) per image, and (6) very low recording rate (one stack every 1–2 min). Other applications will require different settings, in which cell survival will be compromised to get a faster scanning and a better time resolution of a specific process.
20. This will depend on the software utilized. As explained earlier, the possibility of saving individual images separately in tiff format is the best option for subsequent processing.
21. Any software that can read and convert the saved tiff images into tiff stacks will be useful. We use either Scion Image or IDL software to build the stacks and obtain the desired projections and adjustments.

References

1. Cooper, K. W. (1965). Normal spermatogenesis in *Drosophila*, in *Biology of Drosophila* (Demerec, M., ed.), Hafner, New York, pp. 1–61.
2. Tates, A. D. (1971). Cytodifferentiation during spermatogenesis in *Drosophila melanogaster*. An electron microscope study. Ph.D. thesis, Rijkuniversiteit, Leiden.
3. Lifschytz, E. and Hareven, D. (1977). Gene expressions and the control of spermatid morphogenesis in *Drosophila melanogaster*. *Dev. Biol.* **58,** 276–294.
4. Lifschytz, E. and Meyer, G. F. (1977). Characterisation of male meiotic-sterile mutations in *Drosophila* melanogaster. The genetic control of meiotic divisions and gametogenesis. *Chromosoma* **64,** 371–392.
5. Lindsley, D. and Tokuyasu, K.T. (1980). Spermatogenesis, in *The Genetics and Biology of Drosophila, Vol. 2b* (Ashburner, M. and Wright T. R. F., eds.), Academic, London, pp. 225–294.
6. Lifschytz, E. (1987). The developmental program of spermiogenesis in *Drosophila*: a genetic analysis. *Int. Rev. Cytol.* **109,** 211–258.
7. Hackstein, J. H. (1991). Spermatogenesis in *Drosophila*. A genetic approach to cellular and subcellular differentiation. *Eur. J. Cell Biol.* **56,** 151–169.
8. Castrillon, D. H., Gonczy, P., Alexander, S., et al. (1993). Toward a molecular genetic analysis of spermatogenesis in *Drosophila melanogaster*: characteriza-

tion of male-sterile mutants generated by single P element mutagenesis. *Genetics* **135,** 489–505.
9. Fuller, M. (1993). Spermatogenesis, in *The Development of* Drosophila melanogaster (Martinez-Arias, A. and Bate, M., eds.), Cold Spring Harbor Laboratory Press, Plainview, NY, pp. 61–147.
10. Lin, T. Y., Viswanathan, S., Wood, C., Wilson, P. G., Wolf, N., and Fuller, M. T. (1996). Coordinate developmental control of the meiotic cell cycle and spermatid differentiation in *Drosophila* males. *Development* **122,** 1331–1341.
11. Maines, J. and Wasserman, S. (1998). Regulation and execution of meiosis in *Drosophila* males. *Curr. Topics Dev. Biol.* **37,** 301–332.
12. Clarkson, M. and Saint, R. (1999). A *His2AvDGFP* fusion gene complements a lethal *His2AvD* mutant allele and provides an in vivo marker for *Drosophila* chromosome behavior. *DNA Cell Biol.* **18,** 457–462.
13. Kemphues, K. J., Raff, E. C., Raff, R. A., and Kaufman, T. C. (1980). Mutation in a testis-specific beta-tubulin in *Drosophila*: analysis of its effects on meiosis and map location of the gene. *Cell* **21,** 445–451.
14. Gatti, M. and Goldberg, M. L. (1991). Mutations affecting cell division in *Drosophila*. *Methods Cell Biol.* **35,** 543–586.
15. Cenci, G., Bonaccorsi, S., Pisano, C., Verni, F. and Gatti, M. (1994). Chromatin and microtubule organization during premeiotic, meiotic and early postmeiotic stages of *Drosophila* melanogaster spermatogenesis. *J. Cell Sci.* **107,** 3521–3534.
16. Church, K. and Lin, H. P. (1985). Kinetochore microtubules and chromosome movement during prometaphase in *Drosophila* melanogaster spermatocytes studied in life and with the electron microscope. *Chromosoma* **92,** 273–282.
17. Church, K. and Lin, H. P. (1988). *Drosophila*: a model for the study of aneuploidy, in *Aneuploidy*, Part B. Alan R. Liss, Inc., New York, pp. 227–255.
18. Rebollo, E. and Gonzalez, C. (2000). Visualizing the spindle checkpoint in *Drosophila* spermatocytes. *EMBO Rep.* **1,** 65–70.
19. Savoian, M. S., Goldberg, M. L., and Rieder, C. L. (2000). The rate of poleward chromosome motion is attenuated in *Drosophila zw10* and *rod* mutants. *Nature Cell Biol.* **2,** 948–952.
20. Sampaio, P., Rebollo, E., Varmark, H., Sunkel, C. E., and Gonzalez, C. (2001). Organized microtubule arrays in gamma-tubulin-depleted *Drosophila* spermatocytes. *Curr. Biol.* **11,** 1788–1793.
21. Lange, B. M. H., Rebollo, E., Herold, A., and González, C. (2002). Cdc37 is essential for chromosome segregation and cytokinesis in higher eukaryotes. *EMBO J.* **21,** 5364–5374.
22. Nicklas, R. B. and Staehly, C. A. (1967). Chromosome micromanipulation. I. The mechanics of chromosome attachment to the spindle. *Chromosoma* **21,** 1–16.

4

Immunocytological Analysis of Oogenesis

Endre Máthé

1. Introduction

Drosophila oogenesis is a fascinating phenomenon. The coordinated action of many cellular processes produces a fully mature egg containing a maternal dowry that both directs and supports development of the embryo. The ovary is one of the best studied organs of *Drosophila*, and much of our knowledge of oogenesis is contained in several monographs ***(1–4)*** and recent reviews ***(5–8)***. This chapter describes some of the most important cellular processes of oogenesis, and provides detailed methods for their identification and immunocytological analysis.

1.1. Construction of the Egg

The adult female reproductive system of *Drosophila* consists of a pair of ovaries, the genital ducts (common and lateral oviducts, uterus, vagina) and their accessory structures (two spermathecae, two accessory glands, and seminal receptacle), and the external genitalia (*see* **Fig. 1**). The ovaries are direct descendents of the embryonic gonads, whereas all other genital structures derive from a single genital imaginal disc. The formation of embryonic gonads implies the specification of pole plasm (germ plasm) by localized germ-line determinants early in embryogenesis ***(7)***. The pole plasm, in turn, is both necessary and sufficient for the formation of pole cells, the primordial germ cells ***(9)***. Pole cells migrate during gastrulation to reach the gonadal region, where they become surrounded by somatic mesodermal cells and form the embryonic gonads ***(10,11)***. The gonads remain in this undifferentiated state and have no direct connections with the genital disc until the larval–pupal transition ***(1)***. The first connections between the ovaries and lateral oviducts are established 54–60 h after pupariation ***(12)***. The undifferentiated larval ovaries

From: *Methods in Molecular Biology, vol. 247:* Drosophila *Cytogenetics Protocols*
Edited by: D. S. Henderson © Humana Press Inc., Totowa, NJ

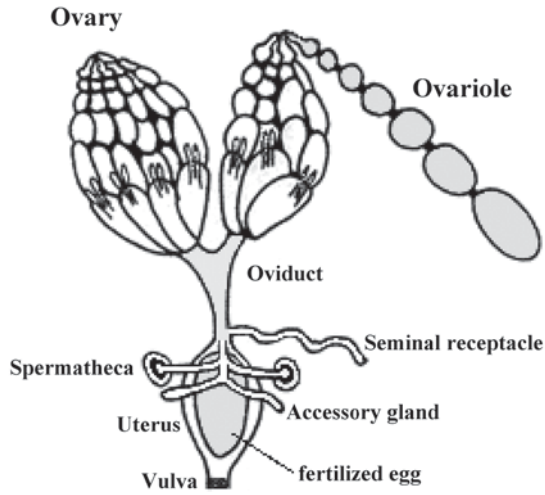

Fig. 1. The internal reproductive organ of the *Drosophila* female. (Adapted from **ref. *2***.)

are relatively small and consist of two cell types: large germ cells and small mesodermal cells; the latter will form the follicle cells, ovarian sheaths (epithelial and peritoneal), and other structures. Differentiation of adult ovaries begins during the mid third larval instar with the appearance of the terminal filaments as a consequence of tunica propria formation around the forming ovarioles ***(1)***. After pupariation, a set of rapid developmental events occurs, which will lead to formation of the mature ovary by the end of pupal life. Differentiation of the genital disc starts after puparium formation, and all of the genital ducts and their accessory structures will be present as primordia after 48 h.

The mature *Drosophila* ovary is composed of 12–16 ovarioles, joined at their tips by terminal filaments. The structural and functional unit of the ovary is the ovariole (*see* **Fig. 2**). Each ovariole is contained within a tube, protected by an ovariolar wall, which consists of tunica propria (or basement membrane), epithelial sheath (bilayered epithelial tissue), and peritoneal sheath (protective tissue). Both the epithelial and peritoneal sheaths contain nervous tissue. The musculature, set between the two layers of epithelial sheath, undergoes rhythmic contractions, pushing the eggs/egg chambers posteriorly. The peritoneal sheath contains tracheoles and holds the ovary together. The formation and differentiation of oocytes takes place in an assembly-line fashion inside the ovarioles. The apical region of the ovariole is called the germarium, and the following part is the vitellarium.

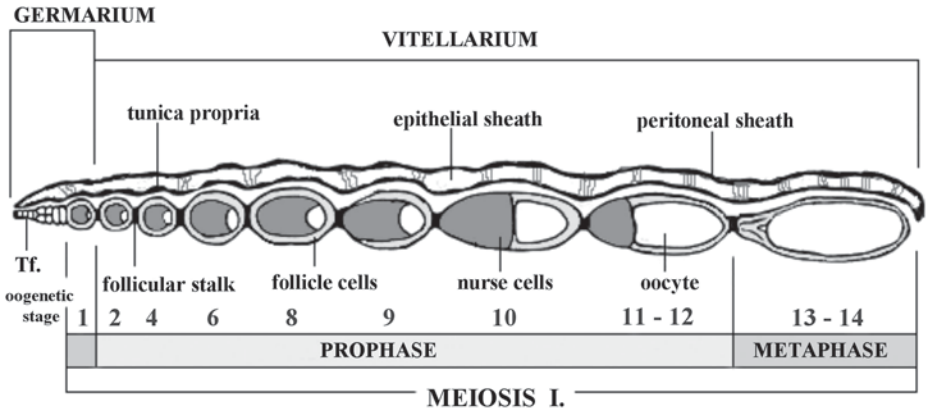

Fig. 2. The formation and development of the egg chambers in ovarioles. Stages 1–14 of oogenesis and the corresponding stages of meiosis are indicated. tf-terminal filament; ovariole wall components: tunica propria, epithelial sheath, and peritoneal sheath. (Adapted from **ref. *13***.)

Oogenesis begins in the germarium with the asymmetrical division of a germ-line stem cell into a daughter stem cell and a cystoblast, as inferred from the partition of a spherical membranous organelle called the spectrosome (*see* **Fig. 3**). Four rounds of mitotic divisions of the cystoblast and its daughters (cystocytes) produce a cluster of 16 cells. Because each of these mitotic divisions is followed by incomplete cytokinesis, the cystocytes remain interconnected through arrested cleavage furrows, thus forming a 16-cell cyst. The arrested cleavage furrows develop into ring canals, and the 16-cell cyst contains 2 cells with 4 ring canals (also named pro-oocytes), 2 cells with 3 ring canals, 4 cells with 2 ring canals, and 8 cells with 1 ring canal each (*see* **Fig. 3**). The ring canals play important roles in the cystocyte divisions and they facilitate the growth and differentiation of the oocyte ***(14)***. The fusome, a continuous vesicular organelle descended from the spectrosome, connects the cystocytes inside the 16-cell cyst via the ring canals (*see* **Fig. 4A**).

Cystocyte divisions are confined to the anterior third of the germarium, known as region 1. As the 16-cell cyst moves posteriorly through regions 2a and 2b of the germarium, it undergoes a change of shape, and one of the two cystocytes with four ring canals differentiates as an oocyte, maintaining a meiotic fate. The other pro-oocyte and 14 cystocytes will become nurse cells through endoreduplication cycles (*see* **Figs. 2** and **4B–E**; *see also* Chapter 6). Each 16-cell cyst acquires a monolayer of follicle cells derived from 2 somatic stem cells located near the junction with region 2b. In region 2b, the 16-cell cysts are initially lens shaped, then become round, and, finally, bud off in

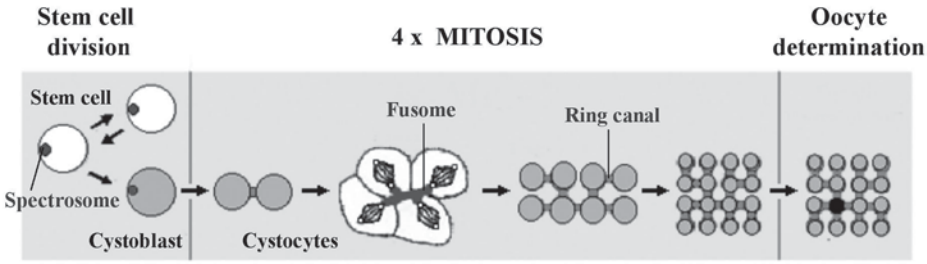

Fig. 3. Schematic representation of the germ-line-specific divisions leading to formation of the 16-cell cyst.

germarium region 3 to form a new egg chamber. This stage 1 egg chamber subsequently enters the vitellarium where it continues to grow and moves further posteriorly.

The vitellarium contains egg chambers from stage 2 to stage 14, which is the mature egg ***(13–16)*** (*see* **Fig. 2**). (The most important morphological features of each stage of oogenesis are listed in **Appendix A**.) The oocyte gradually increases in size during stages 2–10a, acquiring cytoplasm from the nurse cells (*see* **Subheading 1.5.**) and yolk (vitellogenesis) beginning at stage 8. Three

---

Fig. 4. (*opposite page*) **(A)** Stem cell at metaphase stained for tubulin (green), α-spectrin (red), and DNA (TOTO-3, blue). Note the asymmetric nature of this division as inferred from the apical position of the fusome. Scale bar: 5 μm. **(B)** Stage 7 egg chamber stained for lamin (green) and DNA (blue). **(C)** Stage 6 egg chamber stained for tubulin (green), Orbit (red), and DNA (blue). The Orbit protein accumulates behind the oocyte nucleus, whereas the microtubule bundles extend across the cyst. **(D)** Stage 7 egg chamber, stained for actin (red), Filamin (green), and DNA (blue). Notice the subcortical actin network in the oocyte. Scale bar identical for **B–D**: 25 μm. **(E)** Stage 5 egg chamber stained for actin (red) and Filamin (green). Note the four ring canals of the oocyte and the colocalization of the two proteins in the ring canals. Scale bar: 5 μm. **(F)** Stage 4 egg chamber stained with anti-lamin (green) and DNA (red). The nurse cell nuclei contain similar amounts of DNA. The oocyte nucleus, situated at the posterior of the egg chamber, contains the karyosome. **(G)** Stage 10 egg chamber stained as in **(F)**, showing the oocyte nucleus in the anterior dorsal corner. Note the lamin accumulation in the oocyte nucleus. Squamous follicle epithelium covers the nurse cells and columnar epithelium is seen on the oocyte. **(H)** Stage 8 egg chamber stained with anti-tubulin (green), anti-CP190 (red, and panel 2), and DNA (blue, and panel 3). CP190 protein is seen in the nurse cells and accumulates in the oocyte nucleus around stage 8. Note the small size of the karyosome as inferred from the DNA staining (panel 3). **(I)** Cystocyte divisions visualized through staining for tubulin (green), α-spectrin (red, and panel 2), and DNA (blue). The left cyst shows metaphase spindles

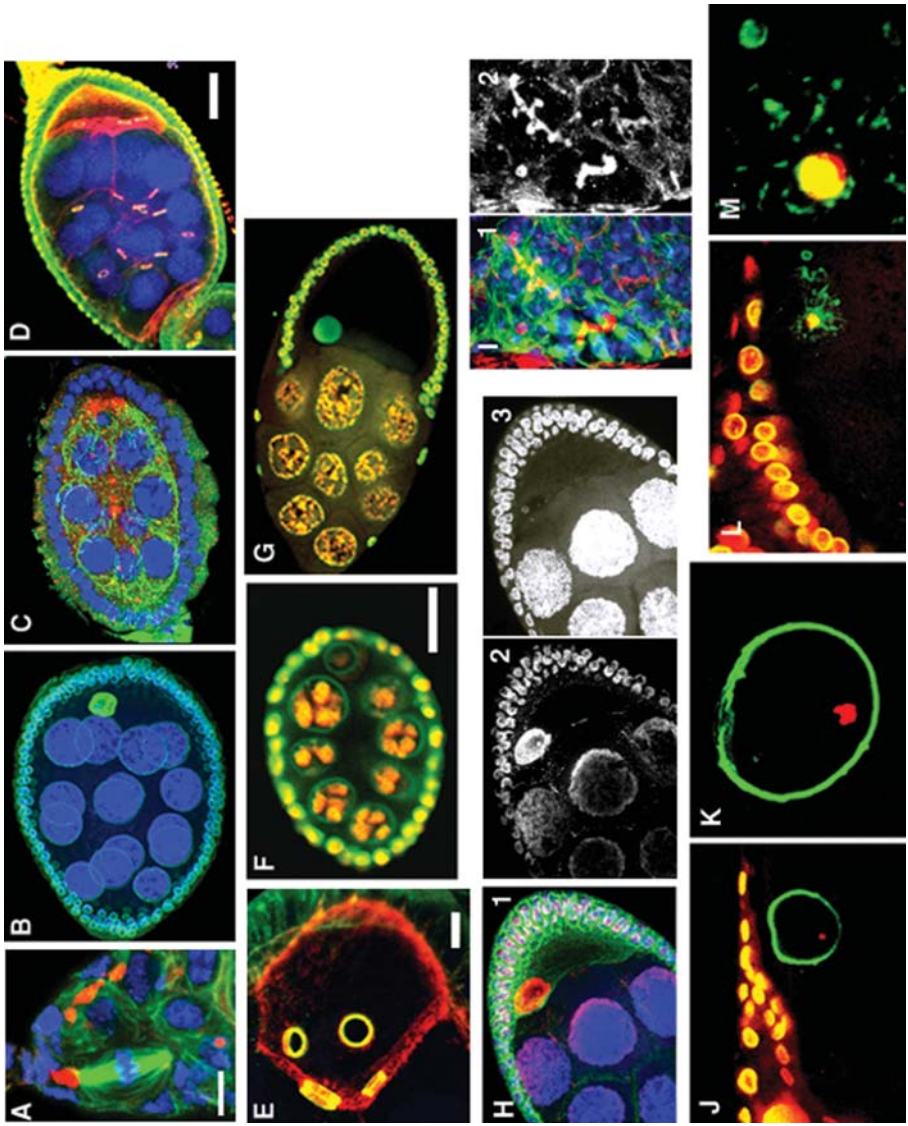

Fig. 4. (*continued*) associated with the fusome at of one of their poles. The right cyst shows fusome "plugs" migrating towards the old fusome. **(J,K)** Stage 13 oocyte. The nuclear lamina of the oocyte nucleus was stained with anti-lamin antibody (green) and the DNA with propidium iodide (red). Note the anterior-dorsal position of the oocyte nucleus with the highly condensed karyosome. **(L,M)** Breakdown of the oocyte nuclear membrane during stage 13, stained as in **(J)** and **(K)**. Lamin becomes dispersed in the cytoplasm during the disassembly of the nuclear envelope. (*See* color plate 3 in the insert following p. 242.)

major yolk constituents have been identified: protein-containing particles, glycogen-rich particles, and lipid droplets. Yolk proteins are synthesized in the fat body ***(17)***, released into the hemolymph, and subsequently taken up by the oocyte through endocytic activity ***(18)***. In addition, yolk proteins are produced by follicle cells ***(19)***. The lipid droplets appear in nurse cells at stage 8 and are transported to the oocyte, whereas the glycogen-rich particles do not appear until stage 13 and are probably synthesized in the oocyte. Maturation of the oocyte occurs in stages 12–14 with the complete resorbtion of the nurse cells, and the completion of eggshell formation, while in the oocyte, meiosis arrests at metaphase I.

The eggshell is a multilayered protein structure deposited by follicle cells ***(20,21)***. The inner layers include the vitelline membrane, the waxy layer, and the inner chorion layer. The outer layers include the endochorion and the exochorion. Once eggshell formation is completed, the follicle cells undergo apoptosis ***(22)*** and are resorbed as the mature egg is released from the ovary. The eggshell has regional specializations like the anterior dorsal appendages and posterior aeropyle (both involved in gas exchange), the micropyle, and the operculum, ringed on three sides by a collar. The collar exhibits ultrastuctural perforations in the chorion and vitelline membrane, and it is easily split, letting the larva escape through the operculum. The micropyle juts out near the ventral collar and surrounds a canal for sperm entry, playing an important role in fertilization.

Egg production depends on the availability of protein ***(1,23)***, sex peptide ***(24,25)***, juvenile hormone ***(26,27)***, ecdysone ***(28,29)***, and the insulin-signaling pathway ***(30,31)***. The newly eclosed *Drosophila* female has a vitellarium consisting of three to six egg chambers, all in previtellogenic stages. Egg chambers/oocytes in vitellogenic stages appear during the first day of adult life, and inseminated females will be able to lay eggs the second day after eclosion. In nutrient-rich conditions, approximately two to three eggs per ovariole per day are produced. The germ-line and somatic stem cells, as well as their progeny, adjust their proliferation rates in response to nutrition without affecting the number of active stem cells ***(31)***. Under conditions of nutrient limitation, egg production can be regulated by programmed cell death at two precise developmental points: (1) in region 2a/2b within the germarium and (2) in stage 8 egg chambers at the onset of vitellogenesis ***(28,29,31)***.

1.2. Asymmetric Germ-Line Divisions

In the adult ovary, the germ-line stem cells lie at the anterior of the tip of the germarium. Genetic ***(32)*** and laser ablation studies ***(33)*** showed that each ovariole contains two to three self-renewing germ-line stem cells that undergo bursts of two to five successive divisions. Germ-line stem cells contain a

spectrosome (the fusome precursor), which arises as the embryonic gonad is formed ***(34)***. The spectrosome associates with one pole of the metaphase spindle, and so is asymmetrically partitioned between the stem cell and cystoblast daughters during cytokinesis ***(35,36)*** (*see* **Figs. 3, 4A,I**).

Cystoblasts/cystocytes also divide asymmetrically, and in doing so, the spectrosome evolves into a branched fusome in the 16-cell cyst ***(5,37)***, accumulating proteins like Bam, ankyrin, α- and β-spectrins, the adducinlike product of the *hu-li tai shao* gene (HtsF), dynein (Dhc64C), and Cyclin A ***(5,35,36)***. Each polarization cycle begins in mitosis, with one pole of the spindle positioned near the fusome (*see* **Fig. 4I**), in a process mediated by cytoplasmic dynein and DLis-1 ***(38–40)***. As the polarization cycle progresses, the preexisting fusome and ring canal are inherited by only one of the two daughter cells. Following mitosis, a "fusome plug" forms in each newly formed ring canal, and then the fusome plug, together with the associated ring canal, moves toward, and finally fuses with the pre-existing fusome. As a result, a highly branched fusome forms within each cyst, with the older cystocytes containing larger networks of fusome.

Following the formation of the 16-cell cyst, the fusome breaks down and disappears (regions 2b–3 of germarium), whereas inside the cyst, a polarized transport is initiated and the nurse cells and oocyte differentiate. Studies on mutants that affect formation of the 16-cell cyst suggest that proper fusome organization is a precondition of oocyte specification. The fusome not only generates a branched pattern of interconnections between cystocytes, it also synchronizes and controls the number of cystocyte divisions.

Immunocytological analysis of stem cell and cystoblast/cystocyte divisions is a very demanding task, because it requires visualization of the spectrosome/fusome together with the spindles, ring canals, nuclei/chromosomes, and centrosomes. Antibodies against these structures are listed in **Appendix B**. Because, as described earlier, the orientation of the spindle with respect to the spectrosome/fusome is determinative for proper development of the germ-line cyst, methods allowing the simultaneous visualization of these two structures are crucial (*see* **Figs. 4A,I**). Such a method is described in **Subheading 3.1.**

1.3. Specification and Determination of the Oocyte

Soon after the 16-cell cyst is formed (in germarium region 1), one of the cells with four ring canals is selected to become the oocyte (in germarium region 2). How this choice is made is still unclear. Whatever mechanisms are involved, oocyte specification requires polarized transport and localization of cytoplasmic proteins and mRNAs, restriction of meiosis, and migration of centrioles into the oocyte ***(3–7)***. A polarized microtubule network, organized by the fusome, facilitates the transport of cytoplasmic factors from the nurse cells

to the oocyte ***(40–42)***. Centriole migration is guided by the fusome ***(43)***, and meiotic entry and progressive restriction of synaptonemal complexes to one cell within the 16-cell cyst are controlled by the BicD and Egl proteins ***(44,45)***.

Further progression of oogenesis requires inactivation of the meiotic checkpoint that detects unrepaired double-strand DNA breaks ***(46)***, and the maintenance and determination of oocyte fate regulated by PAR-1 ***(6,47–51)***. Determination of oocyte fate occurs when the 16-cell cyst, encapsulated by follicle cells, reaches the end of the germarium (region 3) and is accompanied by the anterior–posterior translocation of Bic-D, Orb, centrioles, and the microtubule organizing center (MTOC) within the oocyte. This posterior shift of oocyte markers represents the first sign of polarity within the oocyte itself.

Immunocytological analysis of oocyte specification and determination involves studying the localization of proteins like Bic-D, Orb, PAR-1, PAR-6, Bazooka, γ-tubulin, and Inscuteable (a component of the synaptonemal complex). The sources for antibodies against these proteins are listed in **refs. *45*** and ***51*** and in **Appendix B**. The immunostaining methods detailed in **Subheadings 3.1.–3.4.** can be used to visualize these proteins.

1.4. Morphogenesis and Patterning of Follicle Cells

From the point of view of follicle cells, the formation of the egg chamber involves three interdependent processes: (1) proliferation of follicle cell-specific stem cells, (2) migration and encapsulation of the 16-cell cyst initially by approx 30 follicle cells, and (3) differentiation of follicular epithelium and follicular stalk to separate the egg chambers ***(21)***. Some defects in these processes lead to egg chambers with 2 or more 16-cell cysts. The stem cells of follicle cells are located in the germarium at the transition of regions 2a and 2b. Follicle cell stem cells divide continuously ***(52)*** and are regulated by the terminal filaments ***(53)***. Proliferating follicle cells migrate between successive 16-cell cysts, first contacting the posterior portion and eventually surrounding the entire lens-shaped 16-cell cyst ***(54)***. Follicle cells that contact the germ-line cells fully polarize and form a follicular epithelium, whereas a second group of follicle cells forms the interfollicular stalk. Apical, lateral, and basal polarization cues contribute to the development of the follicular epithelium, and proteins like Crumb and Discs Lost play a determinative role in these processes ***(55)***.

DE-cadherin levels are elevated both in the oocyte and in follicle cells at the anterior and posterior poles and contribute to the posterior positioning of the oocyte in the forming egg chamber ***(54–56)***. The position of the oocyte determines the anterior–posterior polarity of the egg chamber. The follicular stalk attaches adjacent egg chambers to one another as they leave the germarium. Two pairs of polar follicle cells situated at the anterior and the posterior poles of an egg chamber make contact with the follicular stalks. The polar cells are

determined in the germarium, where they cease to divide and accumulate DE-Cadherin. They are the keystones for follicle cell patterning, for they nucleate subsequent patterning of the terminal follicle cells ***(54–57)***.

During stages 2–6, terminal follicle cells are established at the anterior and posterior ends of the egg chamber. Whether anterior or posterior, all terminal follicle cells have the same positional identity and are competent to give rise to anterior cell identity. Main-body follicle cells continue to divide during stages 2–5, whereas in stage 6, endoreduplication and chorion gene amplification are initiated (*see* Chapter 8).

At stage 7, a Gurken signaling event (initiated in the oocyte) specifies posterior follicle cell fate, thus polarizing the anterior–posterior axis of the follicle epithelium ***(58,59)***. During stage 9, the patterning of follicle cells continues and they reorganize into three domains: a small cluster of border cells inside the egg chamber (between the nurse cells and oocyte), a squamous epithelium over the nurse cells, and a columnar main-body epithelium over the oocyte. The border cells detach from the anterior epithelium and migrate through the nurse cells to reach the oocyte. At the same time, the cuboidal main-body follicle cells move posteriorly to form a columnar epithelium over the oocyte. The remaining 30–40 anterior terminal cells flatten over the nurse cells and form a squamous epithelium. During stages 7 and 8, the oocyte nucleus is repositioned in the antero-dorsal corner, and a second Gurken signaling is initiated, an event crucial for the dorsal–ventral patterning of the follicle cells ***(60,61)***. As a consequence, the fate of the dorsal follicle cells is specified, the ventralizing signal is restricted to the ventral follicle cells, and border cell migration is initiated. The main-body follicle cells, executing their posterior migration, are exposed to this Gurken signal as they pass near the oocyte nucleus and, consequently, they adopt a dorsal fate.

The formation of dorsal appendages and operculum depends on the dorsal and anterior patterning of the anterior columnar follicle cells ***(62)***. At stage 10b, the follicle cells migrate centripetally between the nurse cells and the oocyte, enclosing the anterior of the egg. The migrating follicle cells arise at the border between the anterior squamous and the main-body columnar follicle cells, which overlay the border between the nurse cells and oocyte. Their migration occurs concurrently with nurse cell dumping, so that follicle cells cap the oocyte after the nurse cells have expelled their contents. The cells at the leading edge of centripetal migration come to rest at the border cells, and through their coordinated action they create the micropyle ***(63)***.

The immunostaining methods in **Subheadings 3.1.–3.4.** can be used to visualize some of these follicle cell-related processes by using antibodies against lamin, α- or β-tubulins, actin, β-spectrin, DE-cadherin, nonmuscle myosin II heavy chain (MHC), Crumbs, and Discs Lost (*see* **Appendix B**).

1.5. Microtubule and Actin Cytoskeletons

Throughout oogenesis, different polarized microtubule networks are organized within the nurse cell–oocyte complex and mediate important processes related to oocyte determination and differentiation. One such microtubule network is organized in the germarium (*see* **Subheading 1.3.**). During stages 2–6, a common MTOC, situated behind the oocyte nucleus, organizes a microtubule network by focusing the minus ends of microtubules. The plus ends of the microtubules extend through the ring canals into the nurse cells (*see* **Fig. 4C**). No centrosomal proteins of this MTOC are known, except for Centrosomin (Cnn), which accumulates at the MTOC relatively late, at stages 5 and 6 ***(64)***. During stage 7, the terminal follicle cells adopt a posterior fate after receiving the Gurken signal, and their back-signal to the oocyte induces disassembly of the MTOC behind the oocyte nucleus ***(60,61)***. As a consequence, the microtubule network breaks down, and during stage 8, a new microtubule network is organized with microtubules nucleated all around the oocyte cortex, with the exception of the posterior pole ***(40)***. At this time, Cnn is seen relocalized to the anterior and lateral cortical regions of the oocyte ***(64)***. After this reorganization of the microtubule network has occurred, the oocyte nucleus moves along the microtubules, aided by the action of DLis-1 and dynein, from the posterior to a random anterior corner of the oocyte ***(65)***. This new position of the oocyte nucleus defines the dorsal side of the egg chamber through a second Gurken-signaling event (*see* **Subheading 1.4.**). During stages 8 and 9, the microtubule network becomes polarized in such a way that the plus ends of microtubules are enriched at the posterior pole of the oocyte, a process influenced by PAR-1 ***(66)***, Rab11 ***(67)***, and the actin cytoskeleton ***(68)***. This late reorganization of the microtubule network plays an essential role in the localization of anterior and posterior determinants within the *Drosophila* oocyte ***(69,70)***. For details on the localization of anterior and posterior determinants, *see* **refs.** ***7,13,71,*** and ***72***.

The nurse cells and the oocyte are interconnected via ring canals, which are membrane-associated actin cytoskeletal elements. Together with the cortical actin, ring canals play an important role in intercellular cytoplasm transport during oogenesis ***(73)*** (*see* **Figs. 4D,E**). Ring canal assembly is initiated with the arrest of the cleavage furrows at a diameter of 0.5–1 μm, followed by the recruitment of several proteins in a developmentally defined order ***(14,73–76)***. Thus, the ring canals develop an electron-dense outer rim and a proteinaceous inner rim, and their diameter increases to 10 μm by the rapid phase of transport. The glycoprotein D-mucin, anillin, and the kinesin-like protein (KLP) Pavarotti are the first to be recruited next to the contractile actin ring of the cleavage furrows during the cystocyte divisions ***(76–78)***. At the time of the final cystocyte division, another protein (or proteins) that reacts with anti-

phosphotyrosine antibodies can be detected on the outer rim ***(14)***. As soon as the 16-cell cyst enters germarium region 2a, inner rim formation is initiated by the accumulation of Filamin, HtsRC, and actin, and a few hours later, in germarium region 3, the Kelch protein is recruited. The outer rim acquires Filamin at the same time as the inner rim, and as soon as the egg chamber buds off from the germarium, anillin disappears from the outer rim ***(76)***.

Cytoplasm is transported between nurse cells and oocyte in two phases, a slow-initial phase and a rapid-terminal phase ***(3,73,79)***. The slow initial phase occurs during stages 2–10a and seems to be highly regulated ***(80)***. The rapid-terminal phase (also called "dumping") results in the regression of the nurse cells and doubling of the oocyte volume during stages 10b–12. In each nurse cell, a system of actin-based microfilaments forms, connecting the nuclei with the plasma membrane. These microfilaments may serve to tether the nuclei away from the ring canals, because they are too large to pass through ***(81)***. This phase of transport seems to be nonselective and the forces that drive egg chamber elongation during stages 10b–12 may be responsible for it ***(82)***.

The immunostaining methods described in **Subheadings 3.1.–3.4.** work well for visualizing microtubules (using the YL1/2 antibody) and ring canal components. Antibodies against ring canal proteins are described in **refs.** ***74–78***. **Reference** ***14*** describes a rhodamine-conjugated phalloidin-based protocol to visualize actin in egg chambers. To study the effect of cytoskeletal inhibitors, the drugs colchicine (microtubule-specific) and cytochalasin-D (actin-specific) can be employed as described in **refs.** ***41*** and ***80***, respectively. To study microtubule polarity, transgenes that express either the minus-end-directed motor Nod or a plus-end-directed kinesin fused to β-galactosidase can be used as described in **ref.** ***(70)***.

1.6. Female Meiosis

Prophase and metaphase of meiosis I take place during ovarian development (*also see* Chapter 5). Meiotic commitment of the oocyte is established through progressive restriction of the synaptonemal complexes to one of the two pro-oocytes. By the time oocyte fate is determined, the synaptonemal complexes have disappeared. As the egg chamber buds off from the germarium, the oocyte chromosomes begin to condense into a "karyosome" ***(1)***. The karyosome type of chromatin organization is a characteristic of prophase of meiosis I of *Drosophila* females, during which the canonical diplotene and diakinesis phases are not observed ***(83,84)***. During stages 2–6, chromosome condensation continues (*see* **Figs. 4C,F**), and by stages 7 and 8, the karyosome reaches its highest state of compaction with a diameter of 4–7 μm (*see* **Fig. 4H**). In stage 9, the karyosome becomes looser ***(83,84)***, and this reorganization might permit transcription of the *gurken* gene ***(85)***, among others. From stage 10 (*see* **Fig. 4G**), the compact structure of the karyosome is restored and maintained

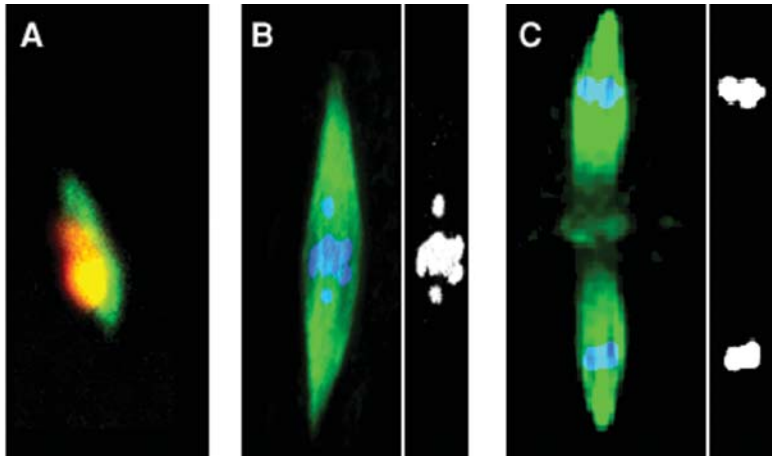

Fig. 5. **(A)** Formation of the meiosis I spindle as visualized by antitubulin (green) and DNA (red) staining. Small spindle, with the karyosome increasing in size. **(B)** Long tapered meiosis I metaphase spindle (green), with the nonexchange fourth chromosomes separated from the metaphase plate (DNA in blue, and right panel). **(C)** Meiosis II metaphase. The twin spindles (green) share the central spindle pole body or midpole (DNA in blue, and right panel). (*See* color plate 2 in the insert following p. 242.)

until stage 13. The mechanism that controls the formation of the karyosome is not known, and no karyosome-specific proteins have been found so far. The chromosome–centrosome passenger protein, CP190, tends to accumulate in the oocyte nucleus, but seems to be excluded from the karyosome ***(86)*** (*see* **Fig. 4H**).

Stage 13 of oogenesis corresponds to prometaphase of meiosis I ***(84)*** and is subdivided into four stages (viz. A, B, C, and D). At stage 13A, the oocyte nuclear membrane is still present, and the karyosome is juxtaposed to the nuclear lamina (*see* **Figs. 4J,K**). The nuclear membrane of the oocyte nucleus breaks down during stage 13B (*see* **Figs. 4L,M**), and an envelopelike array of microtubules appears around the karyosome. During stage 13C (mid-prometaphase), the envelopelike microtubule array transforms into a small bipolar spindle with no visible astral microtubules (*see* **Fig. 5A**). During stage 13D (late prometaphase), the short spindle transforms into a long tapered spindle, with the achiasmate fourth chromosomes positioned between the metaphase plate and spindle poles, whereas the chiasmatic chromosomes are situated at the metaphase plate (*see* **Fig. 5B**). (Full metaphase is sometimes referred to as stage 13E.)

The meiosis I spindle, being anastral and noncentrosomal, is rather unconventional, particularly regarding spindle assembly and the establishment of

bipolarity. The karyosome may act like an initial MTOC, organizing microtubules into a bipolar spindle through the coordinated action of microtubule motors and microtubule-associated proteins ***(87)***. Similar kinds of spindle organization have been observed in chromatin-driven, in vitro spindle assembly assays using centrosome-free extracts ***(88,89)***. Whereas *Drosophila* proteins mediating the establishment of spindle bipolarity have been identified, those involved in a karyosome type of MTOC remain unknown, leaving unanswered the question of how microtubule nucleation occurs.

Two microtubule-associated proteins, D-TACC and Msps, cooperate with the minus-end-directed microtubule motor Ncd to promote the assembly of the meiosis I spindle ***(90)***. A fourth protein, NOD, with a predicted plus-end-directed microtubule motor activity, is localized along the chromosome arms, and is proposed to push achiasmate chromosomes away from the poles, forcing them toward the other chromosomes in the metaphase plate ***(91)***. Full metaphase I is reached at the end of stage 13D, and meiosis I remains arrested throughout stage 14 ***(92)***. Just how this metaphase arrest is maintained is still an open question.

The moment the egg is released from the ovary and passes into the oviduct (ovulation), the metaphase arrest is abolished and meiosis I proceeds into anaphase ***(92)***. Studies on fixed specimens revealed the chromosomes' behavior upon spindle activation to include (1) release of chiasmata and abolition of homologous pairing, (2) abolition of sister-chromatid cohesion along the chromosomal arms, (3) lengthening of the spindle midzone, and (4) transition from meiosis I to meiosis II without daughter nuclei formation ***(84,93)***. Elegant studies of stage 14 live oocytes have shed light on the dynamics of the meiotic spindle after oocyte activation by monitoring the spindle-associated Ncd motor protein tagged with green fluorescent protein (GFP) ***(94,95)***.

Meiosis II is governed by a unique type of spindle apparatus that appears to be an elaboration of the meiosis I spindle ***(93–96)***. The midzone of the meiosis I spindle appears to differentiate into an MTOC by recruiting centrosomal proteins like γ-tubulin, CP190 and Abnormal spindle protein (ASP) ***(93,96,97)***. This newly formed MTOC serves as a central pole for the twin meiosis II spindles (*see* **Fig. 5C**). During metaphase of meiosis II, the kinetochores of the chromosomes are reoriented with respect to the new poles and, subsequently, segregation of daughter chromatids takes place ***(93)***. Upon completion of meiosis II, four haploid nuclei, called polar body nuclei, form in the egg, and inside the polar body nuclei, the chromosomes begin to decondense ***(98)***. The time required to complete both meiotic divisions is estimated at approx 5–10 min ***(94–96)***. Insemination of the egg occurs while anaphase I is still in progress, and both anaphase I and all subsequent meiotic stages proceed identically in unfertilized and fertilized eggs, indicating that spindle activation is independent of fertilization ***(96,98–100)***.

The equal distribution of chromosomes during meiosis I and II is dependent on the maintenance of sister chromatid cohesion ***(101,102)***. At the onset of anaphase I, the chiasmata of homologous chromosomes (referred to as tetrads or bivalents) are released, so that each pair of sister-chromatids (now referred to as dyads or univalents) can segregate to the opposing spindle poles. At the same time as chiasmata are released, the cohesion that holds the sister-chromatid arms of each dyad is similarly abolished. The centromeric cohesion of each dyad is then maintained until the onset of anaphase II, at which time it too is abolished. Thus, during meiosis, chromosome segregation is mediated by two mechanisms at the level of chromosomal cohesion. *Drosophila* proteins responsible for the cohesion of paired homologous chromosomes remain unknown, but they likely include some of the same cohesion proteins that hold together the arms of sister chromatids. At least two *Drosophila* proteins, encoded by the *mei-S332* and *ord* genes, are implicated in centromere cohesion of the dyads ***(103,104)***.

The oocyte nucleus can be easily visualized by staining with anti-lamin antibody using the method described in **Subheading 3.4.** The karyosome can be counterstained with nucleic acid dyes like TOTO-3 or propidium iodide. Analysis of the meiosis I spindle by immunostaining requires special sample preparation and fixation conditions to avoid premature activation of the oocyte. It has been observed that hydration in hypotonic (diluted) Robb's medium ***(105)*** induces physiological changes in oocytes that resembles the normal activation by ovulation ***(106,107)***. The immunostaining method of Theurkauf and Hawley ***(87)*** is based on a prefixation that makes use of normal (undiluted) Robb's medium; therefore, activation of the meiosis I spindle is avoided. Although, this protocol works reasonably well with some antibodies, it requires mass isolation of oocytes. An alternative immunostaining method uses oocytes obtained from females hand-dissected in methanol ***(108)***. This methanol-based method has produced excellent results with several antibodies ***(90)***. A methanol-based method is presented in **Subheading 3.5.** To analyze completion of meiosis I and the meiosis II division, another methanol-based protocol can be used to fix 5- to 10-min-old eggs ***(96)***. A version of this method is described in **Subheading 3.6.** The dynamics of the meiosis I and II spindles can be imaged in live oocytes as described by Endow and Komma using Ncd–GFP transgenic lines ***(94,95)***, whereas the Mei-S332–GFP line of Orr-Weaver and colleagues can be used to follow chromosomes ***(103)***.

1.7. Genetic Dissection of Oogenesis

Much of the progress made during the past two decades in understanding oogenesis is based on the identification of genes whose function is important for oocyte/egg development. Mutations that cause either a non-egg-laying phenotype or a highly abnormal laid-egg morphology are special types of female ster-

ile mutations, because they visibly and directly demonstrate a requirement for the normal functions of the affected genes in oogenesis. About 30% of zygotic lethal mutations can have an ovarian phenotype as well, an observation based on mosaic analysis of such mutations ***(109)***. Furthermore, weaker hypomorphs and conditional alleles of genes identified as zygotic lethals can produce an ovarian phenotype. Any of these mutations may affect either the germ-line or the soma (usually assessed in follicle cells), which can be tested by inducing germ-line and/or follicle cell clones homozygous for the mutation of interest. This can be achieved either by pole cell transplantation ***(9)*** or by mitotic recombination.

1.8. Practical Considerations

It is essential to examine wild-type and mutant ovaries in parallel and under optimal conditions: in well-fed females mated with wild-type or sterile males (for unfertilized eggs). When a new mutation is suspected to be involved in oocyte/egg development, a fertility test should be performed to assess egg morphology and production rate in comparison with wild type. Where mutant females do not lay eggs or the morphology and/or production rate of eggs are apparently altered, then ovarian morphology should be analyzed. For this purpose, ovaries should be dissected from both wild-type and mutant females of the same age and analyzed under a dissecting microscope. Based on morphology, mutations affecting oocyte/egg development can be categorized as rudimentary, tumorous, degenerating, small egg, cup or open chorion, dumpless, dorsalized, ventralized, fused filament, thin chorion, collapsed egg and held-egg mutations ***(3)***. After this examination, usually enough information is gathered to decide which developmental stage(s) and/or process(es) should be analyzed by immunostaining.

The immunostaining methods for oogenesis are based on noncoagulant fixatives like methanol, acetone, formaldehyde, and paraformaldehyde, which rapidly penetrate and convert the cytoplasm into an insoluble gel and render the chromatin resistant to extraction by phosphate-buffered saline (PBS) and Triton X-100 or Tween-20. In general, the immunostaining methods presented in this chapter perform well in various laboratory conditions and with many of the antibodies listed in Appendix B. When new antibodies are tested, it is important to check several fixation conditions and antibody dilutions. By combining these two factors, one should be able to determine the optimal fixation parameters and antibody dilution for a novel antibody.

2. Materials

2.1. Chemicals

1. Heptane-*n* (Sigma-Aldrich). Wear gloves and handle with care; heptane is both an irritant and highly flammable!

2. Methanol (Sigma-Aldrich, protein sequencing grade). Wear gloves and handle with care. Methanol is toxic and highly flammable! Keep aliquots at room temperature and at –20°C.
3. Acetone (Sigma-Aldrich, 100% solution, ACS reagent). Wear gloves and handle with care. Acetone is an irritant and highly flammable! Keep aliquots at –20°C.
4. Dimethyl sulfoxide (DMSO; Sigma-Aldrich, ACS reagent). Make aliquots of 500 µL and store them at –20°C.
5. H_2O_2 (Hydrogen peroxide, Sigma-Aldrich, 30% solution). Wear gloves and handle with care! Keep cold and use fresh.
6. Fetal calf serum (FCS) (Invitrogen). Make aliquots of 500 µL and store them at –20°C.
7. TOTO-3 (Molecular Probes, Eugene, OR). Make aliquots of 10 µL and store them at –20°C.
8. Propidium iodide (Fluka). Make a 1-mg/mL stock solution in water. Wear gloves and handle in a chemical fume hood. Store in a cool dry place and keep tightly closed.
9. Vectashield mounting medium (Vector Laboratories). Keep refrigerated in the dark.
10. *Drosophila* Schneider's medium (Invitrogen).

2.2. Solutions

1. EBR stock solution: 130 m*M* NaCl, 5 m*M* KCl, 2 m*M* $CaCl_2$, and 10 m*M* HEPES, pH 6.9. Store at room temperature for up to 2–3 mo.
2. Buffer B stock solution: 100 m*M* KH_2PO_4/K_2HPO_4 pH 6.8, 150 m*M* NaCl, 450 m*M* KCl, 20 m*M* $MgCl_2 \cdot 6H_2O$.
3. Buffer B fixative solution: 1 vol of 37% formaldehyde (Sigma-Aldrich, molecular-biology grade containing 10–15% methanol), 1 vol of buffer B and 4 vol of distilled H_2O. Store the 37% formaldehyde stock solution at room temperature. It is unstable, tending to polymerize in contact with air. Keep the cap of the bottle tight. If the solution is clear and no precipitate formed, it can be used for up to 6 mo. Wear gloves and work in a fume hood, as the formaldehyde vapor is toxic!
4. 10% Paraformaldehyde (PP) (Polysciences, EM grade) in phosphate-buffered saline (PBS): To prepare 50 mL, weight out 5 g of PP into 40 mL PBS. Dissolve the PP by warming the solution to 60°C. Do not overheat! If the solution turns brownish, discard it and start again! If the PP does not dissolve relatively easily to give a clear solution, then add 1 mL of 1 *N* NaOH, and this should help to get the PP dissolved. Adjust to pH 7 with 1 *N* HCl. Bring the final volume of the solution to 50 mL with PBS and filter-sterilize half of the solution using 0.2-µm filter units. Store the filtered solution in a tightly capped bottle at room temperature and use within 1–2 d, or make frozen aliquots of 500 µL, which are fairly stable for 6 mo. Wear gloves and work in a fume hood, as the PP powder and vapor are toxic!
5. Phosphate-buffered saline (PBS) solution: Dissolve 1 PBS tablet (Sigma) in 200 mL of distilled H_2O.
6. PBT solution: PBS + 0.1% Triton X-100 (Sigma, molecular-biology grade).

7. Di-PBT solution: PBS + 0.2% Triton X-100.
8. Penta-PBT solution: PBS + 0.5% Triton X-100.

2.3. Primary Antibodies

Many antibodies are available to study oogenesis. Some of these are listed in Appendix B. Scientists who carried out relevant studies with a particular antibody are named as the source, and their addresses are available from FlyBase (www.flybase.bio.indiana.edu). Other antibodies can be purchased from the indicated commercial suppliers.

2.4. Secondary Antibodies

The following secondary antibodies are available from Molecular Probes:

1. Alexa 488 anti-rat, Alexa 488 anti-mouse, and Alexa 488 anti-rabbit.
2. Alexa 594 anti-rat, Alexa 594 anti-mouse, and Alexa 594 anti-rabbit.
3. Alexa Fluor 647 anti-mouse, and Alexa Fluor 647 anti-rabbit.
4. Rhodamine-conjugated phalloidin (toxic, wear gloves when handle!).

Cy™5 anti-mouse and Cy™5 anti-rat are available from Jackson Immuno-Research Laboratories.

2.5. Equipment

1. Small Petri dish for dissections (Corning Glass Works, Corning, NY).
2. Fine-tipped watchmaker's forceps (Sigma-Aldrich, style no. 5)
3. Tungsten needles. Tungsten wire can be purchased from Agar Scientific (www.agarscientific.com) and the needle holder can be obtained from Fisher Scientific. The tungsten needles can be sharpened and shaped by electrolysis in either 10% KOH or 10% NaOH with 2–10 V dc. The NaOH and KOH solutions are harmful and toxic, wear gloves and safety goggles. Use only in a chemical fume hood. Keep them tightly closed and store in a cool dry place.
4. Short- and long-pulled glass Pasteur pipets (Bilbate Precision Glass Ltd., England). Heat up the middle of the thinner region of a long glass Pasteur pipet using a Bunsen burner. Holding the two ends, quickly pull apart the Pasteur pipet. Break off the very thin end of the long-pulled Pasteur pipets and they are ready for use.
5. Scalpel blades (Sigma-Aldrich, stainless steel).
6. Grape juice plates for egg collecting.
7. Microscope slides and 24×24-mm^2 cover slips.
8. Egg basket and painting brush for embryo handling.
9. Rotating wheel.
10. 3MM Whatmann paper. Cut into pieces that correspond to the size of the microscope slide.

11. Stereo microscope for dissection.
12. Laser Scanning Confocal microscope.

3. Methods

3.1. Immunostaining of Early Germarial Cells to Stage-12 Egg Chambers

This protocol gives excellent results on germarial stages. Fusome-specific antibodies have performed well, as has the BX69 antitubulin antibody to visualize spindle microtubules of the premeiotic divisions (*see* **Fig. 4**). Many of the ring canal proteins have also been successfully visualized using this protocol.

1. For each staining, dissect out with fine-tipped forceps 5–10 pairs of ovaries from females into 1 mL of EBR solution kept in a small Petri dish. Leave the very end of the abdomen attached to the ovaries to make them more visible during the immunostaining procedure, but try to remove as much fat body tissue as possible (*see* **Notes 1–3**).
2. Transfer the dissected ovaries into a microcentrifuge tube containing 1 mL of EBR solution (*see* **Note 4**).
3. Make the ovaries sink to the bottom by flicking the microcentrifuge tube a few times with your fingers.
4. Retain the ovaries in about 50 µL of EBR solution by removing the rest with a long-pulled glass Pasteur pipet.
5. To carry out the fixation, add into the microcentrifuge tube 100 µL of buffer B fixative and 600 µL of heptane in the indicated order (*see* **Note 5**).
6. Shake the microcentrifuge tube gently by hand for 5 min (*see* **Note 6**).
7. Remove all the fixative with the long-pulled glass Pasteur pipet used in **step 4**.
8. Carry the ovaries through three consecutive washes with PBS by removing the washing solution after each step. Use a new long-pulled Pasteur pipet. Each wash should last at least 3 min. Place the microcentrifuge tube on a rotating wheel and rotate the sample at low speed.
9. Carry the ovaries through three consecutive 5-min washes with PBT.
10. Wash the ovaries in 1 mL of PBT for 1 or 2 h and leave the sample on the rotating wheel.
11. After this last wash, retain the ovaries in approx 50 µL of PBT.
12. Carry out the blocking by adding 900 µL of PBT and 50 µL of FCS (stock solution) into the microcentrifuge tube. Put the microcentrifuge tube on a rotating wheel and rotate at low speed for 30 min at room temperature (*see* **Notes 7** and **8**).
13. After blocking, remove the PBT-FCS solution with a new long-pulled glass Pasteur pipet and leave approx 50 µL of solution over the ovaries.
14. Repeat **steps 12** and **13**.
15. Dilute the primary antibodies with PBT in a total volume of 1 mL and add this solution to the microcentrifuge tube with ovaries.
16. Incubate the ovaries with the primary antibodies overnight at 4°C on the rotating wheel. From this step on, do not shake the sample. Pipet the solutions carefully into the microcentrifuge tube and wrap the tube in aluminum foil (*see* **Notes 9–11**).

17. Carry the ovaries through three consecutive 5-min washes with PBT, rotating the microcentrifuge tube at low speed. Use a new long-pulled Pasteur pipet to remove each wash solution.
18. After the last wash, remove all but approx 50 µL of PBT with the long-pulled glass Pasteur pipet used in **step 17**.
19. Dilute the secondary antibodies with PBS (1 : 200 v/v) in a total volume of 950 µL; then, add this solution to the microcentrifuge tube containing the ovaries (*see* **Note 12**).
20. Incubate the ovaries with the secondary antibodies at room temperature for 2 h on the rotating wheel. Protect the microcentrifuge tubes from light by wrapping in aluminum foil (*see* **Notes 13** and **14**).
21. Remove the secondary antibody solution with a new long-pulled Pasteur pipet.
22. Carry the ovaries through two consecutive 10-min washes with PBT on the rotating wheel at low speed. Remove the washing solution after each step using the long-pulled Pasteur pipet from **step 21**.
23. After the last wash, retain the ovaries in approx 50 µL of PBT, and then add 950 µL of PBS into the tube.
24. For DNA staining, add 1 µL of concentrated TOTO-3 to the microcentrifuge tube and incubate for 45 min at room temperature on the rotating wheel (*see* **Notes 15–17**).
25. Remove the diluted TOTO-3 solution with a long-pulled Pasteur pipet; then, quickly rinse the ovaries with 500 µL of PBS.
26. After this washing step, remove approx 450 µL of PBS with the long-pulled Pasteur pipet.
27. Add two to three drops of Vectashield mounting medium and incubate the samples overnight at 4°C in a dark place (*see* **Note 18**).
28. Transfer two to four ovaries and some mounting medium onto a microscopic slide with a short glass Pasteur pipet.
29. Dissect the ovaries into individual ovarioles and/or egg chambers with fine-pulled tungsten needles (*see* **Notes 19** and **20**).
30. Cover the sample with a 24 × 24-mm^2 cover slip, remove the excess mounting medium with 3MM paper, and seal the edges of the cover slip with nail polish (*see* **Note 21**).
31. Examine the microscopic specimen.
32. The microscopic specimen can be stored in a dark place at 4°C (refrigerator, cold room) for up to several months (*see* **Note 22**).

3.2. Immunostaining of Mid-Germarial Cells to Stage-12 Egg Chambers

This protocol works well to visualize many of the spectrosome–fusome and ring canal components of both the germarium and vitellarium. Cytoskeletal elements like the actin network are well preserved, but spindles in the germarium and microtubule networks are not.

1. For each staining, dissect out with fine-tipped forceps 5–10 pairs of ovaries and place into 1 mL of *Drosophila* Schneider's medium kept in a small Petri dish.

Leave the very end of the abdomen attached to ovaries to make them more visible during the immunostaining procedure, but try to remove as much fat body tissue as possible (*see* **Notes 1–3** and **23**).
2. Transfer the dissected ovaries into a microcentrifuge tube with 1 mL of Schneider's medium and incubate them for 5 min (*see* **Note 4**).
3. Retain the ovaries in approx 50 µL of Schneider's medium by removing the rest of the solution with a long-pulled glass Pasteur pipet.
4. Add 1 mL of PBS to the ovaries and wash them for 10 min by placing the tubes on a rotating wheel.
5. After washing, remove the PBS solution with a long-pulled glass Pasteur pipet and leave approx 50 µL of solution on the ovaries.
6. To carry out the fixation, add 1 mL of buffer B fixative to the microcentrifuge tube (*see* **Note 5**).
7. Shake the microcentrifuge tube gently by hand for 10–20 min (*see* **Note 24**).
8. Remove all the fixative with the same long-pulled glass Pasteur pipet used in **step 5**.
9. Add 1 mL of penta-PBT to the ovaries and incubate them for 30 min on a rotating wheel (*see* **Note 25**).
10. Remove all penta-PBT with the long-pulled glass Pasteur pipet already used in **steps 5** and **8**.
11. Immediately add 1 mL of PBT to the ovaries and incubate them for 30 min on the rotating wheel.
12. After this incubation, retain the ovaries in approx 50 µL of PBT.
13. Carry out the blocking by adding 900 µL of PBT and 50 µL of FCS (stock solution) into the microcentrifuge tube. Put the microcentrifuge tube on the rotating wheel and rotate at low speed for 30 min at room temperature (*see* **Notes 7** and **8**).
14. Follow **Subheading 3.1.** from **step 13**.

3.3. Immunostaining of Stages 2–13

This protocol can be used to visualize many of the spectrosome–fusome and ring canal components in both the germarium and vitellarium. Cytoskeletal elements like the actin network are well preserved, and some anti-tubulin antibodies can be seen to decorate spindle microtubules during the cystocyte divisions.

1. For each staining, dissect out with fine-tipped forceps 5–10 pairs of ovaries from females into 1 mL of EBR solution kept in a small Petri dish. Leave the very end of the abdomen attached to ovaries to make them more visible during the immunostaining procedure, but try to remove as much as possible from the fat body tissue (*see* **Notes 1–3**).
2. Transfer the dissected ovaries into a microcentrifuge tube containing 1 mL of EBR solution (*see* **Note 4**).
3. Make the ovaries sink to the bottom by flicking the microcentrifuge tube a few times with your fingers.
4. Retain the ovaries in approx 50 µL of EBR solution, removing the rest with a long-pulled glass Pasteur pipet.

5. To carry out the fixation, add 100 µL of buffer B fixative and 600 µL of heptane to the microcentrifuge tube in the indicated order (*see* **Note 5**).
6. Shake the microcentrifuge tube gently by hand for 10 min (*see* **Notes 26** and **27**).
7. Remove all the fixative with the long-pulled glass Pasteur pipet used in **step 4**.
8. Carry the ovaries through three consecutive washes with PBS, removing the washing solution after each step. Use a new long-pulled Pasteur pipet. Each washing step should last at least 3 min. Attach the microcentrifuge tube to a rotating wheel and rotate at low speed.
9. After the last wash, retain the ovaries in approx 50 µL of PBS (*see* **Note 28**).
10. Carry out the blocking by adding 900 µL of PBS and 50 µL of FCS (stock solution) into the microcentrifuge tube. Put the tube on a rotating wheel and rotate at low speed for 30 min at room temperature (*see* **Note 8**).
11. After blocking, remove the PBS–FCS solution with a new long-pulled glass Pasteur pipet, and leave approx 50 µL of solution on the ovaries.
12. Repeat **steps 10** and **11**.
13. Dilute the primary antibodies with PBS in a total volume of 1 mL and add this solution to the microcentrifuge tube with ovaries.
14. Incubate the ovaries with the primary antibodies overnight at 4°C. Put the microcentrifuge tube on the rotating wheel. From this step on, do not shake the sample, pipet solutions carefully into the tube and protect the tube by wrapping it in aluminum foil (*see* **Notes 9–11**).
15. Carry the ovaries through two consecutive washes with 1 mL of PBS, rotating the microcentrifuge tubes on a rotating wheel at low speed and removing the washing solution after each step. Use a new long-pulled Pasteur pipet. Each washing step should be 5–10 min.
16. After the last wash, retain the ovaries in approx 50 µL of PBS.
17. Dilute the secondary antibodies with PBS (1 : 200 v/v) in a total volume of 950 µL and add this solution to the microcentrifuge tube containing the ovaries (*see* **Note 12**).
18. Incubate the ovaries with the secondary antibodies at room temperature for 2 h, rotating the microcentrifuge tube on a rotating wheel. Protect the microcentrifuge tube from light by wrapping it in aluminum foil (*see* **Notes 13** and **14**).
19. Remove the secondary antibody solution with a new long-pulled Pasteur pipet.
20. Carry the ovaries through two consecutive washes with 1 mL of PBS, removing the washing solution after each step. Use the long-pulled Pasteur pipet from **step 19**. Each washing step should last for 5–10 min, with the microcentifuge tube rotated at low speed.
21. After the last wash, retain the ovaries in approx 50 µL of PBS and add 950 µL of PBS to the tube.
22. Follow **Subheading 3.1., steps 24–32**, and substitute the PBT with PBS.

3.4. Immunostaining of Stages 1–13

This protocol gives excellent results for stages 1–13. It is based on paraformaldehyde fixation and the combined action of DMSO and di-PBT to make the ovarian tissue highly permeable to antibodies. Use this protocol if

antibody penetration problems are encountered with the methods described in **Subheadings 3.1.–3.3.** Microtubule networks can be nicely visualized in the vitellarium, but the spindle microtubules are not properly preserved in the germarium. The actin network and the structures of the follicle cells, nurse cells, and oocyte nuclei are well preserved by this fixation method.

1. For each staining, dissect out with fine-tipped forceps 5–10 pairs of ovaries from females into 1 mL of di-PBT solution kept in a small Petri dish. Leave the very end of the abdomen attached to ovaries to make them more visible during the immunostaining procedure, but try to remove as much fat body tissue as possible (*see* **Notes 1–3**).
2. Transfer the dissected ovaries to a microcentrifuge tube with 1 mL of di-PBT kept in an ice bath (*see* **Note 4**).
3. Make the ovaries sink to the bottom by flicking the microcentrifuge tube a few times with your fingers.
4. Remove all the di-PBT from the microcentrifuge tube with a long-pulled glass Pasteur pipet (*see* **Notes 29** and **30**).
5. Carry the ovaries through three quick consecutive washes with 1 mL of PBS, removing all the washing solution after each step. Use a new long-pulled Pasteur pipet (*see* **Note 29**).
6. To carry out the fixation, add 350 µL of PBS, 150 µL of 10% PP solution (freshly prepared), and 600 µL of heptane to the microcentrifuge tube in the indicated order (*see* **Note 5**).
7. Shake the microcentrifuge tube vigorously by hand for 1 min and then leave the tube in a rack for 30 s to allow the two phases of the fixative mixture to separate (*see* **Note 31**).
8. Leave 50 µL of the lower phase of the fixative in the microcentrifuge tube to cover the ovaries and remove the rest of the fixative mixture with a new long-pulled glass Pasteur pipet.
9. Immediately add 650 µL of PBS, 300 µL of 10% PP solution, and 50 µL of DMSO in the indicated order. Put the microcentrifuge tube on the rotating wheel and continue to rotate the samples for 20 min at a low speed (*see* **Note 31**).
10. Remove all the second fixative solution with the long-pulled glass Pasteur pipet used in **step 8**.
11. Carry the ovaries through two consecutive quick washes with absolute methanol, removing the washing solution after each step. Use a new long-pulled Pasteur pipet.
12. Add 950 µL of methanol to the microcentrifuge tube and continue to rotate the samples for 30 min at a low speed (*see* **Note 31**).
13. Carry the ovaries through three consecutive quick washes with PBS by removing the washing solution after each step. Use a new long-pulled Pasteur pipet.
14. Carry the ovaries through three consecutive washes with di-PBT by removing the washing solution after each wash. Each washing period should last 5 min (*see* **Note 30**).

15. After the last wash, retain the ovaries in approx 50 µL of di-PBT.
16. Carry out the blocking by adding 900 µL of di-PBT and 50 µL of FCS (stock solution) to the microcentrifuge tube. Rotate the tube at low speed for 1–2 h at room temperature (*see* **Notes 7** and **8**).
17. After blocking, remove the di-PBT–FCS solution with a new long-pulled glass Pasteur pipet, and leave approx 50 µL of solution on the ovaries.
18. Dilute the primary antibodies with di-PBT in a total volume of 950 µL and add this solution to the microcentrifuge tube containing the ovaries.
19. Incubate the ovaries with the primary antibodies overnight at 4°C. Put the microcentrifuge tube with ovaries on the rotating wheel. From this step on, do not shake the sample, pipet solutions carefully and protect the tube by wrapping it in aluminum foil (*see* **Notes 9–11**).
20. Carry the ovaries through three consecutive washes with 1 mL of di-PBT, rotating the tubes at low speed on a rotating wheel, and removing the washing solution after each step. Use a new long-pulled Pasteur pipet. Each washing step should last for 5 min (*see* **Note 30**).
21. After the last wash, retain the ovaries in approx 50 µL of di-PBT.
22. Dilute the secondary antibodies with di-PBT (1 : 200 v/v) in a total volume of 950 µL and add this solution to the microcentrifuge tube containing the ovaries (*see* **Notes 12**, **13**, and **30**).
23. Incubate the ovaries with the secondary antibodies at room temperature for 2 h on a rotating wheel (*see* **Note 14**). Protect the tube from light by wrapping it in aluminum foil.
24. Remove the secondary antibody solution with a new long-pulled Pasteur pipet.
25. Carry the ovaries through two consecutive washes with 1 mL of di-PBT, rotating the microcentrifuge tube on a rotating wheel, and removing the washing solution after each step. Use the long-pulled Pasteur pipet from **step 24**. Each washing step should last for 10 min (*see* **Note 30**).
26. After the last wash, retain the ovaries in approx 50 µL of di-PBT and add 950 µL of di-PBT to the tube (*see* **Note 30**).
27. For DNA staining, add 1 µL of concentrated TOTO-3 and incubate the sample for 45 min at room temperature on a rotating wheel (*see* **Notes 15–17**).
28. Remove the diluted TOTO-3 solution with a long-pulled Pasteur pipet and then quickly rinse the ovaries with 500 µL PBS.
29. Follow the instructions in **Subheading 3.1.** from **step 26**.

3.5. Immunostaining of Stages 13 and 14 to Visualize the Meiotic Spindle

This protocol was designed to carry out immunostaining on meiosis I prometaphase (stage 13) and metaphase (stage 14) oocytes to study the organization of spindles. The protocol is based on staining of the anterior half of mature eggs, obtained after cutting them through the anterior–posterior axis.

1. For each staining, dissect out with fine-tipped forceps 10–20 pairs of ovaries from well-fed females and place in 2 mL of absolute methanol kept in a small

Petri dish. Remove all the adhering tissues from the ovaries and gather the ovaries in another small Petri dish containing 1 mL of absolute methanol (*see* **Notes 2–5** and **32**).
2. Dissect out stage 13 and 14 oocytes from the ovaries by disrupting the ovarioles with tungsten needles.
3. By holding the dorsal appendages with fine-tipped forceps, cut the mature egg in half along its vertical axis with a scalpel or razor blade.
4. Remove the chorion and vitelline membrane from the anterior half of the stage 13 and 14 oocytes. Hold the dorsal appendages with fine-tipped forceps, and with a sharp tungsten needle, push out the anterior half of the egg from the chorion and vitelline membrane (*see* **Note 33**).
5. Immediately place the anterior half of the egg in a microcentrifuge tube containing 1 mL of absolute methanol. Collect approx 25–50 anterior egg parts.
6. Remove the methanol with a long-pulled glass Pasteur pipet, leaving 50 µL to cover the eggs (*see* **Note 5**).
7. Carry the sample through two consecutive quick washes with 1 mL of absolute methanol, removing the wash solution after each step. Use the long-pulled Pasteur pipet from **step 6**.
8. Add 950 µL of methanol to the microcentrifuge tube and rotate the samples for 2 h at a low speed on a rotating wheel (*see* **Note 34**).
9. Carry the sample through three consecutive quick washes with 1 mL of PBS, removing the washing solution after each step. Use a new long-pulled Pasteur pipet (*see* **Note 35**).
10. Carry the samples through three consecutive 5-min washes with 1 mL of PBT as described for **step 9**.
11. After the last wash, retain the ovaries in approx 50 µL of PBT by removing most of the PBT with a long-pulled glass Pasteur pipet.
12. Follow **Subheading 3.1., steps 15–27**.
13. Transfer the egg parts and some mounting medium onto a microscopic slide with a short glass Pasteur pipet.
14. Cover the sample with a 24 × 24-mm^2 cover slip, remove the excess mounting medium with 3MM paper, and seal the edges of the cover slip with nail polish (*see* **Note 21**).
15. Examine the microscopic specimen. Specimens can be stored in a dark place at 4°C (refrigerator, cold room) up to several months (*see* **Note 22**).

3.6. Immunostaining of Meiosis II and the Pronuclear Stage of Embryogenesis

This protocol has been designed to study the completion of female meiosis and the pronuclear stage of early embryonic development ***(95)***.

1. Set up 5 egg-collecting cages with either 100 wild-type or mutant females mated to 50 wild-type males. Feed the flies with yeast paste on grape juice agar plates for 3–4 d at 25°C.

2. On the day of egg collection, synchronize the females' egg-laying activity by collecting eggs at regular intervals as follows: two collections at 30-min intervals and four collections at 10-min intervals. Discard these eggs (*see* **Note 36**).
3. Collect eggs from the synchronized females at regular intervals as follows: six collections at 5-min and 15-min intervals, respectively (*see* **Notes 37** and **38**).
4. Wash the synchronized eggs with normal tap water and put them in an egg basket or sieve mesh.
5. Remove the chorion membrane of the eggs by a treatment with commercial bleach. Monitor the process under a dissecting microscope.
6. Wash the dechorionated eggs thoroughly with normal tap water. Dry the eggs by patting the egg basket onto a filter paper.
7. While the eggs are treated with bleach, make up the fixative in a microcentrifuge tube. The fixative contains 500 µL of methanol and 500 µL of heptane (*see* **Note 5**).
8. With a fine paint brush, transfer the dried eggs from the egg basket into the microcentrifuge tube with the fixative (*see* **Note 38**).
9. Shake the tube for 2 min. Eggs that have lost their vitelline membrane will sink to the bottom of the tube.
10. Remove the fixative mixture from the microcentrifuge tube with a long-pulled glass Pasteur pipet, but leave the eggs covered with 50 µL of the lower phase (methanol) of the fixative mixture.
11. Carry the eggs through two consecutive quick washes with 1 mL of absolute methanol, removing the washing solution after each step. Use the long-pulled Pasteur pipet from **step 10**. Leave 50 µL of methanol on the eggs after each washing step.
12. Add 950 µL of ice-cold methanol to the tube and gently invert several times over a 5-min period.
13. Remove most of the methanol from the tube with a long-pulled glass Pasteur pipet, leaving the eggs covered in 50 µL of methanol.
14. Add 950 µL of ice-cold acetone to the microcentrifuge tube and gently invert several times over a 5-min period (*see* **Notes 5** and **39**).
15. Remove most of the acetone from the tube with a long-pulled glass Pasteur pipet, leaving the eggs covered with 50 µL of acetone.
16. Carry the eggs through three consecutive quick washes with 1 mL of PBS, removing the washing solution after each step. Use a new long-pulled Pasteur pipet.
17. Carry the eggs through two consecutive 5-min washes with 1 mL of PBT. Place the tube on a rotating wheel and rotate at low speed.
18. After the last wash, remove the eggs with a short Pasteur pipet from the microcentrifuge tube and put them in a small Petri dish containing 1 mL of PBT.
19. With a scalpel or razor blade, cut the eggs in half along their longitudinal axis and put them back into the microcentrifuge tube using a short Pasteur pipet (*see* **Note 39**).
20. Wash the eggs again with 1 mL of PBT as described for **step 17**.
21. Carry out the blocking by adding 900 µL of PBT and 50 µL of FCS (stock solution) to the tube. Put the tube on the rotating wheel and rotate at low speed for 1–2 h at room temperature.

22. Follow **Subheading 3.1.**, **steps 15–27**.
23. Follow **Subheading 3.5.**, **steps 13–15**.

4. Notes

1. Oogenesis is tightly controlled (*see* **Subheading 1.**); therefore, it is essential to examine wild-type and mutant ovaries under optimal conditions. Germarial stages can be analyzed in newly emerged and/or 1-d-old females. Well-fed and 1-d-old females contain many egg chambers corresponding to stages 1–8 of oogenesis, whereas females older than 2 d should have fully matured eggs in their ovaries.
2. To study the expressivity and penetrance of an ovarian phenotype, it is advisable to collect and stain samples from several wild-type and mutant females at various time-points (1, 2, 3, 4-d, etc.) and in several independent experiments.
3. Dissect out and proceed to the fixation step as fast as possible, as empirical observations suggest that the quicker you fix the ovaries, the better the cellular structures are preserved. Prolonged prefixation treatments can alter the structure of the ovaries.
4. Unless otherwise indicated, perform the entire immunostaining procedure in a microcentrifuge tube. In addition to practical considerations, like conserving a limited supply of antibodies, the amounts of toxic chemicals and organic solvents used will be greatly reduced.
5. It is important to wear and make use of all the necessary safety and protection equipment, to minimize your exposure to any harmful or toxic chemical. Wear protective gloves and glasses as you proceed to the fixation step.
6. Do not exceed the indicated fixation time. Prolonged fixation may result in poor antibody penetration, leading to weak staining.
7. If an antibody is being tested for the first time, it is possible to substitute the blocking step with a simple incubation in PBT to gain information about the "total" binding capacity of the antibody. In the case of a high signal-to-noise ratio, the staining pattern should reveal the localization of the antibody-specific antigen(s). However, if the signal-to-noise ratio is low, it will be difficult to recognize any specificity; in such situations, blocking with FCS has to be conducted.
8. The precise blocking time with FCS must be determined empirically. In general, 1 h of incubation time is sufficient to achieve good blocking, which will significantly reduce the level of nonspecific staining.
9. Usually, the samples are incubated with the primary antibodies overnight at 4°C. Alternatively, the samples can be incubated for 2–4 h at room temperature. If a particular antibody is showing a low signal-to-noise ratio, try using different incubation times.
10. If a particular primary antibody gives a high background, it can be preadsorbed with excess of fixed ovaries (e.g., incubate an excess of fixed ovaries with the antibody at 10–40 times its final concentration) for 2–3 h. It is important to fix the ovaries according to the same protocol for both the antibody adsorbtion and the immunostaining.
11. In certain circumstances, the primary antibodies can crossreact with each other. This is particularly true for primary antibodies raised in closely related species

like mouse and rat. One way to overcome this problem is to carry out a two-step or multistep incubation with the primary antibodies such that the samples are incubated with only one antibody at a time.

12. The secondary antibodies have to be chosen in light of the available microscope facilities. A set of fluorochrome-conjugated secondary antibodies, suitable for a BioRad Laser-Scanning-Microscope 1024, is listed in **Subheading 2.4.**
13. If a particular secondary antibody gives a high background, it can be preadsorbed with excess of fixed ovaries, as described in **Note 10**.
14. Usually, the samples are incubated in the secondary antibodies at room temperature for 2 h. Alternatively, the samples can be incubated for 2–6 h at room temperature or overnight at 4°C. If a particular antibody is showing a low signal-to-noise ratio, one has to determine empirically the proper incubation times and antibody dilutions.
15. The TOTO-3 dye was chosen for DNA staining, because it is detected in the blue channel, which allows the green and red channels to be used for the detection of cellular protein-specific signals.
16. Propidium iodide can be used instead of TOTO-3, but its signal will be detected in the red channel and, therefore, the secondary antibodies have to be chosen according to what other channels are available on your microscope.
17. For DNA staining, add 1 µL of concentrated propidium iodide (1 mg/mL) to the microcentrifuge tube and incubate the sample for 30 min at room temperature on a rotating wheel.
18. Vectashield mounting medium prevents rapid photobleaching of a wide range of fluorochromes, including those mentioned in this chapter.
19. The dissection of ovaries into individual ovarioles is the most delicate part of the entire immunostaining protocol. With sharp tungsten needles, one can easily disrupt the peritoneal sheath, then remove the epithelial sheath and reach the egg chambers.
20. The germaria can be separated from each other by disrupting the apical region of the ovaries with tungsten needles.
21. Care should be taken not to allow the cover slip to move while removing the excess of mounting medium with 3MM paper.
22. If the microscopic specimens are prepared and stored as advised, they can be re-examined several times, which is of a great importance because details often need to be clarified with respect to a certain staining pattern.
23. If the Schneider's medium is supplemented with FCS (10% final concentration) the isolated germaria can be kept alive for at least 60 min.
24. Do not exceed the 20-min fixation time. Prolonged fixation may result in poor antibody penetration and weak staining. Reducing the fixation time to 10 min may result in a higher signal-to-noise ratio, improving the quality of the immunostaining.
25. The penta-PBT treatment it is crucial step in this protocol, because after the strong fixation, it makes the tissues permeable to antibodies.
26. This fixation time must be adhered to. Longer fixations will result in low antibody penetration.

27. During fixation, the vigorous shaking may alter the cells' internal structures and produce artifacts.
28. After fixation, PBS is used in this protocol to reducing the possibility of extracting proteins from cells through the action of Triton X-100.
29. Prior to fixation it is important to remove all of the wash solution from the ovaries. Empirical observations suggest that complete removal of the wash solution is necessary for successful fixation.
30. If the observed and expected staining patterns are found to be completely different, the DMSO and/or di-PBT treatments might be too "harsh" for the egg chambers/eggs. Leave out or reduce the duration of the DMSO treatment and/or replace the di-PBT solution with PBT or PBS.
31. Exceeding the fixation times will produce artifacts!
32. An alternative methanol-based protocol has been described by Tavosanis et al. ***(108)***. In their protocol, the mature eggs are sonicated in methanol. According to Tavosanis et al., dissect the ovaries in absolute methanol and transfer to a 10-mL plastic tube containing 2 mL of fresh methanol. Sonciate approx 10–20 single ovaries using a Sonifier B-12 (Branson Sonic Power Company) fitted with a cone-shaped probe approx 3–4 mm in diameter at the bottom. Sonicate in five cycles of 1 s each. Transfer oocytes freed of chorion and vitelline membrane to fresh methanol and keep at room temperature for 2 h, then carry through a standard immunostaining protocol.
33. This is the most delicate part of the protocol, and all the chorion and vitelline membrane must be removed completely from the eggs.
34. An alternative fixation can be considered if the antibodies encounter problems in penetrating the eggs. This would include a 10-min treatment with absolute methanol, followed by a treatment with acetone for 10 min, and, finally, a 60-min incubation in absolute methanol.
35. After fixation, a stepwise rehydration can be done by carrying the samples through 70%, 50%, and 30% methanol (diluted with normal water) and PBS. Each step should last at least for 5 min.
36. It is crucial for this experiment to use well-fed females and to synchronize the egg-laying activity of the females. Stick a piece of filter paper to the internal wall of the egg-laying cage and carefully replace the plates. While the eggs are being collected, put only traces of yeast on the plates.
37. An alternative method to collect eggs recently released from ovaries is as follows. Squeeze out the eggs from the uteri of CO_2-anesthetized females by applying slight pressure on abdomens with forceps or a tungsten needle. Dechorionate the eggs on double-sided tape and immediately put them into the fixative mixture.
38. The time interval between egg collection and fixation should not exceed 5 min! It is crucial to wash the eggs and remove the chorion as fast as possible because the eggs/embryos are alive during these procedures.
39. The cold acetone treatment and cutting the eggs/embryos in half greatly improve the antibody penetration, thus allowing structures associated with female meiosis II, the sperm aster, and gonomeric spindle to be visualized by immunostaining.

Acknowledgments

I owe a debt of gratitude to many members of the *Drosophila* community who have provided their knowledge and expertise, which greatly facilitated my effort to put together these immunostaining protocols in a form to provide helpful assistance in performing them by any scientist who may wish to answer questions related to oogenesis. I also would like to express my gratitude to János Szabad, Jaakko Puro, and David M. Glover. By sharing their deep knowledge, they provided the stimulation to put the developmental genetics and cytology of oogenesis in the context of mitosis, meiosis, and, ultimately, the cell cycle. I also acknowledge the Cancer Research Campaign for the support that has made some of this research possible. Finally, I would like to thank my family; this work would have been quite impossible without their constant help and encouragement.

Appendices

Appendix A: Stages of Oogenesis

The main morphological characteristics of the egg chambers/eggs are summarized according to the R.C. King proposed stages of oogenesis ***(1–3)***.

Stage	Duration (h)	Size (μm)	Characteristics
1	9	10 × 10	Round-shaped egg chamber, situated at the end of the germarium; oocyte located at the posterior of the 16-cell cyst; follicle cells form a monolayer on the cyst; no synaptonemal complex in the oocyte nucleus; follicular stalk differentiates as the egg chamber leaves the germarium
2	8	25 × 25	Vitellarium; karyosome formation initiated; oocyte and nurse cells have similar sizes; main-body follicle cells in division; nurse cells begin endoreduplication;
3	8	35 × 35	Karyosome formation completed;
4	6	40 × 50	Condensed karyosome; nurse cell nuclei contain similar amounts of DNA and appear polytene; follicle cells in division
5	5	55 × 75	Highly condensed karyosome; posterior nurse cell nuclei have more DNA than the anterior ones; follicle cells in division

(continued)

Stage	Duration (h)	Size (μm)	Characteristics
6	3	60 × 85	Highly condensed karyosome; nurse cell ploidy equal; follicle cells cease mitosis
7	6	70 × 115	Egg chamber elongates; highly condensed karyosome; nurse cells have higher ploidy at posterior; no yolk visible in the oocyte; first Gurken signal; terminal follicle cells adopt posterior fate
8	6		Nucleus moves into the dorsal anterior corner of the oocyte; highly condensed karyosome; yolk visible in the oocyte; uniform follicle cell layer; lipid droplets in the nurse cells
9	6	Oocyte is about 1/3 of the egg chamber	Decondensed karyosome; follicle cells in process of migration over oocyte, resulting in anterior–posterior gradient of cell thickness; vitelline membrane synthesis initiated
10A	6		Highly condensed karyosome; second Gurken signal; follicle cell layer is columnar over oocyte and squamous over nurse cells; centripetal migration not yet visible
10B	4	Oocyte is about 1/2 of the egg chamber	Highly condensed karyosome; centripetal migration in progress; dorsal follicle cells thicker than the ventral; vitelline membrane extends into opercular region; dumping initiated
11	0.5	Oocyte is about 3/4 of the egg chamber	Highly condensed karyosome; dumping is in progress
12	2		Highly condensed karyosome; dumping completed; nurse cell nuclei remain at the anterior
13	1	Oocyte elongates	Decondensed karyosome; oocyte nuclear membrane breaks down; small meiosis I spindle forms and transforms into a long tapered spindle; glycogen-rich particles in the oocyte; some nurse cell nuclei still remain; dorsal filaments visible at the anterior end
14	> 2 ovulation	Slightly shrunken oocyte	Meiosis I metaphase arrested spindle; no nurse nuclei remain; dorsal filaments complete their elongation; follicle cells degenerate

Appendix B: Epitopes and Antibodies Useful for Studying Oogenesis

Protein recognized	Name of antibody cat. no.	Raised in	Type	Antibody source
Anillin	—	Rabbit	Polyclonal	B. Alberts, C. Field
Anillin	—	Mouse	Monoclonal	B. Alberts, C. Field
Bag-of-marbles (BAM)	BamC cytoplasmic	Mouse, rat	Monoclonal	D. McKearin
	BamF fusome	mouse	Monoclonal	D. McKearin
Ankyrin		Rabbit	Polyclonal	R. Dubreuil
α-Tubulin	YL1/2	Rat	Monoclonal	Harlan Sera Lab
α-Tubulin	N356	Mouse	Monoclonal	Amersham
β-Tubulin	BX69	Mouse	Monoclonal	D. M. Glover
β-Tubulin	1111876	Mouse	Monoclonal	Roche
γ-Tubulin	GTU88	Mouse	Monoclonal	Sigma
γ-Tubulin		Rabbit	Polyclonal	M. Moritz
α-β-Spectrin	S-1390	Rabbit	Polyclonal	Sigma
α-Spectrin	354	Rabbit	Polyclonal	A. Spradling
α-Spectrin	323	Mouse	Monoclonal	A. Spradling
β-Spectrin	337	Rabbit	Polyclonal	A. Spradling
β_{heavy}-Spectrin	243	Rabbit	Polyclonal	D. Kiehart
Dynein heavy chain	PEP1	Rabbit	Polyclonal	T. Hays
Dhc64C	P1H4	Mouse	Monolonal	D. H. S. B. Iowa
DLis-1		Mouse	Monoclonal	R. Steward
HtsF adducinlike	1B1 fusome	Mouse	Monoclonal	H. D. Lipshitz D. H. S. B. Iowa
HtsRC ring canal	655 4A	Mouse	Monoclonal	L. Cooley
Filamin		Rat	Monoclonal	L. Cooley
Phospho-tyrosine	PY20	Mouse	Monoclonal	ICN Biomedicals
Kelch	1B	Mouse	Monoclonal	L. Cooley
Pavarotti-KLP		Rabbit	Polyclonal	D. M. Glover
Cyclin A	Rb270	Rabbit	Polyclonal	D. M. Glover
Orbit		Rabbit	Polyclonal	D. M. Glover
Lamin	T47	Mouse	Monoclonal	D. M. Glover
CP190	Rb188	Rabbit	Polyclonal	D. M. Glover
CNN		Rabbit	Polyclonal	T. Kaufman

(continued)

Name of Protein recognized	antibody cat. no.	Raised in	Type	Antibody source
Bic-D	1B11; 4C2	Mouse	Monoclonal	R. Steward
Egl				R. Steward
Orb	6H8; 4H8	Mouse	Monoclonal	D. H. S. B. Iowa
PAR-1		Rabbit	Polyclonal	D. St. Johnston
Bazooka		Rat	Monoclonal	E. Knust
PAR-6		Rabbit	Monoclonal	J. Knoblich
	Mouse	Polyclonal		
Staufen		Rabbit	Polyclonal	D. St. Johnston
DTACC		Rabbit	Polyclonal	J. Raff
Msps		Rabbit	Polyclonal	H. Okhura
NCD		Rabbit	Polyclonal	S. Endow
MEI-S332		Guinea pig	Polyclonal	T. L. Orr-Weaver
Inscuteable		Rabbit	Polyclonal	J. Knoblich, R. Kraut
Armadillo	N2–7A1	Mouse	Monoclonal	D. H. S. B. Iowa
DE-cadherin	DCAD2	Rat	Monoclonal	M. Takeichi
DN-cadherin	Ex8	Rat	Monoclonal T. Uemura	M. Takeichi
Crumbs	Cq	Mouse	Monoclonal	E. Knust
Disc Lost		Rabbit	Polyclonal	U. Tepass
Nonmuscle myosin heavy chain	656	Rabbit	Polyclonal	D. Kiehart
Vasa	46F11	Mouse	Monoclonal	Y. N. Jan

References

1. King, R.C. (1970) *Ovarian Development in* Drosophila melanogaster. Academic, New York.
2. Mahowald, A.P. and Kambysellis, M.P. (1980) Oogenesis, in *The Genetics and Biology of* Drosophila (Ashburner, M. and Wright, T.R.F., eds.), Academic, New York, Vol. 2d, pp. 141–225.
3. Spradling, A. (1993) Developmental genetics of oogenesis, in *The Development of* Drosophila melanogaster (Bate, M. and Martinez-Arias, A., eds.), Cold Spring Harbor Laboratory Press, Cold Spring Harbor, NY, Vol. 1, pp. 1–70.
4. Matova, N. and Cooley, L. (2001) Comparative aspects of animal oogenesis. *Dev. Biol.* **231,** 291–320.
5. de Cuevas, M., Lilly, M. A., and Spradling, A. C. (1997) Germline cyst formation in *Drosophila*. *Annu.Rev. Genet.* **31,** 405–428.

6. Navarro, C., Lehmann, R., and Morris, J. (2001) Setting one sister above the rest. *Curr. Biol.* 11, R162–R165.
7. Riechmann, V. and Ephrussi, A. (2001) Axis formation during *Drosophila* oogenesis. *Curr. Opin. Gen. Dev.* **11,** 374–383.
8. Endow, S. A. and Komma, D. J. (1997) Spindle dynamics during meiosis in Drosophila oocytes. *J. Cell Biol.* **137,** 1321–1336.
9. Illmensee, K. and Mahowald, A.P. (1974) Transplantation of posterior polar plasm in *Drosophila*: induction of germ cells at the anterior pole of the egg. *Proc. Natl. Acad. Sci. USA* **71,** 1016–1020.
10. Howard, K., Jaglarz, M., Zhang, N., Shah, J., and Warrior, R. (1993) Migration of *Drosophila* germ cells: analysis using enhancer trap lines. *Development* (**Suppl.)** 213–218.
11. Warrior, R. (1994) Primordial germ cell migration and the assembly of *Drosophila* embryonic gonad. *Dev. Biol.* **166,** 180–194.
12. Babcock, B. M. (1971) Oviduct development in *Drosophila*. II. Metamorphic events in normal and ovariectomized females. *Wilhelm Roux. Arch.* **167,** 24–63.
13. van Eeden, F. and St. Johnston, D. (1999) The polarisation of the anterior–posterior and dorsal–ventral axes during *Drosophila* oogenesis. *Curr. Opin. Genet. Dev.* **9,** 396–404.
14. Robinson, D. N., Cant, K., and Cooley, L. (1994) Morphogenesis of the *Drosophila* ovarian ring canals. *Development* **120,** 2015–2025.
15. King, R. C. (1957) Oogenesis in adult *Drosophila melanogaster*. II. Stage distribution as a function of age. *Growth* **21,** 95–102.
16. Cummings, M. R. and King, R. C. (1969) The cytology of the vitellogenic stages of oogenesis in *Drosophila melanogaster* I. General staging characteristics. *J. Morphol.* **128,** 427–442.
17. Gelti-Douka, H., Gingeras, T. R., and Kambysellis, M. P. (1974) Yolk proteins in *Drosophila*: identification and site of synthesis. *J. Exp. Zool.* **187,** 167–172.
18. DiMario, P. J. and Mahowald, A. P. (1986) The effects of pH and weak bases on the in vitro endocytosis of vitellogenin by oocytes of *Drosophila melanogaster*. *Cell Tissue Res.* **246,** 103–108.
19. Brennan, M.D., Weiner, A. J., Goralski, T. J., and Mahowald, A. P. (1982) The follicle cells are a major site of vitellogenin synthesis in *Drosophila melanogaster*. *Dev. Biol.* **89,** 225–236.
20. Margaritis, L., Kafatos, F., and Petri, W. (1980) The eggshell of *Drosophila melanogaster*: I. Fine structure of the layers and regions of the wild-type eggshell. *J. Cell Sci.* **43,** 1–35.
21. Dobens, L. L. and Raftery, L. A. (2000) Integration of epithelial patterning and morphogenesis in *Drosophila* ovarian follicle cells. *Dev. Dynam.* **218,** 80–93.
22. Chao, S. and Nagoshi, R. (1999) Induction of apoptosis in the germline and follicle cell layers of *Drosophila* egg chambers. *Mech. Dev.* **88,** 159–172.
23. Bownes, M. and Blair, M. (1986) The effects of a sugar diet and hormones on the expression of the *Drosophila* yolk-protein genes. *J. Insect Physiol.* **32,** 493–501.

24. Chen, P. S., Stumm-Zollinger, E., Aigaki, T., Balmer, J., Bienz, M., and Bohlen, P. (1988) A male accessory gland peptide that regulates reproductive behaviour of female *D. melanogaster*. *Cell* **54,** 291–298.
25. Soller, M., Bownes, M., and Kubli, E. (1997) Mating and sex peptide stimulate the accumulation of yolk in oocytes of *Drosophila melanogaster*. *Eur. Biochem, J.* **243,** 732–738.
26. Riddiford, L. M. and Ashburner, M. (1991) Effects of juvenile hormones mimics on larval development and metamorphosis of *Drosophila melanogaster*. *Gen. Comp. Endocrinol.* **82,** 172–183.
27. Soller, M., Bownes, M., and Kubli, E. (1999) Control of oocyte maturation in sexually mature *Drosophila* females. *Dev. Biol.* **208,** 337–351.
28. Buszczak, M. B. M., Freeman, M. R., Carlson, J. R., Bender, M., Cooley, L., and Segraves, W. A. (1999) Ecdysone response genes govern egg chamber development during mid-oogenesis in *Drosophila*. *Development* **126,** 4581–4589.
29. Carney, G. E. and Bender, M. (2000) The *Drosophila* ecdysone receptor (EcR) gene is required maternally for normal oogenesis. *Genetics* **154,** 1203–1211.
30. Böhni, R., Riesgo-Escovar, J., Oldham, S., et al. (1999) Autonomous control of cell and organ size by CHICO, a *Drosophila* homolog of vertebrate IRS114. *Cell* **97,** 865–875.
31. Drummond-Barbosa, D. and Spradling, A. C. (2001) Stem cells and their progeny respond to nutritional changes during Drosophila oogenesis. *Dev. Biol.* **231,** 265–278.
32. Wieschaus, E. and Szabad, J. (1979) The development and function of the female germ line in *Drosophila melanogaster*: a cell lineage study. *Dev. Biol.* **68,** 29–46.
33. Lin, H. and Spradling, A. C. (1993) Germline stem-cell division and egg chamber development in transplanted *Drosophila* germaria. *Dev. Biol.* **159,** 140–152.
34. Lin, H. and Spradling, A. C. (1997) A novel group of *pumilio* mutations affects the asymmetric division of germline stem cells in the *Drosophila* ovary. *Development* **124,** 2463–2476.
35. Deng, W. and Lin, H. (1997) Spectrosomes and fusomes anchor mitotic spindles during asymmetric germ cell divisions and facilitate the formation of a polarized microtubule array for oocyte specification in *Drosophila*. *Dev. Biol.* **189,** 79–94.
36. de Cuevas, M. and Spradling, A. C. (1998) Morphogenesis of the *Drosophila* fusome and its implications for the oocyte specification. *Development* **125,** 2781–2789.
37. Storto, P. D. and King, R. C. (1989) The role of polyfusomes in generating branched chains of cystocytes during *Drosophila* oogenesis. *Dev. Genet.* **10,** 70–86.
38. McGrail, M., Gepner, J., Silvanovich, A., Ludmann, S., Serr, M., and Hays, T. S. (1995) Regulation of cytoplasmic dynein function in vivo by the *Drosophila* Glued Complex. *J. Cell Biol.* **131,** 411–425.
39. McGrail, M. and Hays, T. S. (1997) The microtubule motor cytoplasmic dynein is required for spindle orientation during germline cell divisions and oocyte differentiation in *Drosophila*. *Development* **124,** 2409–2419.

40. Cha, B.-J., Koppetsch, B. S., and Theurkauf, W. E. (2001) In vivo analysis of *Drosophila bicoid* mRNA localization reveals a novel microtubule-dependent axis specification pathway. *Cell* **106,** 35–46.
41. Theurkauf, W. E., Alberts, M., Jan, Y. N., and Jongens, T. A. (1993) A central role for microtubules in the differentiation of *Drosophila* oocytes. *Development* **118,** 1169–1180.
42. Grieder, N. C., de Cuevas, M., and Spradling, A. C. (2000) The fusome organizes the microtubule network during oocyte differentiation in *Drosophila*. *Development* **127,** 4253–4264.
43. Bolivar, J., Huynh, J. R., Lopez-Schier, H., Gonzales, C., St. Johnston, D., and Gonzales-Reyes, A. (2001) Centrosome migration into the *Drosophila* oocyte is dependent of *BicD, egl* and the organisation of the microtubule cytoskeleton. *Development* **128,** 1889–1909.
44. Carpenter, A. T. C. (1994) Egalitarian and the choice of the cell fates in *Drosophila melanogaster* oogenesis. *Ciba Found. Symp.* **182,** 223–246.
45. Huynh, J. R. and St. Johnston, D. (2000) The role of *BicD*, *egl*, *orb* and the microtubules in the restriction of meiosis to the *Drosophila* oocyte. *Development* **127,** 2785–2794.
46. Ghabrial, A. and Schüpbach, T. (1999) Activation of a meiotic checkpoint regulates translation of Gurken during *Drosophila* oogenesis. *Nature Cell Biol.* **1,** 354–357.
47. Cox, D. N., Lu, B., Sun, T. S., Williams, L. T., and Jan, Y. N. (2001) *Drosophila par-1* is required for oocyte differentiation and microtubule organization. *Curr. Biol.* **11,** 75–87.
48. Huynh, J. R., Shulman, J., Benton, R., and St. Johnston, D. (2001) PAR-1 is required for the maintenance of oocyte fate in *Drosophila*. *Development* **128,** 1201–1209.
49. Pare, C. and Suter, B. (2000) Subcellular localization of Bic-D : GFP is linked to an asymmetric oocyte nucleus. *J. Cell Sci.* **113,** 2119–2127.
50. Clegg, N. J., Findley, S. D., Mahowald, A. P., and Ruohola-Baker, H. (2001) *Maelstrom* is required to position the MTOC in stage 2–6 *Drosophila* oocytes. *Dev. Genes Evol.* **211,** 44–48.
51. Huynh, J. R., Petronczki, M., Knoblich, J., and St. Johnston, D. (2001) Bazooka and PAR-6 are required with PAR-1 for the maintenance of oocyte fate in *Drosophila*. *Curr. Biol.* **11,** 901–906.
52. Margolis, J. and Spradling, A. C. (1995) Identification and behaviour of epithelial stem cells in *Drosophila* ovary. *Development* **121,** 3797–3807.
53. Forbes, A., Lin, H., Ingham, P., and Spradling, A. C. (1996) *Hedgehog* is required for the proliferation and specification of ovarian somatic cells prior to egg chamber formation in *Drosophila. Development* **122,** 1125–1135.
54. Gonzales-Reyes, A. and St. Johnstone, D. (1998) The *Drosophila* AP axis is polarized by the cadherin-mediated positioning of the oocyte. *Development* **125,** 3635–3644.
55. Tanentzapf, G., Smith, C., McGlade, J., and Tepass, U. (2000) Apical, lateral, and basal polarization cues contribute to the development of the follicular epithelium during *Drosophila* oogenesis. *J. Cell Biol.* **151,** 891–904.

56. Godt, D. and Tepass, U. (1998) *Drosophila* oocyte localization is mediated by differential cadherin-based adhesion. *Nature* **395,** 387–391.
57. Gonzales-Reyes, A. and St. Johnstone, D. (1998) Patterning of the follicle cell epithelium along the anterior-posterior axis during *Drosophila* development. *Development* **125,** 2837–2846.
58. Gonzales-Reyes, A., Elliott, H., and St. Johnstone, D. (1995) Polarization of both major body axes in *Drosophila* by gurken-torpedo signalling. *Nature* **375,** 654–658.
59. Roth, S., Neuman-Silberberg, F. S., Barcelo, G., and Schüpbach, T. (1995) *cornichon* and the EGF receptor signalling process are necessary for both anterior–posterior and dorsal–ventral pattern formation in *Drosophila*. *Cell* **81,** 967–978.
60. Nilson, L. A. and Schüpbach, T. (1999) EGF receptor signalling in *Drosophila* oogenesis. *Curr. Topics Dev. Biol.* **44,** 203–243.
61. van Buskirk, C. and Schüpbach, T. (1999) Versatility in signalling: multiple responses to EGF receptor activation during *Drosophila* oogenesis. *Trends Cell Biol.* **9,** 1–4.
62. Stevens, L. (1998) Twin peaks: Spitz and Argos star in patterning of the *Drosophila* egg. *Cell* **95,** 291–294.
63. Edwards, K., Demsky, M., Montague, R., Weymouth, N., and Kiehart, D. (1997) GFP-moesin illuminates actin cytoskeleton dynamics in living tissue and demonstrates cell shape changes during morphogenesis in *Drosophila*. *Dev. Biol.* **191,** 103–117.
64. Li, K. and Kaufman, T.C. (1996) The homeotic target gene *centrosomin* encodes an essential centrosomal component. *Cell* **85,** 585–596.
65. Swan, A., Nguyen, T., and Suter, B. (1999) *Drosophila Lissencephaly-1* functions with *Bic-D* and dynein in oocyte determination and nuclear positioning. *Nature Cell Biol.* **1,** 444–449.
66. Shulman, J. M., Benton, R., and St. Johnston, D. (2000) The *Drosophila* homolog of *C. elegans* PAR-1 organizes the oocyte cytoskeleton and directs *oskar* mRNA localization to the posterior pole. *Cell* **101,** 377–388.
67. Jankovics, F., Sinka, R., and Erdélyi, M. (2001) An interaction type of genetic screen reveals a role of the *Rab11* gene in *oskar* mRNA localization in the developing *Drosophila melanogaster* oocyte. *Genetics* **158,** 1177–1188.
68. Baum, B., Li, W., and Perrimon, N. (2000) A cyclase-associated protein regulates actin and cell polarity during *Drosophila* oogenesis and in yeast. *Curr. Biol.* **10,** 964–973.
69. Pokrywka, N. J. and Stephenson, E. C. (1995) Microtubules are a general component of mRNA localization systems in *Drosophila* oocytes. *Dev. Biol.* **167,** 363–370.
70. Clark, I., Jan, L. Y., and Jan, Y. N. (1997) Reciprocal localization of Nod and kinesin fusion proteins indicates microtubule polarity in *Drosophila* oocyte, epithelium, neuron and muscle. *Development* **124,** 461–470.

71. Lasko, P. (1999) RNA sorting in *Drosophila* oocytes and embryos. *FASEB J.* **13,** 421–433.
72. Hays, T. and Karess, R. (2000) Swallowing dynein: a missing link in RNA localization? *Nature Cell Biol.* **2,** E60–E62.
73. Mahajan-Miklos, S. and Cooley, L. (1994) Intercellular cytoplasm transport during *Drosophila* oogenesis. *Dev. Biol.* **165,** 336–351.
74. Robinson, D. N. and Cooley, L. (1997) *Drosophila* Kelch is an oligomeric ring canal actin organizer. *J. Cell Biol.* **138,** 799–810.
75. Robinson, D. N., Smith-Leiker, T. A., Sokol, N. S., Hudson, A. M., and Cooley, L. (1997) Formation of the *Drosophila* ovarian ring canal inner rim depends on *cheerio*. *Genetics* **145,** 1063–1072
76. Sokol, N. S. and Cooley, L. (1999) *Drosophila* Filamin encoded by the *cheerio* locus is a component of the ovarian ring canals. *Curr. Biol.* **9,** 1221–1230
77. Field, C. M. and Alberts, B. M. (1995) Anillin, a contractile ring protein that cycles from the nucleus to the cell cortex. *J. Cell Biol.* **131,** 165–178
78. Minestrini, G., Máthé, E., and Glover, D. M. (2002) Mutations that disrupt the sub-cellular localisation of the Pavarotti kinesin-like protein lead to defects in the tubulin and actin cytoskeleton during Drosophila oogenesis. *J.Cell Sci.* **115,** 725–736.
79. Koch, E. A. and King, R. C. (1966) The origin and early differentiation of the egg chamber of *Drosophila melanogaster*. *J. Morphol.* **119,** 283–304.
80. Bohrmann, J. and Biber, K. (1994) Cytoskeleton-dependent transport of cytoplasmic particles in previtellogenic to midvitellogenic ovarian follicles of Drosophila: time lapse analysis using video-enhanced contrast microscopy. *J. Cell Sci.* **107,** 849–858.
81. Cooley, L., Verheyen, E., and Ayers, K. (1992) The *chickadee* gene encodes a profilin required for intercellular cytoplasm transport during *Drosophila* oogenesis. *Cell* **69,** 173–184.
82. Gutzeit, H. (1990) The microfilament pattern in the somatic follicle cells of midvitellogenic ovarian follicles of *Drosophila*. *Eur. J. Cell Biol.* **53,** 349–356.
83. Nokkala, S. and Puro, J. (1976) Cytological evidence for a chromocenter in *Drosophila melanogaster* oocytes. *Hereditas* **83,** 265–268.
84. Puro, J. and Nokkala, S. (1977) Meiotic segregation of chromosomes in *Drosophila melanogaster* oocytes. A cytological approach. *Chromosoma* **63,** 273–286.
85. Neuman-Silberberg, F. S. and Schüpbach, T. (1993) The *Drosophila* dorsoventral patterning gene *gurken* produces a dorsally localized RNA and encodes a TGF alpha-like protein. *Cell* **75,** 165–174.
86. Máthé, E., Bates, H., Huikeshoven, H., Deák, P., Glover, D. M., and Cotterill, S. (2000) Importin-α3 is required at multiple stages of *Drosophila* development and has a stage specific role in the completion of oogenesis. *Dev. Biol.* **223,** 307–322.
87. Theurkauf, W.E. and Hawley, R.S. (1992) Meiotic spindle assembly in *Drosophila* females: behavior of nonexchange chromosomes and the effects of mutations in the nod kinesin-like protein. *J. Cell Biol.* **116,** 1167–1180.

88. Walczak, C. E., Vernos, I., Mitchison, T. J., Karsenti, E., and Heald, R. A. (1998). A model for the proposed roles of different microtubule-based motor proteins in establishing spindle bipolarity. *Curr. Biol.* **8,** 903–913.
89. Walczak, C. E. (2001) Ran hits the ground running. *Nature Cell Biol.* **3,** E69–E71.
90. Cullen, C. F. and Ohkura, H. (2001) Msps protein is localized to acentrosomal poles to ensure bipolarity of *Drosophila* meiotic spindles. *Nature Cell Biol.* **3,** 637–642.
91. Afshar, K., Barton, N. R., Hawley, R. S., and Goldstein, L. S. (1995) DNA binding and meiotic chromosomal localization of the *Drosophila* nod kinesin-like protein. *Cell* **81,** 129–138.
92. Sonnenblick, B. P. (1950) The early embryology of *Drosophila melanogaster*, in *Biology of Drosophila* (Demerec, M., ed.), Wiley, New York, pp. 62–167.
93. Puro, J. (1991) Differential mechanisms governing segregation of a univalent in oocytes and spermatocytes of *Drosophila melanogaster. Chromosoma* **100,** 305–314.
94. Endow, S. A. and Komma, D. J. (1997) Spindle dynamics during meiosis in *Drosophila* oocytes. *J. Cell Biol.* **137,** 1321–1336.
95. Endow, S. A. and Komma, D. J. (1998) Assembly and dynamics of an anstral : astral spindle: the meiosis II spindle in *Drosophila* oocytes. *J. Cell Sci.* **111,** 2487–2495.
96. Riparbelli, M. G. and Callaini, G. (1996) Meiotic spindle organization in fertilized *Drosophila* oocyte: presence of centrosomal components in the meiotic apparatus. *J. Cell Sci.* **109,** 911–918.
97. Wakefield, J. G., Bonaccorsi, S., and Gatti, M. (2001) The *Drosophila* protein Asp is involved in microtubule organization during spindle formation and cytokinesis. *J. Cell Biol.* **153,** 637–648.
98. Máthé, E., Boros, I., Jósvay, K., et al. (1998) The *Tomaj* mutant alleles of *αTubulin67C* reveal a requirement for the encoded maternal specific tubulin isoform in the sperm aster, the cleavage spindle apparatus and neurogenesis during embryonic development in *Drosophila. J. Cell Sci.* **111,** 887–896.
99. Huettner, A.F. (1924) Maturation and fertilization of *Drosophila melanogaster. J. Morphol.* **37,** 385–423.
100. Rabinowitz, M. (1941) Studies on the cytology and early embryology of the egg of *Drosophila melanogaster. J. Morphol.* **69,** 1–49.
101. Orr-Weaver, T. L. (1995) Meiosis in *Drosophila*: seeing is believing. *Proc. Natl. Acad. Sci. USA* **92,** 10,443–10,449.
102. Rieder, C. L. and Cole, R. (1999) Chromatid cohesion during mitosis: lessons from meiosis. *J. Cell Sci.* **112,** 2607–2613.
103. Moore, D. P., Page, A. W., Tang, T. T., Kerrebrock, A. W., and Orr-Weaver, T. (1998) The cohesion protein MEI-S332 localizes to condensed meiotic and mitotic centromeres until sister chromatids separate. *J. Cell Biol.* **140,** 1003–1012.
104. Lopez, J. M., Karpen, G. H., and Orr-Weaver (2000) Sister-chromatids cohesion via MEI-S332 and kinetochore assembly are separable functions of the Drosophila centromere. *Curr. Biol.* **10,** 997–1000.

105. Robb, J. A. (1969) Maintenance of imaginal discs of *Drosophila melanogaster* in chemically defined media. *J. Cell Biol.* **41,** 876–885.
106. Mahowald, A. P., Goralski, T. J., and Caulton, J. H. (1983). In vitro activation of *Drosophila* eggs. *Dev. Biol.* **98,** 437–445.
107. Page, A. W. and Orr-Weaver, T. L. (1997) Activation of the meiotic divisions in *Drosophila* oocytes. *Dev. Biol.* **183,** 195–207.
108. Tavosanis, G., Llamazares, S., Goulielmos, G., and Gonzalez, C. (1997) Essential role for γ-tubulin in the acentriolar female meiotic spindle of Drosophila. *EMBO. J.* **16,** 1809–1819.
109. Szabad, J. (1998) Genetic requirement of epidermal and female germline cells in *Drosophila* in the light of clonal analysis. *Int. J. Dev. Biol.* **42,** 257–262.

5

Cytological Analysis of Oogenesis

Seppo Nokkala and Christina Nokkala

1. Introduction

Female meiosis in *Drosophila* is interesting and exceptional in many respects. First, like all dipterans, *Drosophila* has a polytrophic type of ovary characterized by the presence of nurse cells, which provide ooplasma and yolk to developing oocytes, whereas meiotic chromosomes are metabolically inactive. Meiosis in this type of ovary is characterized by the incorporation of all chromosomes into a karyosome at early meiotic prophase ***(1,2)***. Second, in addition to chiasmatic bivalents, achiasmatic chromosomes also segregate quite regularly from each other; for example, in *Drosophila melanogaster* the tiny fourth chromosomes are always achiasmatic in oogenesis, but nevertheless segregate regularly from each other. Segregation of achiasmatic chromosomes is regular even when the univalent chromosomes are heterologous. The phenomenon is termed "distributive segregation" and is controlled by the distributive system (for review, *see* **refs. *3–6***). To explain achiasmatic segregations, two alternative models have been put forward. One is based on the fact that in female meiosis, conventional diplotene and diakinesis stages are absent and both bivalents and achiasmatic chromosomes are incorporated in a karyosome that persists until prometaphase I. According to the model, physical association of segregating univalents, homologous or heterologous, is established at pachytene while the karyosome is formed and these associations lead to co-orientations of chromosomes on developing spindles ***(4,7,8)***. The other model assumes that univalent chromosomes remain randomly arrayed until the spindle is formed and then become organized so that a univalent orients toward the least crowded pole ***(4–6)***. Based on *in situ* localization of centromeric heterochromatin regions within the karyosome, Dernburg et al. ***(9)*** have presented evidence that pairing of heterochromatic regions of achiasmatic homologous chromosomes

From: *Methods in Molecular Biology, vol. 247:* Drosophila *Cytogenetics Protocols*
Edited by: D. S. Henderson © Humana Press Inc., Totowa, NJ

at pachytene determines their segregation, whereas the segregation of achiasmatic heterologs is determined by a mechanism in which each chromosome orients toward the least crowded pole.

In this chapter, we describe chromosome behavior during female meiosis as revealed from fixed material and cytological methods for analyzing female meiosis in detail ***(7,10)***.

1.1. Behavior of Chromosomes During Female Meiosis

Soon after the 16-cell cyst has formed in the germarium (for details, *see* Chapter 4), the two cells with four ring canals, pro-oocytes, display synaptonemal complexes indicative of pachytene in these cells. Serial reconstructions of synaptonemal complexes reveal that all centromeres are positioned near each other on the same side of the nucleus (i.e., they show chromocentral association) ***(11,12)***. This kind of chromosomal polarity is typical for mitotic cells and is known as Rabl orientation. While still in the germarium, one of the pro-oocytes in the 16-cell cyst is selected to be the oocyte undergoing meiosis, and the other one becomes a nurse cell. In stages 1 and 2, the centromeric regions of bivalents adhere to a common chromocenter ***(13–15)***, followed by incorporation of bivalents into a karyosome during stages 3–6 ***(16)***. Karyosome organization is retained until early stage 13.

During stage 13, the nurse cells degenerate, providing a means to subdivide the stage into five developmental steps, A-E ***(7)***. In stage 13A, the nuclear membrane is still intact and no chromosomal material is seen outside the karyosome. The nuclear membrane disappears at stage 13B, demarcating the start of prometaphase I. Early at this stage, chromosomal material is still arranged in a karyosomelike body, which is then individualized in bivalents in which centromeric regions are still tightly paired. Also, the fourth chromosomes are individualized as a paired structure. The fourth chromosomes and other achiasmate chromosomes are seen detached but still close to each other in mid-prophase, stage 13C. Centromeric regions of chiasmate bivalents are still attached to each other, but pulled toward poles, while the fourth chromosomes are moving toward opposite poles at stage 13D. Full metaphase I is reached at stage 13E, showing a typical arrangement of bivalents and univalents (*see* **Fig. 1**); bivalents with homologous centromeres equidistant from the equatorial plane and chiasmata on the plane, and univalents having stabilized size-dependent positions between a pole and the equatorial plane. The smaller the univalent is, the nearer to the pole it lies ***(7,8)***. Meiosis I is arrested at metaphase I and this stage is found in all eggs at stage 14.

1.2. Metaphase Arrest and Fertilization

To reveal the metaphase arrest, at least one chiasmatic bivalent must be present. If there is no chiasmatic bivalent, as in the *c(3)G* mutant, no typical

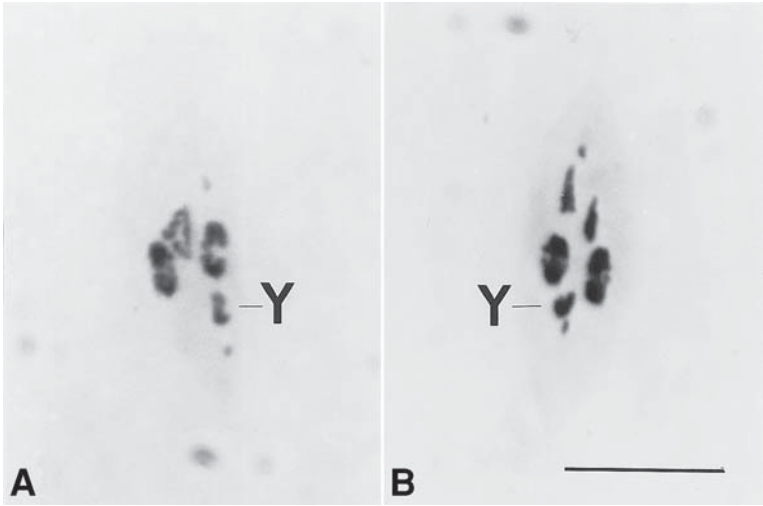

Fig. 1. **(A)** Metaphase I spindles in *In(1)w^{m4}/In(1)dl-49/Y* showing a chiasma in the X chromosome bivalent and the univalent Y chromosome orienting toward the lower pole. **(B)** Metaphase I spindles in *In(1)w^{m4}/In(1)dl-49/Y* showing apparent nondisjunction of univalent X chromosomes caused by the Y chromosome. Bar: 10 µm.

metaphase configuration is formed, but chromosomes move to an anaphase I-like configuration during prometaphase at stage 13E. This configuration is found in the eggs at stage 14, being unable to proceed into meiosis II ***(7)***, apparently because the cell cycle machinery is signaling metaphase arrest. Some of the recombination defective mutants bypass metaphase I arrest and proceed to metaphase II ***(17,18)***.

Metaphase I arrest is released and the meiotic cycle reactivated when the egg is transferred to the uterus. The egg is at anaphase I when sperm enters it, indicating that cell cycle activation is brought about by some unknown component present in the uterus. The meiosis I–late anaphase I spindle (*see* **Fig. 2A**) is transformed to meiosis II spindles (*see* **Fig. 2B**) by organizing the central spindle pole body at the equatorial site ***(19–22)***. Within the spindles, the dyads attain bipolar orientations. As a result of meiotic events, four haploid nuclei are formed, and if the egg is inseminated, fertilization follows. The events of fertilization in wild type or distorted by mutants can be analyzed in detail with the Schiff–Giemsa method described in this chapter (see, e.g., **refs. *10,23***).

2. Materials

2.1. Reagents and Solutions

1. Paraffin, melting point 56–58°C.
2. Chloroform.

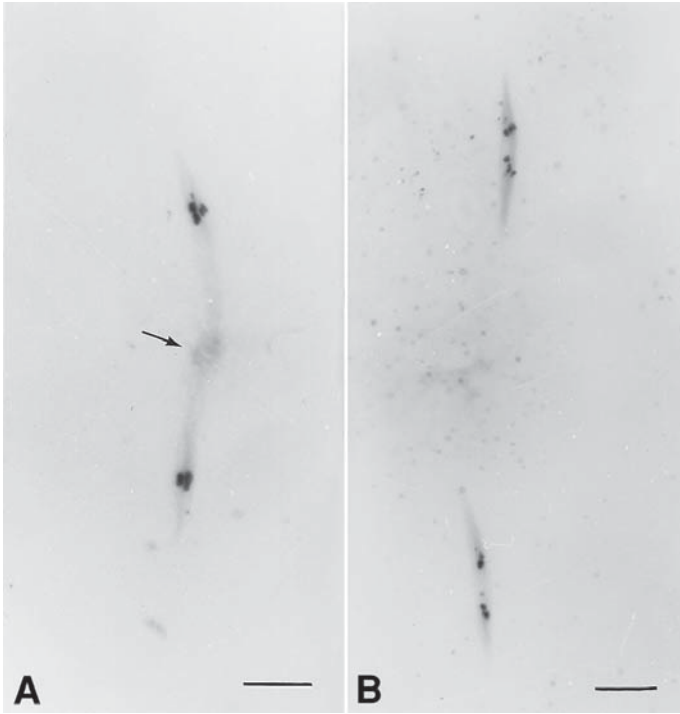

Fig. 2. **(A)** Late anaphase I showing the central spindle pole (arrow). Bar: 10 µm. (Courtesy of J. Puro.) **(B)** Anaphase II spindles. Bar: 10 µm. (Courtesy of J. Puro.)

3. Glacial acetic acid.
4. 45% Acetic acid.
5. 1 *N* HCl; 2 *N* HCl (Merck).
6. Entellan (Merck).
7. Giemsa (Merck).
8. Insect Ringer's solution: 130 m*M* NaCl, 2 m*M* KCl, 0.8 m*M* $CaCl_2 \cdot 2H_2O$, 0.2 m*M* $NaHCO_3$. Store at 4°C.
9. 0.075 *M* KCl.
10. Modified Carnoy fixative: 80% Ethanol : chloroform : glacial acetic acid, 6 : 3 : 1.
11. Schiff's reagent: Add 1 g Basic fuchsin (Merck, C.I. no. 42510) to 200 mL of boiling distilled water. Shake well and allow to cool to approx 50°C, then filter. Add 0.8 g $K_2S_2O_7$ (Merck) and 8 mL of 1 *N* HCl, shake, and allow to stand in the dark over night. On the following day, add 4 spoonfuls of activated charcoal (Merck), shake well, and filter. The filtrate should be colorless. Store protected from light at 4°C.
12. Sörensen's phosphate buffer: Add equal volumes of 67 m*M* NaH_2PO_4 stock solution and 67 m*M* KH_2PO_4 stock solution to reach pH 6.8.

2.2. Equipment

1. Glass vials, approx 25 mm in diameter and 80 mm in height, for fixation and the alcohol series.
2. Inner vials. Prepare from plastic tubes, 15 mm in diameter and 45 mm high. Heat a thin needle over a flame and stick it through the bottom of the tube to make small holes.
3. Facial tissue (Katrin®).
4. Petri dishes (glass), 90–100 mm in diameter, for dissection. Melt enough paraffin in a Petri dish at 60°C to form an approx 0.5-cm layer of solid paraffin when cooled.
5. Petri dishes, 40–50 mm in diameter.
6. Pasteur pipets.
7. Prepare cut Pasteur pipets by cutting the capillary part off in such a way that the new opening is large enough for collecting ovaries.
8. Insect pins; no. 000, 0, and 1 (e.g., Fine Science Tools) or tungsten needles.
9. Fine paint brushes.
10. Microscope slides, cover slips, 18×18, 24×32 mm^2.
11. Filter paper.
12. Scalpels.
13. Staining jars.
14. Fan, blowing cool air.

3. Methods

3.1. Analysis of Egg Chambers of the Germarium to Stage 14

In order to increase the number of egg chambers at stages 12–14, the flies are transferred into new culture vials 2 or 3 d before starting the procedure. Stress caused by the transfer slows down egg laying, and mature (stage 14) and nearly mature eggs (stages 12 and 13) accumulate in the ovaries.

1. Etherize flies and divide females into groups of four to six, and put in small glass vials capped with facial tissue.
2. Transfer a set of females to a Petri dish covered with paraffin. Pipet a small drop of insect-Ringer's solution to a dish near the females.
3. Pick up one female at a time by sticking a thin (no. 000) insect pin through the thorax, and transfer the female near to the drop of Ringer's solution.
4. Using a thicker insect pin (no. 0 or 1), stick the abdomen dorsally between the third and fourth segments and pull the tip of the abdomen with ovaries into the drop. Repeat this for each female in the set.
5. Using an insect pin with a small hook, transfer the tip of each abdomen (containing ovaries) to a small Petri dish containing hypotonic solution (0.075 *M* KCl) for 6 min (for egg chamber stages 2–12) or for 10 min (for stages 13 and 14) (*see* **Note 1**).
6. Using the hooked insect pin, transfer the tips of abdomens into a glass vial containing modified Carnoy fixative. Incubate for at least 2 h at room temperature. If necessary, ovaries can be stored in fixative for several days at 4°C.

7. Decant the fixative away and refill the vial with an equal volume of absolute ethanol. Allow the vial to stand at room temperature for 2 h. Replace the ethanol with an equal volume of 70% ethanol and keep the vial at 4°C overnight.
8. Prepare a decreasing ethanol series—50%, 30%, distilled water, and 1 *N* HCl at room temperature—in glass vials. Put a small plastic tube with small holes in its bottom inside the vial containing 50% ethanol. Take 5–10 abdomens at a time from 70% ethanol and transfer them to 50% ethanol inside the plastic tube. Incubate for 30 min. Using the small plastic tube, transfer the ovaries through 30% ethanol (5 min), distilled water (brief rinse), and into 1 *N* HCl (30 min) at room temperature.
9. For hydrolysis, incubate the ovaries in 1 *N* HCl at 60°C for 8 min.
10. Transfer the ovaries directly into Schiff's reagent for 3–5 min and then into distilled water (*see* **Note 2**).
11. Use the cut Pasteur pipet to transfer abdomens with ovaries and an appropriate amount of distilled water from the inner vial into a small Petri dish.
12. For preparing a slide from stages germarium to stage 12, transfer one abdomen with ovaries into a small drop of distilled water on a clean object slide. Remove all other tissue except ovaries, and if ovaries carry mature eggs, remove these too. Detach the ovarioles from each other. Remove excess water with a piece of filter paper, and pipet a small drop of 45% acetic acid next to the ovarioles (*see* **Note 3**). Use insect pins to move the acetic acid drop over the ovarioles. Wait until all the tissue is transparent, then put a cover slip (18×18 mm^2) on the material. Inspect the slide with a phase-contrast microscope. Wait until all of the streaming under the cover slip ceases, gently press the slide between filter paper, and put the slide on dry ice.
13. For preparing a slide from stages 13 and 14, transfer one abdomen with ovaries into a small drop of distilled water on an object slide. Choose one of the ovaries (carrying the greater number of egg chambers of the desired type) and leave it in the drop while removing all other tissues from the drop. In developing eggs at these stages, the chorion is well developed and has to be removed. For this, cut the eggs in half with insect pins and keep the anterior part in its place with one of the pins. With the second pin, press the egg in an anterior to posterior direction until the yolk enveloped by vitelline membrane comes out from the chorion. Collect dechorionated anterior parts in one place inside the drop. Usually four to six eggs are prepared from one ovary. Then, remove all of the other material from the drop by wiping with an insect pin. Remove excess water around the anterior parts. Pipet a small drop of 45% acetic acid next to the anterior parts. Use insect pins to move the drop onto the anterior parts. Wait until the yolk is transparent and place a cover slip (18×18 mm^2) in its position. Now, the slide can be inspected with phase-contrast optics. The yolk is spread evenly and the most prominent structures seen are remnants of vitelline membrane. Usually, the spindles are situated near these structures. When the streaming under the cover slip is ceased, press the slide gently between the filter paper and place it on dry ice.
14. After freezing the slide for at least 10 min, remove the cover slip with a scapel and immerse the slide in a staining jar filled with absolute ethanol for 5 min at

most. Dip the slide in glacial acetic acid for 18 s (*see* **Note 4**) and air-dry for at least 20 min with a dryer. Store the slide(s) in a dust-free place (e.g., in an incubator [40°C]) at least overnight or longer (air-dried slides can be stored up to 1 yr before Giemsa staining).
15. Incubate the slides in Sörensen's phosphate buffer (pH 6.8) in a staining jar for 5 min.
16. Stain the slides with 4% Giemsa in Sorensen's phosphate buffer for 30 min, rinse briefly in distilled water, and air-dry with a cool fan for 20 min.
17. Mount the slides in Entellan using 24 × 32-mm^2 cover slips.

3.2. Analysis of Anaphase I in Early Embryos

1. Allow inseminated females to lay eggs in fresh culture bottles overnight.
2. Etherize the females and squeeze eggs out of uteri by pressing the abdomen near the uterus with thick insect pins. Repeat collecting at 1- to 2-h intervals.
3. Fix the eggs immediately for 30–60 min in modified Carnoy fixative in small glass vials at room temperature.
4. Add approximately an equal volume of absolute ethanol and allow the fixation to continue overnight at 4°C.
5. Remove the fixative–alcohol liquid and replace with absolute ethanol. Keep at room temperature for 2 h.
6. Replace the absolute ethanol with 70% ethanol and store at 4°C overnight.
7. Using a Pasteur pipet, transfer eggs into an egg basket in a small Petri dish containing 50% ethanol. Incubate for 30 min.
8. Carry the egg basket through 30% ethanol (3–5 min), distilled water (a brief wash), and into 1 *N* HCl for 30 min at room temperature (*see* **Note 5**).
9. Hydrolyze the eggs with 1 *N* HCl (8 min) and stain with Schiff's reagent for 3–5 min. Transfer the eggs in distilled water.
10. Place one egg at a time in a drop of distilled water on a clean microscope slide. Cut the egg into anterior and posterior halves with insect pins. Remove the chorion from both halves and incubate them in 45% acetic acid as described in **Subheading 3.1., step 13**.
11. After previewing the egg halves with a phase-contrast microscope, remove the cover slip with the dry-ice method (*see* **Subheading 3.1., step 14**). Dehydrate the slides in 99% (or 96%) ethanol for 5 min, immerse the slides in glacial acetic acid for 20 s, and air-dry with a fan for 20 min. Store the slides in a dust-free place until stained with Giemsa (*see* **Subheading 3.1.** for instructions).

4. Notes

1. Hypotonic treatment is essential to reveal details (i.e., the positions of bivalents and univalents), in prometaphase I and metaphase I spindles in eggs at stages 13 and 14. If the treatment is too short, all bivalents and univalents are clumped together. If the treatment is too long, chromatids become thin and threadlike making analysis of metaphase figures difficult. Usually, treatment times from 9 to 10 min give optimal results. As whole ovaries are subjected to treatment, individual eggs within ovaries receive slightly varying treatments. Thus, among

eggs within an ovary, there are eggs for which the treatment time is too short. It has been claimed that hypotonic treatment activates the first meiotic spindle, inducing the onset of anaphase *(7)*. However, we have not been able to observe the release of metaphase arrest and the onset of anaphase after treatment with 0.075 *M* KCl solution. On the contrary, chiasmata are seen still to be holding homologs together (*see* **Figs. 1** and **2**), evidencing a metaphase I configuration.

2. The significance of this step is not actually to stain chromosomes, but to affect especially yolk to make it spread evenly. Optimum spreading is achieved when chromatin material appears black or gray colored when inspected with phase-contrast microscopy. If chromatin material appears shiny or bluish, the staining time with Schiff's reagent must be shortened.
3. The size of the acetic acid drop is critical; a drop with a diameter of 4–5 mm gives optimal spreading.
4. After glacial acetic acid treatment for 15–18 s, Giemsa stains the yolk slightly bluish. If the treatment is prolonged, the yolk remains colorless, making the finding of metaphase figures extremely difficult.
5. Alternative: After rehydration in 30% ethanol and rinsing in distilled water, perform the following:
   a. Transfer the eggs to 2 *N* HCl for 2 h, and then into distilled water. Eggs that are at early stages become transparent, whereas older eggs remain opaque.
   b. Cut the transparent eggs in half, remove the chorion, and make squashes in 45% acetic acid with both halves on the same slide.
   c. Remove the cover slip by using the dry-ice method, dehydrate the slide in a 3 : 1 mixture of ethanol and glacial acetic acid for 15 min, and air-dry with a fan for 20 min.
   d. For staining, hydrolyze the slide in 1 *N* HCl at 60°C for 8 min, treat with Schiff's reagent for 10–15 min, and rinse in distilled water, three to four changes, until the water remains colorless.
   e. Stain with 4% Giemsa solution as described in of **Subheading 3.1., step 16**.

References

1. Bier, K., Kunz, W., and Ribbert, D. (1967) Struktur und Funktion der Oocyten-chromosome und Nukleolen sowie der Extra-DNS während der Oogenese panoistisher und meroistischer Insekten. *Chromosoma* **23,** 214–254.
2. Bier, K., Kunz, W., and Ribbert, D. (1967) Insect oogenesis with and without lampbrush chromosomes. *Chromosomes Today* **2,** 107–115.
3. Grell, R. F. (1976) Distributive pairing, in *The Genetics and Biology of Drosophila*, (Ashburner, M. and Novitski, E., eds.), Academic Press, London, Vol. 1a, pp. 435–468.
4. Hawley, R. S. and Theurkauf, W. E. (1993) Requiem for distributive segregation: achiasmate segregation in *Drosophila* females. *Trends Genet.* **9,** 310–317.
5. Hawley, R. S., Irick, H., Zitron, A. E., et al. (1993) There are two mechanisms of achiasmate segregation in *Drosophila* females, one of which requires heterochromatic homology. *Dev. Genet.* **13,** 440–467.

6. Hawley, R. S., McKim, K. S., and Arbel, T. (1993) Meiotic segregation in *Drosophila melanogaster* females: molecules, mechanisms, and myths. *Annu. Rev. Genet.* **27,** 281–317.
7. Puro, J. and Nokkala, S. (1977) Meiotic segregation of chromosomes in *Drosophila melanogaster* oocytes. A cytological approach. *Chromosoma* **63,** 273–286.
8. Theurkauf, W. E. and Hawley, R. S. (1992) Meiotic spindle assembly in *Drosophila* females: behavior of nonexchange chromosomes and the effects of mutations in the nod kinesin-like protein. *J. Cell Biol.* **116,** 1167–1180.
9. Dernburg, A. F., Sedat, J. W., and Hawley, R. S. (1996) Direct evidence of a role for heterochromatin in meiotic chromosome segregation. *Cell* **86,** 135–146.
10. Williams, B. C., Dernburg, A. F., Puro, J., Nokkala, S., and Goldberg, M. L. (1997) The *Drosophila* kinesin-like protein KLP3A is required for proper behavior of male and female pronuclei at fertilization. *Development* **124,** 2365–2376.
11. Carpenter, A. T. C. (1975) Electron microscopy of meiosis in *Drosophila melanogaster* females. Structure, I., arrangement, and temporal change of the synaptonemal complex in wild-type. *Chromosoma* **51,** 157–182.
12. Carpenter, A. T. C. (1979) Synaptonemal complex and recombination nodules in wild-type *Drosophila melanogaster* females. *Genetics* **92,** 511–541.
13. Dävring, L. and Sunner, M. (1973) Female meiosis and embryonic mitosis in *Drosophila melanogaster* I. Meiosis and fertilization. *Hereditas* **73,** 51–64.
14. Nokkala, S. and Puro, J. (1976) Cytological evidence for a chromocenter in *Drosophila melanogaster* oocytes. *Hereditas* **83,** 266–268.
15. Chubyin, V. L. and Chadov, B. F. (1978) The chromocenter in meiotic cells of *Drosophila melanogaster* females with XY-compounds. *Tsitologia* **29,** 168–173.
16. King, R. C. (1970) *Ovarian Development in Drosophila melanogaster*. Academic, New York.
17. McKim, K. S., Jang, J. K., Theurkauf, W. E, and Hawley, R. S. (1993) Mechanical basis of meiotic metaphase arrest. *Nature* **362,** 364–366.
18. McKim, K. S. and Hawley, R. S. (1995) Chromosomal control of meiotic cell division. *Science* **270,** 1595–1601.
19. Puro, J. (1991) Differential mechanisms governing segregation of a univalent in oocytes and spermatocytes of *Drosophila melanogaster*. *Chromosoma* **100,** 305–314.
20. Riparbelli, M. G. and Callaini, G. (1996) Meiotic spindle organization in fertilized *Drosophila* oocyte: presence of centrosomal components in the meiotic apparatus. *J. Cell Sci.* **109,** 911–918.
21. Endow, S. A. and Komma, D. J. (1997) Spindle dynamics during meiosis in *Drosophila* oocytes. *J. Cell Biol.* **137,** 1321–1336.
22. Endow, S. A. and Komma, D. J. (1998) Assembly and dynamics of an anastral : astral spindle: the meiosis II spindle of *Drosophila* oocytes. *J. Cell Sci.* **111,** 2487–2495.
23. Tirián, L., Puro, J., Erdélyi, M., et al. (2000) The *Ketel*^{D} dominant-negative mutations identify maternal function of the Drosophila Importin-β gene required for cleavage nuclei formation. *Genetics* **156,** 1901–1912.

6

Polytene Chromosomes From Ovarian Nurse Cells of *Drosophila melanogaster otu* Mutants

Dmitry E. Koryakov, Natalia I. Mal'ceva, Robert C. King, and Igor F. Zhimulev

1. Introduction

Polytene chromosomes from the salivary gland cells of *Drosophila melanogaster* larvae have been the most useful model for studying the functional morphology of interphase eukaryotic chromosomes since their discovery almost 70 yr ago ***(1)***. The question remains as to whether the polytene structure is universal. How similar is the organization of polytene chromosomes in different tissues, because cell differentiation may lead to diverse functional chromosome states? The greatest difference can be expected to be seen between the chromosomes of the germ-line cells and the cells of somatic tissue.

1.1. Oogenesis and Development of Nurse Cells

Each of the two paired ovaries of the adult *Drosophila* female consists of a cluster of parallel ovarioles, where egg chambers are lying in a single-file arrangement (*see* **Fig. 1A,B**). Each egg chamber contains a branching chain of 16 interconnected cystocytes formed by mitotic division of a germarial cystoblast ***(2)***. Fifteen of the cystocytes differentiate into endopolyploid nurse cells (NCs) (*see* **Fig. 1C**). The function of these germ-line-derived cells is to synthesize RNA and protein molecules, which they transport through a system of ring canals into the oocyte ***(3)*** (*see also* Chapter 4).

The normal development of an egg chamber has been divided into 14 stages ***(4)***. Stages 1–6 are "previtellogenic," with intensive growth of all the cells that form each chamber. At stage 7, the process of transfer of yolk precursors from NCs into the oocyte begins. Vitellogenesis, accelerated growth by the oocyte

From: *Methods in Molecular Biology, vol. 247:* Drosophila *Cytogenetics Protocols*
Edited by: D. S. Henderson © Humana Press Inc., Totowa, NJ

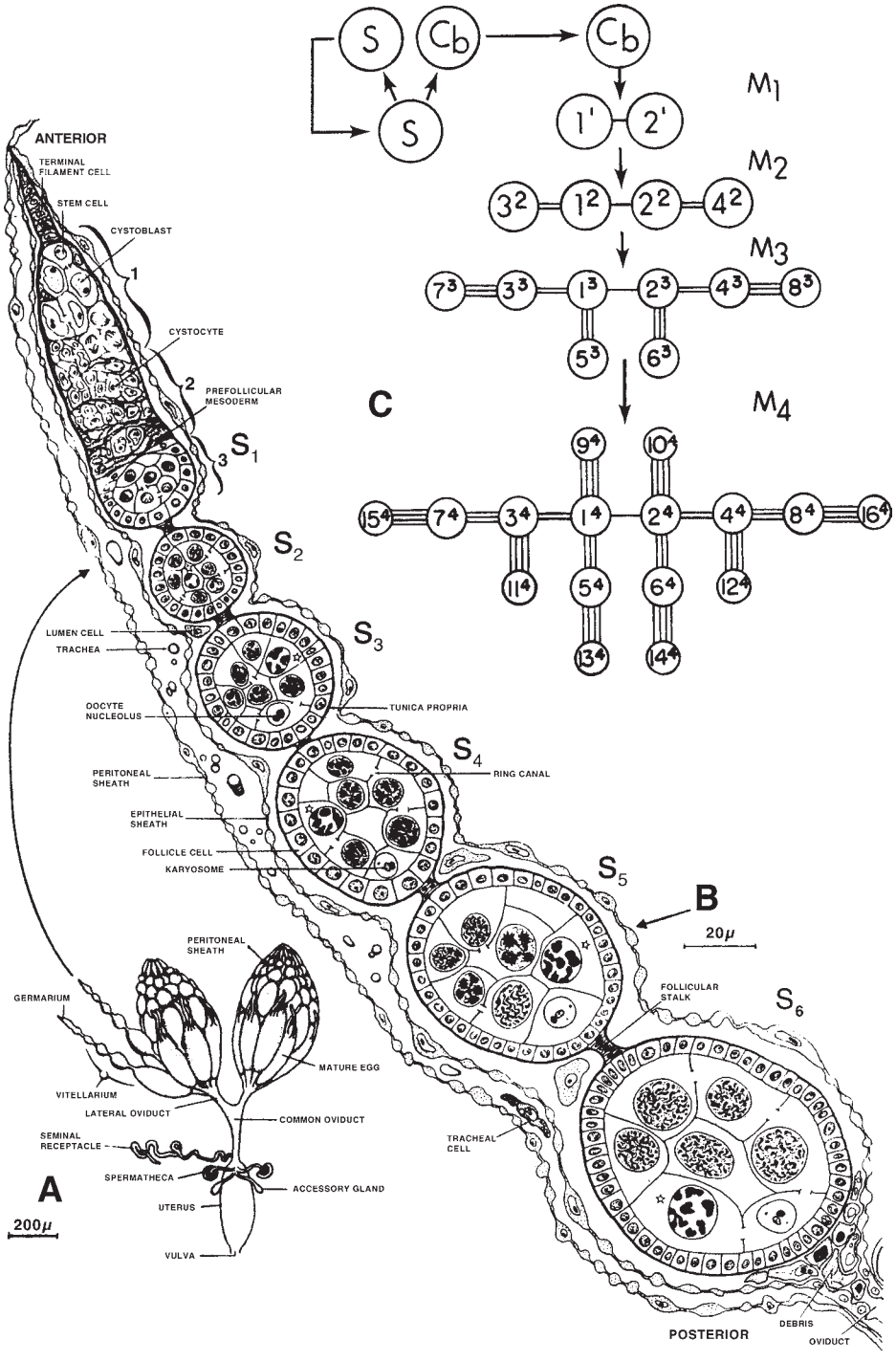
S
Cb
Cb
S
M1
1'
2'
M2
3²
1²
2²
4²
M3
7³
3³
1³
2³
4³
8³
5³
6³
C
M4
9⁴
10⁴
15⁴
7⁴
3⁴
1⁴
2⁴
4⁴
8⁴
16⁴
11⁴
5⁴
6⁴
12⁴
13⁴
14⁴
ANTERIOR
TERMINAL FILAMENT CELL
STEM CELL
CYSTOBLAST
CYSTOCYTE
PREFOLLICULAR MESODERM
S1
S2
S3
S4
S5
S6
LUMEN CELL
TRACHEA
OOCYTE NUCLEOLUS
TUNICA PROPRIA
PERITONEAL SHEATH
RING CANAL
EPITHELIAL SHEATH
FOLLICLE CELL
KARYOSOME
B
20μ
FOLLICULAR STALK
TRACHEAL CELL
DEBRIS
OVIDUCT
POSTERIOR
PERITONEAL SHEATH
GERMARIUM
MATURE EGG
VITELLARIUM
LATERAL OVIDUCT
COMMON OVIDUCT
SEMINAL RECEPTACLE
SPERMATHECA
ACCESSORY GLAND
UTERUS
VULVA
A
200μ

resulting from yolk accumulation, starts at stage 8. By stage 9, NCs also develop unusual nucleoli composed of a shell of interconnected fibers around the periphery of the nucleus. NCs retain more rRNA genes than other polyploid cells and synthesize rRNA at proportionately higher rates ***(5,6)***. By stage 10, NCs reach their maximum size and DNA content (1024–2048C) ***(7)***. Stage 11 is the shortest and marks the beginning of the postvitellogenic period, with apoptosis of NCs, and the completion of the vitelline membrane. During stages 12–14, beta yolk forms, and the egg shell and its appendages are synthesized.

The staging characteristics for *Drosophila* oogenesis were formulated after observations of Feulgen-stained, ovarian whole mounts ***(8)*** (*see* **Subheading 3.1.**). The NC nuclei in chambers belonging to stages 6–10 possessed a dispersed mass of Feulgen-positive threads (*see* **Fig. 1B**, S_6). Nuclei in stages 3 and 4 contained densely staining bulbous structures (*see* **Fig. 1B**, S_3 and S_4). The NCs in stage 5 were at an obviously intermediate state. The nuclei nearest the oocyte contained dispersed chromosomes like those in stage 6, whereas the rest resembled stage 4.

We know that the chromosomes in NCs undergo a cycle of endomitotic DNA replications ***(9)***. In NCs at stages 1–4, the paired homologs go through four endocycles, and the DNA is completely replicated each time with a total DNA content of 64C. At stage 5, the bivalents fall apart, starting with the NCs closest to the oocyte, and the polytene univalents subdivide further to form 32 separate chromatids, each containing the 2C amount of DNA and held together by unreplicated regions. There are three to four replication cycles, depending on the distance of the NC from the oocyte. During these cycles, which take place during stages 6–10, only about 90% of the DNA is replicated ***(9)***.

Fig. 1. **(A)** A dorsal view of the internal reproductive system of an adult egg laying female *Drosophila melanogaster*. Two ovarioles have been pulled loose from the left ovary (From **ref. *2***, Copyright ©1967, used with permission, Wiley-Liss, Inc., a subsidiary of John Wiley & Sons, Inc.). **(B)** A diagram of a single ovariole and its investing membranes. S_1-S_6 = previtellogenic stages of egg chambers; 1, 2, and 3 = regions of the germarium. The distribution of the nucleolar material is drawn in the starred NC nucleus, whereas the other NC nuclei show the appearance of the chromosomal material (From **ref. *2***, Copyright ©1967, used with permission, Wiley-Liss, Inc., a subsidiary of John Wiley & Sons, Inc.). **(C)** A diagram of the steps in the production of a clone of 16 cystocytes. S = stem cell, C_b = cystoblast, M_1–M_4 = four consecutive mitoses. The area in each cell is proportional to the volume of the cell. The canals connecting cells are labeled according to the division at which they were produced (*see* **ref. *3***) (From *A Dictionary of Genetics*, 6th ed, by Robert C. King and William D. Stansfield, ©1985, 1990, 1997, 2002 by Oxford University Press, Inc. Used by permission of Oxford University Press, Inc.)

Table 1
General Characteristics of Ovarian Phenotypes, Terminal Stage of Oogenesis, and Chromosome Morphology for Different *otu* Allelic Compositions

OAC	Q[a]	T[a]	P[a]	O[a]	AS	APC	ARC	P[b]	HP[b]	C[b]	N[b]
7/7	2	0	26	72	p12	p12	12	284	151	76	0
11/11	0	0	53	47	p14	10B	10	89	82	113	266
7/11	1	4	48	47	14	10B	10	23	51	132	331
11/14	0	1	2	97	14	10B	10	—[c]	—[c]	—[c]	—[c]

Abbreviations: OAC = *otu* allelic composition; Q = quiescent germaria; T = ovarian tumors; P = PNC chambers; O = oocyte–NC chambers and mature eggs; AS = most advanced stage of oogenesis; APC = most advanced stage of polytene chromosomes; ARC = most advanced stage in replication cycle; P = pompons; HP = half-pompons; C = condensed; N = normal.

[a] Number per 100 ovarioles; QTPO values for 7/7 and 11/11 were from flies reared at 18°C; values for 7/11 and 11/14 are for flies reared at 23°C.

[b] Number of nuclei of each type observed on 20 slides prepared from 20 ovaries of flies of each genotype

[c] No data available.

Source: Data from ***refs. 13,17,18***.

1.2. Polytene Chromosomes in Developing Nurse Cells

Three mutations that block oogenesis, *fs(2)B*, *fs(2)cup,* and *ovarian tumor* (*otu*), also affect the development of NC chromosomes. Some of their alleles result in the formation of giant banded, polytene chromosomes ***(10–12)***.

The *otu* gene has been shown to transcribe at least two mRNAs and the proteins these translate have multiple functions during oogenesis ***(13–15)***. There are 17 mutant aleleles that have been induced by ethyl methane sulfonate (EMS), and these are divided into three major classes according to their ovarian phenotypes. Ovarian development is blocked earliest in mutants of the quiescent (QUI) class. Homozygotes have quiescent germarial stem cells, so the ovarioles are "agametic." The ovaries from mutants of the oncogenic (ONC) class contain ovarioles with tumorous chambers, and the differentiated class (DIF) produces ovarioles with chambers containing differentiated cells. Some of these chambers lack oocytes and contain a reduced number of cells that resemble NCs in size and morphology. They are called pseudonurse cells (PNC) because they do not have an oocyte to nurse. Other chambers have an oocyte (O) and true NCs, and so they form NC/O syncytia ***(16)***. All mutants carry chambers of all types but in different proportions (*see* **Table 1**). Many of the *otu* alleles are temperature sensitive. If the culturing temperature is lowered from 28°C to 18°C the frequency of NC/O chambers increases significantly in otu^{7}/otu^{7} and otu^{11}/otu^{11} ovaries ***(19)***. Both PNCs and the NCs of NC/O

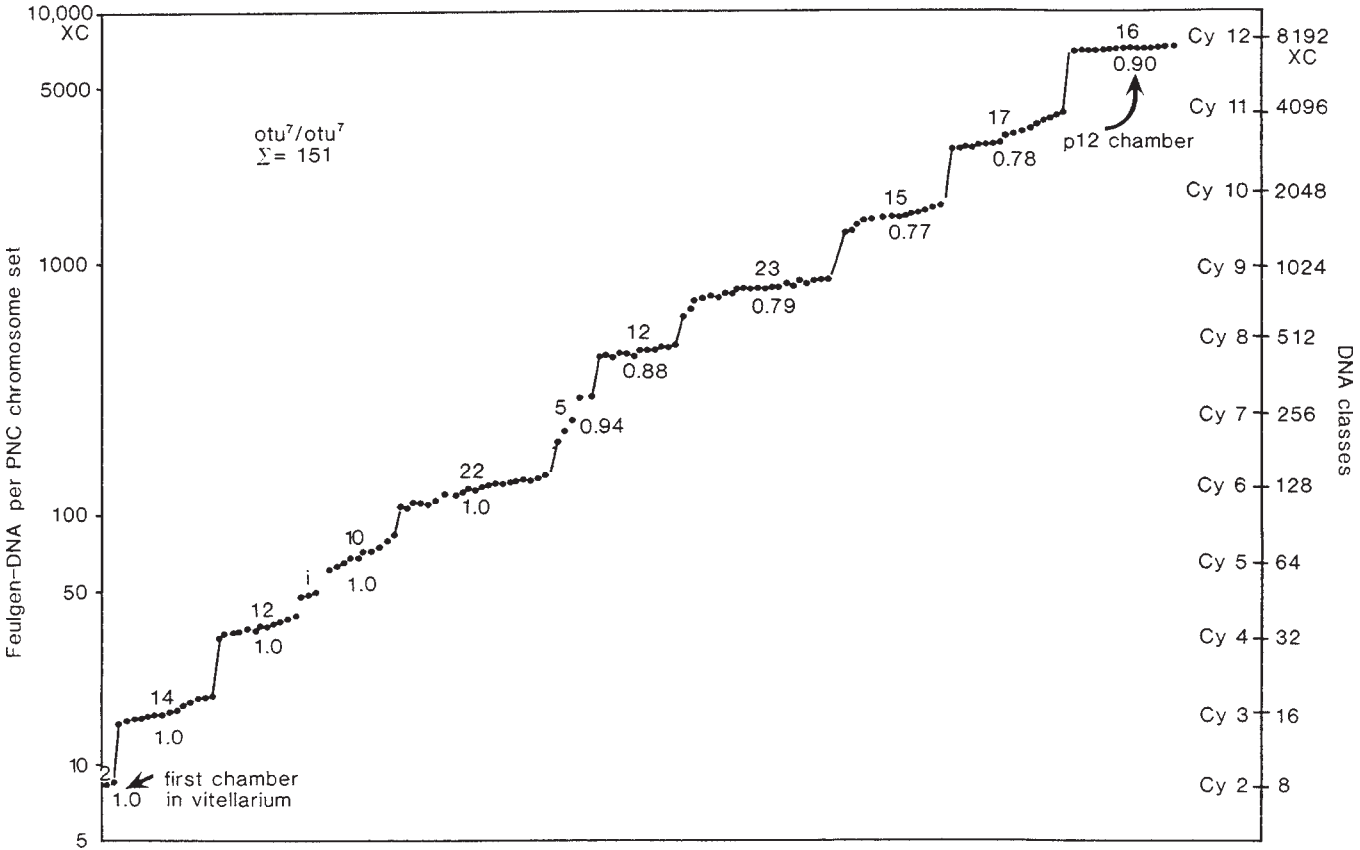

Fig. 2. Measurements of the DNA contents (expressed as multiples of the C value) of 151 sets of PNC chromosomes from an *otu*^{7}*/otu*^{7} ovary. The right vertical axis shows the C values expected after 2–12 endomitotic cycles of DNA replication. The numbers above each "step" show the number of estimates in each series. The decimals show the ratios between the medians for the series and the expected DNA values for the appropriate cycles. A cluster of three nuclei with DNA values intermediate between the cycle 4 and 5 series is labeled with an *i* (Reprinted with permission from **ref. *23***.).

syncytia of certain mutants contain polytene chromosomes ***(11,13,17,19–22)***. The level of polytenization in NCs and PNCs of different *otu* mutants may vary in wide range from 128–512C to 1024C or even 2048–8192C ***(7,23)***.

Oocytes of otu^7 homozygotes are blocked at the p12 stage and die as dwarf, shelled eggs that lack glycogen-rich, beta yolk spheres ***(24)***. Eggs of otu^{11} homozygotes grow to an almost normal size and can be fertilized and laid. However, because the embryos die at an early stage, the defective eggs are called p14's to distinguish them from normal-stage 14's. The otu^7/otu^{11} females are moderately fertile and otu^{11}/otu^{14} females have excellent fertility.

In the NC nuclei of otu^7/otu^7, homologs remain paired; they elongate slowly, and undergo replication cycles while remaining in register. During the first six endocycles, 100% of the DNA replicates; thereafter, only 80–90% replicates during each endocycle (*see* **Fig. 2**). During stages 10–p12, the NC undergo supernumerary DNA replications, and the polytene chromosomes that result reach DNA values of almost 8192C ***(23)***.

We have studied otu^7, otu^{11}, and otu^{14}, and their interallelic combinations and have found chromosomes from otu^7/otu^{11}, otu^{11}/otu^{11}, and otu^{11}/otu^{14} to be of the best quality. The otu^1 (formerly *fs231*) allele belongs to the ONC class. However, in combination with *fs(2)B*, PNCs with polytene chromosomes do occur ***(11)***. Photomaps of PNC polytene chromosomes made by Heino ***(22,25)*** were from females of genotype otu^1/otu^1; *fs(2)B*/+ reared at 18°C.

1.3. Characteristics of Polytene Chromosomes from Ovarian Pseudonurse and Nurse Cells of otu *Mutants*

1.3.1. General Morphology, Chromosome Maps, Puffing Activity, and Protein Localization

The PNC and NC chromosomes from *otu* mutants vary greatly in their length, level of polyteny, and banding pattern (*see* **Fig. 3**). All the chromosomes can be classified by length into four major classes: "pompon" chromosomes (P) (*see* **Fig. 3A,D**) [for use of terms, *see* review by Zhimulev ***(26)***], "half-pompons" (HP) (*see* **Fig. 3B,C**), "condensed" (C) (*see* **Fig. 3G**) and "normal" (N) (*see* **Fig. 3E,F,H**). P chromosomes are the shortest, HP are approximately twice as long as pompons (although still quite short), C chromosomes form a class that includes chromosomes with lengths between HP and N. Class N includes chromosomes with lengths close to those of salivary gland (SG) chromosomes. Also, several groups within each class were distinguished based on chromosome thickness ***(18)***.

The NCs of otu^7/otu^7 flies contain mainly nuclei with P and HP chromosomes. The otu^{11} homozygotes show all the types of chromosome morphology. A heteroallelic combination of otu^7/otu^{11} results in a shift of the

distribution in the direction of the normal class (*see* **Table 1**). Few chromosomes of P and HP classes occur, the percentage of condensed and normal chromosomes increases, and a new group of N extra-large chromosomes appears (*see* **Fig. 3H**) ***(18)***.

Initially, we worked with otu^{11} mutants, so photomaps were made using the N class chromosomes from NCs and PNCs of otu^{11}/otu^{11} females (*see* **Figs. 4–6**). Thorough comparisons of the banding patterns of SG and PNC and NC chromosomes has revealed good correlations except for five regions, where no similarity occurs. These regions are shown by brackets on 2L at 24, 30, and 38 (*see* **Fig. 5**) and on 3L at 66, and on 3R at 95 (*see* **Fig. 6**). In many cases, the corresponding bands in SG chromosomes are split in PNC and NC chromosomes (21C1-2, 22C, 23D1-2, 23E1-2, 30AB, 48F, 51AB, 55C, 57E, 61C, 65D, 66E, 71A and 93F) ***(22,25,27)***.

The PNC and NC chromosomes develop a few large and many very small puffs. The main large puffs are 3CD, 7E, 8C, 11B, 22F, 42AB, 47A, 61AB, and 79D ***(18,22,25,27)***. Telomeric puff 61AB is the largest (*see* **Fig. 7G**). Chromosomes from the NCs of one egg chamber have the same puff pattern (*see* **Fig. 7A–C**), but chromosomes from different stages of egg chamber development show subtle differences in their puff patterns (*see* **Fig. 7D–F**) (Mal'ceva, unpublished data).

To investigate the location of induction of ecdysteron-induced puffs in polytene chromosomes from NCs, ovaries from females of otu^{7}/otu^{11} genotype were incubated for 2–6 h at 25°C or 3–24 h at 16°C in ecdysteron-containing organ culture medium. In another experiment, preincubation of NCs in an ecdysteron-free medium for 12 or 6 h was followed by incubation with ecdysteron for 8 or 6 h, respectively. NC chromosomes did not form puffs in response to ecdysone under these experimental conditions ***(28)***.

It is difficult to induce a heat-shock response in PNC and NC chromosomes. Flies homozygous for otu^{7} were temperature shocked to induce expression of the *hsp* genes, followed by *in situ* hybridization of the *hsp26* probe to polytene chromosomes. In some PNC nuclei, a very faint signal was found ***(29)***. Long incubation in vitro of ovaries from otu^{7}/otu^{11} flies in ecdysteron-containing medium causes formation of tiny *hsp* puffs in 63B, 67B, 83A, and 97D regions ***(28)***.

The PNC and NC chromosomes can be used for immunofluorescent localization of different proteins using antibodies. It is interesting to compare localization of the same proteins in somatic and germ-line cell polytene chromosomes. Data were obtained for Mod (product of the *modulo* gene) and HP1 [heterochromatin protein 1, product of the *Su(var)2–5* gene]. In SG nuclei, anti-Mod antibodies prominently label the nucleolus, although pericentric heterochromatin and the majority of euchromatic bands are also stained. In PNCs, there is

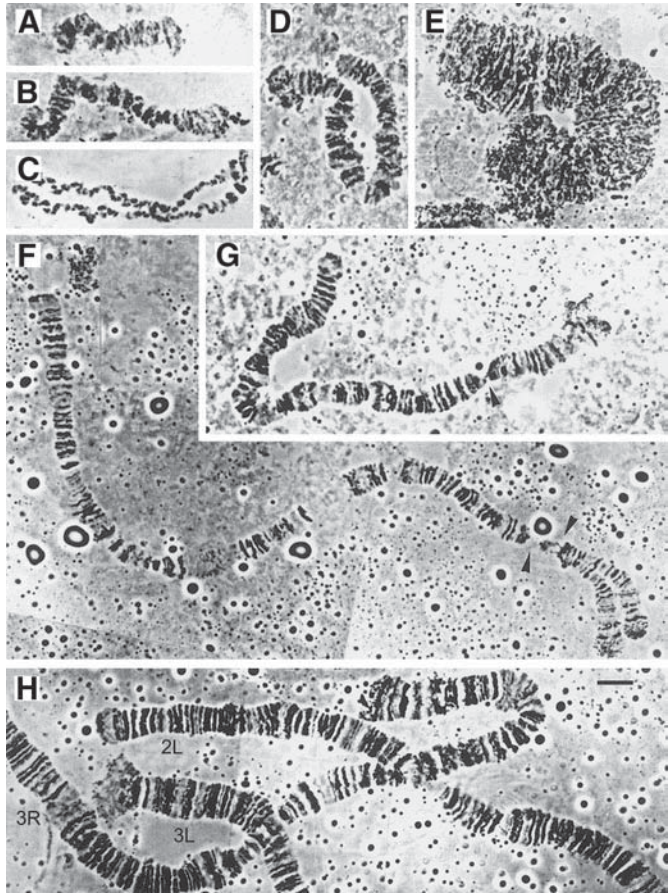

Fig. 3. Types of chromosomal morphology of the 2L chromosome. In all cases (except **c**) the telomere is to the left. **(A)** middle-size pompon chromosome, **(B)** middle-size half-pompon chromosome, **(C)** large half-pompon chromosome, **(D)** extra-large pompon chromosome, **(E)** very thin, beaded polytene chromosome, **(F)** large normal chromosome, arrowheads show the weak points in 36C and D regions, **(G)** large-size condensed chromosome, arrowhead shows the weak point in 36D region, **(H)** extra-large chromosomes with normal banding pattern. Only three-fourths of the 2L chromosome is shown. The bar equals 10 µm. (From **ref. *18***. Copyright ©1997, used with permission, Wiley-Liss, Inc., a subsidiary of John Wiley & Sons, Inc.)

intense staining of nucleoli, but the chromosome arms stain weakly, except for a few dense bands ***(30)***. Localization of HP1 also shows many differences between SG and PNC chromosomes in number and position of sites (Koryakov,

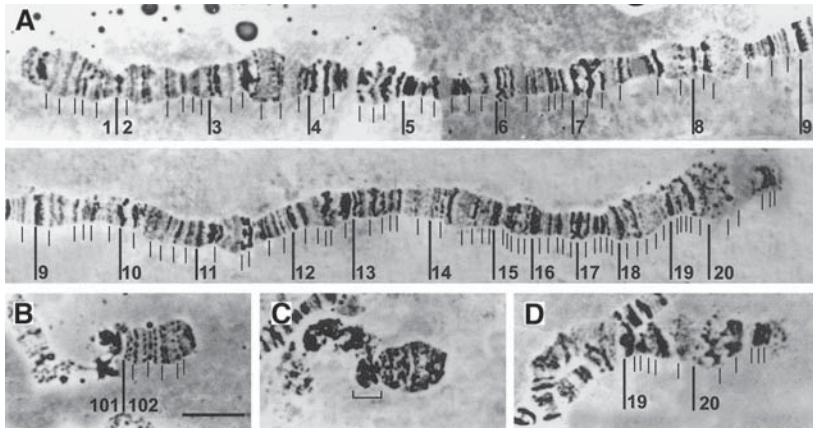

Fig. 4. Photomaps of the X chromosome (sections 1–20) **(A,D)** and chromosome 4 (sections 101–102) **(B,C)** from PNC of an *otu*^{11} mutant. The bracket marks granular material to the left of the 102A region, which often can be seen in chromosome 4. The bar equals 10 μm. (From **ref. *27***. Copyright ©1995, used with kind permission from Kluwer Academic Publishers.)

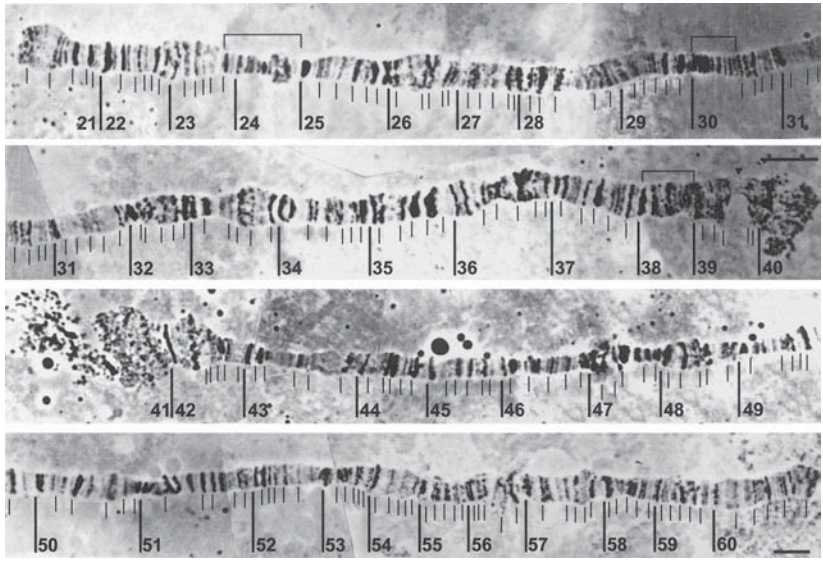

Fig. 5. Photomaps of the left (sections 21–40) and right (sections 41–60) arms of chromosome 2 from PNC of an *otu*^{11} mutant. Brackets show regions where no similarity with the photomaps of SG polytene chromosomes was found. Arrowhead marks weak point in 39DE region. The bar equals 10 μm. (From **ref. *27***. Copyright ©1995, used with kind permission from Kluwer Academic Publishers.)

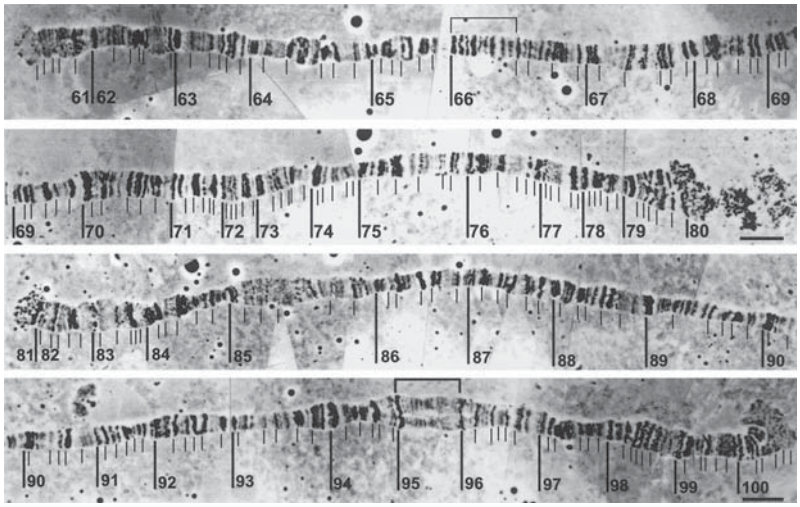

Fig. 6. Photomaps of the left (sections 61–80) and right (sections 81–100) arms of chromosome 3 from PNC of an *otu*^{11} mutant. Brackets show regions where no similarity with the photomaps of SG polytene chromosomes was found. The bar equals 10 μm. (From **ref. *27***. Copyright ©1995, used with kind permission from Kluwer Academic Publishers.)

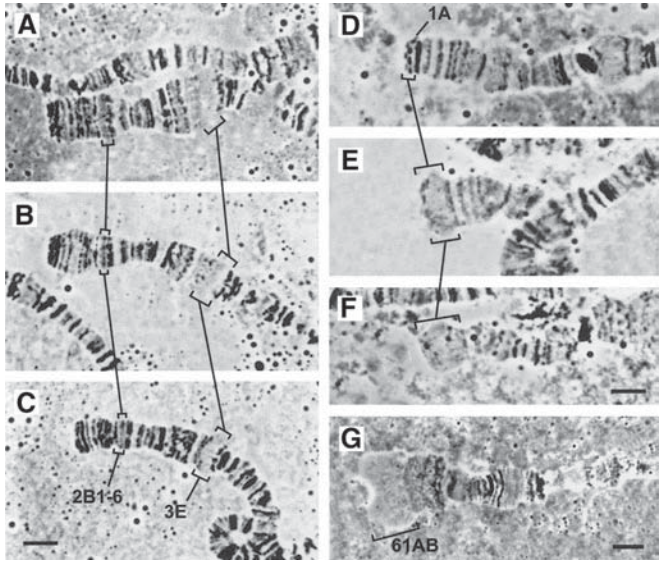

Fig. 7. **(A–C)** Telomeric regions of the X chromosomes with different degrees of polyteny from one egg chamber have the same puff pattern. **(D–F)** Puff formation in 1A region. **(G)** Giant telomeric puff 61AB. The bar equals 10 μm. (Courtesy of N. I. Mal'ceva, unpublished data.)

unpublished data). An example of HP1 localization on a PNC polytene chromosome can be seen in **Fig. 8**.

1.3.2. Heterochromatin Morphology in Pseudonurse and Nurse Cell Chromosomes

Pericentric regions of SG polytene chromosomes are usually involved in nonhomologous associations that result in a structure called the chromocenter. In PNC and NC polytene chromosomes, the chromocenter consists of blocks of polytenized material connected by tiny threads, which can be easily broken during squashing (*see* **ref. *20***, Fig. 8B). Sometimes, bands and even puffs can be seen inside these blocks (*see* **Fig. 9**) ***(27,31–33)***. The pericentric region of the X chromosome in PNC and NC contains a characteristic banding pattern in region 20A–F (*see* **Fig. 4D**), which is rarely seen in SG chromosomes ***(27,31)***. Using a number of chromosome rearrangements and DNA clones with known localization in mitotic heterochromatin, a correspondence was found between polytenized material in PNC autosomes and differentially stained blocks in mitotic chromosomes. The polytenized material in pericentric regions of chromosomes 2 and 3 originates from proximal mitotic heterochromatin rather than proximal euchromatin or material from eu-heterochromatic junction regions (***32–34***, Domanitskaya and Koryakov, unpublished data).

The genetic inactivation of euchromatic genes placed next to pericentric heterochromatin by a chromosomal rearrangement is accompanied by the compaction of corresponding euchromatic chromosome regions (so-called position-effect variegation). A comparative study of the manifestation of position-effect variegation for the polytene chromosomes of SGs and NCs was made using the *Dp(1;1)pn2b* and *Dp(1;f)1337* rearrangements. The percentage frequencies of block formation in the SG and NC nuclei for *Dp(1;1)pn2b* were 92.6% vs 15.8%, respectively; for *Dp(1;f)1337*, these values were 56.8% vs 9.7%, respectively. Therefore, pericentric heterochromatin belonging to germ-line chromosomes is in a configuration that is far less likely to inactivate inserted segments of euchromatin than is heterochromatin from somatic chromosomes ***(18)***.

In polytene chromosomes, there are several sites, which, because of their characteristics, are believed to be the sites of intercalary heterochromatin ***(35)***. Usually, they form weak points where chromosome breaks occur, and they tend to form ectopic contacts with nonhomologous sites and pericentric regions of chromosomes. In PNC chromosomes, breaks were observed in at least 11 sites of the X chromosome, 8 sites of chromosome 2L, 5 sites of 2R, 5 sites of 3L, and 13 sites of 3R, but their frequency is substantially lower in PNC chromosomes than in those from SG cells. In regions 36C, 36D, 39E, and 56F, frequencies of breaks are comparable with those in SG chromosomes (*see* **Figs. 3F,G** and **5**) (***27***; Koryakov, unpublished data).

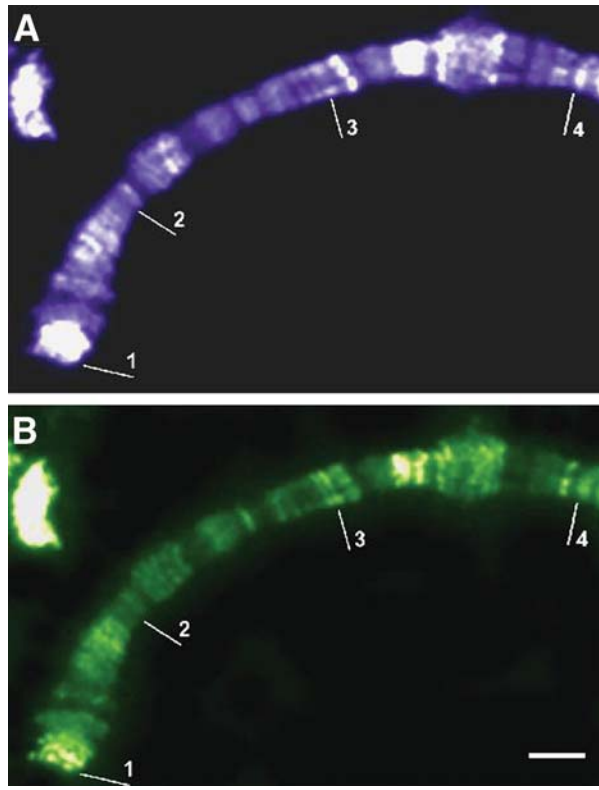

Fig. 8. The distal part of the X chromosome from an *otu*^{11} homozygote with a fluorescence microscope. **(A)** The chromosome was stained with DAPI, so the bright blocks and bands localize DNA. **(B)** The chromosome was stained with the CIA9 antibody against HP1. A comparison of **A** and **B** localizes brightest signals of HP1 to regions 1A, 1F, 2D, 3A, 3C, 3E, and 3F. (Courtesy of D. E. Koryakov, unpublished data.) (*See* color plate 4 in the insert following p. 242.)

The frequency of formation of ectopic contacts between different PNC chromosome regions is 10 times less than in the polytene chromosomes of SG cells. The regions that form ectopic contacts in PNC chromosomes are 2C, 3AB, 9A, 10A, 11A, 11D, 12D, 12E, 26C, 28D, 48D, 49A, 58A, 58F, 59A, 60E, 66E, 67CD, 67E, 69D, 70A, 75F, 76B, 98D, and 99A ***(27)***.

In PNC chromosomes from both *otu* and *fs(2)B* mutants, asynapsis occurs both between the two homologs and between the bundles of chromatids within each homolog. One of the main features of *fs(2)B* chromosomes is the incomplete association (or secondary splitting) of the chromatids. Sometimes, complex reconjugations of parts of different homologs are seen (*see* **Fig. 10**). Such

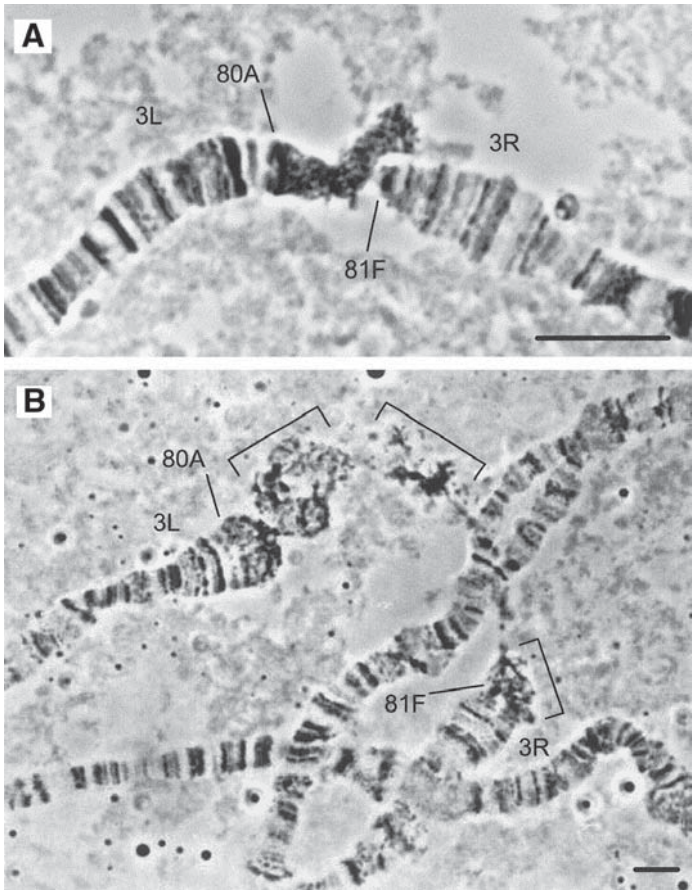

Fig. 9. Structure of the pericentric heterochromatin of chromosome 3. **(A)** Part of the chromocenter with pericentric regions of SG chromosome 3 from an otu^{11} homozygote; **(B)** PNC chromosome 3 from an otu^{11} homozygote carrying *Dp(1;f)1337*. The brackets mark heterochromatic material. The bar equals 10 μm. (Courtesy of D.E. Koryakov and N.I. Mal'ceva, unpublished data.)

splitting of individual homologs is very rare in NC chromosomes of *otu* mutants, with the exception of otu^{11}/otu^{14} (Mal'ceva, unpublished data). Asynapsis between homologs in PNC chromosomes in all of these mutants is much more frequent than in SG chromosomes, especially in regions 19–20, 39–40, 41–42, 79–80, and 81 ***(27)***.

From the above, it is clear that polytene chromosomes of *otu* mutants can serve as a useful model for studying features of gene expression and eu- and heterochromatin behavior.

2. Materials

1. Fly stocks: All fly stocks were cultured at 16°C under uncrowded conditions on protein-rich medium (*see* **item 2**). All experiments were performed with females of either otu^7/otu^{11}, otu^{11}/otu^{11}, or otu^{11}/otu^{11} carrying a Y chromosome (*see* **Note 1**). The X chromosome, bearing the otu^{11} allele carried the *y*, *w,* and sn^3 mutations, whereas the chromosome with otu^7 was free of markers. The *FM3* chromosome was used to balance the stocks. Descriptions of all the markers and the *FM3* balancer can be found in **ref. *36***.

   The flies of the $otu^7/y\ w\ sn^3\ otu^{11}$ genotype were obtained by crossing *FM3/* otu^7 females with $y\ w\ sn^3\ otu^{11}/Y$ males. Therefore, the otu^7 allele was always contributed by the mother and otu^{11} by the father. This point is stressed, because otu^{11}/otu^7 ovaries generate fewer functional oocytes ***(17)***.
2. Culturing medium: 100 g baker's yeast, 50 g corn meal, 40 g ground raisins, 20 g sugar, 10 g agar, 4 mL proprionic acid (serves as fungicide), made up to 1 L. Supplement with live moist yeast on surface.
3. Ephrussi–Beadle solution: 7.5 g NaCl, 0.35 g KCl, 0.28 g $CaCl_2{\cdot}2H_2O$ (or 0.42 g $CaCl_2{\cdot}6H_2O$), and water to 1 L.
4. Leucobasic fuchsin: The methods for preparing this reagent can be found in Chapter 7.
5. Acetic orcein:
   a. Pour 45 mL of 100% acetic acid into a flask, add 1 g of dry orcein. Cork the flask but NOT tightly!
   b. Bring the acid with orcein to VERY WEAK boiling (several bubbles) for 25–30 s.
   c. Add (carefully!) 55 mL of distilled water and heat back to a very weak boiling for 25–30 s.
   d. Cool the flask to room temperature and add 1 *N* HCl in proportion 9 parts of staining solution to 1 part of HCl. Filter this mixture. This stock solution can be kept for months at room temperature.
   e. Mix 2 parts of stock solution with 1 part of 45% acetic acid and filter this mixture. This staining solution is good for weeks.
6. Denaturation solution: 0.07 *N* NaOH, 2X SSC (*see* **item 21**).
7. Hybridization buffer (1.5X): 70% Formamide, 15% dextran sulfate, 3X SSC (*see* **item 21**).
8. Blocking solution: 4X SSC (*see* **item 21**), 0.1% Triton X-100, 2% Blocking Reagent (Roche Diagnostics GmBH, cat. no. 1 096 176) or 4% powdered milk (i.e., 4 g of powdered milk per 96 mL of blocking solution).
9. Cohen and Gotchell medium G: 25 m*M* di-sodium glycerophosphate, 10 m*M* KH_2PO_4, 30 m*M* KCl, 10 m*M* $MgCl_2$, 3 m*M* $CaCl_2$, 160 m*M* sucrose, 0.5% NP-40. This solution can be kept at 4°C for 2–3 d.
10. Formaldehyde fixative: 100 m*M* NaCl, 2 m*M* KCl, 20 m*M* sodium phosphate, 2% NP-40, 2% formaldehyde.
11. Phosphate-buffered saline (PBS)-glycerol: 33 mL of PBS (*see* **item 24**), 67 mL of glycerol.

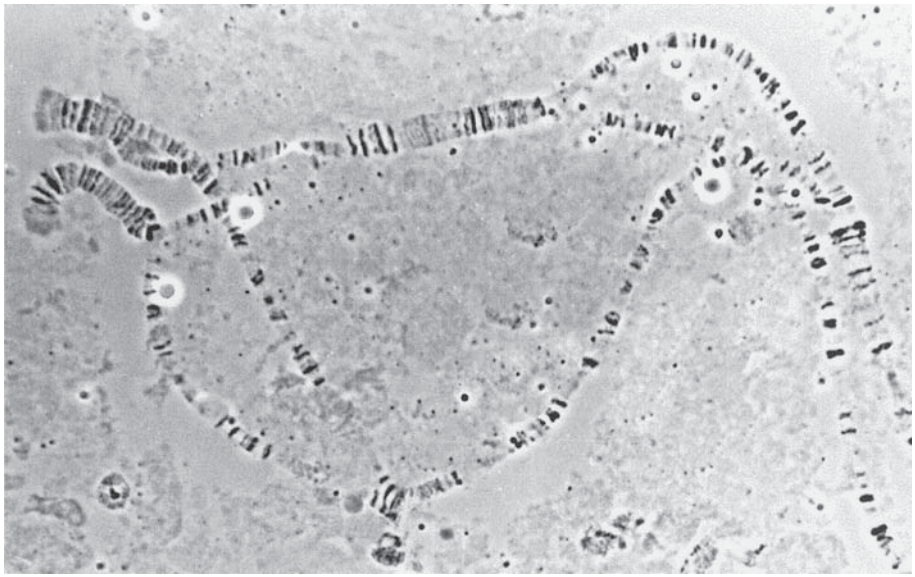

Fig. 10. Example of the complex asynapsis in chromosome 2L from a *fs(2)B* homozygote. The bar equals 10 µm. (From **ref. *27***, Copyright ©1995, used with kind permission from Kluwer Academic Publishers.)

12. TBS–Tween: 10 m*M* Tris-HCl, pH 7.15, 250 m*M* NaCl, 0.05% Tween-20 (*see* **Note 2**).
13. Ether.
14. 45% Acetic acid.
15. 55% Lactic acid.
16. Ethanol (10%, 50%, 70%, 80%, 96%, and 100%).
17. Ethanol-xylene (1 : 1).
18. Xylene.
19. 1 *N* HCl.
20. Water saturated with SO_2.
21. SSC (0.2X, 2X, 3X, 4X): Stock solution 20X SSC contains 3 *M* NaCl and 0.3 *M* sodium citrate, pH 7.0. Other concentrations can be made by dilution of the stock solution.
22. 10% NP-40.
23. 0.1% Triton X-100 in 4X SSC.
24. PBS: 10X Buffer contains 11.5 g Na_2HPO_4, 2 g KH_2PO_4, 80 g NaCl, and 2g KCl per liter of water.
25. Fluoresein-isothiocyanate (FITC)–avidin dissolved in blocking solution (*see* **item 8**) at a final concentration of 25 µg/mL.

26. Biotinylated antiavidin antibodies (e.g., biotinylated, goat antiavidin D from Vector Laboratories, cat. no. BA-0300) dissolved in blocking solution (*see* **item 8**) at a final concentration of 1–10 µg/mL.
27. 4'-6-diamidino-2-phenylidole (DAPI) dissolved in 0.2X SSC (1 µg/mL).
28. Propidium iodide dissolved in 0.2X SSC (5 µg/mL).
29. Vectashield Antifade mounting medium.
30. Salmon sperm DNA.
31. Very fine needles (preferably tungsten), approx 0.2–0.3 mm in diameter, for dissection. Needles with curved tips are sometimes very helpful.
32. Blotting paper.
33. Microscope slides and cover slips.
34. Petri plates.
35. Liquid nitrogen.

3. Methods

3.1. Feulgen-Stained Ovarian Whole Mounts

1. Dissect ovaries in Ephrussi–Beadle solution.
2. Drop approx 20 ovaries into a small vial containing 1 *N* HCl at 60°C; maintain at this temperature for 14 min. To change solutions, gently pour out fluids. Use a clean micropipet to squirt in each new solution. Handle tissue gently.
3. Stain in leucobasic fuchsin until apical portions of the ovary take on a deep violet color (5–60 min).
4. Rinse ovaries two times in water saturated with SO_2, 10% ethanol, 95% ethanol, 100% ethanol, ethanol-xylene (1 : 1), and xylene.
5. Transfer stained ovaries in a drop of xylene to a clean microscope slide. Tease the ovary into its constituent ovarioles. Put a drop of permount over the tissue and cover with a cover slip.

3.2. Orcein-Stained Squashes for Morphological Analysis of Chromosomes

1. To get females of the required genotype, put six to seven pairs of flies per vial with standard medium. Keep at 16°C. At this temperature, the life cycle of flies is approx 30 d.
2. Separate newly emerged females homozygous for the *otu* mutation and put them into vials with fresh medium. Keep the females at 16°C.
3. After 5–11 d, put etherized females in a Petri plate with Ephrussi–Beadle solution and dissect out the ovaries (*see* **Note 1**).
4. Gently transfer whole ovaries to acetic orcein for up to 1 h (*see* **Note 2**).
5. Transfer a stained ovary to a drop of 55% lactic acid on a microscope slide and then using needles separate the ovarioles from peritoneal and tracheolated epithelial sheaths, mature eggs and shelled oocytes, retaining NCs from terminal and subterminal normal stages 7–12 and p12s. Remove all unnecessary materials from the drop. The best NC chromosomes are from stages 9–11 and p12.

6. Cover the drop with a cover slip and spread the chromosomes by gently moving the cover slip back and forth (*see* **Note 3**). Put two to three layers of blotting paper on top of the cover slip and press down gently with your thumb. Remove the excess acid solution with blotting paper.
7. View the chromosomes under a phase-contrast microscope. These preparations remain suitable for analysis for 2–3 wk while stored at 4°C.

3.3. Fluorescent In Situ *Hybridization (FISH)*

3.3.1. Preparation of Squashes

1. Follow **steps 1–3** of **Subheading 3.2.**
2. Transfer a whole ovary to a fresh drop of Ephrussi–Beadle solution. Separate the ovarioles from peritoneal and tracheolated epithelial sheaths, mature eggs, and shelled oocytes, retaining NCs from terminal and subterminal egg chambers.
3. Using tiny needles, transfer five to six selected egg chambers to a drop of 45% acetic acid on a microscope slide. Incubate the egg chambers for a couple of minutes.
4. Cover the drop with a cover slip and make a squash as in **Subheading 3.2., step 6**.
5. Immerse the slide in liquid nitrogen and, when frozen, flip off the cover slip with a razor blade.
6. Give each slide three consecutive 5-min rinses in 96% ethanol.
7. Air-dry the slide.
8. Observe the chromosomes under phase-contrast optics (*see* **Note 4**).

3.3.2. Denaturation of Chromosomes

It is important here, and in **Subheadings 3.3.3.** and **3.3.4.**, to keep the slides MOIST in all steps except where noted.

1. Keep the slides in 2X SSC at 65°C for 60 min.
2. Wash the slides in 2X SSC at room temperature for 5 min.
3. Denature the slides in denaturation solution at room temperature for 1.5 min.
4. After denaturation, immediately transfer the slides to 70% ethanol at –20°C, and keep them there for 5 min.
5. Wash the slides in 80% and 96% ethanol at –20°C for 5 min each.
6. Air-dry the slides.

3.3.3. Hybridization With Probe

1. Mix a biotinylated DNA probe (0.1 µg per slide), competitor DNA (e.g., 0.2–0.3 µg salmon sperm DNA per slide) and water (*see* **Note 5**).
2. Heat the mixture at 100°C for 5 min.
3. Add 2 vol of 1.5X hybridization buffer and mix thoroughly.
4. Heat this mixture at 75°C for 2 min.
5. Drop 30 µL of the mixture per slide, cover with a cover slip, and seal the edges with rubber cement.
6. Keep the slides in a humid chamber with 2X SSC at 37°C overnight.

3.3.4. Detection of Signal

1. Wash the slides three times in 0.2X SSC at 60°C for 15 min.
2. Keep slides in blocking solution at 37°C for 30 min.
3. Drop 25 µL of FITC–avidin per slide, cover with a cover slip, and incubate the slides in a humid chamber at 37°C for 30 min.
4. Wash the slides three times at 42°C for 5 min each with 4X SSC containing 0.1% Triton X-100. After these washes, the slides can be stored in 0.2X SSC at 4°C for at least 48 h.
5. Stain the slides with propidium iodide for 5–10 s or with DAPI for several minutes (*see* **Note 6**).
6. Air-dry the slides, add a drop of antifade reagent to an area of the squash, and cover with a cover slip.
7. View the chromosomes using a microscope appropriate for the DNA stain.

3.3.5. Enhancement of the Signal

The brightness of weak fluorescent signals may be enhanced using the following procedures, one or more times. However, it should be kept in mind that all nonspecific signals will be enhanced as well.

1. Remove the cover slips from the slides to be treated.
2. Wash the slides twice at room temperature for 5 min with 4X SSC containing 0.1% Triton X-100.
3. Drop 25 µL of biotinylated antiavidin per slide, cover with a cover slip, and incubate the slides in a humid chamber at 37°C for 30 min.
4. Wash the slides twice in 4X SSC, 0.1% Triton X-100 at 42°C for 5 min.
5. Follow **Subheading 3.3.4., steps 3–7**.

3.4. Staining Chromosomes With Antibodies to Proteins

We have tested this protocol using antibodies against Mod ***(30)*** and HP1 (Mal'ceva, N. I. and Demakova, O. V., unpublished data; Koryakov, D. E., unpublished data). An example of this staining is shown in **Fig. 8**. This method is based on protocol 30 in **ref.** ***37*** and **ref.** ***38***, with minor changes. It is important AT ALL STEPS of this protocol, except the last, to KEEP THE SQUASHES WET!

3.4.1. Preparation of Squashes

All solutions for this method should be kept at 4°C during all procedures.

1. Follow **Subheading 3.2., steps 1–2**.
2. Dissect whole ovaries in a drop of Cohen and Gotchell medium G (containing NP-40) or in Ephrussi–Beadle solution containing 0.5% NP-40 at room temperature and transfer them to a fresh drop of the same solution. Incubate ovaries in this solution for 3–5 min.

3. Transfer the ovaries to formaldehyde fixative for 10–20 min (*see* **Note 7**).
4. Transfer the ovaries to a drop of 45% acetic acid on a microscope slide and keep there for 2–3 min.
5. Using fine needles, separate ovarioles from peritoneal and tracheolated epithelial sheaths, mature eggs and shelled oocytes, retaining NCs from terminal and subterminal chambers (stages 7–12). Remove all unnecessary tissue material from the drop.
6. Cover with a cover slip and make a squash (*see* **Subheading 3.2., step 6**).
7. Immerse the slide in liquid nitrogen until frozen and flip off the cover slip with a razor blade.
8. Transfer the slide to TBS immediately.
9. Store the slides in TBS at 4°C. If the slides are not to be used within 24 h, then store in PBS-glycerol at –20°C. Slides can be kept in this solution for 1–2 d, and even up to a week.

3.4.2. Staining With Antibodies

1. Remove the slides from storage medium (PBS-glycerol) and wash three times in TBS-Tween at room temperature, 5 min each wash.
2. Remove the slides from TBS-Tween, dry the bottom of the slides quickly with a piece of blotting paper, and add 15–20 µL of primary antibodies to the squash immediately, then cover it with a cover slip (*see* **Note 8**).
3. Keep the slides in a humid chamber at 4°C overnight (*see* **Note 9**).
4. Rinse the slides three times, for 5 min each, with ice-cooled (4°C) TBS-Tween.
5. Remove the slides from TBS-Tween, dry the bottom of the slides quickly with a piece of blotting paper, and immediately add 15–20 µL of secondary FITC-labeled antibodies to the squash, then cover with a cover slip.
6. Keep the slides in a humid chamber at room temperature for 2 h.
7. Rinse the slides three times for 5 min each in TBS-Tween at room temperature.
8. Air-dry the slides.
9. Stain slides with DAPI and view with ultraviolet (UV) light under a fluorescence microscope.

4. Notes

1. Ovarian function is extremely sensitive to nutritional and environmental resources. Presence of males accelerates ovary development and egg maturation ***(6)***. An additional Y chromosome also influences the rate of ovary development and the cytological quality of NC chromosomes. Ovaries of Y-containing females were observed to develop faster and more of their egg chambers reached stage 10 during 4–6 d at 16°C. The percentage of polytene chromosomes of good quality in NCs of Y-containing females is higher. However, polytene chromosomes of the best quality were obtained in a stock homozygous for otu^{11} and carrying *Dp(1;1)pn2B*.
2. Staining times vary widely. We used from 30 min at room temperature to overnight at 4°C and did not find noticeable differences. As NC chromosomes are

more diffuse than SG chromosomes, they are stained weakly and long treatments by acetic orcein may intensify staining. At the same time, cytoplasm is also saturated by orcein, which seriously hampers chromosome exploration.

3. The drop must be large enough for the cover slip to move freely, or chromosomes will be destroyed. If the drop is too large, nuclei will be washed out with excess liquid.
4. During this step, a majority of slides may be rejected, because we use only chromosomes of such length (*see* **Subheading 1.3.1.**) and having banding patterns that can be easily identified with chromosome maps. Unfortunately, these "good" slides constitute no more than 25–30% of all slides made. Others contain too much cytoplasm, which hides chromosomes. Some chromosomes cannot be identified because they look like "luminous cords" without banding patterns. In comparison with SG squashes, where each slide contains dozens of good nuclei, in NC squashes we select slides that contain as few as one to two good nuclei per slide. Putting more than 8–10 egg chambers on a slide adds too much cytoplasm, which prevents chromosome observation.
5. Volumes of components of this mixture depend on the number of slides and the component concentrations. For example, for one slide, you need 1 µL of biotinylated probe at a concentration of 0.1 µg/µL, 2–3 µL of competitor DNA at 0.1 µg/µL, and 7–8 µL of water (i.e., to bring the final volume to 10 µL). To this mixture add 20 µL of hybridization buffer.
6. Duration of staining can vary. You can decrease the concentrations of staining solutions and simultaneously increase the duration of staining to obtain the best results.
7. Time of fixation can be varied widely. It is important for SG chromosomes not to fix them for too long, because this can dramatically decrease chromosome quality. We believe that NC chromosomes must be fixed longer. We fixed ovaries for 10 min in the case of HP1 and 15–20 min in the case of Mod.
8. Protocol 30 in **ref.** ***37*** states that the volume of antibodies should be 40 µL. However, if you use a cover slip and rubber cement, 15–20 µL of antibodies are enough.
9. You can incubate the slides with primary antibodies for 2–4 h at room temperature, but we find it is better to incubate the slides overnight at a lower temperature (4–10°C).

Acknowledgments

This work was supported by grants from the Russian Foundation for Basic Research (02-04-48222), Russian State Program Frontiers in Genetics (2-02), Lavrentiev Grant of Siberian Division of the Russian Academy of Sciences for Young Scientists, and grants of Ministry of Education of Russian Federation (PD-02-1.4-74 and EO2-6.0-37).

References

1. Painter, T. S. (1933) A new method for the study of chromosome rearrangements and the plotting of chromosome maps. *Science* **78,** 585–586.

2. Koch, E. A., Smith, P. A., and King, R. C. (1967) The division and differentiation of *Drosophila* cystocytes. *J. Morphol.* **121,** 55–78.
3. Brown, E. H. and King, R. C. (1964) Studies on the events resulting in the formation of an egg chamber in *Drosophila melanogaster*. *Growth* **28,** 41–81.
4. King, R. C. (1970) *Ovarian Development in* Drosophila melanogaster, Academic, New York.
5. Spradling, A. C. and Orr-Weaver, T. (1987) Regulation of DNA replication during *Drosophila* development. *Annu. Rev. Genet.* **21,** 373–403.
6. Spradling, A. C. (1993) Developmental genetics of oogenesis, in *The Development of* Drosophila melanogaster, (Bate, M. and Martinez-Arias, A., eds.), Cold Spring Harbor Laboratory Press, Plainview, NY, Vol. 1, pp. 1–70.
7. Mulligan, P. K. and Rasch, E. M. (1985) Determination of DNA content in the nurse and follicle cells from wild type and mutant *Drosophila melanogaster* by DNA–Feulgen cytophotometry. *Histochemistry* **82,** 233–247.
8. King, R. C., Rubinson, A. C., and Smith, R .F. (1956) Oogenesis in adult *Drosophila melanogaster*. *Growth* **20,** 121–157.
9. Dej, K. J. and Spradling, A. C. (1999) The endocycle controls nurse cell polytene chromosome structure during *Drosophila* oogenesis. *Development* **126,** 293–303.
10. King, R. C., Burnett, R. C., and Staley, N. A. (1957) Oogenesis in adult *Drosophila melanogaster*. IV. Heredity ovarian tumors. *Growth* **21,** 239–261.
11. King, R. C., Riley, S. F., Cassidy, J. D., White, P. E., and Paik, Y. K. (1981) Giant polytene chromosomes from the ovaries of a *Drosophila* mutant. *Science* **212,** 441–443.
12. Keyes, L. N. and Spradling, A. C. (1997) The *Drosophila* gene *fs(2)cup* interacts with *otu* to define a cytoplasmic pathway required for the structure and function of germ-line chromosomes. *Development* **124,** 1419–1431.
13. Storto, P. D. and King, R. C. (1988) Multiplicity of functions of the *otu* gene products during *Drosophila* oogenesis. *Dev. Genet.* **9,** 91–120.
14. Rodesch, C., Pettus, J., and Nagoshi, R. N. (1997) The *Drosophila ovarian tumor* gene is required for the organization of actin filaments during multiple stages of oogenesis. *Dev. Biol.* **190,** 153–164.
15. Glenn, L. E. and Searles, L. L. (2001) Distinct domains mediate the early and late functions of the *Drosophila* ovarian tumor proteins. *Mech. Dev.* **102,** 181–191.
16. King, R. C. and Storto, P. D. (1988) The role of *otu* gene in *Drosophila* oogenesis. *BioEssays* **8,** 18–24.
17. Storto, P. D. and King, R. C. (1987) Fertile heteroallelic combinations of mutant alleles of the *otu* locus of *Drosophila melanogaster*. *Roux Arch. Dev. Biol.* **196,** 210–221.
18. Mal'ceva, N. I., Belyaeva, E. S., King, R. C., and Zhimulev, I. F. (1997) Nurse cell polytene chromosomes of *Drosophila melanogaster otu* mutants: morphological changes accompanying complementation and position effect variegation. *Dev. Genet.* **20,** 163–174.
19. King, R. C., Mohler, D., Riley, S. F., Storto, P. D., and Nicolazzo, P. S. (1986)

Complementation between alleles at the *ovarian tumor* locus of *Drosophila melanogaster*. *Dev. Genet.* **7,** 1–20.
20. Dabbs, C. K. and King, R. C. (1980) The differentiation of pseudonurse cells in the ovaries of *fs231* females of *Drosophila melanogaster* Meigen (Diptera: Drosophilidae). *Int. J. Insect Morph. Embryol.* **9,** 215–229.
21. King, R. C., Rasch, E. M., Riley, S. F., O'Grady, P. M., and Storto, P. D. (1985) Cytophotometric evidence for the transformation of oocytes into nurse cells in *Drosophila melanogaster*. *Histochemistry* **82,** 131–134.
22. Heino, T.I. (1989) Polytene chromosomes from ovarian pseudonurse cells of the *Drosophila melanogaster otu* mutant. I. Photographic map of chromosome 3. *Chromosoma* **97,** 363–373.
23. Rasch, E. M., King, R. C., and Rasch, R. W. (1984) Cytophotometric studies on cells from ovaries of *otu* mutants of *Drosophila melanogaster*. *Histochemistry* **81,** 105–110.
24. Bishop, D. L. and King, R. C. (1984) An ultrastructural study of ovarian development in the otu^{7} mutant of *Drosophila melanogaster*. *J. Cell Sci.* **67,** 87–119.
25. Heino, T. I. (1994) Polytene chromosomes from ovarian pseudonurse cells of the *Drosophila melanogaster otu* mutant. II. Photographic map of the X chromosome. *Chromosoma* **103,** 4–15.
26. Zhimulev, I. F. (1996) Morphology and structure of polytene chromosomes. *Adv. Genet.* **34,** 1–490.
27. Mal'ceva, N. I., Gyukovics, H., and Zhimulev, I. F. (1995) General characteristics of the polytene chromosomes from ovarian pseudonurse cells of the *Drosophila melanogaster* otu^{11} and *fs(2)B* mutants. *Chromosome Res.* **3,** 191–200.
28. Zhimulev, I. F. and Mal'ceva, N. I. (1997) Action of ecdysterone on salivary gland and nurse cell polytene chromosomes of *Drosophila melanogaster otu* mutant in vitro. *Dros. Inform. Serv.* **80,** 77–82.
29. Heino, T. I., Lahti, V. P., Tirronen, M., and Roos, C. (1995) Polytene chromosomes show normal gene activity but some mRNAs are abnormally accumulated in the pseudonurse cell nuclei of *Drosophila melanogaster otu* mutants. *Chromosoma* **104,** 44–55.
30. Perrin, L., Demakova, O., Fanti, L., et al. (1998) Dynamics of the sub-nuclear distribution of modulo and the regulation of position-effect variegation by nucleolus in *Drosophila*. *J. Cell Sci.* **111,** 2753–2761.
31. Mal'ceva, N. I. and Zhimulev, I. F. (1993) Extent of polyteny in the pericentric heterochromatin of polytene chromosomes of pseudonurse cells of *otu* (*ovarian tumor*) mutants of *Drosophila melanogaster*. *Mol. Gen. Genet.* **240,** 273–276.
32. Koryakov, D. E., Belyaeva, E. S., Alekseyenko, A. A., and Zhimulev, I. F. (1996) Alpha and beta heterochromatin in polytene chromosome 2 of *Drosophila melanogaster*. *Chromosoma* **105,** 310–319.
33. Koryakov, D. E., Alekseyenko, A. A., and Zhimulev, I. F. (1999) Dynamic organization of the beta-heterochromatin in the *Drosophila melanogaster* polytene X chromosome. *Mol. Gen. Genet.* **260,** 503–509.

34. Koryakov, D. E., Domanitskaya, E. V., Belyakin, S. N., and Zhimulev, I. F. (2003) Abnormal tissue-dependent polytenization of a block of chromosome 3 pericentric heterochromatin in *Drosophila melanogaster*. *J. Cell. Sci.* **116,** 1035–1044.
35. Zhimulev, I. F. (1998) Polytene chromosomes, heterochromatin and position effect variegation. *Adv. Genet.* **37,** 1–566.
36. Lindsley, D. L. and Zimm, G. G. (1992) *The Genome of* Drosophila melanogaster, Academic, San Diego, CA.
37. Ashburner, M. (1989) Drosophila: *A Laboratory Manual.* Cold Spring Harbor Laboratory Press, Cold Spring Harbor, NY.
38. Clark, R. F., Wagner, C. R., Craig, C. A., and Elgin, S. C. (1991) Distribution of chromosomal proteins in polytene chromosomes of *Drosophila*. *Methods Cell Biol.* **35,** 203–227.

7

Feulgen–DNA Cytophotometry for Estimating C Values

Ellen M. Rasch

1. Introduction

1.1. Nature of the Task

The genome size of an organism, commonly known as its C value, is defined as the content of DNA (measured by weight or numbers of basepairs) in a single copy of the sequence of DNA found within the cells of an organism (i.e., the amount of DNA in a haploid chromosome set, where 1n = 1C) ***(1)***. A single sperm of *Drosophila melanogaster* contains 0.18 pg DNA, which is the C value for this species ***(2–4)***. By convention, the DNA content of a diploid somatic cell of this species can then be expressed as 2n = 8 = 2C = 0.36 pg DNA for the male diploid genotype of AAXY ***(3)***. And, 2C = 0.40 pg DNA for a diploid *Drosophila* female somatic cell with the genotype of AAXX because the X chromosome contains a bit more DNA than the Y chromosome in this species (*see* **Table 1**). These considerations follow from the "DNA Constancy Hypothesis" formulated in the 1950s ***(5–8)*** that the DNA content of nuclei of a eukaryotic species is essentially constant among the individuals within a given species and constitutes the repository of genetic information for that taxon. For example, genome sizes, expressed as C values, are listed in **Table 1** for 10 different species of *Drosophila*.

Although there is relatively little variation in genome size among prokaryotes ***(1)***, the genome sizes of eukaryotes vary widely among animals and may vary by several thousand-fold among plants ***(9–12)***. The underlying mechanisms that direct these large differences in fundamental genome size for plant and animal species are of increasing interest to students of evolutionary biology, raising questions about the equivalency of genome size, its net genetic information content, and the minimum amount of DNA required for life forms

From: *Methods in Molecular Biology, vol. 247:* Drosophila *Cytogenetics Protocols*
Edited by: D. S. Henderson © Humana Press Inc., Totowa, NJ

Table 1
Estimates of Genome Size for 10 Different Species of *Drosophila* Expressed as C Values in pg DNA per Nucleus[a] and Number of Nucleotide Basepairs (np)

Species	C Value = DNA pg per nucleus	np × 10^8
D. americana	0.30	2.74
D. arizonensis	0.22	2.01
D. eohydei	0.24	2.19
D. funebris	0.23	2.10
D. hydei	0.20	1.83
D. melanogaster (♂)	0.18	1.64
D. melanogaster (♀)	0.20	1.82
D. miranda	0.30	2.74
D. neohydei	0.19	1.73
D. simulans	0.12	1.10
D. virilis	0.34	2.89
Chicken[b]	1.25	11.41
Xenopus laevis[b]	3.15	28.76

[a]Computed by assuming 9.13×10^8 nucleotide pairs per picogram of DNA ***(9)***.

[b]C values are shown for red blood cell (RBC) nuclei of two reference standards.

Source: Adapted from T. R. Gregory, www.genomesize.com/insects. For primary citations, *see* database at this website.

(1,10,13). Also, what is "*junque*" DNA? And, how do different chromatin domains regulate and modulate gene expression in eukaryotic genomes? (*see* **refs. *1,10,14,15***). Because many plant and animal species with relatively small genomes serve as model systems for study by geneticists and developmental biologists, reliable estimates of genome size can provide useful data for these and other current fields of research ***(12,16)***.

Of particular interest are those species with strict regulation of total cell number (eutely) that very often display cells and tissues whose nuclei have undergone repeated cycles of DNA endoreduplication without intervening cycles of nuclear and cytoplasmic division (i.e., mitosis), to result in polyploidy (increase in the number of copies of the diploid chromosome sets) or polyteny (same number of chromosomes, but each chromosome becomes multistranded)—both manifest in giant somatic cell nuclei that contain very large amounts of DNA ***(17–29)***.

1.2. Drosophila *Genome Size*

The C value for *Drosophila melanogaster* is not only useful in its relationship to the net amount of genetic information embedded in its chromosomes ***(1,4,12)***, but it is also needed to study changes in DNA levels associated with alterations in the total amount of genetic coding potential following changes in cell size and cell functions during larval and adult life in this species and its congeners ***(18,28–31)***. Sequencing of the *Drosophila* genome ***(4)*** has now set the future course for the field of molecular developmental biology.

There is a fundamental question in *Drosophila* cytogenetics that can be stated as follows: "What is the functional significance of the selective genome reduplication that is the signature of development in so many dipteran species?" During the life-span of many dipterans, organs other than just the larval salivary glands (Malpighian tubules, gastric folds, fat bodies, hindgut, rectum, and nurse cells of germ-line origin in the ovarioles) regularly show large, densely stained nuclei in certain tissues at certain times during growth and differentiation ***(20,25,26,32–34)***. Analysis of these phenomena requires, in part, the capacity to measure DNA amounts in individual nuclei from extremely small tissue samples, a task admirably suited to cytophotometry, using the sperm C value of 0.18 pg DNA ***(2–4)***. For example, we can now say, with reasonable assurance, that larval hemocytes of *Drosophila* are predominately at the 4C level (0.72 pg DNA), but are almost exclusively at the 2C level (0.36 pg DNA) in adult males (*see* **Fig. 1**). Also, we can say that oenocyte nuclei (*see* **refs. *28–30***) in females remain at the 4C level (0.72 pg DNA) throughout imaginal life (*see* **Fig. 1**), unlike cells of the female adult fat body (AFB), which show a progressive shift from 2C cells to 4C cells to 8C cells and even a few 16C cells that contain about 2.8 pg DNA per nucleus during maturation and senescence (*see* **Fig. 2**). AFB cells in males also show 4C and 8C nuclei during imaginal life. In contrast to the rather staid behavior of DNA in the AFB, analyses of DNA levels in cells of the larval fat body (LFB) show dramatic changes with time ***(31,34)***. The values shown in **Fig. 3** were obtained by measuring the DNA–Feulgen content of individual fat body nuclei from the time of hatching on through the growth and maturation of the fat body in third instar larvae, some 92–96 h after hatching. Mature larvae show more than a hundred-fold increase in the DNA content of their largest nuclei, which may have DNA levels as high as 40 pg per nucleus at the peak of activity in this multifunctional tissue (*see* **Fig. 3**) (***34***; Rasch and Butterworth, unpublished work). As expected ***(29–31)***, there is a marked decrease in nuclear DNA content accompanying organ histolysis that occurs during pupation. Only a few remnant LFB nuclei can sometimes be recognized in the vicinity of the developing AFB in newly eclosed adults (*see* **Fig. 3**). The data in **Fig. 3** were com-

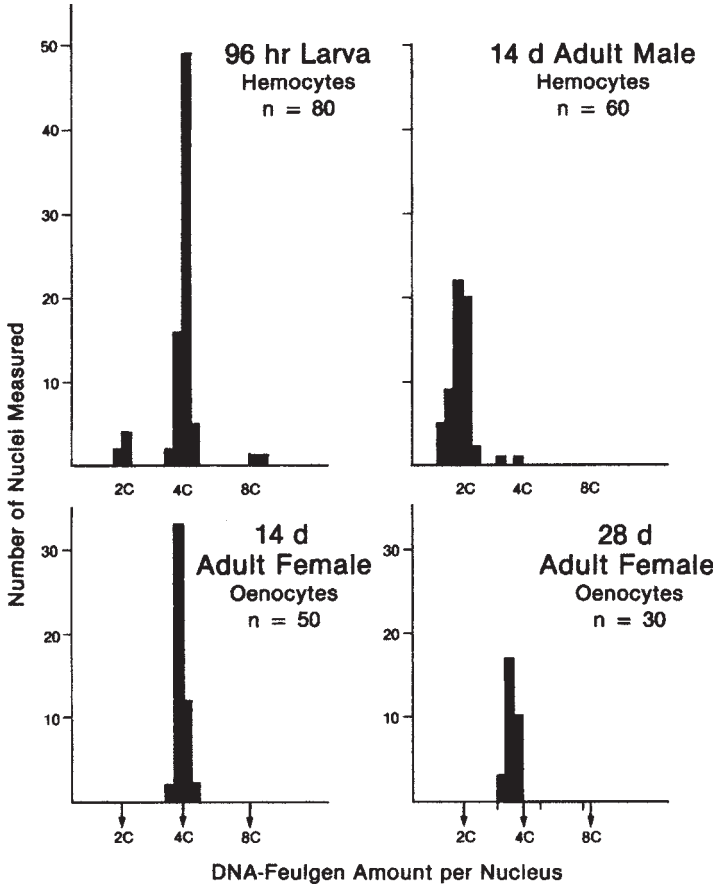

Fig. 1. Histograms of Feulgen–DNA amounts per nucleus for larval and adult hemocytes and oenocytes of *Drosophila melanogaster,* expressed in arbitrary units of relative integrated absorbance, to estimate the extent of genome replication in different tissues at ongoing stages of development. Note differences in frequencies of 2C and 4C hemocyte nuclei at the larval and adult stages. Oenocytes from adult females show only 4C nuclei, presumably holding at an arrested G2 stage of the cell cycle (Rasch, unpublished data).

puted from the average DNA content determined for populations of 50–75 nuclei in fat body cells measured in adipose tissue at each different stage of development. The data on these changes in DNA levels shown represent more than 3000 scans of individual fat body nuclei and are based on measurements of chicken blood cell nuclei used as a reference standard of 2.5 pg DNA ***(2,12,16,31,34)***.

Both cytological and biochemical evidence ***(19,22,23,27,35)*** appear to demonstrate that highly compacted chromatin (constitutive heterochromatin) is sig-

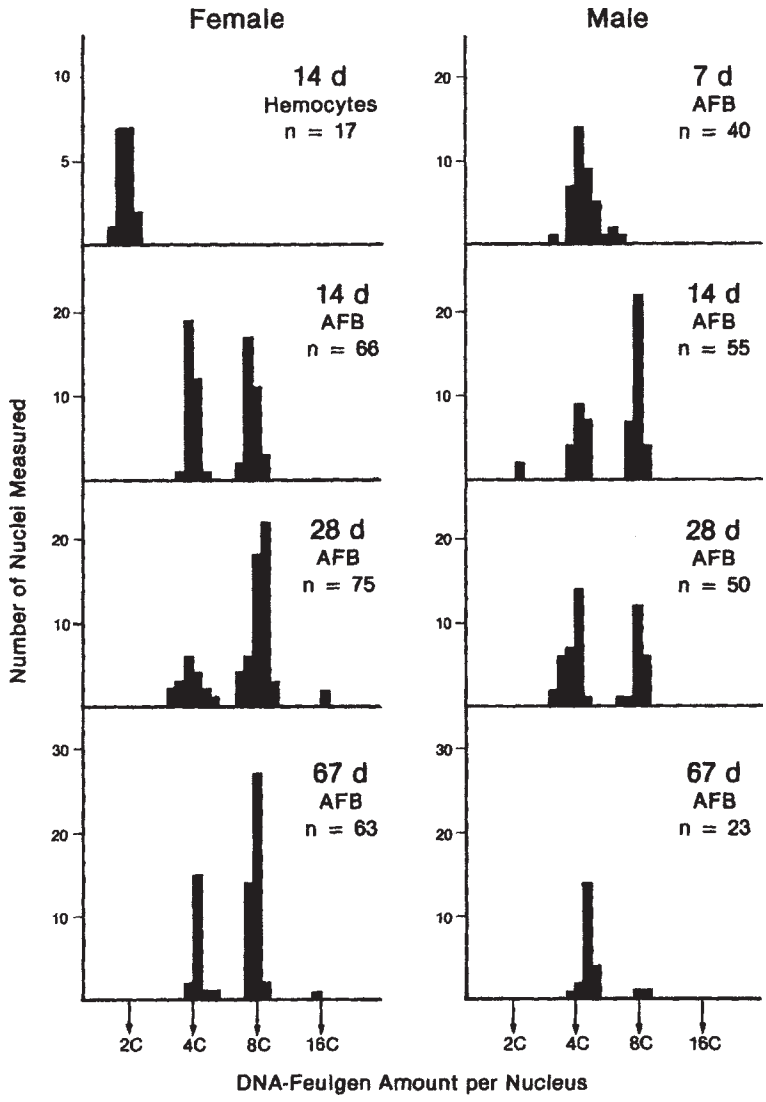

Fig. 2. Histograms of nuclear DNA measurements of fat body nuclei from 14-d, 28-d, and 67-d adult females and males of *Drosophila melanogaster*. The C value for sperm (0.18 pg DNA) was used to identify a shift in nuclear DNA contents from 2C to 4C to 8C during senescence in both female and male adults.

nificantly underreplicated in types of dipteran cells that involve differential replication patterns for (1) euchromatin, (2) compacted chromatin (i.e., heterochromatin), and (3) nucleolar-associated chromatin domains ***(14)***. The functional significance of these anomalies in DNA replication is not understood

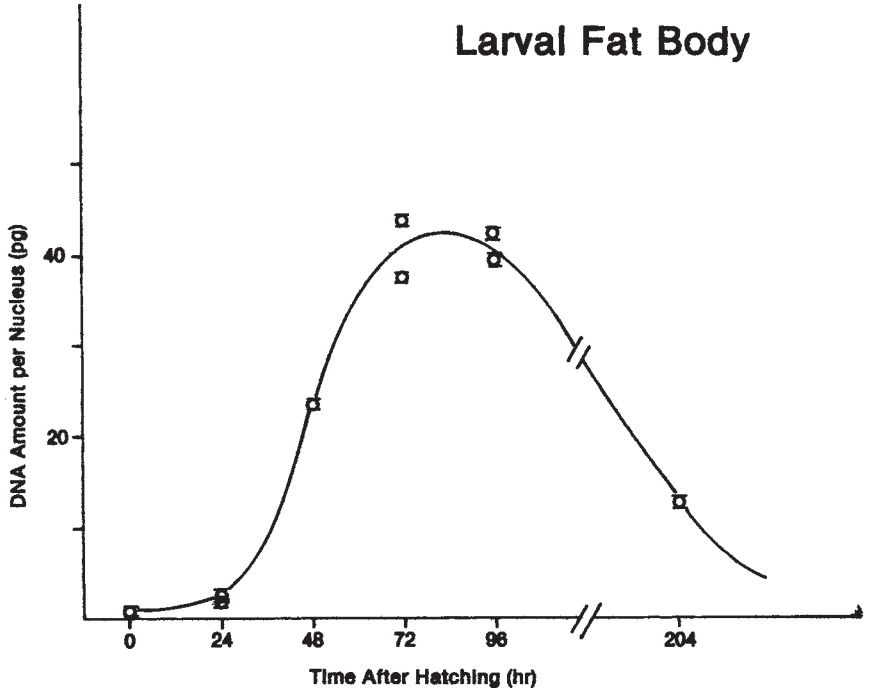

Fig. 3. Changes in average nuclear DNA content of adipose cells during larval development in *Drosophila melanogaster.* Some of the large, somewhat densely stained fat body nuclei approximate 128C and approach up to the 256C DNA levels, suggesting that at least six to seven or more cycles of endoreduplication occur during the course of fat body maturation and senescence ***(31,34)***.

at present, but they do point out that additional critical studies are needed to account, at least in part, for apparent discrepancies between expected DNA levels from replication of the entire genome and the amount of DNA that is detected by DNA–Feulgen cytophotometry in polysomatic dipteran tissues ***(1,10,12,23–25,33,36)***. Perhaps the elegant studies of Gerbi and her co-workers ***(37)*** to identify precise sites of origins of DNA replication for the giant polytene chromosomes of *Sciara coprophila* have now opened the way to apply their strategies to the persistent problem of heterochromatin underreplication in *Drosophila*.

Because manifestations of selective gene replication as well as differential gene activation and selective gene expression are of considerable interest to geneticists and developmental biologists, there is a pressing need to determine C values for a given species and to follow changes in the amounts of DNA per nucleus in particular types of tissue during differentiation. With the "return of

the H-word (heterochromatin)," to quote Lohe and Hilliker ***(14)***, there is a growing interest in the potential role of highly repetitive and/or satellite DNAs and their associated proteins in molecular and cellular biology ***(15)***. In addition, comparisons of C values are of interest in phylogenetic studies of speciation and evolution in many groups of animals ***(1,10)***.

1.3. The Case for Static Microdensitometry

It is often difficult to obtain unequivocal data for genome size in cell systems where the available sample size is too small to yield a reliable estimate based on biochemical assays and counts of cell numbers. It is particularly difficult to resolve DNA levels per cell when tissue samples contain mixtures of diploid cells at various stages of the cell cycle and in tissues consisting of cells with polyploid or polytene chromosomes. Similar problems can often plague analysis of such complex tissue samples by flow cytometry using DNA-specific fluorescent probes in cell systems where the available sample size is too small and/or heterogeneous to yield reliable estimates of DNA amounts per cell.

In these cases, it has been productive to resort to static cytophotometry, and most recently to static, image analysis microdensitometry ***(12)***, employing the DNA–Feulgen reaction with a scanning and integrating cytophotometer of tested accuracy and precision ***(38–41)*** to determine integrated optical density (IOD), which can also be expressed as relative integrated absorbance (RIA), of the Feulgen–DNA dye complex bound to individual nuclei. From such data, it is feasible to obtain reliable estimates of genome size or C values for a diverse array of eukaryotic organisms ***(11,12,16)***.

1.4. Overview

Doing the job at hand requires careful attention to details of tissue preparation, fixation history, staining, and the stoichiometry of the Feulgen–DNA dye complex, as well as well as determining optimal acid hydrolysis conditions and selecting several appropriate reference standards to validate staining and measuring techniques.

Care in setting up, calibrating, and using a microdensitometer are very important, as is the need to reduce flare, nonspecific light loss resulting from scatter, and errors resulting from inhomogeneous distribution of stained chromatin. Relevant particulars about Feulgen staining and the use of a scanning and integrating microdensitometer are described next.

1.5. The Feulgen Reaction for DNA

The Feulgen reaction for DNA was initially described by Feulgen and Rossenbeck in 1924 ***(42)***. They found that a mild acid hydrolysis of fixed tissue sections followed by treatment with Schiff's reagent ***(43)*** resulted in a dis-

Table 2
Hydrolysis Times in 5 *N* HCl for Invertebrate Tissues Prepared in Different Fixatives

Fixative	Hydrolysis time (min)
Alcoholic fixatives	15–20
Formaldehyde vapors	20–25
Formalin fixatives	20–40
Metallic fixatives (e.g., Cr or Hg)	40–60

crete magenta coloring at the sites of DNA in their preparations. Mild acid hydrolysis splits off the purines of DNA so that the residual polynucleotide is identical to apurinic or thymic acid ***(7,44–46)***. The removal of purine bases uncovers potential aldehyde groups present in the 2-deoxyribose molecules. Exposure of the aldehyde groups to Schiff's reagent results in the formation of a very stable, highly chromogenic insoluble compound. Variations in the degree of chromatin compaction within a nucleus are also known to affect the number of sites available for DNA staining after acid hydrolysis ***(7,47–51)***. Kasten has an excellent review of the use of basic fuchsin analogs in the manufacture of Schiff's reagent to identify DNA and the stoichiometry of the Feulgen reaction for DNA ***(52)***. Despite several extensive studies of dye purity and resultant stain intensity ***(52–55)***, the precise mechanism of the Feulgen reaction for DNA is not clearly understood.

Acid hydrolysis removes histone proteins from alcohol–acetic acid fixed chromatin, and some polymer sugar linkages may also be split during acid hydrolysis. Formalin fixation, however, retains the histone proteins of chromatin, as may be demonstrated by the alkaline fast green technique for basic proteins ***(56)***.

1.5.1. Time, Temperature, and Concentration of Acid Hydrolysis are Critical for Successful DNA Staining

Since the introduction of the Feulgen procedure for DNA, HCl has been the hydrolysis agent of choice. Prolonged hydrolysis results in a decrease in staining, presumably caused by chemical alteration, depolymerization, and extraction of the DNA. Acids other than hydrochloric could be used for DNA hydrolysis (phosphoric acid, sulfuric acid, perchloric acid, or trichloroacetic acid). Such a modification to the usual procedure, however, would require empirical cytophotometric determinations for each acid of appropriate concentrations, times, and temperatures for optimal hydrolysis of DNA ***(55)***.

The duration of hydrolysis in 5 *N* HCl at 20–23°C, or the use of the traditional hydrolysis in 1 *N* HCl at 60°C (*see* **ref. *52***), depends, in large part, on the fixation history of the tissue. The values given in **Table 2** are estimates for

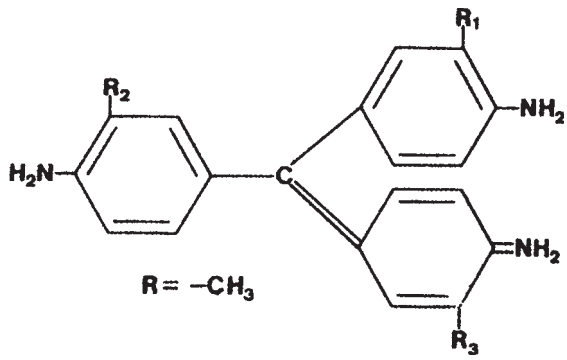

Fig. 4. Diagram of molecular structure of the triarylmethane dyes. Pararosaniline is unmethylated. R_1, R_2, and R_3 represent hydrogen atoms that are sequentially replaced by methyl groups during the synthesis of basic fuchsin analogs. (Adapted from **ref. *55***.)

hydrolysis times in 5 *N* HCl at room temperature (i.e., 20–23°C) using procedures introduced by DeCosse and Aeillo ***(57)***. For each new combination of tissue and fixation procedures, it is necessary to determine appropriate times and temperatures using test tissue samples before processing high-value slide preparations ***(12,16,55)***. The presence of aldehyde groups after mild acid hydrolysis can be demonstrated by using aldehyde-blocking agents ***(58,59)***.

1.5.2. Schiff's Reagents

Spectrophotometric analyses show remarkably similar absorption curves for pararosaniline and its variously methylated derivatives and their synonyms: Pararosaniline (Magenta 0), Rosaniline (Magenta I), Basic Fuchsin (Magenta II) and New Fuchsin (Magenta III) with no, one, two, and three methyl groups, respectively, as illustrated in **Fig. 4**.

Pure fuchsin analogs appear to be equally suitable for Feulgen staining, with respect to their staining intensities (*see* **Note 1**). All fuchsin dyes have nearly identical absorption curves. There is a shift of about 8 nm when comparing the position of the absorption maxima for Pararosaniline and New Fuchsin ***(52,53,55)***. To standardize the Feulgen–Schiff technique, these authors recommend that pure pararosaniline (C.I. 42500) be used to prepare Schiff's reagents (*see* **Note 1**). Others workers have reported satisfactory color generation with the use of Magenta II to prepare Schiff's reagent ***(55)***. Other dyes, such as Azure A or Azure C, have been used to make so-called pseudo-Schiff reagents, but the chemistry and stoichiometry of these dark blue DNA dye complexes have not been adequately explored ***(52)***.

In summary, the Feulgen reaction is not just a "stain" for chromatin like acetocarmine, but it is a specific cytochemical reaction for DNA that is subject

Table 3
Representative Vendors for Basic Fuchsin (C. I. 42500) and/or Pararosaniline (C. I. 42510)

Vendor	Telephone	Website
C and P Sales	(716) 634–3061	www.candpsales.com
Fisher Scientific	(800) 766–7000	www.fishersci.com
Gallard-Schlesinger	(800) 645–3044	www.gallard-schlesinger.com
I. C. N.	(800) 654–0530	www.icnbiomed.com
J. T. Baker	(800) 582–2537	www.jtbaker.com.
Newcomer Supply	(800) 383–7799	www.newcomersupply.com.
Sigma-Aldrich	(800) 325–3010	www.sigmaaldrich.com
Thomas Scientific	(800) 348–2100	www.thomassci.com
VWR	(800) 932–5000	www.vwr.com

to a number of errors, such as differences in (1) the physical state of chromatin domains (i.e., degree of chromatin compaction), (2) preparatory variables such as chemical fixation and "aging" of slides to be compared, and (3) preparatory variables in compounding the Schiff's reagent ***(12)***.

2. Materials

In this and the following sections, most reagents or stains can be obtained from the representative vendors listed with telephone numbers and websites in **Table 3**.

1. Schiff's sulfurous acid leucofuchsin reagent: This can be prepared using **items 3–6** and **8–10** as described in **Subheading 3.1.**, or a premade solution can be purchased from one of the vendors listed in **Table 3**. (Sigma-Aldrich: cat. no. S5133; Fisher Scientific, cat. no. 5532-5001; Thomas Scientific, cat. no. 692-A-1; VWR Scientific Products, cat no. JTU973-1.)
2. 5 *N* HCl: Add 215 mL concentrated acid to 285 mL deionized water.
3. 1 *N* HCl: Add 40.5 mL concentrated acid to 459.5 mL deionized water.
4. 0.01 *N* HCl: Add 1 mL of 1 N HCl to 99 mL deionized water.
5. Basic Fuchsin (pararosaniline chloride, certified, C.I. 42500). Comes as a dry green powder or as small green crystals with a gold metallic luster (*see* **Note 1**).
6. 10% Sodium metabisulfite ($Na_2S_2O_3$; Sigma-Aldrich, cat. no. S-1516) or 10% potassium metabisulfite ($K_2S_2O_3$; Sigma-Aldrich, cat. no. P-2522): Dissolve 10 g in 100 mL deionized water.
7. Sulfite water (1% sodium metabisulfite; make fresh daily): Add 10 mL of 1 *N* HCl to 90 mL of deionized water in a graduated cylinder and decant into a 250 mL-capacity screw-top bottle. Add 10 mL of a stock 10% solution of sodium metabisulfite to another graduated cylinder containing 90 mL of deionized water. Add this solution to the acid solution in the bottle, which generates 200 mL of

Table 4
Alternative to Chromic/Sulfuric Acid for Cleaning Slides and Other Laboratory Glassware

Product	Catalog no.	Vendor
Versa-clean concentrate	04-342	Fisher Scientific
RBS-35 Cleaner	PL 27950	VWR Scientific Products
DeContam	KC85D	ESPI
Micro 90	9031	International Products Corp.
Nochromix	32869-3	Aldrich Chemical Co.

Note: Environmental health and safety regulations restrict the use of chromic/sulfuric acid solutions for routine cleaning of laboratory glassware and glass slides because of the heavy metal contamination and low pH of these solutions. Listed here are several commercially available cleaning agents. Request Material Safety Data Sheets (MSDSs) from the vendor when ordering these materials. When diluting concentrates, remember to wear goggles or a face mask while slowly mixing solutions in a hood and allow to cool to room temperature before capping the container of the diluted solution.

SO_2 rinse water. (Do not inhale noxious fumes!) Distribute the 200 mL into three covered Coplin jars.

8. Decolorizing neutral activated charcoal (100 mesh; Sigma-Aldrich, cat. no. 24,287-6 or Fisher Scientific, neutral Norite A).
9. Filter paper, qualitative grade.
10. Bottles and beakers, 100 mL and 250 mL, to mix and store reagents. Rinse storage bottles with 0.01 *N* HCl before using. Drain to dry.
11. Frosted end slides (e.g., Fisher Scientific, cat. no. 12-544-2) and No. 1 thin cover glasses.
12. Plastic dishes that will hold 72 slides for cleaning.
13. Methanol/formalin/acetic acid (MFA), 85 : 15 : 1 (v/v).
14. D.P.X resin (Bio/Medical Specialties, mspec@artnet.net).
15. Immersion oil and refractive index liquids from n_D 1.520 to 1.580.
16. Staining glassware such as Coplin jars and staining trays.
17. Liquid N_2 or blocks of dry ice (and protective gloves!).
18. "Subbed" slides for *en bloc* Feulgen staining. Cell squashes and dispersal of *en bloc*-stained tissues are best done on frosted end slides that retain penciled labels and carry a thin film of chromed gelatin as a protein "glue" to ensure that tissues will adhere to the slide and not to the cover glass. Slides for subbing should be scrupulously clean before applying the gelatin film.
    To clean the slides:
    a. Use Micro-90 cleaning concentrate (or other product listed in **Table 4**) to prepare a 1% working solution by adding 20 mL of the concentrate to 2 L of deionized water.
    b. Soak 72 slides for 2–3 h (or overnight) in a 1% Micro-90 cleaning solution. Wash the slides thoroughly in several changes of deionized water until the

film of water flows smoothly over surface of the slide and does not break into beads or streaks (i.e., the surface "wets" perfectly).

To coat the slides with gelatin:

a. Add 2 g of chrome alum [chromium potassium sulfate, $CrK(SO_4)_2 \cdot 12H_2O$] to 40 mL of deionized water. Stir to dissolve completely. This 5% stock solution can be stored indefinitely.
b. Sprinkle 0.5 g of gelatin (e.g., Knox brand from supermarket) onto the surface of 100 mL of deionized water in a 250-mL Erlenmeyer flask at room temperature.
c. Incubate the mixture at 60°C to dissolve the gelatin (approx 30 min).
d. When the gelatin is in solution, use a 1-mL pipet to blow 1 mL of 5% chrome alum into the warm gelatin.
e. Decant the "chromed" gelatin solution into a Coplin jar and allow to cool to room temperature before use.
f. Dip each slide into the gelatin solution for 2–3 s.
g. After draining excess solution on the rim of the Coplin jar or onto a piece of absorbent paper, allow coated slides to dry vertically by leaning them against a surface that will keep them at about a 45° angle. Dry overnight. Store the subbed slides in a covered, dust-free slide box.

19. Parlodion (Fisher Scientific Co., cat. no. P35-100): Parlodion is a synonym for pyroxylin (a purified form of nitrocellulose) and is often called celloidin and may be obtained in the form of short, amber-colored strips. **Caution!** Because this is a DOT Class 4.1 flammable solid, due care must be taken to keep it in a flame safety cabinet or under a chemical hood. Keep in the dark; light causes deterioration.
To make 0.25% Parlodion stock solution:
    a. Add 0.25 g of dried pyroxylin strips to 100 mL of a 1 : 1 (v/v) mixture of ethyl ether and absolute ethanol in a glass bottle with a stopper.
    b. Shake for 3–5 min to coat individual strips with the solvent.
    c. Keep the bottled solution either in a flame cabinet or under a hood. It is flammable!
    d. Parlodion strips take 3–5 d to dissolve completely.

3. Methods

3.1. Preparation of Schiff's Reagent

1. Add 10 mL of 1 *N* HCl to 100 mL of distilled water.
2. Add 1.0 g certified Basic Fuchsin (pararosaniline chloride) and shake for 10–15 min.
3. Add 10 mL of 10% sodium metabisulfite solution and shake vigorously for 2–3 min.
4. Let stand at room temperature until the solution turns straw colored, approx 2–3 h. Shake frequently during this period.
5. Place the bottle in a dark cabinet for 48–72 h (*see* **Note 2**).
6. Swirl the solution at least twice a day to suspend the contents.
7. After the desired time, add 0.5 g neutral activated charcoal per 100 mL of reagent.
8. Shake the suspension vigorously for 1–2 min.

9. Filter quickly through coarse filter paper (qualitative grade). The filtrate should be glass clear and colorless. If not, repeat **steps 7–9**.
10. Label 100 mL bottles, filled to the top and closed tightly to minimize air space.
11. Store in a refrigerator until needed (*see* **Notes 3** and **4**). Bring to room temperature before use (*see* **Note 5**).

3.2. Preparation of Tissue for Staining

Use the procedure described in **Subheading 3.3.** to stain tissue squashes (e.g., salivary gland chromosomes), fixed in methanol/acetic acid (3 : 1 v/v) and squashed in 45% acetic or lactic acid. Use also for air-dried droplets of hemolymph, oenocytes, or adult fat body cells. To stabilize the latter types of cells, process them with their reference standards for 15 min in methanol/formalin/acetic acid (MFA) (85 : 5 : 1, v/v), followed by rinsing in several changes of deionized water for at least 5 min before placing the slides into 5 *N* HCl. Deparaffinize sectioned tissues in xylenes and bring them through graded ethanols to deionized water before putting them into acid for DNA hydrolysis (*see* **refs.** ***46,50,51,61*** and **Note 6**).

3.3. Feulgen Reaction for DNA

1. Hydrolyze each set of standards and unknown slides simultaneously in 5 *N* HCl for 20–30 min at 21–23°C (*see* **Note 6**).
2. Dip the slides for 5–10 s in 0.01 *N* HCl (to keep the tissue at ≤pH 2 to keep aldehyde groups available and also to minimize the amount of 5 *N* HCl carried over by the slides that would drop the pH of the Schiff's reagent).
3. Put all of the slides of a set into 1% Schiff's reagent. Allow the tissues to stain at room temperature for 2 h. Faint pink staining will probably be evident after 10–15 min.
4. Rinse the slides in three 5-min changes of sulfite water (made up fresh each day). Keep the Coplin jars covered during each successive 5-min rinse to remove excess Schiff's reagent from the slides.
5. Rinse the slides in running tap water for 10 min. Color will intensify as the excess SO_2 washes out of the tissue.
6. Rinse the slides in three 5-min changes of deionized water.

Decide which of the following steps (**steps 7a** and **8a**, or **steps 7b** and **8b**) is most appropriate for your purposes.

7a. For cytophotometry, dehydrate the slides through a graded series of ethanols to absolute alcohol and air-dry for storage in the dark until mounting in refractive index liquids for measuring.

8a. For cytophotometry, directly after staining, add three to four drops of an appropriate oil to clear the air-dried tissue by matching its refractive index (*see* **Subheading 3.10.**) and add a no. 1 thin cover slip to finish the preparation.

7b. To make permanent preparations, dehydrate the slides through graded ethanols to xylenes.
8b. Clear the slides from **step 7b** in three changes of xylenes, mount in a suitable plastic resin (e.g., D.P.X.). After adding a no. 1 cover slip, allow the preparation to dry overnight before viewing under an oil immersion lens.

3.4. En Bloc *Feulgen Staining*

In many instances, it is easier to do the Feulgen reaction for DNA with tissue fragments [e.g., a lobe of the larval fat body ***(25,30,31)*** or a whole-organ sample such as a pair of larval salivary glands ***(25)***] and then disperse individual cells and nuclei after their staining *en bloc* for the DNA (*see* **Note 7**). Individual Malpighian tubules ***(25,33)*** and ovarioles ***(20,21,62,63)*** (*see* Chapter 6) or testes ***(2,25)***, for example, are very well suited for DNA staining prior to their squashing to obtain banded polytene chromosomes ***(17,20)***, single egg chambers ***(21)*** (*see* Chapter 6) or individual sperm ***(2)***.

3.4.1. Procedure

The staining procedure is much the same as that listed above, but the duration of the steps has to be adjusted to provide enough time for diffusion of materials in and out of the tissue and the exchange of the Schiff's reagent through the barriers imposed by multicellular tissue layers. To avoid nonspecific staining, it is particularly useful to double the number of the bisulfite rinses after completion of the Feulgen staining step. Rinse small tissue pieces in at least three 5-min changes of bisulfite water before rinsing the tissues in deionized water before moving to a final water rinse of 2–4 h in the refrigerator to remove any excess SO_2. If there is residual sulfite in the tissue, it will effectively bleach the magenta Feulgen–DNA complex and the preparation will fade with time.

3.4.2. Dispersing Feulgen-Stained Tissue

1. Place very small pieces of *en bloc*-stained tissue on a clean "subbed" glass slide to swell in roughly 400 µL of 45% acetic acid for 1–2 min.
2. Carefully drain the 45% acetic acid with a small plastic pipet or with a small piece of absorbent paper, taking care not to let the pipet tip or paper touch the tissue.
3. Quickly add a small droplet (200 µL) of fresh 45% acid.
4. Add a 22×22-mm^2 cover glass and squash the tissue onto the slide using the tips of a fine forceps applied with a repeated tapping motion to crack the cells and allow nuclei to disperse and then be held flat by the forces of capillary action under the cover slip.
5. Complete the squashing process using moderate finger pressure applied only downward to avoid shearing the flattened tissue.

6. Freeze the squashes in liquid nitrogen or between two cakes of dry ice. This allows easy removal of the cover slip from the frozen slide by using the sharp edge of a single-edged razor blade to flip the cover glass upward and off the frozen slide.
7. Thaw the still-frozen slide in two changes of absolute ethanol and allow to air-dry for storage in the dark until mounted in refractive index liquids for measuring.

3.5. Coating Slides With Parlodion

Often tissue sections, squashes, or whole-tissue fragments tend to detach from the surface of the slide as it is moved from Coplin jar to Coplin jar of various reagents. This problem can often be solved by applying a thin film of Parlodion (also called celloidin) to coat the slide with a very thin plastic sac that holds the tissue against the slide surface. Such slides can then be carried along with other preparations during acid hydrolysis and through the rest of the steps of Feulgen reaction as detailed in **Subheading 3.4.** (*see* **Note 8**).

1. Put all slides to be coated into absolute ethanol for 2–3 min.
2. Transfer 40 mL of the stock 0.25% Parlodion solution into a 50-mL-capacity coplin jar or glass vial of a size to accommodate dipping of slides.
3. Transfer each slide from the absolute ethanol. Dip it into the coating solution and drain briefly on the edge of the jar.
4. Place each slide directly into 95% ethanol in a Coplin jar to harden the film.
5. Transfer sets of coated slides from 95% ethanol to 70%, 50%, and 20% ethanol solutions.
6. Rinse the slides in several changes of deionized water before proceeding with the acid hydrolysis step of the Feulgen reaction.
7. After coating as many slides as needed, decant the remaining Parlodion solution back into the stock solution bottle and keep stoppered in a safe place for later use.
8. Depending on the number of slides processed and the rate of evaporation of the solvent, the stock solution can be used for a year or more, but may require the addition of more of the 1 : 1 (v/v) ether/absolute ethanol solvent mixture to thin the solution. It should not be poured into a sink for disposal, but must be treated as a hazardous liquid waste.
9. Most of the Parlodion film on a coated slide can be removed after completing the Feulgen reaction to provide a minimal amount of background material when mounting cells in refractive index liquids for cytophotometry (*see* **Note 9**).

3.6. Special Treatment of Sectioned Tissues

Under dire circumstances, when all other methods have failed to keep sectioned material adherent to glass surfaces, perform the following:

1. Mount sections in the usual way on albuminized slides.
2. Allow the sections to expand, drain off excess water, and air-dry overnight.
3. Lay the slides on a paper towel and put onto a shelf in a paraffin oven maintained at 56–58°C.

4. Keep the slides in the oven for 10–15 min to melt the paraffin onto the glass.
5. Take the slides out of the oven and allow the paraffin to solidify at room temperature.
6. Remove the paraffin with three 5-min changes in xylene.
7. Transfer the slides through two changes of absolute ethanol.
8. Coat individual slides by dipping into 0.25% Parlodion.
9. Harden the film in 95% ethanol and rehydrate the tissue to deionized water.
10. Transfer the slides to 5 *N* HCl and proceed with the Feulgen reaction (*see* **Subheadings 3.3.** and **3.4.**).

3.7. Feulgen–DNA Cytophotometry

3.7.1. Basics

The absorption of a chromophore in monochromatic light is proportional to the quantity of the reacted substance, provided that the amount of chromophore taken up is proportional to the amount of original substance present. Quantitative cytophotometry depends on two laws of physics: Lambert's law and Beer's law, which state that the amount of monochromatic light absorbed by a material is related to both its concentration (Beer's law) and its thickness or path length (Lambert's law). That is to say, microdensitometry (cytophotometry) is the measurement of the light absorption of objects under a microscope and can be used to determine the amounts of a histochemical staining reaction in individual nuclei to estimate the cellular content of substances such as DNA ***(12,16,64,65)***.

Quantification of estimates of genome size (the C value) depends on having a reliable method to determine that the amount of Feulgen stain bound to the chromatin of a nucleus is directly proportional to the amount of DNA present. Microdensitometry is concerned with the precise measurement of light-absorbing components in microscopic preparations. Measurement relies on the interaction between photons at specific wavelengths and the chromophores (i.e., chemical substances such as the Feulgen–DNA dye complex that is contained within the nucleus of a cell). Loss of photon energy (absorption) or optical density (OD) results from the interaction of the insoluble stain reaction product with incident light. The transmittance (*T*) of the nonabsorbed incident light to a photosensing element in the system is used to translate the difference between the intensity of incident light entering the object and that of the light leaving the object. In fact, it is only possible to measure the transmittance of an object ***(12,64,65)***.

The conversion of the transmission values (*T*) into absorbance (*A*) is not direct but is expressed as $A = \log (1/T)$. This nonlinear transform is the basis of the relative photometric error (RPE) as a function of specimen transmittance in cytophotometry. The magnitude of the error can be computed as shown in **Fig. 5**. The percent error rises sharply as transmittance is increased (= low-density

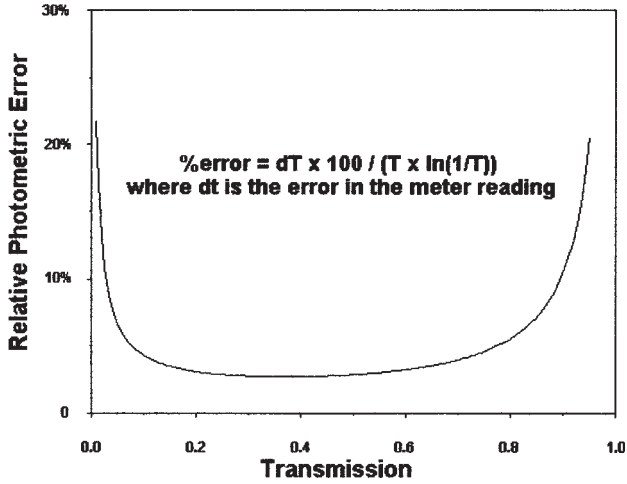

Fig. 5. Relative photometric error as a function of specimen transmittance in cytophotometry. The percent error rises sharply as transmittance is increased and as density is decreased, so that counting of photons is most accurate between the range of 0.2 and 0.8 units of absorbance (A) or optical density (OD). At either extreme of this curve, the changes in percent error are nonlinear (*see* **Note 10**).

object). Conversely, the relative error in counting photons transmitted through a high-density object (= low transmission) is also subject to considerable error (*see* **Note 10**). To minimize this inherent error in photometry, it is important that IOD values remain between 0.15 and 0.85 (i.e., the range over which the relative error is essentially 2–3%) ***(7,12,50,51,64,65)***.

For substances that are uniformly distributed (pure amplitude objects, as in a test tube or a cuvet), there is no difficulty in determining valid IOD values. However, the absorbing material in cells, such DNA in a nucleus, is not normally distributed uniformly, giving rise to the so-called distribution error of cytophotometry ***(12,41,64,65)***, which, if uncorrected, yields erroneous results because of the nonlinear relationship between transmittance and absorption. One solution to this problem is to divide the object into a number of points (pixels), each of which can be regarded as uniform, measure the light transmittance at each point, convert each one to an absorbance, and then sum them to give the total absorbance of the object (i.e., its IOD). The use of either a scanning stage or a Flying Spot microdensitometer provides a feasible way to take multiple sampling of a field that can be summed electronically to yield IOD values for the objects of interest ***(12,38,41,65)***.

By obtaining the relative integrated absorbance expressed in IOD units for populations of Feulgen-stained nuclei from several internal reference "standards"

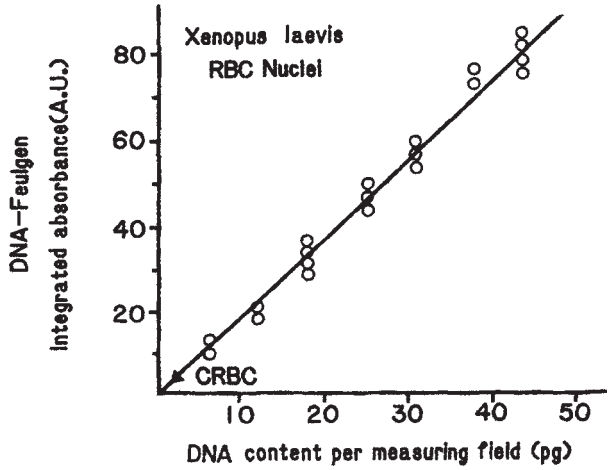

Fig. 6. Relationship between relative integrated absorbance at 560 nm and actual DNA content computed for increasing numbers of *Xenopus laevis* blood cell nuclei. (Reprinted from **ref. *16*** by permission of Wiley–Liss Inc., a subsidiary of John Wiley & Sons Inc. Copyright © 1985.)

of known DNA content ***(2,6,12,16)*** it is possible to establish reliable and reproducible curves to convert IOD values for "unknown" specimens into estimates of the amounts of DNA in picograms per nucleus to obtain C values for various species of *Drosophila* (*see* **Table 1**) or to estimate the number of multiples of the C value present in polysomatic cells of various *Drosophila* tissues at different stages of development (*see* **Figs. 1–3**) or from different genetic stocks (e.g., the *otu* mutants studied by King and his co-workers [***20–22***, ***63***; Chapter 6]).

Representative standard curves over a wide range of DNA levels are shown in **Figs. 6–8**. Erythrocyte nuclei in thin blood films of chicken (2.5 pg DNA per cell), rainbow trout (5.0 pg DNA per cell), and the African clawed toad, *Xenopus laevis* (6.3 pg DNA per cell) are very convenient and readily available reference standards to include with each set of slides to be measured using the Feulgen reaction for DNA.

3.7.2. Scanning Microdensitometry

Feulgen–DNA microdensitometry measurements are taken both of the nucleus within an appropriate mask and, again, of an adjacent clear area of the slide. The difference between the two readings represents the transmittance (T). These readings for "object" and "background" are accomplished electronically by the densitometer to yield data displayed digitally in relative units of IOD as described earlier.

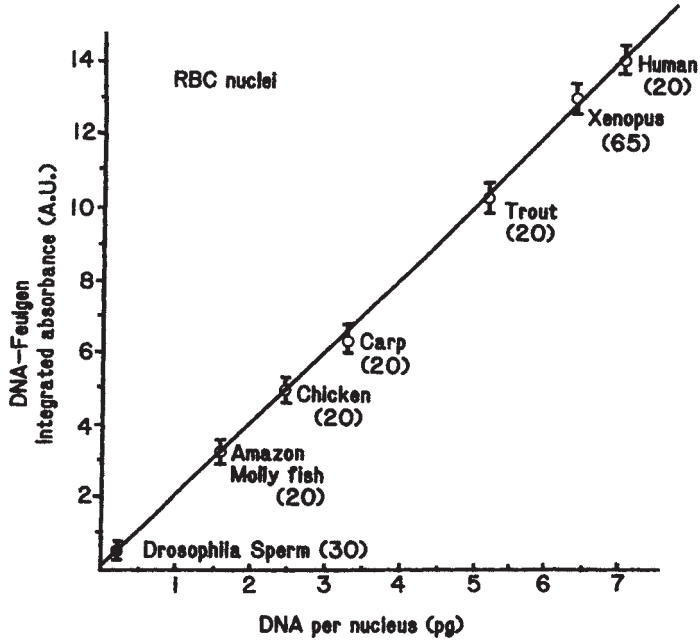

Fig. 7. Calibration curve of genome size estimates by DNA–Feulgen cytophotometry for blood cell nuclei of six vertebrates and *Drosophila* sperm. Values on the ordinate are expressed in arbitrary units (AU) of integrated absorbance at 560 nm. The standard deviation is shown by the vertical bars for each mean. Number of nuclei shown in parentheses. (Reprinted from **ref.** ***16*** by permission of Wiley–Liss Inc., a subsidiary of John Wiley & Sons Inc. Copyright © 1985.)

A single-point measurement, of course, is not representative of the heterogeneous whole of a stained nucleus (the distributional error) nor does it take into account the variations in size of individual nuclei. It is necessary to obtain a series of point densities by scanning the whole nucleus ***(38,39,65)***. The necessary measurements of point densities of a nucleus are required to obtain valid data in IOD units obtained here by a "Flying Spot" instrument (Vickers M86), the scanning spot of which may be from 0.2 to 1.0 μm, depending on the size of the object and the magnification at which it measures each point of its traverse in a raster pattern over the background and over the nucleus. With an instrument of this type, some 40,000 point density samples are accumulated within a 4-s scanning and integrating interval.

Both scanning stage and Flying Spot microdensitometers require careful identification and selection of individual nuclei for measurement and both are time and labor intensive.

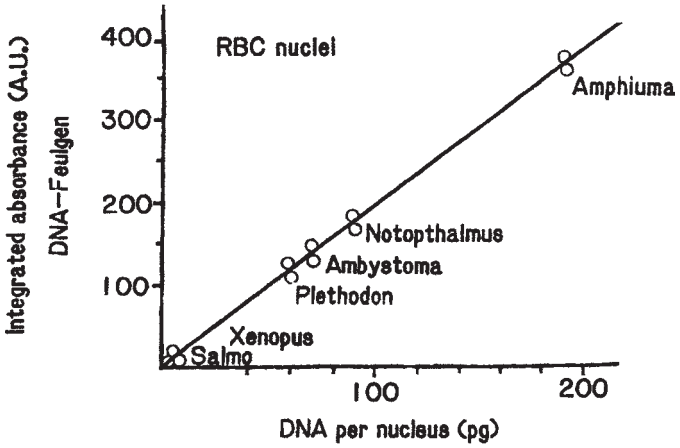

Fig. 8. Calibration curve of genome size estimates by DNA cytophotometry for blood cell nuclei for five species of amphibians and rainbow trout. Values on the ordinate are expressed is arbitrary units (AU) of integrated optical density at 620 nm. Each of the points shown represents the mean obtained from 25–30 individual scans. (Reprinted from **ref.** ***16*** by permission of Wiley–Liss Inc., a subsidiary of John Wiley & Sons Inc. Copyright © 1985.)

It is very likely that genome size determinations in the future will employ Feulgen–DNA image analysis microdensitometry (IAM) ***(12)***. Modern technology using cooled charge-coupled device (CCD) cameras with a dedicated computer and appropriate software has led to increasing application of IAM as a rapid and reliable way to determine genome size and C values for a wide variety of plant and animal species. With a suitable microscope for identification of cells and the ability to select fields for the measurement of multiple nuclei simultaneously, these newer methods offer "accuracy, rapidity, and cost-effectiveness" for genome size determinations ***(12)***. This combination of features may very well lead to a resurgence of interest in the field of genome-size determinations.

3.7.3. Subtractive, Scanning, Integrated Density Measurements

With this particular method, although two scans are necessary for each measurement, it is possible to work with rapidity because a precise "0" density background setting is not required for scanning individual nuclei in a given field. This method has the additional advantage of enabling a stray light electronic compensation to be included at the start of measuring, which will further assist in the reduction of electronic noise. The major difficulty encountered may be the location of a clear background area as large as the mask used for the specimen nucleus. Therefore, the method is most suitable for smears, squashes,

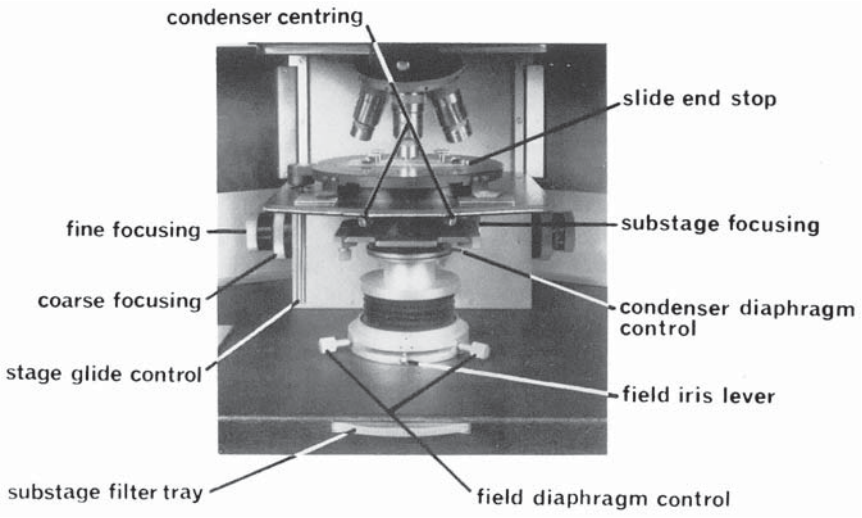

Fig. 9. View of the microscope head of a Vickers M85 scanning microdensitometer to show the optical and mechanical components that must be clean and critically aligned to ensure delivery of monochromatic light through the specimen, as well as an adjacent clear area, to obtain data from more than 40,000 point transmission values automatically sampled (by a 0.2-μm scanning spot) within a 4-s interval. The sum of these point transmission values is transformed to yield the integrated absorbance value for the specimen. A present level of "threshold" optical density can be set to cancel specimen background "noise" ***(51,66)***. The components are identified to aid in alignment of the optics and their ancillary diaphragms. (Adapted from Vickers Instruction Manual, 1977.)

or hemolymph droplets. All values of density of background and object background are registered and shown as digital values on the display panels of the instrument. IOD values and the relative area of absorbing chromophore are stored in keyed files within the computer on disks and can be rendered as hard copy via a suitable interface to a dot matrix or other type of printer ***(12,65,66)***. Several major components used in the following procedure for actual measuring of individual nuclei are shown in **Fig. 9**. Once again, it important to emphasize optic and specimen cleanliness, which, in cytophotometry, verges on sanctity.

1. Turn the masking control knob to "Set" and carefully adjust the Kohler illuminator; place the specimen slide on the stage of the viewing microscope.
2. Select the correct wavelength, bandwidth, and spot size and scanning frame.
3. With the mask and/or specimen-stage controls, place the object within a suitable size of mask centered within the scan frame (reticle in left eyepiece). Then, move to a nearby clear (background) area somewhat larger than the mask size.

4. With the spot manual controls, place the scanning spot in a clear background area within the centered mask and focus carefully to get as sharp an image of the scanning spot as possible. Then, use the fine focus of the microscope to bring the object plane of the specimen to coincide with that of the scanning spot image.
5. Turn the masking control knob to "Scan."
6. Set 0 on the density meter (with photomultiplier blocked) and set background density to 0.05 with the "set" zero control. Set the gating meter to the green line.
7. Switch scanner unit to "Automatic."
8. Press "Integrate" button to scan. Record displays for density and area.
9. Turn the masking control knob to "Set."
10. With specimen-stage controls, move the object from the mask and substitute a clear background area.
11. Turn the masking control knob to "Scan."
12. Press "Integrate" button to scan. Record displays for density and area.
13. Subtract value obtained at **step 12** from value obtained at **step 8**.

The result is in arbitrary IOD units that are dependent on objective magnification and scan frame size. Conversion to absolute units may be accomplished using an appropriate stage micrometer, enabling simple comparisons to be made between results obtained at different magnifications or at different times using the same settings for the instrument. By establishing standard reference curves (*see* **Figs. 6–8**) and always carrying two or more reference standards with each set of "unknowns," results such as the somatic cell genome size or 2C DNA value for an "unknown" species of *Drosophila* from scanning microdensitometry can be stated in picograms of DNA per nucleus with a reasonable degree of confidence in its accuracy ***(2–4,12,16,25)***.

3.8. Possible Pitfalls

Reliable and accurate cytophotometry requires that the microscope be aligned properly to minimize glare and an adequate source of monochromatic light (e.g., 560 nm), near the absorption maximum of the Feulgen–DNA reaction product (560–570 nm). It also requires modulation of ordinary line current fluctuations for the light source and a vibration-free environment for the microscope and other electronic components (*see* **Notes 11** and **12**).

Careful attention must be paid to the optics and the alignment of the microscope used to obtain IOD values of the DNA–Feulgen dye complex bound to nuclei. Variations in transmission across the field of view may be the result of poor optical alignment or dirt on optical surfaces, which can contribute the total noise level of the system. Where the light path through a measured object is asymmetric, conditions of absorption may be changed and lens flare greatly increased. **Figure 9** shows the major components reviewed in the following:

1. Check the symmetry of the light path through the microscope using a phase microscope focusing telescope and a low-power objective to visualize the filament of the light source, the field diaphragm, and the condenser iris diaphragm.
2. Note color fringes as you open and close the diaphragms. Are the red–blue shifts symmetrical at the edges of these apertures as you come up to and away from focus in the object plane?
3. Center components appropriately to eliminate uneven color fringes.

3.9. Stray Light/Glare

Stray light comes from internal reflections, dirt on optics, and so on. Stray light causes small, completely opaque objects to display a definite amount of transmittance. The presence of stray light in the optical path, aside from the principal beam, which reaches the photosensing element, can be directly assessed by "measuring" (with a stationary spot) opaque objects such as small specks of activated charcoal mounted in immersion oil between a slide and a cover slip ***(12,38,51,64)***. Any value for point transmittance appearing on the transmission meter demonstrates the extent of glare in the optic train. The Vickers M86 microdensitometer provides a convenient electronic offset correction for stray light or glare, which is determined as the transmittance of an opaque object mounted in immersion oil, the transmittance value of which is then subtracted by positioning the set infinity knob to a value of zero on the transmittance meter. This offset then defines total darkness for the system.

3.10. Scatter, Refractive Index, and the Becke Line

Nonspecific light loss resulting from scatter from differences in refractive index (n_D) of a specimen and its mounting medium is often one of the most serious errors affecting cytophotometric determinations of DNA–Feulgen amounts in tissue samples ***(12,38,41,49,64)***. Refractive index is a physical property of matter and is a quantitative expression of the degree of change in the velocity of a ray passing through a substance of one refractive index (n_D) to another of a different refractive index. The ray of light is bent from the substance of lower refractive index toward the medium of higher refractive index. That is to say, light is deviated from its initial path either in toward or out from the object of interest if the object and its mounting medium do not have the same refractive index. Look at the fine print on the label of a bottle of microscope immersion oil for which $n_D = 1.515$. The refractive index of the glass used in making oil immersion objectives, glass slides, and cover slips is 1.515. This means that there will be minimal distortion resulting from light scatter as the light from the substage illuminator traverses the condenser and passes through the slide, the object, the cover slip, and microscope optics to the retina of your eye without significant retardation of the incident light (*see* **Note 13**).

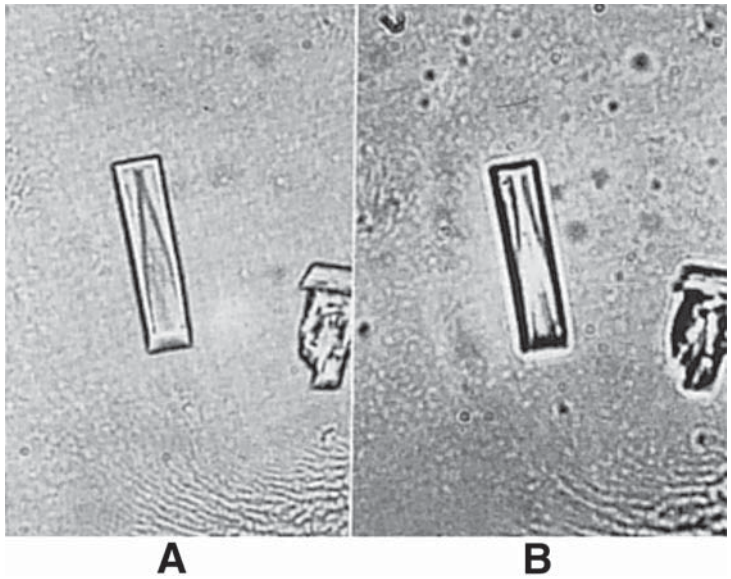

Fig. 10. A crystal of ascorbic acid (vitamin C, n_D = 1.588) mounted in a liquid with n_D = 1.744. **(A)** The specimen is within the focus of the microscope; **(B)** the same specimen, but the focus of the microscope has been raised. The Becke line (bright "halo") appears in both images but is nearer the substance of higher refractive index. The focus of the microscope is raised to show the Becke line (light "halo") bent toward the substance of higher refractive index; that is, it has been displaced outward from the crystal. If the microscope tube is lowered, the Becke line will move inward and the crystal will appear brighter. (Adapted from **ref. *67**.)*

The appearance of bright "halos" around or above nuclear outlines can significantly affect the net amount of light impinging on the light-sensing elements of the system. This bending of light is manifest as the Becke line ***(67)***. Although conditions are not always favorable for its recognition, the phenomenon is clearly evident, when the specimen is of a crystal nature and has straight sides, as shown in **Fig 10**. In this case, taken from Shillaber ***(67)***, a crystal of vitamin C (ascorbic acid), n_D = 1.588, is mounted in a liquid for which n_D = 1.740. In **Fig. 10A**, the specimen is within the focus of the microscope. In **Fig. 10B**, the focus is high to show the Becke line (the bright "halo"), which is nearer the substance of higher refractive index. It is displaced outward from the crystal. If the microscope focus is lowered, the Becke line will move inward and the crystal interior will appear brighter.

The consequences of light refraction in an optical path are clearly illustrated by the changes in appearance of microscopic glass spheres (n_D = 1.468)

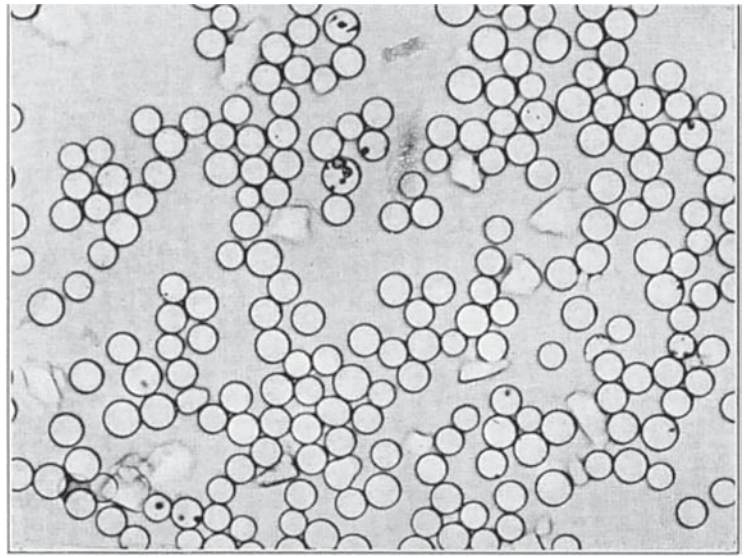

Fig. 11. Photomicrograph of clear glass spheres. The refractive index of the spheres is about 1.468. They are mounted in ethylene glycol (n_D = 1.400). In this micrograph, the focus of the microscope was made as accurately as possible to show how the spheres actually appear under normal lighting conditions. (Adapted from **ref. *67***.)

mounted in ethylene glycol (n_D = 1.400). In **Fig. 11**, the focus of the microscope was made as nearly perfect as possible to give a true idea of how the spheres appear under these conditions. Compare this image with **Fig. 12**, where the microscope focus was raised from the optimum focus. The centers of the individual spheres become brighter as the Becke line bends inward toward the higher refractive index. In **Fig. 13**, the same objects are viewed at a slightly lower optical level and the centers of the spheres appear darker than the surrounding field. Although the amount of incident light is the same for these three views of the spheres, the light bending in and out of the main beam can lead to erroneous transmittance values for small objects such as nuclei.

Refractive index matching is an important part of preparing a specimen for cytophotometry because it determines what a photosensing element will "see" if the specimen and the mounting liquid have the same refractive index, and if that is the same as the microscope slide (n_D = 1.515), the light rays are not refracted and the Becke line does not exist. The specimen itself will be invisible, save for the magenta staining of chromatin by the DNA–Feulgen reaction. For example, the cross-bands of *Drosophila* giant salivary gland chromosomes will appear as pink rungs of a ladder. When a transparent, colorless specimen has low visibility and is neither very small nor very thin, it is generally safe to

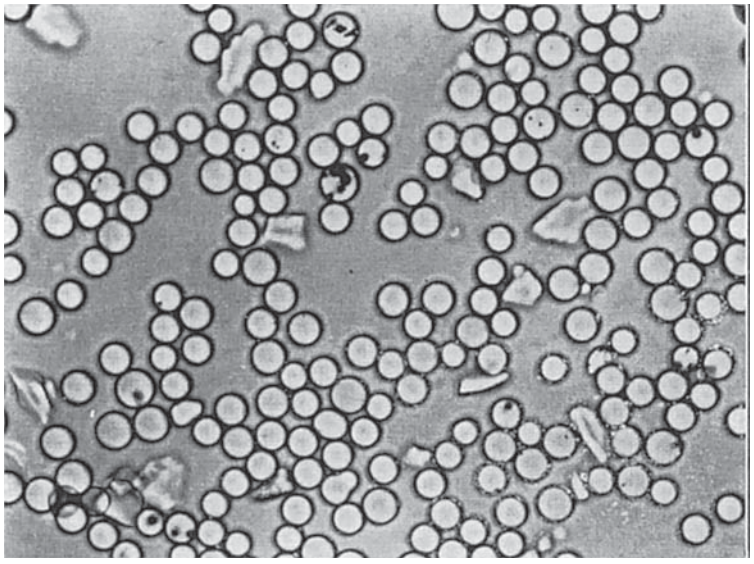

Fig. 12. Photomicrograph of same subject as in **Fig. 11**, but the microscope tube has been raised from the optimum position of focus. Note how the centers of individual spheres become brighter when they are mounted in a liquid with refractive index lower than the n_D of the test objects used here. (Adapted from **ref. 67**.)

assume that its refractive index is very close to that of the mounting liquid and that of glass.

Awareness of the influence of refractive index on estimating DNA content by cytophotometry is an important variable to evaluate before measuring an unfamiliar tissue. The n_D of most biological material ranges from 1.520 to 1.570. For example, refractive index liquid oils of 1.568 and 1.524 were used to compare C values for the very large nuclei of the larval fat body with the DNA levels of the small nuclei of the adult fat body and of oenocytes in *Drosophila* (**Fig. 3** vs **Figs. 1** and **2**). DNA values for individual Feulgen-stained sperm of *Drosophila* are useful as a reference standard for organisms with small genome sizes, but may be significantly underestimated if not matched with refractive index liquids because of their staining density and high refractive index in usual mounting media. **Table 5** lists many commonly used mounting media and their refractive index values.

Sets of oils of different refractive indices are available commercially for use in mounting cells and tissues for cytophotometry (*see* **Note 14**). As stated so simply and succinctly in the procedure outlined by Hardie et al. ***(12)***, "the following steps can be taken to select an oil with the appropriate refractive index for the cell type being analyzed:

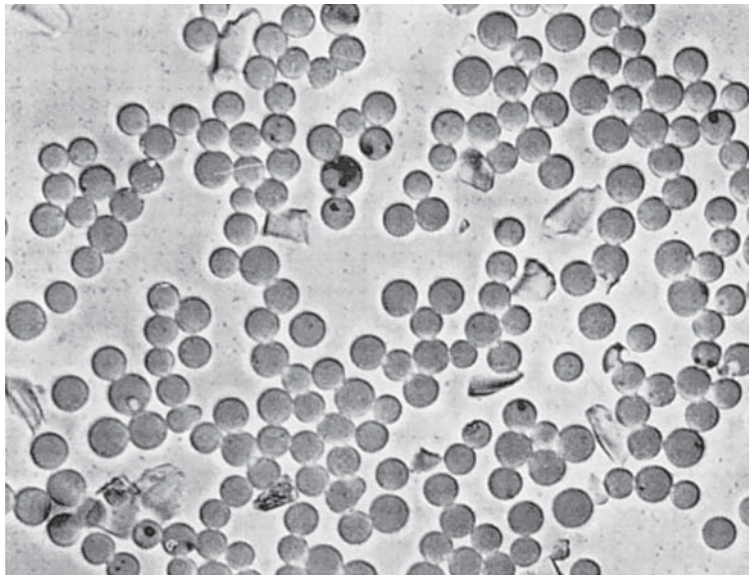

Fig. 13. Photomicrograph of the same object as in **Fig. 11**, but taken at a slightly lower optical level than in **Fig. 12**. The centers of the spheres now appear darker than the surrounding field. The relative density values obtained here would be significantly higher here than those obtained from the same objects mounted in a matching refractive index liquid that would minimize light loss resulting from scatter. (Adapted from **ref. *67***.)

1. Begin by placing a drop of oil with a mid-range refractive index (e.g., $n_D = 1.54$) on the slide and add a cover slip.
2. Focus on a nucleus, which should appear as a pink jewel suspended in space. If membranes are visible, the refractive index is incorrect. (Note that 100× objectives require a second drop of immersion oil, usually $n_D = 1.515$, between the cover slip and the lens.)
3. To determine whether a higher or lower refractive index is needed, focus up and down through the nucleus. In one direction, a bright outline of pink light will be seen on the perimeter of the nucleus. In the other direction, the nucleus will appear to enlarge as the focus moves through it, without any bright light. Take note of which direction of focus (i.e., "up," moving the lens away from the slide, or "down," toward the slide) produces which effect.
4. If the bright light appears when focusing up, then a higher refractive index is required. If the bright light appears during the down focus, then a lower refractive index is needed.

In properly matched preparations with very high transmittance values, or conversely with very low IOD values, the relative photometric error, with regard

Table 5
Refractive Indices of Common Reagents and Mounting Media for Biological Specimens

Alphabetical listing		Listing according to ascending values of n_D	
n_D Temperature 25°C	Name	n_D Temperature 25°C	Name
1.000294	Air[a]	1.000294	Air[a]
1.358	Ethyl alcohol	1.333	Water
1.323	Methyl alcohol	1.323	Methyl alcohol
1.535	Canada balsam (hard)	1.358	Ethyl alcohol
1.477	Castor oil	1.452	Paraffin oil (light)
1.54	Clarite	1.463	Glycerol
1.57	Clarite X	1.468	Olive Oil
1.529	Clove oil	1.477	Castor oil
1.48 (approx)	Glycerin jelly	1.48 (approx)	Glycerin jelly
1.463	Glycerol	1.480	Linseed oil
1.515	Immersion oil[b]	1.491	Xylene
1.480	Linseed oil	1.515	Immersion oil[b]
1.468	Olive oil	1.529	Clove oil
1.452	Paraffin oil (light)	1.535	Canada balsam
1.333	Water	1.54	Clarite
1.491	Xylene	1.57	Clarite X

[a]The index of air is based on that of a vacuum as unity; it is 1.000294. The index of refraction of a substance other than air is usually based on air with an *assumed* index of unity. To convert an index based on air to an index referred to a vacuum as unity, multiply by 1.000294.

[b]The index of flint glass is 1.515. Hence the value of the majority of commercially available immersion oil is 1.515.

Source: Adapted from **ref. *67***.

to the accuracy of readings by the photosensing component of the system, may be in error by as much as 50% or more, simply because of the inaccuracy in readings below IOD values of 0.20 or above 0.80 (*see* **Fig. 5**). It is important to be aware of nonspecific light loss resulting from scatter and the relative photometric error inherent in measuring objects that are very pale or very densely stained. These issues also apply to microdensitometry by image analysis ***(12)***.

3.11. Measuring "Off Peak"

Because a cytophotometer counts molecules with markedly reduced accuracy at either 1% *T* or at 99% *T*, it is always prudent policy to measure objects

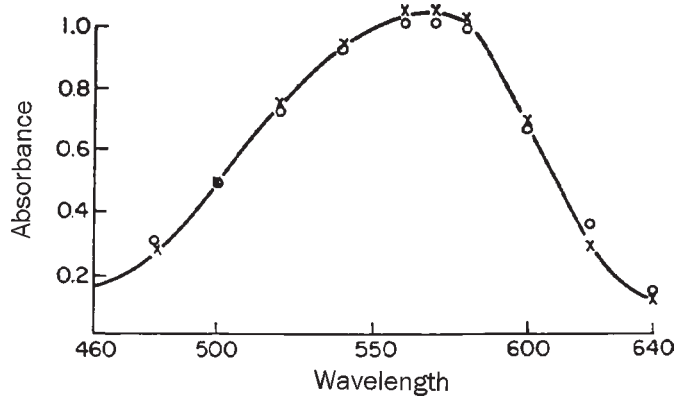

Fig. 14. Absorption curve of the DNA–Feulgen dye complex in a fat body cell of *Drosophila melanogaster*. (Rasch, unpublished data; 1984.)

with IOD values in the range 0.2–0.8. Absorbencies above 1.00 and below 0.15 are subject to rapidly rising error functions at either high density (or low transmission) and at high transmission (and low density). The relative error curve in **Fig. 5** clearly illustrates the magnitude of this potential photometric pitfall.

As shown initially by Swift ***(5)*** in 1950 and subsequently by others ***(50,51,64,68)***, if single-point absorbances for nuclei exceed 1.0 at a wavelength of 560 nm, near the peak absorbance of the Feulgen chromophore, it is both possible and feasible to measure such specimens "off peak" (e.g., at 615 nm or at 620 nm), at which wavelengths absorbance of the Feulgen–DNA reaction product is about half of that at the peak (A_{max}). At the off-peak wavelength, the nuclei will have absorbances in the range 0.40–0.60, instead of 1.0 or above. The wavelength of measuring light must be selected so as to be sufficiently close to A_{max} to allow accurate measurement of the palest nuclei present in the cell sample ***(51,64)***. By measuring on the red side of the Feulgen absorption curve (**Fig. 14**), the slope of the line plotting concentration vs absorbance is greater at 560 nm and lower at 620 nm. This loss in sensitivity, however, is offset by the enhanced accuracy gained with lower and more reliable IOD values.

This shift in wavelength for measuring large, darkly stained nuclei is a valuable tool to have available when comparing DNA levels in polysomatic tissues from maturing larvae of *Drosophila melanogaster* ***(25,31,33,34,36)***. Obviously, when nuclei of an "unknown" are measured off peak, the internal standard reference cell samples for each slide series also must be measured at the same wavelength with the same optical conditions for magnification, electronic gain settings, scanning spot size and mask size, selection ***(12)***.

3.12. Making Blood Smears for Standard Reference Slides

Establishing a standard curve of cells of known DNA content is very important because it demonstrates that the staining procedures are verifiable and that the equipment used for analysis is performing appropriately (*see* **Figs. 7** and **8**). The reference standards chosen should be appropriate for the unknowns to be tested (*see* **Note 15**). The nucleated blood cells of lower vertebrates are very suitable for photometric analysis ***(11,12,16)***. They can be prepared essentially as monolayer blood films using the regular techniques of a hospital hematology laboratory. When making a test slide of *Drosophila* hemolymph, it is practical to let a small droplet air-dry after touching it to a slide that already carries a short film of chicken red blood cell (RBC) nuclei. This makes a much better preparation for cytophotometry than trying to spread (actually shear) insect hemolymph (*see* **Notes 16** and **17**).

3.13. Use of Field Finders

Locating a small area of special interest on a glass slide (e.g., a particular clean region of well-spread individual sperm nuclei), can be a tedious task of scanning a large area of the slide to reposition that same field on the microscope for cytophotometry. Ink marks or circles marked with a wax pencil are sometimes difficult to apply and often rub off. The job can be made much simpler by the use of a slide marked by a numbered and lettered grid (*see* **Fig. 15**). With this tool, it is possible to locate a particular group of cells and record their coordinates in terms of space designations on the surface of a 3 × 1-in. glass slide called a "field finder" (*see* **Note 18**). Gridded slide finders are marked so that they are read right side up (to the viewer) in a conventional microscope when inserted into the clasping jig of the mechanical stage. It is important to position both the "test" slide (the slide with the cells that you want to relocate to measure them) and the gridded slide very carefully so that the corners of the slides are fitted securely within the flat holding arms of the mechanical stage so that repositioning can be accomplished readily and repeatedly without displacement because of stage backlash. To do this, perform the following:

1. Fit the test slide into the clasp of the mechanical stage, being certain that the slide fits snugly against both the vertical and the horizontal axes and the crescent-shaped holding arm of the stage.
2. Scan the slide to find the objects of special interest.
3. Taking care not to disturb the position of the mechanical stage, remove the "test" slide and replace it with the gridded slide. Focus on the field finder without moving or touching the mechanical stage. Note both the vertical and horizontal coordinates of the grid location, reading the site for the position of the cells that you positioned previously as both a letter and a numerical value, noted as a decimal of the letter (e.g., S.2), as shown in **Fig. 15**.

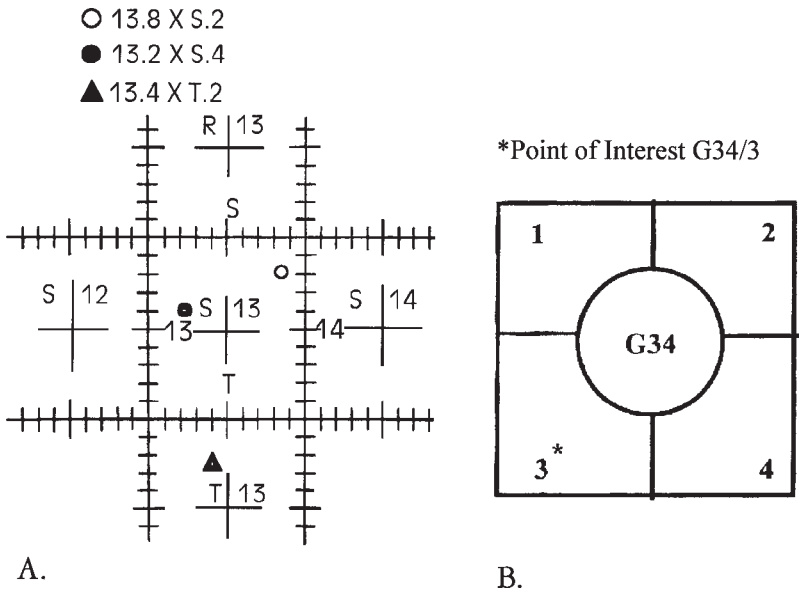

Fig. 15. The Lovins Field Finder **(A)** and the England Finder Grid **(B)** are precision devices for the microscopist to use in relocating fields of interest on a slide-mounted specimen. Each finder has a precision rectangular-coordinate grid pattern protected by a thin cover glass on a special microscope slide. (*See* text and **Note 18** for more details.) The appropriate answers for grid locations of symbols with the Lovins Finder are given at the upper left of **Fig. 14**. The location of the asterisk in the lower left quadrant of the England Finder field of view is read as 34/3*. It does take practice and a bit of time to learn how to read slide coordinates for your prized slide preparation with either of the finders, but the time spent to master this game is a small investment when compared to the time spent trying to relocate a particular group of cells that you *know* is on that slide.

4. Put the slide finder into position on the mechanical stage of the microscope to be used for cytophotometry and relocate the letter–number locus.
5. Remove the field finder and position the "test" slide into the mechanical stage and focus for the object plane without touching or moving the mechanical stage.
6. Again, focus under low power for the object plane, without moving the mechanical stage to identify the group of nuclei to be measured. They should now appear within a 20- to 25-µm radius of the center of the field and might require slight repositioning to go to a 40× high dry objective or to a 100× oil immersion lens for measuring and/or photography.
7. Locate other sites of interest for measuring on the same or other slides by repeating **steps 1–5** with the "test" slide and then the field finder.

Often, it is sufficient to determine the object locus to a letter and one decimal point before putting the test slide on the stage of the cytophotometer using

the coordinates of the gridded slide to position the "test" slide at the same position as the gridded slide that had been used to relocate the desired field. It is also possible to use the letter locus with an estimate of the second decimal point for relocation of a site on the "test" slide initially under low power, before going to oil immersion for final location of the object of interest. This also makes it feasible to find suitable areas for background readings near the nuclei to be measured. To clean a gridded slide, wipe it with a soft cloth or lens paper. Avoid solvents or other chemical cleaners.

4. Notes

1. Useful information about pararosaniline and its methylated analogs (Basic Fuchsin) is available in the 9th edition of *Conn's Biological Stains* ***(69)***. In particular, refer to the chapter on triaminotriphenylmethane dyes (Basic Fuchsins and Rosanilins) pp. 259–266. Also, see Table 19.1—Nomenclature and Synonyms of Stains and Chromogenic Reagents Arranged in Order of *Color Index Numbers*; Table 19.5—Solubility Data; and Table 19.9—Solubilities of Certain Certified Commercial Stains.
2. There is substantial literature on the use of different dye lots in the traditional method of dissolving Basic Fuchsin in boiling water, then adding the metabisulfite ***(49,52,59,60,70)***. Storage of this reaction mixture in the dark may vary from as short a period as 3–4 h up to 30 d, before decolorizing with activated charcoal ***(2,16,70)***. In our experience, storage for 60–72 h in the dark at room temperature is adequate for completion of the reaction that produces leucofuchsin sulfurous acid for Feulgen staining. Longer periods of 96–144 h yielded no increase in the staining intensity of chicken blood cell nuclei (Rasch, unpublished data).
3. Schiff's reagents often show a white, polymorphous precipitate after varying periods of storage in the cold. Formation of the precipitate is less common if the reagent is stored in small bottles, filled to the top to minimize air space and loss of SO_2 from the solution ***(52,58–60)***. Increasing the acid content to 0.2 *N* for 1 g of dye or lowering the dye content to 0.5 g in 0.15 *N* also tends to prevent formation of the white precipitate with certain dye lots of Basic Fuchsin ***(60)***, but may reduce staining intensity due to continuing acid hydrolysis of the DNA in the Schiff's reagent itself.
4. Not all Basic Fuchsins make satisfactory Schiff's reagents. Solutions made from the same batch of the dye may differ considerably in performance, possibly because of conditions and age of the dye lot. Some dye lots are unsatisfactory for staining DNA because the Schiff's reagents prepared from them retain a faint yellow to a dark yellow to yellow to an amber discoloration, despite multiple treatments with decolorizing activated charcoal. Several dye lots of certified Basic Fuchsin for which three to four repeated charcoal treatments did not remove residual discoloration of the reagent include DcFp 8 (yellow), DcFb 14 (dark amber), DcFr 17 (dark yellow), and ACF 37 (medium yellow).

5. Most authors consider that a Schiff's reagent to be used in the Feulgen reaction for DNA has a useful shelf life of some 4–6 mo when stored tightly sealed in a refrigerator. Although unopened bottles of reagent can stain very well even after storage for a year, for quantitative cytophototometry it is prudent to evaluate new batches of Schiff's reagent by doing a trial run with both chicken and trout blood smears before processing a set of high-value *Drosophila* preparations. Evaluating the staining behavior of a Schiff's reagent and determining the optimum duration and temperature for the acid hydrolysis step are critical for reliable and reproducible C-value estimates.
6. To minimize the loss of apurinic acid fragments during the acid hydrolysis of the Feulgen reaction ***(7,44,49)*** some workers ***(40,46,50,61)*** have hydrolyzed their preparations in 4 *N* HCl made with polyethylene glycol (PEG) (molecular weight 8000 (e.g., from Sigma-Aldrich, cat. no. 2139), using 15 g PEG per 50 mL of 4 *N* HCl) for 1 h at 28°C. This is followed immediately by 1 h of Feulgen staining (Schiff's reagent from Sigma-Aldrich) and then given multiple rinses in sulfite water, washed in deionized water, and dehydration in graded alcohols to xylenes for mounting in oil or resin under glass.
7. A few disposable, polypropylene micropipet tips (200 µL capacity) plus several gum rubber pipet bulbs make economical and effective tools for adding or withdrawing small amounts of fixative or other liquid reagents in the immediate vicinity of tissue fragments on a subbed slide. These items are readily available from the vendors listed in **Table 3** (e.g., Fisher Scientific Co., cat. no. 21-197-8E 00 for 200-µL-capacity polypropylene, disposable Redi-Tip micropipet tips and cat. no. 14-065A for 1-mL-capacity gum rubber bulbs). Because of the very small aperture at the tip, the plastic's hydrophobic properties and the fingertip control that a soft rubber bulb affords over the rate of flow at the pipet tip, this homemade micropipet works quite well to facilitate changing solutions without touching tissue specimens. In addition to using micropipets for the multiple protocol steps required for Feulgen staining *en bloc*, we use 1.5-mL-capacity polystyrene "Autoanalyzer" cups (e.g., cat. no. 73.641, color: neutral, Sarstedt, Newton, NC) to hold tissue during the staining process. These cups, or any other short, transparent, plastic vials that have conical bottoms and are free-standing should have "snap off" caps to minimize the loss of SO_2 during the course of the Feulgen reaction and the changing of reagents sequentially with the micropipets. Several different specimens can be processed at the same time through the acid hydrolysis and all of the subsequent steps of the Feulgen staining protocol. The ease of changing solutions and the swirling of tissue fragments upon the addition of each solution in sequence allow both an adequate reagent volume : tissue ratio and sufficient agitation of the specimen to achieve excellent staining for about a dozen sets of different tissue samples simultaneously.

   The multiple wells of the polystyrene or polypropylene trays commonly used for mammalian cell culture can also be used with micropipets to good advantage to accomplish Feulgen staining. These plates are available from most of the vendors listed in **Table 3** (e.g., Fisher Scientific Co., cat. no. 07-200-61 or Corning

Costar No. 3512 for 12 wells per plate or Fisher cat. no. 07-260-740, Corning Costar No. 3527 for 24 wells per plate) and can be used with micropette tips to house different individual tissue specimens (e.g., single ovarioles). However, a glass plate, plastic top, or a thin film of plastic (such as Saran Wrap from a supermarket) should be placed over the tray to prevent dissipation of SO_2 from the Schiff's reagent during the 2-h period of the reaction. The plastic trays can be used with an inverted microscope or with a conventional dissecting microscope to monitor the course of the reaction. A particular advantage of the plastic micropipet tips and the small plastic vials (or wells in a plastic tray) is their adversity to water, which minimizes the hazard of tissues adhering to pipet tips or container walls, as so often happens when using glass surfaces. A customized "tool" kit of micropipets of different holding capacities (20–200 μL) can be easily put together for the particular volumes needed with a given staining protocol. The base of some micropipet tips fit snugly when inserted into the holding rim of a 1 mL rubber bulb. If not, apply a thin film of glycerine around the rim of the pipet base to assure a good fit and adequate suction. Bulbs and pipet tips can be cleaned and recycled for months. Dispo micropipet tips are usually sold in lots of 500–1000 per package. An alternative acquisition plan, perhaps, would be to seek out a colleague in molecular biology who would be willing to make an indefinite loan of a dozen or more polypropylene micropipet tips in return for a good cup of coffee or a cold can of soda.

8. Coated slides are prone to scratches on the face or back of adjacent slides as they are jostled in moving in and out of Coplin jars for the various steps of the Feulgen reaction. Be careful as you move each slide so that rips or tears of the film do not detach tissue fragments from neighboring slides.
9. Almost all of the Parlodion film on a coated slide can be removed after completing the Feulgen reaction by dehydrating coated and stained slides from deionized water through a graded series of ethanols up to absolute ethanol. After three 5-min changes in absolute ethanol, the film is essentially gone and the slide can be cleared in several changes of xylenes before mounting in an appropriate refractive index liquid for cytophotometry.
10. An analogy comes to mind: the chance of shooting a fish in a barrel (photons absorbed) is vastly different when there is only 1 fish (very high transmittance) rather than 50 fish (very low transmittance) available as targets in the same size barrel.
11. To eliminate fluctuations in line current and "noise" in the system, plug the microscope source light and the computer into a voltage regulator (Sola Microcomputer Regulator [MCR], Elk Grove Village, IL). If problems arise with DC power supplies for halogen lamps, such as those used in Vickers M85 microdensitometers, the TENMA model no. 72-6625 regulated 13.8 VDC power supply (20A continuous, 25A surge current capacity) is both useful and economical. It is available from MCM Electronics (www.mcminone.com) and can be fine tuned to deliver somewhat less voltage than regularly used for a 12V lamp (e.g., 11.75V) to obtain a ripple of less than 0.8 mV at the bulb base which significantly pro-

longs the life of the lamp. Simple surge protectors and "line conditioners" are inadequate for the job to be done in modulating voltage shifts during routine operation of the microdensitometer.

12. So-called "body cushions" to eliminate building vibrations are polymer pads, available in several sizes that are mounted on steel plates for strength and weight, but literally soft-cushion a microscope base to make it essentially vibration-free. This feature also recommends their use for image analysis and photomicroscopy. The pads are both suitable and economical for damping building vibrations and are available in various sizes and in four degrees of polymer hardness from Dynamics, Inc. (Allentown, PA).
13. Although the 100× oil immersion lenses for most microscopes have a refractive index (n_D) of 1.515, as do most glass slides and cover slips, and require the use of oil with a n_D of 1.515, some lenses such as those for the Vickers M85 instrument's 40× high dry lens and the 100× oil immersion objective have a n_D = 1.524. It is important to use a matching refractive oil of n_D = 1.524 for immersing both the objective lens and the top lens of the condenser, if double immersion is used to enhance resolution and to minimize distortion of light as a result of scatter.
14. Sets and single 4-oz bottles of refractive index liquids are available from R. P. Cargille Laboratories, Inc. (Cedar Grove, NJ).
15. Convenient blood cell standards may include domestic chicken, RBC 2.5 pg DNA per nucleus; molly fish RBC, 1.6 pg DNA/nucleus; carp, 3.4 pg DNA/nucleus; rainbow trout RBC, 5.1–5.2 pg DNA/nucleus; *Xenopus laevis*, 6.3 pg DNA/nucleus and human lymphocytes 7.0 pg DNA per nucleus. It is very easy to work with a small droplet of blood to put a thin film of standard cells on the bottom half of a slide, leaving the top half free for the addition of an "unknown" cell sample (*see* **ref.** ***12*** for additional suggestions).
16. *See* Hardie et al. ***(12)*** for directions on making blood smears by "pulling" rather than "pushing" a drop of blood along the surface of a glass slide to minimize cell damage.
17. A convenient and readily available listing of genome sizes for many vertebrate and/or invertebrate species is the Animal Genome Size Database imitated and maintained by T.R. Gregory Online at www.genomesize.com.
18. The England Field Finder gridded slide is available from McCrone Microscopes and Accessories, Westmount IL; cat. no. 313 (www.mccrone.com). Although the Lovins Field Finder is no longer manufactured, it might be worth inquiring about its availability as a used item from microscope dealers and microscope repair shops.

Acknowledgments

This research was supported in part by grants from the National Science Foundation (DEB 77-03257, PCM 81-03250, and DEB 00-80921). It is dedicated to Dr. Robert W. Rasch for his continuing encouragement and to Dr. Hewson Swift who mentored my introduction to cytophotometry more than 50 yr ago. I also thank Neil Woodward, David Edwards, Amber McCullough, and Deborah Lee for their expert help in my research program.

References

1. Gregory, T. R. (2001) Coincidence, coevolution or causation? DNA content, cell size, and the C-value enigma. *Biol. Rev.* **76,** 65–101.
2. Rasch, E. M., Barr, H. J., and Rasch, R. W. (1971) The DNA content of sperm of *Drosophila melanogaster*. *Chromosoma* **33,** 1–18.
3. Mulligan, P. K. and Rasch, E. M. (1989) The determination of genome size in male and female germ cells of *Drosophila melanogaster* by DNA–Feulgen cytophotometry. *Histochemistry* **66,** 11–18.
4. Adams, M. D., Celniker, S. E., Holt, R. A., et al. (2000) The genome sequence of *Drosophila melanogaster*. *Science* **287,** 2185–2195.
5. Swift, H. (1950) The constancy of deoxyribose nucleic acid in plant nuclei. *Proc. Natl. Acad. Sci. USA* **36,** 643–647.
6. Mirsky, A. E. and Ris, H. (1951) The desoxyribonucleic acid content of animal cells and its evolutionary significance. *J. Gen. Physiol.* **34,** 451–462.
7. Swift, H. (1953) Quantitative aspects of nuclear nucleoproteins. *Int. Rev. Cytol.* **2,** 1–76.
8. Vendrely, R. and Vendrely, C. (1956) The results of cytophotometry in the study of deoxyribonucleic acid (DNA) contents of the nucleus. *Int. Rev. Cytol.* **5,** 171–197.
9. Britten, R. J. and Davidson, E. H. (1971) Repetitive and non-repetitive DNA sequences and a speculation on the origins of evolutionary novelty. *Q. Rev. Biol.* **46,** 111–138.
10. Gregory, T. R. and Hebert, P. D. N. (1999) The modulation of DNA content: proximate causes and ultimate consequences. *Genome Res.* **9,** 317–324.
11. Gregory, T. R. (2002) Animal Genome Size Data Base. Available at www.genomesize.com.
12. Hardie, D. C, Gregory, T. R., and Hebert, P. D. N. (2002) From pixels to picograms: a beginners guide to genome quantification by Feulgen image analysis densitometry. *J. Histochem. Cytochem.* **50,** 735–749.
13. Butterworth, F. M., Rasch, E. M., and Johnson, M. H. (1985) Is there a limit on in situ, genomic replication in *Drosophila? J. Exp. Zool.* **234,** 325–328.
14. Lohe, A. H. and Hilliker, A.J. (1995) Return of the H-word (heterochromatin). *Curr. Opin. Gen. Dev.* **5,** 746–755.
15. Blackburn, E. H. and Szostok. J.W. (1984) The molecular structure of centromeres and telomeres. *Annu. Rev. Biochem.* **53,** 163–194.
16. Rasch, E. M. (1985) DNA "standards" and the range of accurate DNA estimates by Feulgen absorption microspectrophotometry, in *Advances in Microscopy* (Cowden, R. R. and Harrison, R. W., eds.), New York, NY, pp. 137–166.
17. Alfert, M. (1954) Composition and structure of giant chromosomes. *Int. Rev. Cytol.* **3,** 131–175.
18. Bozcuk, A. N. (1972) DNA synthesis in the absence of somatic cell division associated with ageing in *Drosophila subobscura*. *Exp. Gerontol.* **7,** 147–156.
19. Hammond, M. P. and Laird, C. D. (1985) Chromosome structure and DNA replication in nurse and follicle cells of *Drosophila melanogaster*. *Chromosoma* **91,** 267–278.

20. King, R. C., Riley, S. F., Cassidy, J. D., White, P. E., and Paik, Y. K. (1981) Giant polytene chromosomes from the ovaries of a *Drosophila* mutant. *Science* **212,** 441–443.
21. King, R. C., Rasch, E. M., Riley, S. F., O'Grady, P. M., and Storto. P. D. (1985) Cytophotometric evidence for the transformation of oocytes into nurse cells in *Drosophila melanogaster*. *Histochemistry* **82,** 131–134.
22. Gall, J. G. (1981) Chromosome structure and the C-value paradox. *J. Cell Biol.* **91,** 3s-14s.
23. Rudkin, G. T. and Corlette, S. L. (1957) Disproportionate synthesis of DNA in a polytene chromosome region. *Proc. Natl. Acad. Sci. USA* **43,** 964–968.
24. Rudkin, G. T. (1969) Non-replicating DNA in *Drosophila. Genetics* **61(Suppl.),** 227–238.
25. Rasch, E. M. (1970) DNA cytophotometry of salivary gland nuclei and other tissue systems in Dipteran larvae, in *Introduction to Quantitative Cytochemistry* (Weid, G. W. and Bahr, G. F., eds.), Academic, New York, NY, Vol. 2, pp. 357–397.
26. Renkawitz-Pohl, P. and Kunz, W. (1975) Underreplication of satellite DNA in polyploid ovarian tissue of *Drosophila virilis. Chromosoma* 49, 249–258.
27. Spear, B. B. (1977) Differential replication of DNA sequences in Drosophila chromosomes. *Am. Zool.* **17,** 695–706.
28. Smith, D. S. (1968) *Insect Cells: Their Structure and Function,* Oliver and Boyd, Edinburgh, pp. 183–184.
29. Rizki, T. M. (1978) Fat body, in *The Genetics and Biology of Drosophila* (Ashburner, M. and Wright, T. R. F., eds.), Academic, New York, Vol. 2B, pp. 561–601.
30. Johnson, M. B. and Butterworth, F. M. (1985) Maturation and ageing of adult fat body and oenocytes in *Drosophila* as revealed by light microscopic morphotometry. *J. Morphol*. **184,** 51–59.
31. Butterworth, F. M. and Rasch, E. M. (1986) Adipose tissue of *Drosophila melanogaster*. VII. Distribution of nuclear DNA amounts along the anterior–posterior axis in the larval fat body. *J. Exp. Zool*. **239,** 77–85.
32. Painter, T. S. and Reindorf, E. C. (1938) Endomitosis in the nurse cells of the ovary of *Drosophila melanogaster*. *Chromosoma* **1,** 276–283.
33. Lamb, M. L. (1982) The DNA content of polytene nuclei in midgut and Malpighian tubule cells of adult *Drosophila melanogaster. Roux's Arch. Dev. Biol.* **191,** 381–384.
34. Rasch, E. M. and Butterworth, F. M. (1986) DNA levels in fat body cells of larval and adult *Drosophila melanogaster*. *J. Histochem. Cytochem.* **34,** 22.
35. Spear, B. B. and Gall, J. G. (1973) Independent control of ribosomal gene replication in polytene chromosomes of *Drosophila melanogaster. Proc. Natl. Acad. Sci. USA* **70,** 1359–1363.
36. Dennhofer, L. (1982) Underreplication during Polytenization? *Theor. Appl. Genet*. **63,** 193–199.
37. Bielinsky, A. K., Ezrok, M., Blitzblau, H., et al. (2001) Origin recognition complex binding to a metazoan replication origin. *Molec. Biol. Cell* **12(Suppl.),** 357a.

38. Goldstein, D. J. (1970) Aspects of scanning microdensitometry. I. Stray light (glare). *J. Microsc.* **92,** 1–16.
39. Goldstein, D. J. (1971) Aspects of scanning microdensitometry. II. Spot size, size, focus and resolution. *J. Microsc.* **93,** 15–42.
40. Goldstein, D. J. (1975) Aspects of scanning microdensitometry. III. The monochromater system. *J. Microsc.* **105,** 33–56.
41. Bedi, K. S. and Goldstein, D. J. (1976) Apparent anomalies in nuclear Feulgen–DNA contents, role of systematic microdensitometric errors. *J. Cell Biol.* **71,** 68–88.
42. Feulgen, R. and Rossenbeck, H. (1924) Mikroskopisch-chemischer Nachweis einer Nucleinsaure vom Typus der Thymonuceinsaure und die darauf beruhende elektive Farbung von Zellkernen in mikrokskopisch Praparaten. *Z. Physiol. Chem.* **135,** 203–248.
43. Schiff, H. (1866) Eine neue Reithe organischer Diamine. *Justus Liebigs Ann. Chem.* **140,** 92–137.
44. Jordanov, J. (1963) On the transition of deoxyribonucleic acid to apurinic acid and the loss of the latter from tissues during Feulgen reaction hydrolysis. *Histochemistry (Jena)* **15,** 135–152.
45. Kjellstrand, P. T. T. and Lamm, C. J. (1976) A model of the breakdown and removal of the chromatin components during Feulgen acid hydrolysis. *Histochem. J.* **8,** 419–430.
46. Kjellstrand, P. T. T. (1977) Control of extraction of deoxyribonucleic acid and apurinic acid by polyethylene glycol in Feulgen hydrolysis. *J. Histochem. Cytochem.* **16,** 371–375.
47. Rasch, R. W. and Rasch, E. M. (1973) Kinetics of hydrolysis during the Feulgen reaction for deoxyribonucleic acid. *J. Histochem. Cytochem.* **12,** 1053–1065.
48. Duijdam, W. A. L. and van Duijn, P. (1975) The influence of chromatin compactness on the stoichiometry of the Feulgen Schiff procedures studied in model films. *J. Histochem. Cytochem.* **23,** 882–890.
49. Chieco, P., Jonker, A., Melchorri, C., Vanni, G., and van Noorden, J. F. (1994) A user's guide for avoiding errors in absorbance image cytometry: a review with original experimental observations. *Histochem. J.* **26,** 1–19.
50. Allison, D. C., Ridolpho, P. F., Rasch, E. M., Rasch, R. W., and Johnson, T. S. (1981) Increase of absorption cytophotometric values by control of stain intensity. *J. Histochem. Cytochem.* **29,** 1219–1228.
51. Allison, D. C., Lawrence, G. N., Ridololpho, P. E., O'Grady, B. J., Rasch, R. W., and Rasch, E. M. (1984) Increased accuracy and speed of absorption cytometric DNA measurements by automatic corrections for nuclear darkness. *Cytometry* **5,** 217–227.
52. Kasten, F. H. (1960) The chemistry of the Schiff's reagent. *Int. Rev. Cytol.* **10,** 1–100.
53. Nettleton, G. S. and Martin, A. W. (1979) Separation of fuchsin analogs using thin layer chromatography. *Stain Technol.* **54,** 213–221.
54. Teichmann, J. S., Krick, P., and Nettleton, G. A. (1980) Effects of different fuchsin analogs on the Feulgen reaction. *J. Histochem. Cytochem.* **28,** 1062–1066
55. Schulte, L. and Wittekind, J. (1989) Standardization of the Feulgen-Schiff technique. Staining characteristics of pure fuchsin dyes: a cytophotometric investigation. *Histochemistry* **91,** 321–331.

56. Alfert, M. and Geschwind, I. I. (1953) A selective staining method for the basic proteins of cell nuclei. *Proc. Natl. Acad. Sci. USA* **30,** 991–999.
57. DeCosse, J. J. and Aeillo, N. (1966) Feulgen hydrolysis: effect of acid and temperature. *J. Histochem. Cytochem.* **14,** 601–604.
58. Barka, T. and Anderson, P. J. (1965) *Histochemistry. Theory, Practice and Bibliography,* Harper and Row, New York, NY, pp. 97–100.
59. Pearse, A. G. E. (1968) *Histochemstry: Theoretical and Applied,* Williams and Wilkins, Baltimore, MD, Vol. 1, pp. 254–265 and 647–649.
60. Lillie, R. D. (1951) Simplification of the manufacture of Schiff reagent for use in histochemical procedures. *Stain Technol.* **25,** 163–165.
61. Kotetnikov, V. M. and Litinskaya, L. L. (1981) Comparative studies of Feulgen hydrolysis for DNA: influence of different fixatives and polyethylene glycols. *Histochemistry* **71,** 145–153.
62. Rasch, E. M., King, R. C., and Rasch, R. W. (1984) Cytophotometric studies on cells from the ovaries of *otu* mutants of *Drosophila melanogaster. Histochemistry* **81,** 105–110.
63. Mulligan, P. K. and Rasch, E. M. (1985) Determination of DNA content in the nurse and follicle cells from wild type and mutant *Drosophila melanogaster* by DNA–Feulgen cytophotopmetry. *Histochemistry* **82,** 233–247.
64. Swift, H. and Rasch, E. M. (1956) Microphotometry with visible light, in *Physical Techniques in Biological Research,* Vol. 3 *Cells and Tissues* (Oster, G. and Pollister, A. W., eds.), Academic, New York, pp. 353–400.
65. Sumner, A. T. (1997) Microdensitometry—measurement of staining in cells. *Microsc. Anal.* 15–16.
66. Rasch, E. M. and Rasch, R. W. (1979) Application of microcomputer technology to cytophotometry. *J. Histochem. Cytochem.* **27,** 1384–1387.
67. Shillaber, C. P. (1944) *Photomicrography in Theory and Practice*, John Wiley & Sons, New York, pp. 512–533.
68. Fand, S. B. and Spencer, R. P. (1964) Off-peak absorption measurements in Feulgen cytophotometry. *J. Cell Biol.* **22,** 515–520.
69. Lillie, R. D. (1977) *Conn's Biological Stains*. 9th ed., Waverly, Baltimore, MD, pp. 257–266, 582–584, Table 19.1 (pp. 509–545), Table 19.5 (pp. 554–550), and Table 19.9 (p. 514).
70. de la Torre, I., Velat, G. F., and Dysart, M. F. (1964) The role of hydrogen ion concentration and metabisulfite in the mechanism of the Feulgen reaction. *J. Cell Biol*. **23,** 24a.

8

Fluorescent BrdU Labeling and Nuclear Flow Sorting of the *Drosophila* Ovary

Brian R. Calvi and Mary A. Lilly

1. Introduction

The *Drosophila* ovary has proven to be an excellent model system for addressing many key questions in biology. Among these are questions relating to the cell cycle control of DNA replication and chromosome structure during development. Early studies of ovarian chromosome dynamics employed various histochemical stains and bright-field microscopy ***(1)***. Later, photometric cytometry, ^{3}H-thymidine incorporation, and radioactive *in situ* DNA hybridization were used to study DNA replication and chromatin organization within the ovary ***(2–5)***. Recently, the introduction of fluorescent detection has significantly improved the ability to study chromosome dynamics and DNA replication in the developing ovary ***(6–8)***. In this chapter, we describe two techniques based on fluorescent detection, BrdU labeling and nuclear flow sorting, that have recently been applied to the study of oogenesis. These techniques allow visualization of DNA replication with high resolution by epifluorescence microscopy and accurate measurement of DNA copy number during endocycles of the ovary. We first briefly review the current understanding of cell cycle and chromosome modifications during oogenesis to which these techniques have contributed. For more detailed accounts of oogenesis, the interested reader is referred to previous reviews ***(9–11)***.

The *Drosophila* ovary provides several inherent advantages for the study of the developmental control of DNA replication and chromosome dynamics (*see* **ref.** ***9*** for a review). First, both somatic and germ-line cells modify their cell cycles, chromosome structure, and DNA replication patterns in concert with stages of oogenesis. Unlike what occurs in mammals, the entire process of

From: *Methods in Molecular Biology, vol. 247:* Drosophila *Cytogenetics Protocols*
Edited by: D. S. Henderson © Humana Press Inc., Totowa, NJ

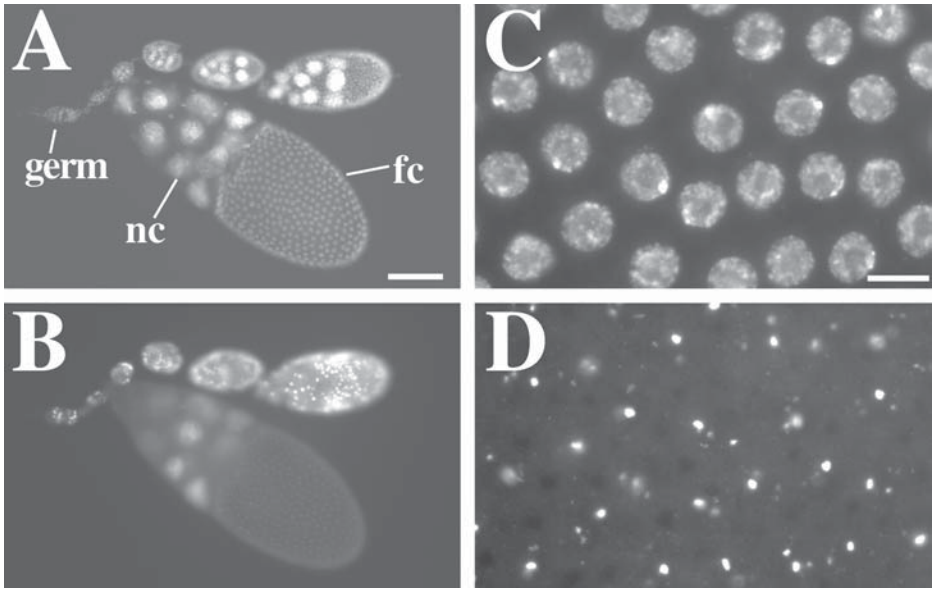

Fig. 1. DAPI and BrdU labeling of *Drosophila* ovaries. **(A)** A low-power fluorescent microscope image of a *Drosophila* ovariole and stage 10B egg chamber labeled with DAPI. The germarium (germ) is anterior and to the left. The largest nuclei in the stage 10B egg chamber are in the nurse cells (nc), whereas those in the follicle cells (fc) are smaller. **(B)** The same ovariole labeled with BrdU. Because mitotic and endocycles are not synchronized, some nuclei within an egg chamber are labeled, whereas others are not. In the stage 10B egg chamber, all follicle cells over the oocyte have foci of BrdU incorporation that correspond to amplifying genes. **(C)** A high-power image of stage 10B follicle cell nuclei labeled with DAPI. The brightest focus in each nucleus is located in the heterochromatic chromocenter. **(D)** The same stage 10B nuclei labeled with BrdU reveals several foci of different intensities. The two brightest spots represent the amplifying chorion genes. The diffuse spots are amplifying loci in other focal planes. Scale bar for **A**, **B** = 100 μm; scale bar for **C**, **D** = 10 μm.

Drosophila oogenesis, from the division of stem cells to the production of a mature egg, takes place throughout the lifetime of the adult female. Therefore, a second advantage is that a single adult female contains numerous egg chambers representing each developmental stage. Egg chambers are comprised of germ-line and somatic cells. Sixteen germ-line cells, a single oocyte and 15 sister nurse cells, are surrounded by an epithelial sheet of somatic follicle cells (*see* **Fig. 1A**). Egg chambers mature within a structure called the ovariole (*see* **Fig. 1A**). Each ovary is comprised of approximately 16 ovarioles that typically contain 7 egg chambers at different stages of development. Because egg cham-

bers migrate posteriorly as they mature, a final advantage is that every ovariole contains an anterior to posterior array of successively older egg chambers.

The prelude to forming an egg chamber begins at the anterior tip of the ovariole in a structure known as the germarium, which contains both germ-line and somatic stem cells (*see* **ref.** ***11*** for a review) (*see* **Fig. 1A**). A germ-line stem cell division at the anterior tip of the germarium gives rise to a primary cystoblast. This cystoblast undergoes four synchronized mitotic division cycles with incomplete cytokinesis as it migrates posteriorly within the germarium. At the end of these divisions, the 16 cells of this germ-line cyst are connected by intercellular bridges called ring canals. All 16 cells enter the premeiotic S-phase, but only the true oocyte continues meiosis. The other 15 cells become nurse cells and begin endocycles in stage 1 of oogenesis. Endocycles are comprised of alternating S- and G-phases without cell division. The somatic stem cells are located in a posterior lateral position within the germarium ***(12)***. These stem cells give rise to a pool of follicle cells that then surround the nurse cell–oocyte complex as it buds off from the germarium to form a stage 1 egg chamber. Fourteen stages of egg chamber development were described by the seminal study of King ***(13)*** and have been adopted as the standard nomenclature in the field.

During stage 1 to stage 10 of egg chamber development, the nurse cells execute approx 10–12 endocycles and arrest with enormous nuclei that have a ploidy of greater than 1000C ***(2,6)*** (*see* **Figs. 1A** and **2**). This high ploidy supports their role as nutritive cells that supply the oocyte with protein and RNA for early embryogenesis. The nurse cells within an egg chamber do not cycle in synchrony with each other. Therefore, BrdU labeling yields egg chambers that have some nurse cell nuclei labeled and others that are not (*see* **Fig. 1B**). Although most euchromatin is replicated during the endocycle, certain heterochromatic satellite sequences are not fully replicated and become progressively underrepresented with succeeding endocycles ***(2–6)***. In stages 1–4, the nurse cell chromosomes adopt a transient pseudopolytene configuration in which the sister chromatids and homologs are synapsed, but then disperse by stage 6 and individual chromosomes cannot be easily identified thereafter ***(8)***. The replicated sisters from each chromosome arm do remain in distinct regions of the nucleus comprising five nuclear domains. In certain mutant strains, the nurse cell chromosomes remain synapsed and form giant polytene chromosomes that have a distinct banded pattern (***14–17***; *also see* Chapter 6).

The somatic follicle cells divide mitotically from stage 1 to stage 6. In stage 6, the follicle cells exit the mitotic cycle and enter the endocycle. Nuclear sorting shows that the majority of follicle cells arrest endocycles with a final ploidy of 16C, and BrdU labeling indicates this arrest occurs before stage 10B ***(6,7)*** (*see* **Figs. 1A,B** and **2**). Follicle cells within an egg chamber do not cycle in

synchrony with one another during mitotic cycles and endocycles. Therefore, with short labeling, some follicle cells are seen to incorporate BrdU while others do not. During stage 9, most follicle cells migrate posteriorly to form a columnar epithelial sheet over the enlarging oocyte. A few follicle cells remain over the nurse cells and become thin and squamous. Also during stage 9, special border follicle cells at the anterior of the chamber migrate posteriorly in between the nurse cells. Their arrival at the nurse cell–oocyte border marks the beginning of stage 10A. During stage 10A, only a few follicle cells are completing the last enodcycle S-phase and label with BrdU.

Stage 10B begins when the most anterior columnar follicle cells over the oocyte begin to migrate to the interior, centripetal position of the egg chamber, which ultimately separates the nurse cells from the oocyte. At the onset of stage 10B, follicle cells begin what amounts to an extended S-phase during which only a few loci re-replicate ***(7,18)***. Two of these loci represent clusters of genes that encode eggshell (chorion) proteins. The cluster on the third chromosome amplifies in copy number to approx 64–100× and the one on the X chromosome to approx 16–20×, above the 16C follicle cell genome (*see* **ref. *10*** for review, and **ref. *19***). The high copy number of these two loci supports rapid biosynthesis of the eggshell later in oogenesis. Because most of the genome is not replicating, BrdU incorporation in these cells appears as four dots (*see* **Fig. 1C,D**). The two most intense spots represent the two chorion loci, and the two faint spots represent unknown loci that amplify to only low levels. BrdU incorporation continues at the third chromosome locus until stage 13, but the X chromosome locus and other loci have much diminished BrdU labeling by stage 12. In conjunction with the tools of *Drosophila* genetics, the ability to monitor the activity of these origins by BrdU has been a useful assay for studying the cell cycle control of replication origin activity (*see* **refs. *20,21*** for examples).

2. Materials

2.1. BrdU Labeling

1. 10 m*M* BrdU (Sigma) in dH_2O. Store at –80°C. These aliquots are good for several freeze–thaw cycles. Surprisingly, BrdU stock goes bad over time at –80°C and should be remade every couple of months. BrdU solution made fresh works best. BrdU is a mutagen and should be handled with care.
2. Mouse anti-BrdU monoclonal antibody (Becton Dickinson).
3. Cy3-Conjugated goat anti-mouse antibody (Jackson ImmunoResearch Laboratories).
4. Glycerol-based antifade solution for mounting ovaries onto microscope slides such as Vectashield (Vector Laboratories).
5. Grace's insect culture medium (Mediatech) brought to room temperature.
6. 2 *N* HCl (8.6 mL concentrated 12 *N* HCl stock per 50 mL H_2O).

7. 100 m*M* Borax neutralization solution: 1.907 g $Na_2B_4O_7 \cdot 10\ H_2O$/50 mL H_2O. Sterilize by filtration and keep stock at 4°C to prevent mold growth.
8. Phosphate-buffered saline (PBS): 130 m*M* NaCl, 3 m*M* NaH_2PO_4, 7 m*M* Na_2HPO_4, pH 7.2. Sterilize by filtration or autoclaving.
9. Phosphate-buffered saline + Triton (PBT): PBS + 0.1% (v/v) Triton X-100.
10. PBT + BSA: PBT + 0.2% (w/v) bovine serum albumen (BSA).
11. PBT + normal goat serum (NGS): PBT + 5% (v/v) NGS. Heat-inactivate NGS at 55°C, 20 min, and store in aliquots at –20°C.
12. PBS + DAPI: PBS + 1 µg/mL 4'6-diamidino-2-phenylindole (DAPI) (Roche).
13. Buffer B for fixation: 100 m*M* KH_2PO_4/K_2HPO_4, pH 6.8, 450 m*M* KCl, 150 m*M* NaCl, 20 m*M* $MgCl_2$.
14. 37% Formaldehyde stock (methanol stabilized). Fresh EM-grade formaldehyde (16%) without methanol can be substituted and volumes should be adjusted accordingly.
15. 5% BSA in dH_2O (distilled water) for pretreating Eppendorf tubes and pipets to discourage sticking of the ovaries.
16. Two fine-tipped dissecting forceps, such as Inox 5 biologie tip (Fine Science Tools).
17. A deep glass dissecting dish such as a 9-well dish with wells that hold 1 mL of solution (Fisher).
18. Short-nose Pasteur pipets.
19. Standard microscope slides, $22 \times 22\text{-mm}^2$ #1 cover slips, and nail polish for sealing.
20. Low-power stereomicroscope for dissections.
21. Epifluorescence microscope.

2.2. Nuclear Flow Sorting

1. Ultra centrifuge equipped with swinging-bucket rotor.
2. Ephrussi–Beadle ringers (EBR): 130 m*M* NaCl, 5 m*M* KCl, 2 m*M* $CaCl_2$, and 10 m*M* HEPES, pH 6.9; autoclave and store at 4°C.
3. 5 mg/mL Collagenase (Type 1A Sigma) diluted in 1X EBR.
4. Nuclear isolation buffer: 15 m*M* Tris-HCl, pH 7.4, 60 m*M* KCl, 15 m*M* NaCl, 250 m*M* sucrose, 1 m*M* EDTA, 0.1 m*M* EGTA, 0.15 m*M* spermine, 0.5 m*M* spermidine. Sterilize with a 0.2-µm filter and store at room temperature.
5. 1X Nuclear isolation buffer with 1.5% NP-40.
6. 100-µm Nitex mesh (Tetko Inc).
7. Three solutions of 0.8 *M*, 1.5 *M*, and 2.5 *M* sucrose dissolved in nuclear isolation buffer.
8. 5-mL plastic pipet cut into 1.5-cm sections.
9. 2-mL Dounce homogenizer (clearance 0.0005–0.0025 in.) (Kontes).
10. 1-mg/mL stock solution of DAPI (4'6-diamidino-2-phenylindole). DAPI should be diluted in 70% ethanol. If the DAPI is diluted in water, it will precipitate over time.
11. 5% BSA in dH_2O for pretreating pipets and tubes.
12. 10-mg/mL Stock solution of RNase A (Sigma-Aldrich) diluted in 0.01 *M* sodium acetate (pH 5.2). Heat to 100°C for 15 min to inactivate DNases.
13. 1 mg/mL Propidium iodide in water.

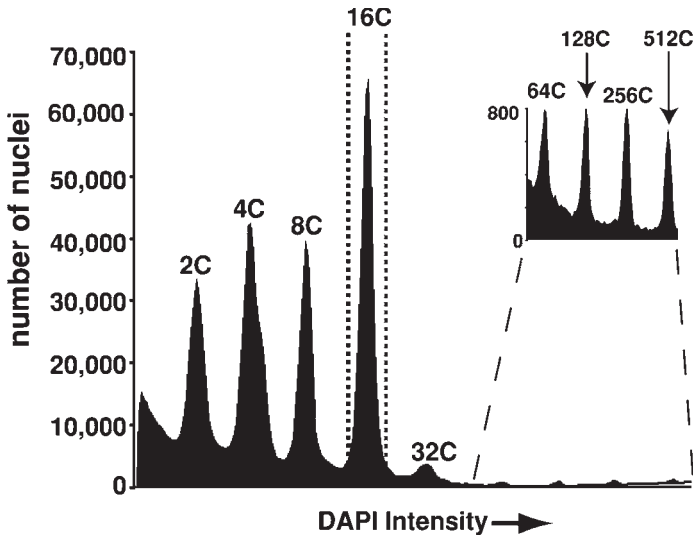

Fig. 2. Flow cytometry (FACS) profile of ovarian nuclei from mature wild-type females. The numbers over the peaks correspond to the DNA copy number (C) of euchromatic sequences. The 2C-32C peaks are composed predominantly of follicle cell nuclei, but the less abundant nurse cell nuclei are also present in these populations. In contrast, the 64C–512C peaks represent only nurse cell nuclei. A blowup of these higher ploidy nurse cell peaks is presented in the right-hand corner of the graph. The 16C follicle cells have been gated (dotted lines) to be collected by FACS.

3. Methods

3.1. BrdU Labeling

1. Three days before dissection, condition *Drosophila* females with males on wet yeast for 2 d, followed by fresh wet yeast for 1 d (*see* **Note 1**).
2. On the day of the experiment, bring enough Grace's medium to room temperature for dissection, incubation, and washes (approx 4 mL per sample). **The tissue must not be chilled before or during BrdU incubation because this inhibits incorporation.** Pretreat tubes and Pasteur pipets with 5% BSA to discourage the sticking of ovaries (*see* **Note 2**).
3. Dissect ovaries in 400 µL of room-temperature Grace's medium in the dissecting dish. After dissecting approximately six pairs of ovaries, puncture the ovarian sheath and partially tease apart the ovarioles at their anterior ends. At the end of this process, most ovarioles should be separated at their anterior tip but remain attached at the posterior near the common duct and uterus. Some mature egg chambers will rupture from the ovariole and break free. Do not be concerned by this.
4. Using a BSA-treated Pasteur pipet, transfer ovaries and free egg chambers from the dissecting dish to a BSA-treated Eppendorf tube. Allow ovaries to settle to

the bottom of the tube for 30 s. Remove Grace's medium with a p1000 Pipetteman and add 1 mL Grace's medium containing 10 µ*M* BrdU. This is prepared by adding 1 µL of 10 m*M* BrdU stock to 1 mL of Grace's. Incubate for 1 h with rocking (as short as 15 min of incubation will yield detectable incorporation).

5. At end of incubation, remove Grace's/BrdU to hazardous waste and rinse the ovaries twice for 3 min (per rinse) in Grace's medium to remove unincorporated label.
6. Fix the ovaries in 1 mL of 6% formaldehyde/buffer B/dH_2O (1 : 1 : 4 using 37% formaldehyde : Buffer B stock : dH_2O) at room temperature for 20 min with rocking.
7. Wash with 1 mL PBT three times, 5 min each rinse with rocking.
8. Acid-treat the ovaries with 1 mL of 2 *N* HCl at room temperature for 30 min with rocking to denature DNA. Alternatively, DNA can be denatured by treating with DNase (*see* **Note 3**).
9. Remove the acid and neutralize the ovaries in 1 mL of 100 m*M* borax (sodium tetraborate) for 2 min.
10. Wash with 1 mL PBT three times, 10 min each wash with rocking.
11. Block the ovaries in 100 µL PBT/5% NGS for 30 min without rocking.
12. Remove the blocking solution and add 100 µL PBT/NGS with 1 : 20 mouse anti-BrdU monoclonal antibody (Becton Dickinson cat. no. 7580). Incubate at 4°C overnight without rocking.
13. The next day, wash with 1 mL PBT/BSA 0.2%, three times for 10 min each wash, followed by three times for 30 min each wash, with rocking.
14. Block the ovaries again with 100 µL PBT/NGS for 30 min.
15. Label with secondary antibody. Remove block and add 200 µL PBT/NGS containing a 1 : 400 dilution of Cy3 goat anti-mouse antibody or other secondary antibody of choice. Mix gently. Incubate in the dark at room temperature for 2 h without rocking.
16. Wash in PBT (without BSA) as in **step 13**.
17. Remove as much PBT as possible and counterstain the nuclei in 100 µL of PBS containing 1 µg/mL of DAPI. Mix gently and let sit at room temperature for 7 min.
18. Remove the PBS/DAPI solution and add 80 µL Vectashield (Vector Laboratories) with a cutoff pipet tip. Gently mix by flicking the tube. Spin full speed in an Eppendorf centrifuge for 3 s. Mix again by flicking the tube but make sure the ovaries remain in the Vectashield. If the ovaries stick on the wall of the tube, spin again briefly. Allow the ovaries to equilibrate in Vectashield for at least 30 min before mounting. At this point, ovaries can be stored at 4°C.
19. Mount the ovaries on microscope slide for observation. With a cut off p200 pipet tip, pipet 23 µL of fresh Vectashield to the middle of the slide. With the same tip, pipet ovaries to one end of slide. Using forceps, pick desired ovarioles and egg chambers into the fresh Vectashield. It is important to transfer ovaries into fresh Vectashield to ensure protection from photobleaching in the microscope. Mount approximately one pair of ovaries per slide. Separate ovarioles completely at this point and remove excess ovary sheath. Spread out and align ovarioles in parallel

by raking forceps through Vectashield. Pipet unused ovaries back into the Eppendorf tube and clean up excess Vectashield that remains on the end of the slide with a kimwipe. Place a 22 × 22-mm^2, #1 cover slip on ovaries. If desired, place a light weight (approx 12 g) on top of cover slip for 3–10 min. This flattens the egg chambers so that more cells are in a single focal plane. Seal the edges of the slide with nail polish and allow to dry for several minutes. Optimal storage of the slides is in the dark at –20°C.

20. Observe incorporation on an epifluorescence microscope equipped with bandpass filters that allow the visualization of DAPI and Cy3 (excitation/emission wavelength (nm): DAPI approx 330/450; Cy3 approx 550/570). BrdU incorporation during mitotic, endocycles, and chorion gene amplification should be visible using a 10× objective (*see* **Fig. 1A–D**). Incorporation will be more apparent under higher-power, 20–100× objective, and an oil immersion lens is recommended. Nuclei should be brightly stained with DAPI, and a focus of more intense DAPI staining should be seen in the heterochromatic chromocenter of polyploid cells (*see* **Fig. 1C**).

3.2. Nuclear Flow Sorting

1. Condition 30–50 females on wet yeast as described in **Subheading 3.1.** (*see* **Note 1**). Processing more than 50 females at a time may result in significantly increased background.
2. It is important to pretreat all materials that will come in contact with the nuclei with a 5% solution of BSA to prevent the nuclei from sticking. This includes Pasteur pipets, Eppendorf tubes, 2-mL Dounce homogenizer, step gradient tube, Pipetteman tips, and the 100-µm Nitex filters. This treatment will greatly increase your yields.
3. Dissect ovaries in 500 µL of cold EBR in a dissection dish. After dissecting approximately five females, transfer the group of ovaries to an Eppendorf tube on ice containing 1 mL EBR. Continue dissecting in groups of five until all the females have been dissected.
4. Digest the ovaries at room temperature in 1 mL of 5 mg/mL collagenase diluted in EBR with rocking for 15 min. After the incubation is complete, rinse the ovaries several times with EBR to remove residual collagenase. This is best accomplished with a Pasteur pipet (*see* **Note 4**).
5. Resuspend the ovaries in 300–500 µL of 1X nuclear isolation buffer with 1.5% NP-40. Using a Pasteur pipet, transfer the ovaries to a 2-ml Dounce homogenizer. Homogenize the ovaries for 10–30 times with a pestle that has a clearance of 0.0005–0.0025 inches. It is not necessary to disrupt the eggshell of older egg chambers.
6. To remove large particulate matter from the solution, including eggshells, filter the homogenate twice through a 100-µm Nitex mesh (*see* **Note 5**).
7. Add DAPI to a concentration of approx 1 µg/mL and incubate for 5 min at room temperature. For a 500 µL sample, this will involve adding to the homogenate 0.5 µL of the 1-mg/mL DAPI stock solution. The DAPI is used to follow the nuclei in the next steps.

8. Build a step gradient with the 0.8-*M*, 1.6-*M*, and 2.5-*M* sucrose solutions in nuclear isolation buffer, starting with 2.5 *M* and finishing with the 0.8-*M* solution on top. We use 300–500 µL for each step in Beckman 11 × 34-mm polyallomar centrifuge tubes. It is important not to disturb the layers when making the gradient. After making the step gradient, three defined layers should be clearly visible when holding the tube up to a light.
9. Gently layer the homogenate on top of the sucrose step gradient, taking care not to disrupt the layers. Centrifuge for 20 min at 20,000*g* in a swinging-bucket rotor. We use a Beckman Optima TLX Ultracentrifuge. Check that the nuclei have pelleted by examining the tube under an ultraviolet (UV) light source. You should see a small pellet of DAPI-bright material at the bottom of the tube.
10. Remove all but 50–100 µL of the sucrose gradient, being careful not to disrupt the nuclei. Resuspend the pellet in 500 µL of nuclear isolation buffer. Disrupt the pellet by pipetting the nuclear isolation buffer up and down several times using a 1 mL Pipetteman. To ensure that the pellet has been resuspended, examine the tube with a UV light source.
11. Add 0.5 µL of the 1-mg/mL DAPI stock solution to obtain a final concentration of 1 µg/mL. Alternatively, nuclei can be stained with propidium iodide (*see* **Note 6**).
12. Store nuclei on ice before sorting. If necessary, nuclei can be stored overnight at 4°C.
13. To obtain a flow cytometry profile, examine the DAPI-stained nuclei excited with a krypton laser with a multiline UV (337–356 nm) source. DAPI emission is collected through a 450/465 bandpass filter. Specifically, we use a Coulter EPICS 752 flow cytometer.

4. Notes

1. *Drosophila* oogenesis is dependent on environment, age, and mating status of the female. Therefore, for both BrdU labeling and nuclear flow sorting, it is critical to use mated females of optimal age that are well fed and watered. This entails conditioning females on wet baker's yeast (the consistency of creamy peanut butter) for 2 d, followed by one more day on fresh wet yeast (a total of 3 d of conditioning). The females should have eclosed from the pupal case at least 3 d and no more than 8 d before the day of dissection (4–6 d post eclosion is optimal in most cases). Because oogenesis proceeds apace only if females have recently mated, males should be present during conditioning.
2. Treat eppendorf tubes and Pasteur pipets with 5% BSA solution to discourage sticking of the ovaries. Pipet 1 mL of 5% BSA into a tube, close the cap and invert, remove the BSA to the next tube to be treated, and so on. Treat pipets by pipetting the solution up and down once.
3. DNase I denaturation is preferred if ovaries are to be labeled for BrdU and an antibody to a protein because most epitopes are not detected after HCl treatment. After formaldehyde fixation in **Subheading 3.1.**, **step 6**, substitute the following for **steps 7–9**. Wash twice, 15 min each, in PBS + 0.6% Trition-X; wash twice, 15 min each, in DNase buffer (66 m*M* Tris-HCl, pH 7.5, 5 m*M* $MgCl_2$, 1 m*M* of 2-mercaptoethanol added fresh), incubate ovaries in 100 µL of DNase I

(12.5 units/mL DNase buffer) at 37°C for 30 min (DNase I: Roche cat. no. 776-785). Proceed to **Subheading 3.1.**, **step 10**.

4. After collagenase treatment, the EBR may become slightly viscous, making it difficult for the ovaries to sink to the bottom of the Eppendorf tube. If this occurs, gently centrifuge the ovaries in a microfuge for 2–3 s to bring them to the bottom of the tube.
5. Crude but effective filters can be easily generated by supergluing a small section of Nitex mesh onto the end of a 1.5-cm section from a 5-mL plastic pipet that has been cut for this purpose. These sieves fit snuggly into 1.5-mL Eppendorf tubes.
6. As an alternative to DAPI, the nuclei can be stained with the nucleic acid dye propidium iodide. However, because propidium iodide (PI) stains both RNA and DNA, it is necessary to remove the RNA before analyzing the nuclei. After resuspending the nuclei in 500 µL of 1X nuclear isolation buffer in **Subheading 3.2.**, **step 10**, add 5 µL of a 10-mg/mL RNase A solution to obtain a final concentration of 100 µg/mL. Incubate for 15 min at room temperature. Next add 2.5 µL of a 1-mg/mL PI stock solution to the nuclei. Let the nuclei stain for at least 15 min at room temperature before the analysis. The RNase A digestion and PI staining can be done concurrently. To obtain a flow cytometry profile, examine the propidium iodide stained nuclei using an argon 488 nm laser collected through a 545/642 bandpass filter.

References

1. Painter, T. S. and Reindorp, E. (1939) Endomitosis in the nurse cells of the ovary of *Drosophila melanogaster*. *Chromosoma* **1,** 276–283.
2. Hammond, M. P. and Laird, C. D. (1985) Chromosome structure and DNA replication in nurse and follicle cells of *Drosophila melanogaster*. *Chromosoma* **91,** 267–278.
3. Beckingham, K. and Thompson, N. (1982) Under-replication of intron$^+$ rDNA cistrons in polyploid nurse cell nuclei of *Calliphora erythrocephala*. *Chromosoma* **87,** 177–196.
4. Beckingham, K. and Rubacha, A. (1984) Different chromatin states of the intron and type 1 intron$^+$ rRNA genes of *Caliphora erythrocephala*. *Chromosoma* **90,** 311–316.
5. Renkawitz-Pohl, R. and Kunz, W. (1975) Underreplication of satellite DNAs in polyploid ovarian tissue of *Drosophila virilis*. *Chromosoma* **49,** 375–382.
6. Lilly, M. and Spradling, A. (1996) The Drosophila endocycle is controlled by Cyclin E and lacks a checkpoint ensuring S-phase completion. *Genes Dev.* **10,** 2514–2526.
7. Calvi, B. R., Lilly, M. A., and Spradling, A. C. (1998) Cell cycle control of chorion gene amplification. *Genes Dev.* **12,** 734–744.
8. Dej, K. J. and Spradling, A. C. (1999) The endocycle controls nurse cell polytene chromosome structure during Drosophila oogenesis. *Development* **126,** 293–303.

9. Spradling, A. C. (1993) Developmental genetics of oogenesis, in *The Development of* Drosophila melanogaster (Martinez-Arias, A. and Bate, M., eds.), Cold Spring Harbor Laboratory Press, Plainview, NY.
10. Calvi, B. R. and Spradling, A. C. (1999) Chorion gene amplification in *Drosophila*: a model for metazoan origins of DNA replication and S-phase control. *Methods* **18,** 407–417.
11. de Cuevas, M., Lilly, M. A., and Spradling, A. C. (1997) Germline cyst formation in Drosophila. *Annu. Rev. Genet.* **31,** 405–428.
12. Margolis, J. and Spradling, A. (1995) Identification and behavior of epithelial stem cells in the Drosophila ovary. *Development* **121,** 3797–3807.
13. King, R. C. (1970) *Ovarian Development in* Drosophila melanogaster, Academic, New York.
14. Koch, E. A. and King, R. C. (1964) Studies on the *fes* mutant of *Drosophila melanogaster. Growth* **28,** 325–369.
15. King, R. C., Riley, S. F., Cassidy, J. D., White, P. E., and Paik, Y. K. (1981) Giant polytene chromosomes from the ovaries of a *Drosophila* mutant. *Science* **212,** 441–443.
16. Keyes, L. N. and Spradling, A. C. (1997) The *Drosophila* gene *fs(2)cup* interacts with *otu* to define a cytoplasmic pathway required for the structure and function of germ-line chromosomes. *Development* **124,** 1419–1431.
17. Heino, T. (1994) Polytene chromosomes from ovarian pseudonurse cells of the *Drosophila melanogaster otu* mutant. II. Photographic map of the X chromosome. *Chromosoma* **103,** 4–15.
18. Calvi, B. R. and Spradling, A. C. (2001) The nuclear location and chromatin organization of active chorion amplification origins. *Chromosoma* **110,** 159–172.
19. Spradling, A. and Mahowald, A. (1980) Amplification of genes for chorion proteins during oogenesis in *Drosophila melanogaster. Proc. Natl. Acad. Sci. USA* **77,** 1096–1100.
20. Royzman, I., Austin, R. J., Bosco, G., Bell, S. P., and Orr-Weaver, T. L. (1999) ORC localization in *Drosophila* follicle cells and the effects of mutations in *dE2F* and *dDP*. *Genes Dev* **13,** 827–840.
21. Schwed, G., May, N., Pechersky, Y., and Calvi, B. R. (2002) *Drosophila* minichromosome maintenance 6 is required for chorion gene amplification and genomic replication. *Mol. Biol. Cell* **13,** 607–620.

9

Studying Nuclear Organization in Embryos Using Antibody Tools

Kristen M. Johansen and Jørgen Johansen

Introduction

One of the major foci in cell biology is to understand the process of nuclear division. In each cell cycle, the chromosomes must be faithfully replicated and the complex nuclear structure has to be duplicated and reorganized ***(1–4)***. Our understanding of the cell cycle and mitosis has increased dramatically in the last several years, as a result of cross-disciplinary approaches combining molecular, cell biological, and genetic techniques (reviewed in **refs. *5–9***). An organism offering a particularly advantageous model system for such studies of mitosis is the early embryo of *Drosophila melanogaster.* The cytoskeleton and mitotic spindle are large and easily visualized, thus facilitating structural analysis. The embryo undergoes 13 rapid and nearly synchronous nuclear divisions giving rise to about 5000 nuclei before cell boundaries form after 3 h of development ***(10–12)***. This syncytial organization of nuclei affords excellent accessibility for experimental perturbations (e.g., using antibodies ***[13–17]*** or pharmacological tools ***[15,18–20]***).

In this chapter, we present approaches that have been optimized for a number of chromosomal and spindle matrix proteins that we have been studying in our laboratory ***(17,21–23)***. These immunostaining protocols are based on techniques developed by Zalokar and Erk ***(24)*** and Mitchison and Sedat ***(25)***. In addition, a number of related immunostaining protocols oriented toward analysis of cytoskeletal proteins ***(26)***, neural antigens ***(27)***, and embryonic proteins ***(28–30)*** have been published and may provide useful additional perspectives. However, it should be emphasized that for any new antigen of interest, it is necessary to optimize the chosen fixative and fixation conditions. Although it

From: *Methods in Molecular Biology, vol. 247:* Drosophila *Cytogenetics Protocols*
Edited by: D. S. Henderson © Humana Press Inc., Totowa, NJ

is beyond the scope of this chapter to review the various principles and advantages of different fixatives, the reader is referred to one of several excellent histology texts for a detailed description of such considerations (e.g., **refs. *31*,*32***).

The strength of *Drosophila* as a model system lies in the wide range of molecular and genetic approaches that can be employed to study a cellular or developmental process. The presence, however, of maternal stores of mRNA and protein can complicate analysis of a protein's function during early development. Employing antibody perturbation approaches, especially in cases where it is not possible to recover germ-line clones, can allow one to block a protein's function during early development and assay the consequences of such perturbation. In these cases it is important to determine whether a particular antibody has function-blocking activity, and also whether the effects observed are indeed the consequence of loss of function or could result instead due to steric interference or indirect effect (note that this latter concern applies to analysis of genetic mutants as well!). A number of protocols have been adapted for injection of nuclei and pole cells ***(33)***, *P*-elements ***(34)***, and mRNA ***(35)***. In cases where dose-response information is required, injection approaches have been developed to facilitate measurement of the volume injected ***(36*,*37)***. The development of various *Drosophila* lines expressing GFP-tagged proteins that allow specific structures to be imaged in living embryos (e.g., microtubules, chromosomes, centrosomes) opens up the exciting prospect of analyzing the consequences of antibody perturbation in real time.

2. Materials

2.1. Standard Embryo Collections

1. Polystyrene Petri dishes (60 × 15 mm [Falcon, no. 351007], 150 × 15 mm [Falcon, no. 351058]). These need not be sterile, but can be washed and reused.
2. Agar (USB no. 10654).
3. Apple juice (any standard grocery store brand will do).
4. Table sugar (standard grocery table sugar).
5. Nipagin (*p*-hydroxybenzoic acid methyl ester, Sigma-Aldrich, no. H6654) 15% in ethanol.
6. Yeast paste (standard grocery baker's yeast dissolved in warm water to form a paste; store at 4°C).
7. Population cage: acrylic wide-mouthed (to accommodate 150 × 15-mm plates) cage of approximate dimensions of 16 × 16 × 16 in.; can be custom-ordered from Owl Scientific Co. or constructed by most in-house shop facilities.
8. Collection bottles: 100 mL Tricornered beakers (Fisher no. 02-593-50B) will fit 60 × 15-mm collection plates. For collections on consecutive days, the beakers will become too wet, so either change flies into fresh beakers daily or cut off the bottom of the beaker and affix a nylon filter to permit airflow.

9. Nylon Spectra/Mesh filters, 70 µm (Fisher, no. 08-670-199).
10. Collection basket: two screen cups (Sigma-Aldrich, no. S1145) and 40 mesh screens (Sigma, no. S0770). Insert a Spectra/Mesh filter above the mesh on one of the baskets.
11. Paintbrush.
12. Distilled water (dH_2O) Squirt bottle.
13. Clorox (dilute 1 : 1 with dH_2O just before use).
14. Plastic weigh boat (Fisher, no. 02-202B).
15. Glass test tube with screw cap (Fisher, no. 14-930AA).
16. Heptane. *(Do not breathe vapor or get on skin; highly flammable.)*
17. 9-in. Pasteur pipets.
18. Phosphate-buffered saline (PBS): 0.9% NaCl, 14 m*M* Na_2HPO_4, 6 m*M* NaH_2PO_4, pH 7.3.
19. Fixative: 4% Paraformaldehyde in PBS. Dissolve 4 g paraformaldehyde in 100 mL PBS by adding 10 *N* NaOH dropwise with stirring until dissolved. Then, add 1 *N* HCl to bring to pH 7.0. Store at 4°C for up to 1 mo. *(Highly toxic; wear gloves and avoid direct contact or inhalation of powder.)*
20. Bouin's Fluid fixative: 0.66% picric acid, 9.5% formalin, 4.7% acetic acid. *(Highly toxic; wear gloves and avoid direct contact or inhalation.)*
21. Methanol containing 5 m*M* EGTA (pH 8.0). *(Avoid contact, inhalation, or ingestion of methanol as it is poisonous and may cause blindness.)*
22. PBST: PBS containing 0.4% Triton X-100. Store at 4°C.
23. Normal goat serum (NGS) (Sigma-Aldrich, no. G6767). Store at –20°C.
24. 5% Sodium azide stock solution (dilute 1:100 for working solution). *(Highly poisonous; avoid contact, inhalation, or ingestion.)*
25. Blocking buffer: PBST containing 1% NGS and 0.05% sodium azide. Prepare fresh.

2.2. Manual Devitellinization

1. Tungsten needle (blunt).
2. Double-sided tape.
3. 60 × 15-mm Petri dish (Falcon, no. 351007).
4. PBST: PBS containing 0.4% Triton X-100. Store at 4°C.

2.3. Antibody Labeling and Detection

1. Rotator (e.g., Fisher, no. 13-688-1D).
2. Primary antibody (as determined by the experimental aim).
3. PBST: PBS with 0.4% Triton X-100. Store at 4°C.
4. Antibody dilution buffer: PBST containing 1% NGS. Prepare fresh.
5. Secondary antibody (select appropriate detection tag as well as specificity for the primary antibody species being used) diluted in PBST with 1% NGS.

For horseradish peroxidase (HRP) detection: We use affinity purified HRP-conjugated goat anti-IgG (heavy and light chain specific) antibody raised against either mouse (Bio-Rad, no. 170-6516) or rabbit (Bio-Rad, no. 170-6515). These antibodies will detect both IgGs and IgMs.

For fluorescent detection we generally use affinity purified antibodies from either Cappell (ICN) or Jackson ImmunoResearch conjugated to either Texas Red, tetramethylrhodamine isothiocyanate (TRITC), fluorescein isothiocyanate (FITC), or cyanine 5 (Cy5). For multiple labelings using monoclonal antibodies, a variety of isotype-specific antibodies are available.

6. PBS. Store at 4°C.
7. 3,3'-Diaminobenzidine tetrahydrochloride (DAB) stock solution: 10 mg/mL DAB in 0.05 *M* Tris-HCl, pH 7.5. *(DAB is a suspected carcinogen; avoid contact, inhalation, or ingestion.)* Store at –20°C protected from light.
8. H_2O_2 (hydrogen peroxide). *(Toxic; avoid contact, inhalation, or ingestion.)* Store at 4°C.
9. PBS containing 0.05% sodium azide.
10. Acrodisc syringe filters (Fisher, no. 09-730-218).
11. Aluminum foil.
12. Hoechst 33258 (Molecular Probes, no. H-3569), 0.2 µg/mL in PBS *(Possible mutagen; avoid contact, inhalation, or ingestion.)* Store at 4°C.

2.4. Mounting Embryos

1. Pasteur pipets.
2. Kimwipes.
3. Glass frosted microscope slides (Fisher, no. 12-544-3).
4. Glass cover slips No. 1½ (Fisher, no. 12-530B).
5. Glycerol containing 5% *n*-propyl gallate. Store at 4°C.
6. Nail polish.
7. Small glass tubes (6 mm outer diameter × 50 mm L) (Fisher, no. 14-958A).
8. Ethanol. *(Avoid contact, inhalation, or ingestion.)*
9. Xylene. *(Toxic and highly flammable; avoid contact, inhalation, or ingestion.)*
10. DEPEX mounting media (Electron Microscopy Sciences, no. 13514). *(Avoid contact, inhalation, or ingestion.)*

2.5. Antibody Perturbation

1. Collection bottles (*see* **Subheading 2.1., item 8**).
2. 60 × 15-mm and 150 × 15-mm apple juice plates.
3. Standard micropipet puller (e.g., Model 700C Vertical Pipet Puller, David Kopf Instruments).
4. Glass filament capillary tubes (1.2 mm outer diameter, 0.68 mm inner diameter, World Precision Instruments, no. M1B120F-4).
5. Inverted microscope (e.g., Model CK2; Olympus Corporation).
6. Micromanipulator (e.g., Model M-152; Narishige Co.).
7. House vacuum and air-pressure lines (700 mm Hg and 30 psi, respectively).
8. Tygon tubing.
9. Two three-way valves.
10. Standard microscope slides.

11. 22×22-mm^2 glass cover slips (Fisher, no. 12-520B).
12. Embryo glue (glue from double-sided or packing tape dissolved in heptane). *(Avoid contact, inhalation, or ingestion.)*
13. Small collection basket.
14. DrieRite™ (Fisher, no. 07-578-3A).
15. Halocarbon oil (Series 95, Halocarbon Products Corporation).

3. Methods

3.1. Embryo Collection, Dechorionation, and Fixation

1. Prepare apple juice plates in 60×15-mm or 150×15-mm Petri dishes for collections from bottles or population cages, respectively (*see* **Note 1**). To a 2-L flask containing a stir bar, add the following:

Agar (*see* **Note 2**)	24 g
Distilled water	750 mL

   Autoclave 20 min on liquid cycle and cool for 45 min with gentle stirring on a stir plate to approx 60°C. Add the following:

Apple juice (prewarmed to ~50°C)	250 mL
Table sugar or sucrose	25 g
Nipagin (15% in ethanol)	10 mL

   Stir until fully mixed and sugar is dissolved, pour plates, and store at 4°C after they have hardened and cooled.
2. For collection plates (*see* **Note 3**), place a dab of yeast paste (baker's yeast dissolved in water) in the center of the plate and place in cage or collection chamber for desired time (*see* **Notes 4** and **5**).
3. Before beginning collection procedures (*see* **Note 6**), prepare a 15-ml screw-cap glass test tube containing 5 mL of your desired fixative (*see* **Note 7**) and 5 mL of heptane (*see* **Note 8**).
4. Wash embryos off of the plate and into a double-tiered collection basket (*see* **Note 9**) using a gentle stream of distilled water from a dH_2O tap or squirt bottle while gently dislodging embryos with a paintbrush. Rinse embryos thoroughly under the dH_2O tap or with a dH_2O squirt bottle. Remove upper basket and thoroughly wash the embryos retained in the lower basket with dH_2O.
5. Freshly prepare 30 mL of a 50% Clorox solution (*see* **Note 10**) and pour into a large plastic octagonal weigh boat. Place the collection basket cup into the weigh boat and agitate gently so the bleach solution disperses the embryos. Incubate 2 min with periodic gentle agitation to disperse embryos.
6. Rinse the embryos thoroughly under the dH_2O tap (or immerse the cup into a tray or beaker of water to thoroughly remove all traces of bleach). With a dH_2O squirt bottle wash embryos off of the side of the collection chamber onto the nylon Spectra/Mesh filter. If using the collection cup, wash the embryos onto the metal rim at the side of the cup. This will enable you to rapidly transfer the embryos to the heptane/fixative test tube by squeezing a small amount of heptane onto the tilted cup's rim with a Pasteur pipet and then pipetting the heptane and embryos quickly back to the 15-mL tube. Alternatively use a paintbrush to pick up and transfer embryos from the filter to

the heptane layer. The embryos will sink through the heptane to the interface between fixative (lower) and heptane (upper) levels (*see* **Note 11**).
7. Orient the tube horizontally to maximize the heptane/fixative interface boundary and agitate vigorously on a shaker for 20 min (*see* **Notes 12** and **13**).
8. Prepare a 15-ml screw-cap test tube with 5 mL methanol containing 5 m*M* EGTA, pH 8.0, and 5 mL heptane.
9. Remove the tube from the shaker, orient vertically, and allow the embryos to float to the interface between the fixative and heptane layers. Transfer embryos to the methanol–EGTA : heptane tube using a 9 in. Pasteur pipet (*see* **Note 14**). Alternatively, if manual devitellinization is required, go to **Subheading 3.2.**
10. Shake the methanol/heptane tube containing the embryos vigorously for 15 s. Allow the tube to stand so that devitellinized embryos can settle to the bottom. Nondevitellinized embryos will remain at the interface (*see* **Note 15**).
11. Draw off all of the fixative, embryos remaining at the interface, and methanol, leaving only the embryos that have settled to the bottom.
12. Repeat washing embryos that sink to the bottom in 10 mL of the following:

    Five washes with methanol/5 m*M* EGTA, pH 8.0.
    Two washes with 50% methanol/5 m*M* EGTA (pH 8.0) : 50% PBS.
    Five washes with PBS (*see* **Note 16**).
13. Using a Pasteur pipet, transfer embryos to 1 mL Blocking Buffer (PBST/1% NGS) in a 1.5-mL microfuge tube (*see* **Notes 17** and **18**) and place tube on a rotator at 4°C for 30 min to several hours (*see* **Note 19**).

3.2. Manual Devitellinization

Some antigen–antibody epitopes are sensitive to methanol; thus, methanol-based methods for mass devitellinization cannot be used. Hand-devitellinization is performed as follows continuing from **step 9** in the fixation protocol in **Subheading 3.1.**

1. Prepare a 60-mm Petri dish by placing a piece of double-sided tape asymmetrically on the bottom surface (*see* **Fig. 1**).
2. Place a drop of embryos from the interface in **Subheading 3.1., step 9** on the doublestick tape, quickly blow on the embryos to spread them out into a monolayer, and rapidly cover embryos in the dish with PBST (*see* **Note 20**).
3. Gently press on the surface of each embryo with a blunt tungsten needle to pop the vitelline membrane and then gently nudge the embryos out of the membrane sac.
4. Gently rotate the Petri dish in a circular motion to collect devitellinized embryos in the center of the dish (*see* **Fig. 1**). Transfer the embryos with a precoated Pasteur pipet (*see* **Note 18**) to a 1.5-mL microfuge tube, allow to settle, and remove the PBST solution.
5. Block embryos as described in **step 13** in **Subheading 3.1.**

3.3. Antibody Labeling and Detection (HRP Method)

1. Using a Pasteur pipet, transfer an aliquot of embryos from the Blocking Buffer tube to a fresh 1.5-mL microfuge tube. Allow embryos to settle and draw off excess Blocking Buffer (*see* **Note 21**).

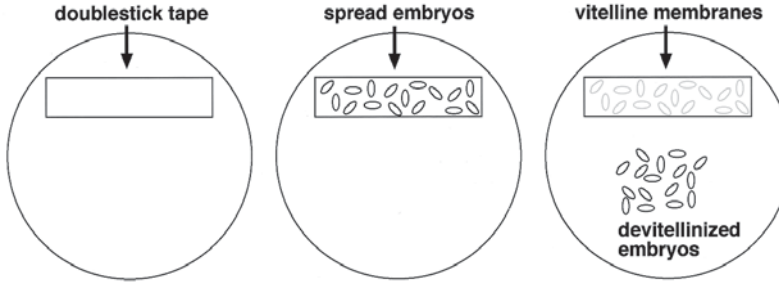

Fig. 1. Setup for manual devitellinization. Place a piece of doublestick tape on one side of a 60 × 15-mm Petri dish. Embryos in a drop of heptane should be dropped onto the tape with the heptane quickly blown away to spread embryos as shown, followed by rapid addition of PBST to minimize the dissolving of the tape glue by the heptane. When done properly, gentle pressure will cause the embryo to pop out of its vitelline case, leaving the membranes stuck to the tape. Gentle swirling of the Petri dish will bring the devitellinized embryos to the middle of the dish for easy retrieval with a "precoated" Pasteur pipet.

2. Prepare 1 mL of primary antibody solution by diluting desired antibody into antibody dilution buffer, add to embryos, and rotate overnight at 4°C (*see* **Note 22**).
3. Allow the embryos to settle to the bottom of the tube. Use a Pasteur pipet to draw off primary antibody solution, rinse briefly with 1 mL of PBST, then wash 3 × 10 min in PBST at 4°C on a rotator.
4. Prepare 1 mL of HRP-conjugated secondary antibody solution by diluting the appropriate secondary antibody (*see* **Note 23**) into antibody dilution buffer, add to embryos, and incubate for 2.5 h at 4°C on a rotator.
5. Allow the embryos to settle, remove the secondary antibody solution, rinse briefly with 1 mL of PBST, then wash twice for 10 min in PBST at 4°C on a rotator.
6. Allow the embryos to settle, draw off the wash buffer, rinse briefly with 1 mL of PBS, and then wash twice for 10 min in PBS (*see* **Note 24**).
7. Prepare substrate solution by adding 10 µL DAB to 1 mL PBS. (Minimize exposure of DAB to light.) Just before use, add 1 µL H_2O_2.
8. Remove the final PBS wash and incubate the embryos in the substrate solution 5–10 min at room temperature on a rotator. Development of a brown precipitate signal can be monitored under a dissecting microscope if desired.
9. Allow the embryos to settle, transfer the DAB solution to hazardous waste collection, briefly rinse the embryos with 1 mL PBS/0.05% sodium azide, then wash once for 10 min in PBS azide.
10. Mount the embryos as described in **Subheadings 3.5.** or **3.6.** (*see* **Note 25**). Results using this approach are shown in **Fig. 2**.

3.4. Antibody Labeling and Detection (Fluorescent Method)

1. Follow **Subheading 3.3., steps 1–3**. Note that for double or triple labelings, where more than one antigen will be detected, it is often possible to combine all

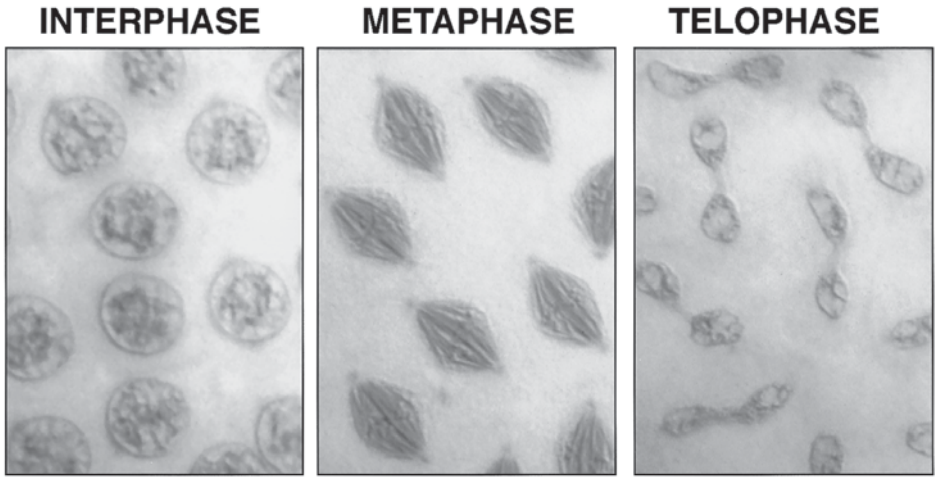

Fig. 2. mAb 2A labeling of *Drosophila* embryonic nuclei representing different stages of the cell cycle, including interphase, metaphase, and telophase. The mAb 2A was detected using an HRP-conjugated secondary antibody as described in **Subheading 2.3.** HRP detection in conjunction with Nomarski microscopy as shown here reveals additional textural details of the structure identified by the mAb 2A. For example, at metaphase the mAb2A can be observed to label centrosomes, spindle matrix fibers, and chromosomes lined up at the metaphase plate.

of the primary antibodies into Blocking Buffer for simultaneous incubation (*see* **Note 26**).

2. Prepare the appropriate fluorochrome-conjugated secondary antibody by dilution into antibody dilution buffer (*see* **Note 27**). Push the diluted secondary antibody solution gently through a syringe filter, taking care to not introduce bubbles into the filtrate (*see* **Note 28**).
3. Add the diluted secondary antibody solution to the embryos, cover the tube with aluminum foil to shield tube from the light (*see* **Note 29**) in this and subsequent incubations, and incubate 2.5 h at 4°C on the rotator.
4. Follow **steps 5** and **6** of **Subheading 3.3.** (*see* **Note 30**).
5. Add 1 mL of PBS containing 0.2 µg/mL Hoechst and rotate 10 min at 4°C.
6. Rinse briefly in PBS, wash once for 10 min in PBS, and mount as described in **Subheading 3.5.** The results using this approach are shown in **Figs. 3** and **4**.

3.5. Mounting Embryos With Glycerol

1. Pick up the antibody-labeled embryos in a Pasteur pipet and dispense onto a microscope slide. Place the bore of the Pasteur pipet flat against the slide and aspirate off excess PBS (*see* **Note 31**). The embryos will be drawn toward the pipet but will remain on the slide. Blot off excess buffer if necessary with a Kimwipe but do not allow the embryos to dry out.

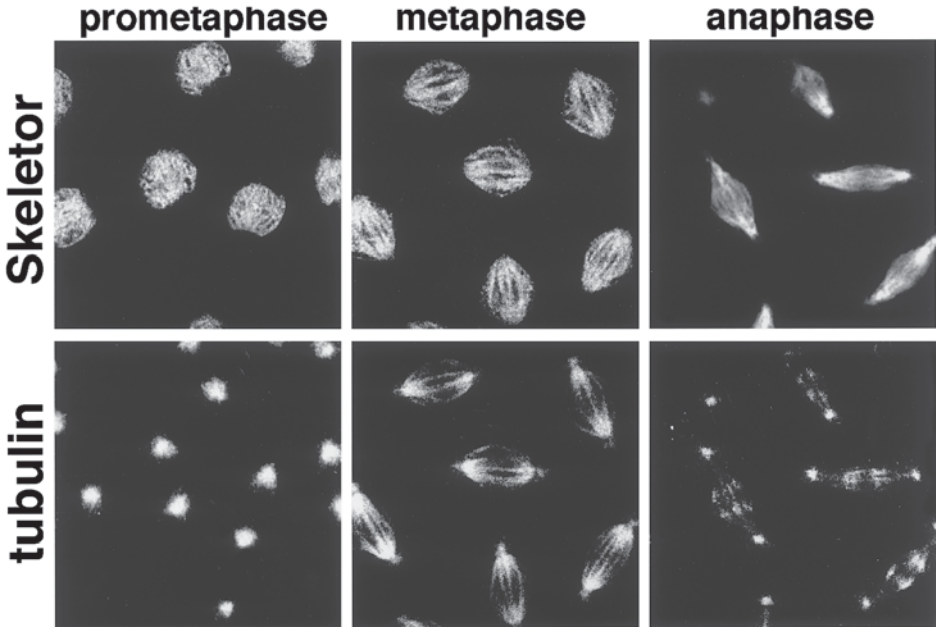

Fig. 3. Double labeling of *Drosophila* embryonic nuclei using confocal fluorescence microscopy in three stages of the cell cycle. The mAb 1A1, an IgM that recognizes the spindle matrix protein skeletor, was detected by TRITC-conjugated anti-mouse IgM secondary antibody. A commercially available anti-α-tubulin antibody, an IgG1 (Sigma-Aldrich, T-9026), was detected by FITC-conjugated anti-mouse IgG1 antibody in order to visualize microtubules.

2. Place two to three drops of glycerol containing 5% *n*-propyl gallate onto the embryos (*see* **Note 32**). Gently spread the embryos with a 200 µL pipet tip so they are not piled in one cluster.
3. Gently place a $22 \times 40\text{-mm}^2$ No. 15 cover slip onto the embryos, taking care not to trap bubbles. Seal the edges with nail polish (*see* **Note 33**.).
4. Image the embryos immediately using a fluorescent microscope or store in slide boxes at –20°C in the dark for fluorescently labeled preparations or at either –20°C or room temperature for HRP-labeled preparations (*see* **Note 34**).

*3.6. Mounting HRP-Labeled Embryos With DEPEX (***see** *Note 35)*

1. Transfer HRP-labeled embryos to a 1 mL glass tube (*see* **Note 36**.)
2. Dehydrate the embryos through successive extractions with 1-mL of increasing concentrations of ethanol as follows: 10%, 50%, 90%, and two washes of 100% ethanol (*see* **Note 37**).
3. Withdraw the ethanol and resuspend the embryos in xylene (*see* **Note 38**). Allow the embryos to settle and replace the xylene with a fresh 1-mL aliquot

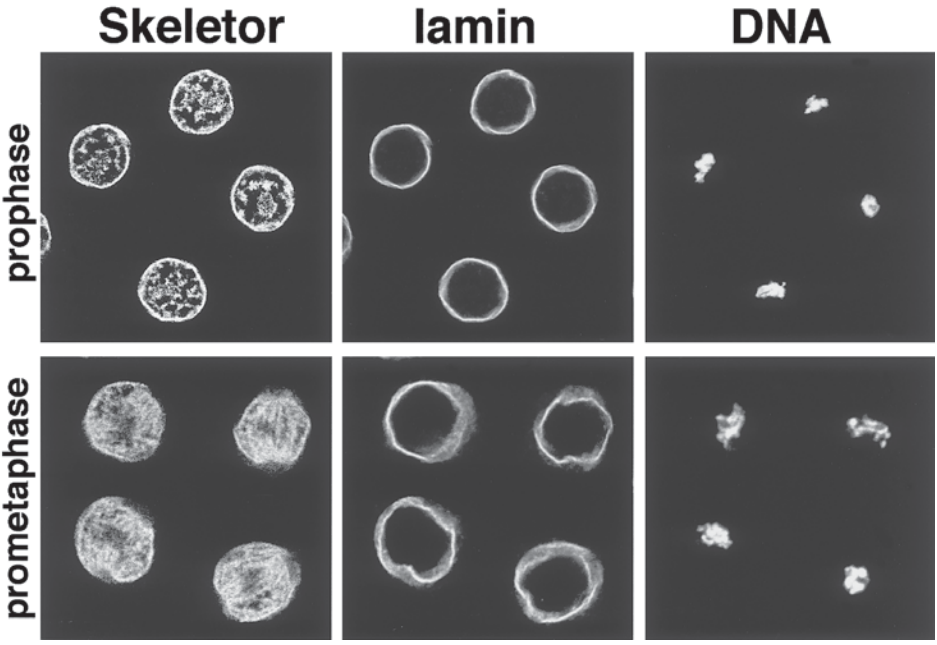

Fig. 4. Triple labeling of *Drosophila* embryonic nuclei using confocal fluorescence microscopy in two stages of the cell cycle. The mAb 1A1, an IgM that recognizes the spindle matrix protein skeletor, was detected by TRITC-conjugated anti-mouse IgM secondary antibody. A rabbit polyclonal antibody raised against lamin (generous gift of Dr. P. Fisher) was detected by FITC-conjugated anti-rabbit IgG secondary antibody. Hoechst was used to stain the DNA.

of xylene. If the embryos do not settle, repeat the ethanol extractions (*see* **Note 37**).

4. Using a Pasteur pipet, place the embryos onto a microscope slide in several drops of xylene, and quickly aspirate off much of the excess xylene, and rapidly place five to seven drops of DEPEX mounting medium on the embryos (*see* **Note 39**). Spread embryos using a P200 tip, place a 22×40-mm^2 cover slip over the embryos, being extremely careful not to trap any bubbles (*see* **Note 40**).
5. Place a weight onto the cover slip (we use a brass weight of approx 1.5 mm diameter weighing approx 170 g) to assist even spreading of the DEPEX mountant completely to the edges of the cover slip and leave undisturbed overnight until the mountant has fully hardened. Hardened mountant that has oozed out from under the cover slip can be trimmed away using a sharp razor blade.
6. Image embryos using standard light or Nomarski microscopy or store slides at room temperature.

3.7. Antibody Perturbation of Embryonic Development by Microinjection

1. Prepare antibody solution for injection (*see* **Note 41**). Aliquot antibody and store at –80°C or use for injections immediately (*see* **Note 42**).
2. Set up four collection bottles with approx 250 flies in a 25°C humidified incubator (or at your desired temperature) and allow them to lay 2–4 d before collecting for injections. Change the plates daily.
3. Allow the flies to prelay on a fresh plate for 30 min before changing to the collection plate. Allow flies to lay on the collection plate for 30 min (*see* **Note 43**).
4. Prepare injection needle as follows: Using a standard micropipet puller, pull glass filament capillary tubes to give a tip diameter less than 6 µm.
5. Prepare a second glass capillary tube with a tip diameter greater than 40 µm to be used later for vacuuming leaked cytoplasm (*see* **Note 44**).
6. Load the injection needle with antibody solution by placing the back end of the capillary tube in a microfuge tube containing antibody solution. Capillary action will draw the solution into the needle (*see* **Note 45**). Alternatively, the needle can be loaded by back-filling with a heat-pulled Pasteur pipet or Hamilton syringe. If bubbles are present, they can be removed by applying a vacuum for 1–10 min (*see* **Note 46**).
7. Prepare several cover slips by applying "embryo glue" (*see* **Note 47**) to the edge of a 22×22-mm^2 cover slip with a Pasteur pipet, spreading it along the edge as if buttering toast in a rectangular pattern slightly larger than the dimensions covered by the spread embryos. Make several such cover slips and allow to air-dry.
8. After the 30-min collection, align embryos on a cover slip as follows: Wash the embryos into a small collection basket and dechorionate as described in **Subheading 3.1., step 5** (*see* **Note 48**). Place the Spectra/Mesh nylon filter on top of a paper towel briefly to remove excess water.
9. Prepare an apple juice agar pad by excising a rectangular block of agar (approx 40 mm × 10 mm) from an apple juice plate poured as described in **Subheading 3.1.** (*see* **Note 49**.). Align approx 75 embryos in 2 parallel rows without touching each other, as shown in **Fig. 5** (*see* **Note 50**).
10. Gently lower the glue edge of a cover slip (prepared in **step 7**) onto the arrayed embryos to transfer them to the cover slip.
11. Desiccate the embryos 8–12 min by placing the cover slip, embryo-side down, in a sealed jar containing DrieRite (*see* **Note 51**). Prop the cover slip so as not to allow embryos to contact the DrieRite or it will stick to the glue.
12. Place the cover slip on a slide (embryos up) and cover embryos with a thin layer of halocarbon oil. Place the slide on the microscope stage with the embryos oriented along the cover slip edge closest to the micromanipulator.
13. Connect the injection needle to a pressure injection system constructed by attaching the needle holder to a three-way valve leading to air and vacuum systems. A second three-way valve left open to the air is inserted between the air/vacuum line and the needle, thus allowing for manual regulation of either air or vacuum pressure by simply placing a finger over its opening. If the tip of the pulled injection needle is too small (<1 µm), connect the needle at an angle of 8°–10° to a

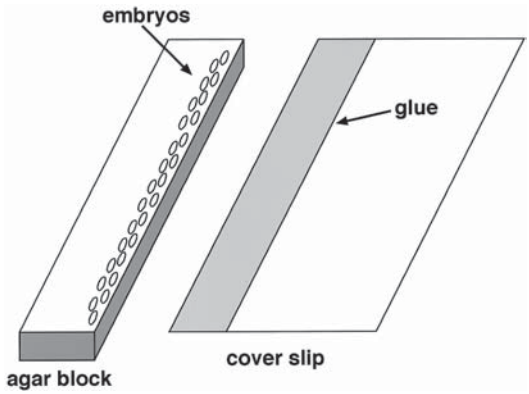

Fig. 5. In preparation for injection, embryos are lined up in two rows along the edge of a block of apple juice agar that has been excised from an apple juice plate. The alignment shown here is intended for a lateral injection site. "Embryo glue" is applied to the edge of a cover slip, providing a sticky surface on which to pick up the embryos from the agar block to immobilize them for injection. Once affixed to the cover slip, the cover slip will be placed on a slide and overlayed with a thin layer of halocarbon oil. (Adapted from **ref. *35***).

micromanipulator mounted on an inverted microscope stage. Gently break the tip of the injection needle by touching the needle tip against the debris of broken cover slips that have been secured with doublestick tape on a glass slide while monitoring the process under the microscope.

14. Position the injection needle so it is aligned perpendicularly with the first embryo. Set the three-way valve regulating air and vacuum pressure to the air setting. By moving the stage towards the injection needle, insert the needle into the embryo and cover the open three-way valve to allow the air pressure to force the injection solution into the embryo. Withdraw the needle quickly and carefully to minimize the loss of cytoplasm (*see* **Note 52**).
15. After completion of the set of microinjections, vacuum away any leaked cytoplasm using the larger bored capillary tube prepared in **step 5**.
16. If the embryos express a fluorescently tagged protein (e.g., green-fluorescent protein [GFP] or any of its color variants), the embryos can be directly observed using confocal microscopy. If the embryos are to be fixed in preparation for antibody or Hoechst staining, after incubating for the desired time, dry excess oil from the back of the cover slip, place the cover slip in a 60-mm Petri dish, and wash several times with PBST to remove as much halogen oil as possible. Add fixative : heptane (50 : 50) to the Petri dish and rotate for 20 min to allow fixation. Manually devitellinize the embryos as described in **Subheading 3.2., step 3**. Proceed with labeling and detection as described in **Subheading 3.4.** The result from Hoechst staining of one such perturbed antibody-injected embryo is shown in **Fig. 6**.

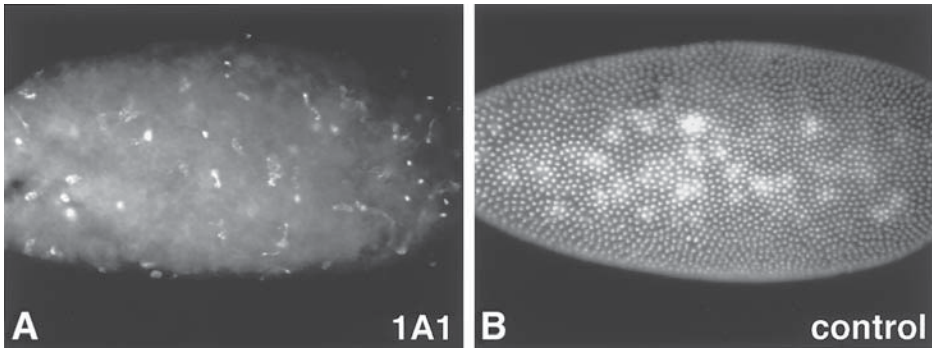

Fig. 6. Results from an antibody perturbation experiment. The mAb 1A1 recognizing the skeletor protein **(A)** or a control IgM antibody that does not stain *Drosophila* embryos **(B)** were injected into early, syncytial embryos as described in **Subheading 3.7.** Embryos were allowed to develop for 2.5 h at 20°C prior to fixation, devitellinization, and Hoechst staining. DNA staining revealed many fewer nuclei and severe chromosomal abnormalities in the antiskeletor antibody-perturbed embryos, whereas the control-injected set continued to develop indistinguishably from wildtype.

4. Notes

1. Change plates daily for best results and monitor humidity. If flies are "drying out" in the population cage, add a "spa" by moistening a Terri-towel in a weigh boat and place it in a corner of the cage.
2. The least expensive grade of agar can be used. (Flies are not picky!)
3. Collection plates must be at the collection temperature before use. Females will not lay eggs well on cold plates!
4. "Feeding" plates should be fully spread with yeast, and changed more frequently if flies are laying heavily. If staging is critical, it is essential to do a "prelay" collection of 1 h before exchanging the prelay plate with the collection plate, as females will retain fertilized eggs for some time if they feel conditions for laying eggs are not optimal.
5. Collection times will depend on desired stage of analysis; see **ref.** ***38*** for a staging guide.
6. It is essential to process embryos rapidly and avoid large aggregations to prevent anoxic effects ***(39)***, which can lead to a range of defects, most notably chromosome bridging at anaphase ***(26)***. Therefore, it is important to have your fixation tube ready immediately after dechorionation. We use a 15-ml test tube because when attached horizontally to a shaker, it provides an extensive interface between fixative and heptane layers, thus allowing embryos to spread out in a monolayer (*see* **Subheading 3.1., step 7**).
7. There are many different fixes available with respective advantages and disadvantages. One should experiment with several different fixatives to determine

which preserves both antigenicity of the protein of interest as well as morphological structure (*see* **refs.** ***31*** and ***32*** for detailed descriptions of different fixatives and the principle of fixation for each). We have obtained best results with Bouin's Fluid fixative, which is a precipitative fixative characterized by its rapid penetration and efficient fixing action on the nucleus. The combination of fixative agents in Bouin's Fluid (picric acid is precipitative, acetic acid enables rapid penetration and dissolves lipids, formalin crosslinks proteins) is particularly effective. 4% Paraformaldehyde fixes tissues primarily by crosslinking, and although it has moderate penetration, its fixing action is slow. Where mass devitellinization is performed, it should be noted that methanol not only induces removal of the vitelline membrane but also acts as a fixative, precipitating proteins and solubilizing lipids.

8. Heptane is essential for creating small holes in the vitelline membrane, thus allowing penetration of the fixative into the embryo.
9. Many different collection baskets of different sizes have been described ***(26,28,37)*** with various advantages for ease of use. We use a double-collection-basket system comprised of two screen cups (Sigma-Aldrich, no. S1145) where the top cup contains a single 40 mesh screen (Sigma-Aldrich, no. S0770) to trap any adult flies that might have stuck to the apple juice plate. Embryos wash through his mesh to the lower cup, in which we have installed a 70-µm nylon filter (Spectra/Mesh) above the 40 mesh screen to trap the embryos. This double-cup system fits nicely into a 250-mL beaker to allow manipulations with a paintbrush and squirt bottle to wash embryos into the basket.
10. Bleach loses its potency after dilution and with aging. Buy small bottles of Clorox to increase inventory turnover. If problems arise with embryos failing to sink in methanol at later stages (**Subheading 3.1.**, **step 10**), suspect that the bleach is not at the proper strength and visually monitor for dechorionation under a dissecting microscope.
11. Work rapidly to prevent anoxic effects. These techniques expose embryos to heptane prior to their exposure to fixative, which facilitates even fixation. If you observe gradients of fixation, suspect problems with crowding of embryos or fixation penetrance and try either fixing fewer embryos at a time and/or pretreating embryos (30–60 s) with heptane only before adding fixative to the tube.
12. A convenient method for vigorous agitation available in most laboratories is to securely tape your tube to the arm of a shaking water bath set at 220 rpm.
13. The duration for fixation should be empirically determined to optimize results for any given antigen–antibody interaction. In some cases, shorter times may give adequate fixation and better penetration. Longer times may be necessary, but beware of overfixation, which would lead to reduced antibody penetration.
14. Draw up a small quantity of heptane and then try to pick up the embryos at the interface. Before releasing pressure on the pipet bulb, pick up more heptane from the top layer. This heptane will "bubble up" through the Pasteur pipet, dispersing the embryos contained within the pipet, and, usually, causing them to settle nicely at the interface between the fixative and the heptane layers contained within the

pipet. Squeeze out the fixative layer back into the fixation test tube and transfer only the embryo layer to the new methanol–EGTA/heptane tube. It may take several rounds of this aspiration to move all of the embryos. With practice, you can transfer the embryos with a minimum of either the fixative or heptane layers.

15. If embryos are slow to settle or the yield seems especially low, the tube can be shaken vigorously for an additional 15 s.
16. Embryos will settle more slowly upon introduction into the aqueous buffers. Failure of the majority of the embryos to sink within several minutes may indicate incomplete extraction of heptane from the embryos and indicates a need for further methanol extractions.
17. Because many commercially available and commonly used secondary antibodies are raised in goats, we generally employ normal goat serum (NGS) in our blocking buffers. However, it is critical in your design that blocking agents and antibodies be compatibly matched. For example, if your primary antibody was raised in goat, you could not use goat serum to block nonspecific sites. Typically, match the blocking buffer serum type with that of the species used to generate the secondary antibodies in your experiment.
18. After aspirating off the final PBS wash, "precoat" the Pasteur pipet with the Blocking Buffer before transferring the Blocking Buffer to the embryos. Use the precoated pipet to transfer the embryos in Blocking Buffer to the 1.5 mL microfuge tube. Failure to "precoat" Pasteur pipets can result in embryos sticking to the pipet surface.
19. In most cases, embryos can be stored at 4°C in Blocking Buffer containing 0.05% sodium azide for several weeks without significant loss of staining resolution.
20. The amount of heptane transferred in the drop and the speed at which embryos are spread and covered with PBST are critical and will need to be determined with practice. Too much heptane will seriously dissolve the doublestick tape surface, resulting in embryos being mired in the tape and sliding out from under the tungsten needle in **Subheading 3.2., step 3**, without devitellinization. Too little heptane and the embryos will not stick sufficiently to the surface to allow needle pressure to pop the embryos out of the vitelline case. With the correct amount, the vitelline membrane will stick firmly to the doublestick tape surface, but the tape will still be firm enough to support the applied pressure.
21. Best results will typically be obtained if you do not exceed approx 30–50 µL volume of embryos. Use of too large a volume of embryos may result in weak or variable staining.
22. Primary antibody dilution should be empirically determined by comparing results from a dilution series. If the primary antibody was raised in rabbit, affinity purification is recommended due to high backgrounds in *Drosophila* staining typically found to be present in rabbit serum.
23. Secondary antibody should be directed against the species in which the primary antibody was raised and should be affinity purified (commercially available as such).
24. The presence of Triton X-100 or sodium azide will inhibit the HRP reaction.
25. Typically, we use HRP detection only for single labeling studies because multiple labeling is more easily performed using fluorescent tags (*see* **Subheading 3.4.**).

However, if so desired, it is possible to use enzyme-linked secondary antibodies to do double-labeling experiments by employing an alkaline phosphatase-conjugated secondary antibody against the second primary antibody that will give a blue-black reaction product distinguishable from the brown HRP reaction product. The reader is referred to Johansen et al. ***(40)*** for an example of such double labeling.

26. Double and triple labelings require careful selection of isotype- and species-specific secondary antibodies and care must be taken that in no case are secondary antibodies raised in a host in which one of the primary antibodies were raised. However, should that prove impossible it may be possible to judiciously select a defined order for sequential incubation with primary and secondary antibodies to avoid such crossreactivity.
27. Most commercially available secondary antibodies work well at 1 : 200–1 : 400 dilution, but should be empirically determined for each lot. Select only affinity-purified antibodies and test for crossreactivity with *Drosophila* embryos in the absence of any primary antibodies. We have not had any problems with affinity-purified antibodies from Bio-Rad, ICN/Capell, or Jackson ImmunoResearch, but have observed background problems in non-affinity-purified antibodies from other sources.
28. Filtration removes fluorescent aggregates that may appear as speckles in the epifluorescent images. Presence of bubbles in the filtrate may denature proteins, compromising antibody performance.
29. From this stage onward, cover the tube to protect from light and minimize quenching of the fluorescent signal.
30. Failure to remove Triton X-100 will reduce or eliminate the Hoechst staining signal.
31. By keeping the edge of the pipet opening pressed against the microscope slide, you can aspirate off the buffer without removing the embryos. This will not work if the pipet tip is chipped or cracked.
32. *n*-Propyl-gallate is added to reduce quenching of the fluorescent signal and is not necessary for the mounting of HRP-labeled preparations.
33. Use brightly colored nail polish instead of clear in order to observe whether the edges are fully sealed.
34. Some signals, particularly labeling deep in the interior such as the nervous system, may require overnight clearing for maximal visibility and resolution. Although most labelings will be immediately obvious, we recommend also viewing your preparation after allowing for overnight clearing.
35. DEPEX-mounted slides are considerably more difficult to prepare but provide exceptional clearing and resolution and when properly mounted, will store indefinitely.
36. Xylene solvent will dissolve plastic microfuge tubes.
37. It is critical to use absolute ethanol for the final extractions. Any remaining aqueous buffer (e.g., from 95% ethanol) will prevent complete penetration by the xylene and the embryos will not sink in the next step. Therefore, use only a freshly

opened bottle of 100% ethanol or use 100% ethanol stored over dehydration beads.

38. Xylene is highly volatile and a respiratory irritant. This work should be performed in a hood.
39. The xylene will evaporate extremely rapidly so it is crucial that these steps be performed quickly to prevent the embryos from drying out.
40. If even small bubbles should form beneath the cover slip, the slide will not be permanent, as the size of the bubbles will continue to grow over time. However, after overnight clearing even if bubbles are present you should at least be able to obtain images from many of the embryos that are not yet overtaken by bubbles.
41. In order to have sufficient antibody for effective perturbation, it is recommended that it be concentrated such that it will give strong embryo staining when used as described in **Subheading 3.3.** at a dilution of 1 : 1000 or more. High concentrations of antibody may be difficult to inject, however, because of increased viscosity. Thus, optimal conditions must be established balancing high antibody titer with ease of injection without needle clogging. Antibodies can be purified using one of several commercially available kits (e.g., Pierce or Bio-Rad).
42. Whereas it is convenient to prepare antibody and store for later use and it is preferable to compare different experiments using the same "lot" of antibody, some antibodies do not store well. Thus, it is critical to assay for antibody activity after storage. Antibodies that are aliquotted for storage must not contain preservatives such as sodium azide or thimerosal if they are to be used for microinjection.
43. Best results are obtained if there is minimal disturbance of the flies or incubator during collection periods. In addition, we consistently find low yields of eggs on overcast or rainy days, suggesting that egg-laying behavior may be sensitive to barometric pressure.
44. Prepare needles on the same day as the injections are to be performed in order to maintain tip sharpness. However, 5–10 needles should be prepared before beginning injections so as to have replacement needles handy, if needed.
45. Leaning the capillary tube at a 45° angle will help prevent bubbles from becoming lodged in the pipet.
46. We use in-house outlets for air (30 psi) and vacuum (700 mm Hg) systems.
47. Embryo glue is made by extracting double-sided tape or brown packing tape in heptane overnight.
48. Because of the relatively small numbers of embryos obtained within a 30-min collection, it is easier to use a smaller collection basket constructed from a plastic scintillation vial from which the bottom has been removed. Drill a hole into its cap and use to secure a small square of Spectra/Mesh screen (70 μm mesh size) over the mouth of the vial. Embryos can be washed and dechorionated in this smaller basket and the filter can be removed after dechorionation for easier access to embryos.
49. Using an apple juice pad will facilitate the orientation of the embryos because they can be nudged into position with a forceps prior to picking them up on the cover slip (*see* **Subheading 3.7., step 10**).

50. For antibody perturbation, we typically inject laterally in order to achieve a centralized injection site. However, alternatively, embryos can be aligned with either anterior or posterior ends oriented toward the cover slip edge if injection into one of the poles is desired instead.
51. The time required for desiccation will depend on the genotype of the embryos, the temperature, and the ambient humidity. Typically, we desiccate for 8 min ± 30 s. If significant cytoplasm leakage occurs after injection, try desiccating for slightly longer periods.
52. Proper desiccation will enable injections to be performed without cytoplasmic leakage. Typically, we inject 1 nL volume per injection.

Acknowledgments

We thank Dr. Paul Fisher for his generous gift of anti-lamin antibody and Drs. Linda Ambrosio and Kwang-Hyun Baek for advice in setting up our microinjection system. We thank Dong Wang and Melissa Blacketer for critical reading of the manuscript. This work was supported by National Science Foundation (NSF) grant MCB-0090877 and National Institutes of Health (NIH) grant GM62916 to KMJ.

References

1. Laskey, Fairman, R. A., M. P., and Blow, J. J. (1989) S Phase of the cell cycle. *Science* **246,** 603–608.
2. McIntosh, J. R. and Koonce, M. P. (1989) Mitosis. *Science* **246,** 603–608.
3. Pines, J. (1999) Four-dimensional control of the cell cycle. *Nature Cell Biol.* **1,** E73–E79.
4. Hinchcliffe, E. H. and Sluder, G. (2001) "It Takes Two to Tango": understanding how centrosome duplication is regulated throughout the cell cycle. *Genes Dev.* **15,** 1167–1181.
5. Cross, F., Roberts, J., and Weintraub, H. (1989) Simple and complex cell cycles. *Annu. Rev. Cell Biol.* **5,** 341–395.
6. Norbury, C. and Nurse, P. (1992) Animal cell cycles and their control. *Annu. Rev. Biochem.* **61,** 441–470.
7. Vidwans, S. J. and Su, T. T. (2001) Cycling through development in *Drosophila* and other metazoa. *Nature Cell Biol.* **3,** E35–E39.
8. Pines, J. and Rieder, C. L. (2001) Re-staging mitosis: a contemporary view of mitotic progression. *Nature Cell Biol.* **3,** E3–E6.
9. Scholey, J. M., Rogers, G. C., and Sharp, D. J. (2001) Mitosis, microtubules, and the matrix. *J. Cell Biol.* **154,** 261–266.
10. Zalokar, M. and Erk, I. (1976) Division and migration of nuclei during early embryogenesis of *Drosophila melanogaster. J. Microsc. Biol. Cell.* **25,** 97–106.
11. Foe, V. E. and Alberts, B. M. (1983) Studies of nuclear and cytoplasmic behavior during the five mitotic cycles that precede gastrulation in *Drosophila* embryogenesis. *J. Cell Sci.* **61,** 31–70.

12. Foe, V. E. (1989) Mitotic domains reveal early commitment of cells in *Drosophila* embryos. *Development* **107,** 1–22.
13. Warn, R. M., Flegg, L., and Warn, A. (1987) An investigation of microtubule organization and functions in living *Drosophila* embryos by injection of a fluorescently labeled antibody against tyrosinated α-tubulin. *J. Cell Biol.* **105,** 1721–1730.
14. Kiehart, D. P., Ketchum, A., Young, P., et al. (1990) Contractile proteins in *Drosophila* development. *Ann. NY Acad. Sci.* **582,** 233–251.
15. Buchenau, P., Saumweber, H., and Arndt-Jovin, D. J. (1993) Consequences of topoisomerase II inhibition in early embryogenesis of *Drosophila* revealed by in vivo confocal laser scanning microscopy. *J. Cell Sci.* **104,** 1175–1185.
16. Mermall, V. and Miller, K. G. (1995) The 95F unconventional myosin is required for proper organization of the *Drosophila* syncytial blastoderm. *J. Cell Biol.* **129,** 1575–1588.
17. Johansen, K. M., Johansen, J., Baek, K.-H., and Jin, Y. (1996) Remodeling of nuclear architecture during the cell cycle in *Drosophila* embryos. *J. Cell. Biochem.* **63,** 268–279.
18. Edgar, B., Odell, G. M., and Schubiger, G. (1987) Cytoarchitecture and the patterning of fushi tarazu expression in the *Drosophila* blastoderm. *Genes Dev.* **1,** 1226–1237.
19. Raff, J. W., Whitfield, W. G., and Glover, D. M. (1990) Two distinct mechanisms localize cyclin B transcripts in syncytial *Drosophila* embryos. *Development* **110,** 1249–1261.
20. Planques, V., Warn, A., and Warn, R. M. (1991) The effects of microinjection of rhodamine-phalloidin on mitosis and cytokinesis in early stage *Drosophila* embryos. *Exp. Cell. Res.* **192,** 557–566.
21. Jin, Y., Wang, Y., Walker, D. L., et al. (1999) JIL-1: a novel chromosomal tandem kinase implicated in transcriptional regulation in *Drosophila*. *Mol. Cell* **4,** 129–135.
22. Wang, Y., Zhang, W., Jin, Y., Johansen, J., and Johansen, K.M. (2001) The JIL-1 tandem kinase mediates histone H3 phosphorylation and is required for maintenance of chromatin structure in *Drosophila*. Cell **105,** 433–443.
23. Walker, D. L., Wang, D., Jin, Y., et al. (2000) Skeletor, a novel chromosomal protein that redistributes during mitosis provides evidence for the formation of a spindle matrix. *J. Cell Biol.* **151,** 1401–1411.
24. Zalokar, M. and Erk, I. (1977) Phase-partition fixation and staining of *Drosophila* eggs. *Stain Technol.* **52,** 89–95.
25. Mitchison, T. J. and Sedat, J. (1983) Localization of antigenic determinants in whole *Drosophila* embryos. *Dev. Biol.* **99,** 261–264.
26. Theurkauf, W. E. (1994) Immunofluorescence analysis of the cytoskeleton during oogenesis and early embryogenesis. *Methods Cell Biol.* **44,** 489–505.
27. Patel, N. H. (1994) Imaging neuronal subsets and other cell types in whole-mount *Drosophila* embryos and larvae using antibody probes. *Methods Cell Biol.* **44,** 445–487.

28. Rothwell, W. F. and Sullivan, W. (2000) Fluorescent analysis of *Drosophila* embryos, in *Drosophila Protocols* (Sullivan, W., Ashburner, M., and Hawley, R. S., eds.), Cold Spring Harbor Laboratory Press, Cold Spring Harbor, NY, pp. 141–157.
29. Rebay, I. and Fehon, R.G. (2000) Generating antibodies against *Drosophila* proteins, in *Drosophila Protocols* (Sullivan, W., Ashburner, M., and Hawley, R.S., eds.), Cold Spring Harbor Laboratory Press, Cold Spring Harbor, NY, pp. 389–411.
30. Spector, D. L, Goldman, R. D., and Leinwand, L. A. (1998) Immunofluorescence methods for *Drosophila* tissues, in *Cells: A Laboratory Manual* (Spector, D. L, Goldman, R. D., and Leinwand, L. A., eds.), Cold Spring Harbor Laboratory Press, Cold Spring Harbor, N pp. 107.1–107.9.
31. Humason, G.L. (1997) *Animal Tissue Techniques,* W.H. Freeman, San Francisco.
32. Horobin, R. W. (1982) *Histochemistry,* Gustav Fischer Verlag, New York.
33. Santamaria, P. (1986) Injecting eggs, in *Drosophila: A Practical Approach.* (Roberts, D.B., ed.), IRL, Oxford, pp. 159–173.
34. Spradling, A. C. (1986) P element-mediated transformation, in *Drosophila: A Practical Approach.* (Roberts, D. B., ed.), IRL, Oxford, pp. 175–197.
35. Baek, K.-H. and Ambrosio, L. (1995) An efficient method for microinjection of mRNA into *Drosophila* embryos. *BioTechniques* **17,** 1024–1026.
36. Lee, G. M. (1989) Measurement of volume injected into individual cells by quantitative fluorescence microscopy. *J. Cell Sci.* **94,** 443–447.
37. Kiehart, D. P., Crawford, J. M., and Montague, R. A. (2000) Quantitative microinjection of *Drosophila* embryos, in Drosophila *Protocols* (Sullivan, W., Ashburner, M., and Hawley, R. S., eds.), Cold Spring Harbor Laboratory Press, Cold Spring Harbor, NY, pp. 345–359.
38. Campos-Ortega, J. A. and Hartenstein, V. (1997) Stages of *Drosophila* embryogenesis, in *The Embryonic Development of Drosophila* melanogaster. Springer-Verlag, New York, pp. 9–102.
39. Foe, V.E. and Alberts, M.M. (1985) Reversible chromosome condensation induced in *Drosophila* embryos by anoxia: visualization of interphase nuclear organization. *J. Cell Biol.* **100,** 1623–1636.
40. Johansen, K. M., Kopp, D. M., Jellies, J., and Johansen, J. (1992) Tract formation and axon fasiculation of molecularly distinct peripheral neuron subpopulations during leech embryogenesis. *Neuron* **8,** 559–272.

10

Whole-Mount Fluorescence *In Situ* Hybridization to Chromosomes of Embryos

Daryl S. Henderson

1. Introduction

Whole-mount fluorescence *in situ* hybridization (FISH) to chromosomes of *Drosophila* embryos is used to pinpoint the position of a chromosomal segment of interest, specified by the DNA probe(s), within a "preserved" three-dimensional nuclear structure. This technique has been used to (1) visualize the relative positions of homologous loci during the onset of somatic chromosome pairing ***(1,2)***, (2) establish whether separation of sister chromatids had occurred in mutants arrested at the metaphase/anaphase transition ***(3–5)***, (3) karyotype zygotes ***(6)***, and (4) ascertain the ploidy of nuclei of a checkpoint mutant ***(7)***. The basic embryo-FISH technique can be combined with antibody staining to permit simultaneous detection of both a hybridized DNA probe and a specific subcellular structure, such as the nuclear envelope, permitting spatial relationships to be defined ***(8,9)***. Protocols for both techniques are included in this chapter.

Probably the most important consideration when planning an embryo-FISH experiment is the choice of DNA probe. Although the exact selection will depend heavily on the biological question that is to be addressed, some general comments about probes can be made (*see also* Chapter 18).

The longer the target sequence available to the probe, the better the signal that will be produced. Thus, satellite DNA repeats, which in genomic DNA can extend for megabases (Mb), can make excellent probes. Simple satellite DNA probes have another advantage: They can be produced by automated synthesis (e.g., as a 50–60-mer oligonucleotide consisting of 10–12 repeats of a 5-nt sequence). Be aware, however, that many satellite sequences and

From: *Methods in Molecular Biology, vol. 247:* Drosophila *Cytogenetics Protocols*
Edited by: D. S. Henderson © Humana Press Inc., Totowa, NJ

other repetitive DNAs reside at multiple chromosomal loci ***(10)***, which may limit their experimental utility. Some single-locus repetitive DNAs are listed in **Table 1**.

Several embryo-FISH studies have used unique DNAs as probes, typically derived from approx 80- to 100-kb genomic fragments cloned in P1 vectors ***(8,9,14)***. Such large DNAs must be broken into small fragments, either by digestion with multiple "4-base cutter" restriction enzymes (e.g., *Alu*I, *Hae*III, *Mse*I, *Msp*I, *Rsa*I, and *Sau*3AI; ***14***) or by sonication ***(8)***, to enable their penetration into the embryo. Probe fragments having a mean size of 200–300 bp are reported to work best ***(1)***. Unique genomic sequences totaling <10 kb have also been used successfully for embryo-FISH, although in those cases, the fluorescence signals were detected using a microscope equipped with a highly sensitive cooled charge-coupled device (CCD) camera ***(15,16)***.

Chromosomes in syncitial nuclei adopt a polarized or Rabl orientation in interphase, in which centromeric regions are localized to one side the nucleus (apically, toward the embryo surface) and telomeric regions are positioned toward the opposite side (basally, toward the embryo interior; *see* **refs. *17*** and ***18***). In effect, the anaphase configuration of the previous mitosis is maintained until prophase of the next mitosis. Consequently, in interphase, each gene locus tends to occupy a particular axial position in the nucleus. Highly repetitive DNAs most often reside in pericentric regions of chromosomes, and probes to such repeats will produce FISH signals apically ***(9)***, although Y^L-linked satellites would be expected to show an axial distribution in accordance with their positions along the chromosome arm. In the case of the AAGAG satellite cluster associated with the bw^D mutation at the tip of the right arm of chromosome 2, in syncitial embryos it assumes a basal position in the nucleus, characteristic of the chromosome end, and shows preferential association with the nuclear envelope (NE) ***(14)***. However, the characteristic associations of heterochromatic DNAs with the nuclear periphery and nucleolus seen in interphase nuclei of postsyncitial developmental stages are not observed in precelluarized embryos, most probably because heterochromatin has not yet formed. Moreover, certain DNA–NE associations that have been observed in the interphase of cycle 13 syncitial embryos do not persist into telophase, and in telophase new DNA–NE associations can form ***(9)***.

Probe DNA can be labeled using a variety of enzymatic methods that incorporate either hapten- or fluorophore-coupled deoxyribonucleotide triphosphates (dNTPs) into the probe fragments. The most commonly used labeling methods are random priming ***(19,20)*** (*see* **Subheading 3.1.**), nick-translation ***(21)***, and 3'-end labeling ("tailing") catalyzed by terminal deoxyribonucleotidyl transferase (TdT) ***(22)***. FISH methods using hapten-coupled dNTPs offer greater versatility and are generally more sensitive than direct methods using

Table 1
Examples of Single-Locus Repetitive DNAs

Chromosome	DNA probe	Locus	Comments	Ref.
X	359-bp satellite	X heterochromatin	Some labeling of chromosomes 2 and 3 on metaphase squashes showing heavy labeling of X ***(10)***.	***10***
Y^L	AATAC satellite	h5–h6	~3.5 Mb	***10,11***
Y^S	AATAAAC satellite	h22	~1.6 Mb	***10,11***
2L	Histone gene cluster	39D–E	100–150 copies per chromosome	***1***
2R	AACAC satellite	Pericentric heterochromatin		***11,12***
2R	5S rDNA	56F1,2		
3R	CCCGTACTCGGT *dodeca satellite*	Pericentric heterochromatin		***13***
4			*See* **Note 1**	

fluorophore-coupled dNTPs. The most widely used haptens are biotin and digoxigenin (DIG). After hybridization to chromosomes, biotin moieties of the probe are detected using fluorescently labeled avidin or streptavidin, both of which bind biotin with high affinity. DIG moieties are detected using anti-DIG antibodies (from Roche). Commonly used fluorochromes include fluorescein isothiocyanate (FITC), tetramethyl rhodamine isothiocyanate (TRITC), and various cyanine dyes (e.g., Cy2, Cy3, Cy5, and Alexa® Fluors). A wide range of fluorochrome-conjugated avidin and streptavidin reagents are available from numerous vendors (e.g., Vector Laboratories, Sigma-Aldrich, Jackson ImmunoResearch, Molecular Probes), whereas the range of fluorophore-conjugated anti-DIG antibodies is fairly limited (e.g., FITC, TRITC, and amino-methylcoumarinacetic acid [AMCA]). Although the exact choice of fluorophores will depend on both your microscope's light sources and filter sets, typically even basic laser scanning confocal microscopes are configured to allow imaging of both green-fluorescent (e.g., FITC, Cy2) and red-fluorescent (e.g., TRITC, Cy3) dyes.

An emerging technology, quantum dots (QDs), may some day supplant organic dyes as fluorophores for biological imaging. Core–shell QDs consist of a luminescent semiconductor dot core (e.g., CdSe) capped by a thin inorganic shell (e.g., ZnS) that prevents surface quenching and increases photostability of the core (e.g., **refs. *23*** and ***24***). QDs emit at different wavelengths depending on dot size, but different color dots can be excited at a single wavelength, which has important implications for multicolor FISH. Furthermore, QDs are intensely fluorescent at concentrations comparable to organic dyes and can be visualized by both conventional fluorescence and confocal microscopy. They are highly photostable and do not require antifade reagents. At least two QD–streptavidin conjugates are now available commercially, from Quantum Dot Corporation (Hayward, CA [www.qdot.com]). Qdot™ 585 would substitute for lissamine rhodamine B or TRITC conjugates, and Qdot™ 605 would substitute for Texas Red.

Protocols for preparation of embryos are given in **Subheadings 3.2.** and **3.3.** The FISH method (**Subheadings 3.4–3.6.**) is essentially that of Hiraoka et al. ***(1)*** incorporating minor modifications of Sigrist et al. ***(3)***. The protocol for combined immunostaining and FISH (**Subheading 3.7.**) is modified from Gemkow et al. ***(8)***.

2. Materials

1. Probe DNAs (*see* **Table 1**).
2. Biotin–14-dATP, 0.4 m*M* stock solution (Life Technologies) or biotin–16-dUTP or other appropriate hapten-labeled nucleotide (*see* **Note 2**).
3. FITC–avidin D and FITC anti-avidin D antibodies (the latter is optional; Vector Laboratories) (*see* **Note 3**).

4. Oligolabeling buffer (OLB) for labeling with biotin–14-dATP: Prepare from the following stock solutions:

   Solution A: 1.25 *M* Tris-HCl, pH 8.0, 125 m*M* $MgCl_2$, 250 m*M* β-mercaptoethanol, and 0.5 m*M* each dNTP (minus dATP; Roche). Solution A can be prepared as follows: To 485 µL of Solution O, add 9 µL of β-mercaptoethanol, 2.5 µL of 100 m*M* dCTP, 2.5 µL of 100 m*M* dGTP, and 2.5 µL of 100 m*M* dTTP. Store at –20°C. Do not add dATP to solution A (*see* **Note 4**).

   Solution B: 2 *M* HEPES, pH 6.6. Store at 4°C.

   Solution C: Random hexamer $pd(N)^6$ (Amersham Pharmacia Biotech) dissolved at 90 A_{260} units per milliliter in 1 m*M* Tris-HCl, 1 m*M* EDTA, pH 7.5. Store at –20°C.

   Solution O: 1.25 *M* Tris-HCl, pH 8.0, 125 m*M* $MgCl_2$.

   Mix solutions A, B and C in a ratio of 2 : 5 : 3 to give OLB. Store at –20°C.
5. Klenow fragment of DNA polymerase I (5 U/µL; Roche).
6. Reagents for ethanol precipitation to remove unincorporated nucleotides following the labeling reaction (*see* **Note 5**).
7. Vacuum filter glass funnel with fritted glass base and clamp (e.g., Fisherbrand, Millipore, or Kontes).
8. Nitex nylon mesh, approx 120-µm pore size.
9. Distilled water and distilled water containing 0.1% Tween-20 (v/v).
10. 50% Concentrated household bleach (e.g., Clorox) (i.e., bleach solution having a final concentration of approx 3% sodium hypochlorite.
11. Glass vial with snap cap (16 mL, Wheaton) or glass scintillation vial.
12. Phosphate-buffered saline (PBS): 137 m*M* NaCl, 2.7 m*M* KCl, 8 m*M* Na_2PO_4, 1.5 m*M* KH_2PO_4, pH 7.4. To make 1 L of 10X PBS stock solution, add 80 g NaCl, 2 g KCl, 2 g KH_2PO_4 and 11.4 g Na_2PO_4 to approx 800 mL of distilled water. Adjust to pH 7.4 with 10 *N* NaOH and add distilled water to 1 L.
13. PBST: 1X PBS, 0.1% Tween-20.
14. Fixative: 3.7% Formaldehyde in PBS. Dilute 1 vol of 37% (w/w) formaldehyde (e.g., Sigma-Aldrich) in 9 vol of PBS. Formaldehyde is mutagenic and carcinogenic. Wear gloves and work with formaldehyde in a fume hood.
15. Methanol.
16. Heptane.
17. Prehybridization rinse solution: 4X SSC, 0.1% Tween-20, 20% formamide (e.g., Fisher Super Pure Grade). Deionize the formamide using ion-exchange resin AG501-X8 (BioRad). 20X SSC is 3 *M* NaCl, 0.3 *M* Na_3-citrate, pH 7.0.
18. Hybridization solution: 4X SSC, 0.1% Tween-20, 50% formamide.
19. Wash solutions:
    a. 4X SSC, 0.1% Tween-20, 40% formamide.
    b. 4X SSC, 0.1% Tween-20, 30% formamide.
    c. 2X SSC, 0.1% Tween-20, 20% formamide.
    d. 2X SSC, 0.1% Tween-20, 10% formamide.
    e. 2X SSC, 0.1% Tween-20. (This solution is also used prior to hybridization, at **Subheading 3.3., step 7**.)

20. Propidium iodide (PI) solution: 1 mg/mL PI in PBS. Store in the dark at 4°C. Spin at >10,000*g* for 5 min in a microcentrifuge before use. Other appropriate DNA stains can be used, depending on your microscope's light sources and filter sets (e.g., Sytox dyes and TOTO-3, from Molecular Probes).
21. 10 mg/mL RNase A. Required if using PI to stain DNA.
22. Mouse monoclonal antibody against *Drosophila* nuclear lamin Dm_0 [e.g., ADL84; ***(25)***] and a rhodamine-labeled secondary antibody (e.g, goat or donkey anti-mouse [Jackson ImmunoResearch] [optional]).
23. Fetal calf serum (FCS) (required for immuno-FISH). Store in aliquots at –20°C.
24. Microscope slides and cover slips.
25. Vectashield mounting medium (Vector Laboratories) or similar.
26. Nail polish, clear.

3. Methods

3.1. Labeling of DNA Probe by Random Priming

This is but one method to label probe DNA. Other methods include nick translation (*see* **Note 6**) and 3'-endlabeling using TdT (*see* **Note 7**).

1. Denature 100–500 ng of satellite DNA [e.g., Y chromosome repeats $(AATAAAC)_n$ or $(AATAC)_n$ or *dodeca satellite*] in water or 10 m*M* Tris-HCl, 1 m*M* EDTA, pH 8.0 (TE) buffer by heating at 100°C for 10 min in a 0.5-mL Eppendorf Safe-Lock microcentrifuge tube.
2. Add 18 µL of denatured DNA to a 0.5-mL microcentrifuge tube containing 5 µL of OLB and 1 µL of biotin–14-dATP. (For AT-rich DNAs, dilute 1 vol of 0.4 m*M* biotin–14-dATP with 4 vol of 0.4 m*M* unlabeled dATP.) (*See* **Note 2**.)
3. Add 1 µL of Klenow enzyme (5 U) to give a total reaction vol of 25 µL and incubate at 37°C for 1–2 h or overnight at room temperature.
4. Stop the reaction by adding 2 µL of 200 m*M* EDTA, pH 8.0 (and/or by heating at 65°C for 10 min).
5. Remove unincorporated nucleotides by ethanol precipitation (*see* **Note 5**) or other means (e.g., with a spin column). If the probe is not to be used right away, store at –20°C.

3.2. Collection and Dechorionation of Embryos

1. Place an approx 6×6-cm^2 swatch of Nitex mesh between the glass funnel and fritted base of a vacuum filter apparatus, and clamp the funnel to the base. Attach the assembly to a vacuum system. Wet the Nitex mesh with distilled water and check for leakage.
2. Collect embryos (1–3 h old) from a population cage or egg collection bottle and transfer them to the glass funnel using a paintbrush and by squirting them with a stream of distilled water containing 0.1% Tween-20. Fine-mesh sieves (e.g., with 425- and 125-µm openings) can also be used at this point to screen out unwanted debris. Rinse the embryos several times with water/0.1% Tween-20, applying suction to remove each wash.

3. To dechorionate the embryos, add several milliliters of 50% bleach solution and leave the embryos for 3–4 min. Replenish the bleach solution if there is leakage from the vacuum filter and occasionally stir the embryos using a paintbrush (*see* **Note 8**).
4. Remove the bleach solution by suction and then rinse the embryos thoroughly with distilled water containing 0.1% Tween-20 and then with distilled water, applying suction to remove each rinse.
5. Gently lift the funnel while applying suction and rinse any remaining embryos from the funnel wall onto the Nitex mesh.

3.3. Fixation and Devitellization of Embryos

1. Using a fine paintbrush, transfer the dechorionated embryos from the Nitex mesh to a glass vial (e.g. scintillation vial) containing approx 3 mL of fixative (3.7% formaldehyde in PBS) overlayed with approx 5 mL of heptane. Dab the embryos into the heptane so they fall from the brush and sink to the fixative–heptane interface. Gently agitate the vial on a blood tube roller or other mixer for 10–15 min at room temperature.
2. Using a Pasteur pipet, remove all of the fix and all but approx 1 mL of the heptane. Dispose of these solutions into appropriate chemical waste containers.
3. Add approx 5 mL of methanol and shake the vial vigorously for approx 1 min. Devitellinized embryos will sink to the bottom of the vial. They can be helped to sink by tapping the vial.
4. Using a cut-off 200–µL pipet tip and pipetter, transfer the devitellinized embryos in methanol to a 0.5-mL microcentrifuge tube.
5. Remove the old methanol and rinse the embryos in three changes of fresh methanol (approx 300 µL each).
6. Rehydrate the embryos by washing them three times in approx 300 µL of PBST (5 min each wash).
7. Rinse the embryos three times in approx 300 µL of 2X SSC, 0.1% Tween-20.

3.4. Hybridization

1. Incubate the embryos in 4X SSC, 0.1% Tween-20, 20% formamide for 10 min at room temperature. Embryos will take on a translucent appearance in formamide.
2. Incubate the embryos in 4X SSC, 0.1% Tween-20, 50% formamide for 10 min at room temperature.
3. Remove the previous solution and replace with fresh 4X SSC, 0.1% Tween-20, 50% formamide, and incubate the embryos for 1 h at 37°C. Near the end of the prehybridization, boil the biotin-labeled probe (prepared in **Subheading 3.1.**) for 5–10 min to denature duplex DNA.
4. Remove as much prehybridization solution as possible and add approx 25 ng of probe in 25 µL of hybridization solution (4X SSC, 0.1% Tween-20, 50% formamide) to an embryo volume of approx 15 µL. Mix gently (*see* **Note 9**). For unique sequence DNAs, use approx 250–1000 ng of probe.
6. Denature the chromosomal DNA by placing the embryos in a 70°C water bath, heating block, or thermocycler for 15 min (*see* **Note 10**).
7. Hybridize at 30–37°C overnight (12–18 h) with gentle agitation (*see* **Note 11**).

3.5. Posthybridization Washing

Embryos are sequentially washed in solutions of increasing stringency to remove nonspecifically bound probe.

1. Transfer the embryos to a 1.5-mL microcentrifuge tube using a Pasteur pipet.
2. Discard as much of the old hybridization solution as possible, then briefly rinse and then wash the embryos in fresh hybridization solution (4X SSC, 0.1% Tween-20, 50% formamide) for 20 min at room temperature. Use approx 0.5–1 mL of wash solution for all washes and gently agitate the embryos (e.g., on a rotating wheel).
2. Wash in 4X SSC, 0.1% Tween-20, 40% formamide for 20 min at room temperature.
3. Wash in 4X SSC, 0.1% Tween-20, 30% formamide for 20 min at room temperature.
4. Wash in 2X SSC, 0.1% Tween-20, 20% formamide for 20 min at room temperature.
5. Wash in 2X SSC, 0.1% Tween-20, 10% formamide for 20 min at room temperature.
6. Rinse twice in 2X SSC, 0.1% Tween-20.

3.6. Detection of Bound Probe

1. Incubate the embryos in 1 : 100 FITC–avidin D in 2X SSC, 0.1% Tween-20, 100 µg/mL RNase A overnight at 4°C on a rotating wheel (*see* **Notes 3**, **12**, and **13**). In this and the following steps, keep the tube covered with aluminum foil to prevent exposure to light.
2. Wash the embryos twice in 2X SSC, 0.1% Tween-20 for 20 min at room temperature.
3. Wash the embryos once in PBS for 5 min.
4. Incubate the embryos in 1 : 1000 propidium iodide solution in PBS for 5 min.
5. Rinse the embryos in PBS for 5 min.
6. Mount the embryos in Vectashield or similar mountant.

In case of weak FISH signals, *see* **Notes 13** and **15**.

3.7. Combined FISH and Immunostaining

1. Proceed as described in **Subheadings 3.1–3.5.**
2. After completing **Subheading 3.5., step 6**, rinse the embryos twice with PBST.
3. Block the embryos in approx 1 mL of 10% FCS in PBST for 1 h at room temperature. Mix gently (e.g., on a rotating wheel).
4. Remove the blocking solution and incubate the embryos in 1 : 10 to 1 : 100 mouse monoclonal anti-*Drosophila* lamin antibodies in 10% FCS in PBST for 4–6 h at room temperature or overnight at 4°C (*see* **Note 14**).
5. Wash the embryos in five changes of PBST, 30 min each wash.
6. Incubate the embryos in 1 : 100 FITC–avidin D and in an appropriate concentration of goat or donkey anti-mouse rhodamine-labeled secondary antibodies in 10% FCS in PBST, for 2–3 h at room temperature or overnight at 4°C (*see* **Note 13**).
7. Wash the embryos in five changes of PBST, 20–30 min each wash.
8. Mount the embryos in Vectashield or similar mounting medium and seal the cover slip with clear nail polish.

4. Notes

1. Gemkow et al. ***(2)*** have developed a simple technique to "paint" chromosome 4 using a combination of fluorochromes. YOYO-1 (a green-fluorescent dye; Molecular Probes) stains all chromosomes, whereas TOTO-3 (Molecular Probes) selectively stains chromosome 4. An advantage of this method is that it does not require denaturation of chromosomal DNA. However, it does require a light source capable of exciting TOTO-3 (e.g., 633 nm spectral line of a He–Ne laser) and an appropriate filter set.
   a. Dechorionate and fix embryos as described in **Subheadings 3.2.** and **3.3.**
   b. Incubate embryos in 100 µg/mL RNase A in PBST for 3–5 h at 37°C.
   c. Remove the RNase solution and replace with PBST containing 0.1 µ*M* YOYO-1 and 0.2 µ*M* TOTO-3 for 30 min (at room temperature).
   d. Mount in Vectashield mounting medium.
2. I have suggested biotin–dATP assuming an AT-rich satellite DNA is used as a probe; biotin–16-dUTP could also be used. Although hapten-conjugated dNTPs are normally efficient substrates for polymerases, they do not entirely substitute for their natural counterparts (*see* **ref. *26*** and references therein). This is particularly evident at high ratios of modified dNTP : unmodified dNTP, which can cause DNA synthesis to abort ***(26)***. For this reason and because not all incorporated biotin moieties will be accessible to avidin anyway because of steric hindrance, the biotin-dATP in the labeling reaction should be diluted with unlabeled dATP in a ratio of 1 : 4 (*see* **Subheading 3.1., step 2**). For AT-rich DNA probes, the amount of biotin–dATP could be reduced even further. Consider that the G-C-rich *dodeca satellite* (CCCGTACTCGGT) probe produces a strong FISH signal when labeled even with biotin–dUTP ***(13)***.
3. Fluorophore-labeled egg white avidin and bacterial streptavidin are available from numerous sources (e.g., ExtrAvidin®–FITC conjugate, Sigma-Aldrich). These are highly purified and chemically modified avidins with low nonspecific binding compared to the native proteins.
4. Biotin–14-dATP will be added just prior to the labeling reaction (*see* **Subheading 3.1., step 2**). If labeling with biotin–16-dUTP or digoxigenin–11-dUTP, for example, then dTTP would be left out of the mix instead of dATP.
5. Removal of unincorporated label helps to increase the signal-to-noise ratio. Ethanol precipitation can be done as follows:
   a. Transfer the stopped reaction to a 1.5-mL microcentrifuge tube and add 1 µL of 20 mg/mL glycogen (molecular-biology grade; e.g., Sigma-Aldrich, G 1767) and TE to bring the volume to 100 µL. Glycogen is suitable as a carrier for nucleic acid molecules as small as eight nucleotides ***(27)***.
   b. Add 0.5 vol (50 µL) of 7.5 *M* ammonium acetate and mix.
   c. Add 2.5 vol (400 µL) of absolute ethanol, vortex briefly, and hold at –70°C for 1 h to precipitate the labeled DNA.
   d. Centrifuge at maximum speed (12,000*g*–16,000*g*) in a microcentrifuge at 4°C.
   e. Aspirate the supernatant, rinse the pellet in 1 mL of 70–80% ice-cold ethanol, and allow the pellet to air-dry (but do not overdry). Resuspend the DNA in an

appropriate volume of formamide to give approx 2 ng/µL (for satellite DNAs). Store the labeled probe at –20°C if not being used right away. After denaturation, add the probe DNA to an equal vol of 8X SSC, 0.2% Tween-20 to yield probe in 4X SSC, 0.1% Tween-20, 50% formamide suitable for hybridization.

6. Nick translation ***(21)*** can be used as an alternative method to label DNA. In this case, it is necessary to optimize digestion with DNase I to produce suitably sized probe fragments. Simple protocols for doing this in the context of FISH probes are described in **refs. *28*** and ***29***.
7. For short oligos and small DNA fragments, 3'-end labeling (or tailing) using TdT is required. A protocol for this can be found in ***(30,31)***.
8. Bleach and heptane will damage the brush, so dedicate a single paintbrush for this purpose.
9. This amount of probe (approx 25 ng) is sufficient for highly repetitive DNAs. Larger amounts are required for unique DNAs. For example, Gemkow et al. ***(8)*** used 600–1000 ng of DNA from a P1 clone.
10. Temperatures typically from 70°C–91°C are used to denature chromosomal DNA. For example, Hiraoka et al. ***(1)*** and Sigrist et al. ***(3)*** used 70°C for 15 min in 4X SSC, 0.1% Tween-20, 50% formamide. Gemkow et al. ***(8)*** used 80°C for 15 min in 4X SSC, 100 m*M* sodium phosphate, pH 7.0, 0.1% Tween-20, 50% formamide. Dernburg recommends denaturation at 91°C for 2 min in 3X SSC, 10% dextran sulfate, 50% formamide ***(30)***.
11. A 37°C hybrization temperature should work for most probes, including *dodeca satellite*, 359-bp satellite, and unique DNAs. Lower temperatures may work better for A-T rich sequences. Lohe et al. ***(10)*** listed hybridization temperatures for satellite DNAs that may serve as a guide; bear in mind that they used a different hybridization solution.
12. If the embryo DNA is to be stained with a fluorophore that binds RNA as well as DNA (e.g., propidium iodide), include RNase A (0.5–1 mg/mL) at this step.
13. FITC–avidin D (1 : 100 dilution of stock) and FITC-anti-avidin D (1 : 100) can be added together to amplify the signal ***(13,32)***.
14. Immunostaining after the harsh conditions of FISH works well in the case of the lamin Dm protein, which is abundant in interphase and forms a stable polymer concentrated at the nuclear periphery. Dernburg and Sedat ***(31)*** reported that a surprising number of other proteins can also be immunostained after FISH, including tubulin, nuclear pore proteins, topoisomerase II, and GAGA factor.
15. Gemkow et al. ***(8)*** reported having successfully adapted the tyramide reaction for enhancing FISH signals ***(33,34)*** to whole-mount *Drosophila* embryos. Their protocol assumes a DIG-labeled probe was used, but biotin-labeled probes also can be detected by using streptavidin–horseradish peroxidase (HRP) conjugate (Perkin-Elmer Life Sciences):
    a. Prepare the embryos as described in **Subheading 3.7., steps 1–3**.
    b. Incubate with a 1 : 500 dilution of HRP-coupled anti-DIG antibody (Roche) for 3–4 h at room temperature or overnight at 4°C.

c. Remove antibody solution and wash the embryos extensively in PBST for 2–3 h, changing the wash solution every 20 min.
d. Remove the final wash and add tyramide buffer: 100 m*M* sodium phosphate buffer, pH 7.2, 10 m*M* imidazole, 5% polyvinyl alcohol (PVA) 30,000–70,000 MW (Sigma-Aldrich).
e. Add 0.2 µg/mL Cy3-labeled tyramide (FITC-, TRITC-, and Cy5-labeled tyramides are also available; Perkin-Elmer Life Sciences) and incubate the embryos for 15 min at room temperature.
f. Start the peroxidation reaction by adding 0.001% H_2O_2. Incubate for 45 min.
g. Stop the reaction by washing the embryos in several changes of PBST.

References

1. Hiraoka, Y., Dernburg, A. F., Parmelee, S. J., Rykowski, M. C., Agard, D. A., and Sedat, J. W. (1993) The onset of homologous chromosome pairing during *Drosophila melanogaster* embryogenesis. *J. Cell Biol.* **120,** 591–600.
2. Gemkow, M. J., Verveer, P. J., and Arndt-Jovin, D. J. (1998) Homologous association of the Bithorax-Complex during embryogenesis: consequences for transvection in *Drosophila melanogaster*. *Development* 125, 4541–4552.
3. Sigrist, S., Jacobs, H., Stratmann, R., and Lehner, C. F. (1995) Exit from mitosis is regulated by *Drosophila fizzy* and the sequential destruction of cyclins A, B and B3. *EMBO J.* **14,** 4827–4838.
4. Stratmann, R. and Lehner, C. F. (1996) Separation of sister chromatids in mitosis requires the *Drosophila* pimples product, a protein degraded after the metaphase/anaphase transition. *Cell* **84,** 25–35.
5. Bhat, M., Philp, A. V., Glover, D. M., and Bellen, H. J. (1996) Chromatid segregation at anaphase requires the *barren* product, a novel chromosome-associated protein that interacts with topoisomerase II. *Cell* **87,** 1103–1114.
6. Dernburg, A. F., Daily, D. R., Yook, K. J., Corbin, J. A., Sedat, J. W., and Sullivan, W. (1996) Selective loss of sperm bearing a compound chromosome in the *Drosophila* female. *Genetics* **143,** 1629–1642.
7. Forgarty, P., Campbell, S. D., Abu-Shumays, R., et al. (1997) The *Drosophila grapes* gene is related to checkpoint gene *chk1/rad27* and is required for late syncitial division fidelity. *Curr. Biol.* **7,** 418–426.
8. Gemkow, M. J., Buchenau, P., and Arndt-Jovin, D. J. (1996) FISH in whole-mount *Drosophila* embryos. RNA: activation of a transcriptional locus, DNA : gene architecture and expression. *Bioimaging* **4,** 107–120.
9. Marshall, W. F., Dernburg, A. F, Harmon, B., Agard, D. A., and Sedat, J. W. (1996) Specific interactions of chromatin with the nuclear envelope: positional determination within the nucleus in *Drosophila melanogaster*. *Mol. Biol. Cell* **7,** 825–842.
10. Lohe, A. R., Hilliker, A. J., and Roberts, P. A. (1993) Mapping simple repeated DNA sequences in heterochromatin of *Drosophila melanogaster*. *Genetics* **134,** 1149–1174.
11. Bonaccorsi, S. and Lohe, A. (1991) Fine mapping of satellite DNA sequences along the Y chromosome of *Drosophila melanogaster*: relationships between satellite sequences and fertility factors. *Genetics* **129,** 177–189.

12. Csink, A. K. and Henikoff, S. (1998) Large-scale chromosomal movements during interphase progression in *Drosophila*. *J. Cell Biol.* **143,** 13–22.
13. Carmena, M., Abad, J. P., Villasante, A., and Gonzalez, C. (1993) The *Drosophila melanogaster dodecasatellite* sequence is closely linked to the centromere and can form connections between sister chromatids during mitosis. *J. Cell Sci.* **105,** 41–50.
14. Dernburg, A. F., Broman, K. W., Fung, J. C., et al. (1996) Perturbation of nuclear architecture by long-distance chromosome interactions. *Cell* **85,** 745–759.
15. Gunawardena, S. and Rykowski, M. (1994) Looking at diploid interphase chromosomes. *Methods Cell Biol.* **44,** 393–409.
16. Gunawardena, S., Heddle, E., and Rykowski, M. C. (1995) "Chromosome puffing" in diploid nuclei of *Drosophila melanogaster*. *J. Cell Sci.* **108,** 1863–1872.
17. Foe, V. E. and Alberts, B. M. (1985) Reversible chromosome condensation induced in *Drosophila* embryos by anoxia: visualization of interphase nuclear organization. *J. Cell Biol.* **100,** 1623–1636.
18. Marshall, W. F., Fung, J. C., and Sedat, J. W. (1997) Deconstructing the nucleus: global architecture from local interactions. *Curr. Opin. Genet. Dev.* **7,** 259–263.
19. Feinberg, A. P. and Vogelstein, B. (1983) A technique for radiolabeling DNA restriction endonuclease fragments to high specific activity. *Anal. Biochem.* **132,** 6–13.
20. Feinberg, A. P. and Vogelstein, B. (1984) "A technique for radiolabeling DNA restriction endonuclease fragments to high specific activity." Addendum. *Anal. Biochem.* **137,** 266–267.
21. Rigby, P. W. J., Dieckmann, M., Rhodes, C., and Berg, P. (1977) Labeling deoxyribonucleic acid to high specific activity *in vitro* by nick translation with DNA polymerase I. *J. Mol. Biol.* **113,** 237–251.
22. Schmitz, G. G., Walter, T., Seibl, R., and Kessler, C. (1991) Nonradioactive labeling of oligonucleotides in vitro with the hapten digoxigenin by tailing with terminal transferase. *Anal. Biochem.* **192,** 222–231.
23. Pathak, S., Choi, S.-K., Arnheim, N., and Thompson, M. E. (2001) Hydroxylated quantum dots as probes for in situ hybridization. *Am. J. Chem. Soc.* **123,** 4103–4104.
24. Goldman, E. R., Balighian, E. D., Mattoussi, H., et al. (2002) Avidin: a natural bridge for quantum dot-antibody conjugates. *Am. J. Chem. Soc.* **124,** 6378–6382.
25. Stuurman, N., Maus, N., and Fisher, P. A. (1995) Interphase phosphorylation of the *Drosophila* nuclear lamin: site-mapping using a monoclonal antibody. *J. Cell Sci.* **108,** 3137–3144.
26. Augustin, M. A., Ankenbauer, W., and Angerer, B. (2001) Progress toward single-molecule sequencing: enzymatic synthesis of nucleotide-specifically labeled DNA. *J. Biotechnology* **86,** 289–301.
27. Hengen, P. N. (1996) Carriers for precipitating nucleic acids. *Trends Biochem. Sci.* **21,** 224–225.
28. Leversha, M. A. (2001) Mapping of genomic clones by fluorescence *in situ* hybridization. *Methods Mol. Biol.* **175,** 109–127.

29. Watters, A. D., Stacey, M. W., and Bartlett, S, J. M. (2002) A modified nick translation method used with FISH that produces reliable results with archival tissue sections. *Mol. Biotechnology* **20,** 257–260.
30. Dernburg, A. (1998) Whole-mount fluorescence in situ hybridization to *Drosophila* chromosomal DNA. In *Cells: A Laboratory Manual*, Vol. 3., *Subcellular Localization of Genes and Their Products* (Spector, D. L., Goldman, R. D., and Leinwand, L. A., eds.), Cold Spring Harbor Laboratory Press, Plainview, NY, pp. 115.1–115.18.
31. Dernburg, A. F. and Sedat, J. W. (1998) Mapping three-dimensional chromosome architecture in situ. *Methods Cell Biol.* **53,** 187–233.
32. Spathas, D. H. and Ferguson-Smith, M. A. (1993) A simplified one-step procedure for enhanced detection of biotinylated probes with fluorescein conjugates. *Trends Genet.* **9,** 262.
33. Raap, A. K., Vandecorput, M., Vervenne, R., Van Gijlswijk, R., Tanke, H. J., and Wiegant, J. (1995) Ultra-sensitive FISH using peroxidase-mediated deposition of biotin- or fluorochrome tyramides. *Hum. Mol. Genet.* **4,** 529–534.
34. Van Gijlswijk, R., Wiegant, J., Raap, A. K., and Tank, J. H. J., (1996) Improved localization of fluorescent tyramides for fluorescence *in situ* hybridization using dextran sulfate and polyvinyl alcohol. *Histochem, J. Cytochem.* **44,** 389–392.

11

Orcein Staining and the Identification of Polytene Chromosomes

John Tonzetich

1. Introduction

Acetic orcein staining of polytene chromosomes was introduced in 1941 ***(1)*** shortly after the initial studies on aceto-carmine-stained chromosomes by Bridges ***(2)*** and has remained a standard method of preparation. Orcein dye can be purchased in both its natural form as extracted from two species of lichens, *Rocella tinctoria* and *Lecanora parella*, and a synthetic form. The mechanism of staining is not clearly understood because the stain itself is a variety of phenazones, which may interact at an acid pH with negatively charged groups or possibly interact hydrophobically with chromatin. Acetic acid fixation accommodates stretching of the chromosomes in the interband regions during a squash, thus providing for a higher resolution of the banding structure. The later addition of lactic acid to aceto-orcein ***(3)*** kept the glands softer in the fix and allowed for easier spreading of chromosomes. The method and its variations have appeared more recently in several publications ***(4,5)***.

Drosophila polytene chromosomes are found in a number of larval tissues, including the midgut, hindgut, and the fat body, but the largest chromosomes are found in the salivary glands of the third instar. They are referred to as interphase chromosomes and are structurally more comparable to highly amplified interphase chromatin than to mitotic chromosomes because the gland grows by endoreplication of DNA, thus increasing cell size rather than cell number. Each of the homologs is tightly synapsed in this somatic tissue and undergoes approx 10 rounds of endoreplication, producing 1024 chromatids closely associated in parallel arrays. The extent of polyteny varies depending on the position of cells (those in the narrower neck of the glands have a lesser

From: *Methods in Molecular Biology, vol. 247:* Drosophila *Cytogenetics Protocols*
Edited by: D. S. Henderson © Humana Press Inc., Totowa, NJ

C value), the growth conditions, and the strain of fly ***(6)***. The average length of the chromosome arms is approx 200 µm but varies with the amount of stretching ***(7)***. The mean width is about 3 µm. All of the chromosome arms are associated at their centromeric regions, forming a centralized structure known as the chromocenter from which the chromosome arms radiate. The Y chromosome, which is heterochromatic and not highly endoreplicated, is completely contained within the chromocenter and is therefore not discernible. In males, the single X-chromosome consists of half the number of chromatids and typically stains visibly lighter than the paired X's in females. A nucleolus can often be seen associated with the X and Y chromosomes by a fine strand of chromatin. In *Drosophila melanogaster* the X chromosome is acrocentric, and the second and third chromosomes are metacentric, and the fourth chromosome is a very short, dotlike, acrocentric. The karyotypes of many *Drosophila* species can be traced to the rearrangements of six linkage groups designated A–F ***(8)***

The polytene chromosomes of *D. melanogaster* contain approx 3000 bands. The distinctive banding pattern of each chromosome has been carefully delineated in cytogenetic maps both by light ***(9)*** and electron microscopy ***(10)***. The standard system of map nomenclature ***(2)*** divides the 4 chromosomes into 102 divisions, each of the chromosome arms containing 20 divisions (X: 1–20; 2L: 21–40; 2R: 41–60; 3L: 61–80; 3R: 81–100) excepting the small fourth chromosome, which is divided into divisions 101–102. Each numerical division is further subdivided into six lettered sections (A–F), each section containing approximately six consecutively numbed bands. The bands vary in size and clarity, the more evident bands typically delimiting map subdivisions. Similar but less detailed maps have been published for many *Drosophila* species ***(11)***.

2. Materials

1. Texas banana agar: Mix 20 g agar, 30 g dried brewer's yeast, and 1 L water. Autoclave. Add two blended bananas and 100 mL Karo syrup. Allow to cool slightly and add 5 mL propionic acid in 45 mL water. Pour into vials.
2. Yeast–glucose–agar ***(4)***: Mix 30 g agar, 100 g glucose, 100 g dried brewer's yeast, and 1 L water. Autoclave or boil to thicken. Cool slightly and add 5 mL propionic acid in 34 mL of water. Pour into vials.
3. Carolina instant fly food (Carolina Biological Supply). Add equal parts dried food flakes and water to vials.
4. *Drosophila* Ringers: To 1 L of water, add 7.5 g NaCl, 0.35 g KCl, and 0.21 g $CaCl_2$.
5. PBS (phosphate-buffered saline): To 1 L of water, add 8 g NaCl, 0.2 g KCl, 1.15 g Na_2HPO4, and 0.2 g NaH_2PO_4, pH 7.4.
6. 0.8% NaCl.
7. 45% Acetic acid.

8. No. 5 forceps (Fine Science Tools).
9. Lactic–acetic-Orcein (after Lim): Mix 1 g Gurr's natural orcein (Bio/Medical Specialties, Santa Monica, CA) in 50 mL concentrated lactic acid and allow to sit at room temperature for several hours, then filter. Mix 1 g of natural orcein in 50 mL glacial acetic acid and heat for several hours below boiling. Filter. Mix two acidic stains and water in 1 : 1 : 1 ratio.
10. Subbed slides: Prepare a 0.1% gelatin solution at 65°C; cool and add chromium potassium sulfate to 0.01%. Dip slides in solution, dry and store at 4°C.
11. Probe-On-Plus slides (Fisher).
12. Siliconized cover slips: Rinse cover slips in a solution of 5% dichlorodimethylsilane in chloroform (Sigma-Aldrich). Note that this solution is highly volatile and toxic. Rinse extensively in water and bake at 180°C for 2 h.
13. Permount (Fisher).

3. Methods

3.1. Culture Conditions and Preparation of Squashes

The best polytene chromosomes spreads are produced from late, third instar larvae that have been well fed with yeast and grown in uncrowded cultures. Culture media can be any one of the three mentioned in **Subheading 2.**

1. For larger chromosomes, culture second and third instar larvae at 18°C and feed additional yeast (*see* **Note 1**.)
2. Using a dissecting needle, select large, third instar larvae that have migrated from the medium but are not about to pupate or have everted their spiracles. Place larvae in a container (Petri dish, Syracuse watch glass) that has a thin layer of PBS, *Drosophila* Ringers, or 0.8% saline and shake the container to rinse away media adhering to the body wall.
3. Determine the sex of the larva if necessary by looking for the gonadal area (*see* **Fig. 1**).
4. Transfer a single larva using forceps to a glass slide containing a large drop of *Drosophila* Ringers or 45% acetic acid (*see* **Note 2**) and place the slide on the stage of a dissecting scope with transmitted light (*see* **Note 3**).
5. Firmly grasp the head end of the larva at the base of the mouth hooks with a pair of forceps and quickly grasp the tail end about three-quarters along the length of the body with a second pair of forceps. Pull off the head end (*see* **Note 4**).
6. Remove the glands (*see* **Fig. 2**) as quickly as possible and place in a second drop of 45% acetic acid. Clean off fatty tissue, although the small thin strips along the length of the gland can remain without affecting the preparation Also remove the narrow ducts at the anterior end of the glands.
7. Allow glands to sit in 45% acetic acid fix for 2–5 min.
8. Remove the glands to a drop of lactic–acetic-orcein stain on a slide and allow to stain for 5 min. Do not let stain evaporate.
9. Prepare a clean slide for the squash by wiping with a Kimwipe. No lint should be seen on the slide (*see* **Note 5**).

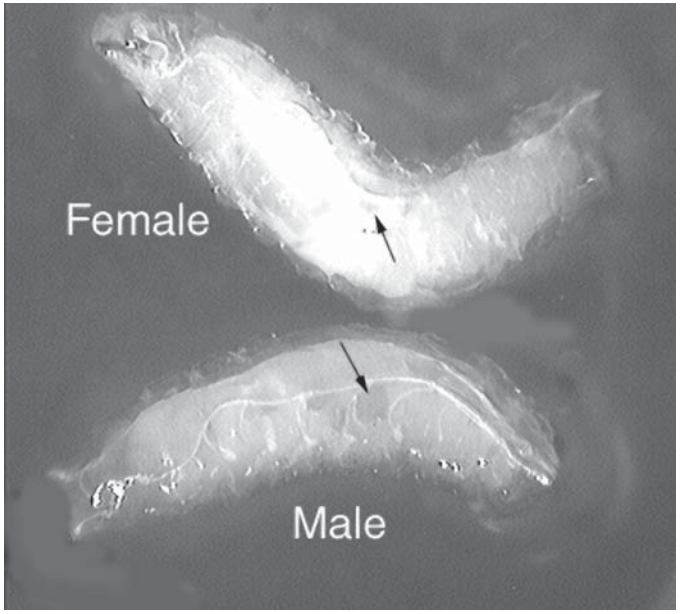

Fig. 1. Male and female larvae with gonadal area visible through body wall as indicated by arrow. Male exhibits a large oval translucent area, whereas the female exhibits a very small translucent spot, sometimes difficult to locate. (Dissecting microscope at 25×; reduced from original magnification.)

10. Add a small drop (20 µL) of 1 : 2 : 3 fixative to the slide and transfer the two glands from the stain to the drop (*see* **Note 6**).
11. Drop a clean cover slip on the preparation, allow fixative to spread, and gently tap the cover slip with a dissecting needle or blunt pencil while observing the preparation under the dissecting scope.
12. Holding a piece of bibulous paper along one edge of the cover slip, gently score the surface of the cover slip in a spiral or zigzag pattern to spread the chromosomes. Be careful not to shift the cover slip, as the motion will shear the chromosomes into fragments.
13. Blot the squash by pressing down with your thumb on a piece of bibulous paper overlaying the cover slip. Again, be careful not to allow the cover slip to shift.
14. Seal the edges of the cover slip with nail polish. For a permanent mount, see **Note 7**.
15. Store slides in the refrigerator for the short term or in the freezer for the long term.

3.2. Identifying Chromosomes

Maps of salivary gland chromosomes can be found in a number of publications ***(2,9,10–15,17)***, the most commonly used being **ref. *9***. Learning to identify chromosomes is a matter of time and is based on the recognition of specific

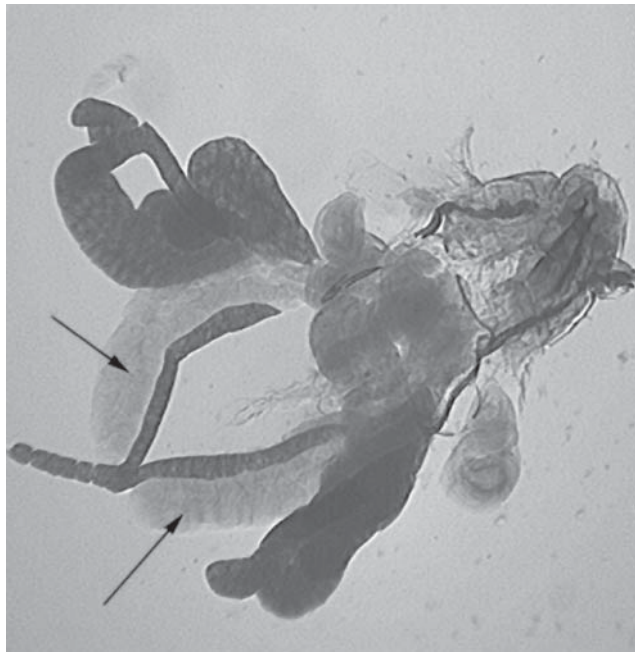

Fig. 2. Dissected head end of larva with salivary glands indicated by arrow. Note fat tissue attached to both sides of glands. (Dissecting scope at 30×; reduced from original magnification.)

aspects of the banding patterns. Difficulties encountered as a result of local variations in banding pattern can occur depending on the strain of fly, puff formation, and the intensity of staining that can obscure finer banding and doublets. Other phenomena such as ectopic pairing, asynapsis, excessive stretching, and specific regions varying in stage of constriction also create variable patterns ***(6)***.

The easiest way to begin to identify the chromosomes is to resolve the banding patterns of the telomeric ends of the chromosomes and then look for additional landmarks as described by Bridges ***(2)*** and Lefevre ***(9)***. Generally, these landmarks are puffs, constrictions, and uniquely shaped or banded regions. The telomeric ends of each of the chromosome arms excepting the dot chromosome are presented in **Fig. 3** as a simple way of first identifying each chromosome (*see* also Chapter 12).

4. Notes

1. Higher temperatures (20–25°C) may be required for culture of specific strains of flies.

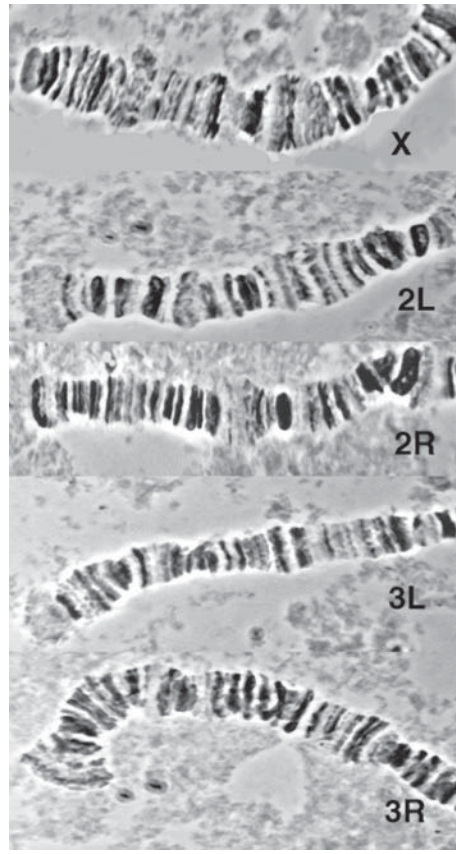

Fig. 3. Telomeric ends of the X chromosome, left and right arms of the second chromosome (2L, 2R), and left and right arms of the third chromosome (3L, 3R). Orcein stained chromosomes observed at 1000× using phase contrast (reduced from original magnification).

2. Forty-five percent acetic acid is preferred because dissection in salines is known to induce additional puffing in chromosomes.
3. The use of transmitted light from an opaque reflecting surface below the microscope stage allows for stronger contrasts such that the slightly translucent glands are distinctly visible. The fat bodies appear as dark opaque sheets of tissue.
4. The glands appear as two long, slightly translucent sacs that connect to a common tube near the mouth. Large sheets of fat tissue may be connected laterally. Do not use the glands if they shrink on fixation or become grainy in appearance or damaged in removal.
5. If a permanent spread is being made, the squash is made on a subbed slide or a commercially available Probe-On-Plus slide (Fisher) to which tissues adhere.

6. Squashes may be made directly in the stain, thus allowing for further staining. Squashing in fixative provides a cleaner background.
7. In order to remove the cover slip for a permanent spread, use siliconized cover slips. Allow slides to sit at room temperature for several hours and then freeze by dipping in dry ice-ethanol bath for 1 h. Flip off cover slip with razor blade and place slide in 95% ethanol (room temperature) for 5 min and then in 100% ethanol for 10 min. Seal a cover slip over preparation with Permount.

References

1. La Cour, L. F. (1941) Acetic-orcein: a new stain-fixative for chromosomes. *Stain Technol.* **16,** 169–173.
2. Bridges, C. B. (1935) Salivary chromosome maps with a key to the banding of the chromosomes of *Drosophila melanogaster*. *J. Hered*. **26,** 60–64.
3. Nicoletti, B. (1959) An efficient method for salivary gland chromosome preparation. *Dros. Inform. Serv.* **33,** 181–182.
4. Ashburner, M. (1989) Drosophila, *A Laboratory Manual,* Cold Spring Harbor Laboratory, Cold Spring Harbor, NY, pp. 28–32.
5. Pardue, M. L. (1994) Looking at polytene chromosomes, in *Methods in Cell Biology* (Goldstein, B, L. S. and Fryberg, E. A., eds.), Academic, San Diego, CA, Vol. 44, pp. 333–370.
6. Richards, G. (1985) Polytene chromosomes, in *Comprehensive Insect Physiology, Biochemistry and Pharmacology* (Kerbut, G. A. and Gilbert, L. I., eds.), Pergamon, Oxford, Vol. 2, pp. 255–300.
7. Zhimulev, I. F. (1996) Morphology and structure of polytene chromosomes, in *Advances in Genetics* (Hall, J. C. and Dunlap, J. C. eds.), Academic, San Diego, CA, Vol. 34, pp. 260–280.
8. Sturtevant, A. H. and Novitski, E. (1941) The homologues of the chromosomal elements of the genus *Drosophila*. *Genetics* **26,** 517–541.
9. Lefevre, G., Jr. (1976) A photographic representation and interpretation of the polytene chromosomes of *Drosophila melanogaster* salivary glands, in *The Genetics and Biology of Drosophila* (Ashburner, M. and Novitski, E., eds.), Academic, New York, pp. 31–66.
10. Sorsa, V. (1988) Electron microscopic mapping of polytene chromosomes, in *Chromosome Maps of Drosophila*, CRC, Boca Raton, FL, Vol. II, Ch. 16, pp. 29–107.
11. Sorsa, V. (1988) Polytene maps of *Drosophila,* in *Chromosome Maps of Drosophila*, CRC, Boca Raton, FL, Vol. 1, Ch. 14, pp. 155–194.
12. Bridges, C. B. (1938) A revised map of the salivary gland X-chromosome of *Drosophila melanogaster. J. Heredity* **29,** 11–13.
13. Bridges, C. B. and Bridges, P. N. (1939) A new map of the second chromosome: a revised map of the right limb of the second chromosome of *Drosophila melanogaster*. *J. Heredity* **30,** 475–476.
14. Bridges, P. N. (1941) A revised map of the left limb of the third chromosome of *Drosophila melanogaster*. *J. Heredity* **32,** 64–65.

15. Bridges, P. N. (1942) A new map of the salivary gland 2L-chromosome of *Drosophila melanogaster*. *J. Heredity* **33,** 403–408.
16 Ashburner, M. (1972) Puffing patterns in *Drosophila melanogaster* and related species, in *Developmental Studies on Giant Chromosomes* (Beerman, W., ed.), Springer-Verlag, New York, pp. 101–151.
17. Lindsley, D. L. and Grell, E. H. (1968) Genetic variations of *Drosophila melanogaster*. Carnegie Institution of Washington Publication No. 627.

12

Salivary Chromosome Analysis of Aberrations[†]

Adelaide T. C. Carpenter

1. Introduction

Even with the advent of sequenced genomes, the ability to locate aberration breakpoints onto the salivary chromosome map remains one of the singular strengths of *Drosophila* as a research organism. Salivary chromosome analysis is not difficult, yet many people are reluctant to attempt to do it: and if they do begin they may flounder for lack of a clear idea of what they should be trying to do. I hope this chapter will both encourage more people to try and also make the learning easier. Once mastered, doing salivary cytology is fun and rewarding: and you will never again have your research set back 6 mo because the "deficiency" stock someone sent you was not what it was supposed to be; as a matter of course you will have checked it out first!

2. Materials

2.1 Solutions

1. Dissecting saline: 0.7% NaCl in water (*see* **Note 1**).
2. Lacto-aceto-orcein: You can probably borrow some from a co-worker when you first begin but eventually you are going to have to make your own. There are many recipes, the following is mine:

   Put 2 g of Gurr's synthetic orcein into 100 mL of 1 part 45% acetic acid, 1 part concentrated lactic acid. Reflux for 1 h (boiling beads help). Cool; do not filter. Store at room temperature in a glass bottle with a frittered glass stopper. Good until used up. This is the "rough" stain; it should give excellent staining and handling characteristics as is although each batch of stain will differ slightly.

[†]Dedicated to Dan L. Lindsley in appreciation for his much good advice, especially about the old shirt.

From: *Methods in Molecular Biology, vol. 247:* Drosophila *Cytogenetics Protocols*
Edited by: D. S. Henderson © Humana Press Inc., Totowa, NJ

Place 1 mL in an Eppendorf tube, centrifuge it for 10 min in a microfuge to pellet the suspended stain crystals, and try it (*see* **Subheading 3.1.**). As long as it is not shaken it does not need to be filtered or centrifuged again, but if chunks of crud appear on the preparations you have shaken it; recentrifuge. If it is not satisfactory, the modification in **Note 2** is at least one place to start.

Note: I am now using Lefevre's ***(1)*** no-cook orcein (slightly modified from the original recipe), with excellent results. Take 2 g of Gurr's synthetic orcein; add 50 mL glacial acetic acid, 30 mL of lactic acid, and 20 mL of distilled water. Let it sit on your desk for a couple of days, shaking it whenever you think of it. Centrifuge as above before use.

3. Fixative: One part glacial acetic acid to three parts 95% ethanol (*see* **Note 3**).

2.2. Larvae

1. Once you get really skilled you will be able to use nearly anything, but give yourself every advantage at the beginning. Start a fresh culture on the most nutritious food available to you, seeded with yeast; limit larval competition by using only one to three female parents per vial (discard or transfer them to fresh food after 3–5 d); be ready to begin work as soon as the first larvae crawl up out of the food (*see* **Note 4**).
2. Outcross the aberration stock to wild type (*see* **Note 5**). If the aberration stock already has a balancer with a larval marker, fine, but I do not recommend bothering to rebalance a stock to introduce one: once you have the hang of making the preparations it is easy to make enough of them to be 95% confident of having at least one nonbalancer (i.e., 5) in only a few minutes, and if this part has not become routine yet then you need the practice! Indeed, some aberrations (usually deficiencies) delay development. If you have not gotten a nonbalancer preparation out of say the first 20 larvae up, stop work and try again the next day on the delayed, crawled-up larvae (*see* **Note 6**).

2.3. Dissecting Equipment

1. The tools for dissecting salivary glands out of larvae are nearly as varied as the people doing the dissection. I use two pairs of Dumont no. 5 Inox forceps, at least one pair of which must be in excellent shape; two thick, three-well depression slides (Pyrex); a black plastic plate 6.5 × 3.5 × 0.25 in.; and, most importantly, I wear a clean, old, well-washed long-tailed cotton shirt. Dissections are of course done under a dissecting microscope; exact ranges of magnifications are not critical but should be near 0.8× to 4.0× objective lenses with 10× oculars. Work is very much easier if the light source is attached to the microscope head and the microscope is set up so that the light is pointing directly toward you. This means that the microscope post is toward you. So what?
2. A box of ordinary microscope slides (frosted end on at least one side is helpful for writing labels) and a box of 18 × 18-mm cover slips, thickness no. 1. Neither needs to be pre-cleaned or coated.

3. A clean index card for the staining, rough paper toweling for cleaning the forceps and a good paper towel for the squashing. The best squashing towels I have found are the ones that have their edges folded in about 30 mm (*see* **Note 7**).
4. A white plastic (or ceramic) plate roughly the same size as the black one for doing the tapping out.
5. A tool for tapping out. I use the back end of my forceps (put the tip cover back on first so you do not risk ramming them into the microscope head), but just about anything that is firm and not too pointy can be used. However, it is easier to get consistently proper-force taps if this implement has a bit of weight (*see* **Note 8**).

2.4. Compound Microscope

Does not have to be fancy but should have phase-contrast lenses and condensor and, at a minimum, a low-magnification dry lens (16× is fine) and a 100× oil-immersion lens. A 40× high-dry lens is useful as is a 63× oil. Mount them in the order 100×–63×–16×–40× to lower the chance of swinging the 40× through the oil by mistake. Photographic capability is not needed. Because orcein is a red dye, a green filter will be helpful for increasing contrast. The stage must be translatable and vernier markings on it are very nearly vital.

2.5. Polytene Maps

The assignment of alpha-numeric to salivary-chromosome band in universal use in the *Drosophila* community is that of C. B. Bridges, and the maps to use for final assignments of breakpoints are the high-resolution drawings originally published in **refs. *2–6*** and reprinted in both **ref. *7*** and **ref. *8*** (Academic Press also sells a booklet of just the maps separately). Some form of these maps should be available at the microscope for direct comparison with the actual preparation. However, these high-resolution maps are only useful once you know where in the genome you are—they are of too high magnification for scanning work. A low-resolution map of all five arms is also vital to have with you at the microscope; in my experience, both in my own work and in teaching salivary analysis to others, the very best map to use to find your way between and along the arms is the low-magnification drawing of Bridges ***(9)*** (reproduced as **Fig. 1**). Although they are occasionally useful, I do NOT recommend using Lefevre's photographs ***(1)*** for routine work. Bridges's drawings are averages of what the banding patterns look like; Lefevre's photographs are of only one cell (for each section) and are badly overstained anyway—they had to be, for the photography, but you do not want to be emulating that! Rather, you should aim at just enough staining to be able to see the bands. How long to stain has to be determined empirically (different batches of stain vary substantially) and also depends on the ambient temperature but is normally between 5 and 10 min. Moreover, many regions were revised between the low- and the

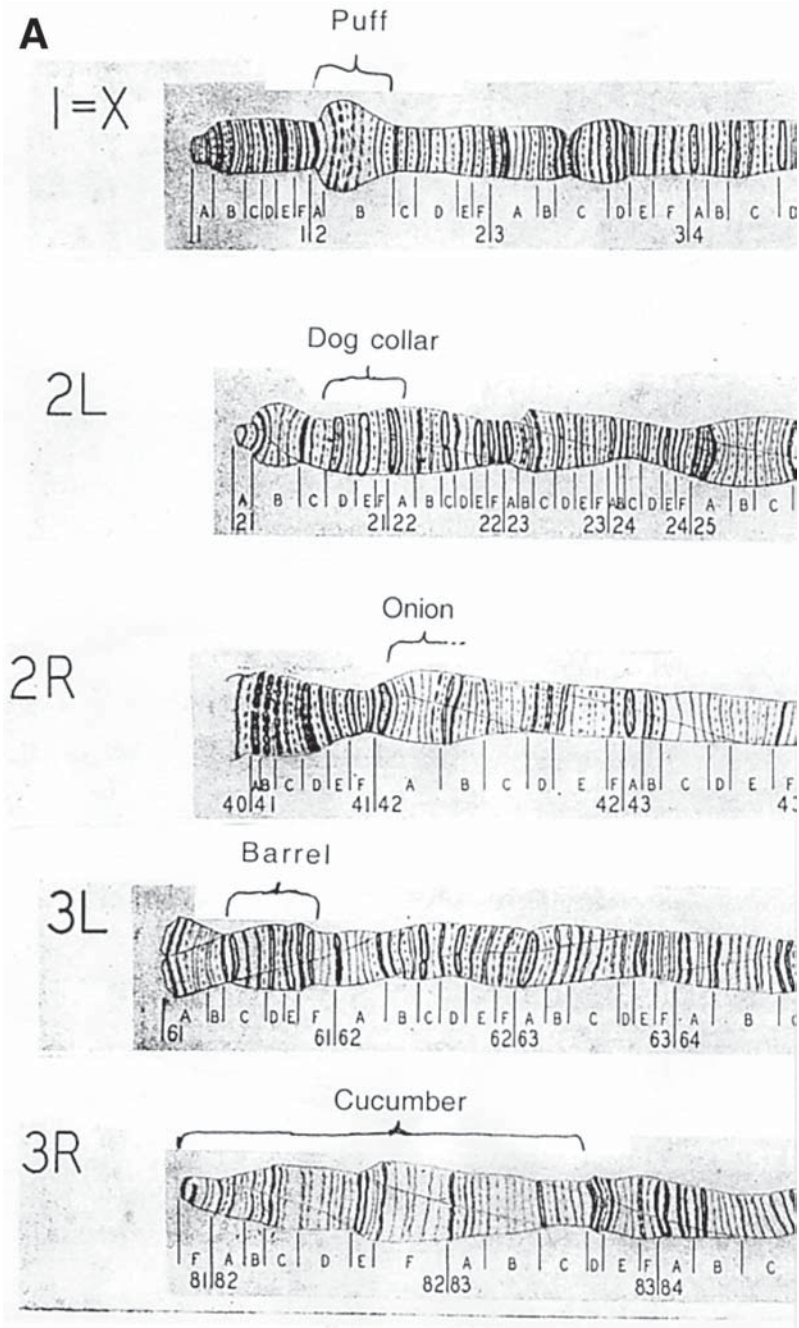

Fig. 1. **(A–F)** The 1935 low-magnification map of *Drosophila melanogaster* salivary chromosome bands originally published by Bridges ***(2)***; for use, photocopy each

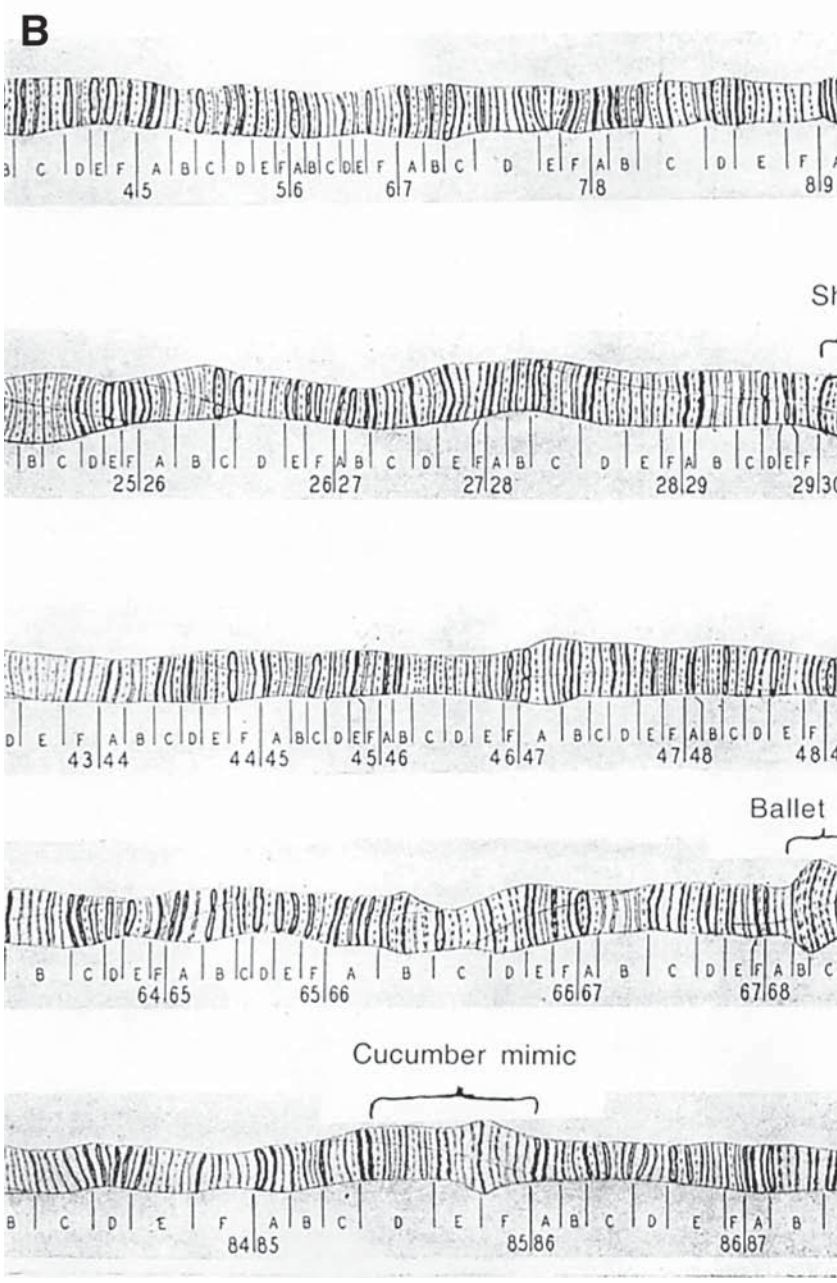

Fig. 1. (*continued*) of the segments and assemble them into one long map. (Reprinted with the permission of Oxford University Press from **ref. *9***.)

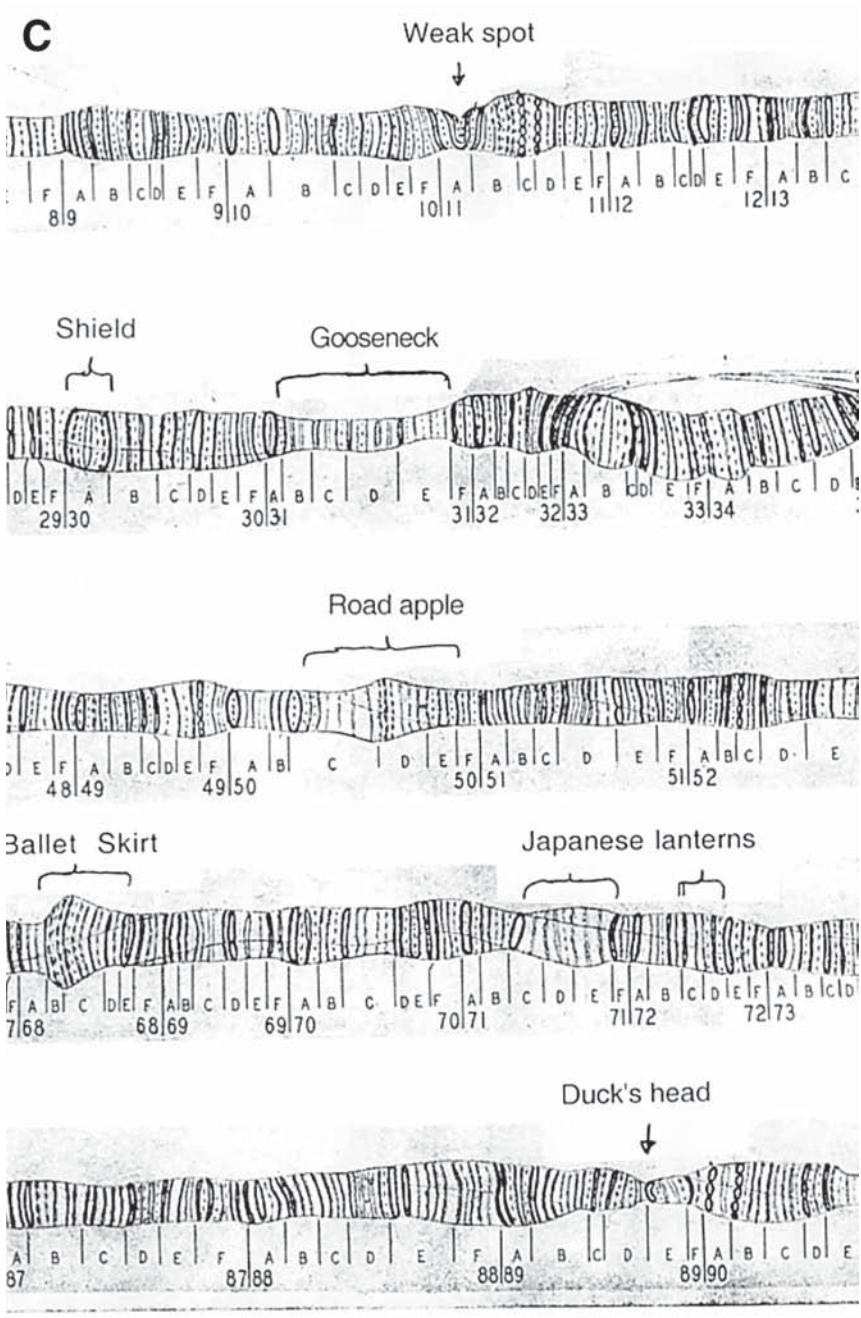

Fig. 1. (*continued*)

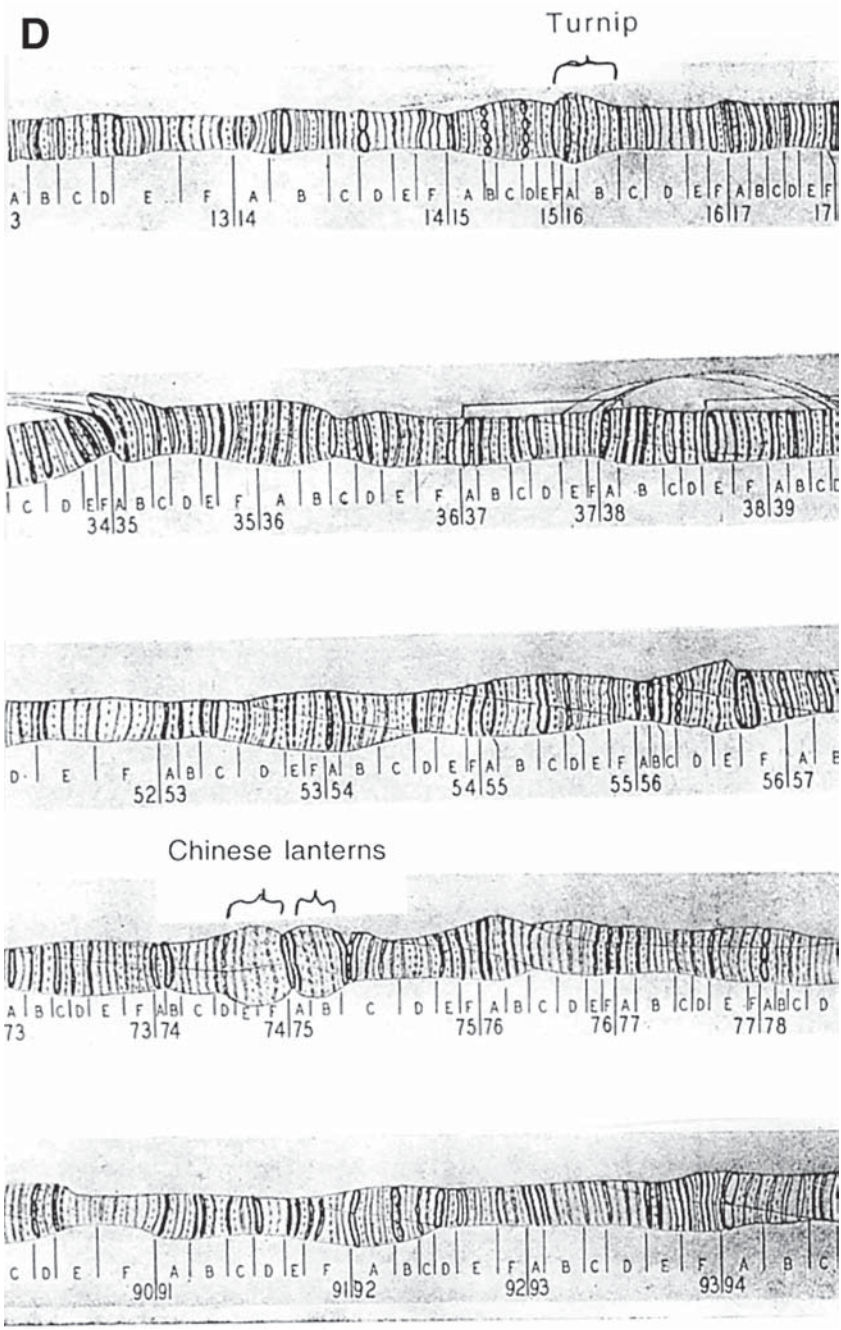

Fig. 1. (*continued*)

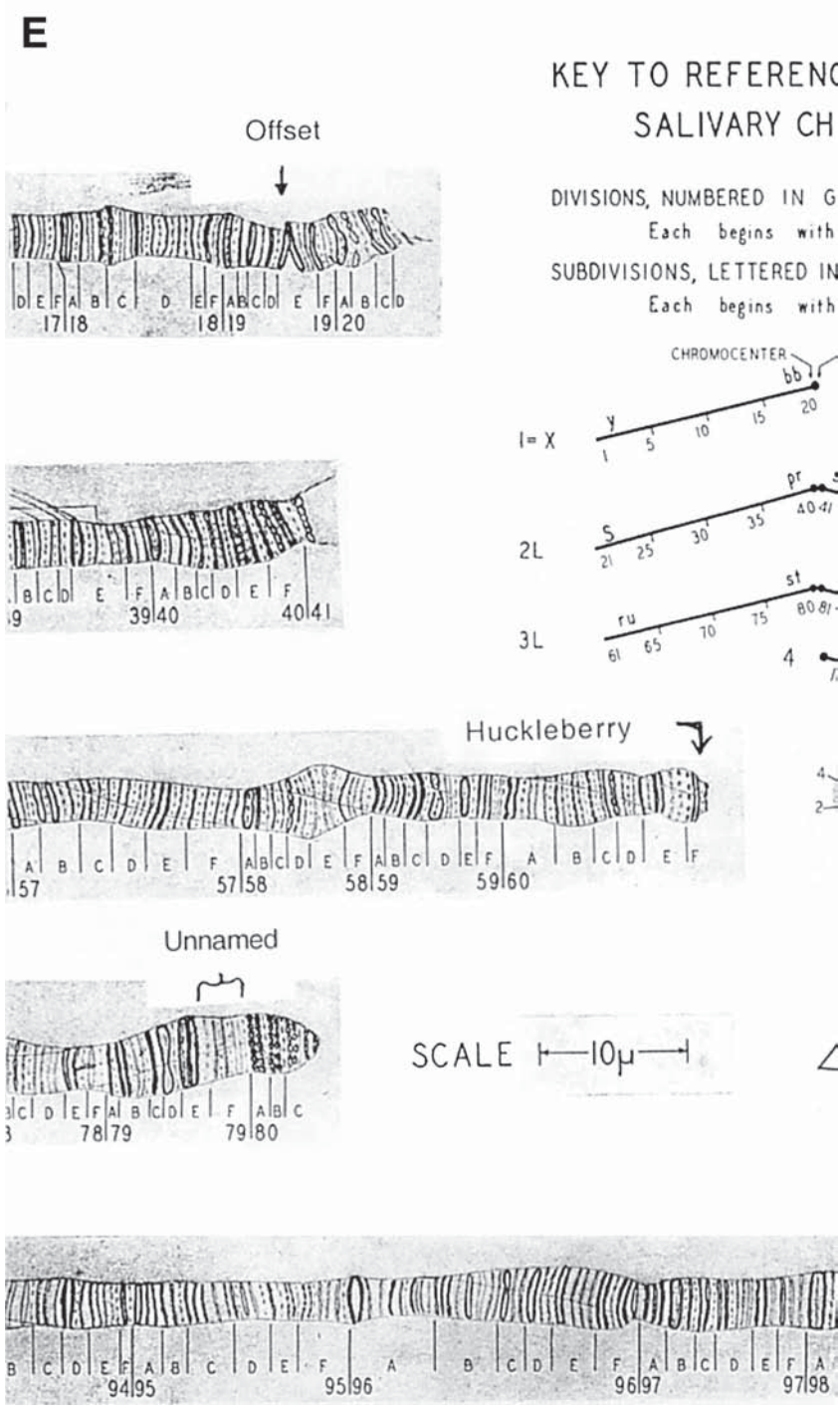

Fig. 1. (*continued*)

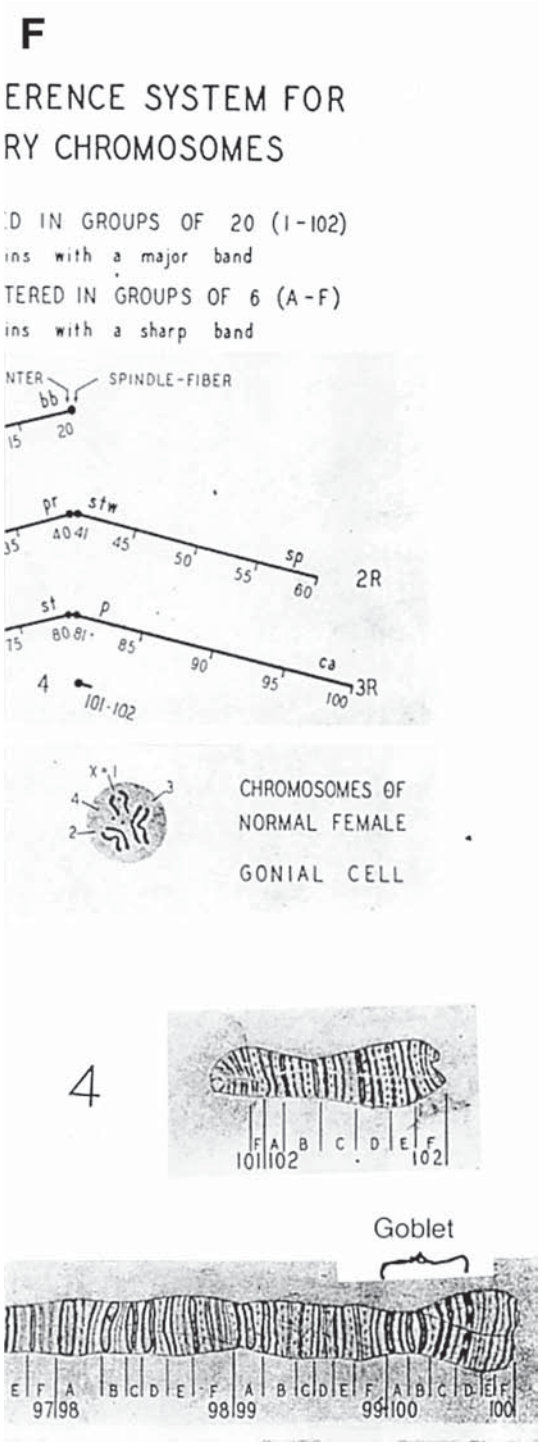

Fig. 1. (*continued*)

high-resolution maps, and Lefevre did not always make that explicit. It is the revised Bridges maps we are to follow (*see* **Note 9**).

3. Methods

3.1. Preparation of Salivary Gland Chromosome Squashes

1. Set up for work: Make fixative, put on old shirt, find forceps, and so forth. Half-fill two wells of one depression slide with saline; half fill the middle well of the other depression slide with fixative (*see* **Note 10**). Put both slides onto the black plastic plate (or your local equivalent), long sides adjacent with the saline slide further away; transfer 6–10 larvae from their vial into one of the wells of saline.

   Age and condition of the larvae are very important. The older the larva the more highly polytene its salivary chromosomes and, therefore, the easier to see banding patterns; however, larvae that are beginning to pupate are also beginning to degrade their salivary chromosomes—these are not useful for routine analysis. Take larvae that have crawled up out of the food onto the glass wall but which are still actively moving; larvae that have slowed down, and especially those that have everted their spiracles, are too old (*see* **Note 11** about gluelessness). The larvae should still be quite active once they are in the saline. Discard at this point any that are not.

   Cultures do not always go so well that larvae crawl up out of the food to pupate, however. When this happens, you must dig those mature larvae out of the food (use the dissecting microscope to see them) (*see* **Note 12**).
2. Using the dissecting microscope at medium magnification, move one larva from the holding saline well into the other ("dissecting") saline well. With your nondominant hand and the poorer pair of forceps, grasp the larva about halfway along its length; with your dominant hand and the better pair of forceps, catch the "nose" of the larva just behind the end of the black mouthparts (*see* **Note 13**). Once you have both grabs solid, pull the forceps apart, gently but firmly. The larva will come apart too, and if you have placed your forceps correctly and pulled steadily enough, the larva's breakpoint will be next to the nose forceps; the mouthparts, with associated larval structures including the salivary glands, will pull free of the rest of its carcass (*see* **Note 14**). While you still have the body in your body forceps, discard it.
3. The salivary glands are the long paired translucent structures; they usually have white, opaque, mostly flat fat bodies attached to them. Seeing all of this requires a black background, hence the black plate or equivalent. The very best dissection is one in which the fat strips itself off the glands as they emerge from the larval body; unfortunately, this is more luck than skill. Fortunately, it is not necessary to get every scrap of fat off the glands for aberration analysis. However, do remove not only mouthparts and so forth from the glands but also at least the large flat bits of fat—and as much of the side strips as come off easily. Do not waste much time on this, however.
4. Grasp the glands by their common anterior duct, if they are still joined; otherwise, do pick both up together but try to minimize the amount of saline being

carried over. Do not squeeze them. Lift the glands from the saline; move the plate so that the fixative well is visible through the microscope and immediately transfer the glands into the fixative. Prod them under the surface with the transferring forceps; make sure any accompanying saline is diluted away from the glands. Those forceps are now contaminated with fixative; we will clean them later.

5. Pick up a cover slip, breathe on it gently, and carefully rub it with your shirt tail to clean it. Hold it so that the room light reflects off the surface so you can see, and rub off, any bits of lint. Put the cover slip on some convenient piece of clean paper (e.g., an index card) and deposit onto its center 8 microliters of stain in one drop (*see* **Note 15**). All of this should take 10–15 s and the glands should have been in the fixative long enough; look at them. Gone from translucent to white? Fine (*see* **Note 11**). Move the glands up the side of the well to the surface of the fixative with the contaminated forceps; from there, it is relatively easy to lift them out of the liquid using surface tension to hold them to one tine of the forceps to minimize transfer of fixative into the stain. If both glands do not come at once, transfer the first to the stain and come back for the second (*see* **Note 16**). Do not leave the glands in the fixative longer than necessary.

   If the stain runs away from the glands then you have transferred fixative across too; use the forceps tip to move the stain back over the glands and try not to bring so much over the next time.
6. Clean the forceps by wiping them well with rough paper toweling (*see* **Note 17**); alternatively, run them through a piece of filter paper (*see* **Note 18**). If, during subsequent dissections, the glands or other internal larval parts start to turn opaque while they are still in the saline you have brought back fixative on the forceps; stop, discard saline and larvae, wash that depression slide and your forceps thoroughly, add fresh saline, and begin again.
7. Go back to the saline wells, move another larva over into the dissecting well, and proceed from **step 2** to dissect, and begin staining, a second set of glands while the first one is staining. How long the glands should sit in the stain before squashing depends on the particular batch of stain, temperature, and so forth, but it is usually around 5 min; I get another five larvae dissected and into stain by the time the first one is ready for squashing—your early mileage may differ. It is better to understain than to overstain, so if you have only done three by the time the first has been 5 min in stain stop there and start the squashing steps on it—then on each of the others in turn.
8. Clean a slide with breath and shirt tail just as you did for the cover slip; holding the frosted end, set the other end against the index card near the first cover slip so that the body of the slide is above it and gently lower the frosted end until the slide just touches the top of the drop of stain—at that point, the whole cover slip will rise to flatten against the slide. Turn the slide cover-slip upward, put it onto the white tapping-out plate, and put both under the dissecting microscope under high magnification. Focus on the glands, which should be visibly flattened pinkish cells at this point. The stain should extend more or less evenly to the edges of the cover slip and be featureless. If there are dark lumps in it you have shaken

your container of stain; throw these preparations away, recentrifuge your stain, and begin again. If there are darker but nonlumpy regions of stain, check them for included bits of lint. As long as it is not actually among the cells, a small piece of included lint does not preclude a good squash but a large one anywhere does. By all means, prove this for yourself but also try harder to be truly clean for the next preparation (*see* **Note 19**).

9. Just touch the edge of the cover slip with the first two fingers of your nondominant hand: This keeps the cover slip from slipping during the tapping-out. This does usually mean that you get stain onto those finger tips. Because the stain is strongly acidic, this can result in acid burns if it is not washed off, so always wash your hands and those fingers thoroughly when you have finished work (*see* **Note 20**).
10. Take your tapping tool in your other hand. The first series of taps is to break the cell membranes by hydrostatic pressure from the stain; these first taps therefore should hit the cover slip just outside the gland. Hit down, hit-and-bounce-back, hit firmly but not too hard (*see* **Note 21**); and watch what is happening to the glands. You should see the cell outlines disappear. Tap in different places for each tap. Usually around five taps is enough—you should be able to see the nuclei (densely stained dots) floating free but still all within the area the gland began over. If they are already scattered you have tapped too hard or too close or have large lint; if the cells will not break open you have fixed too long or gotten fixative into the saline.
11. The next series of taps are to break the nuclear envelopes—but not yet to spread out the chromosomes. Tap directly over the glands, harder than before, five or six times on different places. Stop and look. Most of the nuclei should now be invisible; tap more if many are not. The total time for both types of taps should not be more than about 5 s (*see* **Note 22**).
12. Take the squashing paper towel, folded edges up; fold over the top 30 mm or so and place the slide inside this fold, slide-edge snug against the inside of the top fold (*see* **Note 23**), with the cover slip up and within the area of the side fold (*see* **Note 24**). With the slide near the edge of your bench, put the ball of your thumb directly over where the cover slip is and press down firmly; then roll your thumb to the left and to the right. These actions are both pressing and wicking the stain out from under the cover slip (onto the towel); this flow will spread out the chromosome arms. Whether just one thumb's pressure is enough depends on your size and thumb strength; I myself rest the heel of the other hand directly atop the squashing thumbnail and press down with that hand—forearm strength only, no need for whole-body weight. It is important for the squash to be quick and firm; it is the initial outrush of stain that gives a good spread. No amount of remedial squashing will transform a poor squash into a good one. However, really firm pressure is not needed. If your thumb gets sore, you are pressing too hard (*see* **Note 25**).
13. All of the tapping and squashing should have taken as much or slightly less time than it took to dissect the gland in the first place, so the next staining gland is

ready for tapping and squashing: Do that, then the next, and so forth. Once you have the whole set squashed, examine them with the compound microscope; you may have your perfect preparation in this set—and if you do not, you need the immediate feedback of what did not work while you can remember what the "did not work" was.

14. Before you begin your next round of dissections, discard and replace the solutions in the wells.

3.2. Preliminary Examination of Slides

1. Assemble your preparations, salivary-band maps, compound microscope, lots of paper and a sharp pencil. Put the first slide under the compound microscope cover slip up; check Köhler illumination and set the condensor for phase for your low-magnification objective lens—usually phase 2. Find the glands and scan across them for quality of spreading. Look for regions where well-spread nuclei are common. Usable preparations typically fall into one of two categories: Either the nuclei at the edge are overstretched but the ones in the middle are fine; or the nuclei around the edges are fine but the ones in the middle are underspread. Any nucleus in which you can identify the region of interest is usable, but first you want to find your aberration, and to do that you need to be able to identify all of the chromosomes in one to several cells, even if you already think you know what kind of aberration you have and where it is! You may be wrong. Thus, the first step is to find regions with nuclei that look somewhat like starfish under low power. If there are none, toss that slide and look at the next one. Once you have switched to oil it is inconvenient to have to go back to low power (*see* **Note 26**), because the oil on the slide changes the point of focus for the 16× lens—much better to do your scanning at 16× first, jotting down likely-looking regions by stage coordinates.
2. Now switch over to 40× dry (or 63× oil). Are the chromosomes flat as opposed to curling around themselves? If not flat, do not waste more time on that preparation, go to another, hopefully better, one. Is the banding pattern clear and crisp? If the thicker bands are dark black smudges, you have overstained and will not be able to make the finest discriminations. All published photographs of salivary banding give the appearance of overstaining as a side effect of the photography; you want your preparations to look much less stained than that.
3. Look at the nuclei; identify ALL of the chromosome arms and scan them for abnormalities. At the beginning, you will find it helpful to make a line sketch of all of the chromosomes with the positions of the landmarks indicated—this helps you to keep straight what regions you have identified and cleared as normal versus regions identified but suspect versus regions not identified yet. Jot down the stage coordinates of every nucleus from which you get information; as the analysis proceeds you will be refining your ideas of what is going on, and when you change your mind (as you will several times during any analysis) it is very helpful to be able to go back to see how you were mistaken earlier! If you were. It may well be the second determination that is wrong. Do not forget to check the heterochromatin and chromosome 4.

Learning how to distinguish between the basic arm landmarks (each arm has landmarks at its tip, middle, and base, and they all have distinctive names that help to keep them straight; a sample of the named landmarks are indicated on **Fig. 1**) is the one part of learning the chromosomes when it is really helpful to have a coach to check that you have identified all of them correctly. If you have to learn all by yourself, be especially careful not to accept an arm identity by only one landmark until you are really very sure what it looks like under a variety of circumstances—instead, always check for at least one other landmark for that arm, preferably two, and eliminate the other arms by two or more landmarks as well.

3.3. Detailed Examination of Aberrations

1. Find all five tips, bases, middles in the first well-spread nucleus. If you already know which region to be looking in, locate it and see what you can tell about it, but do not try to get too detailed yet. Is it making a buckle (loop)? Then it may be a deficiency (or a duplication or a small inversion)—but completely normal regions can make buckles (just look around the rest of the genome); you need to see a buckle in at least most cells before you can conclude "deficiency" (or whatever). Is it making a joint with another chromosome? Then it may be a translocation—again, you need to see joints (or asynapsis) in all cells before you conclude "translocation." Is it making a joint with its own or other arm? Then, suspect inversion (large). If you do not know which region to be looking in, look around and make mental or physical note of anything that looks suspicious, then go immediately to another nucleus and check it out as though it were the first—compare, anything in common? then go to a third, and so on. If you have really found your aberration then you should be able to identify it in *each and every nucleus* (*see* **Note 27**). The only exceptions to this rule are very small deficiencies and inversions, which will sometimes lie sideways to your plane of view and be detectable; at other times the normal homolog will lie uppermost and the chromosome will look completely normal. Here, you must find chromosomes with that region asynapsed before you will be confident that you know your aberration!
2. Still at intermediate power, once you think you know what type of aberration you have, check around the rest of the genome to make sure that there is nothing else major heterozygous! You will never be able to eliminate the possibility of extraneous small deficiencies or solely heterochromatic translocations, but you can eliminate most other aberrations (*see* **Note 28**).
3. If you have a translocation or a large inversion, work out to the letter division where all the breakpoints are. This is done as follows.

   Figure out which arm by the major tip–mid–base landmarks. If you are lucky, your break will be near a landmark; if not—you will have to work your way in to it, using the low-magnification maps, matching up what you see with the maps. Worry about only the darkest bands here, generally the ones that start letter divisions. Work your way in from both directions (sequentially). You should get to the same place! If you do not, try again on another nucleus. Keep at this until you

are reasonably confident that you can see the correlation between the maps and your chromosomes so that when you go to high power and the detailed maps you will be looking in the right region! Do not worry too much about what the junction of the synapsed aberration looks like at this point, but do keep track of any nuclei in which that junction looks particularly informative; you will come back to those later. It is a good idea to be making drawings of the bandings at this stage, although it gets a bit tedious if you are dealing with a breakpoint very distant from landmarks in both directions; it is very much easier to draw the chromosomes and the dark bands (just the darkest bands at this stage, with as much morphology as you can see in them), and label the drawing with what bands you think they are, than to try to keep track in your head. Some regions are particularly prone to long stretches of similar-looking banding patterns; if you really get stuck trying to fit the banding patterns on your chromosomes to the Bridges maps, Lefevre's photographs ***(1)*** may help (or the excellent ones that were available in the Encyclopedia of Drosophila), but use them only to sort out which Bridges bands are which and switch back to his drawings immediately; you will learn your way around the chromosomes much faster. You will also begin to recognize additional banding patterns that are sufficiently distinctive to be within-arm landmarks that are closer to your region of interest than the "formal" landmarks are.

4. Once you are confident that you know pretty much where all your breakpoints are, switch over to 63× or 100× and oil—and the high-magnification drawings. Now you are ready to try to figure out exactly where the breakpoints are (*see* **Note 29**).

   Aberrations whose breakpoints are far apart frequently synapse up completely, so all you have to do is find nuclei where the breakpoint is lying completely flat, as a cross; draw the bands (now all the bands that you can see, not only at the breakpoint but also far enough back on all four arms so that you are sure that you are in the right place); and identify them from the high-magnification maps. You will never find all of the bands that Bridges drew in (or not without going to lengths described in **Subheading 3.4., step 2**), but try to see, and identify, as many as you can, not only at the breakpoint but also nearby—the nearby ones will give you a feel for what you can hope to resolve at the breakpoint in that preparation (*see* **Note 30**). The assumption is as follows: If bands on the homologs are synapsed, they are the same band. Get your first drawing labeled up as detailed as you can, then go find another clear nucleus and start from scratch, complete with drawing it too. Then go find a third. If all three agree and you are satisfied with the level of detail, stop. However, if they differ very much at all, keep on finding more informative nuclei and also go back to the ones you have done to see if you can figure out why they differ—in the end all your drawings must either agree or else have an explanation of why they do not agree (e.g., 69B twisted and hard to see in this nucleus). Keep in mind that you will very likely never be sure exactly where a breakpoint is from orcein cytology, just keep trying to refine it. For example, 69C is a letter division of faint bands; in most nuclei

you will probably only be able to see 69C1,2 and 69D1–3, but if you look around long enough you will find one with C4,5 visible, and if you are lucky they will be synapsed so you will know which side of them the break is, and if you are very lucky you will see C8,9 too—your final description of the breakpoints should reflect exactly how much information you have been able to gather and not one whit more. For example, if you are sure that 69C1,2 is on one side of the breakpoint and 69D1–3 is on the other side, then that breakpoint is given as 69C3–11 (*see* **Note 31**).

5. The conventions I use for describing breakpoints (I have never seen the conventions written down) are "range I cannot see on the left"; "range I cannot see on the right" [e.g., for an In(2LR) 30B11–12; 60F3–4 (interband) means that I saw 30B9,10 distal to the break and 30C1,2 proximal to it but did not see 30B11 or 12, whereas on 2R I saw 60F3 proximal and 60F4 distal; "(interband)" means that the breakpoint appears to be in an interband—as always, the possibility that the break is actually a little bit into a band that looks unaffected cannot be excluded]; for a deficiency, 70D2; 70D4 means that I have seen that 70D1 and 70D5 are still present and D2–4 are absent.
6. If you are having trouble getting a good fit for all four arms around the breakpoint, the most likely problem is that you are in the wrong place entirely; go back a stage and recheck where your breaks are at the gross level. However, although the banding patterns are really quite remarkably constant there are differences between larvae, and for some regions, the maps seem to have been drawn from unusually old or young ones: For those regions, the patterns of dark versus lighter bands in my preparations very rarely match the high-magnification maps. I have found Sorsa's drawings of electron microscope (EM) banding patterns ***(10,11)*** to be very helpful in such cases (*see* **Note 32**).
7. Fully-synapsed aberrations are frequently rather bunched up, bandwise, and relatively little detail can be seen. Partly asynapsed chromosomes can be helpful here; you can frequently see many more of the faint bands in the asynapsed parts, which you can then find synapsed in other nuclei so you know which they are as well as that they exist. Sometimes the banding patterns of the two parent chromosomes are sufficiently different so that a *tentative* identity of bands up to the breakpoint can be made from the asynapsed junction chromosome, but this should be backed up by finding synapsis—and also by getting the same breakpoint from the reciprocal junction chromosomes! This latter is very important, both as a check of the accuracy of the first determination and also as a check that your translocation or inversion does not have a small deficiency at one end—or a small additional inversion. Nuclei that are fully synapsed on one side but asynapsed on the other are most useful here; keep looking for them and refining your information (*see* **Note 33**).

3.4. Small Aberrations

1. Small inversions and deficiencies are more difficult; they rarely lie flat, they often do not synapse completely, and when they do synapse completely they do not lie flat at all. Here you have to work from partly synapsed chromosomes, and,

moreover you really do need to have at least one nucleus with the aberration completely asynapsed—because a small deficiency can look like a small inversion and vice versa, when synapsed, but when asynapsed, the difference is obvious. If you find a particularly pesky one that synapses too well, try doing your squashes over a balancer (after having satisfied yourself that you know where the aberration is over wild type!); pick a balancer that has a breakpoint within a couple of number divisions but not much closer, because you are going to need to be able to compare the banding patterns of the asynapsed normal (balancer) chromosome with your aberration, so you need to be able to *find* that region in the absence of being able to work down from the tips and so forth very easily. To prepare yourself for this, when you get a good balancer preparation from your outcrosses, amuse yourself by trying to find that chromosome's landmarks in it. It is very important to be comparing normal and aberration chromosomes in the very same nucleus here; although the variation in fine-scale banding patterns (i.e., which faint bands are visible, whether a grainy band looks grainy) differs less within one larva than between them, there still does exist within-larva variation (*see* **Note 34**). For these you *have* to get asynapsed, well-stretched chromosomes to ask whether all of the faint bands are still there, but really small deficiencies/inversions are just plain invisible by this technique.

2. As you will very quickly notice, bunched-up, unstretched chromosomes only show the darkest bands, whereas stretched ones show the fainter ones; overstretched ones show them all. Once you know your region very well—so that you can find it in overstretched chromosomes—even these become of use if you really, really have to get a breakpoint down to the band (*see* **Note 35**).

3.5. Heterochromatic Breakpoints

1. Euchromatic–heterochromatic breakpoints have the additional problems that the euchromatic bands on both sides of the breakpoint are underreplicated and that heterochromatin itself makes bands; never, never, never assign a band identity in a euchromatic–heterochromatic aberration without seeing it synapsed with the homolog, and always, always, always work in to that breakpoint from both sides. You will always have larger uncertainty ranges when the "other" breakpoint is in heterochromatin.
2. Sometimes you will be able to tell which arm the heterochromatic break is in and sometimes you will not. Heterochromatin synapses with other heterochromatin freely and also frequently stretches and breaks during the squashing procedure. If you see some nuclei with your arm stretched out but with a fuzzy patch and others with that region of the arm pulled back to the chromocenter, you very likely have a heterochromatic break! If you often see that region of euchromatin associated with the heterochromatin of, for example, 2R, then it is likely that the heterochromatic break is in 2R heterochromatin. However, this is something you cannot be really sure of unless you find a cell where that heterochromatin is being banded and also gives you a synapsed-up "cross" configuration; this is much more likely to occur if the heterochromatic break is just barely into the heterochromatin in the first place. Many people seem to take the "association = iden-

tity" route because there are relatively few aberrations in FlyBase where arm of heterochromatic break has not been at least guessed at, but for at least many heterochromatic aberrations you will find that any arm may be associated with the euchromatic break if you look at enough nuclei. I myself use the new terminology "Ab(euchromatic arm;h), euchromatic breakpoint" unless I'm reasonably certain I have seen convincing cells. Of course, if you have information from the aberration's genetic behavior you should say so [e.g., "T(2;3) inferred from genetics"].

3. The *Su(UR)ES* system ***(12)*** can be very helpful if you really have to know more about an heterochromatic breakpoint.
4. A few other descriptions of how to do salivary cytology can be found in **refs. *1*,*13*** and Chapter 11.

4. Notes

1. Atmospheric CO_2 provides enough buffering as long as the solution is made up at least the day before. The quality of water seems to be irrelevant; even hard tap water is satisfactory in my hands. This can be kept for months or years but discard when something is visibly growing in it.
2. Take an Eppendorf tube, pipet in 1.00 mL "rough" stain, add 30 µL of concentrated lactic acid, 90 µL of glacial acetic acid, and 90 µL of water; this gives the "final" stain. Shake well, spin down for 10 min in a microfuge, and try it.
3. This must be made up fresh for each session, but the ratio does not need great accuracy; eyeballing "3 vs 1" with Pasteur pipets is good enough. Mix the components thoroughly.
4. You want the fattest, happiest larvae possible; in my experience, good food is more important than temperature, but high temperature gives poorer larvae than lower—if you can, rear these cultures at 20–22°C (room temperature).
5. Unless you are really confident in your virgining ability, take the females from the balanced aberration stock.
6. However, do check to be sure that the preparations you think are balancer really are (look up that balancer's breakpoints and find some distinctive feature); your aberration chromosome may be more complicated than you expect it to be—if so, it too may exhibit asynapsed regions.
7. If your institution does not stock these, make your own. Start with a piece of absorbent toweling about 300 × 200 mm, fold it in half across the longer dimension, then fold each long side in approx 30 mm.
8. I cannot get proper tapping with, for example, the eraser end of a pencil, although some people swear by this tool.
9. Many of the errors I have encountered in checking the cytology of others can be traced to their having used the wrong map.
10. The fixative solution tends to creep up and over the sides of its well; having it separate from the wells of saline keeps it from getting into the saline. If the fixative ever does get into either of the saline wells, STOP, discard all saline and larvae, wash the wells, and start over; preparations made from such contaminated saline will be too poor to use.

11. If the central part of each gland is a much denser white than the rest, this indicates that the gland has started producing glue already; old ones will seep this material out into the fixative. Both such glands are too old to give good preparations; toss them at this point. Old glands can also be detected at the time of dissection by their slightly knobby surface texture.
12. A trick that gets those foody larvae up onto the walls which you may not be able to apply for political-correctness reasons is to blow (or have a friend blow) a puff of cigarette smoke into the vial, replace the plug, and wait 3–5 min.
13. Yes, yes the larva will be thrashing around after the first grab; the trick here is to do the transfer to the dissecting well, turn the larva loose, then do the two grabs in very quick succession. If you miss the "nose" grab, release the body grab too and start from the beginning.
14. If the larva ruptures anywhere else, so that the salivary glands do not float free, do not waste time trying to dig them out; toss the whole larva and start fresh with a new one.
15. My only use for a Pipetman!
16. Usually the gland(s) just float off the forceps into the stain, but if you need to use the other pair of forceps to encourage them off, do so.
17. Do not prick yourself! But do rub all contaminated surfaces well.
18. This does not always work as well and can bend the tips.
19. Simple care is sufficient; I do my own salivary preparations at my fly-pushing microscope, in a room full of stocks plugged with cotton. However, I leave some time for the dust to settle before starting cytology if I have just been handling cultures and their cotton plugs. Do not, however, try to make these or any other cytological preparations while wearing a fluffy sweater!
20. Alternately, or if your skin is particularly sensitive, wear a glove on this hand.
21. If the cover slip breaks, you have tapped too hard.
22. This technique of tapping and looking works quite well for preparations for in situs too; however, do it on the black plate and move the forceps' end to block the direct light for looking—so that the cells show as white fuzz before the first tapping. This white fuzz will disappear if the first tapping has successfully broken the cell membranes.
23. This guards against the cover slip slipping during squashing.
24. This guards against having the slide break from slight irregularities in the bench surface.
25. At this point, you can actually see the spread chromosomes with dissecting-microscope magnifications (highest magnification against a white background).
26. You must not go back to a high-dry 40× lens now—you will get oil on it!
27. Or at least be able to say that there is something wrong there but cannot say what because another arm is lying over it, and so forth.
28. Do not panic if you see some regions perpetually in knots; some regions synapse ectopically with great regularity. The proximal half of 2L is particularly prone to this, but other regions do too. If in doubt, look at a preparation from a different aberration or from wild type.

29. However, first take a break; rest your eyes—it is very important to force yourself to take eye-rest breaks very often, especially when first sitting down to compound microscope work. No lens is completely flat, and 100× lenses induce motion sickness quite quickly. If you ever start to feel even slightly nauseous, *stop working immediately* and do not come back to the microscope until the next day at the earliest. Your effective working time will increase quickly, but only if you do not push it!
30. If you are having trouble seeing any of the fainter bands, you are probably overstaining your preparations.
31. If there seems to be about the same distance between C1,2 and the breakpoint as between the breakpoint and D1–3 you may *guess* that the breakpoint is rather near the middle of C, but you do not *know* that so the formal description remains 69C3–11—unless you have seen some of the lighter bands and are as sure as you can be that you have identified them correctly.
32. You do not want to be trying to find your breakpoint from those maps very often; they are too detailed for by-the-microscope use.
33. Using aberration/balancer larvae can be very useful here—with the right balancer! (I.e., one that is not broken in the region where the aberration is.)
34. You also need to be sure that you are looking at the aberration chromosome and not the balancer!—particularly if you are having trouble convincing yourself that there is no aberration there after all.
35. To produce overstretched preparations deliberately, do the tapping as normal but just before you squash use the back end of your forceps to move the cover slip laterally about 1 mm.

References

1. Lefevre, Jr, G. (1976) A photographic representation and interpretation of the polytene chromosomes of *Drosophila melanogaster* salivary glands, in *The genetics and biology of Drosophila*, vol. 12 (Ashburner, M. and Novitski, E., eds.), Academic, New York, pp. 31–66.
2. Bridges, C. B. (1938) A revised map of the salivary gland X-chromosome of *Drosophila melanogaster. J. Heredity* **29,** 11–13.
3. Bridges, C. B. and Bridges, P. N. (1939) Reference map of the salivary gland 2R-chromosome of *Drosophila melanogaster. J. Heredity* **30,** 475–476.
4. Bridges, P.N. (1941) A revised map of the left limb of the third chromosome of *Drosophila melanogaster. J. Heredity* **32,** 64–65.
5. Bridges, P. N. (1941) A revision of the salivary gland 3R-chromosome map of *Drosophila melanogaster. J. Heredity* **32,** 299–300.
6. Bridges, P.N. (1942) A new map of the salivary gland 2L-chromosome of *Drosophila melanogaster. J. Heredity* **33,** 403–408.
7. Lindsley, D. L. and Grell, E. H. (1968) *Genetic Variations of* Drosophila melanogaster, Carnegie Institution of Washington, Washington, D.C.
8. Lindsley, D. L. and Zimm, G. G. (1992) *The Genome of* Drosophila melanogaster, Academic, New York.

9. Bridges, C. B. (1935) Salivary chromosome maps with a key to the banding of the chromosomes of *Drosophila melanogaster. J. Heredity* **26,** 60–64.
10. Sorsa, V. (1988) *Chromosome maps of Drosophila* I. CRC, Boca Raton, FL.
11. Heino, T. I., Saura, A. O., and Sorsa, V. (1994) Maps of the salivary gland chromosomes of *Drosophila melanogaster. Dros. Inform. Serv.* **73,** 621–678. Also www.helsinki.fi/~saura/EM for EM photographs.
12. Belyaeva, E. S., Zhimulev, I. F., Volkova, E. I., Alekseyenko, A. A., Moshkin, Y. M., and Koryakov, D. E. (1998) *Su(UR)ES:* a gene suppressing DNA underreplication in intercalary and pericentric heterochromatin of *Drosophila melanogaster* polytene chromsomes. *Proc. Natl. Acad. Sci. USA* **95,** 7532–7537.
13. Kennison, J. A. (2000) Preparation and analysis of polytene chromosomes. in *Drosophila Protocols* (Sullivan, W., Ashburner, M., and Hawley, R. S., eds.), Cold Spring Harbor Laboratory Press, Cold Spring Harbor, NY. pp. 111–117.

13

In Situ Hybridization to Polytene Chromosomes

Robert D. C. Saunders

1. Introduction

Since its development by Pardue and Gall ***(1)***, the technique of *in situ* hybridization to polytene chromosomes has played a central role in the molecular genetic analysis of *Drosophila melanogaster*. The power of *in situ* hybridization is largely the result of the scale of polytene chromosomes and, consequently, the high degree of resolution they offer the researcher. The use of radiolabeled probes has now been largely superseded by faster, nonradioactive signal detection methods, generally using biotin- or digoxygenin-substituted probes that also offer greater resolution, because there is less scatter of signal with immunochemical and immunofluorescent detection than with silver grains. The utilization of *in situ* hybridization technology is of particular interest to those engaged in chromosome walking or genome mapping projects, in which it is essential to check all clones along a chromosome walk by *in situ* hybridization in order to identify clones containing repetitive DNA and to avoid the isolation of clones derived from outside the region of interest. It is also useful when orienting a chromosome walk and when determining if a particular clone is derived from DNA uncovered by a deficiency. At least one *Drosophila* genome mapping project ***(2,3)*** relied on *in situ* hybridization to accurately map sets of overlapping cosmids (contigs) to the polytene chromosome map, whereas another ***(4)*** used *in situ* hybridization as the sole means of ordering yeast artificial chromosome (YAC) clones along the genome.

The complete genome sequence of *D. melanogaster* was published in 2000 ***(5,6)***. What role is there for this technique in the postgenomic era? In fact, there are still situations in which verification of polytene chromosome location is important. Examples of such applications are mapping

From: *Methods in Molecular Biology, vol. 247:* Drosophila *Cytogenetics Protocols*
Edited by: D. S. Henderson © Humana Press Inc., Totowa, NJ

chromosome rearrangement breakpoints and work involving related *Drosophila* species.

In this chapter, the use of biotin-labeled probes for *in situ* hybridization to polytene chromosomes is described.

2. Materials

1. Clean microscope slides (*see* **Note 1**).
2. Clean siliconized cover slips, 24-mm square (*see* **Note 1**).
3. Clean siliconized cover slips, 22 mm × 50 mm (*see* **Note 1**).
4. Compressed air can (e.g., Dust-Off®; Falcon Safety Products, Inc. Sommerville, NJ).
5. 0.7% NaCl.
6. 45% Acetic acid.
7. 1 : 2 : 3 Fixative: 1 vol Lactic acid, 2 vol distilled water, 3 vol glacial acetic acid.
8. Liquid nitrogen.
9. 2X SSC: 300 m*M* NaCl, 30 m*M* sodium citrate, pH 7.0.
10. 70 m*M* Sodium hydroxide, freshly prepared from pellets.
11. 70% and 96% Ethanol.
12. Coplin jars, or similar, for incubating slides.
13. Oligolabeling buffer: Prepare as described in **refs. *7*** and ***8*** using the following solutions:
    a. Solution A: Add 9 µL of β-mercaptoethanol, 12.5 µL of 20 m*M* dATP, 12.5 µL of 20 m*M* dCTP, 12.5 µL of 20 m*M* dGTP to 0.47 mL of solution O.
    b. Solution B: 2 *M* HEPES, pH 6.6.
    c. Solution C: Random hexanucleotides (Pharmacia) at a concentration of 90 A_{260} units/mL.
    d. Solution O: 1.25 *M* Tris-HCl, pH 8.0, 125 m*M* $MgCl_2$.

    Prepare oligolabeling buffer by mixing solutions A, B, and C in the proportions 2 : 5 : 3. Oligolabeling buffer and its constituents should be stored at –20°C.
14. TE: 10 m*M* Tris-HCl, pH 8.0, 1 m*M* EDTA.
15. 1 m*M* Biotin–16-dUTP (Roche). Store at –20°C (*see* **Note 2**).
16. 50X Denhardt's solution: 5 g Ficoll, 5 g polyvinyl pyrrolidone, 5 g bovine serum albumin (BSA), water to 500 mL. Filter and store at –20°C.
17. 2X Hybridization solution: 8X SSC, 2X Denhardt's solution, 20% dextran sulfate, 0.8% sonicated salmon sperm DNA. Store at –20°C.
18. Plastic box with tightly fitting lid, lined with moist tissue paper.
19. Detek-1 streptavidin–horseradish peroxidase detection kit (Enzo), or ExtrAvidin–horseradish peroxidase conjugate (Sigma-Aldrich). The Enzo dilution buffer is phosphate-buffered saline (PBS) supplemented with 1% BSA, 5 m*M* EDTA (*see* **Note 2**).
20. PBS: 8 g NaCl, 0.2 g KCl, 1.44 g Na_2HPO_4, 0.24 g KH_2PO_4 per 1 L.
21. PBS-TX: PBS containing 0.1% Triton X-100.
22. DAB solution: 0.5 mg/mL Diaminobenzidine in PBS, supplemented with 0.01% H_2O_2. DAB is a potent mutagen. Care should be taken at all times when working with solutions containing DAB. Gloves should be worn and DAB should be dis-

pensed in the fume hood. DAB should be inactivated in 50% bleach before disposal (*see* **Note 2**).
23. 0.89% Giemsa's staining solution in methanol/glycerol (Gurrs/BDH). Use as a 1 : 20 dilution in 10 m*M* sodium phosphate buffer, pH 6.8.
24. DPX mountant (Fluka).
25. Diamond pencil.
26. Nail polish.
27. Polytene chromosome maps (*see* **Note 3**).

3. Methods

3.1. Preparation of Polytene Chromosomes

Preparation of chromosomes from various species and tissues is broadly the same: tissues are dissected from appropriate staged animals and generally fixed in an organic acid fixative. The preferred fixative for *Drosophila* salivary gland chromosomes is 45% acetic acid, followed by 1 : 2 : 3 lactic acid : water : acetic acid. The choice of fixative is not immutable, however; for example, many drosophilists use merely 45% acetic acid.

Use only slides with good quality chromosomes. These appear flat and gray, with clear banding. Chromosomes that appear bright and reflective under dry-phase examination will have poorer morphology, hindering accurate interpretation (*see* **Note 4**). The region of the slide where the chromosomes are located should be visible when the slide is dry and it should be marked with a diamond pencil on the reverse side of the slide.

Drosophila stocks should be maintained on a medium suitable for the species in use. The best larvae are collected from well-yeasted, uncrowded cultures. Select large third instar larvae that are still crawling and have not everted their anterior spiracles.

1. Dissect out the salivary glands in a drop of 0.7% NaCl and transfer them to a drop of 45% acetic acid. Allow to fix for approx 30 s.
2. Transfer the glands to a drop of 1 : 2 : 3 fixative on a clean siliconized cover slip. Fix for 3 min, then pick up the cover slip with a clean slide, by touching it to the drop. The slide does not have to be coated or "subbed" before use.
3. Spread the chromosomes by tapping the cover slip with a pencil in a circular motion. Check the chromosomes using phase contrast. When the chromosomes are suitably spread, fold the slide in blotting paper and press gently to remove excess fix. Leave the slide at room temperature for 1 h to overnight. This step squashes the chromosomes as the fix evaporates, and the cover slip sinks toward the surface of the slide. Alternatively, the slide can be squashed firmly between blotting paper and frozen immediately. Take care not to allow the cover slip to slide sideways or the chromosomes will be overstretched (*see* **Note 4**).
4. Freeze the slide in liquid nitrogen. While the slide is still frozen, flip off the cover slip with a scalpel blade and proceed to **step 5**.

5. Place the slide in 70% ethanol for 5 min. Transfer the preparation through two 5-min changes of 96% ethanol and air-dry. The chromosomes can be stored desiccated at room temperature.

3.2. Pretreatment and Denaturation of Chromosomes

I will describe two protocols used to denature polytene chromosomes prior to hybridization. The first uses alkali treatment and the second uses heat to denature the chromosomes. Although the latter is a quicker method, some probes can give a rather dispersed signal compared with chromosomes prepared using alkali denaturation.

3.2.1. Alkali Denaturation

1. Incubate the slides in 2X SSC at 65°C for 30 min. This step is intended to help preserve the morphology of the chromosomes.
2. Transfer the slides to 2X SSC at room temperature for 10 min, then denature the chromosomes by incubating the slides in 70 m*M* NaOH for 2 min. The 70 m*M* NaOH must be freshly prepared, using NaOH pellets rather than a concentrated stock solution.
3. Rinse the slides in 2X SSC.
4. Dehydrate through ethanol as described in **Subheading 3.1., step 5** and air-dry. The slides should be used the same day.

3.2.2. Heat Denaturation

1. Place the slides directly in gently boiling 5 m*M* Tris-HCl, pH 7.5 for 2 min.
2. Place the slides in cold 70% ethanol for 5 min. Transfer the preparation through two 5-min changes of 96% ethanol and air-dry. Denatured slides should be used the same day.

3.3. Preparation of Labeled Probe

Probes are most conveniently prepared by the random priming method of Feinberg and Vogelstein ***(7,8)***. The DNA can be in the form of intact plasmid, lambda, cosmid, or YAC clones, or a restriction fragment isolated by agarose gel electrophoresis. In the latter case, the gel used should be cast using low-melting-point agarose, and the band should be excised in a minimum volume of gel. Three volumes of sterile distilled water are then added, and the mixture boiled for 7 min before adding it to the labeling reaction. Alternatively, the DNA can be extracted from the gel, using a variety of methods, typically "freeze-squeezing," phenol extraction, or a proprietary method such as Geneclean (*see* **Note 5**).

3.3.1. Synthesis of Biotinylated Probes by Random Priming

1. Place 5 µL oligolabeling buffer and 1 µL 1 m*M* biotin–16-dUTP in a microcentrifuge tube.

2. Boil 100–500 ng DNA in 20 µL water or TE for 3 min, then add 18 µL to the tube.
3. Add 1 µL (5 units) of Klenow fragment of DNA polymerase I and incubate the reaction at room temperature for 1 h to overnight.
4. Ethanol-precipitate the labeled DNA and resuspend it in 50 µL sterile distilled water; then, add 50 µL 2X hybridization solution and mix well. This is sufficient probe for five slides. Any unused probe may be stored at –20°C (*see* **Note 6**).

3.3.2. Synthesis of Probes from PCR Amplified DNA

Probes can be made from DNA amplified by the polymerase chain reaction (PCR), using additional PCR cycles in the presence of a biotinylated nucleotide.

1. Remove unincorporated nucleotides from the amplified DNA (e.g., by gel electrophoresis).
2. Set up the PCR using the same conditions used to amplify the probe DNA, but with the following changes. Substitute biotin–16-dUTP for the TTP in the PCR. Five cycles of synthesis are usually sufficient. Increasing the length of the polymerization step to 10 min is advised, because the concentration of biotin–16-dUTP is low.

3.4. Hybridization

1. Boil the probe for 3 min by suspending the tube in boiling water and quench on ice. Check the volume after boiling and restore to the initial volume with sterile distilled water.
2. Pipet 20 µL of the probe onto the chromosomes. Cover the chromosomes and probe with a clean siliconized cover slip. There is no need to seal the cover slip.
3. Place the slides in a plastic box lined with moist tissue to prevent evaporation from the preparation, seal the lid, and place in a 58°C incubator overnight.
4. Remove the slides from the humid box. Dip them in 2X SSC to allow the cover slip to slide off, then wash them in 2X SSC, 53°C, for 1 h. Three changes of wash solution should be made.

3.5. Signal Detection

1. Take the slides from the final wash and pass them through two 5-min washes in PBS.
2. Wash the slides for 2 min in PBS-TX
3. Rinse in PBS. Do not allow the slides to dry out during signal detection.
4. Make a 1 : 250 dilution of streptavidin–horseradish peroxidase conjugate in the buffer supplied with the Enzo kit. Alternatively, ExtrAvidin–horseradish peroxidase conjugate (Sigma) can be used, at the same dilution. Apply 50 µL to the chromosomes and cover with a 22×50 mm^2 cover slip. Replace the slides in the humid box and incubate at 37°C for 30 min.
5. Wash off unbound streptavidin conjugate by passing the slides through the PBS and PBS-TX washes described in **steps 1–3**. Drain the slides, but do not allow them to dry.

6. Place 50 µL of DAB solution onto the chromosomes and cover with a 22×50-mm^2 cover slip. This solution should be made up fresh because hydrogen peroxide decays rapidly. Take care when working with DAB, as it is a potent carcinogen. Follow the guidelines for use and disposal described in **Subheading 2., item 22**.
7. Incubate at room temperature for 10–15 min in the humid box. Rinse the slides in PBS and examine under phase contrast. The signal appears blackish-brown, sometimes quite refractile in strong cases. If the signal seems weak, add more DAB solution and incubate longer. If the signal is strong enough, rinse the slide well with distilled water (*see* **Note 7**).
8. Stain in Giemsa's stain for 1 min, rinsing off excess stain in running water for a few seconds. Allow the slides to air-dry. Check that the staining is sufficiently intense. Overstained chromosomes can be destained in 10 m*M* sodium phosphate buffer, pH 6.8, and understained chromosomes can be restained. The preparation should be mounted under a siliconized cover slip with DPX mounting medium. DPX is a xylene-soluble mountant, which does not affect either the Giemsa stain or DAB deposit, and the slides should last for many years. It is convenient to seal the edges of the cover slip with nail polish to prevent immersion oil from seeping under the cover slip.

The preparations should be examined under phase contrast. Some results are shown in **Fig. 1**, although photographic reproduction is most successful with color film.

4. Notes

1. Make sure the slides and cover slips are scrupulously clean, especially of lint from any tissue paper used to clean them; thus, only lint-free tissue paper should be used. It is good practice to clean slides and cover slips immediately prior to use by dipping in ethanol and wiping. Excess ethanol and lint can be removed by using a photographer's compressed air can (e.g., Dust-Off).
2. The biotin-labeling methods of probe preparation are not the only methods available to the researcher. Other labeling systems include the digoxygenin system (Roche), and alternatives to random priming for incorporation of label, such as photobiotin labeling, can be used. When selecting a detection system for an experiment, several factors must be kept in mind. First, the durability of the specimen is important. Signals visualized with horseradish peroxidase and DAB offer the advantage of long-term stability, compared with the fluorescent methods, an important feature when engaged in long-range chromosome walking or genome mapping. Second, one should assess the degree of sensitivity required for a given experiment. For example, methods for directly labeling probe DNA with fluorescent dyes, although quicker, do not offer the same degree of sensitivity as the two-step detection systems. Third, when choosing a method that employs an enzymatic reaction for detection, such as alkaline phosphatase or horseradish peroxidase, care should be taken to select a substrate whose reaction product is both stable and insoluble in the mountant in use and that contrasts well with the chromosome counterstain.

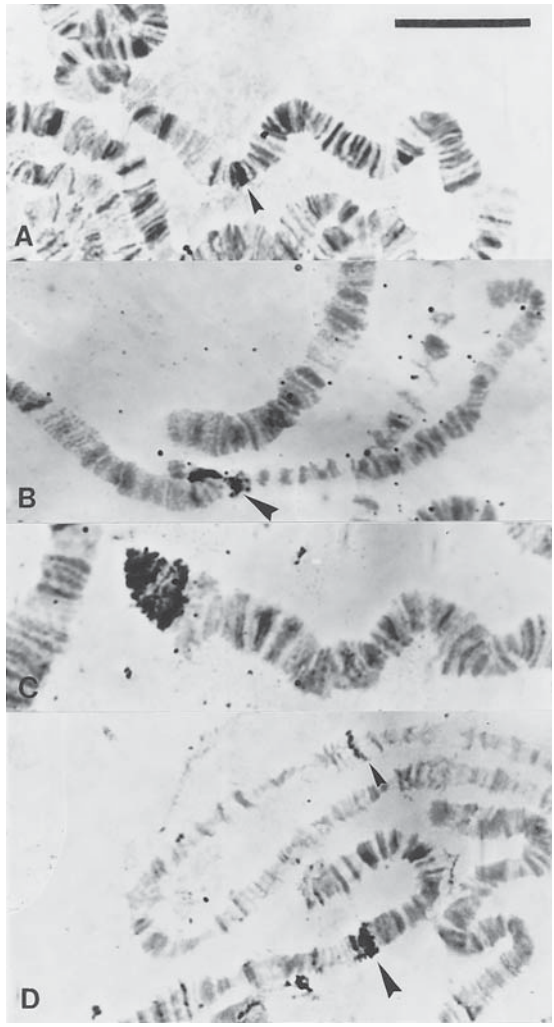

Fig. 1. *In situ* hybridization of biotin-labeled probe DNA to *D. melanogaster* polytene chromosomes. The signals have been detected using streptavidin–horseradish peroxidase conjugate, with DAB as the substrate, and the chromosomes are counterstained with Giemsa. **(A)** Mapping a cosmid clone, using a 2.8-kb restriction fragment as a probe. The signal is indicated by the arrow and lies in bands 96A21–25. **(B)** Mapping a clone relative to a chromosome rearrangement. The probe is a cosmid/phage containing an insert derived from bands 96B1–10, hybridized to *T(Y;3)B197/+* chromosomes. The signal lies on chromosome 3, in bands 96B1–10, proximal to the breakpoint. **(C)** Hybridization of PCR amplified DNA derived from microdissection of division 1 ***(9)***. **(D)** Hybridization of PCR amplified DNA derived from microdissection of subdivision 25A ***(9)***. Scale bar: 20 μm.

3. Polytene chromosome maps are available for many *Drosophila* species. Sorsa ***(10)*** has compiled a list of all maps of drosophilid polytene chromosomes. For *D. melanogaster*, the 1935 Bridges map ***(11)*** and the Lefevre ***(12)*** photomap are indispensable. These are available from Academic Press, in a folder together with the Bridges' revised maps ***(13–15)***.
4. One of the most important factors in successful *in situ* hybridization experiments is the quality of the polytene chromosomes. There are many ways in which polytene chromosomes can be prepared, differing mostly in the manner by which the chromosomes are spread and squashed. Allowing the cover slip to slip sideways when spreading causes the chromosome arms to stretch. Overstretched chromosomes can make analysis of the *in situ* hybridization difficult. Poor chromosome morphology can also result from denaturing chromosomes for too long in alkali and from other, poorly understood, fixation problems. If the chromosome morphology is repeatedly found to be puffy and swollen, try the alternative denaturation method of boiling, which often preserves the morphology better than alkali denaturation.
5. The presence of repetitive DNA within a cloned segment of DNA can prevent easy determination of the chromosomal site of origin of the clone. The use of sibling species can resolve this problem. For example, *D. simulans* and *D. mauritiana* polytene chromosomes have been used ***(2)*** in mapping cosmids containing cloned segments of *D. melanogaster* DNA. This is possible because the sibling species have different amounts of repetitive DNA and different populations of transposable elements.
6. High background on preparations is generally associated with poor incorporation of a biotinylated nucleotide and inefficient removal of unincorporated nucleotides prior to hybridization.
7. If no signal is seen when using a biotinylated probe, test the probe as follows. Make a dot blot with a series of dilutions of unlabeled probe DNA and a series of dilutions of probe DNA. Hybridization under standard filter hybridization conditions followed by signal detection using the same system as used for *in situ* hybridization will indicate whether the problem lies in probe preparation or in signal detection. A systemic problem where no signals are obtained with a variety of probes may indicate that the working DAB solution has decayed. Generally, this can be rectified by using fresh hydrogen peroxide. Stocks of hydrogen peroxide should be replaced regularly.

References

1. Pardue, M.-L., Gerbi, S.A., Eckhardt, R. A., and Gall, J. G. (1969) Cytological localization of DNA complementary to ribosomal RNA in polytene chromosomes of *Diptera*. *Chromosoma* **29,** 268–290.
2. Siden-Kiamos, I., Saunders, R. D. C., Spanos, L., et al. (1990) Towards a physical map of the *Drosophila melanogaster* genome: mapping of cosmid clones within defined genomic divisions. *Nucleic Acids Res.* **18,** 6261–6270.
3. Kafatos, F. C., Louis, C., Savakis, C., et al. (1991) Integrated maps of the *Drosophila* genome: progress and prospects. *Trends Genet.* **7,** 155–161.

4. Ajioka, J. W., Smoller, D. A., Jones, R. W., et al. (1991) *Drosophila* genome project: one-hit coverage in yeast artificial chromosomes. *Chromosoma* **100,** 495–509.
5. Adams, M. D., Celniker, S. E., Holt, R. A., et al. (2000) The genome sequence of *Drosophila melanogaster*. *Science* **287,** 2185–2195.
6. Benos, P. V., Gatt, M. L., Ashburner, M., et al. (2000) From sequence to chromosome: the tip of the X chromosome of *D. melanogaster*. *Science* **287,** 2220–2222.
7. Feinberg, A. P. and Vogelstein, B. (1983) A technique for radiolabeling DNA restriction endonuclease fragments to high specific activity. *Anal. Biochem.* **132,** 6–13.
8. Feinberg, A. P. and Vogelstein, B. (1984) Addendum to Feinberg and Vogelstein (1983). *Anal. Biochem.* **137,** 266–267.
9. Saunders, R. D.C., Glover, D. M., Ashburner, M., et al. (1989) PCR amplification of DNA microdissected from a single polytene chromosome band: a comparison with conventional microcloning. *Nucleic Acids Res.* **19,** 9027–9037.
10. Sorsa, V. (1988) *Chromosome maps of* Drosophila, CRC Press, Boca Raton, FL.
11. Bridges, C. B. (1935) Salivary chromosomes. With a key to the banding of the chromosomes of *Drosophila melanogaster*. *J. Heredity* **26,** 60–64.
12. Lefevre, G. (1976) A photographic representation and interpretation of the polytene chromosomes of *Drosophila melanogaster* salivary glands, in *The Genetics and Biology of Drosophila*, (Ashburner, M. and Novitski, E., eds), Academic, New York, Vol. 1a, pp. 31–66.
13. Bridges, C. B. (1938) A revised map of the salivary gland X-chromosome. *J. Heredity* **29,** 11–13.
14. Bridges, C. B. and Bridges, P. N. (1939) A new map of the second chromosome: a revised map of the right limb of the second chromosome of *Drosophila melanogaster*. *J. Heredity* **30,** 475–476.
15. Bridges, P. N. (1941) A revision of the salivary gland 3R-chromosome map of *Drosophila melanogaster*. *J. Heredity* **32,** 299–300.

14

Combined Immunostaining and FISH Analysis of Polytene Chromosomes

Sergey Lavrov, Jérôme Déjardin, and Giacomo Cavalli

1. Introduction

Polytene chromosomes result from subsequent cycles of DNA replication that are not followed by nuclear division. In *Drosophila*, this occurs in the majority of larval tissues and is most prominent in salivary glands, where up to eleven rounds of replication events may occur. Because the replicated chromatids remain tightly aligned, this process leads to pairing of up to 2048 DNA strands, giving rise to a highly reproducible banding pattern ***(1)***. This exceptional structure allows cytological analysis of genes and their associated proteins with a relatively high resolution. Up to 5000 condensed bands separated by less condensed interband chromatin regions can be well resolved with electron microscopy, whereas conventional optical microscopy techniques allow about 1000 bands and interbands to be distinguished. Because the size of *Drosophila* genomic euchromatin is about 120 Mb, the level of resolution on a linear scale is in the order of 10–50 kilobases (kb), depending on the local degree of condensation of the chromosomal region of interest. Therefore, polytene chromosomes represent a formidable tool for cytological analysis of biological processes. Moreover, polytene chromosome assays can be readily implemented in most laboratories, because they require only standard transmission and fluorescence microscopy equipment and reagents and do not demand great technical expertise.

Polytene chromosomes can be used in many different experimental approaches. Early studies used them to investigate chromosome structure and organization. More recently, practical applications have often aimed at identifying the cytological position of cloned genes and transgene insertions by *in situ* DNA

From: *Methods in Molecular Biology, vol. 247:* Drosophila *Cytogenetics Protocols*
Edited by: D. S. Henderson © Humana Press Inc., Totowa, NJ

hybridization or at determining by immunostaining techniques whether proteins of interest are chromosomally associated. Double-labeling experiments allow one to study colocalization of chromosome-associated proteins ***(2,3)***. Polytene chromosome assays are also useful for mapping domains of protein–protein interaction. This can be done by studying colocalization of interacting polypeptides in the presence of different types of mutation in each of them ***(4,5)***. Other applications involve dynamic studies of protein distribution in response to environmental stimuli such as heat shock ***(6,7)***, induction of gene expression by transcriptional activators ***(8,9)*** and treatment by agents like ribonucleases ***(10)*** or chemical inhibitors of transcription ***(11)***.

One common application is to determine whether a particular DNA sequence is associated with a protein of interest. Mapping the chromosomal location of transcriptional regulators can indicate if they are associated with loci containing putative target genes. A direct proof of binding to a regulatory element can be obtained by showing that a transgenic copy of the element induces an ectopic binding site on polytene chromosomes. Traditionally, this is achieved by two separate experiments. First, the transgene insertion is mapped by *in situ* DNA hybridization. Second, on separate preparations, immunostaining is performed in the transgenic line and compared to a wild-type background. Finally, the binding pattern is analyzed in order to determine if an additional binding site can be detected in the region of insertion of the transgene. This approach has been successfully used in many cases ***(12–14)***, but it has the major disadvantage that DNA hybridization and protein immunostaining are done on separate slides. Therefore, it can only be applied if the number of binding sites for the protein of interest is relatively small and, in particular, in the absence of endogenous binding sites in the cytological region of interest. Unfortunately, many chromosomal proteins display hundreds of binding sites in the genome ***(15,16)***. In this case, it is almost impossible to unambiguously determine if the transgene induces an ectopic binding site. We describe here a method that combines immunostaining of proteins and fluorescent *in situ* hybridization (immuno-FISH) for direct visualization of a specific DNA fragment and a protein of interest on the same chromosome. This method allows more refined mapping of protein binding sites compared to genes of interest and it can be widely used to map binding to both endogenous genes and transgenic insertions.

The method consists of two parts: In the first part, fluorescent protein staining of polytene chromosome preparations is performed. After immunostaining, a FISH protocol is applied in order to detect the DNA of interest with a different fluorochrome from the one used for immunostaining. Some protein epitopes and antibodies survive the FISH procedure and this allows image acquisition of DNA and protein staining on one slide using specific filter sets. When the protein staining does not survive FISH, it is still possible to do the experiment

by sequentially performing immunostaining followed by acquisition of a series of images on slide positions that can be precisely monitored using the "xy" scale of the microscope stage or more accurate devices. After image acquisition, a FISH experiment is performed on the same slide and images are acquired at the same slide coordinates for analysis of *in situ* DNA labeling. Finally, the separately acquired images are accurately merged using imaging software. This somewhat complicated procedure has the advantage of allowing immuno-FISH experiments to be performed on any protein of interest, regardless of the stability of the antibody under the relatively harsh conditions used for FISH experiments.

2. Materials

2.1. Fluorescent Immunostaining

1. Fly growth medium: Use bottles with rich medium (e.g., [1] 80 g fresh yeast, 80 g wheat flower, 11 g agar, 50 mL Moldex, and water to 1 L final volume, or [2] 8 g agar, 18 g dried yeast, 10 g soybean meal, 7 g molasses, 80 g malt extract, 80 g cornmeal, 6.3 mL propionic acid, and water to 1 L final volume).
2. Dissection stainless-steel tweezers no. 5.
3. Tris-HCl, pH 7.5, Tris-HCl, pH 8.5, Triton X-100 and 1 *N* KOH, Nonidet P40 (NP-40), Tween-20, glycerol, NaCl powder, nonfat dry milk powder (can be obtained directly from grocery stores).
4. Poly-L-lysine-coated slides. They can be purchased commercially (e.g., Merck Eurolab, cat. no. 711909) or prepared in the laboratory. For laboratory preparation, start with 100–200 slides in racks. Soak the slides in corrosive detergent solution for 2 h. Wash in running tap water for 2 h. Wash twice in bidistilled water (ddH_2O). Dip twice in 95% ethanol. Air-dry. Dip the slides in poly-L-lysine solution (slide adhesive solution, 0.1% [w/v] in water; Sigma-Aldrich, P 8920). Withdraw the rack; the solution should cover the slides uniformly and stay on the slides. Air-dry the slides.
5. Standard cover slips, 22 × 22 mm (Corning or others).
6. Latex gloves.
7. Pencil (HB type).
8. Solution 1: 0.1% Triton X-100 in phosphate-buffered saline (PBS), pH 7.5. Dissolve in PBS from a 10% Triton X-100 (w/v in ddH_2O) stock solution. Store at room temperature (RT) in the dark.
9. 37% Formaldehyde stock solution: Weigh 1.85 g of paraformaldehyde and dissolve in a final volume of 4.93 mL ddH_2O. Add 70 µL of 1 *N* KOH and dissolve by heating to 60°C. Store in 100-µL aliquots at –80°C. This solution is stable for several months. To test its stability, thaw aliquots by boiling for 1 min. If a precipitate forms or the color of the solution becomes brownish, it should be discarded and prepared again.
10. Solution 2: 3.7% Formaldehyde, 1% Triton X-100 in PBS, pH 7.5. Prepare by adding 400 µL of PBS (pH 7.5) and 50 µL of 10% Triton X-100 to 50 µL of 37% formaldehyde stock. This solution should be made fresh every 2–3 h.

11. Solution 3: 3.7% Formaldehyde, 50% acetic acid. Prepare by adding 50 µL of 37% formaldehyde stock solution to 200 µL of ddH_2O and 250 µL of glacial acetic acid. Prepare fresh every 2–3 h.
12. Slide racks.
13. Liquid nitrogen.
14. Diamond-tip pen.
15. Razor blade.
16. Protective glasses.
17. Methanol.
18. PBS, pH 7.5.
19. Block solution: 3% Bovine serum albumin (BSA) (fraction V; Sigma-Aldrich, A-2934), 0.2% (w/v) NP-40, 0.2% (w/v) Tween-20, and 10% w/v nonfat dry milk (from any grocery store) in PBS. To make 500 mL: Add 15 g BSA powder to 440 mL of PBS and dissolve by magnetic stirring. Add 1.0 g NP-40 and dissolve by stirring. Add 1.0 g of Tween-20 and dissolve by stirring. Add 50 g of nonfat dry milk and dissolve by stirring. The solution should have a homogeneous milky aspect. Store at –20°C in 50-mL aliquots.
20. Wash solution A: 300 m*M* NaCl, 0.2% (w/v) Tween-20, and 0.2% (w/v) NP-40 in PBS. To make 1 L, dissolve the following in 1 L of PBS: 9.55 g NaCl, 2.0 g NP-40 and 2.0 g Tween-20.
21. Wash solution B: 400 m*M* NaCl, 0.2% (w/v) Tween-20, 0.2% (w/v) NP-40 in PBS. To make 1 L, dissolve the following in 1 L of PBS: 15.4 g NaCl, 2.0 g NP-40, and 2.0 g Tween-20.
22. 200X 4',6-diamidino-2-phenylindole (DAPI) (Sigma-Aldrich, D 9542) stock solution: For a 200X stock, dissolve DAPI in 180 m*M* Tris-HCl (pH 7.5) at 0.1 mg/mL. Store frozen in 100-µL aliquots and protect from light. Working solution can be made by diluting an aliquot of stock in PBS or in 50 m*M* Tris-HCl, pH 7.5, at a concentration of 0.5 µg/mL.
23. Mowiol mounting medium: Add 2.4 g Mowiol 4-88 (Calbiochem no. 475904) to 6 g of glycerol and 6 mL of H_2O. Mix for 3 h and add 12 mL of 0.2 *M* Tris-HCl, pH 8.5, and incubate for 30 min at 60°C with mixing. Pellet insoluble material by centrifugation at 5000*g* for 15 min. Add Diazabicyclo[2,2,2]octane (DABCO) (Merck no. 803456) to 2.5% (w/v) as an antibleaching agent. Make 500-µL aliquots and store at –20°C.

2.2. Postfixation by Formaldehyde or EGS

1. 3.7% Formaldehyde in PBS: Prepare fresh from 37% stock solution (*see* **Subheading 2.1., item 9**); add 50 µL of stock to 450 µL of PBS.
2. 50 m*M* Ethylene glycol-bis[succinic acid *N*-hydroxysuccinimide ester] (EGS) (Sigma-Aldrich, E-3257). Prepare fresh in PBS.

2.3. Fluorescent In Situ Hybridization

1. Hybridization solution: 2X SSC, 10% (w/v) dextran sulfate, 50% formamide, 0.8 mg/mL salmon sperm DNA. 20X SSC stock solution is 3 *M* NaCl, 0.3 *M*

sodium citrate, pH 7.0; 50% dextran sulfate stock solution is prepared by stirring 25 g of dextran sulfate in 50 mL final volume of sterile H_2O (store at 4°C). Salmon sperm DNA solution at 8 mg/mL is prepared according to **ref. *17***. To make 10 mL of hybridization solution, mix 2 mL of 50% dextran sulfate, 5 mL formamide, 1 mL of DNA solution, and 1 mL of 20X SSC. Add water to 10 mL. Store in 500-µL aliquots at –20°C.

2. Detection solution: 50 m*M* Tris-HCl, pH 7.5, 4% (w/v) BSA. Prepare before use by dissolving 80 mg of BSA powder in 2 mL of 50 m*M* Tris-HCl.
3. BioNick labeling system (Gibco-BRL, cat. no. 18247-015).
4. 3 *M* Sodium acetate, pH 5.3.
5. 70% and 96% Ethanol.
6. TE: 10 m*M* Tris-HCl, 1 m*M* EDTA, pH 8.0.
7. Fluorescein isothiocyante (FITC)- or Texas Red-conjugated streptavidin (Vector Laboratories, cat. nos. SA-5001 and SA-5006).
8. Biotinylated antistreptavidin antibodies (Vector Laboratories, cat. no. BA-0500; optional).

3. Methods

3.1. Fluorescent Immunostaining of Polytene Chromosomes

3.1.1. Preparation of Third Instar Larvae

1. Add a drop of live baker's yeast and a paper filter moistened with a few drops of water to bottles containing fly food.
2. Let the flies lay eggs just to the point where larvae will hatch under uncrowded conditions (<100 larvae/bottle). This takes 7 d after egg lay at 18°C. We recommend this temperature in order to maximize the degree of polyteny, but higher temperatures can be chosen if needed, with relatively modest loss of size of the chromosomes.
3. For salivary gland preparations, use third instar larvae that are still crawling and have not yet started to pupariate.

3.1.2. Chromosome Squashes

1. Dissect one pair of salivary glands in solution 1. Try to get rid of most of the fat body cells without wasting more than a couple of minutes and, if possible, without separating the two glands.
2. Using tweezers, transfer the glands to ~40 µL of solution 2 on a cover slip.
3. Fix the glands homogeneously by moving them slowly into solution 2 for the appropriate time (*see* **Note 1**).
4. Move the glands into 40 µL of solution 3 on a 22 × 22-mm cover slip. At this step, the glands often stick to the tweezers. Carefully remove them with a second pair of tweezers and leave in the solution for 2 min, 45 s.
5. Pick up the cover slip with a microscope slide with the poly-L-lysine side facing the glands and quickly flip the slide in order to avoid liquid spillage and sliding of the glands sideways. The glands are visible as an opaque halo. Keep hold of

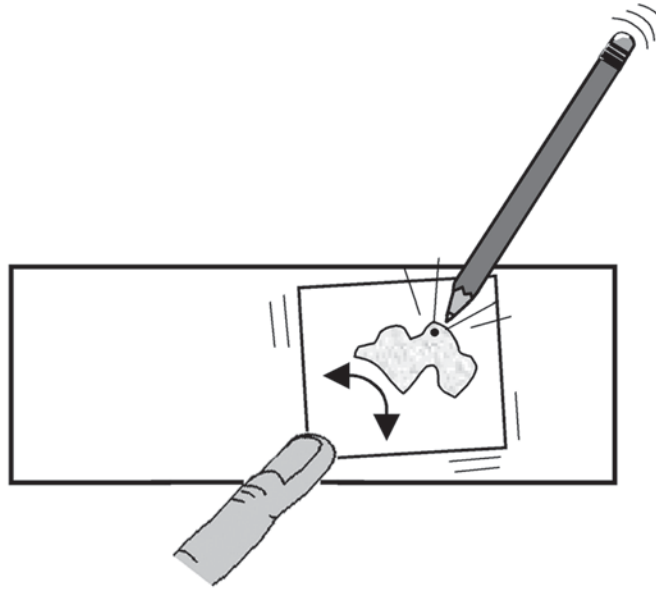

Fig. 1. A schematic representation of the procedure for spreading polytene chromosomes is shown. The squashed salivary glands are represented as a gray halo below the cover slip. The pencil is held with the right hand while the left-hand finger moves the cover slip.

the bottom left corner of the cover slip with a finger (wear Latex gloves in order to avoid acid burns). Tap on the cover slip with the tip of a pencil (it should be a soft tip like "HB" or softer, avoid "2H" type pencils) while moving the cover slip in order to obtain a lateral oscillation of about 2–4 mm amplitude (*see* **Fig. 1**). This results in cells and nuclei opening and in chromosome spreading. Start tapping right at the spot where the glands are located and then gradually move to the other areas of the cover slip. The tapping direction should be along the vertical axis. This is continued for 10–15 s, until the liquid excess has run off and the cover slip starts to stick on the slide. Tapping should be performed using the right pressure, which requires adjustment by trial and error. This step is the only difficult handling of the whole experiment and it is done slightly differently in different laboratories.

6. Squash the chromosomes and remove excess fixative by evenly pressing the slide (cover slip down) onto blotting paper (some laboratories have developed special devices for application of even pressure, but in our experience, a simple thumb pressure at the cover slip position is sufficient). Examine the preparation under phase contrast. Good preparations should contain nicely banded, well-spread chromosomes, some of which should be nonfragmented. High levels of fragmentation indicate that either the pressure was excessive or the cover slip was moved too harshly during the spreading procedure. On the other hand, the widespread presence of chromosomes wrapped in unbroken nuclei is diagnostic of insuffi-

cient tapping pressure. After observing the spread chromosomes, mark the position of the cover slip on the back of the slide using a diamond-tip pen.
7. Wear protective glasses and gloves. Freeze the slides by immersion in liquid nitrogen. Quickly flick off the cover slip with a razor blade or a scalpel and dip the slides into PBS.
8. Wash the slides twice for 15 min in PBS by slowly shaking the rack (at 100–150 rpm in an orbital shaker).
9. Proceed with the immunostaining or keep the slides (up to 1 mo) in 100% methanol at 4°C.

3.1.3. Immunostaining

1. Wash the stored slides twice for 15 min in PBS. Transfer to block solution and shake by slowly rotating for 1 h at RT or overnight at 4°C.
2. Add to each slide 20 µL of affinity-purified primary antibodies diluted in block solution (*see* **Note 2**). Cover with a cover slip, avoiding bubble formation. Incubate for 1 h at RT in a humid chamber (we use a box containing wet blotting paper). All subsequent steps are performed at RT.
3. Rinse in PBS; cover slips will fall off. Rinse one more time.
4. Wash by shaking thoroughly for 15 min in an orbital shaker in wash solution A, then repeat this step in wash solution B (*see* **Note 3**).
5. Rinse twice in PBS.
6. Add 20 µL of fluorescent secondary antibody (*see* **Note 4**) diluted in block solution containing 2% normal serum (*see* **Note 5**). Cover with a cover slip and incubate for 40 min in a humid chamber in the dark. Perform all subsequent steps in the dark in order to prevent bleaching of the fluorochrome.
7. Repeat **steps 3–5**.
8. Stain for 10 min in 40 µL of DAPI solution (0.5 µg/mL in PBS). Wash 5 min in PBS.
9. After immunostaining, the simplest protocol would be to proceed directly to FISH. However, the epitope–antibody or the primary–secondary antibody interactions may not survive the harsh conditions applied during FISH. Postfixation by either formaldehyde or EGS-dependent crosslinking of proteins to chromosomal DNA may preserve these interactions. Treatment with either one of these two reagents may be sufficient to preserve the epitope–antibody interaction. However, in some cases, even this postfixation step is not sufficient, leading to loss of the fluorescent signal. Therefore, the need for postfixation and its efficacy should be tested for every new epitope–antibody combination. There are three possibilities: (1) There is no need for postfixation between immunostaining and FISH. One example is shown in **Fig. 2** for histone H4 acetylated at Lysine 12. In this case, one should proceed from **Subheading 3.1.3., step 7** directly to FISH (**Subheading 3.4.**); (2) postfixation before FISH is needed in order to preserve the immunostaining signal (one example is shown in **Fig. 3** for the Polyhomeotic protein). In this case, proceed from **Subheading 3.1.3., step 7** to **Subheading 3.3.**; (3) the immunostaining signal is lost, even when postfixation is used. In this last case, acquire images of selected immunostained chromosomes (**Subheading 3.2.**),

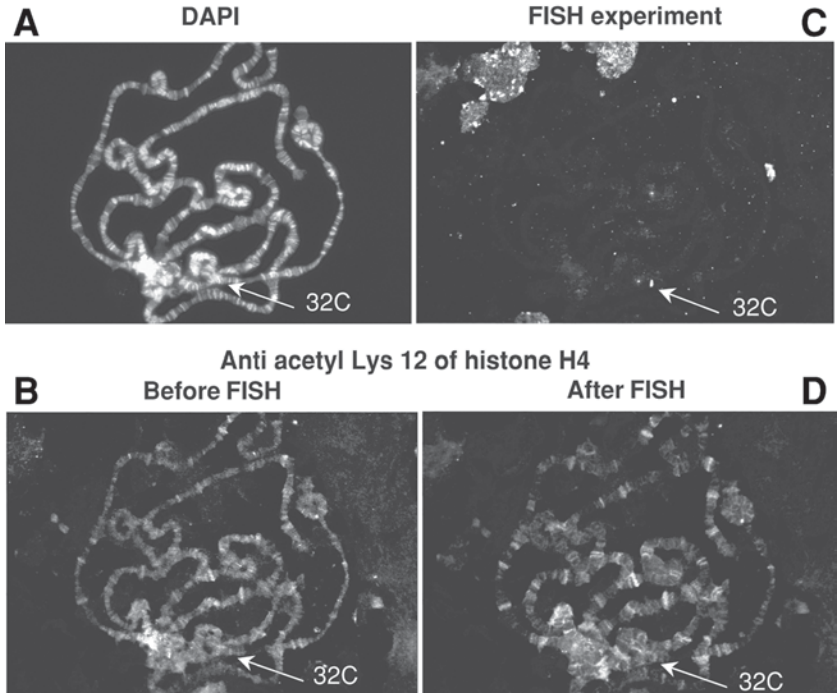

Fig. 2. Survival of the labeling of the histone H4 acetyl Lysine 12 epitope to FISH after immunostaining: **(A)** Chromosomal DNA banding as seen by DAPI counterstaining. **(B)** Immunostainning was performed and a picture taken before FISH. **(C)** FISH experiment using a 3.5-kb probe containing *lacZ* sequences. A *lacZ*-containing transgene present in the line is inserted at position 32C. Streptavidin–FITC was used for detection. **(D)** The same chromosome was recorded in the antibody channel after FISH. The antibody staining survives this treatment. In this particular case, the immunostained bands are sharper than before FISH, probably because of reduction of background immunostaining upon the harsh treatments during the FISH procedure. Anti-acetyl-histone H4 (Lys12) rabbit polyclonal IgG was from Upstate Biotechnology (cat. no. 06-761) and was used at a dilution of 1 : 100. Donkey anti-rabbit (Jackson ImmunoResearch, cat. no. 3 711-165-152) was used at a dilution of 1:350. The FISH signal was amplified as described in **Note 6**.

proceed to FISH (**Subheading 3.4.**), and record FISH images. Finally, produce overlay images with the help of image analysis software like Adobe Photoshop (**Subheading 3.5.**).

3.2. Cytological Analysis of Immunostained Slides

1. Mount the preparations in 40 µL Mowiol or in 99.5% glycerol for cytological examination and image acquisition.

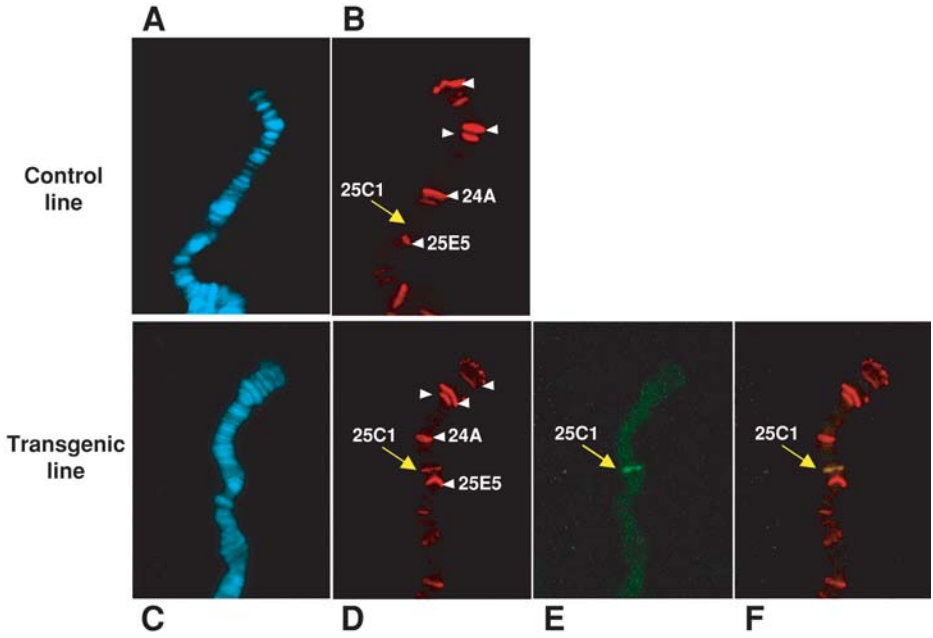

Fig. 3. Immuno-FISH with the Polyhomeotic (PH) protein. **(A,B)** Immunostaining was performed in a control fly line that does not contain any transgene in order to detect the endogenous banding pattern of the protein. DAPI is shown in **(A)** and PH is shown in **(B)**. The cytology of the PH endogenous binding sites (arrowheads) is indicated by numbers. No endogenous band is seen at 25C1, the site where the transgene of interest is located (yellow arrow). **(C–F)** Immuno-FISH is performed in a transgenic line containing at 25C1, a regulatory element that binds PH protein (in this case, the Fab-7 region, which regulates the *Abdominal-B* gene of the Bithorax-Complex ***[8,18]***). PH survives FISH after postfixation with formaldehyde, which was performed between immunostaining and FISH. **(C)** shows DAPI staining. **(D)** shows the PH immunostaining signal after FISH. (E) shows the FISH signal generated by a probe of approx 13 kb spanning the transgene and **(F)** shows the merge between **(D)** and **(E)**. A yellow signal is seen at the transgene position, indicating colocalization between PH and the transgenic DNA. The anti-PH antibody is described in **ref. *19*** and was used at a 1 : 500 dilution. The FISH signal in this case was obtained without amplification. (*See* color plate 5 in the insert following p. 242.)

2. Examine the slides under a microscope. Good chromosome spread images are acquired using a DAPI filter and the corresponding antibody filter. The position of each chromosome set is recorded. This can be done manually by using the scale of the microscope stage. We used a conventional photonic microscope (Leica DMR8) with a stage connected to a "Leica Sensor Control Display" device. This device measures the *xy* position of the object with an accuracy of ± 1 µm.

Formatting of the acquired image will depend on the image acquisition device. We recommend storing the image files in "TIFF" format and in "Indexed color" mode for subsequent image processing as described in **Subheading 3.5.**

3.3. Postfixation of the Immunostaining Signal

Either formaldehyde or EGS can be used as fixing agents in order to prevent signal degradation during the FISH procedure. We usually try formaldehyde first and only test EGS whenever formaldehyde does not work. A critical point is postfixation time. Longer times will, in general, better preserve the immunostaining signal, but they will reduce the efficiency of *in situ* hybridization. We usually perform postfixation for 15 min at 37°C, as indicated in **Subheading 3.3.1.**, **step 2** and **Subheading 3.3.2.**, **step 2**, but this time can be reduced to 10 min as tested empirically. As stated in **Subheading 3.1.3.**, some epitopes do not need postfixation. In this case, proceed to **Subheading 3.4.**

3.3.1. Postfixation by Formaldehyde

1. Wash the slides in PBS for 5 min (*see* **Note 7**).
2. Incubate the chromosomes in 20 µL of 3.7% formaldehyde in PBS under a cover slip for 15 min at 37°C in a humid chamber in the dark (*see* **Note 8**).
3. Wash three times in PBS, 5 min each, and proceed to **Subheading 3.4.**

3.3.2. Postfixation by EGS

1. Wash the slides in PBS for 5 min (*see* **Note 7**).
2. Incubate the chromosomes in 20 µL of 50 m*M* EGS solution (freshly made in PBS) under a cover slip for 10–30 min at 37°C in a humid chamber in the dark (*see* **Note 8**).

3.4. FISH of Polytene Chromosomes

3.4.1. Preparation of the Slides for FISH

1. Wash the slides three times in 2X SSC, 5 min each wash (if the epitope–antibody interaction survives FISH, perform all the steps in the dark).
2. Dehydrate the chromosomes by passing the slides twice in 70% ethanol, 5 min each wash, and twice in 96% ethanol, 5 min each wash.
3. Allow the slides to air-dry and store at 4°C overnight (maintain the slides in a flat position to favor flattening of the chromosomes).

3.4.2. Preparation of the Hybridization Probe

1. Label 1 µg of DNA by biotinylation using the BioNick (BRL) nick-translation kit, according to manufacturer's instructions.
2. After the nick-translation reaction, add to the sample 1/10 vol of 3 *M* sodium acetate, pH 5.3, and ethanol precipitate by adding 2.5 vol of cold 96% ethanol and incubating at –80°C for 1 h or at –20°C overnight. After centrifugation in a

4°C microfuge at maximum speed for 30 min, wash the biotinylated DNA pellet once with 70% ethanol, dry the pellet, and dissolve in 20 µL of TE.
3. Mix the solution of biotinilated DNA with 200 µL of hybridization buffer. The mixture is stable at –20°C.

3.4.3. Hybridization

1. If the antibody staining survives FISH, perform all steps in the dark. Just before hybridization, incubate the slides in 2X SSC for 45 min at 70°C (do not put slides into hot SSC; instead, put them into SSC at room temperature and then put the slide rack into a 70°C water bath). Dehydrate by passing through 70% ethanol (twice for 5 min each) and 96% ethanol (twice for 5 min each). Air-dry the slides.
2. Denature the DNA by incubating the slide in 100 m*M* NaOH for 10 min. Wash the slides three times in 2X SSC (1 min, 1 min, and 5 min) and dehydrate by passing through 70% ethanol (twice for 5 min each) and 96% ethanol (twice for 5 min). Air dry slides.
3. Denature an aliquot (approx 10 µL per slide to be hybridized) of the hybridization mixture containing biotinylated probe DNA for 5 min at 80°C, then snap-cool on ice. Prewarm the hybridization mix again to 37°C. Load 6–10 µL of the mixture on the slide, cover by a cover slip, and seal with rubber cement in order to prevent liquid evaporation. Hybridize overnight in a dark humid chamber at 37°C.

3.4.4. Washing and Detection

1. After hybridization, remove the rubber cement and then remove the cover slips by immersion in one bath of 2X SSC.
2. Wash in 2X SSC three times at 42°C, 5 min each, and then 5 min at RT.
3. Add 40 µL of FITC-conjugated streptavidin (for green staining) or Texas Red-conjugated streptavidin (for red staining). Dilution ranges from 1 : 30 to 1 : 100 (to be tested by a serial dilution experiment) in the detection solution.
4. Incubate for 1 h at RT in a dark humid chamber. Perform all subsequent steps in the dark.
5. Wash in 2X SSC three times at RT, 5 min each, and once in PBS for 5 min. (Optional: The FISH signal from fluorescent-coupled streptavidin may be amplified using biotinylated anti-streptavidin antibodies; *see* **Note 6**.)
6. Stain the slides for 10 min in 40 µL of DAPI solution (0.5 µg/mL in PBS). Wash 5 min in PBS.
7. Mount with Mowiol and acquire FISH images at the fluorescence microscope.

3.5. Analysis of FISH Images and Mounting of Immunostaining and FISH Pictures

We perform this step using Adobe Photoshop software, version 5.0 or higher. Some basic knowledge of this software is needed in order to mount the immuno-FISH pictures. The following instructions are one example of how to do it, but other procedures or imaging software may also be used.

1. Select the best chromosomes for image analysis. In cases where the antibody staining survives FISH, from the digital camera attached to the microscope acquire three pictures for every selected chromosome with appropriate filter sets: one for the antibody staining, one for the FISH signal, and one for DAPI staining. If the antibody staining does not survive FISH, image acquisition of immunostained chromosomes at marked slide coordinates will already have been done as described in **Subheading 3.2.**, and at this stage of the experiment, separate acquisition of the FISH and DAPI images is performed on the same chromosomes.
2. At this stage, three images are available for every chromosome: a DAPI staining, an immunostaining, and a FISH staining. These images are 8-bit "Indexed Color" tiff format files.
3. In order to produce properly aligned color pictures, open all three files in Adobe Photoshop. Convert all images from "Indexed Color" to "RGB" color mode (Menu: Image → Mode).
4. Choose one file (usually it is the DAPI stain) and transfer the content of the other two files to it. This can be done by selecting each image to be transferred (Menu: Selection → Select all), then "Copy" and "Paste" to the target image. The resulting image will look the same, but now it is color coded. This means that each of the three layers contains three channels: red, green, and blue. Save this three-layered file as a new file with a different name, with the .psd extension.
5. Align the three image layers by moving the layer content by the arrow keys ("Move" tool from the Photoshop toolbox) (*see* **Note 9**). The morphologically common details on all images, such as the chromosome contours, should coincide. Finally, crop the image to the zone of interest ("Crop" tool from Photoshop toolbox) and save the file.
6. Create pseudocolor pictures for each layer. From the "Image" menu, go to "Adjust" → "Levels." The dialog window shows the color channels on top, the input levels in the middle and the output levels at the bottom. In order to obtain the correct color for the DAPI image, select from "channels" the red one and set the output level at zero. Thus, only blue and green are left, resulting in a cyan color. Then, go to the input levels and adjust in order to obtain the proper staining intensity. Confirm by clicking "OK." In order to obtain a red color for the file corresponding to the red fluorochrome staining, go back to the layers and select the appropriate one. Select again "Adjust" → "Levels." Set the output level of the green and the blue channels to zero. Now, only the red is left. Select the input levels in order to adjust the intensity and confirm. For the green color, repeat this step, but now setting to zero the output levels of the red and the blue channels.
7. Visualize each channel by selecting or unselecting each of them in the "Layers" dialog box (the icon of an eye appears in a check box flanking the appropriate layer upon selection). For a view of the overlay image, switch the view mode from "normal" to "superimposed."

4. Notes

1. The fixation time in solution 2 needs to be adjusted for each individual antigen. Thirty seconds are good for most antigens. Longer times may be required for very basic proteins. For example, 5 min are required for histone staining.
2. Primary antibody dilutions have to be empirically adjusted using serial dilutions. When testing new antibodies, one should first determine the optimal working concentration in a Western blot experiment. In most cases, the optimal concentration for polytene chromosomes ranges between 10-fold and 100-fold higher than the one used for Western blot. Signal intensity and background level depend critically on primary antibody concentration, therefore careful analysis of this parameter is required. Note that the optimal dilution often differs from the ones used in immunostaining of other tissues. Use affinity-purified antibodies whenever possible. For antisera, it is recommended to preabsorb against embryos.
3. If background problems persist, the NaCl concentration can be raised to 550 m*M*.
4. For the secondary antibody, optimal working dilutions should also be tested, but this parameter is less critical than for primary antibodies and it is often close to the manufacturer's instructions. Always include a negative control slide with secondary antibody in the absence of primary antibody.
5. The serum used for incubation with secondary antibody should be from the same species as the one in which the antibody has been raised.
6. In FISH experiments, the signal from the fluorescent-coupled streptavidin can be amplified. In this case, after incubation with the streptavidin conjugate and washing (*see* **Subheading 3.4.4., steps 3–5**), incubate slides with biotinylated antistreptavidin antibodies (Vector Laboratories), diluted in the same buffer and in the same concentration as streptavidin. After antibody staining, wash the slides as in **Subheading 3.4.4., step 5** and again incubate with the streptavidin conjugate (**Subheading 3.4.4., steps 3–5**).
7. Postfixation of the immunostained signal can be also performed after cytological analysis of immunostaining, if necessary. In this case, after image acquisition of Mowiol-mounted slides, remove the Mowiol and cover slips by washing in PBS for 1 h with mild shaking. Wash once more in PBS for 5 min. After this step, proceed to **Subheading 3.3.1., step 1** or **Subheading 3.3.2., step 1**, as appropriate.
8. The time of postfixation should be optimized. Longer fixation times improve the stability of the immunostaining signal after FISH. However, they will correspondingly reduce accessibility of the chromosomal DNA to the labeled probe during FISH and thus reduce the FISH signal. We often found 15 min to be the best compromise between preservation of immunostaining and FISH sensitivity. However, we suggest performing preliminary experiments with postfixation times ranging from 10 to 30 min.
9. Alignment of the three image layers in the Photoshop compound image file is necessary—in particular, in the case of separate immunostaining and FISH-staining image acquisition. However, this is often needed even in case of acquisition of all images at the same time, because acquisitions with different filters may result in images that are offset by a few pixels. This is the result of suboptimal microscope settings and can be corrected by proper microscope adjustment.

Acknowledgments

We thank all laboratory members for discussion and critical reading of the manuscript. Work in our laboratory is supported by the CNRS, by the Association pour la Recherche sur le Cancer, by the Fondation pour la Recherche Médicale, by the Fondation Annette-Schlumberger pour l'Education et la Recherche, and by the Human Frontier Science Program Organisation.

References

1. Ashburner, M. (1989) *Drosophila: A Laboratory Handbook*. Cold Spring Harbor Laboratory Press, Cold Spring Harbor, NY.
2. Franke, A., Decamillis, M., Zink, D., Cheng, N. S., Brock, H. W., and Paro, R. (1992) Polycomb and polyhomeotic are constituents of a multimeric protein complex in chromatin of Drosophila-Melanogaster. *EMBO J.* **11,** 2941–2950.
3. Rastelli, L., Chan, C. S., and Pirrotta, V. (1993) Related chromosome binding sites for *zeste*, suppressors of *zeste* and *Polycomb* group proteins in *Drosophila* and their dependence on *Enhancer of zeste* function. *EMBO J.* **12,** 1513–1522.
4. Platero, J. S., Hartnett, T., and Eissenberg, J. C. (1995) Functional analysis of the chromodomain of HP1. *EMBO J.* **14,** 3977–3986.
5. Platero, J. S., Sharp, E. J., Adler, P. N., and Eissenberg, J. C. (1996) *In vivo* assay for protein–protein interactions using *Drosophila* chromosomes. *Chromosoma* **104,** 393–404.
6. Weeks, J. R., Hardin, S. E., Shen, J., Lee, J. M., and Greenleaf, A. L. (1993) Locus-specific variation in phosphorylation state of RNA polymerase II in vivo: correlations with gene activity and transcript processing. *Genes Dev.* **7,** 2329–2344.
7. Nowak, S. J. and Corces, V. G. (2000) Phosphorylation of histone H3 correlates with transcriptionally active loci. *Genes Dev.* **14,** 3003–3013.
8. Zink, D. and Paro, R. (1995) *Drosophila Polycomb*-group regulated chromatin inhibits the accessibility of a *trans*-activator to its target DNA. *EMBO J.* **14,** 5660–5671.
9. Cavalli, G. and Paro, R. (1999) Epigenetic inheritance of active chromatin after removal of the main transactivator. *Science* **286,** 955–958.
10. Richter, L., Bone, J. R., and Kuroda, M. I. (1996) RNA-dependent association of the *Drosophila* maleless protein with the male X chromosome. *Genes Cells* **1,** 325–336.
11. Egyhazi, E., Ossoinak, A., Pigon, A., Holmgren, C., Lee, J. M., and Greenleaf, A. L. (1996) Phosphorylation dependence of the initiation of productive transcription of Balbiani ring 2 genes in living cells. *Chromosoma* **104,** 422–433.
12. Zink, B., Engström, Y., Gehring, W. J., and Paro, R. (1991) Direct interaction of the *Polycomb* protein with *Antennapedia* regulatory sequences in polytene chromosomes of *Drosophila melanogaster*. *EMBO J.* **10,** 153–162.
13. Chan, C. S., Rastelli, L., and Pirrotta, V. (1994) A *Polycomb* response element in the *Ubx* gene that determines an epigenetically inherited state of repression. *EMBO J.* **13,** 2553–2564.

14. Rozovskaia, T., Tillib, S., Smith, S., et al. (1999) Trithorax and ASH1 interact directly and associate with the trithorax group-responsive bxd region of the Ultrabithorax promoter. *Mol. Cell. Biol.* **19,** 6441–6447.
15. Tsukiyama, T., Becker, P. B., and Wu, C. (1994) ATP-Dependent nucleosome disruption at a heat-shock promoter mediated by binding of GAGA transcription factor. *Nature* **367,** 525–532.
16. Gerasimova, T. I. and Corces, V. G. (1998) Polycomb and trithorax group proteins mediate the function of a chromatin insulator. *Cell* **92,** 511–521.
17. Sambrook, J., Fritsch, E. F., and Maniatis, T. (1989) *Molecular Cloning: A Laboratory Manual, 2nd ed.*, Cold Spring Harbor Laboratory Press, Cold Spring Harbor, NY.
18. Gyurkovics, H., Gausz, J., Kummer, J., and Karch, F. (1990) A new homeotic mutation in the *Drosophila* bithorax complex removes a boundary separating two domains of regulation. *EMBO J.* **9,** 2579–2585.
19. Strutt, H. and Paro, R. (1997) The *Polycomb* group protein of *Drosophila melanogaster* has different compositions at different target sites. *Mol. Cell. Biol.* **17,** 6773–6783.

15

Electron Microscopy of Polytene Chromosomes

**Valery F. Semeshin, Elena S. Belyaeva,
Victor V. Shloma, and Igor F. Zhimulev**

1. Introduction

Most studies of the structure and function of Dipteran salivary gland polytene chromosomes are based on the phenomenon of the relative constancy of the banding pattern characteristic of each species. This made possible the building of cytological maps of polytene chromosomes widely used in genetic and molecular genetic research. The most detailed maps of the salivary gland polytene chromosomes of *Drosophila melanogaster* were those made in the 1930s to 1940s by Bridges and Bridges using the light microscope (LM) (*see* **ref. *1***). More recently, Sorsa and his colleagues ***(2–4)*** presented revised electron microscope (EM) maps covering the entire salivary gland chromosome set of *D. melanogaster*. To carry out this extremely laborious work, they used a squash/thin-sectioning EM technique. We consider this approach to be the best for precise mapping of politene chromosome regions. Moreover, chromosomes prepared by this method can be used for autoradiographic study, *in situ* hybridization and protein localization at the EM level, as described in this chapter.

1.1. EM Mapping and Sources of Errors

In ultrathin sections of polytene chromosomes, large thick bands can usually be seen easily. Visualization of thin faint bands depends mainly on two factors: (1) the method of fixation and treatment prior to embedding and (2) the thickness of the sections analyzed.

From: *Methods in Molecular Biology, vol. 247:* Drosophila *Cytogenetics Protocols*
Edited by: D. S. Henderson © Humana Press Inc., Totowa, NJ

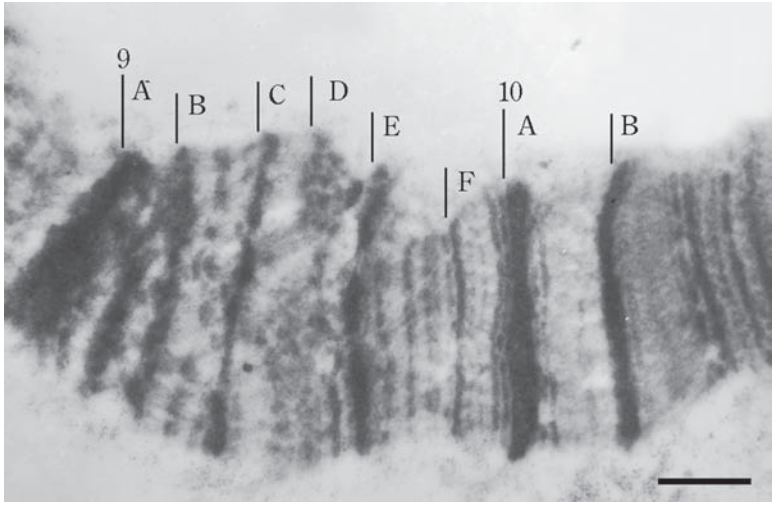

Fig. 1. The 9A-10B region of the X chromosome. The chromosome was fixed in 3 : 1 ethanol/acetic acid. Scale bar: 1 μm.

1.1.1. Chromosome Fixation

In our experience ***(5–7)***, fixation of salivary glands in 3% glutaraldehyde produces contracted chromosomes in which it is very difficult to discern many thin bands (*see also* **ref. *8***). Fixation in 3% formaldehyde preserves the visibility of thin bands; however, it makes squashing of the glands difficult and results in poorly spread chromosomes. This is also the case for glutaraldehyde fixation. Salivary gland treatment with 45% acetic acid, the fixative used by Bridges, allows the detection of thin bands but results in the formation of doublets of thick bands. Treatment with 60% lactic acid significantly reduces the number of observable thin bands. Long-term storage of preparations in 96% ethanol ***(9)*** results in a drastic contraction of the bands. Only fixation in a 3 : 1 mixture of alcohol (ethanol or methanol) and acid (acetic or propionic) gives the desired result, allowing both good chromosome spreading and visualization of the greatest number of the bands. The polytene chromosome in **Fig. 1** is an example. Comparison of this electron micrograph with the revised map of Bridges ***(1)*** reveals a characteristic difference: Most of the bands indicated as doublets by Bridges appear as singlets in **Fig. 1**. After analyzing many other chromosome regions, we concluded that practically all heavy bands are single and that fixation in 45% acetic acid or in a hydrated 3 : 1 mixture of alcohol : acetic acid leads to the formation of double vacuolated bands. We consider such vacuolization to be an artifact of fixation. It should be noted that the best

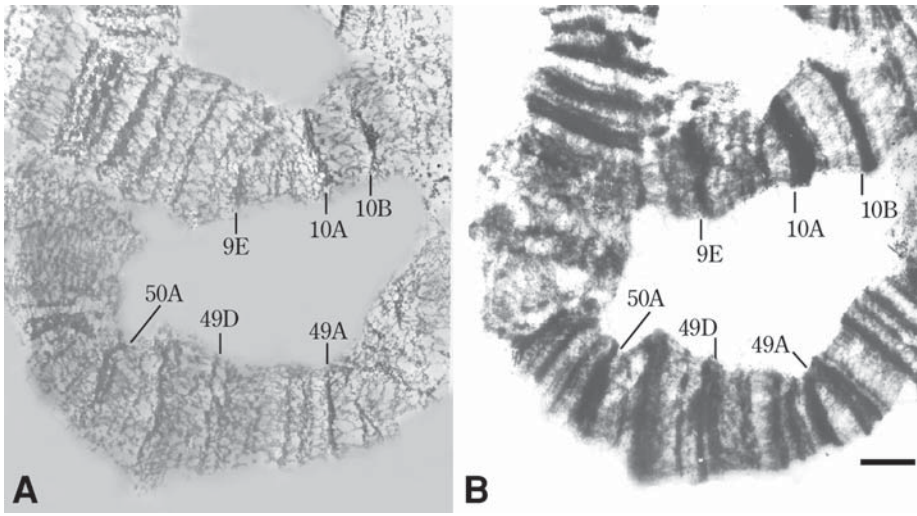

Fig. 2. Banding pattern of polytene chromosome regions in serial sections of different thickness: **(a)** 50–70 nm and **(b)** 120–150 nm. Scale bar: 1 μm.

way to detect thin bands, like those in **Fig. 1**, is through analysis of serial sections of many chromosomes.

1.1.2. Thickness of Sections

Accuracy of polytene chromosome mapping as well as interpretation of the observed images depends both on the DNA content and the degree of DNA decompaction in a given structure. Therefore, section thickness plays an important role in the analysis of banding pattern ***(10)***. **Figure 2** shows thin (50–70 nm) and thick (120–150 nm) sections in two regions, namely 9–10 and 48–49 of the *D. melanogaster* X and 2R chromosomes, respectively, made from the same Araldite block. In the 50- to 70-nm ultrathin section (*see* **Fig. 2A**) it is difficult to identify very thin bands and to interpret the structure of large bands. In the thick section, two bands positioned close to each other may look like a single band (*see* **Fig. 2B**). Although neither image furnishes a detailed picture of the banding pattern, the comparison nevertheless demonstrates a clear advantage of the thick section over the thin one. In the thin section, many of the large bands exhibit a reticular, fine flaky structure. Faint bands are tightly juxtaposed to large ones and it is quite impossible to determine the exact number of bands, as they look like an indivisible network of chromatin. In the 120- to 150-nm sections, faint bands cover a larger cross section, which facilitates their detection (compare the 9E–10A region in **Figs. 1** and **2**). The same conclusion

was made earlier by Berendes ***(8)***, who proposed to use even thicker sections (150–200 nm). However, large neighboring bands in such sections often look fused.

Finally, the detectability of bands depends on the extent of stretching of the polytene chromosome. Therefore, the quality of chromosome structure should be monitored using the light microscope before sectioning is done with an ultratome.

1.1.3. Mapping Rules

The diversity of band morphology of polytene chromosomes requires that certain mapping rules be followed for correct interpretation of the data obtained. Such rules were formulated earlier ***(11)*** and can be summarized as follows:

1. The banding pattern of a region has to be reproducible in serial sections of at least two or three chromosomes. Single dense structures of very small size (approx 1/20 of chromosome diameter) with approximately equal length and width are not regarded as bands.
2. The best fixative is a 3 : 1 alcohol : acid mixture. Vacuole like formation in large bands increases with increasing fixative hydration, which gives rise to doublet artifacts.
3. In estimating the number of bands taking part in puff development, the beginning and end stages of the process should be included in the analysis and the chromosomes of larvae at different developmental stages should be studied.
4. The optimum thickness of sections used for mapping is 120–150 nm.

1.2. EM Autoradiography

The most convincing demonstration of transcriptional activity in a particular chromosome region can be obtained in autoradiographical experiments. Using ^{3}H-uridine as a precursor of RNA synthesis, it was shown that puffing regions are the most transcriptionally active sites on polytene chromosomes (for a review, *see* **ref. *12***). As for interbands, the light microscope has insufficient resolving power to decide between activity and inactivity. However, this question can be addressed by EM autoradiography (**Subheading 3.2.**). We applied the thin-section squash technique to precisely localize where ^{3}H-uridine had incorporated into chromosome structures ***(13)***. The results showed a good correspondence between LM and EM data: Maximum incorporation was observed over the puffing regions and minimum incorporation was found over the dense bands. Silver grains occurred also over the interbands and diffuse thin bands. An example of such labeling is shown in **Fig. 3**. To get a reliable result, this investigation was performed on serial sections of a large number of chromosomes.

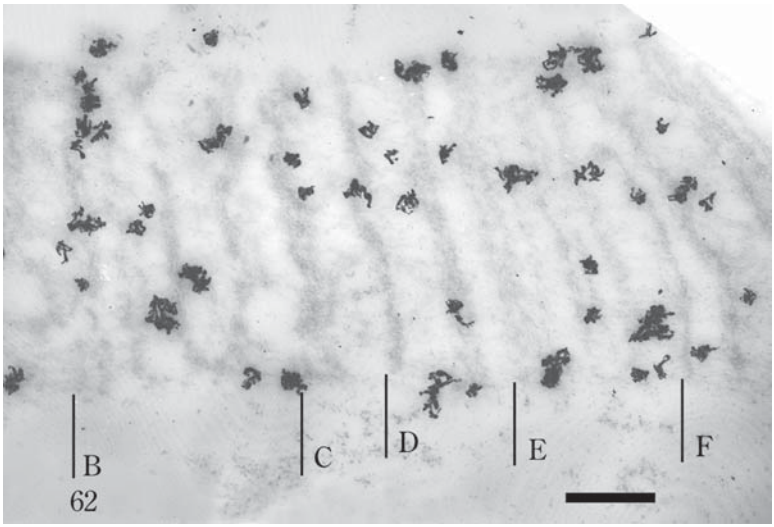

Fig. 3. Electron microscope autoradiography of the 62B–F region of the *D. melanogaster* 3L chromosome. Scale bar: 1 μm.

1.3. EM In Situ *Hybridization to Polytene Chromosomes*

In situ hybridization methods have become indispensable tools in molecular cytogenetics because they allow for the localization of specific sequences of DNA and RNA in cells, linking molecular information to structural studies ***(14,15)***. In *Drosophila*, these techniques are especially suitable because of the existence of giant polytene chromosomes, which also show a distinct and reproducible banding pattern. Originally, *in situ* hybridization studies employed radioactively labeled DNA probes and light microscopy ***(16)***. Subsequently, methods for detection of nucleic acids by biotin-labeled ***(17–19)*** or digoxygenin-labeled ***(20)*** probes were developed. Attempts to increase the resolution of the method led to the elaboration of nonradioactive *in situ* hybridization at the ultrastructural level ***(21,22)***. As for polytene chromosomes, Wu and Davidson ***(21)*** developed a method using colloidal gold spheres photochemically crosslinked to single-stranded DNA fragments. Another approach was taken by Kress et al. ***(23)***, who used biotinylated DNA probes to surface-spread *Drosophila* chromosomes. Neither of these methods gained wide recognition, probably because of technical difficulties.

Here, we describe a method of *in situ* hybridization for standard squashes of *D. melanogaster* polytene chromosomes (**Subheading 3.3.**). Digoxygenin-labeled DNA probes were chosen because the intensity of their hybridization signal was shown to be greater than that obtained with biotin-labeled probes

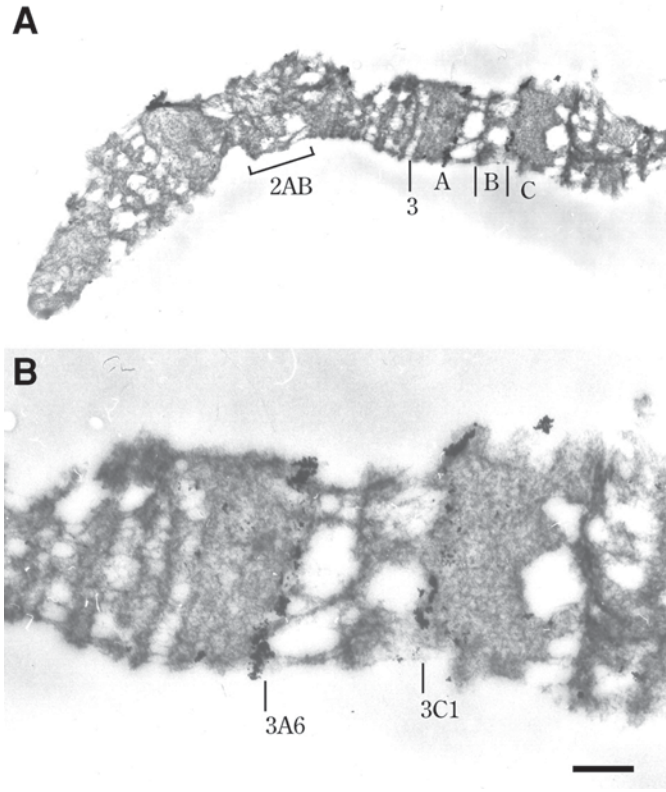

Fig. 4. Electron micrograph *in situ* hybridization of the 3AC region of the X chromosome with a Carnegie-20 DNA probe. **(A)** General view of the telomeric region of the X chromosome and **(B)** magnified fragment. The transgenic strain with a P-lArB construction inserted in the 3A4–6 region was used. P-lArB contains DNA of the *rosy* gene. The Carnegie-20 plasmid carries 7.2 kb of the *rosy* gene and approx 700 bp of the *Drosophila white* gene. Hybridization signal appears in both the 3A4–6 and 3C1 regions, corresponding to the P-lArB insert and the endogenous *white* gene, respectively. Scale bar: 1 μm.

(20). In comparison with EM specimens prepared by conventional methods, the denaturation, saline washes, and hybridization steps of this method affect chromosome structure: The large bands swell and become indistinctly gray and they occasionally fuse with neighboring bands (*see* **Fig. 4**). However, the chromosome regions remain recognizable and the localization of label on the chromosome correlates well with the results obtained with other methods.

Our attempts to perform postembedding *in situ* hybridization using ultrathin sections of chromosomes embedded in Araldite *M* or LR White were unsuc-

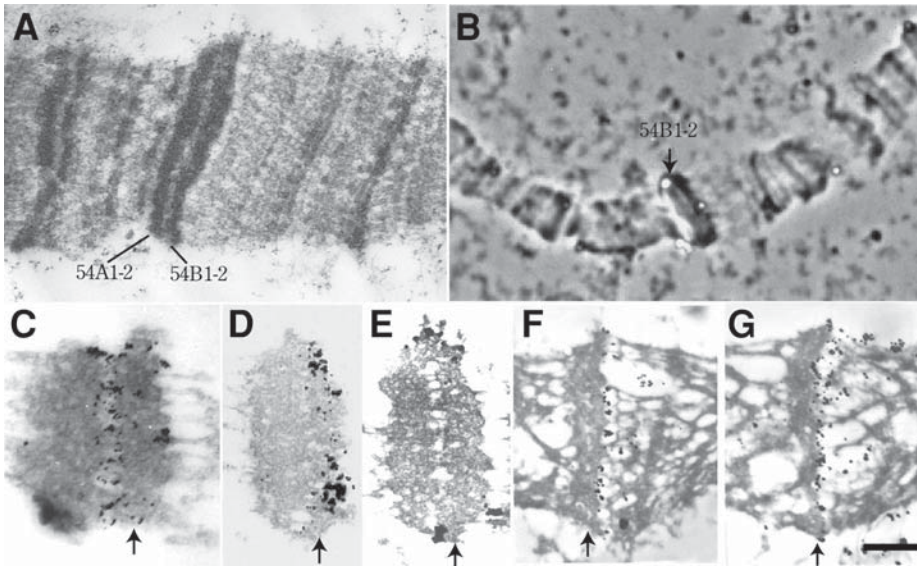

Fig. 5. Localization of the *mbl* gene in the 54AB region of chromosome 2R by EM *in situ* hybridization; **(A)** EM map of the 54AB region; **(B)** light microscope and **(C–G)** EM *in situ* hybridization pictures. The 54B1–2 band is indicated by the arrow. The *mbl* gene covers >100 kb ***(26)***. DNA probes from the 3' (S4), middle (+62), and 5' (mblH1) parts of the gene were used. The locations of hybridization signals are consistent with the molecular data ***(26)***; the S4 probe is localized in the interband region 54A1–2/B1–2 **(C)**, +62 probe in the 54B1–2 band **(B,D,E)**, and the *mbl*H1 probe in the 54B1–2/B3 interband **(F,G)**. In ultrathin serial sections, the distribution of gold particles is different for the dense and decondensed regions: in interbands, label can be found in all sections of series **(F,G)** but in condensed bands, only in the first one to two sections **(D,E)**. Data indicate that the *mbl* gene is orientated in the direction from centromere to telomere, consistent with data from the *Drosophila* genome sequencing project. Scale bar: 1 μm.

cessful ***(24)***, perhaps because the antibodies conjugated to the gold particles penetrated poorly into the epoxy resin ***(25)***. This possibility is supported by our observation that the hybridization signal is differentially distributed along the chromosome thickness in pre-embedding *in situ* hybridization experiments. When DNA is detected in large condensed bands, gold particles are seen mainly on the chromosome surface in the first sections of a series (*see* **Fig. 5D,E**); when it is detected in the decompacted regions, such as puffs or interbands, the gold label is more or less evenly distributed along the chromosome thickness and it is seen in all of the serial sections (*see* **Fig. 5C,F,G**). Fine mapping of DNA probes with respect to chromosome banding pattern is facilitated when photographs obtained by both EM *in situ* hybridization and the conventional

EM method are compared. The high resolution and specificity of probe location was shown for the P-lArB insertion and the *white* gene in a *D. melanogaster* transformed line (*see* **Fig. 4**). The method was also used for the fine mapping of the *mbl* gene, localized in the 54AB region of polytene chromosome 2R, which we were able to orientate on the chromosome (*see* **Fig. 5**).

1.4. EM Immunolocalization of Proteins in Polytene Chromosomes

Another powerful approach for investigating polytene chromosome organization is to precisely localize proteins in bands, interbands, and puffs. For this purpose, the method of indirect immunofluorescent (IF) analysis is widely used.

However, the potential of IF labeling is limited by the low resolving capacity of the light microscope. Overlapping of the fluorescence signals makes it difficult to finely localize antibodies in the loose regions of polytene chromosomes, which are, as a rule, composed of a series of fine bands hardly discernible under the light microscope. Some of the bands, the so-called minibands, are recognizable only at the ultrastructural level. Similarly, fluorescence signals cannot be resolved in regions where closely situated large bands are separated by fine interbands. There was a growing realization that such difficulties might be overcome by using electron microscopy. Assurance was provided by the localization of RNA polymerase B ***(27)***, acetylated isoforms of histone H4 ***(28)***, as well as a 74-kDa acidic chromosomal protein ***(29)*** by immuno-EM methods.

To improve and simplify the method, we attempted to localize a number of proteins specific to puffs, interbands, and bands, using conventional IF methodologies ***(30)*** in combination with the pre-embedding technique for gold-conjugated antibodies (*see* **Subheading 1.3.**). An example of its potential is presented in **Fig. 6**. We used monoclonal antibodies against the Z4 protein, which is located presumably in interbands ***(31)***. Our experiments confirmed this conclusion (*see* **Fig. 6**) as well as the absence of Z4 from the regions of large puffs. High specificity, discrete localization of immunogold label, and its conformity to IF patterns were shown for a number of other antibodies against different proteins distributed in fine bands, puffing bands, and puffs (i.e., in loosened chromosome regions). This method is described in **Subheading 3.4.**

In contrast, our attempts to detect proteins in dense bands using the immunogold EM method were unsuccessful. For example, using the IF technique, the SuUR (Suppressor of Underreplication) protein was localized to the bands of intercalary heterochromatin ***(32)***. Overexpression of the gene encoding SuUR in the GAL4–UAS system produced intensive IF staining of the majority of dense bands (*see* **Fig. 7A,B**). However, immunogold EM analysis of SuUR showed the gold particles to be distributed over the edges of the dense bands; the label was absent from the internal parts of these bands (*see* **Fig. 7C**). Similar results were obtained when antibodies against other proteins known to be associated with these bands were used.

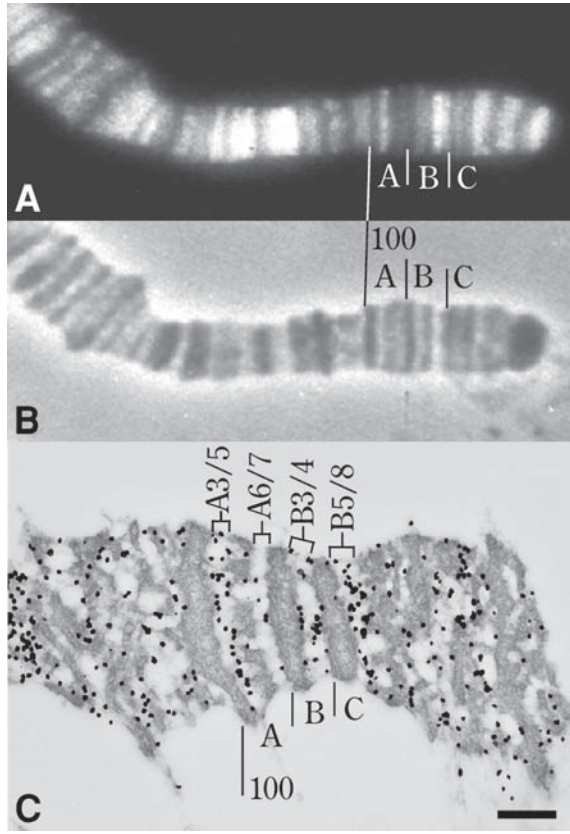

Fig. 6. Immunolocalization of the Z4 protein in the 100AC region of the 3R chromosome: **(A)** immunofluorescence, **(B)** phase contrast, and **(C)** immunogold EM images. Scale bar: 1 µm.

Taken together, these results indicate that the immunogold EM method did not enable detection of proteins in the dense regions of polytene chromosomes. Antibodies conjugated to gold particles apparently cannot penetrate into the compacted structures. Antibodies can interact only with the surface of the band, where they remain bound. A similar observation was made in our EM *in situ* hybridization study of digoxygenin labeled probes of band DNA (*see* **Subheading 1.3.**). Finally, it seems that antibody molecules may also become nonspecifically bound in loose chromosome regions. This is evidenced by the weak fluorescence shown by such regions and their labeling in ultrathin sections.

The advantage of the immunogold EM method is that it allows investigation of the fine topography and protein composition of interbands, thin or puffing bands,

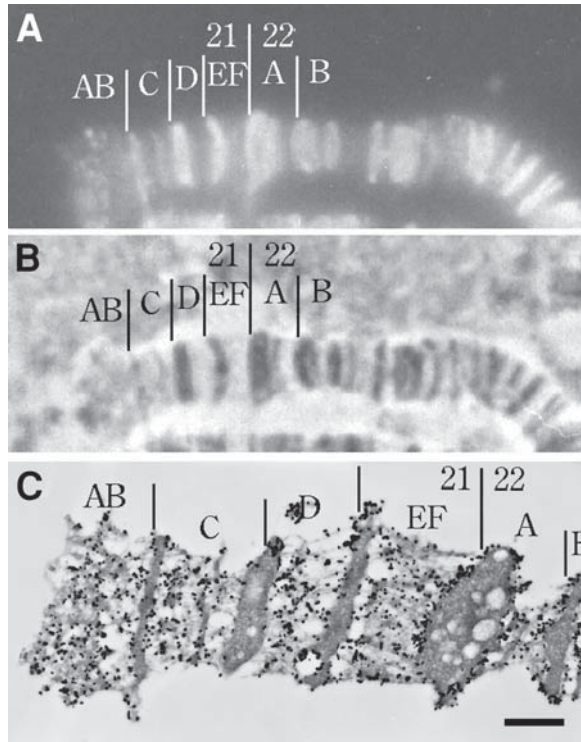

Fig. 7. Immunolocalization of antibody against the SuUR protein in the 21DE region of 2L chromosome 2L. The *SuUR* gene is overexpressed in the GAL4-UAS system: **(A)** immunofluorescence, **(B)** phase contrast, and **(C)** immunogold EM images. Scale bar: 1 µm.

and puffs. It is known that intense transcription of polytene chromosome sites is accompanied by band decondensation and puffing. Therefore, the immunogold EM method is suitable for localization of proteins involved in transcription.

2. Materials

1. Culturing medium for larvae: 50 g Corn meal, 40 g ground raisins, 20 g sugar, 100 g baker's yeast, 8–10 g agar, 4 mL propionic acid, 1 L water.
2. Standard fly culture vials.
3. Saline solution for salivary gland dissections: 7.5 g NaCl, 0.35 g KCl, 0.21 g $CaCl_2$, double-distilled or deionized water to 1000 mL.
4. ^{3}H-Uridine (1 mCi/mL, specific activity 44 Ci/m*M*); for autoradiography.
5. Alcohol : acid fixative: 3 vol of 96% ethanol : 1 vol glacial acetic acid. Prepare fresh and keep at 4°C.
6. Formaldehyde fixative: 100 m*M* NaCl, 2 m*M* KCl, 10 m*M* NaH_2PO_4, pH 7.2–7.4, 2% formaldehyde. Prepare fresh.

7. Phosphate-buffered saline (PBS): 137 m*M* NaCl, 3 m*M* KCl, 8 m*M* NaH_2PO_4, 2 m*M* KH_2PO_4, pH 7.2.
8. PBST: PBS + 0.1% Tween-20.
9. 20X SSC (standard saline citrate): 3 *M* NaCl, 0.3 *M* Na-citrate, pH 7.0.
10. Denaturation solution: 70% Formamide in 2X SSC.
11. Hybridization buffer: 50% Deionized formamide, 1% dextran sulfate, in 2X SSC.
12. Blocking solution: 0.1% Bovine serum albumin (BSA) in PBST.
13. DIG DNA labeling kit, for incorporation of digoxygenin 11-dUTP (Roche).
14. Genius 1 buffer: 150 m*M* NaCl, 100 m*M* maleic acid (Roche).
15. Genius 2 buffer: Genius 1 buffer containing 0.5% Genius blocking reagent.
16. Antidigoxigenin-gold (0.8 nm) sheep IgG (Roche).
17. Silver enhancement reagents (Roche).
18. Gold (10 nm)-conjugated goat anti-rabbit IgG (Sigma-Aldrich). Dilute 1 : 50 in blocking solution following the manufacturer's recommendations.
19. Gold (10 nm)-conjugated goat anti-mouse IgG (Sigma-Aldrich). Dilute 1 : 50 in blocking solution.
20. Ilford L-4 emulsion (England) and Kodak D-19 developer solution.
21. Araldite M, Araldite M Hardener, and Araldite M Accelerator (Fluka).
22. Silicone solution (Serva).
23. 45% Acetic acid.
24. 2% Uranyl acetate in 70% ethanol (*see* **Note 1**).
25. Ethanol series: 20%, 35%, 50%, 70%, and 96%.
26. Butanol.
27. Xylene.
28. Butanol : xylene (1 : 1, v/v).
29. Chloroform.
30. Siliconized microscopic slides (Superfrost slides, Erie Scientific Co.).
31. Siliconized cover slips (18×18 mm^2).
32. Copper EM grids (1000 μm mesh).
33. Curved watchmaker's forceps, finely sharpened.
34. Needles for tissue dissections, stiff and very fine.
35. Diamond pencil.
36. Cups of aluminum foil or of thin plastic (*see* **Note 2**).
37. Objective marker (*see* **Note 3**).
38. Petri dishes.
39. Liquid nitrogen.

3. Methods

3.1. Preparation of Thin Sections of Polytene Chromosomes

3.1.1. Dissection, Squashing, Staining, and Dehydration

1. Grow larvae at 18°C in culturing media under uncrowded conditions (40–50 larvae in a standard test tube). At 18°C, their development is delayed up to 10 d; however, the chromosomes become thicker than at 25°C.

2. Wash two to three larvae briefly in saline solution. Transfer them to a fresh portion of the same saline solution and dissect out the salivary glands with watchmaker's forceps or sharp stiff needles. Carefully remove the fat body. This should take approx 1 min.
3. Transfer the glands immediately to a small glass cup with alcohol : acid (3 : 1, v/v) fixative. The volume of fixative should not be less than 1.0 mL; the cup must be carefully closed and kept on ice. Continue with dissecting the remaining larvae, changing the saline solution for each larva. Rinse your dissecting instruments in distilled water after each round of dissection. Collect the salivary glands in the fixative, but do not put more than 15 in 1 cup. Fix them for 15 min to several hours.
4. Transfer a couple of salivary glands to a drop of 45% acetic acid (about 10 µL) on a siliconized cover slip. Incubate for 30–60 s.
5. Cover the glands with a siliconized microscope slide; turn the slide over, and gently presquash the glands by tapping over the cover slip with a blunt needle or a pencil eraser. Slightly move the cover slip in a circular motion with a needle.
6. Cover the squash with filter paper and squash hard with your finger or thumb. Examine the quality of the squash (chromosome spreading) under phase contrast. If it is unsatisfactory, repeat the squashing once more, first adding a small drop(s) of 45% acetic acid to the edge of the cover slip. If the result is satisfactory, use a diamond pencil to mark on the back side of the slide the field containing the chromosomes.
7. Freeze the slide in liquid nitrogen and remove the cover slip with a razor blade. Immediately place the slide in 96% ethanol.
8. Change the 96% ethanol two to three times, incubating the slide for 10 min in each change.
9. Collect the slides in 2% uranyl acetate/ethanol solution for contrasting, keeping them in this solution for 12–24 h at room temperature or longer at 4°C (*see* **Note 1**).
10. Dehydrate the squashes in a series of alcohol–xylene: two changes in 96% ethanol; two changes in butanol; two changes in butanol : xylene (1 : 1); two changes in xylene, 10 min in each.

3.1.2. Embedding in Epoxy Resin

1. Prepare the Araldite mixture: Combine Araldite *M* and Araldite M Hardener (1 : 1, v/v), warm at 60°C, and mix using a glass rod; add 2% of Araldite M Accelerator and mix again carefully. Fill aluminum foil cups with this mixture (*see* **Note 2**). In the following text the mixture of three Araldite M Components will be designated as Araldite.
2. Saturate the squashes with epoxy resin. To do this, incubate the slides in xylene : Araldite (1 : 3, v/v) and then in xylene : Araldite (3 : 1, v/v) for 10 min each.
3. Remove excess Araldite from the slide using filter paper. Be careful not to touch the marked region of the slide.
4. Place the marked region of the slide with Araldite in the center of the foil cup.
5. Press the cup against the slide and remove excess Araldite by filter paper.

6. Put the slides on a plate and polymerize the epoxy at 60°C for 24 h.
7. Freeze the slide in liquid nitrogen, detach the Araldite block from the slide, and remove it from the foil cup.
8. Set the Araldite block into the hole of the plastic holder (*see* **Note 2**) and select a chromosome by using a phase-contrast microscope.
9. Draw the chromosome contour. This will be useful for further identification of the chromosome region under the EM.
10. Scratch out a square with maximum dimensions of 0.2×0.2 mm^2 around selected chromosome using the objective marker (*see* **Note 3**).
11. Saw out the marked part of the block using a fret-saw (*see* **Note 3**). It is possible to get up to 10 small blocks from 1 initial embedding.
12. Trim a pyramid with a razor blade first roughly and then precisely with a new razor blade of high quality or with a glass knife using an Ultratome or Pyramitome.

3.1.3. Preparation of EM Grids

1. Dip a carefully cleaned microscopic slide in 0.25% Formvar solution in chloroform. Slowly pull the slide out of the solution and dry it for 1–2 min.
2. Cut the film along the slide edges with a razor blade and dip the filmed slide slowly at an angle of about 5°–10° into a Petri dish filled with distilled water. Allow the film to float onto the water surface (*see* **Note 4**).
3. Place the EM grids on the film.
4. Lower another microscope slide onto the film with grids at an angle of about 60° and pull it from the Petri dish.
5. Remove excess water with filter paper and dry the grids.
6. Stabilize the Formvar film by carbon coating to a thickness of approx 30–50 nm.
7. Store the slides with grids in special box or in a covered Petri dish to keep them free of dust.

3.1.4. Thin Sectioning of Chromosomes

1. Insert a trimmed block in the ultratome holder and orientate the pyramid surface in parallel with the knife's edge. For identification of chromosome regions in the EM, it is very important to section a block without distortions. Remember also that the diameter of a *Drosophila* polytene chromosome is approx 3–5 µm and only the first 15–20 sections have chromosome material.
2. Cut thin sections with the ultramicrotome. If the first two to three sections are incomplete (i.e., less than one-third of the area of the pyramid square), reorientate the pyramid to get more complete sections. If the size of the first sections reach at least half the area of the pyramid square, continue sectioning.
3. Using curved forceps, pick up 10–15 serial sections on a Formvar-coated grid. The simplest way to do this is by touching the grid with suitable chromosome sections.
4. Remove water from the grid using filter paper. Collect the specimens in a grid box.
5. Analyze the grids and, if suitable, photograph in the EM at 60–80 kV.

3.2. EM Autoradiography

1. Dissect salivary glands in saline solution as described in **Subheading 3.1.1., step 2** and collect them in a separate cup in saline solution.
2. Transfer 10–15 glands into saline solution containing ^{3}H-uridine and incubate for 5 min.
3. Fix the glands either in cold ethanol : acetic acid (3 : 1, v/v) for 15 min or in 45% acetic acid for 3–5 min.
4. Squash, stain, and dehydrate the glands as described in **Subheading 3.1.1., steps 4–10**.
5. Embed the glands in epoxy resin as described in **Subheading 3.1.2., steps 1–7**.
6. Check for ^{3}H-uridine incorporation by coating the Araldite blocks with liquid photographic emulsion. Expose in the dark for 72–120 h and then develop them with Kodak D-19 developer (3 min).
7. Choose specimens with high levels of labeling and remove the emulsion with warm water.
8. Proceed from **Subheading 3.1.2., step 8** continuing through to **Subheading 3.1.4., step 4**.
9. Assemble the grids with sections on a narrow strip of plexiglass using scotch tape. Prepare two to three similar strips with "empty" grids (i.e., without sections). These will be used to test the thickness and distribution of the emulsion.
10. Melt a portion of Ilford L-4 emulsion at 40°C in a dark room, dilute it with double-distilled water, and gently mix to homogeneity using a clean glass rod.
11. Cover "empty" grids with emulsion and check the distribution of silver grains under the EM. This test is to ensure that the emulsion gives a monolayer of halide silver crystals. If necessary, continue diluting the emulsion until the desired consistency is obtained. When working with photographic emulsion, follow the manufacturer's instructions.
12. Cover the grids having the sections with the same emulsion: Dip the plexiglass strip into the liquid emulsion, pull it out, and allow the emulsion to dry.
13. Expose the grids in a dark box for 2–2.5 mo.
14. Develop the preparations with Kodak D-19 developer (3 min).
15. Examine chromosome labeling under EM at 80 kV.

3.3. EM In Situ Hybridization of DNA to Polytene Chromosomes

The method is based on techniques developed by de Frutos et al. ***(20)*** for the light microscope with some modifications according to **ref. *24***.

3.3.1. Preparation of Polytene Chromosomes

1. Dissect and squash the salivary glands as described in **Subheading 3.1.1., steps 2–8**.
2. Collect and store the squashes in 70% ethanol. To spare the morphology of the polytene chromosomes, do not allow them to dry.
3. Postfix the chromosomes in 70% ethanol : formaldehyde : acetic acid (90 : 5 : 5, v/v/v) for 10 min before denaturation.

4. Wash and hydrate the squashes in an ethanol series (50%, 35%, and 20%) for 10 min each and collect them in 2X SSC.
5. Warm the squashes in 2X SSC for 2 min at 65°C.
6. Denaturate the chromosomes in 70% formamide diluted with 2X SSC at 65°C for 2 min.
7. Chill the squashes quickly in 2X SSC at 4°C.

3.3.2. Preparation of Probe

1. Place 1 µg of DNA in a microcentrifuge tube and add sterile distilled water to 15 µL (*see* **Note 5**).
2. Denature the DNA by boiling in a water bath for 5 min, then immediately place the tube on ice.
3. Add 2 µL of DIG DNA labeling mix (10X conc.), 2 µL hexanucleotide mix (10X conc.), and 1 µL (5 units) of Klenow fragment of DNA polymerase I. Incubate the reaction at 37°C for 1 h or overnight.
4. Ethanol-precipitate the labeled DNA and resuspend it in 50 µL of sterile distilled water.
5. Denature the DNA probe by boiling in a water bath for 5 min, then immediately put the tube on ice and add an equal volume of 2X hybridization buffer.

3.3.3. Hybridization

1. Drop 20 µL of hybridization mix on the slide, cover with a cover slip (avoid bubbles!), and seal with rubber cement. The amount of digoxigenin (DIG)-labeled DNA probe must be approximately 20 ng per slide.
2. Incubate the slides in a humid chamber overnight at 37°C.
3. Gently remove the cover slips in 2X SSC and wash the slides at room temperature as follows:
   a. Twice in 2X SSC for 5 min each.
   b. Twice in PBS for 5 min each.
   c. In PBS + 0.1% Triton X-100 for 3 min.
   d. Three times in PBS for 5 min each.
   e. Twice in Genius 1 buffer for 5 min each.
   f. In Genius 2 buffer for 30 min.
   g. In Genius 1 buffer for 5 min.
4. Drop on the slide anti-DIG-Gold diluted with PBST (1 : 30) and incubate under a cover slip in a humid chamber for 1 h at room temperature.
5. Wash slides at room temperature:
   a. Three times in PBST, 5 min each.
   b. Twice in PBS for 5 min.
   c. Six times in double-distilled water for 3 min each.
6. Incubate squashes with Silver Enhancement Reagent for 20 min, or longer, at room temperature under a cover slip. Check the appearance of the signal under a light microscope.

7. Wash the slides six times in double-distilled water.
8. Dehydrate the slides in 20%, 35%, 50%, and 70% ethanol for 10 min each.
9. Stain the chromosomes with uranyl acetate and dehydrate them as described in **Subheading 3.1.1., steps 9** and **10**.
10. Embed, mark and thin-section the chromosomes as described in **Subheadings 3.1.2–3.1.4.**

3.4. Immunogold EM Localization of Proteins on Polytene Chromosomes

3.4.1. Preparation of Polytene Chromosomes

1. Dissect the salivary glands in saline solution containing 1% Tween-20.
2. Transfer part of glands to a drop (30–50 µL) of formaldehyde fixative and fix them for 20–30 s.
3. Transfer the glands to a drop (30–50 µL) of 45% acetic acid containing 10% formaldehyde and fix them for 30–40 s.
4. Squash the glands as described in **Subheading 3.1.1., steps 4–6**.
5. Freeze the slide in liquid nitrogen.
6. Remove the cover slip with a razor blade and place the slide in 1.5% formaldehyde in PBS (postfixative), for 30 min.
7. Collect the slides in PBS at 4°C.

3.4.2. Incubation With Antibodies

1. Incubate the squashes in 0.1% BSA in PBST (blocking solution), using 50 µL per slide under a cover slip, in a humid chamber for 30 min at room temperature.
2. Gently remove the cover slip. Place 50 µL of primary antibodies (in blocking solution) on the slide and cover the squash with a cover slip (*see* **Note 6**). Keep the slides in a humid chamber for 2 h at room temperature or overnight at 4°C.
3. Remove the cover slip in PBST and wash the slide three times in PBST, 5 min each wash.
4. Place 50 µL of a 1 : 50 dilution of secondary antibodies conjugated with gold on each squash, cover with a cover slip, and incubate in humid chamber for 2 h at room temperature or overnight at 4°C.
5. Follow **Subheading 3.3.3., steps 5–10**.

4. Notes

1. Because the staining solution is saturated with uranyl acetate, this salt gives a sediment in bright light. To prevent or decrease sedimentation, add acetic acid to 0.2–0.3%. Keep it in a dark and cool place. It is possible to use the solution many times over several months.
2. To simplify and facilitate the embedding procedure, we use home-made cups of aluminum foil, as shown in **Fig. 8**. The most suitable thickness of foil for making such cups is 0.07–0.10 mm.
3. Technique of chromosome selection, marking and sawing small blocks is shown in **Fig. 9**. Using large Araldite blocks allows one to select the best quality chro-

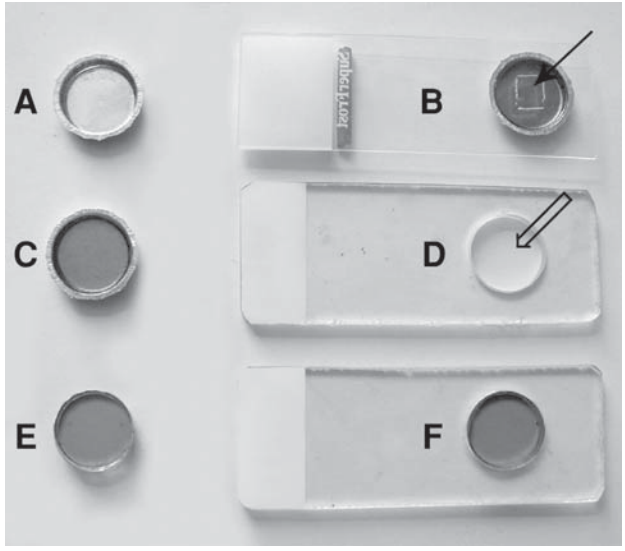

Fig. 8. Technique of chromosome embedding in epoxy–resin: **(A)** cup of aluminum foil; **(B)** slide with a squash to which the cup filled up with Araldite is attached. The square on the back side of the squash shows the field with chromosomes (arrow); **(C)** the cup with hard Araldite block after polymerization at 60°C for 24 h; the block was detached from the slide with a scalpel after dipping it in liquid nitrogen; **(D)** plastic holder for Araldite block; diameter of the hole (double arrow) is the same as the Araldite block after stripping the foil **(E)**; **(F)** Araldite block is inserted in the plastic holder for analysis under the light microscope.

mosomes under the light microscope with high magnification (100×). The selected chromosomes can be marked using a special objective marker (*see* **Fig. 9A**), which was devised by A. Yu. Kerkis ***(33,34)***.

4. Thickness of grid's film can be evaluated by its color. Usually, we use yellow or goldish film, with a thickness of 80–100 nm. Thickness of the film depends on the temperature and humidity of air in the room. Hot air and dry air make the film thinner, whereas low temperatures and humid air make it thicker. Change the concentration of Formvar to establish the desirable film thickness.
5. For best results, the DNA for *in situ* hybridization must be prepared in the form of restriction or polymerase chain reaction fragments with lengths ≥500 bp.
6. The antibody concentration has to be found experimentally using immunofluorescent techniques; it must not be less than 3–5 µg/mL.

Acknowledgments

We thank V.A. Melnikov and A. Yu. Kerkis for help and technical advice throughout the work, and E.N. Andreyeva for assistance with immunofluorescence

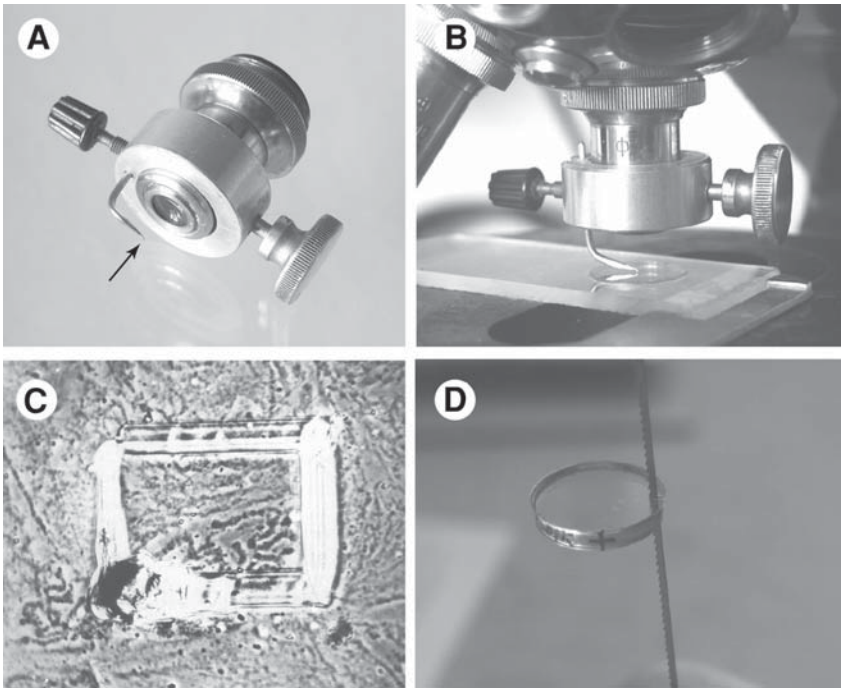

Fig. 9. Chromosome marking, sawing and trimming of small blocks from a large one: **(A)** Objective marker with sharp curved needle (arrow); the needle point is focused in the center of objective with low magnification (10×). **(B)** Chromosome contoured in Araldite block by the objective marker. **(C)** General view of the marked place under the microscope (10×). **(D)** Sawing of small Araldite block for trimming by a fret-saw.

analysis. This work was supported by grants from Russian Foundation for Basic Research (02-04-48222), Russian State Program Frontiers in Genetics (2-02), Lavrentiev Grant of Siberian Division of the Russian Academy of Sciences for young scientist and grants of the Ministry of Education of Russian Federation (PD02-1.4-74 and EO2-6.0-37).

References

1. Lindsley, D. L. and Zimm, G. G. (1992) *The Genome of* Drosophila melanogaster. Academic, San Diego, CA.
2. Saura, A. O. (1986) Electron microscopic mapping of the second polytene chromosome of *Drosophila melanogaster*: Ph.D. dissertation, University of Helsinki.
3. Sorsa, V. (1988) *Chromosome Maps of* Drosophila, CRC, Boca Raton, FL.
4. Heino, T. I., Saura, A. O., and Sorsa, V. (1994) Maps of the salivary gland chromosomes of *Drosophila melanogaster. Dros. Inform. Serv.* **73,** 619–738.
5. Semeshin, V. F., Zhimulev, I. F., and Belyaeva, E. S. (1979) Cytogenetic study on

the 9E–10A region of the X chromosome of *Drosophila melanogaster*. I. Morphology of the region and mapping of deletions involving the 10A1–2 band. *Genetika* **15,** 1784–1792 (in Russian).
6. Zhimulev, I. F., Semeshin, V. F., and Belyaeva, E. S. (1981) Fine cytogenetical analysis of the band 10A1–2 and the adjoining regions in the *Drosophila melanogaster* X-chromosome. I. Cytology of the region and mapping of chromosome rearrangaments. *Chromosoma* **82,** 9–23.
7. Zhimulev, I. F. (1996) Morphology and structure of polytene chromosomes. *Adv. Genet.* **34,** 1–490.
8. Berendes, H. D. (1970) Polytene chromosome structure at the submicroscopic level. I. A map of region X, 1–4E of *Drosophila melanogaster*. *Chromosoma* **29,** 118–130.
9. Atherton, D. and Gall, J. (1972) Salivary gland squashes for *in situ* nucleic acid hybridization studies. *Dros. Inform. Serv.* **49,** 131–133.
10. Semeshin, V. F., Demakov, S. A., Perez Alonso, M., Belyaeva, E. S., Bonner, J. J., and Zhimulev, I. F. (1989) Electron microscopical analysis of *Drosophila* polytene chromosomes. V. Characteristics of structures formed by transposed DNA segments of mobile elements. *Chromosoma* **97,** 396–412.
11. Semeshin, V. F., Baricheva, E. M., Belyaeva, E. S., and Zhimulev, I. F. (1985) Electron microscopical analysis of *Drosophila* polytene chromosomes. II. Development of complex puffs. *Chromosoma* **91,** 210–233.
12. Zhimulev, I. F. (1999) Genetic organization of polytene chromosomes. *Adv. Genet.* **39,** 1–599.
13. Semeshin, V. F., Zhimulev, I. F., and Belyaeva, E. S. (1979) Electron microscope autoradiographic study on transcriptional activity of *Drosophila melanogaster* polytene chromosomes. *Chromosoma* **73,** 163–177.
14. Pardue, M. L. (1986) *In situ* hybridization to DNA of chromosomes and nuclei, in Drosophila: *A Practical Approach* (Roberts, D.B., ed.), IRL, Oxford, pp. 111–137.
15. Wilkinson, D. G. (1992) The theory and practice of *in situ* hybridization, in *In Situ Hybridization: A Practical Approach* (Wilkinson, D. G., ed.), IRL, Oxford, pp. 1–13.
16. Gall, J. G. and Pardue, M. L. (1969) Formation and detection of RNA-DNA hybrid molecules in cytological preparations. *Proc. Natl. Acad. Sci. USA* **63,** 378–383.
17. Langer-Safer, P. R., Levine, M., and Ward, D. C. (1982) Immunological method for mapping genes on *Drosophila* polytene chromosomes. *Proc. Natl. Acad. Sci. USA* **79,** 4381–4385.
18. Engels, W. R., Preston, C. R., Thompson, P., and Eggleston, W. E. (1986) In situ hybridization to *Drosophila* salivary gland with biotinylated DNA probes and alkaline phosphate. *Focus* **8,** 6–8.
19. Pliley, M. D., Farmer, J. L., and Jeffrey, D. E. (1986) *In situ* hybridization of biotinylated DNA probes to polytene salivary chromosomes of Drosophila species. *Dros. Inform. Serv.* **63,** 147–149.
20. de Frutos, R., Kimura, K., and Peterson, K. (1990) *In situ* hybridization of *Drosophila* polytene chromosomes with digoxigenin–dUTP labeled probes. *Meth. Mol. Cell. Biol.* **2,** 32–36.

21. Wu, M. and Davidson, N. (1981) Transmission electron microscopic method for gene mapping on polytene chromosomes by *in situ* hybridization. *Proc. Natl. Acad. Sci. USA* **78,** 7059–7063.
22. Hutchison, N. J., Langer-Safer, P. R., Ward, D. C., and Hamkalo, B. A. (1982) *In situ* hybridization at the electron microscopic level: hybrid detection by autoradography and colloidal gold. *J. Cell Biol.* **95,** 609–618.
23. Kress, H., Meyerowitz, E. M., and Davidson, N. (1985) High resolution mapping of *in situ* hybridized biotinylated DNA to surface-spread *Drosophila* polytene chromosomes. *Chromosoma* **93,** 113–122.
24. Semeshin, V. F., Artero, R., Perez-Alonso, M., and Shloma, V. (1998) Electron microscopic *in situ* hybridization of digoxigenin–dUTP labeled probes with *Drosophila melanogaster* polytene chromosomes. *Chromosome Res.* **6,** 405–410.
25. Binder, M. (1992) *In situ* hybridization at the electron microscope level, in *In Situ Hybridization: a Practical Approach* (Wilkinson, D.G., ed.), IRL, Oxford, pp. 105–120.
26. Begemann, G., Paricio, N., Artero, R., Kiss, I., Perec-Alonso, M., and Mlodzik, M. (1997) *muscleblind*, a gene required for photoreceptor differentiation in *Drosophila*, encodes novel nuclear Cys_3 His-type zinc-finger-containing proteins. *Development* **124,** 4321–4331.
27. Sass, H. and Bautz, F, E. K. (1982) Immunoelectron microscopic localization of RNA polymerase B on isolated polytene chromosomes of *Chironomus tentans*. *Chromosoma* **85,** 633–642.
28. Turner, B. M., Franchi, L., and Wallace, H. (1990) Islands of acetylated histone H4 in polytene chromosomes and their relationship to chromatin packaging and transcriptional activity. *J. Cell Sci.* **96,** 335–346.
29. Hill, R. J., Mott, M., and Steffensen, D. M. (1987) The preparation of polytene chromosomes for localization of nucleic acid sequences, proteins, and chromatin conformation. *Int. Rev. Cytol.* **108,** 61–118.
30. Clark, R. F., Wagner, C. R., Craig, C. A., and Elgin, R, S. C. (1991) Distribution of chromosomal proteins in polytene chromosomes of *Drosophila. Methods Cell Biol.* **35,** 203–227
31. Saumweber, H., Symmons, P., Kabisch, R., Will, H., and Bonhoeffer, F. (1980) Monoclonal antibodies against chromosomal proteins of *Drosophila melanogaster*. Establishment of antibody producing cell lines and partial characterization of corresponding antigens. *Chromosoma* **80,** 253–275.
32. Makunin, I. V., Volkova, E. I., Belyaeva, E. S., Nabirochkina, E. N., Pirrotta, V., and Zhimulev, I. F. (2002) The *Drosophila* Suppressor of Underreplication protein binds to late-replicating regions of polytene chromosomes. *Genetics* **160,** 1023–1034.
33. Kristolyubova, N. B. and Kerkis, Yu, A. (1968) The application of the "light" radioautography for electron microscopy investigations *Cytology* **10,** 1497–1499 (in Russian).
34. Kerkis, A.Yu., Zhimulev, I.F., and Belyaeva, E.S. (1975) A method of electron microscopic autoradiography for studying the structural and functional organization of definite regions of polytene chromosomes. *Cytology* **17,** 1330–1331 (in Russian).

16

Analysis of Mitosis in Squash Preparations of Larval Brains

Orcein, Giemsa, Hoechst 33258, DAPI, Quinacrine, and N-Banding

Laura Fanti and Sergio Pimpinelli

1. Introduction

The cytology of mitotic chromosomes has proved to be essential for research into different aspects of *Drosophila* biology. Cytological approaches are routinely used to study mutations that affect chromosome behavior or structure. Moreover, cytological methods are essential for analyzing heterochromatin (*see* **ref. *1*** for review). This material is largely refractory to both genetic and molecular analyses because of the absence of recombination and because of its high content of repetitive DNA sequences. In addition, heterochromatin cannot be analyzed effectively on polytene chromosomes because it is underreplicated and included in the chromocenter. However, by applying high-resolution banding techniques (e.g., quinacrine, Hoechst, and N-banding) and fluorescence *in situ* hybridization (FISH) to mitotic chromosomes, one can precisely determine the breakpoints of heterochromatic rearrangements and map different types of heterochromatic DNA sequences.

Several squashing techniques have been developed for the preparation of larval brain mitotic chromosomes ***(2,3)***. Here, we describe a series of squashing protocols that we routinely use for different experimental purposes and that can be successfully applied for chromosome preparation in other *Drosophila* and mosquito species ***(4–9)***.

2. Materials

2.1. Fixation of Mitotic Chromosomes

1. Physiological solution: 0.7% NaCl in distilled water. Autoclave and store at 4°C.
2. Hypotonic solution: 0.5% Tri-sodium citrate dihydrate in distilled water. Autoclave and store at 4°C.

From: *Methods in Molecular Biology, vol. 247:* Drosophila *Cytogenetics Protocols*
Edited by: D. S. Henderson © Humana Press Inc., Totowa, NJ

3. Fixative solution: Methanol/acetic acid/distilled water in the ratio 11 : 11 : 2 (v/v/v). Methanol is poisonous. It may be harmful by inhalation, ingestion, and skin absorption. Handle it in a chemical fume hood.
4. Liquid nitrogen. **Caution:** Liquid nitrogen is very dangerous because of its extreme temperature; wear cryo-mitts and a face mask.
5. Siliconized microscope slides.
6. Cover slips, 20×20 mm^2 or 22×22 mm^2.
7. Thin forceps (e.g., Dumont no. 5 Biologie).
8. Razor blade.
9. Absolute ethanol.

2.2. Orcein Staining

1. Physiological solution (*see* **Subheading 2.1., item 1**).
2. 1 m*M* Colchicine.
3. 35 × 10-mm Petri dish.
4. Hypotonic solution (*see* **Subheading 2.1., item 2**).
5. Fixative solution (*see* **Subheading 2.1., item 3**).
6. 2% Aceto-orcein solution: This solution is prepared by boiling synthetic orcein powder (Gurr) in 45% acetic acid for 45 min in a reflux condenser. To obtain good staining, it is important to remove the particulate matter from the aceto-orcein solution before use either by filtration through blotting paper or by centrifugation in a microcentrifuge.
7. Nail polish or depilatory wax (can be found in most cosmetic shops).

2.3. Giemsa Staining

1. 2% Giemsa in a phosphate buffer at pH 7.0. We routinely use Giemsa from Merck, but other Giemsa brands work just as well.
2. Euparal.

2.4. Hoechst Staining

1. Hoechst buffer (HB): 150 m*M* NaCl, 30 m*M* KCl, 10 m*M* Na_2PO_4, pH 7.0. Store at room temperature.
2. Hoechst solution: 0.5 µg/mL Hoechst 33258 dissolved in HB.
3. Mounting solution: 160 m*M* Na_2HPO_4, 40 m*M* sodium citrate, pH 7.0.
4. Rubber cement.

2.5. DAPI Staining

1. DAPI (4',6-diamidine-2-phenylindole dihydrochloride) stock solution: 100 µg/mL DAPI in distilled water. It can be stored in the dark at 4°C. It is a carcinogen and an irritant. It may be harmful by inhalation, ingestion, and skin absorption. Wear gloves and use it in a chemical fume hood.
2. 20X SSC: 3 *M* NaCl, 0.3 *M* sodium citrate, pH 7.0. Sterilize by autoclaving and store at room temperature.

3. DAPI staining solution: 0.2 µg/mL DAPI dissolved in 2X SSC. Store at 4°C.
4. Vectashield-1000 (Vector Laboratories) or similar mounting medium containing glycerol and antifading compounds.

2.6. Quinacrine Staining

1. Absolute ethanol.
2. Quinacrine solution: 0.5% Quinacrine dihydrochloride (Gurr) dissolved in absolute ethanol.
3. Rubber cement.

2.7. N-Banding

1. 1 *M* $Na_2H_2PO_4$ solution, pH 7.0, for heat treatment.
2. Giemsa solution: 4% Giemsa (Merck) in sodium phosphate buffer at pH 7.0.
3. Euparal or similar mounting medium.

3. Methods

3.1. Orcein Staining

1. Transfer third instar larvae into drops of approx 50 µL of physiological solution placed on a siliconized slide and dissect the brains at room temperature (*see* **Note 1**).
2. Transfer the brains to a 35 × 10-mm covered Petri dish containing 2 mL of physiological solution and a drop of 1 m*M* colchicine and incubate for 1.5 h at 25°C (*see* **Note 2**).
3. Transfer the brains to a drop of hypotonic solution for 10 min at room temperature (*see* **Note 2**).
4. Transfer the brains to freshly prepared fixative solution for approx 20 s (check, however, the fixation under the dissecting microscope and continue to incubate the brains until they begin to become transparent).
5. Transfer four fixed brains individually into four small drops of 2% aceto-orcein placed on a very clean, dust-free nonsiliconized 20 × 20 or 22 × 22-mm^2 cover slip and leave for 1–2 min.
6. Lower a very clean, dust-free slide onto the cover slip, which will adhere because of the surface tension. Invert the sandwich and squash between two or three sheets of blotting paper. To prevent the cover slip from sliding and the consequent damage to the preparation, squashing should be carried out in two steps. First, exert a gentle pressure to remove the excess of aceto-orcein and then squash very hard.
7. Seal the edges of the cover slip with either nail polish or melted depilatory wax (*see* **Note 3**) (*see* **Fig. 1A–C** for examples of orcein-stained chromosomes).

3.2. Fixation of Mitotic Chromosomes for Giemsa, Hoechst, DAPI, and Quinacrine Staining and N-Banding

1. Transfer third instar larvae into drops of approx 50 µL of physiological solution placed on a siliconized slide and dissect out the brains at room temperature (*see* **Note 1**).

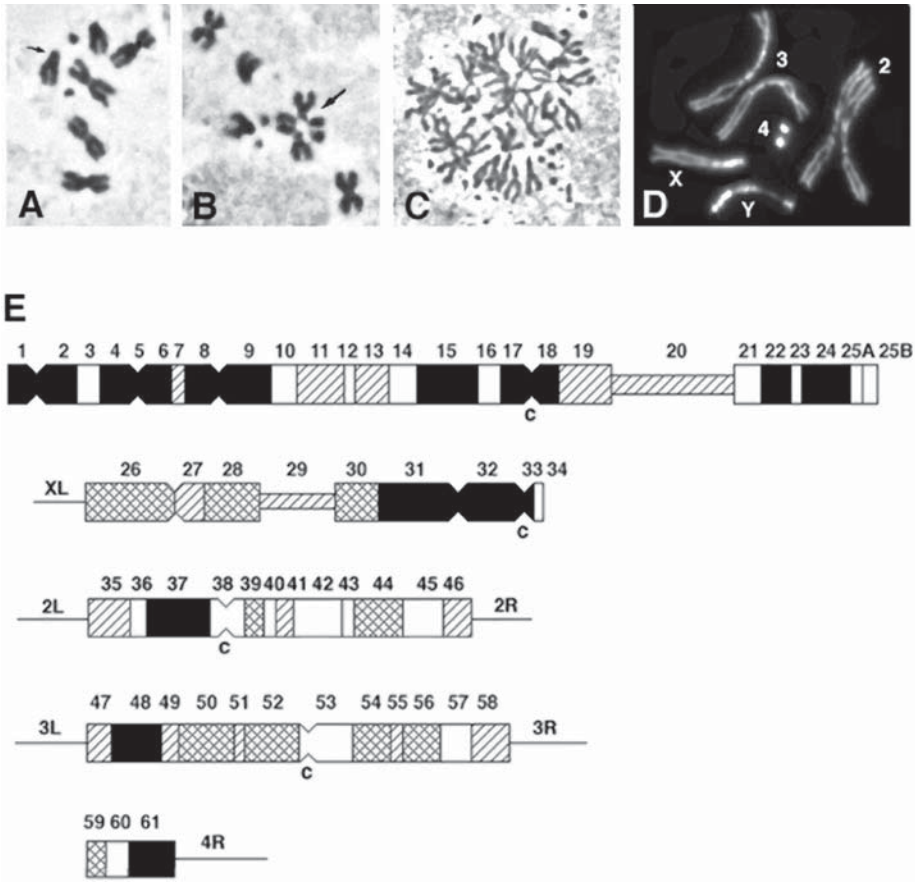

Fig. 1. Examples of orcein- and DAPI-stained mitotic chromosome preparations of *D. melanogaster* neuroblasts. **(A)** Colchicine- and hypotonic-treated wild-type female metaphase; **(B)** colchicine- and hypotonic-treated female metaphase showing an autosomal symmetrical exchange (arrow); **(C)** colchicine- and hypotonic-treated mutant female metaphase showing a high degree of polyploidy; **(D)** DAPI-stained male metaphase; **(E)** cytological map of *D. melanogaster* heterochromatin. The diagrams are representative of prometaphase neuroblast chromosomes stained with Hoechst 33258 or DAPI. Only the heterochromatic portions of chromosomes are shown, with euchromatin depicted as a thin line. The entirely heterochromatic Y chromosome, the X chromosome, and the second, third, and the fourth chromosome heterochromatin are schematically represented from top to bottom. "C" indicates the position of the centromere; the location of the fourth chromosome centromere has not been precisely determined. Filled segments indicate bright fluorescence, cross-hatched segments indicate moderate fluorescence, hatched segments indicate dull fluorescence, and open segments indicate no fluorescence. These segments or bands are designated h1 to h61, as indicated.

2. Transfer the brains to a drop of hypotonic solution for 10 min at room temperature (*see* **Note 2**).
3. Transfer the brains to freshly prepared fixative solution for approx 20 s (check, however, the fixation under the dissecting microscope and keep the brains in the fixative until they begin to become transparent).
4. Transfer four fixed brains individually into four small drops of 45% acetic acid placed on a very clean, dust-free siliconized 20 × 20 or 22 × 22-mm^2 cover slip and leave for 1–2 min.
5. Lower a very clean, dust-free slide onto the cover slip, which will adhere because of the surface tension. To prevent the cover slip from sliding and the consequent damage to the preparation, squashing should be carried out in two steps. First, exert a gentle pressure to remove excess acetic acid and then squash very hard.
6. Freeze the slide in liquid nitrogen.
7. Flip off the cover slip with a razor blade and immediately immerse the slide in absolute ethanol at room temperature. Air-dry the slides and store them at 4°C until further processing.

3.3. Giemsa Staining (see Note 4)

1. Rehydrate the air-dried slides in Hoechst buffer (HB) for 5 min at room temperature.
2. Stain in Giemsa staining solution for 10 min at room temperature (*see* **Note 5**).
3. Differentiate the chromosome preparations by washing the slides in tap water (*see* **Note 6**) and then air-dry the slides.
4. Mount in Euparal or similar medium.

3.4. Hoechst Staining (see Note 7)

1. Rehydrate the air-dried slides in Hoechst buffer (HB) for 5 min at room temperature.
2. Stain in Hoechst solution for 10 min at room temperature.
3. Wash briefly (approx 5 s) in HB.
4. Air-dry the slides, keeping them in a vertical position.
5. Mount either in HB or mounting solution.
6. Seal around the edges of the cover slip with rubber cement.
7. To reduce fluorescence fading, store the slides in the dark at 4°C for 1–2 d before observation (*see* **Note 8**).

3.5. DAPI Staining

1. Rehydrate the slides for 5 min in 2X SSC at room temperature.
2. Stain in DAPI solution for 5 min at room temperature.
3. Wash briefly (approx 5 s) in 2X SSC solution.
4. Air-dry the slides, keeping them in a vertical position.
5. Mount in Vectashield-1000 or in a similar medium containing glycerol and antifading compounds. For examples of DAPI-stained chromosomes, *see* **Fig. 1D,E**.

3.6. Quinacrine Staining (see Note 9)

1. Immerse the slides with fixed chromosomes in absolute ethanol for 5 min.
2. Stain the slides in quinacrine solution for 10 min.
3. Wash the slides twice (5 s each wash) in absolute ethanol.
4. Air-dry the slides, keeping them in a vertical position.
5. Mount in distilled water.
6. Seal around the edges of the cover slip with rubber cement.
7. Store the slides in the dark at 4°C before observation to reduce fluorescence fading and to improve the degree of differentiation (*see* **Note 8**).

3.7. N-Banding (see Note 10)

1. Immerse the slides with fixed chromosomes in 1 *M* $Na_2H_2PO_4$, pH 7.0, at 85°C, and incubate for 15 min.
2. Transfer the slides to distilled water at room temperature.
3. Stain the slides in Giemsa solution for 20 min at room temperature.
4. Differentiate the chromosome preparations by washing the slides in tap water (*see* **Note 6**).
5. Air-dry the slides.
6. Mount in Euparal or similar medium.
7. Examine the slides using phase-contrast optics.

4. Notes

1. Use two fine forceps (e.g., Dumont no. 5 Biologie) to easily dissect the brains. The larval mouth parts and the posterior part of the larval body should be grasped and then pulled apart. Because the brain usually remains attached to the head together with several imaginal discs and the salivary glands, the more rigid mouth parts should be completely removed with the forceps.
2. Colchicine incubation followed by hypotonic treatment permits one to obtain a large number of good metaphase figures (200–400 per brain) that can be analyzed for chromosome morphology, presence of chromosome aberrations and degree of ploidy. However, to examine the degree of chromosome condensation, the colchicine must be omitted because this substance disrupts spindle microtubules and induces metaphase arrest and overcontraction of chromosomes. Hypotonic treatment improves metaphase chromosome spreading and causes sister-chromatid separation, allowing examination of chromosome condensation. Because hypotonic shock disrupts anaphase ***(10)***, these figures are almost always absent in hypotonically treated brains. To observe all phases of mitosis and to evaluate the mitotic index and frequency of anaphases, the dissected brains should be squashed in aceto-orcein without colchicine treatment and hypotonic shock, although in such preparations, chromosome morphology is not so well defined ***(11)***.
3. Well-sealed slides can be stored for 1–2 mo at 4°C without substantial deterioration.
4. Giemsa staining is required for permanent preparations. This can be done by staining fixed chromosomes.

5. The timing of Giemsa staining varies with the Giemsa brand and should be adjusted to obtain the desired staining.
6. Because Giemsa stain is additive, if the chromosomes are not sufficiently stained, the slide can be stained again in 2% Giemsa until the desired staining is obtained.
7. This protocol ***(5,12)*** is a modified version of the protocol described by Latt ***(13)*** for mammalian chromosomes. Other protocols have been described ***(14,15)***.
8. Fluorescence fading depends on both the lamp and the filter sets used for epifluorescence. If the degree of fading is too high, the slides may be mounted in Vectashield-1000 or in a similar medium containing glycerol and antifading compounds.
9. This quinacrine staining protocol was developed by Gatti et al. ***(5)***. Other quinacrine banding techniques have been described by Vosa ***(16)***, Ellison and Barr ***(17)*** and Faccio Dolfini ***(18)***.
10. The N-banding procedure is essentially that of Funaki et al. ***(19)*** with minor modifications ***(7)***. Best results are obtained when fixed preparations are aged for 2–5 d at 4°C before processing.

References

1. Gatti, M. and Pimpinelli, S. (1992) Functional elements in *Drosophila melanogaster* heterochromatin. *Annu. Rev. Genet.* **26,** 239–275.
2. Ashburner, M. (1989) Drosophila: *A Laboratory Handbook.* Cold Spring Harbor Laboratory Press, Cold Spring Harbor, NY.
3. Gonzalez, C. and Glover, D. M. (1993) Techniques for studying mitosis in *Drosophila*, in *The Cell Cycle: A Practical Approach* (Fantes, P. and Brooks, R., eds.), IRL, Oxford, pp. 143–175.
4. Gatti, M., Tanzarella, C., and Olivieri, G. (1974) Analysis of the chromosome aberrations induced by X-rays in somatic cells of *Drosophila melanogaster*. *Genetics* **77,** 701–719.
5. Gatti, M., Pimpinelli, S., and Santini, G. (1976) Characterization of *Drosophila* heterochromatin. Staining and decondensation with Hoechst 33258 and quinacrine. *Chromosoma* **57,** 351–375.
6. Pimpinelli, S., Pignone, D., Gatti, M., and Olivieri, G. (1976) X-ray induction of chromatid interchanges in somatic cells of *Drosophila melanogaster*: variation through the cell cycle of the pattern of rejoining. *Mutat. Res.* **35,** 101–110.
7. Pimpinelli, S., Santini, G., and Gatti, M. (1976) Characterization of *Drosophila* heterochromatin. II. C- and N-banding. *Chromosoma* **57,** 377–386.
8. Bonaccorsi, S., Santini, G., Gatti, M., Pimpinelli, S., and Coluzzi, M. (1980) Intraspecific polymorphism of sex chromosome heterochromatin in two species of the *Anopheles gambiae* complex. *Chromosoma* **76,** 57–64.
9. Bonaccorsi, S., Pimpinelli, S., and Gatti, M. (1981) Cytological dissection of sex chromosome heterochromatin of *Drosophila hydei*. *Chromosoma* **84,** 391–403.
10. Brinkley, B. R., Cox, S. M., and Pepper, D. A. (1980) Structure of the mitotic apparatus and chromosomes after hypotonic treatment of mammalian cells in vitro. *Cytogenet. Cell Genet.* **26,** 165–176.

11. Gatti, M. and Baker, B. S. (1989) Genes controlling essential cell cycle functions in *Drosophila melanogaster*. *Genes Dev.* **3,** 438–453.
12. Gatti, M. and Pimpinelli, S. (1983) Cytological and genetic analysis of the Y chromosome of *Drosophila melanogaster*. I. Organization of the fertility factors. *Chromosoma* **88,** 349–373.
13. Latt, S. A. (1973) Microfluorimetric detection of deoxyribonucleic acid replication in human metaphase chromosomes. *Proc. Natl. Acad. Sci. USA* **70,** 3395–3399.
14. Holmquist, G. (1975) Hoechst 33258 fluorescent staining of *Drosophila* chromosomes. *Chromosoma* **49,** 333–356.
15. Hazelrigg, T., Fornili, P., and Kaufman, T. C. (1982) A cytogenetic analysis of X-ray induced male steriles on the Y chromosome of *Drosophila melanogaster*. *Chromosoma* **87,** 535–559.
16. Vosa, C. G. (1970) The discriminating fluorescence patterns of the chromosomes of *Drosophila melanogaster*. *Chromosoma* **31,** 446–451.
17. Ellison, J. R. and Barr, H. J. (1971) Differences in the quinacrine staining of the chromosomes of a pair of sibling species: *Drosophila melanogaster* and *Drosophila simulans*. *Chromosoma* **44,** 424–435.
18. Faccio Dolfini, S. (1974) The distribution of repetitive DNA in the chromosomes of cultured cells of *Drosophila melanogaster*. *Chromosoma* **44,** 383–391.
19. Funaki, K., Matsui, S., and Sasaki, M. (1975) Location of nucleolar organizers in animal and plant chromosomes by means of an improved N-banding technique. *Chromosoma* **49,** 357–370.

17

Analyzing Chromosome Function by High Frequency Formation of Dicentric Chromosomes In Vivo

Kami Ahmad and Kent G. Golic

1. Introduction

The generation of dicentric chromosomes by site-specific recombination is a technique that has been used to study a number of different chromosomal phenomena, including: (1) the segregation of acentric chromosome fragments ***(1,2)***, (2) the behavior and resolution of chromosome bridges during cell division ***(3,4)***, and (3) cellular responses to a broken chromosome end ***(4)***. Its greatest advantage is that it allows quantitative experiments on the behavior and cellular consequences of this class of chromosome rearrangement. Furthermore, recombinase-mediated dicentric chromosome formation is specific in that the timing of formation and specification of the chromosomes that are involved are defined by controlled expression of a recombinase and the location of recombinase target sites, respectively. Choice of target sites provides a sophisticated degree of control over the genetic aneuploidy that can result from cell division after a dicentric chromosome is produced. Use of such a predictable, quantitative system can be quite powerful. For example, efficient production of dicentric Y chromosomes aided in the cell cycle analysis of DNA damage responses in *Drosophila* somatic cells, with significant differences from experiments performed with random (X-ray) methods ***(4)***.

The yeast FLP/*FRT* site-specific recombination system has been successfully imported by *P*-element transformation into *Drosophila* and operates with high efficiency and specificity ***(5)***. The precise and predefined recombination mediated by this system has been extensively used for deletion of parts of *P*-element constructs or of genomic sequences between two *P* elements, transgene activation, transgene episome generation, mosaic clonal analysis,

From: *Methods in Molecular Biology, vol. 247:* Drosophila *Cytogenetics Protocols*
Edited by: D. S. Henderson © Humana Press Inc., Totowa, NJ

generation of defined chromosomal rearrangements, and insertion of DNA into specified locations within the genome ***(6,7)***. Two components are introduced into flies to achieve FLP-mediated recombination: a transgene that will produce the FLP recombinase, and transgenes that carry the FLP Recombination Target (*FRT*) sites. Production of FLP (typically from a heat-shock-inducible *hsFLP* transgene) results in recombination between pairs of *FRT* sites. *FRT* sites are asymmetric; thus, the possible recombination products from any two sites can be predicted given the relative orientation of the two sites (direct or inverted) in the genome.

The frequency of recombination events varies according to the distance between the two *FRT* sites, the linkage relationship (cis/trans on homologs or heterologs), the sequence context of each site, and their chromosomal context ***(8–11)***. In most circumstances, recombination between two nearby *FRT*s is extremely frequent, approaching 100% efficiency. Dicentric chromosome formation results from exchange between two *FRT*s that lie in an inverted relative orientation on the same chromosome arm of replicated sister chromatids (*see* **Fig. 1**). The chromosomal material distal to the *FRT* sites is released as an acentric inverted duplication fragment, whereas the proximal material forms a dicentric chromosome. In the following mitotic division, the acentric fragment fails to segregate to daughter cells, whereas the dicentric portion forms a chromosome bridge as the two sister centromeres are pulled to opposite poles. The genetic consequences of this division are the loss of all genetic material distal to the *FRT* sites and loss or duplication of more proximal material if the dicentric chromosome breaks at any location other than the site of sister-chromatid fusion. In most cases, the loss of chromosomal material is significant and the resulting daughter cells are severely aneuploid.

A pair of inverted *FRT*s in 8F of the X chromosome was used to test the efficiency of dicentric formation and to examine its phenotypic consequences ***(8)***. Heat-shock-induced production of FLP in larvae resulted in substantial pupal lethality and produced defects in the eyes, wings, tergites, and bristles in the individuals that eclosed as adults. This syndrome was consistent with the production of aneuploid cells after dicentric formation and division, and aneuploidy specifically for the X chromosome was confirmed by consequent loss of a distal *yellow*$^+$ marker. There was no evidence that rearrangements in other parts of the genome occurred. Approximately 90% of mitotic figures in larval brain tissue showed dicentrics (*see* **Fig 1B,C**), demonstrating that the frequency of unequal sister-chromatid exchange between *FRT*s was very high. Although FLP-mediated recombination is expected to be a reversible reaction, dicentric formation might be favored if the freed reciprocal acentric and dicentric products drift apart, which would preclude their reunion by another round of recombination.

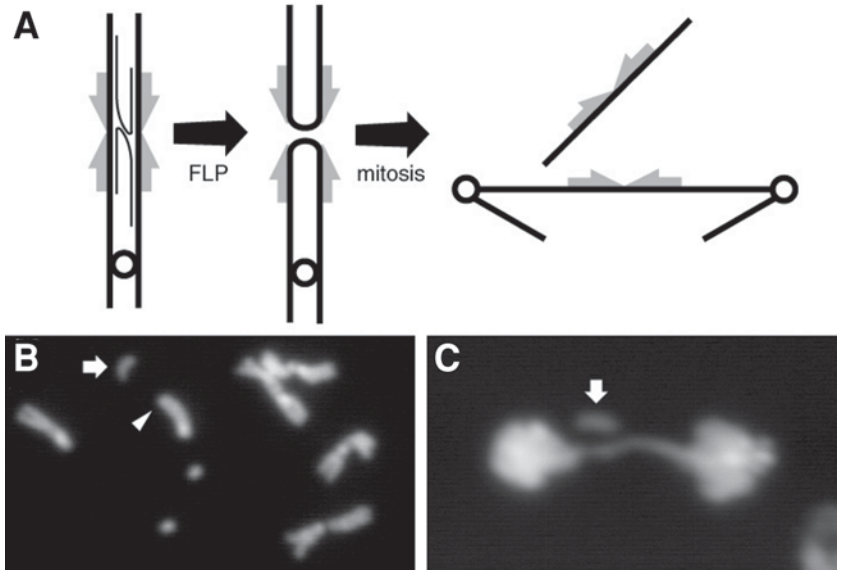

Fig. 1. Dicentric formation by FLP-mediated unequal sister chromatid exchange. **(A)** Recombination between inverted *FRT*s (gray half-arrows) on replicated sister chromatids produces a dicentric chromosome and an acentric fragment. **(B)** An acentric fragment (arrow) and a truncated dicentric chromosome (arrowhead) can be seen after FLP recombination on the X chromosome. **(C)** A dicentric bridge spans the two poles of division in anaphase, whereas the acentric fragment (arrow) fails to segregate.

High-efficiency dicentric chromosome formation has been used to address several questions related to chromosome function. Dicentric formation on a nonessential, marked Y chromosome was used to analyze the operation of cell cycle checkpoint responses to the single double-strand break produced by mitotic breakage of the dicentric ***(4)***. The chromosomal specificity of the double-strand break allowed clear determination of the features of cellular responses, separable from the consequences of aneuploidy that are invariably associated with the induction of DNA damage by random methods. Other experiments have focused on the distal acentric fragment for the analysis of chromsome segregation. Chromosomal material separated by radiation-induced chromosome breakage from a very small minichromosome exhibits centromere activity, but the distal portion of a normal X chromosome (released by site-specific recombination) does not ***(1)***. A similar system was used to show that the bw^D heterochromatic satellite block does confer weak centromeric activity to a released acentric fragment ***(2)***.

All of these studies used existing *P*-element insertion lines and markers to construct strains suitable for the intended dicentric experiment. The following protocols outline the development and characterization of a strain competent for dicentric formation. A particular example, beginning with a single *FRT*-bearing *P*-element insertion on chromosome 3 is presented. A similar protocol can be developed for any insertion of an *FRT*-bearing construct, using appropriate balancer strains. The rationale for various steps is included in **Subheading 4.**

2. Materials

2.1. Fly Strains

1. Transposase strain: w^{1118}*; Sb P[Δ2–3, ry*$^{+}$*]*99B*/TM6B*.
2. Recovery strain: w^{1118}.
3. Extraction strain (for chromosome 3): w^{1118}*; Sb/TM6B*.
4. *FRT*-bearing insertion line: w^{1118}*; P[>*w^{hs}*>]*(67A)1C (*see* **Note 1**).
5. FLP source: w^{1118} *; P[70FLP, ry*$^{+}$*]*4A.

2.2. Fly Manipulations

1. Standard fly food in vials and milk bottles.
2. Water bath equilibrated at 38±0.5°C.
3. Standard dissecting microscope, anesthetizer, and fly manipulation tools.
4. Waterproof marker.

2.3. Mitotic Characterization

1. No. 5 dissection forceps.
2. Dissection dish.
3. Phosphate-buffered saline (PBS), pH 7.0.
4. 0.5% Sodium citrate solution, pH 7.0.
5. 45% Acetic acid.
6. Glass microscope slides.
7. 22-mm^2 siliconized glass cover slips.
8. 25-mm^2 No. 1 1/2 glass cover slips.
9. Whatman filter paper.
10. Dry ice.
11. Razor blade.
12. 0.5 µg/mL 4',6-Diamidino-2-phenylindole (DAPI) in PBS.
13. Coplin staining jars.
14. Glycerol mounting medium.
15. Compound fluorescence microscope, equipped with 100× objective lens and a filter set for DAPI.

2.4. Time-Course Analysis

1. No. 5 dissection forceps.
2. Compound microscope and dissecting microscope equipped for color photography.

3. Methods

3.1. Fly Strains

All strains are grown on standard fly food medium ***(12)*** at 25°C. Crosses for the generation of dicentric chromosomes are performed in vials.

3.2. Fly Manipulations

3.2.1. Generation of Lines Carrying Duplicate P-Element Insertions

1. G0 cross: Mate flies from a single-copy *P[>w^{hs}>]* insertion line (the element is marked with a w^{hs} marker and gives an orange eye color) to flies from the transposase strain to mobilize the construct. Collect male progeny with Stubble bristles (genotype: w^{1118}*/Y; P[>*w^{hs}*>]*45*/Sb P[Δ2–3, ry*$^{+}$*]*99B*)*.
2. G1 cross: Mate individual males to three virgin w^{1118} females in a vial. About 50–100 such matings should be sufficient to produce multiple independent lines competent to form dicentric chromosomes ***(8)***. Examine only the Sb^{+} G2 progeny (lacking transposase) from each vial; they are expected to either have white eyes (lacking the *P[>*w^{hs}*>]* element), orange eyes like the parent insertion (therefore most likely the same insertion), or other shades of w^{+} (new insertions). Flies with eyes darker than the parent orange color are candidates for duplicated *P* elements (*see* **Note 2**.)
3. G2 cross: Dark-eyed flies are crossed to the extraction strain w^{1118}*; Sb/TM6B* to map and balance the new insertion chromosome. Because each G1 cross gives independent mutagenic events but the progeny from within each cross may not be independent, the G2 crosses are designated accordingly. Assign each G1 cross vial that produces interesting progeny a number, and the kept individual progeny from each vial a letter (e.g., each G2 cross will be labeled 1A, 1B, 2A, etc.) to indicate their relationships. Each G2 cross will produce w^{1118}*; 3*/TM6B* males and females (where * indicates a chromosome that potentially carries a transposed *P* element).
4. G3 mapping cross: Map the *P*-element insertion by crossing w^{1118}*; 3*/TM6B* males with dark eyes to w^{1118} females. Some new insertions will be unlinked to chromosome 3 and will give w^{+} progeny that also carry *TM6B*; discard these lines. Lines where the darker eye color is linked to chromosome 3 are examined further to identify lines with two adjacent *P* elements in an inverted orientation that are usable for dicentric formation.
5. G3 stock construction: Cross pigmented w^{1118}*; 3*/TM6B* males and virgin females *inter se* to generate a balanced insertion stock.

3.2.2. Identification of Lines Suitable for the Generation of Dicentric Chromosomes

1. G4 cross: Mate males from one of the new insertion lines (w^{1118}*; 3*/TM6B*) to females carrying a FLP source (w^{1118}*; P[70FLP, ry*$^{+}$*]*4A) in vials. Label the vials with a waterproof marker. Allow these cultures to continue for 5 d (until

crawling third instar larvae are present). At this time, there should be numerous larvae crawling in the food.
2. Discard the parents.
3. Immerse the vials in a 38°C water bath (such that they are covered up to the height of the plug in the vial) for 60 min. This induces the *70FLP* gene and catalyzes recombination at *FRT*s.
4. Return the vials to 25°C.
5. Adult progeny will begin emerging about 10 d after the cross was first set up. Examine the eyes, bristles, wings and abdomens of progeny up until d 18 of the cross. Lines with two adjacent *P[>w^{hs}>]* insertions in an inverted relative orientation show a characteristic phenotypic syndrome when FLP is produced during development. This syndrome includes roughened eye facets, irregular notches in the wing margins, missing and shortened bristles, and etched tergites on the dorsal side of the abdomen. Lines that do not produce these phenotypes are discarded (*see* **Note 3**).

3.3. Mitotic Characterization

1. Repeat the G4 cross from **Subheading 3.2.2.** to generate larvae carrying inverted *FRT*-bearing *P* elements and the *70FLP* gene. Allow the culture to continue until crawling larvae appear (typically 5–6 d after setting up the cross).
2. Discard the parents.
3. Immerse the vials in a 38°C water bath for 60 min.
4. Return the vials to 25°C for 4 h.
5. Fill two wells of a dissection dish with PBS, a third well with 0.5% sodium citrate, and a fourth with 45% acetic acid.
6. Select *w^{1118}; 3*/P[70FLP, ry^{+}]*4A larvae from the heat-shocked vials for dissection. Sibling progeny that carry *TM6B* can be excluded by scoring for the *Tubby* marker.
7. Rinse the larvae in one well of the dissection dish filled with PBS.
8. Grasp a larva about halfway along its length with one pair of forceps, and with another pair of forceps, grab the anterior tip of the larva. Pull firmly but gently on the anterior end, so that the mouth-hooks and anterior structures come out. These usually include the salivary glands, some fat bodies, imaginal discs, and brain. Tease apart the brain from the other structures.
9. Transfer a brain to sodium citrate and incubate for 10 min.
10. Transfer the brain to 45% acetic acid for 1–2 min.
11. Transfer the brain to a drop of 45% acetic acid on the middle of a glass slide. Cover with a siliconized cover slip.
12. Fold a piece of Whatman filter paper in half and place it around the prepared slide. Place the sandwich on a benchtop, place your thumb on the filter paper directly over the cover slip, and press down very hard for 30 s.
13. Remove the filter paper and place the glass slide on a block of dry ice. Incubate for 5 min.
14. Remove the slide from the dry ice and, using a razor blade, quickly pop off the cover slip from the frozen slide.

15. Immediately immerse the slide in a Coplin jar filled with PBS. Slides can be collected at this point over a period of a few hours.
16. Transfer the slides to a Coplin jar filled with a DAPI solution. Incubate for 5 min.
17. Transfer the slides to a Coplin jar with PBS to rinse for 5 min.
18. Remove the slides and tamp off any remaining liquid. Cover the stained sample with a small drop of glycerol and place a regular cover slip on top. Gently flatten the preparation under a sheet of Whatman filter paper and seal with nail polish.
19. When the nail polish has dried, the sample can be examined using a fluorescence compound microscope. Scan through the tissue for metaphase and anaphase figures. In metaphase figures where dicentic formation has occurred, a released acentric fragment can often be easily seen (*see* **Fig. 1**). In anaphase figures, a dicentric chromosome forms a distinctive bridge between the two groups of segregating nuclei and should also be apparent. The frequency of these aberrant mitoses gives a quantitative estimate of the frequency of dicentric formation (typically 70–95%). The presence of chromosome bridges confirms the identification of a *P*-element insertion line that can produce dicentric chromosomes (*see* **Note 4**.)

3.4. Time-Course Analysis

1. Repeat the G4 cross from **Subheading 3.2.2.** to generate larvae carrying adjacent *FRT*s and the *70FLP* gene. Allow the culture to continue 2–3 d after setting up the cross.
2. Transfer the parents to a new vial and discard the old vial.
3. On the appropriate day for the tissue of interest, immerse the vials in a 38°C water bath for 60 min (*see* **Note 5**).
4. Return the vials to 25°C.
5. For analysis of imaginal discs, wait until crawling larvae appear in the vial. Select w^{1118}*; 3*/P[70FLP, ry*$^{+}$*]*4A larvae and dissect as described in **Subheading 3.3.** (*see* **Note 6**).
6. For analysis of adult structures, examine adults as they eclose. The approximate stage of development when dicentric chromosomes were formed can be deduced based on when those flies eclosed after heat-shock induction. For example, adults that eclose 10 d after the heat shock were typically embryos or young larvae at the time of heat shock.
7. Photograph adult body parts with a dissecting or compound microscope equipped with a camera.

4. Notes

1. The *P[>*w^{hs}*>]*, *P[RS5]*, and *P[RS3]* constructs (which carry a w^{hs} marker gene and two *FRT*s) have been successfully used in this technique. A hypomorphic marker gene, such as w^{hs}, is required for this protocol. The location of many existing *FRT*-bearing *P*-element insertions can be found in Flybase (www.flybase.bio.indiana.edu).
2. Some new single-copy insertions will also be included in this category, although many, in fact, do carry two insertions near the starting insertion site ***(8)***. Occasionally, Sb^{+} G2 progeny may have mosaic expression of the w^{hs} marker. These

are often recombinants that carry *P[>w^{hs}>]* and the *P[Δ2–3]* transposase source or, less likely, insertions that are subject to position effect variegation. Discard these.

3. Heat-shock induction of the *70FLP* gene in this protocol is timed to maximize the incidence of dicentric chromosomes as cells in these tissues proliferate. The severity of these defects will depend on the frequency at which dicentric chromosomes are formed and the amount of aneuploidy that results after cell division with the dicentric and acentric products. However, lines in which dicentrics form at moderate to high frequencies should easily be spotted. Even dicentric chromosomes that produce no aneuploidy can give high incidences of roughened eyes and notched wings. The overcrowding of progeny in vials should be avoided.
4. The behavior of the released acentric fragment can be quantitatively examined in the anaphase spreads of these preparations. Comparison to a normal control strain is necessary to separate squashing artifacts from consequences of dicentric formation.
5. Cell division in many imaginal discs continues until the prepuparium stage, but proliferation of some tissues is more restricted ***(13)***. Induction of FLP should be timed to maximize the production of dicentric chromosomes when the tissue of interest is actively proliferating. For example, the cell division schedules in the eye-antennal imaginal disc during larval development are well characterized. This allowed cell cycle analysis of the consequences of cell division with a dicentric chromosome ***(4)***. Dicentric formation in male germ line stem cells can be obtained by heat shocking a 1- to 2-d-old culture. Dicentric formation in the female germline can be induced by heat-shocking females at virtually any point of development prior to or even after eclosion.
6. Any tissue can be examined from these larvae. Cell division and cell death rates can be estimated by examining imaginal discs, which are mitotically active in this period. Even the examination of the postmitotic but polytenizing salivary glands can be useful: The site of unequal sister-chromatid exchange can be mapped quite precisely by preparing polytene spreads from crawling larvae in which *70FLP* was induced 2–3 d after egg laying ***(2)***.

Acknowledgments

Work in the laboratory of K. G. G. was supported by grant RO1 GM60700 from the National Institutes of Health and by the Stowers Institute for Medical Research.

References

1. Williams, B. C., Murphy, T. D., Goldberg, M. L., and Karpen G. H. (1998) Neocentromere activity of structurally acentric mini-chromosomes in *Drosophila*. *Nature Genet.* **18,** 30–37.
2. Platero, J. S., Ahmad, K., and Henikoff, S. (1999) A distal heterochromatic block displays centromeric activity when detached from a natural centromere. *Mol. Cell* **4,** 995–1004.
3. Ahmad, K. and Golic, K. G. (1998) The transmission of fragmented chromosomes in *Drosophila melanogaster*. *Genetics* **151,** 1041–1051.

4. Ahmad, K. and Golic, K. G. (1999) Telomere loss in somatic cells of *Drosophila* causes cell cycle arrest and apoptosis. *Genetics* **151,** 1041–1051.
5. Golic, K. G. and Lindquist, S. (1989) The FLP recombinase of yeast catalyzes site-specific recombination in the *Drosophila* genome. *Cell* **59,** 499–509.
6. Golic, K. G. (1993) Generating mosaics by site-specific recombination, in *Cellular Interactions Development: A Practical Approach* (Hartley, D., ed.), Oxford University Press, New York, pp. 1–31.
7. Rong, Y. S. and Golic, K. G. (2000) Site-specific recombination for the genetic manipulation of transgenic insects, in *Insect Transgenesis: Methods and Applications* (Handler, A. and James, T., eds.) CRC, Boca Raton, FL, pp. 53–75.
8. Golic, K. G. (1994) Local transposition of *P* elements in *Drosophila melanogaster* and recombination between duplicated elements using a site-specific recombinase. *Genetics* **137,** 551–563.
9. Ahmad, K. and Golic, K. G. (1996) Somatic reversion of chromosomal position effects in *Drosophila melanogaster*. *Genetics* **144,** 657–670.
10. Golic, K. G. and Golic, M. M. (1996) Engineering the Drosophila genome: chromosome rearrangements by design. *Genetics* **144,** 1693–1711.
11. Golic, M. M., Rong, Y. S., Petersen, R. B., Lindquist, S. L., and Golic, K. G. (1997) FLP-mediated DNA mobilization to specific target sites in *Drosophila* chromosomes. *Nucleic Acid Res.* **25,** 3665–3671.
12. Matthews, K. (1994) Care and feeding of *Drosophila melanogaster*, in *Methods in Cell Biology* (Goldstein, L. S. B. and E. A. Fyrberg, A., eds.), Academic, New York, Vol. 44, pp. 13–32.
13. Cohen, S. M. (1993) Imaginal disc development, in *The Development of* Drosophila melanogaster (Bate, M. and Matinez Arias, A., eds.), Cold Spring Harbor Laboratory, Plainview, NY, Vol. 2, pp. 747–841.

18

Analysis of Chromosomes of the Larval CNS by FISH and BrdU Labeling

Amy K. Csink

1. Introduction

The central nervous system (CNS) of the third instar larva is the most convenient tissue in which to examine both mitotic chromosomes and the diploid interphase nucleus. It contains a mixture of cell types at various degrees of differentiation. Here, methods for examining the diploid nuclei of the third instar larva are presented. One method employs BrdU incorporation to label nuclei during the S-phase. A second uses fluorescence *in situ* hybridization (FISH) to determine where certain sequences are located. Both can be used on either mitotic chromosomes or interphase nuclei. These two methods can be used by themselves or in combination. When used in combination, a researcher can identify which cells have recently undergone the S-phase and examine the specific positions of various chromosomal regions in the interphase nucleus.

There are many reasons why one may wish to examine nuclear organization in tissue of the *Drosophila* larvae instead of primary tissue culture or established cell lines. For instance, it is quite possible that events associated with differentiation are correlated with changes in nuclear structure. Additionally, cells receive cell cycle and developmental cues from their neighbors, and disruption of these spatial arrangements may be problematic. However, when using cells from tissue, cell cycle synchronization is not possible. One would like to be able to determine, at least approximately, the cell cycle stage of a specific nucleus in a mixture of heterogeneous cells, such as is commonly encountered in tissue. Questions concerning the nuclear organization found at specific times in the cell cycle and at specific times of

From: *Methods in Molecular Biology, vol. 247:* Drosophila *Cytogenetics Protocols*
Edited by: D. S. Henderson © Humana Press Inc., Totowa, NJ

development can then be addressed. Changes in nuclear organization during the cell cycle has been extensively studied during the blastoderm stage of embryogenesis ***(1)***. However, there are a number of features of this stage that are exceptional. The cells are undergoing an unusually rapid cell cycle and have little or no G1 stage. They remain in the Rabl orientation, an organization that is often not found in nuclei from cells of more mature tissue. Finally, the level of transcription is low, which may influence the position of a specific chromosomal region ***(2)***.

In this chapter, a procedure for FISH to larval CNS cells is presented. This procedure is very similar to a number of other procedures that have been previously published for both polytene and interphase nuclei ***(3–5)***, but is one known to be compatible with BrdU labeling of nuclei. The combined FISH–BrdU method simply includes the anti-BrdU antibody at the final step. A procedure for doing only BrdU is also included. Precise methods for the BrdU feeding of larvae are described, as well as a way to pulse-feed larvae with BrdU. This procedure has been combined with quantitative analysis of 4',6-diamidine-2-phenylindole (DAPI) fluorescence to more precisely determine the cell cycle stage of individual nuclei in a squash. Although this aspect of the technique is not discussed here, a discussion of this application can be found in **ref. *6***.

2. Materials

2.1. Larvae Collection and Prelabeling Treatment

1. *Drosophila* media (Carolina Biological Supply Co.): You will need bags of both the blue and white instant foods. Cultures for egg-laying are done in plastic bottles (Applied Scientific) that can fit a 35-mm culture dish on top.
2. Grape plates for egg-laying: 100 mL Welch's grape juice, 100 mL bi-distilled water (ddH_2O), 8 g agar. Melt in a microwave, cool to approx 60°C, and add 1 mL acetic acid and 1 mL 100% ethanol. Mix and pour into 35-mm culture dishes. Store in plastic boxes at 4°C for up to 5 d. Bring plates to room temperature before use.
3. Sucrose food: 20% Sucrose in phosphate-buffered saline (PBS), 1.5% agar. Aliquot approx 10 mL into small plastic vials. Plug with cotton.
4. PBS, pH 7.0: To make 1 L of 10X PBS, pH 7.0, mix 75.97 g NaCl, 12.46 g $Na_2HPO_4{\cdot}2H_2O$, and 4.8 g $NaH_2PO_4{\cdot}2H_2O$. Dissolve in distilled water (dH_2O). Autoclave.

2.2. BrdU Feeding

1. 5-Bromo-2'-deoxyuridine (BrdU; Sigma-Aldrich, B-5002) solution. Make a 20-mg/mL stock solution in 40% ethanol. This may take a while to dissolve and may need to be warmed to 37°C. Stock solution is good for at least 1 mo and is stored at –20°C. This stock solution is then diluted to the desired con-

centration in water and used to rehydrate the food as described in **step 2** (*see* **Note 1**).
2. BrdU feeding dish: Crush blue Carolina food into a fine powder using a mortar and pestle. Measure 0.3 g of crushed food into a 35-mm Petri dish and add 1.6 mL of BrdU solution.

2.3. Pulse Feeding

Dark blue food: For 1.6 mL of BrdU solution, add 150 µL bromophenol blue (BPB, 3 mg/mL in PBS) to BrdU solution before adding to blue Carolina food.

2.4. Dissection

1. Siliconized cover slips: Place 18 × 18-mm^2 cover slips in cover slip racks (Molecular Probes). Use four containers large enough to hold the cover slips in racks. Pour 95% ethanol into two of these and 1% Aquasil (Pierce) in distilled water into the other two. Dip the rack into the Aquasil, then the ethanol. Repeat using the other two washes. Between washes, tap the base of the holder on a paper towel to remove excess. Multiple racks can be stepped through the washes. Allow to air-dry in a covered container that is slightly propped open to minimize dust. Take care that the cover slips remain as dust-free as possible (*see* **Note 2**).
2. MAW fixative: In a 2-mL microfuge tube, mix 800 µL acetic acid, 800 µL methanol, 73 µL ddH_2O. This remains fresh for only 3 h, after which it should be remade.
3. *Drosophila* Ringer's solution: 182 m*M* KCl, 46 m*M* NaCl, 3 m*M* $CaCl_2$, 10 m*M* Tris-HCl. Adjust to pH 7.2 with HCl and autoclave.

2.5. Hybridization

1. 20X SSC: 3 *M* NaCl, 0.3 *M* Na-citrate. Adjust to pH 7.0 with NaOH and autoclave.
2. Humid chambers: Plastic boxes with close-fitting lids are lined with damp filter paper. Slides are propped off the bottom with broken plastic pipets.
3. 1 *M* Triethanolamine-HCl (TEA): Mix 132.7 mL of triethanolamine (Sigma-Aldrich, T-1377) in approx 800 mL dH_2O. Bring pH to 8.0 with concentrated HCl and adjust the volume to 1 L. Store in the dark.
4. Acetic anhydride.
5. 70 m*M* NaOH (freshly made).
6. Hybridization mix: In a microfuge tube, mix 210 µL of formamide, 63 µL of 20X SSC, 77 µL dH_2O, 40 mg dextran sulfate (MW 500K). Thoroughly mix and dissolve at 65°C for about 30 min. This can be stored at –20°C for 3 mo.
7. Probes: Probe DNA can be a synthesized oligonucleotide of a repetitive sequence, a polymerase chain reaction (PCR)-amplified repetitive sequence or a cloned stretch of unique or repetitive genomic sequence. The synthetic oligonucleotide should be 45–70 bp in length. PCR amplification has worked for the rDNA repeats and the 359-bp repeat from *D. melanogaster* using divergent primers. For a unique genomic region, the best probes are the cosmids and P1s from the Drosophila Genome Project (www.fruitfly.org). In determining the probe to use for

specific genomic regions, one must consider size and uniqueness. I have found that as little as 15 kb can be detected using our microscope, but this can be unreliable. Fifty kilobases is good and 100 kb is very good. However, it is often difficult to find a larger clone that is unique for the region of interest. Each P1 or cosmid must be tested for uniqueness on mitotic diploid spreads and location accuracy on polytenes. For the P1s, I have found that even if one avoids the clones described as repetitive or chromocentral on polytenes, only about one in five are unique on mitotics. In general, it is probably better to go for something a bit smaller, like a cosmid, if there is a well-annotated one in your region of interest.

Probe DNA can be labeled by a number of methods, including (1) oligonucleotide-primed incorporation using the Klenow fragment of DNA polymerase I, (2) incorporation of label during PCR to genomic DNA for repetitive sequences, and (3) terminal transferase. Oligonucleotides must be labeled by terminal transferase. In order to use terminal transferase to label large genomic clones, the DNA must first cut down to 50- to 150-bp fragments using a 4-bp restriction enzyme mix ***(5)***.

There are two types of label: direct and indirect. Direct has the fluorochrome on the nucleotide. These are sold by Amersham (Fluoro Red or Green) and are available as rhodamine or fluorescein isothiocyanate (FITC) conjugates. These are very convenient, but although I have not seen a difference with sensitivity, they can have greater background artifacts. Also, one must be careful of light exposure in earlier steps of the hybridization procedure. The indirect method incorporates biotin–dUTP or digoxygenin (DIG)–dUTP and then detects it with fluorochrome-conjugated streptavidin or anti-DIG antibodies, respectively.

In considering the fluor choice, you must take into account the capabilities of your microscope system. For the basic BrdU detection, you will use the FITC and DAPI filters sets for BrdU and total DNA detection. This then leaves you with the rhodamine and Cy5 for probes, or if you do not have a scope with far red abilities, only rhodamine.

8. Formamide: Formamide must be of very high quality. Unfortunately, this is the major expense associated with this procedure. We use formamide from Fluka (47671) that is packed under nitrogen. It can be stored at 4°C until opened. After opening, formamide should be stored at –20°C. It can be aliquoted or defrosted at each use and then refrozen. When defrosting, minimize exposure to oxygen by not stirring or shaking it. If it does not freeze solid when it is returned to –20°C, it's no good. Formamide is a hazardous chemical and should be handled and disposed of properly.
9. Fluorochromes for detection of biotin- and digoxygenin-labeled probes: Streptavidin–Cy5 is from Jackson ImmunoResearch and made up to a concentration of 0.83 mg/mL in 50% glycerol. Anti-DIG Fab conjugated to FITC or rhodamine is from Roche and is made up at 0.2 mg/mL in 50% glycerol. All are aliquoted and stored at –20°C. Aliquots should not be refrozen, but stored at 4°C and will last 2 mo at this temperature. The aliquots stored at –20°C are good for at least 2 yr. Final dilution should be in PBS with 1% BSA (Sigma-Aldrich, A-7638).

10. Anti-BrdU–FITC antibodies: These can be obtained from a number of companies, including Roche and BioMeda. Anti-BrdU that is not conjugated to a fluor can also be purchased and a secondary antibody with your fluor of choice can be used. Follow the manufacturer's recommendations for preparation, storage and dilution. Final dilution should be in PBS with 1% BSA (Sigma-Aldrich, A-7638).

2.6. BrdU Detection Without FISH

PBS-TX: 1X PBS with 0.3% Triton-X 100.

3. Methods

3.1. Larvae Collection and Prelabeling Treatment

1. Place 50–80 females and at least 10 males on white Carolina instant food with about 1 mL of yeast paste of peanut butter consistency. Grow for 2–3 d, changing to new food (with yeast paste) every day.
2. In the morning of the third or fourth day, move the flies to a plastic bottle (without food) with approx 20 air holes poked in it. Tape a grape plate with large dollop of yeast paste to the opening of the bottle. Allow flies to "dump" eggs for 2–3 h. This will help get rid of eggs that are being held and make the subsequent collections more synchronous. Discard this grape plate and replace it with a new one having approx 50 µL of yeast paste. Collect embryos on grape plates at 2-h intervals. Maintain the collection plates at 25°C in a larger Petri dish. Collections can be done similarly during succeeding days for at least a week. Allow flies to dump eggs each morning.
3. After 24 h, move larvae from grape plates to vials (30–50 larvae/vial) containing white instant food and a dollop of yeast paste.
4. Allow the larvae to develop at 25°C. At 95–100 h after egg deposition (AED), pick larvae out of the food. This can be done by scraping out the top layer of food into a watch glass containing Ringer's and picking out the larvae with a forceps. Larvae should be crawling in the food. Never take larvae crawling up the sides, as they have finished eating. (Of course, if they are properly synchronized, they should not be at that stage yet.) Rinse the larvae in Ringer's to remove adhered food. Place larvae on sucrose food for 2 h. Proceed with BrdU labeling.

3.2. BrdU Feeding

1. Pick larvae off the sucrose food, give them one final rinse with Ringer's, and place them on the culture plates containing BrdU-laced food. Let them eat for the desired time interval at 25°C (*see* **Note 1**). Place the BrdU culture plates in larger Petri dishes.
2. Remove the larvae from the food and rinse them in Ringer's or PBS. If you have labeled for less than about 3 h, make sure the larvae have blue food in their guts.

3.3. Pulse Feeding

1. Take larvae from the sucrose food as described in **Subheading 3.2.** Place them on dark blue food mixture for 15–20 min. The BrdU concentration should be from 1 to 2 mg/mL.
3. Remove the larvae to a dish of PBS and rinse. Select only those larvae with blue food visible in the crop, but not in the gut. Place them on crushed white instant food.
4. After 2 h from the beginning of BrdU feeding, transfer the larvae to a dish of PBS, and rinse. Select only those larvae with no blue food visible in their bodies. Place on crushed blue instant food (with no BPB or BrdU). If necessary, the larvae can then be examined for light blue food in the gut to ensure that they have continued eating.
5. Dissect after the desired "chase" time.

3.4. Dissection

1. If BrdU labeling is not being done, wandering third instar larvae can simply be collected from any food cultures. In either case, the larvae should be rinsed in Ringer's.
2. Use a multiwell depression plate. All solutions should fill the well about two-thirds. Put 0.7% NaCl in a well and either 1% (for interphase nuclei) or 0.5% (for mitotic spreads) sodium citrate solution in the well next to it. Dissect the larval CNS (brain lobes and ventral ganglion) in NaCl by pulling on the mouth-hooks. If you will be looking at interphase nuclei to examine nuclear structure, make sure that you remove the imaginal discs, because you will not be able to tell what tissue you are examining once you squash it. This precaution is not necessary if you will be looking at mitotic spreads.
3. Move the CNS into sodium citrate solution. For interphase cells, incubate the CNS for 5 min (in 1% sodium citrate); for mitotic spreads, incubate for 10 min (in 0.5% sodium citrate).
4. Clean a slide with 95% ethanol. Wipe with lint-free lens paper. Place 7 µL of 45% acetic acid on a siliconized 18×18-mm^2 cover slip. Place fresh (less than 3 h old) MAW fixative in a well. Move brains to MAW for 30–60 s. If carryover of sodium citrate into the fixative is significant, decant the fixative using a micropipet and replace with additional fixative.
5. Move the CNS to acetic acid on a cover slip. It does not matter if the tissue falls apart at this point. If the squash is for mitotic figures, leave the CNS in the acetic acid for 1 min before squashing.
6. Pick up the cover slip with the slide so that the sample is in the middle of the slide. Move the cover slip slightly to spread the cells and wick out excess acetic acid with the edge of bibulous paper. Squash between folds of bibulous paper. Squash slightly for interphase and harder for mitotics.
7. Immerse the slide in liquid nitrogen until it stops sizzling. Remove the cover slip with a razor blade. Air-dry the slide.
8. Examine slides under phase contrast to determine if the squash was successful. Store in the dark until ready to hybridize.

3.5. FISH to CNS Nuclei

All washes are done in slide-staining boxes or Coplin jars.

1. Immerse the slides in 2X SSC at 65°C for 30 min. Wash at room temperature in the following: 2X SSC for 2 min, two washes of 70% ethanol for 5 min, and two washes of 95% ethanol for 5 min. Air-dry.
2. For each slide, dilute 0.3 µL RNAse (Roche DNAse free, 10 mg/mL) in 40 µL of 2X SSC. Pipet onto the sample on each slide and cover with a 22×22-mm^2 cover slip. Incubate in a humid chamber at 37°C for 1 h. Wash at room temperature in the following: 2X SSC for 2 min (cover slips will float off here), two washes of 70% ethanol for 5 min, and two washes of 95% ethanol for 5 min. Air-dry.
3. Prepare 200 mL of 0.1 *M* TEA from 1 *M* stock in a 500-mL flask. Quickly add 320 µL of acetic anhydride to the TEA, swirl, and pour on top of the slides in a rack in a staining box. Incubate at room temperature for 10 min. Wash at room temperature as follows: two washes of 2X SSC for 5 min, two washes of 70% ethanol for 5 min, and two washes of 95% ethanol for 5 min. Air-dry. Slides can be prepared to this point and stored at 4°C for 1 d.
4. Denature the chromosomes in NaOH as follows. It is important that the denaturation time be precisely 3 min and that you hybridize the slides immediately after drying. Wash at room temperature in the following: 70 m*M* NaOH (freshly prepared) for 3 min, 2X SSC for 5 min, two washes of 70% ethanol for 5 min, and two washes of 95% ethanol for 5 min. Air-dry.
5. Denature the probe(s) in a 0.5-mL microfuge tube at 95°C for 3 min and then quick-cool on ice. For each slide, you should have a probe volume of 2 µL. If you are using single-stranded oligonucleotide probes, denaturation is not necessary. Use 5–30 ng of each probe per slide.
6. Add 10 µL of hybridization mix for each slide to the probes. Mix by pipetting.
7. Pipet 12 µL of hyb-probe mix onto the area of the slide containing the tissue. This is often still visible as a slight clouding. Cover with a 22×22-mm^2 cover slip, with as few bubbles as possible. Seal the edges with rubber cement. Incubate in a humid box for 5 h to overnight (*see* **Note 3**). Remember to keep the slides in the dark if you have direct labeled probes.
8. Prewarm the formamide mix to the desired temperature (25–37°C).
9. Remove the rubber cement and float off the cover slips in 2X SSC at room temperature.
10. Incubate the slides in two washes of 2X SSC, 50% formamide at 25–37°C for 30 min.
11. Wash at room temperature: in PBS for 1 min, in two washes of PBS, 5 min each, in PBS with 0.1% Triton-X 100 for 5 min, and in PBS for 5 min.
12. It is very important not to let the slides dry at all during this step and the next. Do each slide one at a time. Remove a slide from PBS. Aspirate off excess PBS, and on each slide, pipet 100 µL of PBS with 1% BSA. Cover with 40×22-mm^2 cover slip. Incubate at room temperature in a humid box for 30 min.
13. Turn down the lights. Dilute streptavidin–Cy5 1:600, anti-DIG–rhodamine 1:300 and/or anti-BrdU–FITC in PBS with 1% BSA.

14. Float off the cover slips in PBS. Remove the slide from PBS. Aspirate off excess PBS and pipet on 100 µL of the detection mix. Cover with a 40 × 22-mm^2 cover slip and incubate at room temperature for 1 h in a dark humid box. Wash at room temperature in the following: two washes of PBS, 5 min each, PBS with 0.1% Triton-X 100 for 5 min, and PBS for 5 min.
15. Stain in DAPI. Remove the slides from the final PBS wash and immediately treat in the following washes: dH_2O for 10 s, 0.4 µg/mL DAPI in dH_2O for 20 s, dH_2O for 10 s. Air-dry. Shield from excess light by putting a box over the slides while they are drying.
16. Immediately after air-drying, mount in 10 µL of Vectashield (or other glycerol-based mountant with antifade) under a 22 × 22-mm^2 cover slip. Seal the edges with nail polish. Store slides at 4°C (*see* **Note 4**).
17. Image using fluorescence microscopy (*see* **Note 5**).

3.6. BrdU Detection Without FISH

1. At room temperature in slide-staining boxes, treat the slides in the following washes: PBS-TX for 5 min, 2 *M* HCl in PBS-TX for 30 min, PBS-TX for 10 min, and three washes in PBS for 5 min each.
2. It is very important not to let the slides dry at all during this step and the next. Do each slide one at a time. Aspirate off excess PBS, and onto each slide, pipet 100 µL of PBS with 1% BSA. Cover with a 40 × 22-mm^2 cover slip.
3. Incubate at room temperature in a humid box for 1 h. Float off the cover slips in PBS.
4. Aspirate off excess PBS. On each slide, pipet 100 µL of anti-BrdU FITC in PBS with 1% BSA. Cover with a 40 × 22-mm^2 cover slip. Incubate at room temperature in the dark in humid box for 2 h.
5. Treat the slides in the following washes: PBS for 5 min, PBS with 0.3% Triton-X for 5 min, and PBS for 5 min.
6. Stain in DAPI. Remove the slides from the final PBS wash and immediately treat the slides in the following washes: dH_2O for 10 s, 0.4 µg/mL DAPI in dH_2O for 20 s, dH_2O for 10 s. Air-dry. Shield from excess light by putting a box over the slides while they are drying.
7. Mount in 10 µL of Vectashield immediately after air-drying. Seal the edges with nail polish. Store slides at 4°C in the dark.

4. Notes

1. BrdU is toxic to larvae at too high a concentration or if they are exposed to it for too long. We have used concentrations from 0.4 to 2 mg/mL. When concentrations less than 0.4 mg/mL were used, incorporation could not be easily detected after 2 h of feeding. When larvae were fed 1 mg/mL BrdU from 95 to 105 h AED until pupation, 95% pupated and 12% emerged. When larvae were pulse-fed as described in this procedure (using 1 mg/mL BrdU), all of the larvae emerged and were fertile. Further information concerning effects of BrdU on various parameters can be found in **ref. *6***. A detailed description of the time-course of incorporation in CNS nuclei can also be found there.

2. It is important that the slides, tools, and working surface be relatively dust-free and clean. The dissecting scope and working surface should be wiped down with a damp cloth prior to use. Care should be taken to keep slides and cover slips covered.
3. Temperature of hybridization and/or formamide concentration in both the hybridization mix and wash may need to be changed depending on the probe. For instance, the $(AATAT)_n$ (45 bp) oligo probe only works at 25°C in 40% formamide, whereas $(AAGAG)_n$ works fine at 37°C, 50% formamide. In general, we hybridize genomic probes at 35°C and 50% formamide. It is very important that the temperature of the incubation not spike above the desired hybridization temperature and that the formamide wash is never above the hybridization temperature. Because of this, hybridizations and posthybridization formamide washes are done in high-precision water baths. Slides are placed in a humid chamber and weighted down in a water bath. The water level is just below the lid and the bath is kept covered.
4. Slides will easily last at least 2 wk at 4°C without loss of signal or degradation. After that, the direct labeled probes seem to begin to disperse. However, in my experience, the indirect labeled signals last at least a few months, as does the DAPI and BrdU-FITC labeling.
5. Our lab uses a Deltavision system from Applied Precision, Inc. (www.api.com/products/bio/deltavision), which records epifluorescence images on a charge-coupled device (CCD) camera. This is a three-dimensional deconvolution microscope that allows images to be taken at very high resolution and is a commercial version of the technology developed by the Sedat and Agard group *(7)*. Such a complicated setup is not necessary for this procedure, but there are certain aspects that are very helpful. First, unlike a confocal microscope, the number of different fluors that can be imaged is limited only by the availability of the colors and the filter sets, not by the need to include different lasers. The setup described can collect images excited at four different wavelengths from ultraviolet to far red. This is especially important if you wish to examine the relative positions of two different chromosomal regions during the S-phase. Second, the cooled CCD camera along with deconvolution software allows the detection of very weak signal with minimal background noise from the camera.

References

1. Marshall, W. F., Fung, J. C., and Sedat, J. W. (1997) Deconstructing the nucleus: global architecture from local interactions. *Curr. Opin. Genet. Dev.* **7,** 259–263
2. Foe, V. E., Odell, G. M., and Edgar, B. A. (1993) Mitosis and morphogenesis in the *Drosophila* embryo: point and counterpoint, in *The Development of* Drosophila melanogaster (Bate, M. and Martinez Arias, A., eds.), Cold Spring Harbor Laboratory Press, Plainview, NY, Vol. 1, pp. 149–300.
3. Ashburner, M. (1989) Drosophila: *A Laboratory Manual*, Cold Spring Harbor Laboratory Press, Cold Spring Harbor, NY.
4. Gatti, M., Bonaccorsi, S., and Pimpinelli, S. (1994) Looking at *Drosophila* mitotic chromosomes. *Methods Cell Biol.* **44,** 371–391.

5. Marshall, W. F., Dernburg, A. F., Harmon, B., Agard, D. A., and Sedat, J. W. (1996) Specific interactions of chromatin with the nuclear envelope: positional determination within the nucleus in *Drosophila melanogaster*. *Mol. Biol. Cell* **7,** 825–842.
6. Csink, A. K. and Henikoff, S. (1998) Large-scale chromosomal movements during interphase progression in *Drosophila*. *J. Cell Biol.* **143,** 13–22.
7. Agard, D. A., Hiraoka, Y., Shaw, P., and Sedat, J. W. (1989) Fluorescence microscopy in three dimensions. *Methods Cell Biol.* **30,** 353–377.

19

Immunostaining of Squash Preparations of Chromosomes of Larval Brains

Laura Fanti and Sergio Pimpinelli

1. Introduction

Immunostaining of mitotic chromosomes of larval neuroblasts by antibodies directed against specific proteins is a powerful tool for analyzing their distribution in both euchromatin and heterochromatin. This approach is particularly important for the structural analysis of heterochromatin because the high content of repetitive DNA and the absence of meiotic recombination render this material difficult to manipulate by standard genetic and molecular methods. Sensitive chromosome banding techniques have elaborated a cytogenetic map of *Drosophila melanogaster* heterochromatin ***(1,2)***, which is now resolved into 61 distinct bands designated h1–h61 (*see* Chapter 16). The relationship between these bands and the locations of 30 genetically defined heterochromatic loci, the major satellite DNA clusters, and 12 different middle repetitive DNA families have been determined ***(3,4)***.

More recently, we have undertaken a systematic study of the distribution of different types of chromosomal proteins in heterochromatin. To this end, we have optimized sensitive techniques to detect the binding sites of chromosomal proteins on both mitotic and polytene chromosomes (*see* **Fig. 1**). These techniques permit analyses of the in vivo interactions of chromosomal proteins with each other or with specific DNA sequences in heterochromatin and euchromatin. By combining immunostaining, high-resolution fluorescence *in situ* hybridization (FISH), and banding techniques (*see* Chapter 16), it is possible to perform accurate mapping of proteins, high and middle repetitive DNA sequences, and heterochromatin-encoded genes. Comparative analysis of the distribution patterns of all these elements permits one to obtain important

From: *Methods in Molecular Biology, vol. 247:* Drosophila *Cytogenetics Protocols*
Edited by: D. S. Henderson © Humana Press Inc., Totowa, NJ

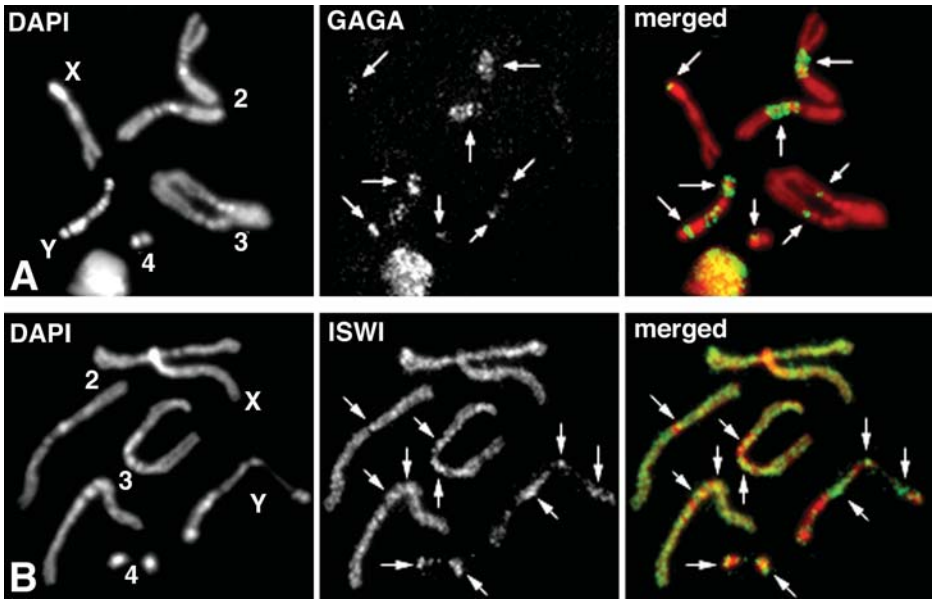

Fig. 1. Examples of mitotic chromosomes of *Drosophila* larval brains immunostained with specific antibodies directed against the GAGA **(A)** and ISWI **(B)** proteins. **(A)** the GAGA immunopattern reveals that the protein is present at specific heterochromatic regions (arrows) and apparently absent from euchromatin. **(B)** The immunopattern produced by anti-ISWI antibodies shows that the protein is present along the euchromatin and is located at specific heterochromatic regions of the autosomes and the Y chromosome (arrows). The X and Y chromosomes are indicated; the numbers indicate the autosomes. (*See* color plate 6 in the insert following p. 242.)

information about both the molecular composition of different heterochromatic domains and their structural similarities with euchromatic domains.

To cytologically analyze the distribution of chromosomal proteins along the mitotic chromosomes, it is necessary to devise fixation procedures that do not alter the protein composition of the chromosomes. The classical methanol/acetic acid fixation procedures used on mitotic chromosomes permit one to obtain good chromosome preparations for classical staining, fluorescent banding, and FISH analysis ***(1,2,4–6)***, even though they remove a substantial portion of chromosomal proteins. Localization by indirect immunofluorescence requires fixation procedures that not only preserve the protein component of chromosomes but also leave the protein epitopes exposed and recognizable by the specific primary antibody. Therefore, depending on the fixation procedure, two artifactual cases of negative results can arise: the protein has been extracted or the protein is present but not detectable because its epitope(s) is masked.

Another case that can arise is that of poor quality immunopatterns. This can depend on the primary antibody or, again, on the fixation procedure used.

Here, we describe a series of fixation procedures that we developed for the immunolocalization of several chromosomal proteins. Other protocols for certain proteins have been described by other authors *(7,8)*. We found that all steps of the fixation procedures can be critical for a specific protein, including hypotonic treatments, concentrations of fixative chemicals, incubation times, and modalities of chromosome squashing. We also found cases in which the treatment of fixed chromosomes with DNase I before immunostaining strongly improved the fluorescence intensity of the immunopatterns. In conclusion, we want to stress that for a given protein, it is necessary to develop a fixation procedure that maximizes epitope exposure to the specific primary antibody without affecting the protein's localization. One consequence of these differential fixation requirements is that for several proteins, it is impossible to perform double immunostaining even though primary antibodies produced in different species are available.

2. Materials

2.1. Fixation of Mitotic Chromosomes

1. Physiological solution: 0.7% NaCl in distilled water. Autoclave and store at 4°C.
2. Hypotonic solution: 0.5% Tri-sodium citrate dihydrate in distilled water. Autoclave and store at 4°C.
3. Fixative solution 1: 2% Formaldehyde, 45% acetic acid in distilled water. All fixative solutions have to be freshly prepared. Formaldehyde is highly toxic and carcinogenic. It is harmful to breathe the vapors and it may irritate the skin. Acetic acid is also harmful. Wear gloves and use these substances in a chemical fume hood.
4. Fixative solution 2: Methanol/acetic acid/distilled water (5 : 2 : 1, v/v/v). Methanol is poisonous. It may be harmful by inhalation, ingestion, and skin absorption. Use it in a chemical fume hood.
5. Fixative solution 3: methanol/acetic acid/distilled water (5 : 2 : 3, v/v/v).
6. Chromosome isolation buffer: 120 mg $MgCl_2 \cdot 6H_2O$, 1 g citric acid, 1 mL Triton X-100, and distilled water to 100 mL. Sterilize by filtration and store in aliquots at –20°C.
7. Fine forceps (e.g., Dumont no. 5 Biologie).
8. Microscope slides, siliconized and nonsiliconized.
9. Siliconized cover slips, 18×18 mm^2.
10. Cover slips (nonsiliconized), 24×24 mm^2.
11. Razor blade.
12. Cold methanol (stored at –20°C).
13. Cold acetone (stored at –20°C).
14. Liquid nitrogen. **Caution:** Wear cryo-mitts and a face mask.

15. 1 mg/mL DNAse I stock solution (from bovine pancreas, grade II; Roche).
16. 10X Nick-translation (NT) buffer (for DNase I treatment): 0.5 *M* Tris-HCl, pH 7.8–8.0, 50 m*M* $MgCl_2$, 0.5 mg/mL bovine serum albumin (BSA). Store at –20°C.
17. 10X Phosphate-buffered saline (PBS): 80 g NaCl, 2 g KCl, 2.4 g KH_2PO_4, 14.4 g Na_2PO_4, and distilled water to 1 L. Autoclave and store at 4°C.

2.2. Fluorescent Immunostaining of Fixed Chromosome Preparations

1. 10X PBS (*see* **Subheading 2.1., item 17**).
2. PTX solution: 1X PBS, 1% Triton X-100, freshly prepared.
3. Dried nonfat milk.
4. PBS/BSA solution: 1X PBS, 1% BSA. Sterilize by filtration and store in aliquots at –20°C.
5. Primary antibodies. They lose activity every time they are thawed; therefore, it is advisable to store antibodies frozen in aliquots, and once thawed, to store them at 4°C.
6. Fluorochrome-linked secondary antibodies. They are light sensitive.

2.3. DAPI Staining and Preparation Mounting

1. DAPI (4',6-Diamidine-2-phenylindole dihydrochloride) stock solution: 1 mg/mL DAPI in distilled water. It can be stored in the dark at 4°C. It is a carcinogen and an irritant. It may be harmful by inhalation, ingestion, and skin absorption. Wear gloves and use it in a chemical fume hood.
2. 20X SSC: 3 *M* NaCl, 0.3 *M* sodium citrate, pH 7.0. Sterilize by autoclaving and store at room temperature.
3. DAPI staining solution: 3 µL of DAPI stock solution in 60 mL of 2X SSC. It can be used for up to a week if stored in the dark at 4°C.
4. Antifade: 233 mg DABCO (1,4-diazabicyclo-[2,2,2]-octane), 200 µL of 1 *M* Tris-HCl, pH 7.5–8.0, 9 mL sterile glycerol, 800 µL sterile H_2O. DABCO may be harmful by inhalation, ingestion and skin absorption. Wear gloves and handle it in a fume hood.
5. Nail polish.

3. Methods

3.1. Fixation of Mitotic Chromosomes: Method 1 (see Note 1)

1. Transfer third instar larvae into drops of approx 50 µL of physiological solution placed on a siliconized slide and dissect out the brains (*see* **Note 2**).
2. Transfer the brains to a drop of hypotonic solution for 8 min at room temperature (*see* **Note 3**).
3. Transfer the brains to fixative solution 1 for 8 min.
4. Transfer four fixed brains into corresponding four small drops of the same fixative solution and place on a clean 18 × 18-mm^2 siliconized cover slip.

5. Lower a clean nonsiliconized slide on the cover slip, invert the sandwich, and squash gently for about 1 min between two sheets of blotting paper.
6. Freeze the slide in liquid nitrogen and flip off the cover slip with a razor blade.
7. Immerse the slide in 1X PBS at room temperature (*see* **Note 4**).

3.2. Fixation of Mitotic Chromosomes: Method 2 (see Note 5)

1. Transfer two or three third instar larvae into a drop of approx 50 µL of physiological solution placed on a siliconized slide and dissect the brains (*see* **Note 2**).
2. Transfer the brains into hypotonic solution for 2–10 min (*see* **Note 3**).
3. Transfer the brains to a drop (approx 9 µL) of fixative solution 2 or 3, placed on a 18 × 18-mm^2 siliconized cover slip (*see* **Note 5**).
4. Mash the brains using a couple of syringe needles to make a homogeneous suspension during fixation (*see* **Note 6**).
5. Lower a clean nonsiliconized slide on the cover slip, invert the sandwich, and squash very gently between four or five sheets of blotting paper.
6. Freeze the slide in liquid nitrogen and flip off the cover slip with a razor blade.
7. Immediately immerse the slide in 1X PBS at room temperature (*see* **Note 4**).

3.3. Fixation of Mitotic Chromosomes: Method 3 (see Note 7)

1. Transfer third instar larvae into drops of approx 50 µL of physiological solution placed on a siliconized slide and dissect out the brains (*see* **Note 2**).
2. Transfer the brains (8–10 brains) to hypotonic solution for 10 min.
3. Transfer the brains to a 9-µL drop of chromosome isolation buffer placed on a clean 18 × 18-mm^2 siliconized cover slip.
4. Mash the brains using a couple of syringe needles to make a homogeneous suspension and leave for 4 min (*see* **Note 6**).
5. Lower a clean nonsiliconized slide onto the cover slip, invert the sandwich, and squash very gently between four or five sheets of blotting paper.
6. Freeze the slide in liquid nitrogen and flip off the cover slip with a razor blade.
7. Immediately immerse the slide in cold methanol (–20°C) for 5 min.
8. Remove excess methanol by leaning the slide on a sheet of blotting paper and immediately immerse it in cold acetone (–20°C) for 1 min.
9. Immerse the slide in 1X PBS at room temperature (*see* **Note 4**).

3.4. Fixation of Mitotic Chromosomes: Method 4 (see Note 8)

1. Transfer third instar larvae into drops of approx 50 µL of physiological solution placed on a siliconized slide and dissect out the brains (*see* **Note 2**).
2. Transfer the brains to a drop of hypotonic solution for 8 min at room temperature (*see* **Note 3**).
3. Transfer the brains to fixative solution 1 for 8 min.
4. Transfer four fixed brains to corresponding four small drops of the same fixative solution placed on a clean 18 × 18-mm^2 siliconized cover slip.

5. Lower a clean nonsiliconized slide onto the cover slip, invert the sandwich, and squash gently for about 1 min between two sheets of blotting paper.
6. Freeze the slide in liquid nitrogen and flip off the cover slip with a razor blade.
7. Immerse the slide in 1X PBS at room temperature (*see* **Note 4**).
8. Stain the slide in DAPI staining solution for 4 min and wash in 1X PBS for 5 min.
9. Mount the slide in a drop of 1X PBS and seal the cover slip with rubber cement.
10. Look at the preparation under a photomicroscope, take pictures of good mitotic chromosomes, and save as many images as possible (*see* **Note 9**).
11. Remove the rubber cement and put the slide in a Coplin jar containing 1X PBS and let the cover slip fall from the slide into the jar.
12. Onto the slide, put 100 µL of 1 % DNase I stock solution in 1X NT buffer for 8 min at room temperature (*see* **Note 10**).
13. Wash the slide in 1X PBS three times for 5 min each.

3.5. Fluorescent Immunostaining on Fixed Chromosomes

1. Put the slides with fixed chromosomes in PBS in a Coplin jar containing PTX solution for 10 min.
2. Incubate the slides in 1X PBS with dried nonfat milk for 30 min (about 1 spoon of milk in 40 mL of 1X PBS).
3. Clean the slides in 1X PBS for 3 min.
4. Dilute the primary antibodies in PBS/BSA at a concentration appropriate for the antibody.
5. Put 10–15 µL of the antibody solution on the mitotic preparation and incubate for 1 h at room temperature and overnight at 4°C in a humid chamber.
6. Wash the slide three times in PBS for 5 min each wash.
7. Dilute the fluorochrome-conjugated secondary antibodies in PBS/BSA at the recommended concentration.
8. Put 10–15 µL of the secondary antibody solution on the mitotic preparation and incubate for 1 h at room temperature in a humid chamber.
9. Wash the slides three times in 1X PBS for 5 min in the dark.

3.6. DAPI Staining and Mounting

1. Stain the slides in DAPI staining solution at room temperature for 4 min (*see* **Note 11**).
2. Wash the slides in 1X PBS for 30 s.
3. Drain the slides of liquid and mount in a drop of antifade solution using a 24×24-mm^2 nonsiliconized cover slip (*see* **Note 12**).
4. Put the slide between two sheets of blotting paper and press gently to remove excess antifade solution.
5. Seal the preparation with nail polish (*see* **Notes 13–15**).

4. Notes

1. This protocol has been successfully used for immunostaining with antibodies directed against MODULO and ISWI proteins ***(9,10)***.

2. To easily dissect the brains, use two thin forceps (e.g., Dumont no. 5 Biologie). The larval mouth parts and the posterior part of the larval body should be grasped and then pulled apart. Because the brain usually remains attached to the head together with several imaginal disks and the salivary glands, the more rigid mouth parts should be completely removed with the forceps.
3. The duration of hypotonic treatment is critical. Some proteins can be removed by the hypotonic shock and cannot be visualized after immunostaining. Therefore, it can be useful to omit this step or to change the length of this treatment in some cases.
4. The slides can be stored in PBS at 4°C for 1 d before immunostaining.
5. This protocol uses two fixative solutions that differ only in the distilled water content and the time of hypotonic treatment. For example, hypotonic treatment for 2 min followed by fixation with solution 2 has been successfully used for immunostaining with antibodies directed against Heterochromatin Protein 1 (HP1) ***(11)***. Hypotonic treatment for 10 min followed by fixation with solution 3 has been successfully used for immunostaining with antibodies directed against the GAGA protein ***(12)***. Fixation in acetic acid is another treatment that can remove proteins from mitotic chromosomes. Varying the proportion of acetic acid with respect to the other components of the fixative may be necessary in some cases.
6. Brains fixed in solutions containing a low concentration of acetic acid become hard and need to be broken up before squashing. However, this procedure is very sensitive to ambient temperature and humidity. Therefore, to avoid excessive drying of the tissues during their disruption, it is sometimes necessary to increase the quantity of squashing solution placed on the siliconized cover slip.
7. This protocol has been successfully used for immunostaining with antibodies directed against histone proteins (Fanti et al., unpublished work).
8. This protocol has been successfully used for immunostaining with antibodies directed against TRITHORAX and POLYCOMB proteins (Fanti et al., unpublished work).
9. Because one of the steps of this protocol involves treating the chromosome preparations with DNase I, which will affect the fluorescence intensity of the DNA-binding DAPI fluorochrome, it is important to take pictures before the treatment to record good images of chromosomes that will later be merged with images of the immunosignals.
10. Sometimes the protein epitope recognized by the antibody can be masked because of protein–DNA folding. In this case, a light treatment with DNase I after protein fixation may enhance the protein–antibody interaction. This treatment does not produce artifactual alterations to the immunopatterns.
11. Alternatively, you can use Hoechst 33258 (0.5 µg/mL) dissolved in Hoechst buffer (HB). In this case, wash the slides in HB for 5 min, stain them in Hoechst solution for 10 min, and wash again in HB. HB is 150 m*M* NaCl, 30 m*M* KCl, 10 m*M* Na_2HPO_4, pH 7.0.
12. Vectashield (H-1000; Vector Laboratories) can also be used.
13. The slides should be stored in the dark at 4°C for 1–2 d before microscopic observation. This treatment reduces fluorescence fading.

14. Chromosome preparations are analyzed using a computer-controlled epifluorescence microscope equipped with a cooled CCD camera. The fluorescent signals, recorded separately as gray-scale digital images, are pseudocolored and merged using the Adobe Photoshop program.
15. The immunostained slides can be used for FISH. To perform the sequential immunostaining and FISH technique, store the immunostained slides for a week at 4°C and then remove the nail polish with acetone. (However, for this purpose, it would be better to seal the immunostained slides with rubber cement that can be easily removed.) Then, the slides must be washed many times in 1X PBS. Finally, standard FISH techniques can be performed.

Acknowledgments

We thank C. Goday for useful suggestions in elaborating some of the immunostaining procedures. We thank S. Elgin, P. Harte, R. Paro, V. Pirrotta, J. Pradel, J. Tamkun, B. Turner, and C. Wu for giving us the above cited antibodies.

References

1. Gatti, M., Pimpinelli, S., and Santini, G. (1976) Characterization of *Drosophila* heterochromatin. I. Staining and decondensation with Hoechst 33258 and quinacrine. *Chromosoma* **57,** 351–375.
2. Pimpinelli, S., Santini, G., and Gatti, M. (1976) Characterization of *Drosophila* heterochromatin. II. C- and N-banding. *Chromosoma* **57,** 377–386.
3. Gatti, M. and Pimpinelli, S. (1992) Functional elements in *Drosophila melanogaster* heterochromatin. *Annu. Rev. Genet.* **26,** 239–275.
4. Pimpinelli, S., Berloco, M., Fanti, L., et al. (1995) Transposable elements are stable structural components of *Drosophila melanogaster* heterochromatin. *Proc. Natl. Acad. Sci. USA* **92,** 3804–3808.
5. Gatti, M., Tanzarella, C., and Olivieri, G. (1974) Analysis of the chromosome aberrations induced by X-rays in somatic cells of *Drosophila melanogaster*. *Genetics* **77,** 701–719.
6. Holmquist, G. (1975) Hoechst 33258 fluorescent staining of *Drosophila* chromosomes. *Chromosoma* **49,** 333–336.
7. Pak, D. T. S., Pflumm, M., Chesnokov, I., et al. (1997) Association of the origin recognition complex with heterochromatin and HP1 in higher eukaryotes. *Cell* 91, 311–323.
8. Platero, J. S., Csink, A. K., Quintanilla, A., and Henikoff, S. (1998) Changes in chromosomal localization of heterochromatin-binding proteins during the cell cycle in *Drosophila*. *J. Cell Biol.* **140,** 1297–1306.
9. Perrin, L., Demakova, O., Fanti, L., et al. (1998) Dynamics of the sub-nuclear distribution of Modulo and the regulation of position-effect variegation by nucleolus in *Drosophila*. *J. Cell Sci.* **111,** 2753–2761.
10. Deuring, R., Fanti, L., Armstrong, J. A., et al. (2000) The ISWI chromatin-remodeling protein is required for gene expression and the maintenance of higher order chromatin structure in vivo. *Mol. Cell* **5,** 355–365.

11. Fanti, L., Giovinazzo, G., Berloco, M., and Pimpinelli, S. (1998) The heterochromatin protein 1 prevents telomere fusions in *Drosophila*. *Mol. Cell* **2,** 527–538.
12. Huang, D. W., Fanti, L., Pak, D. T., Botchan, M. R., Pimpinelli, S., and Kellum, R. (1998) Distinct cytoplasmic and nuclear fractions of *Drosophila* heterochromatin protein **1,** their phosphorylation levels and associations with origin recognition complex proteins. *J. Cell Biol.* **142,** 307–318.

20

Visualizing Mitosis in Whole-Mount Larval Brains

Daryl S. Henderson

1. Introduction

The central nervous system (CNS) of the third instar larva is a tissue of choice for studying conventional mitotic cycles in *Drosophila*. For example, squash preparations of the larval CNS are routinely used to investigate chromosome structural and numerical anomalies in late larval lethal mutants (e.g., **refs.** ***1***,***2***; also *see* Chapters 16–18), to study heterochromatin (e.g., **refs.** ***3–5***), and to localize chromosomal proteins by immunostaining (*see* Chapter 19). Mitotic chromosomes are not unduly harmed upon squashing, and for many experimental purposes it is advantageous to have them flat and well spread. However, the same cannot be said of the mitotic spindle, which is distorted or destroyed in squash preparations. A simple method for live analysis of mitosis in larval brain cells involves "pulverizing" dissected brain tissue with fine scalpel blades to produce a monolayer of cells for short-term (approx 1 h) study ***(6)***. The method can be used to visualize any mitotic proteins/structures for which green fluorescent protein (GFP)-expressing strains are available, and both wild type and mutants can be studied with equal facility. However, a potential drawback is that both the mechanical disrupting of tissue and nonphysiological culture medium used could have adverse effects on mitosis. Moreover, information about relative spindle geometry in a developmental context (e.g., **ref.** ***7***) is lost. A complementary approach to the above methods is to use whole-mount preparations of fixed brains to obtain a three-dimensional (albeit static) view of mitosis. This chapter describes a protocol for immunostaining whole-mount larval brains for analysis by laser scanning confocal microscopy.

The third instar larval CNS can be seen as a prominent pair of spherical lobes (the supraesophageal ganglia) broadly joined basally to a somewhat

From: *Methods in Molecular Biology, vol. 247:* Drosophila *Cytogenetics Protocols*
Edited by: D. S. Henderson © Humana Press Inc., Totowa, NJ

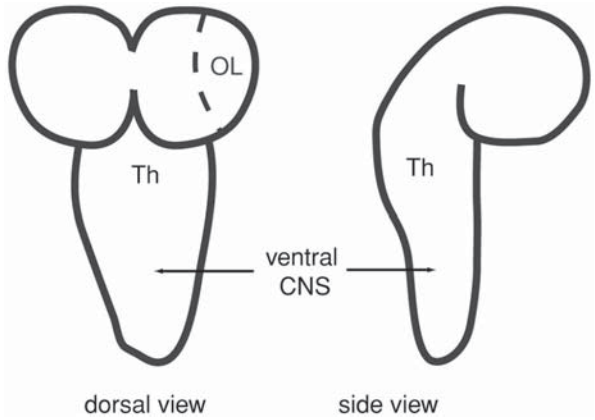

Fig. 1. Drawings of the larval CNS, viewed dorsally and laterally. The supraesophageal ganglia at the anterior (top of figure) are fused to the ventral CNS. The dotted line shown in one ganglion delimits the region of the optic lobe anlagen (OL) where extensive cell proliferation occurs ***(6,8,9)***. The thoracic neuromere region is indicated (Th). A detailed illustration of a larval brain can be found in **ref. *10***.

wedge-shaped protuberance, the ventral CNS (*see* **Fig. 1**). The supraesophageal ganglia will metamorphose into the brain and optic lobes of the adult head (reviewed in **ref. *8***). The ventral CNS is organized into a series of fused ganglia called neuromeres, with each neuromere corresponding to a different anatomical segment of the fly. A bulge in the ventral CNS (i.e., the thick end of the "wedge") corresponds mainly to the three thoracic neuromeres, where extensive ongoing cell proliferation begins soon after hatching ***(9,11)***. Concentrated there and in the optic regions of the CNS are numerous neuronal stem cells, or neuroblasts, that divide continuously throughout most of larval development ***(11)*** but do not appear to be required for larval function.

Thoracic neuroblasts are relatively large cells that divide asymmetrically approximately every 55 min (at 25°C) to produce another neuroblast and a smaller ganglion mother cell (GMC) ***(9)***. The GMC divides in turn, symmetrically, to produce two smaller postmitotic ganglion cells that will differentiate into adult neurons ***(9)***. Mitosis occupies about one-fourth of the neuroblast division cycle in wild type (approx 15 min at 24°C; for details, *see* **ref. *6***). The superficial location of large numbers of actively dividing neuroblasts at the periphery of the CNS is a tremendous experimental advantage for imaging in three dimensions. Consequently, the optic lobes and the thoracic neuromeres of the ventral CNS are especially good regions to view mitotic cells (*see* **Note 1**).

The protocol described here was adapted from a method devised by Audibert et al. ***(12)*** for preserving and visualizing mitotic spindles in imaginal discs. Its

most important elements are the dissection and fixation conditions. Dissection should be done quickly so that the larval brain (or whole "head") can be immersed in fixative without delay. The fixative solution differs from some others commonly used in that it contains both a high concentration of formaldehyde (10% [w/v] rather than 3.7%) and the chelating agent EGTA [ethylene glycol bis(β-aminoethyl ether) tetraacetic acid)]. EGTA helps to stabilize spindles by sopping up calcium ions, which promote microtubule disassembly (e.g., **ref. *13***).

2. Materials

1. Forceps (e.g., Dumolux no. 5; Fine Science Tools).
2. Microscope slides and cover slips. Clean them in ethanol and keep them free of dust.
3. Glass scintillation vial with screw cap or similar glass vial (approx 10–16 mL).
4. Dust-off® (Falcon Safety Products, Inc., Sommerville, NJ) or similar compressed gas to blow dust from slides and cover slips.
5. Phosphate-buffered saline (PBS): 6 m*M* NaH_2PO_4, 6 m*M* Na_2HPO_4, 150 m*M* NaCl, pH 7.5. Autoclave or filter-sterilize (*see* **Note 2**).
6. PBST: PBS containing 0.1% (v/v) Tween-20 (polyoxyethylene-sorbitan monolaurate, Sigma-Aldrich) (*see* **Note 3**).
7. Fixative: 10% (w/v) Formaldehyde, 1 m*M* EGTA in PBS, pH 7.5, freshly prepared. To make 10 mL of fixative, add 2.7 mL of 37% (w/w) formaldehyde solution, pH 7.5, and 100 µL of 100 m*M* EGTA, pH 7.5, to 7.1 mL of PBS (*see* **Notes 4** and **5**).
8. Permeablization solution: PBS containing 0.3% (v/v) Tween-20.
9. Blocking solution: 10% Fetal calf serum (FCS) in PBST. To make approx 10 mL, add 1 mL of FCS to 9 mL PBST, filter-sterilize using a 0.2-µm syringe filter, and store at 4°C (*see* **Note 6**).
10. Primary and secondary antibodies (*see* **Tables 1** and **2**) (*see* **Notes 7** and **8**).
11. Propidium iodide (PI) solution: 1 mg/mL PI in PBS, or other DNA fluorochrome appropriate for your microscope.
12. 10 mg/mL RNase A (DNase-free): RNase A can be bought that is free of contaminating DNase activity. If in doubt, boil for 10–15 min to inactivate any DNases. Store in aliquots at –20°C. RNase A is required if staining DNA with PI.
13. Vectashield (Vector Laboratories) or similar antifade mounting medium.
14. Clear nail polish.

3. Methods

Initially, manipulate whole heads (e.g., the anterior fourth of the larva) rather than brains. Proceed with batches of three to five heads of a particular genotype through to at least **step 7** before starting on a second batch of either the same or a different genotype. The aim is to minimize the time spent on dissection initially so as to get the tissue into fixative as quickly as possible. Quick fixation helps to maintain good spindle morphology; it may be less important for other mitotic structures/epitopes.

Table 1
Some Useful, Commercially Available Antibodies for Visualizing Mitotic Structures/States in *Drosophila*

Mitotic structure	Antibody	Source
Mitotic spindle/α-tubulin	YL1/2, rat monoclonal	Abcam, Cambridge,UK; ab9265
	DM 1A, mouse monoclonal	Sigma-Aldrich; T-9026
Centrosome/γ-tubulin	GTU88, mouse monoclonal	Sigma-Aldrich; T-6557
Histone H3 phosphoepitope ("mitosis marker")	Rabbit polyclonal	Upstate (www.upstatebiotech.com); 06-570
Cyclins A and B	Mouse monoclonal	DSHB (www.uiowa.edu/~dshbwww) (*see* **Note 7**)

Table 2
Noncommercial Antibodies Against *Drosophila* Mitotic Structures/Epitopes

Protein/Epitope (gene)	Localization/ staining	Ref.[a]
Bub1 (*bub1*)	Kinetochores	***(14,15)***
ROD (*rough deal*)	Kinetochores	***(16)***
ZW10 (*zeste-white 10*)	Kinetochores	***(16,17)***
3F3/2 phosphoepitopes[b]	Kinetochores/spindle poles	***(14,15,18)***
ASP (*abnormal spindle*)	Centrosomes	***(15,19)***
CNN (*centrosomin*)	Centrosomes	***(15,19)*** (*see also* Chapter 25)
CP190 (*centrosome-associated protein 190*)	Centrosomes (chromatin in interphase)	***(15,19,20)***
Prod (*proliferation disrupter*) of chromosomes 2 and 3	Pericentric heterochromatin	***(15)***

[a]Studies that include immunostainings of whole-mount larval brains.
[b]Anti-3F3/2 antibody recognizes conserved phosphoepitopes on kinetochores not yet attached to spindle microtubules. The epitopes are apparently sensitive to mechanical tension and normally disappear from the kinetochore at the onset of anaphase (*see* **ref. *21***).

1. Wash three to five third instar larvae of the desired genotype in PBS to remove any adhering food.
2. Using two pairs of fine forceps, remove the "head" from each larva in fresh PBS. Grasp a larva with one pair of forceps about one-quarter of the way from the anterior end. Grasp the larva with a second pair of forceps just posterior to the first pair, and pull the forceps in opposite directions to open the larva. Do not bother to dissect out the brain at this time. However, make sure that the brain is sufficiently exposed so that it is readily bathed in fixative. This may require tearing and pulling back some of the larval cuticle and partially everting the anterior tissues.
3. Immediately after each dissection, transfer the head to a glass scintillation or similar vial containing approx 2 mL of fixative. Fix the heads for 15–20 min, gently swirling every few minutes. The goal is to dissect all the heads within 5 min so that the first head is fixed for 20 min and the last for approx 15 min.
4. Carefully remove the fixative with a Pipetman or Pasteur pipet and then quickly rinse the heads twice in 2 mL of PBS, and then wash once in 2 mL of PBS for at least 5 min.
5. Transfer a single head to a dissection dish (or Petri dish) with fresh PBS and dissect out the brain and remove any attached imaginal discs and other unwanted material. Transfer the brain to a 1.5-mL microcentrifuge tube containing 1 mL of PBST. Repeat this dissection step for the remaining brains, placing them all together in the same microcentrifuge tube.

6. Remove the PBST and replace with 1 mL of permeabilization solution. Incubate for 10 min on a blood mixer/rotating wheel.
7. Remove the permeabilization solution and replace with 1 mL blocking solution. Incubate for 30–60 min at room temperature on a rotating wheel.
8. Incubate the brains in 1 mL of blocking solution containing an appropriate dilution of primary antibodies (*see* **Note 9**). Incubate overnight at 4°C with gentle agitation. If you intend to stain the DNA with PI (or other fluorochrome that binds RNA as well as DNA), include RNase A to a final concentration of 0.5–1 mg/mL (*see* **Note 10**).
9. Remove the primary antibodies and wash the brains six times in PBST at room temperature, 10 min each wash on a rotating wheel. Be careful not to discard any brains with the used wash solution.
10. After removing the final wash of **step 9**, add 1 mL of blocking solution and an appropriate concentration of fluorophore-conjugated secondary antibodies (*see* **Notes 9** and **11**). Incubate the brains for 2–4 h at room temperature on a rotating wheel. In this and all subsequent steps, keep the tubes in the dark (e.g., wrapped in aluminum foil) as much as possible.
11. Remove the secondary antibodies and wash the brains four times in PBST, 15 min each wash.
12. Wash the brains twice in PBS, 15 min each wash on a rotating wheel.
13. If staining the DNA with PI, incubate the brains in PBS containing 1/1000 concentration of PI solution for 5 min.
14. Remove the PI solution and rinse the brains in PBS.
15. Mount each brain on a clean, dust-free cover slip in Vectashield mounting medium with its ventral side facing the cover slip. Gently lower a clean slide onto the cover slip until it touches the mounting medium, and then pick up the cover slip with the slide. Seal the edges of the cover slip with clear nail polish and view using a laser scanning confocal microscope.

4. Notes

1. It is often assumed that all cells of the larval CNS are diploid. However, there is evidence for some brain cells normally becoming polyploid. First, DNA–Feulgen cytophotometric analyses of nuclear DNA content showed instances of 8C nuclei among expected 2C and 4C nuclei (the latter would correspond to cells in G2) in a population of *D. melanogaster* larval neural cells ***(22)***. Second, certain glial cells in abdominal neuromeres A3–7 were observed to replicate their DNA apparently without dividing during larval life ***(23)***. Such cells, and possibly others elsewhere in the larval CNS, may be endoreplicating.
2. PBS tablets (e.g., Sigma-Aldrich or Oxoid) are very convenient for making PBS solutions. Simply dissolve the tablets in distilled water and autoclave.
3. Triton X-100 can be used as a detergent in place of Tween-20 at the same concentration.
4. There are two ways to prepare the fixative. In the first, adjust the pH of approx 12 mL of fresh 37% (w/v) formaldehyde to pH 7.5 and then mix 2.7 mL with EGTA,

pH 7.5, and PBS, pH 7.5, as described in **item 7**; Or mix 2.7 mL of fresh 37% formaldehyde (not pH adjusted) with EGTA and approx 6 mL of PBS and then adjust the pH with drops of a 1.4 : 1 (v/v) solution of 1 *N* NaOH : 1 *N* KOH ***(12)***.

5. EGTA is very acidic and only slightly soluble in water at this concentration. However, it will go into solution at higher pH. To make 50 mL of 100 m*M* EGTA, add 1.9 g of EGTA (Sigma-Aldrich) to 40 mL of water. On a stirrer, add 10 *N* NaOH until the solution begins to clear and then add 1 *N* NaOH dropwise to achieve pH 7.5. Add water to 50 mL. Store at 4°C.
6. Fetal calf serum (FCS) is a rich growth medium, so it is important to keep the blocking solution free of microbes. If the blocking solution has been exposed to nonsterile conditions and then left for many weeks at 4°C, it is worth passing it again through a 0.2-μm syringe filter.
7. The Developmental Studies Hybridoma Bank (DSHB) at the University of Iowa, Iowa City, is an excellent source of inexpensive monoclonal antibodies (discounted for educational, nonprofit institutions). DSHB carries many monoclonals raised against *Drosophila* proteins, including some directly relevant to cell cycle studies (available at www.uiowa.edu/~dshbwww).
8. When starting out, try using antibodies against α-tubulin to stain the spindle (*see* **Table 1**) and propidium iodide to stain the DNA of wild-type brains. Metaphase and anaphase spindles are fairly easy to identify down the microscope, and if your spindles are not bipolar and nicely formed, then your fixation may be suspect.
9. Dilutions will vary depending on the titer of the primary and secondary antibodies and must be determined experimentally. Typically, dilutions of secondary antibodies will be in the range of 100-fold to 500-fold, but follow the supplier's guidelines.
10. RNase can be added instead to the incubation with secondary antibodies (**step 10**).
11. If background fluorescence is found to be a problem, the secondary antibodies can be preadsorbed on larval brains dissected, fixed, and permeabilized as described in **steps 1–6**. For example, dilute the secondary antibodies 1 : 8 in 3 vol of blocking solution for every volume of fixed tissues and incubate for 2 h at room temperature ***(12)***.

Acknowledgments

This protocol (or variations thereof) passed through the able hands of a number of my former colleagues in David Glover's laboratory, then in Dundee, Scotland. Although I am not certain of the history, I believe it was Mar Carmena who originally adapted it from Audibert et al. I have introduced some minor changes to the protocol, but others who may also have contributed modifications include Tom Howard, Hiro Ohkura, and Alastair Philp.

References

1. Baker, B. S., Smith, D. A., and Gatti, M. (1982) Region specific effects on chromosome integrity of mutations at essential loci in *Drosophila melanogaster*. *Proc. Natl. Acad. Sci. USA* **79,** 1205–1209.

2. Gatti, M. and Baker, B. S. (1989) Genes controlling essential cell-cycle functions in *Drosophila melanogaster*. *Genes Dev.* **3,** 438–453.
3. Bonaccorsi, S. and Lohe, A. (1991) Fine mapping of satellite DNA sequences along the *Y* chromosome of *Drosophila melanogaster*: relationships between satellite sequences and fertility factors. *Genetics* **129,** 177–189.
4. Lohe, A. R., Hilliker, A. J., and Roberts, P. A. (1993) Mapping simple repeated DNA sequences in heterochromatin of *Drosophila melanogaster*. *Genetics* **134,** 1149–1174.
5. Csink, A. and Henikoff, S. (1996) Genetic modification of heterochromatic association and nuclear organization in *Drosophila*. *Nature* **381,** 529–531.
6. Savoian, M. S. and Rieder, C. L. (2002) Mitosis in primary cultures of *Drosophila melanogaster*. *J. Cell Sci.* **115,** 3061–3072.
7. Ceron, J., Gonzalez, C., and Tejedor, F. J. (2001) Patterns of cell division and expression of asymmetric cell fate determinants in postembryonic neuroblast lineages of *Drosophila*. *Dev. Biol.* **230,** 125–138.
8. Truman, J. W. (1990) Metamorphosis of the central nervous system of *Drosophila*. *J. Neurobiol.* **21,** 1072–1084.
9. Truman, J. W. and Bate, M. (1988) Spatial and temporal patterns of neurogenesis in the central nervous system of *Drosophila melanogaster*. *Dev. Biol.* **125,** 145–157.
10. Ito, K., Urban, J., and Technau, G. M. (1995) Distribution, classification, and development of *Drosophila* glial cells in the late embryonic and early larval ventral nerve cord. *Roux's Archiv Dev. Biol.* **204,** 284–307.
11. Datta, S. (1995) Control of proliferation activation in quiescent neuroblasts of the *Drosophila* central nervous system. *Development* **121,** 1173–1182.
12. Audibert, A., Debec, A., and Simonelig, M. (1996) Detection of mitotic spindles in third-instar imaginal discs of *Drosophila melanogaster*. *Trends Genet.* **12,** 452–453.
13. Schilstra, M. J., Bayley, P. M., and Martin, S. R. (1992) The effect of solution composition on microtubule dynamic instability. *Biochem. J.* **277,** 839–847.
14. Basu, J., Bousbaa, H., Logarihino, E., et al. (1999) Mutations in the essential spindle checkpoint gene *bub1* cause chromosome missegregation and fail to block apoptosis in *Drosophila*. *J. Cell Biol.* **146,** 13–28.
15. Donaldson, M. M., Tavares, A. A. M., Ohkura, H., Deak, P., and Glover, D. M. (2001) Metaphase arrest with centromere separation in *polo* mutants of *Drosophila*. *J. Cell Biol.* **153,** 663–675.
16. Scaërou, F., Starr, D. A., Piano, F., Papoulas, O., Karess, R. E., and Goldberg, M. L. (2001) The ZW10 and Rough Deal checkpoint proteins function together in a large, evolutionarily conserved complex targeted to the kinetochore. *J. Cell Sci.* **114,** 3103–3114.
17. Williams, B. C. and Goldberg, M. L. (1994) Determinants of *Drosophila* zw10 protein localization and function. *J. Cell Sci.* **107,** 785–798.
18. Bousbaa, H., Correira, L., Gorbsky, G. J., and Sunkel, C. E. (1997) Mitotic phosphoepitopes are expressed in Kc cells, neuroblasts and isolated chromosomes of *Drosophila melanogaster*. *J. Cell Sci.* **110,** 1979–1988.

19. Barbosa, V., Yamamoto, R. R., Henderson, D. S., and Glover, D. M. (2000) Mutation of a *Drosophila* gamma tubulin ring complex subunit encoded by *discs degenerate-4* differentially disrupts centrosomal protein localization. *Genes Dev.* **14,** 3126–3139.
20. Cullen, C. F., Deak, P., Glover, D. M., and Ohkura, H. (1999) *mini spindles*: a gene encoding a conserved microtubule-associated protein required for the integrity of the mitotic spindle in *Drosophila*. *J. Cell Biol.* **146,** 1005–1018.
21. Daum, J. R., Tugendreich, S., Topper, L. M., et al. (2000) The 3F3/2 antiphosphoepitope antibody binds the mitotically phosphorylated anaphase-promoting complex/cyclosome. *Curr. Biol.* **10,** R850–R852.
22. Rasch, E. M. (1970) DNA cytophotometry of salivary gland nuclei and other tissue systems in dipteran larvae, in *Introduction to Quantitative Cytochemistry* (Weid, G. W. and Bahr, G. F., eds.), Academic, New York, Vol. 2, pp. 357–397.
23. Prokop, A. and Technau, G. M. (1994) BrdU incorporation reveals DNA replication in non dividing glial cells in the larval abdominal CNS of *Drosophila*. *Roux's Arch. Dev. Biol.* **204,** 54–61.

21

Immunostaining of Whole-Mount Imaginal Discs

Brigitte de Saint Phalle

1. Introduction

The imaginal discs of *Drosophila melanogaster* are saclike clusters of cells that generate the epidermal structures of the adult head, thorax, and external genitalia during metamorphosis. Imaginal disc precursor cells are segregated from larval cells during embryogenesis and follow an autonomous developmental program within the larva ***(1–4)***. They divide extensively while undergoing pattern formation and cell determination but retain their sac-like shape through the third instar ***(5,6)***. The approximate location of the 19 imaginal discs in the third instar larva are shown in **Fig. 1A**. A schematic cross section of a typical disc with squamous epithelial cells on one side and columnar epithelial cells on the other is shown in **Fig. 1B**. During metamorphosis in the pupa, the sac everts and the columnar epithelial cells form the eyes, antennae, wings, halteres, and other adult epidermal structures ***(6)***. For excellent reviews of work on imaginal discs prior to 1993, see **ref. *8***, and for more recent work, see a new book ***(9)*** with emphasis on pattern formation.

Imaginal discs are a good experimental system for studying development because they are simple structures that can be easily dissected from larvae. Genetic screens for disc-specific mutations have been used to study growth control ***(3,10–12)***, pattern formation ***(5,13–15)***, cell determination ***(3,16)*** and morphogenesis ***(6,17)***. Discs have been transplanted and cultured in vitro for studies of fate mapping and transdetermination ***(13,18,19)***. Molecular-genetic analysis of development in discs has greatly contributed to our understanding of signal transduction pathways in cell differentiation ***(16,17)***. Mosaic analysis in discs is an excellent tool for the study of lethal mutations in the context of normal development (*see* Chapter 17). Recent studies have shown that signaling from the peripodial membrane, traditionally ignored in the study of discs,

From: *Methods in Molecular Biology, vol. 247:* Drosophila *Cytogenetics Protocols*
Edited by: D. S. Henderson © Humana Press Inc., Totowa, NJ

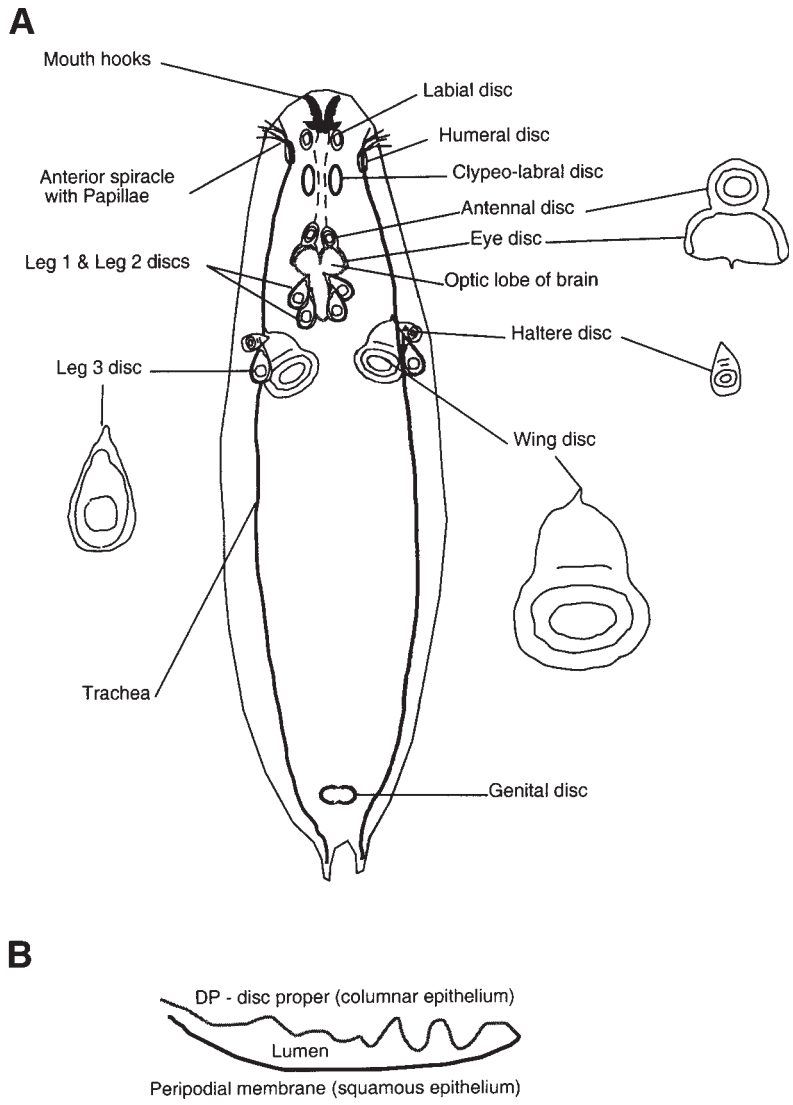

Fig. 1. Schematic of third instar larva showing the location of the imaginal discs. (Adapted from **ref.** *7*.)

is crucial to disc development. These studies have begun to elucidate the mechanisms of long-distance signaling ***(17,20–23)***.

Imaginal discs are anatomically simple enough to examine by light microscopy without sectioning. Two methods are commonly used to identify cell components for observation. Enzymatic detection is very sensitive and inexpensive

and can be used with a simple light microscope. An enzyme is localized by adding its soluble substrate that precipitates and leaves an insoluble colored product at the enzyme site. For example, the most commonly used reporter for gene expression is β-galactosidase, detected with X-gal. Enzyme-labeled antibodies can be used to detect any antigen. The enzymes usually employed as labels are horseradish peroxidase (HRP) detected with 3,3'-diaminobenzidine (DAB), and alkaline phosphatase detected with 5-bromo-4-chloro-3-indolyl phosphate (BCIP)/nitro blue tetrazolium (NBT). For a discussion of enzymatic detection and protocols *see* **refs. *24*** and ***25***; for fly-specific protocols, *see* **refs. *26*** and ***27***. The other technique, labeling of cell components with fluorescent tags, is more flexible and fluorescence microscopy provides better resolution. The protocols in this chapter are for immunofluorescent multiple labeling. Electron microscopy requires entirely different fixation and staining protocols.

The first step is to stabilize the discs by fixation. Fixation preserves the physical structure of tissue and prevents digestion by enzymes or bacteria. The process of fixation is complex and not well understood. Some fixatives stabilize tissue by precipitating and clumping proteins (e.g., ethanol, methanol), whereas other crosslink proteins (e.g., formaldehyde, glutaraldehyde) and trap associated components. Artifacts of fixation include changes in the volume of tissues, extraction of proteins, lipids, and nucleic acids, and chemical modification of proteins, which can affect the interaction of antibody and antigen ***(28–30)***. Any fixation protocol is a compromise: Physical structure is preserved better with a hard fix, but staining is better with a light fix that does not affect antigenicity or preclude antibody access. For light microscopy, the usual approach, adopted in this chapter, is to crosslink proteins with a light formaldehyde fix and allow stain/antibody access by permeabilizing cell membranes with detergent. If an antigen is modified by aldehyde fixation, there are various alternatives such as antigen retrieval (essentially undoing some the crosslinks by microwaving or with proteases) or the use of nonaldehyde fixatives ***(25)***. Ultimately, finding the best fixation for a given antigen is an empirical procedure. For an example of modifications required for visualizing microtubules in discs, *see* **ref. *31***. Histology texts and electron microscopy texts are sources of data on fixation procedures. There is an enormous amount of practical information on internet histology forums and other forums. Internet data are unedited personal information, usually without references and with no guarantee of accuracy, but it can be extremely valuable. It is a particularly good way of locating additional sources of information.

Once the sample is fixed, the cellular components of interest are labeled for detection. Staining with antibodies is the most common method for attaching fluorescent labels because antibodies can be raised against so many cellular components. Primary antibodies can be labeled (direct detection) or a labeled

secondary antibody against the IgG of the primary antibody host can be used to mark the antibody–antigen complex (indirect detection). Direct detection eliminates background staining, by a secondary. For multiple staining it enables the investigator to use antibodies from the same host of the same class and subclass without elaborate blocking, and it eliminates the potential for interactions associated with secondaries. However, direct labeling of an antibody requires sufficient quantity of antibody and time and effort from the investigator for quality control (for protocols, *see* **ref. *24***). Convenience and flexibility make indirect detection the usual choice. Affinity-purified secondaries are commercially available for a variety of hosts with a variety of fluorescent tags. Secondary antibodies that have been enzymatically digested into Fab fragments containing only the antigen-binding site, labeled and unlabeled, are commercially available. Using Fab fragments improves tissue penetration and removes the sites on the heavy chain that are often the target of secondaries and that bind cell surface receptors. Therefore, using Fab fragments may reduce crossreaction and cell surface binding.

There are nonimmunological fluorescent probes for many components of the cell (e.g., 4',6-diamidine-phenylindole [DAPI] and Hoechst fluorescent dyes that bind DNA). An excellent source of information is the *Handbook of Fluorescent Probes and Research Chemicals* from Molecular Probes and references therein ***(32)***. For a noncommercial reference, *see* **refs. *33*** and ***34***. Many protocols for using nonimmunological fluorescent probes are compatible with antibody-based staining, but harsher protocols may destroy antigens or alter their location or appearance. For example, fluorescence *in situ* hybridization (FISH) protocols extract cell proteins and denature DNA, so staining after FISH should always be compared with the results of normal staining as a control to see if enough useful information has been retained for each antigen.

The protocol in this chapter for immunostaining of whole-mount imaginal discs is a good starting point. It works well with a wide variety of antigens and preserves the fluorescence of green fluorescent protein (GFP). **Subheading 4.** suggests ways of customizing the protocol for different antigens. Although imaginal discs have only two layers of cells, they have folds and the nuclei are at different levels. This produces a high background level of out-of-focus light, which can be dramatically reduced by using a confocal microscope, or removed computationally by deconvolution. For a short introduction to microscopy, *see* Sections 9 and 10 of **ref. *35*** and references therein.

2. Materials

1. Two no. 5 forceps (Fine Science Tools), one should be Biologie (extrafine tips).
2. Insect medium, such as Schneider's medium (Sigma-Aldrich).
3. 20% Bovine serum albumin (BSA) (Sigma-Aldrich), on ice.
4. 10X Phosphate-buffered saline (PBS): 80 g NaCl, 2 g KCl, 2 g KH_2PO_4, pH 7.3, on ice.

5. Fixative: 4% Formaldehyde fixative made fresh from paraformaldehyde (*see* **Note 1**). Dissolve 0.65 g Na_2PO4 in 80 mL of double-distilled water in a flask. Add 4 g of paraformaldehyde (Polysciences), cap the flask loosely, and heat to 60–70°C in a fume hood. Stir until the paraformaldehyde has dissolved, cool, add 0.4 g NaH_2PO_4, dissolve, then add double-distilled water to 100 mL and filter through a 22-μm filter. Adjust to pH 7.4 if necessary. This solution is not stable and should be made fresh (*see* **Notes 2** and **3**).
6. Wash solution: 1X PBS, 1% BSA, 0.1% Triton X-100 (Fisher Biotech, electrophoresis grade), 0.03% sodium azide (*see* **Notes 3** and **4**).
7. Block-permeabilization solution: 1X PBS, 1% BSA, 0.3% Triton X-100, 0.03% sodium azide (i.e., wash solution with extra Triton X-100) (*see* **Notes 3** and **4**).
8. 100X DAPI stock: 10 mg DAPI/100 mL methanol. Store in the dark at –20°C (*see* **Note 3**).
9. Final clearing solution: 1X PBS, 0.03% Brij35 (Sigma-Aldrich), 0.03% sodium azide (*see* **Note 3**).
10. Slides and cover slips of the appropriate thickness for the microscope to be used.
11. Vectashield mounting medium (Vector Laboratories).
12. Clear nail polish.

3. Methods

3.1. Dissection (see Note 5)

1. Select a third instar larva. Third instar larvae are large, wandering larvae that have anterior spiracles with papillae. The anterior spiracles are located on either side of the black mouth hooks and, in third instar larvae, the fingerlike papillae make them look like hands. (First instar larvae have no papillae.) *See* **Fig. 1**.
2. In cold PBS, hold the larva with one forceps at about mid-body, and pull the head off with the other forceps. How you grasp the head determines which discs you get. Grasp the mouth hooks and spiracles to pull out all discs (except the genital disc). The wing, haltere, and T3 leg disc are usually associated to the main tracheal trunk, which resembles a white cord. The remaining disc complexes are with the mouth hooks and associated structures and may also come with the salivary glands, brain, and part of the gut. If you grasp just the mouth hooks and pull abruptly, you can get only the eye-antennal discs attached to the mouth hooks. **Figure 1** shows the approximate locations of the discs, and the groupings that are likely to be together.
3. Carefully pull away the salivary glands, fat bodies, brain, gut, and excess material if any is attached to the discs (*see* **Note 6**).
4. Transfer the discs to a 0.5-mL Eppendorf tube containing 500 μL of PBS on ice. Ten microliters of 20% BSA added to the PBS will keep the discs from sticking to the Eppendorf tube.

3.2. Fixation

1. Remove the PBS from the disc complexes by aspirating with a syringe or vacuum device and add 500 μL of fixative. Fix for 20 min at room temperature (RT).

2. Wash three times with the wash solution for 10 min each wash. Fixed tissue can be stored for only a short time at 4°C in aqueous solution (*see* **Note 7**).

3.3. Staining (see Note 8)

This protocol assumes that the first and second primary antibodies have been raised in different hosts. If this is not the case, *see* **Note 9**. Fluorescent labels for the secondary antibodies should be chosen to the capabilities of the microscope that will be used.

The protocol specifies staining serially for two antigens. Serial staining offers a great deal of flexibility, which is particularly useful when still experimenting with a stain. Conditions can be varied for each antibody; the sample can be divided and stained differently after the first staining, or postfixed, and so on. The downside is that it takes longer, and during the extra steps, there is more opportunity for dissociation of antibody–antigen complexes and even reversal of crosslinks in the fix. Postfixation can prevent this problem but may affect staining for some antibodies.

Antibodies are diluted in the wash solution. All blocking, incubation, and clearing steps are done in 0.5-mL eppendorf tubes on a rotator. Storage between steps should be at 4°C in the wash solution because formaldehyde crosslinks are not stable in aqueous solutions and there can be exchange between antibodies and antigens. Try to minimize the length of time between steps; for stainings that take more than 1 d, do one of the washes at 4°C overnight.

1. Block and permeabilize in block-permeabilization solution for 1–2 h at room temperature or 4 h at 4°C (*see* **Note 10**).
2. Incubate with host 1 primary antibody 1 (e.g., rabbit anti-lamin) in Wash solution for 1–2 h at RT (*see* **Note 11**).
3. Clear by washing three times with the wash solution for 20 min each (a minimum of 60 min for all washes). If using a labeled primary antibody, skip steps 4 and 5.
4. Incubate with anti-host 1 secondary antibody in the wash solution for 1–2 h at RT.
5. Clear by washing three times with Wash solution for 20 min each (a minimum of 60 min for all washes). If using a labeled primary antibody, skip **steps 6** and **7**.
6. Incubate with anti-host 2 secondary antibody in the wash solution for 1–2 h at RT.
7. Clear by washing three times with the wash solution for 20 min each (a minimum of 60 min for all washes).
8. **Optional:** If you are not already using a fluorophore that excites in the ultraviolet (UV) range and have a DAPI filter, incubate with DAPI (1 µg/mL final concentration) for 10 min. It is a good way to locate cell nuclei.
9. Final clear by washing three times with the final clearing solution for 20 min each (a minimum of 60 min for all washes). The substitution of Brij35 (which does not fluoresce) for Triton X-100 and the removal of the BSA should reduce background (*see* **Note 12** for staining controls for single- and multiple-label staining).

3.4. Mounting

1. Remove the aqueous solution and incubate the tissue in mounting medium at RT for at least 20 min (*see* **Note 13**). This enables the mounting medium to penetrate the tissue and improves imaging by eliminating a sudden optical transition from glycerol to aqueous. It will also minimize the amount of water present, which can act to quench fluorescence in glycerol-based media.
2. Remove the mounting medium and add fresh moutant.
3. Transfer the discs to a clean slide (*see* **Note 14**). Add enough mounting medium to just cover the discs—a mound should be clearly visible. The amount of material depends on the size of the cover slip used. A 22×22-mm^2 cover slip can hold 25–30 µL of material.
4. Place a clean cover slip of the appropriate thickness for your microscope over the discs and wait until the mountant spreads to the edge of the cover slip. Seal with clear nail polish and allow to dry thoroughly (*see* **Note 15**).
5. Image the slide immediately or store at –20°C for up to a week.

3.5. Troubleshooting

Table 1 provides a brief description of some common staining problems and references to parts of the chapter where these are discussed.

4. Notes

1. Paraformaldehyde is insoluble polymerized formaldehyde. It is solubilized by depolymerizing it in a reaction catalyzed by base. The resulting solution contains formaldehyde in the form of methylene hydrate, HO–CH_2–OH (formaldehyde, HCHO, is a gas). The solution is not stable: Formic acid can be produced and the formaldehyde can evaporate or repolymerize ***(28,30)***. Electron-microscopy-grade formaldehyde solutions are expensive and are also not stable once the ampoule is opened. It is less expensive and more convenient to dilute commercial formaldehyde (37% [w/w], Fisher certified ACS) in PBS. Commercial formaldehyde is stabilized in monomeric form by the addition of up to 15% methanol and is stored at room temperature (an opened bottle is good for up to 1 yr). Unfortunately, most references do not recommend fixing with stabilized formaldehyde because it is largely monomeric and will, therefore, only crosslink proteins directly and because of the methanol content (up to 1.5% when diluted). Methanol coagulates proteins and extracts lipids, altering membranes and destroying organelles, but is the effect of 1.5% methanol for 20 min observable at the level of light microscopy? I have not been able to detect any difference using confocal microscopy or deconvolution microscopy for specimens fixed with stabilized formaldehyde versus freshly made formaldehyde. However, in the absence of any published, rigorous comparison, I have recommended the old fashioned method adapted from Kiernan ***(28)***.
2. Some protocols specify detergent in the fixative. Although this may speed fixation and give access to proteins that might be degraded quickly, solubilizing

Table 1
Staining Problems

Problem	Possible cause	Try
Poor staining throughout	Antigen not preserved. Antigenicity affected by fix. Poor tissue preservation or old sample. Antibody not effective at dilution used.	Different fixation. Longer fixation, use sample immediately. Optimize antibody solutions (*see* **Subheading 1**, **Notes 7** and **8**, and also positive controls for primary antibodies in **Table 2**).
Poor staining, patchy	Tissue not fully permeabilized.	*See* **Note 10**.
Poor staining, interior of sample	Over-fixation.	Try softer fix (shorter duration or lower temperature).
High background	Nonspecific staining by primary or secondary antibody; autofluorescence.	Determine origin of background from staining controls (**Table 2**), then treat accordingly (*see* **Notes 10** and **11**).
Antigen shows up in multiple channels	Microscopy artifact. Interaction of stain components.	Change fluorophores/filter set. *See* staining controls (**Table 2**).

Table 2
Staining Controls

Control for	Positive control	Negative control	Prevention
Autofluorescence	Not applicable	Unstained specimen	0.1% Sodium borohydride in PBS has been used to reduce autofluorescence
Nonspecific staining (primary antibody)/ stain failure	1. GFP-tagged antigen 2. Stain with a different antibody against the primary antibody	1. Pre-immune serum or normal serum from the same animal species used to make the antigen 2. Deficiency mutant 3. Add sufficient antigen to bind all the antibody	Try different fix Affinity-purify the antibody Preadsorb against discs Vary the blocking agent Dilute the primary antibody
Nonspecific staining (secondary antibody)	Stain with primary antibody that is well characterized	Stain with secondary antibody only	Label primary antibody Optimize dilution of secondary antibody Preadsorb against discs Block with normal serum from same animal species as used to generate the secondary antibody
Interaction between reagents in multiple staining (staining pattern for antigen A appears in channel for antigen B or antigens appear to be colocated)	Not applicable	Single stain	Use different fluorophores or improved filters Use secondaries that have been preadsorbed against other species Use different antibody Use labeled primary antibody Try different stain order Block with normal serum from the same animal species used to make the offending secondary, and postfix

phospholipid membranes could also affect membrane-associated antigens. For a brief discussion *see* **ref. *36***.

3. Cautions on fixatives, preservatives, and stains: Fixatives fix the investigator's tissues as readily as they fix samples. They are toxic if absorbed through the skin or swallowed. Exposure to fumes or dust can irritate or destroy tissue in the eyes, mucous membranes, and respiratory tract. *Formaldehyde* or formalin, the traditional name for formaldehyde in aqueous solution, is also a carcinogen. It is harmful if absorbed through the skin, swallowed, or inhaled. *Paraformaldehyde* (powdered polymeric formaldehyde) is highly toxic. Avoid skin contact, do not breathe dust, or get it in the eyes. Use in a fume hood, wearing gloves and eye protection. *Methanol* can cause blindness if ingested. Avoid breathing the fumes. *Sodium azide* (used as a preservative) may be fatal if swallowed or absorbed through skin. It is harmful if inhaled. Keep sodium azide away from acids, heat, sparks, and flame. It is an explosion hazard, sensitive to mechanical impact; avoid rough handling. It reacts with copper and lead to produce explosive azides; explosions in laboratory plumbing containing these metals are possible. *DAPI* may be carcinogenic. It may be harmful if absorbed through the skin, swallowed, or inhaled.
4. Bovine serum albumin (BSA) is specified as a blocking agent. BSA will produce unacceptably high background if an antibovine secondary is required. Replace with normal serum from an appropriate species. This issue is discussed in **Note 10**.
5. Dissecting discs takes practice. To avoid deterioration, the discs should be fixed as quickly as possible after dissection; 20 min in cold PBS is the recommended maximum time for dissecting. Dissecting in serum-free insect medium preserves discs better than PBS, if you are slow. The fine forceps required to grasp with precision are very delicate and one way to minimize tip damage is to dissect in a drop of liquid on a plastic pad made from solidified rubber cement or aquarium sealant in a Petri dish. I dissect in a glass three-well spot plate (Hampton Research). I use the first well to pull the larvae apart, the second to clean up the discs, and the third for storing discs.
6. A method for handling large numbers of larvae is to cut off and discard the posterior half and then evert the anterior half by reaching inside, grasping, and pulling on the mouth hooks and papillae. The disc complexes will thus be exposed to fixative immediately. Further dissection can be done during fixation, or after.
7. Formaldehyde crosslinks are reversible in aqueous solution and the tissue will deteriorate noticeably in a matter of weeks at 4°C. Poor tissue preservation is shown by distortion of structure, excessive squashing, misshapen nuclei, and collapsed tissue. After fixation, discs can be stored in methanol or ethanol at 4°C if your antigen(s) is compatible with alcohol. At high concentration, alcohol extracts proteins and lipids, damages membranes, and destroys organelles and some antigens, including GFP. Before staining, rehydrate in a series of 90%, 75%, 50%, 25%, and 0% alcohol/PBS (15 min each).
8. Immunostaining artifacts can arise from fixation or from the staining process itself. The major causes of staining problems are poor penetration of the tissue by

antibodies, nonspecific antibody binding, and interactions between reagents in multiple label stains. The protocol provided here makes no assumptions about the antibodies that will be used, but staining artifacts at each step can be minimized for a specific antibody. Some controls used to detect staining artifacts are discussed in **Notes 9–11** and summarized in **Table 2**.

9. Antibodies: Nonspecific staining, which occurs when an antibody binds targets other than its antigen, creates background noise that can overwhelm the antibody–antigen signal. Affinity-purified antibodies are the best choice for staining tissue. In multiple-labeling experiments, it is preferable to use primary antibodies from different hosts, avoiding closely related hosts like rat and mouse. Secondaries that have been adsorbed to minimize crossreaction with other species are available commercially for multiple-label staining. Ideally, secondary antibodies should all be raised in the same host so they do not interact with each other. Secondaries that distinguish same-host antibodies by class and subclass are also available commercially. I have had good results with antibodies from Jackson ImmunoResearch Laboratories. It is common practice to reuse diluted antibodies, especially rare or expensive ones. This adds an element of uncertainty: At each use, the titer of antibody is reduced; also, diluted antibodies are not stable. Usually, the initial titer of antibody is high enough to get more than one successful stain and, with controls, the quality of the stain can be monitored. In accordance with Murphy's Law, deterioration becomes noticeable when you are looking at a particularly interesting sample.
10. *Permeabilization:* 0.3% Triton X-100 is used to solubilize membranes and give antibodies access to the cell proteins of the discs. Irregular staining, particularly where there is stain failure in the interior of the tissue rather than exterior, indicates poor penetration of tissue. IgM antibodies are particularly susceptible to penetration problems because each antibody has five Y-shaped units, each one as large as an IgG antibody. If there is poor staining of the interior of the discs after staining at high titer overnight at 4°C, permeability can be increased by increasing the time of incubation in the blocking solution, the amount of detergent, using another detergent, or using a harsher method of permeabilization, like methanol. However, these measures can also affect membrane-bound antigens. Some protocols specify detergent in the fixative. Although this may speed fixation and give access to proteins that might be degraded quickly, solubilizing phospholipid membranes could also affect membrane-associated antigens. For a brief discussion, *see* **ref. *36***.

    Blocking: Blocking is a way to reduce background staining due to nonspecific binding by antibodies. BSA was chosen as a source of nonimmune antibody for blocking any epitopes in the tissue that are capable of binding a variety of IgG. If an antibovine secondary antibody is used, BSA will increase the background instead of reducing it. Ideally, the blocking reagent should be normal serum from the host of the labeled secondary antibody and all secondaries should be from the same host to prevent interaction between them.
11. *Incubation:* Antibodies exhibit nonspecific binding if used in excess or incubated for too long. To get the strongest stain with an acceptable amount of

background, test the antibody at a variety of dilutions. The time of incubation should permit diffusion of the antibody throughout the tissue. One to two hours at room temperature (or 4–8 h at 4°C) is a good starting point, but some reactions can require up to 24 h at 4°C. If staining is still uneven there may be a problem with permeabilization of the discs.

Clearing/washing: Any unbound antibody remaining in the tissue will add to the background directly if the antibody is labeled or indirectly by binding labeled secondary far from the location of antigen.

12. Controls are used to identify staining artifacts. **Table 1** lists the major staining artifacts with controls and some methods of prevention.

Controls for single labeling: Autofluorescence is not usually a problem in discs, although other structures (e.g., the trachea and spiracles) autofluoresce. Autofluorescence should not vary under constant fixation conditions and probably only needs to be examined once for a particular microscope and filters.

The controls for primary antibodies address two issues: identification of staining as a result of antibody–antigen binding (positive controls) and identification of staining as a result of nonspecific binding (negative controls). If characterizing a new antibody for immunofluorescence, read a fuller treatment of the testing involved, such as **ref. *25***. For a primary antibody that has already been characterized for immunofluorescence, using a different fixative may alter antigen-binding sites and nonspecific binding may occur because of epitopes found in this particular tissue (with this particular fix). The best negative control is preimmune serum or normal serum from the same host as the primary. A positive control is required if the staining pattern for the antigen is an issue in the experiment (or to verify stain failure). If the antigen has a distinctive staining pattern, it may be easy to evaluate, a diffuse staining pattern may always remain a challenge.

Staining with only the secondary will show background staining as a result of nonspecific binding by the secondary, which can occur in addition to binding to the target host. A secondary antibody that exhibits significant nonspecific binding in the presence of the primary antibody can be incubated against discs to remove the crossreacting IgG. In my experience, commercial labeled secondaries produce very little background except when I have tried to amplify a signal using biotinylated secondary plus a tertiary stain, which produced a punctate background.

Additional controls for multiple labeling: Additional problems occur with multiple labeling: Reagents can crossreact or different fluorophores may not be completely isolated by the microscope. In both cases, the single-label staining pattern of an antigen will differ from the multiple-labeling staining. It is very useful to be thoroughly familiar with the appearance of a single-label stain for each antibody, and it pays to look at the single-label stain in multiple channels to check for microscopy artifacts. If the artifact is the result of the interaction between staining reagents, labeled primaries are a good solution. Another solution is to use secondary antibodies that have been adsorbed against the IgG of the other species. Blocking can also improve the stain dramatically at the cost of

extra steps. As a example of a worst-case scenario, you can stain with two monoclonal antibodies of the same class and subclass using the following baroque method:

1. Stain with the first monoclonal and the corresponding labeled secondary.
2. Block open anti-mouse target sites on the labeled secondary with 20% normal mouse serum.
3. Block unoccupied mouse target sites on the primary (and the mouse serum from the previous step) with fivefold excess of unlabeled anti-mouse *monovalent* Fab fragments.
4. Postfix to prevent exchange during subsequent staining. (Do not omit this step, it is crucial.)
5. After all of this, the second monoclonal will not be captured by the first labeled secondary and the second anti-mouse secondary will not have access to target sites on the first monoclonal.

13. Antifade agents work by reducing the generation and/or diffusion of reactive oxygen species. Many formulations are available commercially, like Vectashield, specified in this protocol. There are various others available in the literature; for a selection, *see* **ref. *36***.
14. Slides, even precleaned slides, are often dusty. By Murphy's Law, a vividly fluorescent particle of dust will be colocated with the most interesting data. Slides can be cleaned with detergent (e.g., 5% sodium dodecylsulfate [SDS] in water), rinsed thoroughly with double-distilled water to remove all traces of detergent, and dried. Cover slips from a newly opened box or a box that is kept closed are much likelier to be clean.
15. If only a few discs are mounted, they may become compressed vertically. To avoid compressing the discs, use small pieces of a no. 1.5 cover slip in the corners to support the cover slip. (If the discs move as you focus, try putting a drop of 500 µg/mL poly-L-lysine [Sigma-Aldrich] in water on the slide where the discs will be mounted and allow to dry.) Even better preservation of the three-dimensional structure is possible by embedding the discs in an acrylamide pad, a technique originally developed for high-resolution microscopy of chromatin structure ***(37,38)***.

References

1. Harbecke, R., Meise, M., Holz, A., et al. (1996) Larval and imaginal pathways in early development of *Drosophila*. *Int. J. Dev. Biol.* **40,** 197–204.
2. Fuse, N., Hirose, S., and Hayashi, S. (1994) Diploidy of *Drosophila* imaginal cells is maintained by a transcriptional repressor encoded by escargot. *Genes Dev.* **8,** 2270–2281.
3. Cohen, S. M. (1993) Imaginal disc development, in *The Development of* Drosophila melanogaster (Bate, M. and Martinez Arias, A., eds.), Cold Spring Harbor Laboratory Press, Plainview, NY.
4. Hayashi, S., Hirose, S., Metcalfe, T., and Shirras, A. D. (1993) Control of imaginal disc development by the *escargot* gene of *Drosophila*. *Development* **118,** 105–115.

5. Wolff, T. and Ready, D. F. (1993) Pattern formation in the *Drosophila* retina, in *The Development of* Drosophila melanogaster (Bate, M. and Martinez Arias, A., eds.), Cold Spring Harbor Laboratory Press, Plainview, NY.
6. Fristrom, D. and Fristrom, J. W. (1993) Metamorphic development of the adult epidermis, in *The Development of* Drosophila melanogaster (Bate, M. and Martinez Arias, A., eds.), Cold Spring Harbor Laboratory Press, Plainview, NY.
7. Bryant, P. J. and Levinson, P. (1985) Intrinsic growth control in the imaginal primordial of *Drosophila*, and the autonomous action of a lethal mutation causing overgrowth. *Dev. Biol.* **107,** 355–363.
8. Bate, M. and Martinez Arias, A. (eds.), (1993) *The Development of* Drosophila melanogaster, Cold Spring Harbor Laboratory Press, Plainview, NY.
9. Held, L. I. (2002) *Imaginal Discs: The Genetic and Cellular Logic of Pattern Formation.* Cambridge University Press, Cambridge.
10. Hipfner, D. R. and Cohen, S. M. (1999) New growth factors for imaginal discs. *BioEssays* **21,** 718–720.
11. Kurzik-Dumke, U., Gundacker, D., Renthrop, M., and Gateff, E. (1995) Tumor suppression in *Drosophila* is causally related to the function of the *lethal(2) tumorous imaginal discs* gene, a *dnaJ* homolog. *Dev. Genet.* **16,** 64–76.
12. Kylsten, P. and Saint, R. (1997) Imaginal tissues of *Drosophila melanogaster* exhibit different modes of cell proliferation control. *Dev. Biol.* **192,** 509–522.
13. Brook, W. J., Diaz-Benjumea, F. J., and Cohen, S. M. (1996) Organizing spatial pattern in limb development. *Annu. Rev. Cell Dev. Biol.* **12,** 161–180.
14. Russell, M. A., Ostafichuk, L., and Scanga, S. (1998) Lethal *P–lacZ* insertion lines expressed during pattern respecification in the imaginal discs of *Drosophila*. *Genome* **41,** 7–13.
15. Weigmann, K., Cohen, S. M., and Lehner, C. F. (1997) Cell cycle progression, growth and patterning in imaginal discs despite inhibition of cell division after inactivation of the *Drosophila* Cdc2 kinase. *Development* **124,** 3555–3563.
16. Dickson, B. and Hafen, E. (1993) Genetic dissection of eye development in Drosophila, in *The Development of* Drosophila melanogaster (Bate, M. and Martinez Arias, A., eds.), Cold Spring Harbor Laboratory Press, Plainview, NY.
17. Agnes, F., Suzanne, M., and Noselli, S. (1999) The *Drosophila* JNK pathway controls the morphogenesis of imaginal discs during metamorphosis. *Development* **126,** 5453–5462.
18. Maves, L. and Schubiger, G. (1998) A molecular basis for transdetermination in *Drosophila* imaginal discs: interactions between wingless and decapentaplegic signaling. *Development* **125,** 115–124.
19. Li, C. and Meinertzhagen, I. A. (1997) The effects of 20–hydroxyecdysone on the differentiation in vitro of cells from the eye imaginal disc from *Drosophila melanogaster*. *Invertebr. Neurosci.* **3,** 57–69.
20. Ramirez-Weber, F. A. and Kornberg, T. B. (1999) Cytonemes: cellular processes that project to the principal signaling center in *Drosophila* imaginal discs. *Cell* **97,** 599–607.

21. Ramirez-Weber, F. A. and Kornberg, T. B. (2000) Signaling reaches to new dimensions in *Drosophila* imaginal discs. *Cell* **103,** 189–192.
22. Gibson, M. C. and Schubiger, G. (2000) Peripodial cells regulate proliferation and patterning of *Drosophila* imaginal discs. *Cell* **103,** 343–350.
23. Cho, K. O., Chern, J., Izaddoost, S., and Choi, K. W. (2000) Novel signaling from the peripodial membrane is essential for eye disc patterning in *Drosophila*. *Cell* **103,** 331–342.
24. Lane, D. and Harlow, E. (1988) *Antibodies: A Laboratory Manual.* Cold Spring Harbor Laboratory Press, Cold Spring Harbor, NY.
25. Harlow, E. and Lane, D. (1999) *Using Antibodies: A Laboratory Manual.* Cold Spring Harbor Laboratory Press, Plainview, NY.
26. Sullivan, W., Ashburner, M., and Hawley, R. S. (2000) Drosophila *Protocols.* Cold Spring Harbor Laboratory Press, Plainview, NY.
27. Ashburner, M. (1989) Drosophila: *A Laboratory Manual.* Cold Spring Harbor Laboratory Press, Cold Spring Harbor, NY.
28. Kiernan, J. A. (1990) *Histological and Histochemical Methods: Theory and Practice*, 2nd ed., Pergamon, New York.
29. Hayat, M. A. (1981) *Fixation for Electron Microscopy.* Academic, New York.
30. Hayat, M. A. (1989) *Principles and Techniques of Electron Microscopy: Biological Applications*, 3rd ed., CRC, Boca Raton, FL.
31. Audibert, A., Debec, A., and Simonelig, M. (1996) Detection of mitotic spindles in third-instar imaginal discs of *Drosophila melanogaster*. *Trends Genet.* **12,** 452–453.
32. Haugland, R. P. (1996) *Handbook of Fluorescent Probes and Research Chemicals*, 6th ed., Molecular Probes, Inc., Eugene, OR.
33. Mason, W. T. (1999) *Fluorescent and Luminescent Probes for Biological Activity: A Practical Guide to Technology for Quantitative Real-Time Analysis*, 2nd ed., Academic, San Diego, CA.
34. Chazotte, B. (1998) Nonimmunological fluorescent labeling of cellular structures, in *Cells: A Laboratory Manual* (Spector, D. L., Goldman, R. D., and Leinwand, L. A., eds.), Cold Spring Harbor Laboratory Press, Plainview, NY.
35. Spector, D. L., Goldman, R. D., and Leinwand, L. A. (eds.) (1998) *Cells: A Laboratory Manual,* Cold Spring Harbor Laboratory Press, Plainview, NY.
36. Jacobson, K. A. (1998) Preparation of cells and tissue for fluorescence microscopy, in *Cells: A Laboratory Manual* (Spector, D. L., Goldman, R. D., and Leinwand, L. A., eds.), Cold Spring Harbor Laboratory Press, Plainview, NY.
37. Urata, Y., Parmelee, S. J., Agard, D. A., and Sedat, J. W. (1995) A three-dimensional structural dissection of *Drosophila* polytene chromosomes. *J. Cell Biol.* **131,** 279–295.
38. Bass, H. W., Marshall, W. F., Sedat, J. W., Agard, D. A., and Cande, W. Z. (1997) Telomeres cluster de novo before initiation of synapsis: a three-dimensional spatial analysis of telomere positions before meiotic prophase. *J. Cell Biol.* **137,** 5–18.

22

Wing Somatic Mutation and Recombination Test

Heloísa Helena Rodrigues de Andrade,
Maria Luíza Reguly, and Mauricio Lehmann

1. Introduction

The *Drosophila* wing somatic mutation and recombination test (SMART; also known as the wing spot test) provides a rapid means to assess the potential of a chemical to induce loss of heterozygosity (LOH) resulting from gene mutation, chromosomal rearrangement, chromosome breakage, or chromosome loss. This bioassay makes use of the wing-cell recessive markers *multiple wing hairs* (*mwh*, 3–0.3) and *flare* (*flr*^{3}, 3–38.8) in transheterozygous *mwh* +/+ *flr*^{3} animals. When a genetic alteration is induced in a mitotically dividing cell of a developing wing disc, it may give rise to a clone(s) of *mwh* and/or *flr*^{3} cells (i.e., a "spot") visible on the wing surface of the adult fly. The total number of clones induced in a group of chemically treated flies gives quantitative data concerning the whole genotoxic activity of a compound, whereas the types of clone can reveal the mutational mechanisms involved in clone production. Variations on the SMART system described in this chapter have been used to measure frequencies of spontaneous LOH in mutants defective in meiotic recombination and disjunction, DNA repair, and cell proliferation ***(1–3)***.

Single *flr*^{3} or *mwh* spots (both small and large clones) indicate the occurrence of either a point mutation (in *flr*$^+$ or *mwh*$^+$), a chromosomal alteration (e.g., a deletion of *flr*$^+$ or *mwh*$^+$), or mitotic recombination. On the other hand, twin spots (i.e., patches of adjacent *flr*^{3} and *mwh* cells) are exclusively derived from mitotic recombination. Twin spots therefore give a preliminary indication of the recombinagenic action of a compound. It is also useful to distinguish small single spots (one to two mutant cells) from large single spots (≥ three

From: *Methods in Molecular Biology, vol. 247:* Drosophila *Cytogenetics Protocols*
Edited by: D. S. Henderson © Humana Press Inc., Totowa, NJ

mutant cells); this is because small spots are produced during the last one to two rounds of cell division in the pupa, whereas large spots are produced earlier, during larval feeding. There is also another reason to evaluate small spots separately: Genetic deficiencies resulting from chromosomal aberrations most often result in only small clones, regardless of the time of initiation, as the affected cells appear to proliferate slowly if at all ***(4)***.

Almost 300 chemicals have been evaluated in the wing spot test (documented in approx100 publications; reviewed in **ref. *5***). These include various antineoplastic drugs, small alkylating agents, bulky adduct-forming compounds, crosslinking agents, clastogenic intercalating and nonintercalating topoisomerase inhibitors, antimetabolites that disturb nucleotide pools, DNA synthesis inhibitors, and nucleoside analogs. The genotoxic effects of these representative compounds are, in general, strong and dose related ***(5)***.

Aneuploidogenic compounds tested in the SMART have typically shown weak effects. This was the case for the microtubule antagonists chloral hydrate ***(6)*** and vincristine ***(7)***, which induce significant increases only in the frequencies of small single spots. Such a weak response of the SMART to detect somatic monosomy was also found for vinblastine ***(4,7)*** and vinorelbine ***(8)***, although significant increases in the frequencies of large single clones were observed for both compounds ***(4,8)***. Monosomic cells, if they remain viable, would have greatly reduced reproductive rates and so be expected to yield small single spots ***(4,9)***. For spindle poisons such as docetaxel, which disrupt microtubule assembly, a significant increase in small single spots has been observed. Consequently, this enhancement could be taken as evidence that docetaxel induces monosomic cells resulting from its interaction with microtubules, which is a behavior expected for a compound that has microtubule-stabilizing activity and is a potent inhibitor of cell division.

Application of the SMART to deriving qualitative or quantitative structure–activity relationships has been achieved for several groups of chemicals: Antiparasitic nitrofurans ***(10)***, tricyclic antidepressants ***(11,12)***, pyrolysis products ***(13,14)***, pyrrolizidine alkaloids and nitrosamines ***(15–17)***, antineoplasic drugs ***(18–20)***, and polycyclic aromatic hydrocarbons ***(21)***. In this context, the wing SMART has proved to be sufficiently sensitive to be able to establish relationships between chemical structure and differential recombinational or mutagenic responses. The wing spot test is also well suited for testing complex mixtures, such as airborne aerosol extracts ***(22)***, plant extracts ***(23)***, beverages such as coffee ***(24,25)***, herbal teas and wines ***(26,27)***, as well as tannic acid ***(28)***. Although both caffeine and tannic acid were determined to be genotoxic in the wing SMART ***(24,26)***, they also both showed antigenotoxic activity in combination with several known strong mutagens ***(25,28,29)***. Thus, the SMART can

also be used to assess the effects of nongenotoxic chemicals, which may act as modulators when combined with genotoxins. Such approaches identified the protective effects of chlorophyllin ***(30,31)***, ascorbic acid ***(32)***, novo-biocin ***(33)***, antipyretic analgesics ***(34)***, sodium thiosulfate ***(35)***, epigallocatechin ***(36)*** and tannic acid ***(28)***. In the latter case, however, treatment conditions appear to be critical, because tannic acid was able to enhance the genotoxicity of both nitrogen mustard (HN2) and methyl methanesulfonate (MMS) when applied as a posttreatment ***(28)***. In a similar vein, vanillin (VA) has been shown to have opposite effects on different genotoxic expressions of mitomycin C (MMC). VA significantly enhanced the recombinagenicity of MMC (to approx 170%) while reducing its mutagenicity (to approx 80%) ***(37)***. In view of these antagonistic effects, the clear overall effect of VA was to increase considerably the level of mitotic recombination induced by MMC ***(37)***.

All in all, the applicability of the SMART to studies of antigenotoxic effects is reinforced by the demonstration that some modulators that decrease the incidence of mutational effects are equally able to increase the occurrence of mitotic recombination. This means that modulating agents must be evaluated not only in terms of their action on mutagenic events (point and chromosomal mutations) but also in relation to their effects on mitotic recombination. Because the transheterozygous flies express all these genetic end points, the SMART has an additional advantage over other assays: It makes it possible to draw a more complete picture of the pharmacological behavior of modulating agents, such as described earlier for VA.

Standard strains of *Drosophila* can transform certain chemicals, termed "progenotoxins," into reactive metabolites. This enables an array of genotoxins requiring bioactivation to be readily detected in the wing spot test, including pyrolysis products ***(13,14)***, hydrazines ***(25,38)***, vicinal dihaloalkanes ***(4,39,40)***, heteroaromatics such as aflatoxin B_1 ***(4,40,41)***, pyrrolizidine alkaloids ***(17,42)*** and nitrosamines ***(15)***. The wing spot test is also well suited as a model system to study nitrosation by sodium nitrite in vivo ***(43)***.

In 1989, Frölich and Würgler ***(44)*** constructed new strains with high constitutive bioactivation by introducing chromosomes 1 and 2 of a strain in which cytochrome P450 levels are increased compared to the standard tester strains. In particular, the CYP6A2 level is increased ***(45)*** primarily as a result of mutation of the cytochrome P450 regulatory gene *Rst(2)DDT*. The levels of other cytochrome P450 proteins may also be affected in this mutant, but this has not been demonstrated. With promutagens such as aflatoxin B_1, urethane ***(44,46)*** and *N*-nitrosopyrrolidine ***(21,47)***, which are readily detected with standard strains, high bioactivation resulted in steeper dose–response curves. High bioactivation strains are particularly useful for testing polycyclic aromatic hydrocarbons, their nitro derivatives, and other aromatic chemicals, which

require metabolic activation and frequently show a weak response with standard strains ***(21,48)***. The most striking case is that of dimethyl-4-aminoazobenzene (butter yellow), which gave positive results only with high bioactivation.

Finally, the situation for environmental contaminants is not documented to the same extent as that for chemical compounds. In spite of this, several studies revealed advantages of the wing SMART as a method to evaluate the impact of possible environmental changes. The test appraised environmental contamination, including airborne particulate matter, at two different sites on two dates in Mexico City, using the ST and HB crosses. The extracts showed genotoxic activity predominantly in the HB cross, indicating the presence of indirectly acting genotoxins. A good correlation with the same extracts in the *Salmonella* microsome assay reinforces the suitability of the wing spot test to detect genotoxicity associated with airborne particles ***(21,49,50)***. More recently, the SMART was also applied to monitor the genetic toxicity of surface waters under the influence of urban and industrial discharges in the Caí river (Porto Alegre City, Brazil), proving its sensitivity to detect contamination from urban discharges ***(51,52)***.

The broad spectrum of genetic end points monitored as LOH in somatic cells—including point mutations, deletions, unbalanced half-translocations, mitotic recombination, chromosome loss, and nondisjunction—makes the wing SMART a most versatile in vivo test. It is also technically simple, quick and inexpensive to do, and allows flexibility in the choice of both route of administration of the test chemical and time of exposure. In addition, it allows analysis of an extensive sample size, because microscopic inspection covers approx 50,000 cells per fly. Moreover, statistical procedures applicable to the SMART are well established, and different statistical tests can be applied according to the peculiarities that specific sets of data may show.

2. Materials

1. *Drosophila* tester strains:
   a. *mwh*: The marker *multiple wing hairs* (*mwh*, 3–0.3), which is a completely recessive, homozygous viable mutation, is kept in a homozygous *mwh* strain. The *mwh* mutation is located near the tip of the left arm of chromosome 3 and in homozygous condition produces multiple trichomes per cell instead of the normally unique trichome.
   b. *flr^3/In(3LR)TM3, ri p^p sep l(3)89Aa bx^{34e} e Bd^S*: The marker *$flare^3$* (*flr^3*, 3–38.8) is a recessive mutation that affects the shape of the wing hairs, producing a trichome that has the shape of a flare. It is also located on the left arm of the chromosome 3, but in a more proximal position. All three extant mutant alleles of *flr* are recessive zygotic lethal. By contrast, homozygous *flr* cells in the wing imaginal discs are viable and produce mutant trichomes. Because of their zygotic lethality, theses alleles are kept in stocks over balancer chromosomes carrying multiple inversions (TM3).

   c. High bioactivation (HB) line: *ORR/ORR; flr^3/In(3LR)TM3, ri p^p sep l(3)89Aa bx^{34e} e Bd^S*. The ORR strain has chromosomes 1 and 2 from a DDT-resistant Oregon R(R) line, which are responsible for a high constitutive level of cytochrome P(CYP)6A2 ***(47,53)***. This cross improves the performance of the wing SMART in the case of promutagens activated via cytochrome P450-dependent metabolic pathways. More detailed descriptions of the genetic markers and the balancer chromosome can be found in **ref. *53***.
2. Plastic vials (Carolina Biological Supply; cat. no. CE-17-3120 or similar).
3. Plastic foam vial plugs (Carolina Biological Supply; cat. no. CE-17-3122 or similar).
4. *Drosophila* Instant Medium (Carolina Biological Supply, Burlington, NC, USA; cat. no. CE-17-3200) or mashed potatoes (Knorr Co. or similar) (*see* **Note 1**).
5. Microscope at 400× magnification, bright field.
6. Stereomicroscope at 8× magnification.
7. Water bath.
8. Heating plate (optional).
9. Balance (capacity: 500 g; readability: 0.1 g).
10. Microscope slides, frosted at one end at 25 × 75 mm).
11. Cover slips (24 × 32 mm).
12. Tweezers (Sigma-Aldrich; cat. no. T5790 or similar).
13. Fine-meshed stainless-steel strainer.
14. Metal cubes (approx 40 mg each) for weights.
15. Ethanol, 70%.
16. Faure's solution: 30 mg Gum arabic, 20 mL glycerol, 50 mg chloral hydrate, 50 mL water.
17. Nail polish.
18. Live baker's yeast.
19. Sucrose or sugar (crystalline).
20. Agar–agar (powdered).
21. Powdered cellulose (Merck), used for acute treatment.

3. Methods

3.1. Culturing and Treatment of Tester Strains

Set up the following two crosses by mating 80 virgin females with 40 males per vial:

1. Standard cross (**ST**): Cross *flr^3/TM3, Bd^S* females to *mwh/mwh* males.
2. High-bioactivation cross (**HB**): Cross *ORR/ORR; flr^3/TM3, Bd^S* females to *mwh/mwh* males.

3.1.1. Chronic Exposure: 3-D-Old Larvae Treated for 48 H

1. After 3 d put the parental flies in culture bottles containing a solid agar base (3% [w/v] agar–agar in water) covered completely with an approx 5-mm layer of live baker's yeast supplemented with sucrose.

2. Eight hours later remove the flies from the bottles.
3. Wash out the 3-d-old larvae (72 ± 4 h after the beginning of oviposition) with tap water through a fine-meshed stainless-steel strainer.
4. Put the larvae, in equal batches of approx 100, into plastic vials containing 1.5 g of *Drosophila* Instant Medium.
5. Use 5 mL of the test compound solutions to rehydrate the 1.5 g of dry instant medium (*see* **Note 1**). Include a negative control, using water or solvent.

The treated individuals remain in the vials until the emergence of the surviving adult flies.

3.1.2. Acute Exposure: 3-D-Old Larvae Treated for 2–6 H

1. Follow **Subheading 3.1.1., steps 1–3**.
2. Put the 3-d-old larvae into plastic tubes that have one end covered with fine nylon gauze.
3. Place the tube into a 50-mL beaker containing 0.3 g of powdered cellulose and 1.5 mL of mutagen solution. The larvae will immediately start to feed through the gauze on the wet powdered cellulose.
4. Two to six hours later, remove the larvae by rinsing them with tap water.
5. Flush the larvae into a culture vial containing 1.5 g of dry *Drosophila* Instant Medium wetted with 5 mL of distilled water.

The standard procedure for the wing spot assay employs the chronic exposure. However, when the compound under investigation is chemically unstable, the acute exposure must be used.

3.2. Preparation of Wings

1. Collect the emerged adult flies, both *mwh +/+ flr*^{3} *and mwh +/TM3, Bd*^{S} genotypes, from both the **ST**, and **HB** crosses and store in 70% ethanol. *TM3* heterozygotes are identified by the *Bd*^{S} serration on the wing extremity.
2. Rinse the flies in water and then transfer them into a drop of Faure's solution on a slide.
3. Detach the wings from the body.
4. With tweezers, line up on a clean slide 10 female and 10 male wings per slide, ensuring that they are spread out.
5. Keep the wings in a dust-free environment (e.g., in a Petri dish) for at least 24 h, or for 1 h on a hot plate (60°C), because they need to be firmly glued to the slide.
6. Put a droplet of Faure's solution on a cover slip, and with the drop hanging, lower it on top of the wings.
7. Place several metal cubes on top of the cover slip for at least 24 h at room temperature, or for 1 h on a hot plate (60°C), while the preparation dries and hardens.
8. Seal the cover slip with nail polish to obtain a permanent preparation.

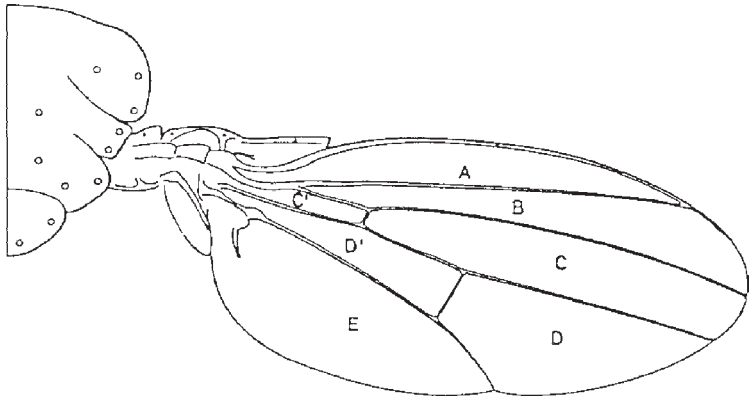

Fig 1. Wing areas, **A–E**, inspected for spots.

3.3. Microscopic Analysis of Wings

1. Inspect both the dorsal and the ventral surfaces of the wings under 400× magnification for the presence of single spots (*mwh* or *flr* phenotype) or twin spots (a *mwh* clone adjacent to a *flr* clone).
2. Note the position of the spots according to the sector of the wing (*see* **Fig. 1**).
3. Score clones only in the distal wing compartment. Record the size of each spot (the number of affected cells), its type (whether it is a *mwh* or *flr* spot, or a twin spot), and its frequency (*see* **Note 2**).

The classification of small spots consisting of one or two affected cells poses some problems. Practice is needed to detect small single spots. Because they are more frequent in untreated controls, it is important to differentiate true mutants from developmental disturbances in trichome pattern formation (*see* **Notes 3–5**).

mwh: Classify as a *mwh* clone all cases in which a wing cell shows a *mwh* phenotype (i.e., ≥ three hairs) (*see* **Fig. 2**). Do not count groups of cells showing two hairs without any occurrence of one or more cells having three hairs. In cases of one three-hair cell alongside one or more cells with two hairs, count all cells as *mwh* (*see* **Fig. 2B**).

flr: *flr* single spots are very infrequent because they probably arise from relatively rare events such as point mutations at the locus, interstitial deletions, and perhaps double crossing-over. The expression of *flr* in large single clones is quite variable, ranging from pointed, shortened, and thickened hairs to amorphous, sometimes balloon-like extrusions of melanotic chitinous material (*see* **Fig. 2C**).

Twin spots: Manifest *flr* and *mwh* phenotype in the same clone. Consider as twin clones: (1) one or more *mwh* cells adjacent to one or more *flr* cells, as well as those separated by one or two wild-type hairs; and (2) clones formed by *flr* cells

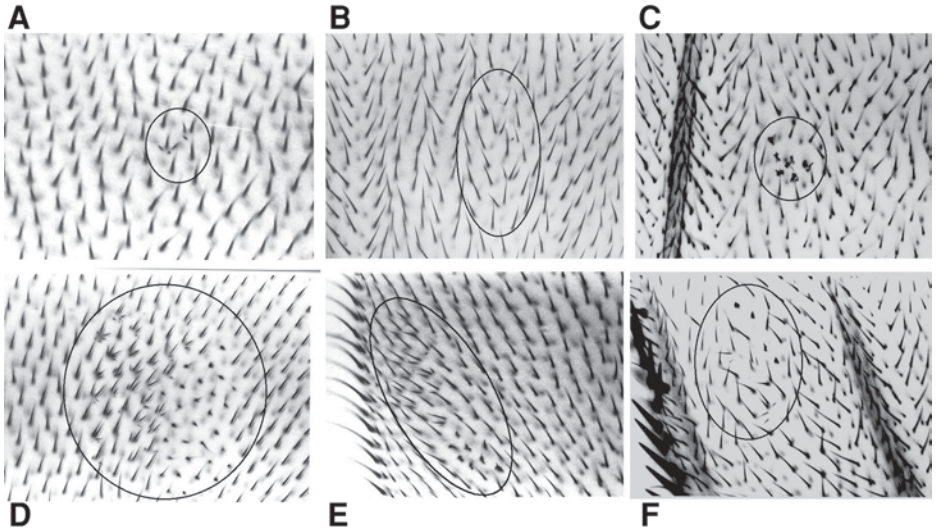

Fig 2. Different types of clones and their variations: **(A)**Small single spot with two cells expressing *mwh* phenotype; **(B)** large single spot with five cells expressing *mwh* phenotype. (Note that this is a spot that contains just one three-hair cell alongside four cells with two hairs.); **(C)** large single spot with six cells expressing *flr* phenotype; **(D)** twin spot with 30 cells expressing *mwh* phenotype alongside 30 cells expressing *flr* phenotype; **(E)** twin spot with 14 cells expressing *mwh* phenotype and 8 cells expressing *flr* phenotype; **(F)** twin spot with 4 cells expressing *mwh* phenotype and 4 cells expressing *flr* phenotype.

and cells containing one or more two-hair cells, as in this case, cells with two hairs are considered as *mwh* (*see* **Fig. 2D,E,F**).

3.4. Statistical Analysis

The statistical methods used to analyze SMART data, which make it possible to characterize a result as positive, weakly positive, negative, or inconclusive, were first presented by Frei and Würgler ***(54)***.

Some biological aspects of the wing spot test must be pointed out before considering the statistical analysis. First, the number of target cells in the wing primordium is not precisely known. However, we know that during the larval and early pupal stages, cells of the wing primordia undergo approx 12 rounds of division, beginning with some 10–30 cells after embryogenesis and ending up with approx 30,000 cells when cell division ceases at the onset of metamorphosis ***(54)***. In chronic exposure experiments, the number of clones per wing divided by the number of cells contained in a wing provides an overall estimate of the clone induction frequency per cell and per cell division. Second, clone

size reflects time of induction, according to the number of cell division cycles undergone between induction and metamorphosis. For continuous exposure, the expected clone size distribution in the ideal situation therefore corresponds to a geometric series with frequencies decreasing by a factor of 2 as clone size (measured in numbers of cells) increases by a factor of 2 ***(55)***.

In experiments designed to assess the mutagenicity of a given chemical, most often a treatment series is compared with a control series. One might like to decide whether the compound used in the treatment should be considered as mutagenic or nonmutagenic. The formulation of two alternative hypotheses allows one to distinguish among the possibilities of a positive, weakly positive, inconclusive, or negative result of an experiment. In the null hypothesis (H_0), one assumes that there is no difference in the mutation frequency between the control and treated series. Rejection of the null hypothesis indicates that the treatment resulted in a statistically increased mutation frequency. The alternative hypothesis (H_A) postulates *a priori* that the treatment results in an increased mutation frequency compared to the spontaneous frequency. This alternative hypothesis is rejected if the observed mutation frequency is significantly lower than the postulated increased frequency. Rejection indicates that the treatment did not produce the increase required to consider the compound as mutagenic. If neither of the two hypotheses is rejected, the results are considered inconclusive, as one cannot accept at the same time the two mutually exclusive hypotheses. In the practical application of the decision procedure, one defines a specific alternative hypothesis requiring that the mutation frequency in the treated series be *m* times that in the control series, which is then used together with the null hypothesis. It may happen in this case that both hypotheses have to be rejected. This would mean that the treatment is weakly mutagenic, but leads to a mutation frequency that is significantly lower than *m* times the control frequency ***(54)***.

3.4.1. Distinguishing Different Spot Types

In the wing spot assay, it is customary to assess genotoxicity not only for the total number of spots recovered, but also to distinguish twin spots from single spots, because twin spots are uniquely produced by mitotic recombination, whereas single spots can be produced by various mechanisms.

To assess negative results, empirically chosen multiplication factors (*m*) were originally introduced for testing ***(4,54)***; these are *m*=2 for both total spots and small single spots, because of their high spontaneous frequencies, and *m*=5 for both the rare spontaneous large single spots and twin spots ***(56)***.

3.4.2. Optimal Sample Size

In order to minimize the chance of inconclusive results, the statistical tests should be made sufficiently powerful. This can be achieved by planning

optimal experimental sample sizes. For an experiment with $p<5\%$, and tested in both directions, we need a control sample of such a size as to make the expected average yield be 32.5 spots on all control flies together. This figure is independent of stocks and test systems and is determined exclusively by theoretical parameters (i.e., the significance level [$p<5\%$] and the minimal risk [doubling effect]) we have opted for as well as the power we require (95% correct decisions). In the standard *mwh/flr*^{3} wing spot test with a spontaneous frequency regularly of approx 0.6 spots per fly, this corresponds to an optimal sample size of 55 flies (both wings analyzed) ***(56)***.

Determination of the optimal sample size depends on (1) the optimally sufficient number of spots expected in the control sample, which is a theoretical parameter, and (2) the mean frequency of spontaneous spots per individual, which is an empirical parameter. Although the former is independent of the particular strain or strain combinations used in experimentation, the latter is not. Therefore, working groups using the present method to find the optimal experimental sample size should base their sample size estimations on the specific spontaneous spot frequencies, which their strains or strain combinations show ***(56)***.

3.4.3. Pooling Data from Different Experiments

Normally, two or more experiments are performed with a test compound, and if no statistical differences are found between them, the data are pooled. Depending on the data, one can use different statistical tests to check for homogeneity/heterogeneity. In this case, if the individual series do not show overdispersion, the chi-squared test for proportion may be used. On the other hand, if there is overdispersion within samples, the Kruskal–Wallis H-test is more reliable, because the chi-squared (χ^2) test may be too liberal (Frei, personal communication) (*see* **Note 6**).

Pooled negative controls may be useful to estimate parameters (e.g., an optimal estimation of spontaneous spot frequencies). However, because of the possibility of heterogeneity among control samples, it is always advisable to carry out a parallel control and, for significance testing, to compare the experimental samples with the parallel control (Frei, personal communication).

3.4.4. Optimal Design

In order to minimize the risk of false-positive or false-negative test results, the minimum necessary requirements are (1) that each treatment series be accompanied by a concurrent control series, (2) that for each experiment the *ratio* between the number of treated flies and the number of control flies examined be the same, and (3) that for the control and the treatment group in each experiment, the *ratio* between females and males examined be the same ***(56)***.

3.4.5. Which Statistical Test to Use

To test the two hypotheses, several tests are suitable and almost equivalent: (1) The conditional binomial test (Kastenbaum and Bowman test) is recommended if the spot number is small; (2) the χ^2 test for proportions is used if the expected number of mutations in the control and treatment series are not too small (say, ≥5 each); (3) the *G* test (log-likelihood ratio test) and (4) the *U*-test (Mann–Whitney test) with correction for ties are used if the individual variability (within experiments, within sexes) contributes significantly to overdispersion.

3.4.6. The χ^2 Test for Proportions

3.4.6.1. Assessment of Positive Results: Testing Against the Null Hypothesis (H_0)

H_0: No difference between control and treatment group.

In an experiment with N_c untreated flies in the control and N_t treated flies in the treatment series, we test against the null hypothesis H_0 that wing spots are not increased in frequency in the experimental group. The expectation of n_c spots for the control flies and the expectation of n_t spots for the treated flies is, in each case, proportional to the numbers of flies in each group, n being the total number of mutations recovered in both series together.

Provided the respective expected numbers of mutations in the control and treatment series are not too small (say, ≥5 each), the χ^2 test for proportions may be used to test against H_0 and H_A. It may be recalled that with a sufficiently large n, the χ^2 test is equivalent to the binomial test. Frei and Würgler ***(54)*** proposed to use the χ^2 test with Yates' continuity correction, because with that approximation, the probabilities P_0 and P_A, corresponding to the respective calculated χ^2 values, become almost the same as with the conditional binomial test.

To illustrate how the calculations are carried out, we use the data from a treatment with docetaxel (0.005 m*M*) and the corresponding control data published in **ref. *18***. We test against the proportionality $p_0 : q_0$ among the observed total spots, whereby p_0 and q_0 are the proportions of control and treated flies respectively (note: $p_0 + q_0 = 1$).

The number of flies in the control was $N_c = 100$; the total number of spots in this series was $n_c = 46$, which gives the frequency of spots per fly for the control:

$$f_c = n_c/N_c = 46/100 = 0.460 \quad (1)$$

In the experimental series, the number of flies was $N_t = 60$; the number of spots was $n_t = 47$, with a resulting frequency of spots per fly of

$$f_t = n_t/N_t = 47/60 = 0.783 \quad (2)$$

From the data, one estimates that the frequency in the experimental series is 1.703 times the frequency in the control:

$$m_e = f_t/f_c = 1.703 \tag{3}$$

The proportion of wing spots expected in the control is

$$p_0 = N_c/(N_c + N_t) = 100/(100 + 60) = 0.625 \tag{4}$$

and in the experimental series is

$$q_0 = 1 - p_0 = N_t/(N_c + N_t) = 60/(100 + 60) = 0.375 \tag{5}$$

if the general incidence were the same in the two groups. Considering the number of spots in the control and experimental series together ($n = 93$) and applying Yates' correction, it is possible to test against H_0 by calculating

$$\begin{aligned}\chi^2 &= \{[(|n_c - p_0 n| - 1/2)^2]/p_0 n\} + \{[(|n_t - q_0 n| - 1/2)^2] / q_0 n\} \\ &= \{[(|46 - 0.625 \times 93| - 1/2)^2] / 0.625 \times 93\} \\ &+ \{[(|47 - 0.375 \times 93| - 1/2)^2] / 0.375 \times 93\} = 6.200\end{aligned} \tag{6}$$

Use a χ^2-table and look up the probability $p = \alpha$ of the calculated χ^2. The test is one sided as long as we are only interested in proving an increase in spot frequency in the treated group. A two-sided test ($p=2\alpha$) is indicated in comparisons whose interest lies in significant disproportions in both directions (e.g., if we ask whether the two sexes in a treatment group react differently).

$\chi^2 = 6.200$ exceeds the value $\chi^2_{(\alpha = 0.05,\ \nu = 1)} = 2.706$ tabulated for the one-sided test; thus, H_0 is rejected.

3.4.6.2. Assessment of Negative Results: Testing Against the Alternative Hypothesis (H_A)

H_A: Treated flies have *m*-times more spots than untreated ones.

One may be interested in "proving" that a substance is not hazardous. In this case, one tries to exclude the possibility that the spots observed could be the results of a mutagenic effect of the substance. A minimal risk cannot be excluded, but one may be able to exclude significantly a certain multiple (m) of the spontaneous frequency; that is, one may be able to demonstrate that the effect is significantly below a doubling of the spontaneous frequency (m=2, used for small single and total spots).

Under this hypothesis, the expected spot numbers are also proportional to the fly numbers ($p_A : q_A$), but they differ in addition, because the theory postulates that spots are found in proportions 1 : m in control and treated groups (note: $p_A + q_A = 1$).

For testing against H_A, the expectations change according to the multiple m we are testing against (here, $m = 2$, because $m_e = 1.7$). So, we have

$$p_A = N_c / (N_c + mN_t) = 100 / (100 + 2 \times 60) = 0.45455 \quad (7)$$

and

$$q_A = 1 - p_A = mN_t / (N_c + mN_t) = 2 \times 60 / (100 + 2 \times 60) = 0.54545 \quad (8)$$

which represent the respective proportions in which the spots would be expected in the control and experimental series if H_A was true. Again, using Yates' correction, we test against this hypothesis by calculating

$$\begin{aligned} \chi^2 = \{[(|n_c - p_A n| - 1/2)^2] / p_A n\} + \{[(|n_t - q_A n| - 1/2)^2] / q_A n\} = \\ = \{[(|46 - 0.45455 \times 93| - 1/2)^2] / 0.45455 \times 93\} \\ + \{[(|47 - 0.54545 \times 93| - 1/2)^2] / 0.54545 \times 93\} = 0.452 \end{aligned} \quad (9)$$

which is less than the value $\chi^2_{(\beta = 0,05,\, \nu = 1)} = 2.706$ tabulated for the one-sided test and, thus, H_A, is accepted. Having rejected H_0 and accepted $_A$ we conclude the test substance has a significant mutagenic effect (*see* **Note 7**).

3.4.7. The Conditional Binomial Test

In an experiment, the number of mutations in the control series can theoretically take any value, from 0 to n, and the number of mutations in the treated series can have any value, from n to 0. One calculates the binomial distributions (based on p_0, q_0, and n under H_0, and based on p_A, q_A, and n under H_A, already calculated for the χ^2 test) to determine the probabilities with which all the different possible results of an experiment are expected, with n mutations overall.

The respective significance levels at which we decide to test for rejection of H_0 and H_A were denoted by α and β, respectively. Conceptually, both tests are one sided. The opposite nature of the hypotheses requires that the cumulative probabilities (P_0 and P_A) be calculated from the opposite extreme ends of the respective binomial distributions ***(54)***.

According to the rationale set out, H_0 is rejected in the binomial test if

$$P_0 = \sum_{i=0}^{n_c} \binom{n}{i} p_0{}^i \, q_0{}^{n-i} = \sum_{r=n_t}^{n} \binom{n}{r} q_0{}^r \, p_0{}^{n-r} \leq \alpha \quad (10)$$

and, by analogy, H_A is rejected if

$$P_A = \sum_{i=0}^{n_t} \binom{n}{i} q_A{}^i \, p_A{}^{n-i} = \sum_{r=n_c}^{n} \binom{n}{r} p_A{}^r \, q_A{}^{n-r} \leq \beta \quad (11)$$

The tables of Kastenbaum and Bowman ***(57)*** for the conditional binomial test can be used for the test of both hypotheses. For rejection of H_0 and H_A, the frequencies q_0 and p_A, respectively, should be used to look up the corresponding limit numbers in the tables. H_0 is rejected if the number of mutations in the treated group (n_t) is larger than or equal to the tabulated value; H_A is rejected if

Table 1
Calculation Steps of the Mean *mwh* Clone Size Class ($\hat{i}$), With and Without Clone Size Correction, Induced After Treatment With 0.05 m*M* of Camptothecin[b]

	Treatment							
	Negative Control[b] (4% ethanol + 4% Tween-80) *N* = 78 flies			Camptothecin 0.05 m*M*[b] *N* = 20 flies			Camptothecin, 0.05 m*M*, control corrected	
Clone size category (i)[a]	Freq.	*mwh* spot number	Freq × i	Freq.	*mwh* spot number	Freq × i	Corrected frequency	Freq × i
1 (1 cell)	0.192	15	1 × 0.192 = 0.192	0.60	12	1 × 0.6 = 0.60	0.6–0.192 = 0.408	0.408
2 (2 cells)	0.218	17	2 × 0.218 = 0.436	1.10	22	2 × 1.1 = 2.20	1.1–0.218 = 0.882	1.764
3 (3–4 cells)	0.026	2	3 × 0.026 = 0.078	1.60	32	3 × 1.6 = 4.80	1.6–0.026 = 1.574	4.722
4 (5–8 cells)	0.013	1	4 × 0.013 = 0.052	1.20	24	4 × 1.2 = 4.80	1.2–0.013 = 1.187	4.748
5 (9–16 cells)	0.013	1	5 × 0.013 = 0.065	0.90	18	5 × 0.9 = 4.50	0.9–0.013 = 0.887	4.435

6 (17–32 cells)	0.013	1	6 × 0.013 = 0.078	0.95	19	6 × 0.95 = 5.70	0.95–0.013 = 0.937	5.622
7 (33–64 cells)	0	0	0	0.35	7	7 × 0.35 = 2.45	0.35–0 = 0.35	2.45
8 (65–128 cells)	0	0	0	0.50	10	8 × 0.5 = 4.00	0.5–0 = 0.50	4.00
9 (129–256 cells)	0	0	0	0.95	19	9 × 0.95 = 8.55	0.95–0 = 0.95	8.55
10 (> 256 cells)	0	0	0	0.35	7	10 × 0.35 = 3.50	0.35–0 = 0.35	3.50
Σ	0.475	37	0.907	8.50	170	41.10	8.025	40.199
Mean *mwh* clone size class ($\hat{i}$) Σ(Freq. × Cat.)/Σ Freq.		1.90			4.84			5.01

[a] *mwh* clones from single and twin spots were classified according to the number of cells they contain.
[b] Data were extracted from Cunha et al. ***(19)***.

Table 2
Clone Induction Frequency per 10^5 Cells and per Cell Division as Well as the Percentage of Recombination, With and Without Clone Size Correction, After Chronic Treatment with 0.5 m*M* of Camptothecin[a]

	Historical negative control (4% ethanol + 4% Tween-80)	Camptothecin (0.5 m*M*)
mwh/flr^3		
No. of flies (N)	78	20
Total *mwh* clones[b] (n)	37	170
Mean *mwh* clone size class[b–d] ($\hat{i}$)	1.89 [–]	4.84 [5.01]
Geometric mean of clone size[b–d] ($2^{\hat{i}-1}$)	1.86 [–]	14.22 [16.11]

	Without clone size correction[c–e] $f_t = (n/NC) \times 10^5$	With clone size correction[c–e] $f'_t = (2^{(\hat{i}-2)}) \times f$	Without clone size correction[c–e] $f_t = (n/NC) \times 10^5$	With clone size correction[c–e] $f'_t = (2^{(\hat{i}-2)}) \times f$
Clone induction frequencies (per 10^5 cells per cell division)	$f_t = 37/(78 \times 48{,}000) \times 10^5 = 0.97$ [–]	$f'_t = (2^{(1.89...-2)}) \times 0.97... = 0.91$ [–]	$f_t = 170/(20 \times 48{,}8000) \times 10^5 = 17.42$ [16.45]	$f'_t = 2^{(4.84...-2)} \times 17.41... = 124.31$ [132.42]

	Without clone size correction[c,d] $(1-f_h/f_t) \times 100$	With clone size correction[c,d] $(1-f'_h/f'_t) \times 100$
Recombination (%) in *mwh/flr*^{3} flies[f]	$(1-1.54.../17.42...) \times 100 = 91.18$ [94.24]	$(1-1.77.../124.31...) \times 100 = 98.58$ [98.98]

Table 2 *(continued)*
Clone Induction Frequency per 10^5 Cells and per Cell Division as Well as the Percentage of Recombination, With and Without Clone Size Correction, After Chronic Treatment with 0.5 m*M* of Camptothecin[a]

	Historical negative control (4% ethanol + 4% Tween-80)	Camptothecin (0.5 m*M*)
mwh/TM3		
No. of flies (N)	80	20
Total *mwh* clones[b] (n)	23	15
Mean *mwh* clone size class[b–d] ($\hat{i}$)	1.70 [–]	2.20 [2.51]
Geometric mean of clone size[b–d] ($2^{\hat{i}-1}$)	1.62 [–]	2.30 [2.86]

	Without clone size correction[c–e] $f_h = (n/NC) \times 10^5$	With clone size correction[c–e] $f'_h = (2^{(\hat{i}-2)}) \times f$	Without clone size correction[c–e] $f_h = (n/NC) \times 10^5$	With clone size correction[c–e] $f'_h = (2^{(\hat{i}-2)}) \times f$
Clone induction frequencies (per 10^5 cells per cell division)	$f_h = 23/(80 \times 48{,}800) \times 10^5$ = 0.59 [–]	$f'_h = 2^{(1.7...-2)} \times 0.58...$ = 0.48 [–]	$f_h = 15/(20 \times 48{,}800) \times 10^5$ = 1.54 [0.95]	$f'_h = 2^{(2.20...-2)} \times 1.54...$ = 1.77 [1.35]

[a]Data extracted from Cunha et al. ***(19)***.
[b]Considering *mwh* clones from *mwh* single spots and from twin spots.
[c]In order to render the table more easily read, only two decimals are shown.
[d]Numbers in square brackets are control corrected.
[e]C = 48,800 (i.e., approx number of cells examined per fly).
[f]Recombinational frequency is calculated only in *mwh/flr*^{3} markers using the clone induction frequencies obtained in *mwh/TM*3 flies, in which this event is suppressed.

the number of mutations in the control group (n_c) is larger than or equal to the tabulated value ***(54)***.

3.4.8. The U-Test of Wilcoxon, Mann, and Whitney

If individual variability (within experiments, within the same sex) contributes significantly to overdispersion, the fidelity of the aforementioned tests may be seriously affected (*see* **Note 8**). This is particularly the case for antimutagenicity or comutagenicity experiments, where the so-called positive control is compared with the cotreatment or posttreatment series to check if the modulator is modifying the genotoxic effect of a specific mutagen, or in cases where two experimental conditions (e.g., genotypes) are investigated. Pronounced individual variability can be the result of differential individual sensitivity and/or variable uptake of compounds. In this case, the U-test of Wilcoxon, Mann, and Whitney (also called Wilcoxon II) based on the number of spots recovered in individual flies is indicated ***(56)***.

3.5. Clone Parameters

3.5.1. Mean mwh Clone Size Class

Clones can be classified into size classes (i), delimited by powers $2^{\hat{\imath}-1}$, according to the number of *mwh* cells they contain. For continuous exposure in the ideal case, the mean clone size class is $\hat{\imath} = 2$ and the mean clone size is $2^{\hat{\imath}-1} = 2$ cells (geometric mean). In practice, the clones may be smaller or larger than theoretically expected. For compounds that are applied chronically, but are otherwise either unstable, bioactivated with delay, or inactivated rapidly during the last one to two rounds of cell division in the pupa, a correction of the estimated clone induction frequency may be appropriate according to the mean size of the clones ***(55)***.

Considering *mwh* clones from *mwh* single spots and from twin spots, it is possible to calculate the mean *mwh* clone size class *(î)*. This figure represents the clone size class in which the majority of clones induced by a specific treatment is located.

To illustrate how it is possible to find out the mean *mwh* clone size class, we use some data extracted from Cunha et al. ***(19)*** as shown in **Table 1**. To calculate the mean clone size (geometric mean), one has just to apply the $\hat{\imath}$, found in a specific treatment, in the formula $2^{\hat{\imath}-1}$. For example, the geometric mean of the clones found in the treatment with 0.05 m*M* of camptothecin is $2^{(4.84-1)} = 14.32$.

3.5.2. Clone Induction Frequencies Per Cell and Per Cell Division

At the end of wing development, the wing consists of approx 30,000 cells. Wing development starts with some 30 cells in the embryo. We can estimate

that there may be approx 10 rounds of cell division until metamorphosis. At each cell division round, the number of cells is doubled. Summing up the individual cell divisions gives C = 30 + 60 + 120 + 240 + 480 + 960 + 1920 + 3840 + 7680 + 15,360 ≈ 30,000, which is also the final number of cells present in the adult wing. In other words, there are as many cells in the adult wing as there are cell divisions of precursor cells during development. There is one cell generation in passing from 30 to 60 cells, one passing from 60 to 120, and so on. In the last (i.e., the 10th generation), the primordium passes from approx 15,000 to the final 30,000 cells (Frei, personal communication).

The *mwh* clone frequency per fly makes it possible to estimate the induction frequency per cell and per cell division. An appropriate estimation of the induction frequency is obtained if the *mwh* clones per fly frequency is divided by the number of cells (48,800) present in both wings (*see* **Table 2**). We use 48,800 (24,400 per wing) instead of 60,000 cells (2 × 30,000—considering both wings), because in screening for wing spots, we do not examine all the cells in a wing; there are approx 24,400 cells in the wing area we inspect for spots (*see* **Fig. 1**).

It seems desirable to estimate clone frequencies in the SMART as induction frequencies per cell and per cell generation. It has been proposed that, depending on the time of induction, such frequency determinations should include a clone size correction. However, if the interpretation is correct, that small clone size in balancer heterozygotes reflects the presence of a chromosomal deficiency and not, or not only, a late time-point of induction in the course of development, a clone size-dependent correction of the clone induction frequency may be meaningless or may even falsify the result. Such would not only be the case for balancer heterozygotes, but to a certain extent also for inversion-free individuals, because in the latter, the same chromosomally aberrant clones are to be expected in addition to those produced by recombination. Cautious use of the clone size correction is therefore suggested, because in the case of particularly small clones, clone size-corrected induction frequencies may be underestimations, mainly in balancer heterozygous flies. In the case of particularly large clones, however, the uncorrected frequencies may be underestimations. In critical cases, therefore, one would probably determine both values to indicate the possible range of these estimates, as indicated in **Table 2** ***(55)***.

3.5.3. Quantification of Recombinagenicity

The relative frequency of twin spots may give some idea of the recombinagenicity of a compound. Genotoxic chemicals can give quite different results in this respect ***(33)***. Under the assumption that mitotic crossing over is proportional to the physical distance on the chromosome between the centromere and marker genes, one would expect approx 50% of twin spots (recombination between *flr*^{3} and the centromere) and 50% of *mwh* single spots to be caused by mitotic crossing over ***(9)***.

Some data have shown that twin spot identification depends on clone size. Ramel and Magnusson ***(33)*** have already pointed out that for chemicals producing predominantly small spots, the lack of the *flr*^{3} genotype expression in small clones leads to considerable biases, because small twin spots cannot be readily identified.

For an unbiased evaluation of recombinagenicity, it is therefore preferable to compare the *mwh* clone frequencies in the two genotypes *mwh/flr*^{3} and *mwh/TM3* (*see* **Table 2**). The difference in clone induction between the two genotypes is a quantitative measure of recombinagenicity ***(9)***.

4. Notes

1. It is also possible to use other types of medium, especially mashed potato—in this case, use 1.0 g of mashed potato, and 5 mL of the test solution.
2. In balancer heterozygous flies, induced LOH leads to only single *mwh* spots, reflecting predominantly point mutation and chromosome aberration, because the products of mitotic recombination involving the *TM3* chromosome and its structurally normal homologs are probably inviable ***(58)***. Note that because the *TM3* balancer chromosome carries *flr*$^+$, only *mwh* clones are observed.
3. Large clones mostly show an elongated shape and usually extend parallel to the longitudinal axis of the wing.
4. Marked clones on the wing blade appear in general as contiguous, noninterrupted spots.
5. In some cases, the spots are split into two or more cell groups of different size arranged along the axis of the main growth direction. In this case, those separated by three or more wild-type cell rows are scored as separate spots.
6. Heterogeneity tests are two-sided (e.g., comparisons among controls or among repetitions or between sexes).
7. Testing against both the null hypothesis and the alternative hypothesis allows four possible diagnoses:
   a. If H_0 is accepted and H_A rejected: negative.
   b. If H_0 and H_A are accepted: inconclusive.
   c. If H_0 is rejected and H_A accepted: positive.
   d. If H_0 and H_A are rejected: weak positive.
8. Aggregated data pooled over individuals, sex and experiments may show overdispersion; that is, there may be more variability in the data than theoretically expected. The statistical comparison of pooled control and treatment totals may then be too liberal because false-positive results (as well as of false-negative ones in decision procedures) are more likely to occur. Hence, such testing would increase the overall chance for conflicting diagnoses in critical situations ***(56)***.

References

1. Baker, B. S., Carpenter, A. T. C., and Ripoll, P. (1978) The utilization during mitotic cell division of loci controlling meiotic recombination and disjunction in *Drosophila melanogaster*. *Genetics* **90,** 531–578.

2. Baker, B. S. and Smith, D. A. (1979) The effects of mutagen-sensitive mutants of *Drosophila melanogaster* in nonmutagenized cells. *Genetics* **92,** 833–847.
3. Szabad, J. and Bryant, P. J. (1982) The mode of action of "discless" mutations in *Drosophila melanogaster*. *Dev. Biol*. **93,** 240–256.
4. Graf, U., Würgler, F. E., Katz, A. J., et al. (1984) Somatic mutation and recombination test in *Drosophila melanogaster*. *Environ. Mol. Mutagen.* **6,** 153–188.
5. Vogel, W., Graf, U., Frei, H., and Nivard, M. M. J. (1999) The results of assays in *Drosophila* as indicators of exposure to carcinogens, in *The Use of Short- and Medium-Term Tests for Carcinogens and Data on Genetic Effects in Carcinogenic Hazard Evaluation* (McGregor, D. B., Rice, J. M. and Venitt, S., eds.), IARC, pp. 427–470.
6. Zordan, M., Osti, M., Pesce, M., and Costa, R. (1994) Chloral hydrate is recombinogenic in the wing spot test in *Drosophila melanogaster*. *Mutat. Res.* **322,** 111–116.
7. Vogel, E. W. and Nivard, M, M. J. (1993) Performance of 181 chemicals in a *Drosophila* assay predominantly monitoring interchromosomal mitotic recombination. *Mutagenesis* **8,** 57–81.
8. Tiburi, M., Reguly, M. L., Schwartsmann, G., Cunha, K. S., Lehmann, M., and Andrade, H. H. R. (2002) Comparative genotoxic effect of vincristine, vinblastine, and vinorelbine in somatic cells of *Drosophila melanogaster*. *Mutat. Res.* **519,** 141–149.
9. Frei, H. and Würgler, F. E. (1996) Induction of somatic mutation and recombination by four inhibitors of eukaryotic topoisomerases assayed in the wing spot test of *Drosophila melanogaster. Mutagenesis* **11,** 315–325.
10. Moraga, A. A. and Graf, U. (1989) Genotoxicity testing of antiparasitic nitrofurans in the *Drosophila* wing somatic mutation and recombination test. *Mutagenesis* **4,** 105–110.
11. van Schaik, N. and Graf, U. (1991) Genotoxicity evaluation of five tricyclic antidepressants in the wing somatic mutation and recombination test in *Drosophila melanogaster. Mutat. Res.* **260,** 99–104.
12. van Schaik, N. and Graf, U. (1993) Structure-activity relationships of tricyclic antidepressants and related compounds in the wing somatic mutation and recombination test in *Drosophila melanogaster*. *Mutat. Res.* 2**86,** 155–163.
13. Yoo, A., Ryo, H., Todo, T., and Kondo, S. (1985) Mutagenic potency of heterocyclic amines in the *Drosophila melanogaster* wing spot test and its correlation to carcinogenic potency. *Jpn. J. Cancer Res.* (*Gan*) **76,** 468–473.
14. Graf, U., Wills, D., and Würgler, F. E. (1992) Genotoxicity of 2-amino-3-methylimidazo (4,5-f) quinoline (IQ) and related compounds in *Drosophila. Mutagenesis* **7,** 145–149.
15. Negishi, T., Shiotani, T., Fujikawa, K., and Hayatsu, H. (1991) The genotoxicities of *N*-nitrosamines in *Drosophila melanogaster* in vivo: the correlation of mutagenicity in the wing spot test with the DNA damages detected by the DNA repair test. *Mutat. Res.* **252,** 119–128.
16. Frei, H., Lüthy, J., Brauchli, J., Zweifel, U., Würgler, F. E., and Schlatter, C. (1992) Structure/activity relationships of the genotoxic potencies of sixteen pyrrolizidine alkaloids assayed for the induction of somatic mutation

and recombination in wing cells of *Drosophila melanogaster*. *Chem. Biol. Interact.* **83,** 1–22.
17. Campesato, V. R., Graf, U., Reguly, M. L., and Andrade, H. H. R. (1997) The recombinogenic activity of integerrimine, a pyrrolizidine alkaloid from *Senecio brasiliensis*, in somatic cells of *Drosophila melanogaster. Environ. Mol. Mutagen.* **29,** 91–97.
18. Cunha, K. S., Reguly, M. L., Graf, U., and Andrade, H. R. R. (2001) Taxanes: the genetic toxicity of paclitaxel and docetaxel in somatic cells of *Drosophila melanogaster*. *Mutagenesis* **16,** 79–84.
19. Cunha, K. S., Reguly, M. L., Graf, U., and Andrade, H. H. R. (2001) Comparison of camptothecin derivatives presently in clinical trials: genotoxic potency and mitotic recombination. *Mutagenesis* **17,** 141–147.
20. Cunha, K. S., Reguly, M. L., Graf, U., and Andrade, H. H. R. (2001) Somatic recombination: a major genotoxic effect of two pyrimidine antimetabolitic chemotherapeutic drugs in *Drosophila melanogaster. Mutat. Res.* **514,** 95–103.
21. Delgado-Rodriguez, A., Ortíz-Marttelo, R., Graf, U., Villalobos-Pietrini, R., and Gómez-Arroyo, S. (1995) Genotoxic activity of environmentally important polycyclic aromatic hydrocarbons and their nitro derivatives in the wing spot test of *Drosophila melanogaster*. *Mutat. Res.* **341,** 235–247.
22. Graf, U. and Singer, D. (1989) Somatic mutation and recombination test in *Drosophila melanogaster* (wing-spot test): effects of extracts of airborne particulate matter from fire-exposed and non-fire-exposed building ventilation filters. *Chemosphere* **19,** 1094–1097.
23. Pimentel, A. E. P., Cruces, P, M. M., and Zimmering, S. (1991) Evaluation of the mutagenic potential of tepezcohuite in the *Drosophila* wing spot test. *Mutat. Res.* **264,** 115–116.
24. Graf, U. and Würgler, F. E. (1986) Investigation of coffee in Drosophila genotoxicity test. *Food Chem. Toxicol.* **24,** 835–842.
25. Abraham, S. K. (1994) Antigenotoxicity of coffee in the Drosophila assay for somatic mutation and recombination. *Mutagenesis* **9,** 383–386.
26. van Schaik, N., Grant, A., Rubenchik, I., and Graf, U. (1984) Use of Drosophila test systems for genotoxicity testing of herbal tea. *Immunol. Hematol. Res.* **3,** 199–202.
27. Graf, U., Alonso Moraga, A., Castro, R., and Díaz Carrillo, E. (1994) Genotoxicity testing of different types of beverages in the *Drosophila* wing somatic mutation and recombination test. *Food Chem. Toxicol.* **32,** 423–430.
28. Lehmann, M., Graf, U., Reguly, M. L., and Andrade, H. H. R. (2000) Interference of tannic acid on the genotoxicity of mitomicin C, methylmethanesulfonate, and nitrogen mustard in somatic cells of *Drosophila melanogaster*. *Environ. Mol. Mutagen.* **36,** 195–200.
29. Abraham, S. K. and Graf, U. (1996) Protection by coffee against somatic genotoxicity in Drosophila: Role of bioactivation capacity. *Food Chem. Toxicol.* **34,** 1–14.

30. Olvera, O., Zimmering, S., Arceo, C., and Cruces, M. (1993) The protective effects of chlrophyllin in treatment with chromium (VI) oxide in somatic cells of *Drosophila. Mutat. Res.* **301,** 201–204.
31. Negishi, T., Nakano, H., Kitamura, A., Itome, C., Shiotani, T., and Hayatsu, H. (1994) Inhibitory activity of chlorophyllin on the genotoxicity of carcinogens in *Drosophila. Cancer Lett.* **83,** 157–164.
32. Cederberg, H. and Ramel, C. (1989) Modifications of the effect of bleomycin in the somatic mutation and recombination test in *Drosophila melanogaster*. *Mutat. Res.* **214,** 69–80.
33. Ramel, B. and Magnusson, J. (1992) Modulation of genotoxicity in *Drosophila*. *Mutat. Res.* **267,** 221–227.
34. Sato, T., Nagaoka, K., Nagase, H., Niikawa, M., and Kito, H. (1996) The effect of several antipyretic alalgesics on mitomycin C-induced mutagenesis using the wing spot test in *Drosophila melanogaster*. *Jpn. Toxicol, J. Environ. Health* **42,** 136–141.
35. Katz, J. (1989) Sodium thiosulfate inhibits cisplatin-induced mutagenesis in somatic tissue of *Drosophila. Environ. Mol. Mutagen.* **13,** 97–99.
36. Hayatsu, H., Inada, N., Kakutani, T., et al. (1992) Suppression of genotoxicity of carcinogens by (–)-epigallocatechin gallate. *Prev. Med.* **21,** 370–376.
37. Santos, J. H., Graf, U., Reguly, M. L., and Andrade, H. H. R. (1999) The synergistic effects of vanillin on recombination predominate over its antimutagenic action in relation to MMC-induced lesions in somatic cells of *Drosophila melanogaster. Mutat. Res.* **444,** 355–365.
38. Torres, C., Ribas, G., Xamena, N., Creus, A., and Marcos, R. (1992) Genotoxicity of four herbicides in the *Drosophila* wing spot test. *Mutat. Res.* **280,** 291–295.
39. Kramers, P. G. N., Gryseels, A, B. J. M., Jordan, P., et al. (1991) Review of the genotoxicity and carcinogenicity of antischistosomal drugs: is there a case for a study of mutation epidemiology? Report of a task group on mutagenic antischistosomals. *Mutat. Res.* **257,** 49–89.
40. Romert, L., Magnusson, J., and Ramel, C. (1990) The importance of glutathione and glutathione transferase for somatic mutations in *Drosophila melanogaster* induced *in vivo* by 1,2-dichloroethane. *Carcinogenesis* **8,** 1399–1402.
41. Shibahara, T., Iyehara Ogawa, H., Ryo, H., and Fujikawa, K. (1995) DNA-damaging potency and genotoxicity of aflation M_1 in somatic cells *in vivo* of *Drosophila melanogaster*. *Mutagenesis* **10,** 161–164.
42. Frei, H., Lüthy, J., Brauchli, J., Zweifel, U., Würgler, F. E., and Schlatter, C. (1992) Structure/activity relationships of the genotoxic potencies of sixteen pyrrolizidine alkaloids assayed for the induction of somatic mutation and recombination in wing cells of *Drosophila melanogaster*. *Chem. Biol. Interact.* **83,** 1–22.
43. Guzmán-Rincón, J., Espinosa, J., and Graf, U. (1998) Analysis of the *in vivo* nitrosation capacity of the larvae used in the wing somatic mutation and recombination test of *Drosophila melanogaster. Mutat.Res.* **412,** 69–81.
44. Frölich, A. and Würgler, F. E. (1989) New tester strains with improved bioactivation capacity for the *Drosophila* wing-spot test. *Mutat. Res.* **216,** 179–187.

45. Saner, A., Weibel, B., Würgler, F. E., and Sengstag, C. (1996) Metabolism of promutagens catalyzed by *Drosophila melanogaster* CYP6A2 enzyme in *Saccharomyces cerevisiae*. *Environ. Mol. Mutagen.* **27,** 46–58.
46. Frölich, A. and Würgler, F. E. (1990) Genotoxicity of ethyl carbamate in the *Drosophila* wing spot test: dependence on genotype-controlled metabolic capacity. *Mutat. Res.* **244,** 201–208.
47. Graf, U. and van Schaik, N. (1992) Improved high bioactivation cross for the wing somatic mutation and recombination test of *Drosophila melanogaster*. *Mutat. Res.* **271,** 59–67.
48. Frölich, A. and Würgler, F. E. (1990) Drosophila wing-spot test: improved detectability of genotoxicity of polycyclic aromatic hydrocarbons. *Mutat. Res.* **234,** 71–80.
49. Graf, U. and Singer, D. (1992) Genotoxicity testing of promutagens in the wing somatic mutation and recombination test in *melanogaster, D. Rev. Int. Contam. Ambient.* **8,** 15–27.
50. Delgado-Rodriguez, A., Ortíz-Marttelo, R., Graf, U., Villalobos-Pietrini, R., Gómez-Arroyo, S., and Graf, U. (1999) Genotoxicity of organic extracts of airborne particles in somatic cells of *Drosophila melanogaster*. *Chemosphere* **39,** 33–43.
51. Silva, R. M. (1999) Genotoxicidade associada a amostras de água do rio Caí sob influência de dejetos urbanos, Dissertação de Mestrado. Universidade Federal do Rio Grande do Sul, Porto Alegre, Brazil.
52. Amaral, V. S. (2001) Monitoramento do impacto de dejetos industriais em amostras de água do rio Caí através do teste SMART em *Drosophila melanogaster*, Dissertação de Mestrado, Universidade Federal do Rio Grande do Sul, Porto Alegre, Brazil.
53. Lindsley, D. L. and Zimm, G. G. (1992) *The Genome of* Drosophila melanogaster, Academic, San Diego CA.
54. Frei, H. and Würgler, F. E. (1988) Statistical methods to decide whether mutagenicity test data from *Drosophila* assays indicate positive, negative or inconclusive result. *Mutat. Res.* **203,** 297–308.
55. Frei, H., Clements, J., Howe, D., and Würgler, F. E. (1992) The genotoxicity of the anti-cancer drug mitoxantrone in somatic and germ cells of *Drosophila melanogaster*. *Mutat. Res.* **279,** 21–33.
56. Frei, H. and Würgler, F. E. (1995) Optimal experimental design and sample size for the statistical evaluation of data from somatic mutation and recombination tests (SMART) in *Drosophila. Mutat. Res.* **334,** 247–258.
57. Kastenbaum, M. A. and Bowman, K. O. (1970) Tables for determining the statistical significance of mutation frequencies. *Mutat. Res.* **9,** 527–549.
58. Szabad, J., Soós, I., Polgár, G., and Brutlag, D. L. (1983) Testing the mutagenicity of malondialdehyde and formaldehyde by the *Drosophila* mosaic and the sex-linked recessive lethal tests. *Mutat. Res.* **113,** 117–133.

23

Analysis of Histoblasts

Mekkara Mandaravally Madhavan and Kornath Madhavan

1. Introduction

The epidermal cells, a derivative of ectoderm during embryogenesis of insects, contribute to the distinct cuticular pattern and form of the different stages that appear during their ontogeny. The type of cuticular products is the result of gene expression of the individual epidermal cells that lie immediately underneath these outgrowths ***(1)***. In hemimetabolous insects, the larval epidermal cells (LECs) present at the time of hatching from the egg and their descendants are responsible for the different cuticular patterns seen in the nymph and adult. In contrast, in many holometabolous insects, such as *Drosophila*, the distinct and different cuticular patterns exhibited by the larva and adult have a dual orgin; that of the larva is derived from the LEC and that of the adult is derived from the imaginal discs ***(2)***. The prospective integument of the adult head, thorax, genitalia, and analia is derived from imaginal discs ***(3–5)***. Each of the adult abdominal segments is derived mainly from three pairs of diploid histoblast nests (i.e., a pair of anterior dorsal [ADN], posterior dorsal [PDN] and ventral [VN] nests), located among the polytene LEC of the abdominal segments of the larva (*see* **Figs. 1**, **2A–C**, and **3A,B**). In addition, there is a pair of inconspicuous spiracular nests (SN) in each of the abdominal segments; during metamorphosis these nests (*see* **Fig. 3C**) develop into the paired spiracles on the lateral sides of the adult abdominal segment ***(3,6–9)***.

In the following, we describe the contributions of histoblasts in the formation of adult abdominal segments of *Drosophila*. The tergal area of each of the abdominal segments, depending on the presence or absence and the type of cuticular outgrowths, show distinct regions (*see* **Fig. 4A,B**). Histological studies and deletion of different histoblast nests indicate ***(8,10,11)*** that the descendents of the ADN form the hairy and bristled region of the tergum, whereas

From: *Methods in Molecular Biology, vol. 247:* Drosophila *Cytogenetics Protocols*
Edited by: D. S. Henderson © Humana Press Inc., Totowa, NJ

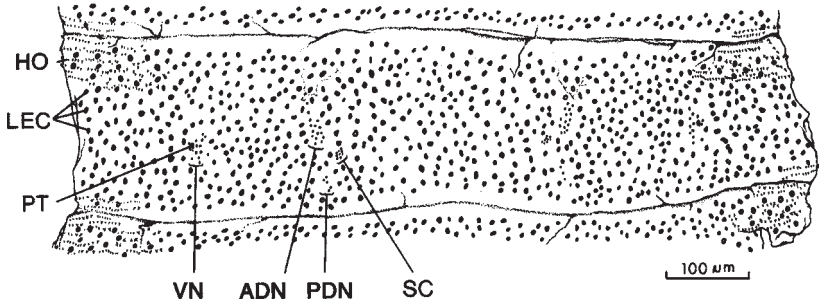

Fig. 1. Camera lucida drawing of a whole mount of the epidermis of the fourth abdominal segment of a 44 h old larva (same segment as shown in **Fig. 2A**). The whole mount was prepared after dissecting the larva mid-ventrally, treated with Feulgen's reagent, which tints the nuclei and shows the distribution of the paired anterior dorsal (ADN), posterior dorsal (PDN), and ventral (VN) histoblast nests among the larval epidermal cells (LECs). HO, ventral bands of hooks; SC, cluster of small cells of unknown function; PT, polytene cell in the midst of the VN. (From **ref. *7***, reproduced with permission of Springer-Verlag.)

those of the PDN contribute to the intersegmental membrane and the acrotergite ***(12)*** respectively (*see* **Fig. 4B**). The paired VN give rise to the sternum of the abdominal segments. The sternum contains a median sclerotized patch of cuticle, the sternite, with bristles and hairs, whereas the remaining area, the pleura, contains only hairs. The spiracles derived from the spiracular nests are located contralaterally in the pleura (*see* **Fig. 5A**). The location of these nests underneath the larval cuticle can be recognized externally in the third instar larvae and early puparia, by their closeness to larval muscle attachment sites, which appear as small depressions on the cuticle (*see* **Fig. 5B**).

The microscopic hairs, which decorate the tergite, sternite, and pleural regions, show distinct morphological features. The tergite and sternite hairs are long and thin with a narrow base and their shafts appear to arise sharply from the general body cuticle (*see* **Fig. 6A,B**). In contrast, the cuticle around the bases of the pleural hairs is membranous and thrown into folds. As a result, these hairs appear broad based (*see* **Fig. 6E**). The shaft of the pleural hairs appears forked with unequal arms (*see* **Fig. 6D**).

One of the main questions in the development of organisms is to understand, in cellular and molecular terms, how the component cells cooperate to generate a specific size and pattern in the resulting tissue or organ, and we are beginning to understand this. The development of the integument of the abdomen of *Drosophila* is suited for such studies because the histoblasts are an integral part of the larval abdominal epidermis and appear as a single layered epithe-

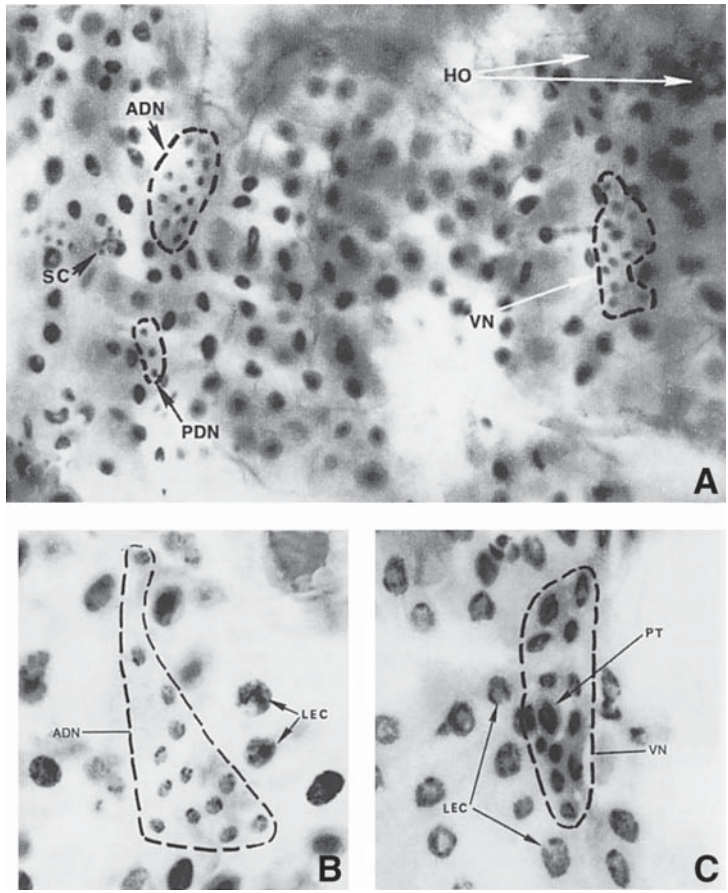

Fig. 2. **(A)** Whole mount of the right fourth abdominal hemisegment of a 44 h old larva showing the anterior dorsal (ADN), posterior dorsal (PDN), and ventral (VN) nests of histoblasts (enclosed by the dashed line), ventral band of hooks (HO), and cluster of small cells (SC) of unknown function. **(B)** Whole mount of the abdominal epidermis of the second segment of a 44-h-old larva showing the left anterior dorsal histoblast nest (ADN, enclosed by dashed line) among the larval epidermal cells (LECs). **(C)** Tangential section passing through the epidermis of the third abdominal segment of a 17-h-old larva showing the ventral nest (VN, enclosed by dashed line). See the polytene cell (PT) in the midst of the histoblasts, and the surrounding LECs. All preparations were stained with Feulgen's reagent and counterstained with fast green. (From **ref. *7***, reproduced with permission of Springer-Verlag.)

lium and thereby provides an excellent opportunity to examine cell–cell interactions and cell communication in a flat epithelial sheet (*see* **Fig. 1**). Further, this epithelium is more amenable to surgical manipulations and whole-mount

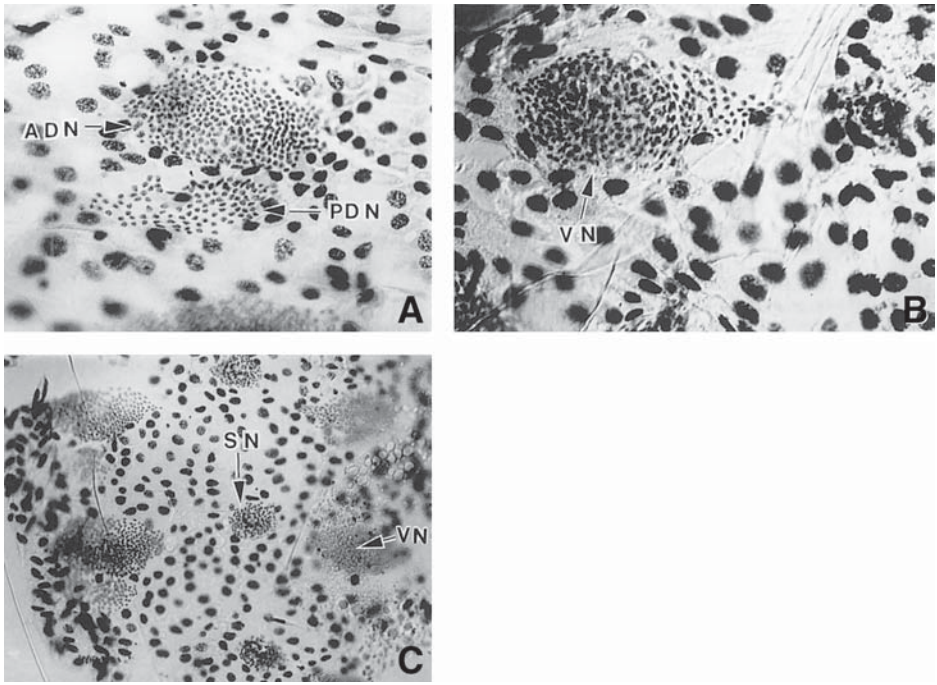

Fig. 3. **(A)** Appearance of the anterior dorsal (ADN), posterior dorsal (PDN), **(B)** ventral (VN), and **(C)** spiracular nests (SN) of wild type (18 h after pupariation) in whole-mount preparations stained with Feulgen's reagent. (From **ref. *9***, reproduced with permission of Springer-Verlag.)

histological preparations, compared to the pseudostratified epithelium of imaginal discs. Because there is no muliplication of the LECs or the histoblasts during the entire larval life of *Drosophila*, the spatial pattern established during late embryonic development is maintained in the larval epidermis. Thus, it is possible to uncouple mitosis from other processes occurring during the 96-h-long larval life. During metamorphosis, the histoblasts divide and begin to replace sequentially the LECs that undergo programmed cell death (apoptosis) ***(8,10)***. This facilitates visualization of the sequence of interactions, over a long period, of these two cell types side by side as they occur.

We now review the limited number of published studies on histoblasts, which illustrate their suitability for probing many problems in developmental biology. We also indicate where lacunae exist in the nonutilization of this model system for such studies.

When the different histoblast nests are deleted by γ-irradiation, the surrounding LECs survive metamorphosis and secrete cuticle and cuticular outgrowths

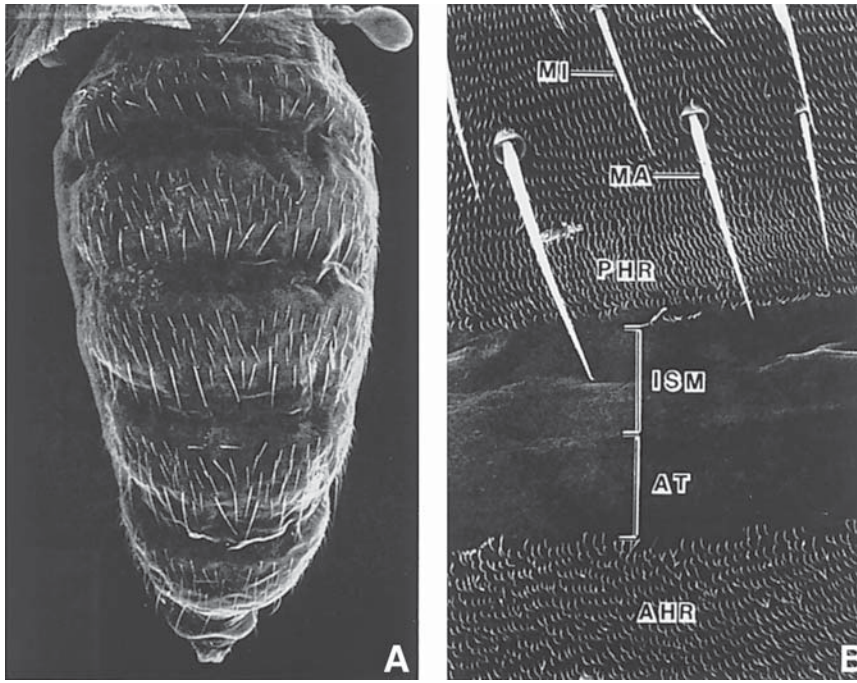

Fig. 4. **(A)** Scanning electron microscopic (SEM) picture of the dorsal view of a stretched abdomen of a female adult fly exposing the fairly wide and usually folded intersegmental hairless regions, alternating with tergites, which are decorated with cuticular outgrowths. **(B)** An enlarged view of the posterior of the third and anterior of the fourth tergite and the intersegmental region showing the details of the cuticular landscape. AHR, anterior hairy region, AT, acrotergite, ISM, intersegmental membrane, MA, macrochaeta, MI, microchaeta, PHR, posterior hairy region. (From **ref. *8***, reproduced with permission of the Company of Biologists.)

(hairs) characteristic of their positions in the abdominal segment (*see* **Fig. 7A–D**). This indicates that the LEC may contain the blueprint for the adult abdominal cuticlar pattern ***(13)***. Whether this information is transmitted to the histoblasts and, if so, how that is done are details yet to be worked out.

Formation of the tergite and median sternite by the paired histoblast nests also offers an opportunity to analyze the roles of mitosis, cell growth, cell migration, and cell death in histoblasts in the realization of the final size of these sclerotized cuticular tissues. So far, no studies have been published on these aspects.

During metamorphosis of *Drosophila*, one of the intrinsic signals that allows the replacement of LECs by the histoblasts could come from differential titers of juvenile hormones and ecdysones. Although there is no record of studies on

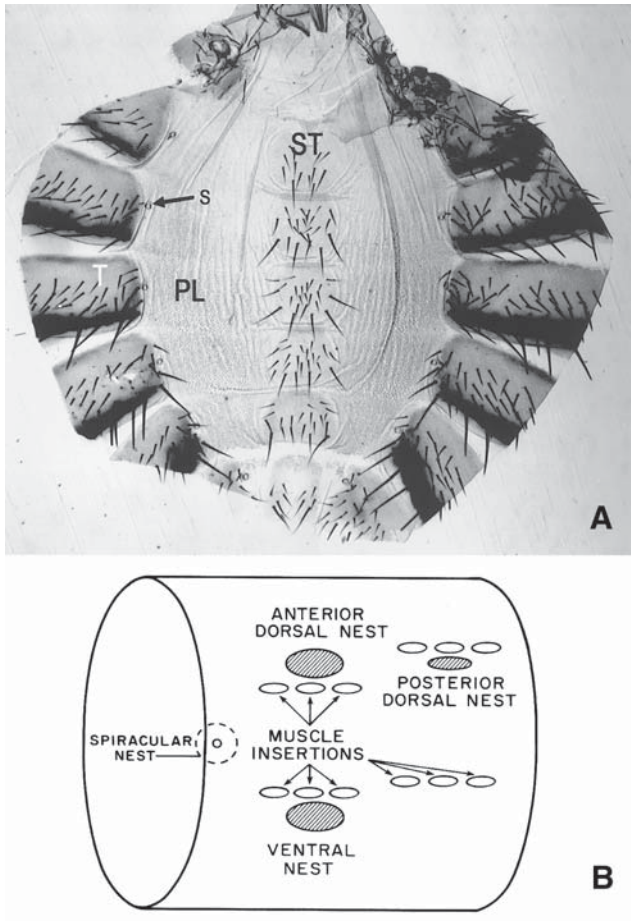

Fig. 5. **(A)** Whole mount of the unstained abdominal cuticle of an adult female fly. The abdomen was cut mid-dorsally and the cuticle was spread to show the median sternites (ST), pleura (PL), and paired spiracles (S). T, cut portion of tergite. **(B)** Diagrammatic representation of the relative positions of the three histoblast nests and nearby muscle attachment sites in the left side of a hemisegment of a third instar larval epidermis. (From **ref.** ***10***, reproduced with permission of Springer-Verlag.)

the role of ecdysones on the dynamics of growth and differentiation of histoblasts, a few studies indicate that juvenile hormone and its synthetic analogs do affect mitosis in them and secretion of adult abdominal cuticle and its outgrowths ***(14–17)***.

Mitotic recombination using X-ray irradiation during different stages of embryonic and postembryonic development has been used extensively to gen-

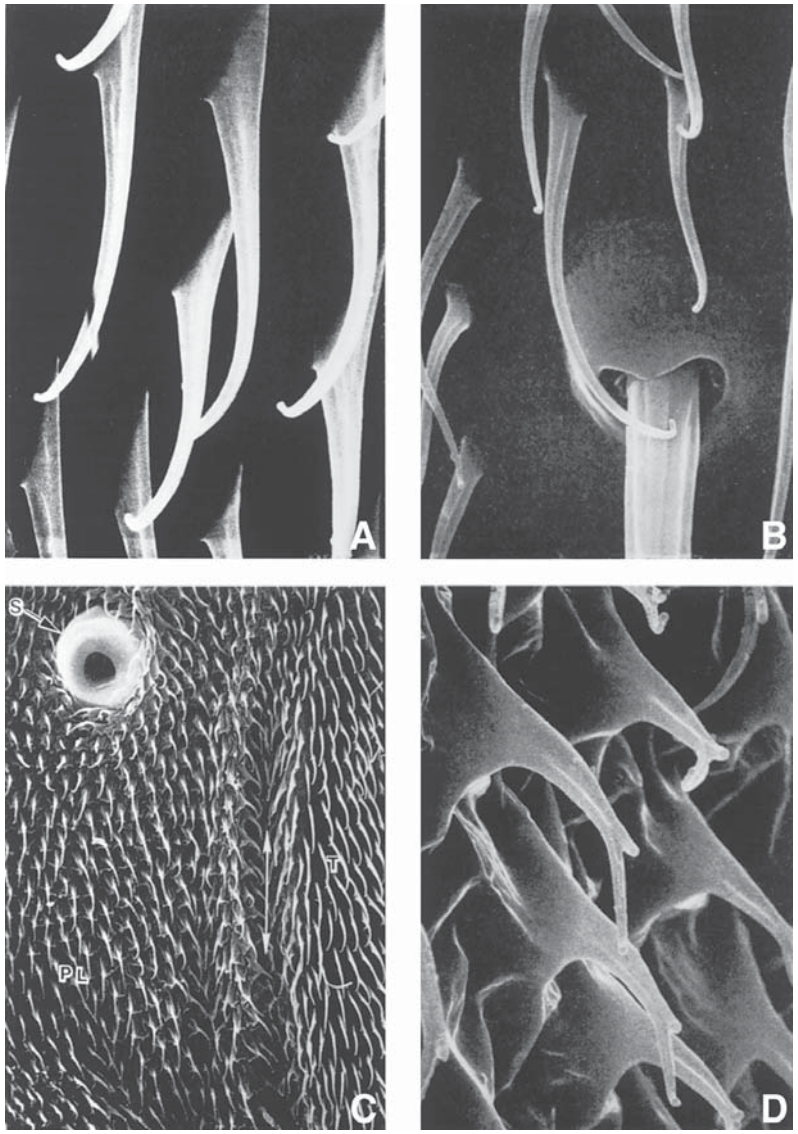

Fig. 6. SEM pictures of adult abdominal hairs showing their distinct morphology: **(A)** tergal hairs and **(B)** sternal hairs. These are long and narrow and project abruptly from the cuticle. **(C)** The relative positions of the spiracle in the pleura and the tergo-pleural border line (arrow). PL, pleural region; S, spiracle; T, tergal region. **(D)** Note that the cuticle around the bases of the pleural hairs is thrown into folds and the hairs appear broad based, in constrast to those of the tergite and sternite. The shafts of the hairs are forked. (From **ref. *8***, reproduced with permission of the Company of Biologists.)

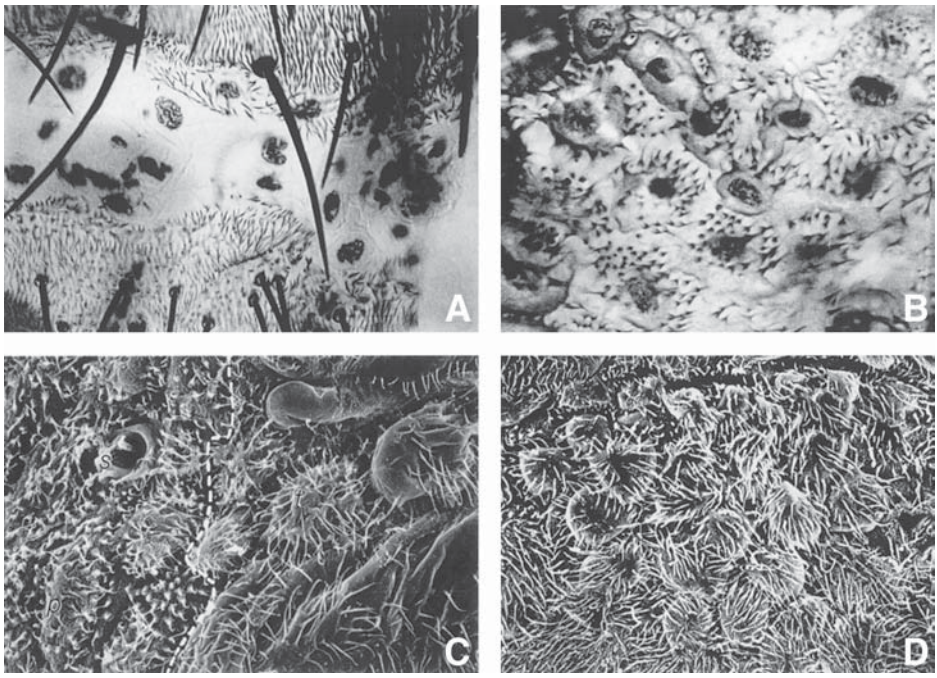

Fig. 7. **(A)** and **(B)** are Feulgen-stained whole-mount preparations and **(C)** and **(D)** are SEM images of regions of abdominal segments of adults resulting from larvae that received γ–radiation. **(A)** Posterior of the third and anterior of the fourth hemitergite and their intersegmental region. Persisting LECs, which are immediately posterior to the macrochaetae, secrete hairs, whereas those in the intersegmental region secrete smooth cuticle. **(B)** Pleural region. Note that the hairs secreted by the surviving polytene LECs show bulbous bases. **(C)** The tergopleural border (dashed line) of the left fourth hemisegment showing two different kinds of hair secreted by the tergal (t) and pleural (p) LECs. S, remnant of spiracle. **(D)** Third sternite region showing surviving LECs bearing hairs, which, similar to those on the tergite, are narrow, long, and without folds at their bases. (From **ref.** ***13***, reproduced with permission of the Company of Biologists.)

erate genetically marked twin spots to estimate the primordial cell numbers in, and growth dynamics of, different histoblast nests ***(18)***. Madhavan and Schneiderman ***(7)*** have also studied these features of the histoblasts from histological observations and have compared the advantages and disadvantages of these two protocols. More recently, FLP/FRT (*see* Chapter 17) and SMART (*see* Chapter 22) methods have been employed to generate mitotic recombination in the imaginal cells.

Although extensive studies have been done in the identification of genes, their products and their role in pattern formation, regulation of size, and cell

death in the cuticular structures resulting from the imaginal discs of *Drosophila*, such studies have only just begun in the histoblasts. Madhavan and Madhavan ***(9)*** observed that mutation in epidermal growth factor receptor (EGFR), a transmembrane receptor tyrosine kinase (RTK), affects mitosis, spreading and differentiation of adult epidermal cells derived from the various histoblast and spiracular nests (*see* **Figs. 8A–C** and **9**). Further, the need for EGFR becomes critical after pupation, and the requirement continues throughout pharate adult development for the correct development of the abdominal integument and spiracle. It is reported that Wingless (Wg) determines tergite and sternite cell fates ***(19,20)***, and EGFR acts synergistically with Wg ***(20)***. Kopp et al. ***(20)*** have also shown that Decapentaplegic (DPP) opposes Wg and EGFR signaling, thus promoting pleural fate in the adult abdominal epidermal cells. This explains the wild-type abdominal cuticular pattern observed in the DPP mutant adult flies.

The expression of the selector gene *engrailed* (*en*) determines the posterior compartment of the tergite ***(21)***. Under the influence of *en,* all cells in the posterior compartment secrete Hedgehog (Hh). This protein enters into the anterior compartment of this segment and that of the following, forms concentration gradients, and at least partly dictates the stereotypic anterior–posterior landscape and affinities of cells of the adult tergite ***(22–25)***. The details of what finally controls the polarity of the cuticular outgrowths on the tergum and sternum are still unclear ***(26)***.

It is possible that the reluctance to apply histological and molecular histological methods to this system could be the result of the difficulty in making planar whole-mount preparations of histoblasts and LECs, and in the identification of the smaller and fewer cells of histoblast nests during larval stages (*see* **Fig. 1**) and metamorphosis. We believe that our stepwise description of the methods on whole-mount preparation of the integument during different stages of development of *Drosophila* will enable the reader to obtain a flat preparation, wherein the location of different histoblast nests and the surrounding LECs can clearly be seen after conventional nuclear and cytoplasmic staining, or specific molecular and immunological staining protocols can be applied for diverse analyses of these two types of cell, during the epigenesis of the abdominal segments.

2. Materials

1. Wild or mutant strains of *Drosophila*.
2. Egg collection plates (per 1 L): Dissolve 22.5 g of Bacto-agar (Difco) and 25 g of sucrose in 750 mL of boiling water. Add 250 mL of apple juice. Cool to approx 60°C and pour into Petri dishes (50 × 9 mm) halfway without air bubbles. Let the contents harden, cover and store at 4°C. Bring to room temperature before use.

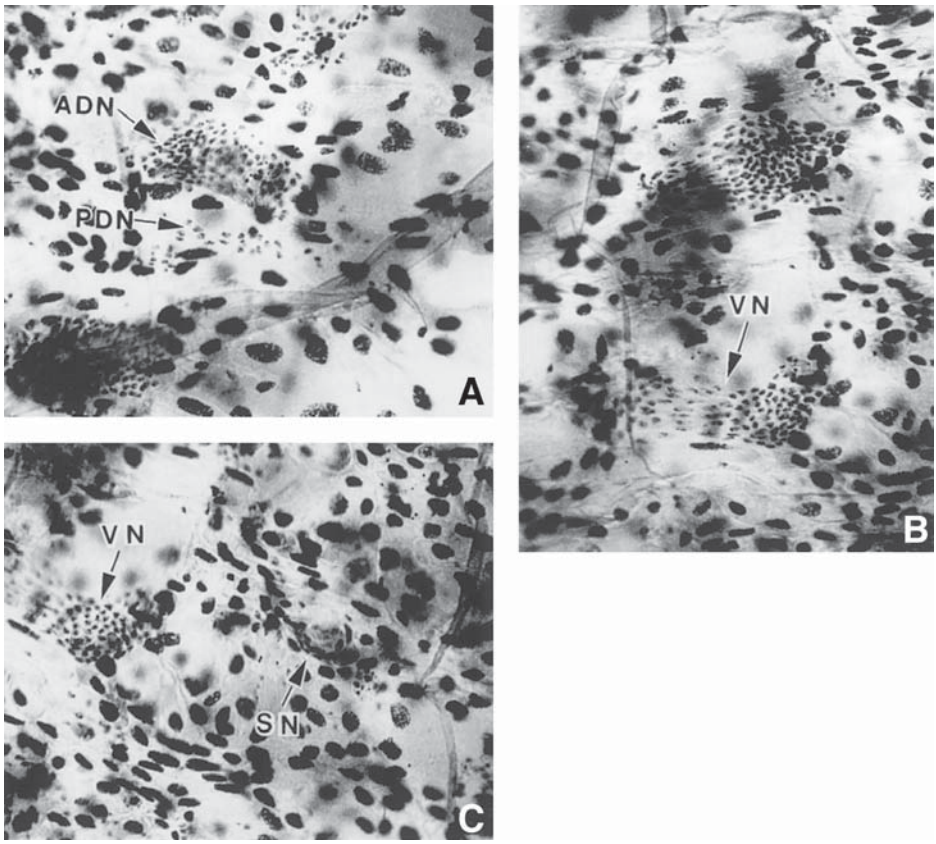

Fig. 8. Feulgen-stained whole-mount preparation from the EGFR mutant (*torpedo*) animal 18 h after pupariation showing a conspicuous reduction in the number of cells in the **(A)** anterior dorsal (ADN) and posterior dorsal (PDN), **(B)** ventral (VN), and **(C)** spiracular (SN) nests. Compare the appearance of these nests to those of the wild-type animal of the same stage of development in **Fig. 3**. (From **ref. *9***, reprinted with permission of Springer-Verlag.)

3. *Drosophila* Ringer's solution ***(27)***: 130 m*M* NaCl, 4.7 m*M* KCl, 1.9 m*M* $CaCl_2$. Dissolve 7.5 g NaCl, 0.35 g KCl, and 0.21 g $CaCl_2 \cdot 2H_2O$ in 1000 mL of distilled water. Store at 4°C in a stoppered bottle.
4. Kahle's fixative: Mix 12 mL of filtered formalin, 32 mL of absolute ethanol, 2 mL of glacial acetic acid, and 60 mL of water. Store in a stoppered bottle at room temperature.
5. Pasteur pipets, small paintbrushes, Sharpie pens.
6. Watchmaker's forceps (#3).
7. Straight iridectomy scissors.

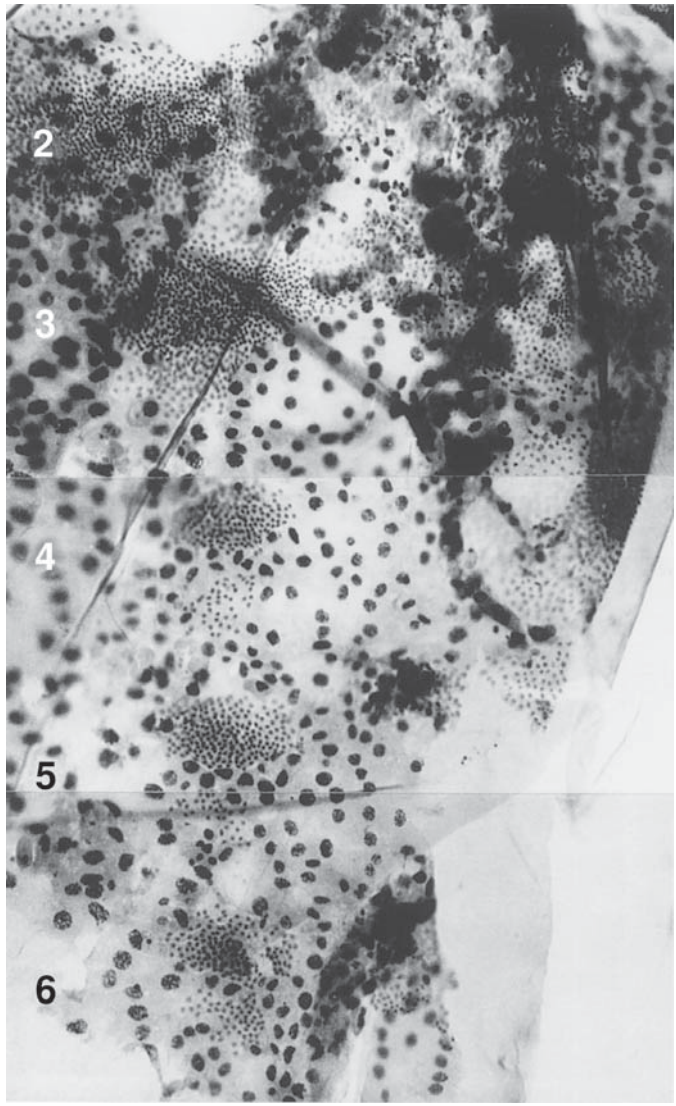

Fig. 9. Feulgen-stained whole-mount preparation of the abdominal integument of an EGFR mutant (*torpedo*) pharate adult, 25 h after pupariation. The photo montage of the right dorsal histoblast nests of the second to sixth segments shows a range of defects as a result of the mutation. The anterior dorsal and posterior dorsal nests of segments 2 and 3 have fused together, show a normal number of cells, and have started to spread in all directions, replacing the larval epidermal cells, as in the wild type at this stage of development. However, the dorsal nests of segments 4, 5, and 6 contain fewer cells, still remain apart, and are yet to spread actively. (From **ref. *9***, reproduced with permission of Springer-Verlag.)

8. Sharp, steel dissecting needles.
9. Small Stender dishes (36 × 19 mm).
10. Glass depression slides.
11. Precleaned RITE ON (frosted at one end) microslides (Fisher Scientific).
12. No. 1 Glass cover slips (22 × 22 mm^2) (Fisher Scientific).
13. Small plastic Petri dishes (50 × 9 mm)
14. Filter paper (42.5 mm in diameter) to line the Petri dishes.
15. Ethanol: 30%, 50%, 70%, 90%, 95%, and 100%.
16. Schiff's Feulgen reagent ***(28)*** (*see also* Chapter 7): Put 1 g of basic fucshin in a 500-mL Erlenmeyer flask. Add 200 mL of boiling distilled water to dissolve the stain (*see* **Note 1**). Stir for 5 min, cap with aluminum foil, and cool to exactly 50°C. Filter and add 20 mL of 1 *N* HCl to the filtrate. Cool to 25°C and add 1 g of sodium metabisulfite ($Na_2S_2O_5$). Stir well. Keep the solution in a stoppered and aluminum-foil-covered bottle in the dark for 20 h at room temperature. The solution should appear straw colored after this period. Add 1 g of activated charcoal and stir for 2 min. Filter; the filtrate should be clear (*see* **Note 2**). Store the clear filtrate in another stoppered bottle covered with aluminum foil at 4°C. This can be used as long as it remains colorless. Bring the solution to room temperature before use.
17. 6 *N* HCl: Add 50 mL of concentrated (12 *N*) HCl to 50 mL of distilled water. Stir.
18. Bleaching solution: Make stock solutions of 100 mL each of 10% potassium bisulfite ($K_2S_2O_5$) and 1 *N* HCl in distilled water. Just before use, add 5 mL $K_2S_2O_5$ to 90 mL of distilled water and stir well. To this, add 5 mL of 1 *N* HCl and mix well. Keep in a stoppered bottle.
19. 1% Fast green in 70% ethanol.
20. Xylene.
21. Permount mounting medium (Fisher Scientific).
22. Water mounting medium (Fisher Scientific).
23. Brass bars (5 × 1 × 1 cm^3).
24. 1 *N* NaOH: Dissolve 4 g NaOH in 100 mL of distilled water. Store in a bottle with a nonglass stopper.
25. Small hot plate (10 cm in diameter).

3. Methods

1. Keep fly stocks in an incubator maintained at 25 ± 1°C and 65% relative humidity.
2. Transfer well-fed adults from a stock culture food bottle to a fresh food bottle (without live yeast grains), cap it with an egg collection plate, and make two precollections of eggs of 1 h each using separate plates. This procedure will remove older eggs retained in the oviducts of the flies. Replace the second precollection plate with a fresh one and collect eggs for 30 min. This will allow emergence of a synchronized population of larvae from these eggs. Repeat this step until one gets enough eggs.
3. Keep the eggs in the plates for 21 h. Remove any prehatched larvae and collect freshly hatched ones for the next 10 min and transfer them to a new vial of food to continue further development. Under these conditions, the first, second, and

third instars last 0–24, 24–48, and 48–96 h after hatching from the egg respectively (*see* **Note 3**).

4. Collect freshly pupariated animals (white puparia) from the wall of the culture vial, 96 h after hatching of first instar larvae.
5. Transfer white puparia with a wet paintbrush to Petri dishes lined with moistened filter paper and allow to develop to desired stages of pharate pupal and pharate adult development. The pupal molt and adult emergence occur 12 and 96 h after puparium formation, respectively.

3.1. Whole-Mount Preparation of Larval Integument

1. To make whole-mount preparations of the larval integument, collect cleaned larvae of appropriate age (*see* **Note 4**) and place them in a Petri dish lined with moist filter paper.
2. Keep a Stender dish half-filled (2 mL) with distilled water and allow the water to reach 50°C on a hot plate.
3. Transfer, using watchmaker's forceps, a larva to this hot water and leave it there for 5–10 s so that it is killed and straightened.
4. Immediately, transfer this larva to a depression slide containing a few drops of Ringer's solution.
5. Under the dissecting microscope (100 ×) keep the larva on its back and hold its anterior end (with the black mouth hooks) with forceps and make a transverse cut with iridectomy scissors immediately posterior to the holding point. Similarly, make a transverse cut at the posterior end, anterior to the posterior paired spiracles.
6. Hold the anterior cut end of the larva with forceps firmly and make a clean midventral longitudinal slit starting from the posterior to the anterior end.
7. Continue to hold the anterior end of the larva with forceps, and using another forcep carefully remove all the major internal organs (digestive, nervous, and reproductive systems and the extensive sheets of fat body) as much as possible without disturbing and damaging the integument and its attached muscles.
8. Transfer the carcass to a Stender dish half-filled with Ringer's solution. Holding the carcass to the bottom of the dish, flush out the remaining tissue debris by carefully squirting Ringer's solution several times at the inner surface of the integument.
9. Remove the medium with the floating debris and repeat the cleaning process outlined above (**step 8**) with fresh Ringer's solution. Repeat this step six to eight times so that all possible loose debris is removed from the integument, resulting in a clean filet containing the cuticle, LECs, histoblasts, and muscle fibers attached to the body wall.
10. Transfer quickly the clean filet to another Stender dish containing a drop of Kahle's fixative with fast green (*see* **Note 5**). Hold the filet to the bottom for 2 min so that it remains flattened (*see* **Fig. 1** for the appearance of a representative extended segment) and submerged while being fixed.
11. Gently add more fixative to the dish and cover it and leave it for 12–24 h at room temperature. Make sure the filet is immersed completely in the fixative.

12. Carefully remove the fixative and replace it with decreasing concentrations of ethanol, starting with 70% and finally with distilled water. Keep the tissue in each of these solutions for 5 min.
13. Remove the distilled water and replace it with 2 mL of 6 *N* HCl for 10 min for hydrolysis. Replace the acid and rinse briefly with distilled water once.
14. Remove the water immediately and add 2 mL of Schiff's reagent and cover the dish. Keep this in a lightproof box for 90 min at room temperature.
15. Remove the Schiff's reagent and quickly add the bleaching solution. After 2 min, replace with fresh bleaching solution and repeat twice more.
16. Replace the bleaching solution with filtered tap water. Remove the water after 2 min and repeat this 10 times. After the last rinse, keep the tissue in filtered tap water for 30 min. Make sure that during all of these steps the tissue remains submerged in the medium.
17. At the end of this period, check nuclear staining in the tissues of the integument under the dissecting microscope. The nuclei of LECs, histoblasts (*see* **Fig. 2A,B**), and muscles should appear as dark magenta dots.
18. Replace tap water with 30%, 50%, and 70% ethanol and keep the stained tissue in each of the above for 3 min.
19. If counterstaining of the cytoplasm of the tissue is needed, replace the 70% ethanol with fast green stain for 1–2 min.
20. Transfer the integument to a fresh dish containing 90% ethanol and process it through 100% ethanol twice, keeping it for 5 min in each of these solutions.
21. While it is in the last change of 100% ethanol, add an equal amount of xylene and swirl the solutions to mix well. Leave the tissue in it for 5 min.
22. Replace the ethanol–xylene mixture with fresh xylene and leave the tissue for 5 min; repeat this twice.
23. Place a small drop of Permount mounting medium in the center of a microslide. Gently and carefully introduce the dehydrated and stained integument into this drop by holding the integument on one end and slowly inserting it into the medium at a slant. Gently sway the tissue two or three times in the medium so that the carried-over xylene mixes with the Permount.
24. After a minute, transfer the integument to a drop of Permount on a labeled slide. Gently push down the specimen to the bottom of the medium with the cuticular surface facing upward (*see* **Note 6**).
25. Hold the cover glass on its edge and bring it down slowly so that its middle area touches the mounting medium first, and taking care not to trap air bubbles.
26. Press the top of the cover glass gently with the tip of a dissecting needle, so that the integument remains flat at the bottom and allows the medium to fill under the surface of the cover glass up to its edges.
27. Keep the slide on a flat surface to dry. Carefully place a brass bar in the center of the cover glass for 24 h. This allows the specimen to remain flat.

3.2. Whole-Mount Preparation of Pupal and Pharate Adult Integument

Allow the white puparia to develop 0–8, 12–28, and 40–96 h after puparium formation, and use these stages for whole-mount preparations of histoblast

nests and LECs with the following modification of procedures used for larvae (*see* **Notes 7** and **8**).

1. Place 0- to 4-h-old scrubbed and cleaned puparia on a depression slide containing a drop of Ringer's solution to make the appropriate cut. Because the puparial case becomes brittle and begins to apolyse from the underlying pupal cuticle by 4–6 h after pupariation and because the separating pupal integument tends to curl down during fixation and subsequent processing, it is necessary to heat specimens which are 5 h or older after puparium formation, as described in **Subheading 3.1., steps 2** and **3**, before making the following cuts.
2. Cut the pupariated animals either dorso-ventrally in the mid line (resulting in left and right halves) or laterally (resulting in dorsal and ventral halves).
3. Transfer each of these halves to a Stender dish, half-filled with Ringer's solution. Remove the unwanted debris of internal organs by gently squirting Ringer's solution as described in **Subheading 3.1., steps 8** and **9**. Trim anterior and posterior ends of these halves to prevent potential folding of cuticle during subsequent processing.
4. Fix, process, stain and counterstain, and dehydrate the filets in labeled and separate dishes as described in **Subheading 3.1., steps 10–22**. Retain the puparial case during these steps so that it can cradle and protect the fragile integument from damage while handling.
5. Remove the puparial case from stages 8 h after pupariation and beyond.
6. Trim off the head and thoracic regions from the abdominal segments.
7. Mount the stained abdominal segments as described in **Subheading 3.1., steps 23–27** (*see* **Figs. 3**, **7A,B**, **8**, and **9**).

3.3. Whole-Mount Preparation of Unstained Abdominal Cuticle of Adults

1. Preserve adult flies in 70% ethanol for 3–7 d.
2. Separate the abdomen in 70% ethanol and make either a mid-ventral or mid-dorsal longitudinal cut in it to obtain a complete dorsal or ventral view of the adult cuticular pattern, respectively.
3. Transfer individual pieces to separate Stender dishes with 70% ethanol. Using forceps and without damaging the cuticle, remove the internal organs and fat body as much as possible.
4. Pass the specimen through the descending grades of ethanol (70%, 50%, and 30%) and finally through distilled water, keeping the specimen in each of the solutions for 2 min (*see* **Subheading 3.1., step 12**).
5. Transfer the piece to a dish on a hot plate (50°C) containing 1 *N* NaOH and cook for 2–3 min. Now the tissues attached to the cuticle will become translucent.
6. Transfer the cooked integument to a dish containing distilled water. Under the dissecting microscope, holding the skin to the bottom of the dish, carefully squirt water several times to remove all the digested tissue remains.
7. Mount the clean cuticle in water mounting medium following **Subheading 3.1., steps 23–27** (*see* **Fig. 5A**).

4. Notes

1. Never add the stain to boiling water because it will boil over.
2. If the filtrate is slightly pinkish, add again 1 g of activated charcoal, stir, and filter.
3. The different larval instars can be indentified externally following Bodenstein's description ***(6)***. In the first instar, there are no anterior spiracles, whereas in the second, these appear as closed enlargements at the tip of the lateral tracheal trunks. The anterior spiracles of the third instar have seven to nine fingerlike processes with open ends. To a limited extent, the size of the mouth hooks can also be used to recognize the different larval instars. The mouth hook with 1 tooth of the first instar is the smallest, whereas the largest with 9–12 teeth is seen in third instar.
4. Scoop a sample of food with larvae from the surface of the food and place it in a Petri dish containing distilled water. Swirl the water around to separate the larvae from food particles. Pick up the larvae with forceps and transfer them to a Petri dish with distilled water and scrub them with a paintbrush and wash them again. Transfer the cleaned larvae to a new Petri dish lined with moist filter paper.
5. Add a few drops of 1% fast green solution (in 70% ethanol) to the Kahle's fixative and mix well. The stain in the fixative colors the tissue for its easy recognition during subsequent processing.
6. This two-step (**steps 23** and **24**) procedure prevents subsequent collection of air bubbles on and around the specimen.
7. Distinguishing features of the major stages of metamorphosis ***(6)*** are as follows:

   2 h Fully tanned puparium;
   12 h Pupation;
   49 h Beginning of pale yellow eye pigmentation of developing adults;
   69 h Beginning of pigmentation of bristles (chaetae) in head, thorax, and appendages;
   96 h Adult with pigmented bristles in head, thorax, and abdomen and is ready to eclose.

   All hours are after white puparium formation. If more detailed staging of metamorphosis is necessary, refer to **ref. *29***.
8. In other hours of metamorphosis, the forming pupal and adult epidermis is fragile and, thus, it is very difficult to keep them as intact sheets during processing.

Acknowledgments

We thank John Buckingham and Joel Villa of the Audio-Visual Services of the College for expert art work. We also thank the late Howard Schneiderman for years of sharing his wisdom. The studies referred from our laboratory were supported by grants from the Whitehall Foundation and Monsanto Company.

References

1. Wigglesworth, V. B. (1972) *The Principles of Insect Physiology*, 7th ed., Chapman & Hall, London.

2. Williams, C. M. (1950) The metamorphosis of insects. *Sci. Am.* **182,** 24–28.
3. Bryant, P. J. (1978) Pattern formation in imaginal discs, in *The Genetics and Biology of Drosophila*, (Ashburner, M. and Wright, T. R. F., eds.), Academic, New York, Vol. 2C, pp. 229–335.
4. Cohen, S. M. (1993) Imaginal disc development, in *The Development of* Drosophila melanogaster (Bate, M. and Martinez Arias, A., eds.), Cold Spring Harbor Laboratory Press, Plainview, NY, Vol. 2, pp. 747–841.
5. Fristrom, D. and Fristrom, J. W. (1993) The metamorphic development of the adult epidermis, in *The Development of Drosophila melanogaster* (Bate, M. and Martinez Arias, A., eds.), Cold Spring Harbor Laboratory Press, Plainview, NY, Vol. 2, pp. 843–897.
6. Bodenstein, D. (1950) The postembryonic development of *Drosophila,* in *Biology of* Drosophila (Demerec, M., ed.), Wiley, New York, pp. 275–367.
7. Madhavan, M. M. and Schneiderman, H. A. (1977) Histological analysis of the dynamics of growth of imaginal discs and histoblast nests during the larval development of *Drosophila melanogaster*. *Roux's Arch. Dev. Biol.* **183,** 269–305.
8. Madhavan, M. M. and Madhavan, K. (1980) Morphogenesis of the epidermis of the adult abdomen of *Drosophila*. *J. Embryol. Exp. Morphol.* **60,** 1–31.
9. Madhavan, K. and Madhavan, M. M. (1995) Defects in the adult abdominal integument of *Drosophila* caused by mutations of *torpedo*, a DER homolog. *Roux's Arch. Dev. Biol.* **204,** 330–335.
10. Roseland, C. and Schneiderman, H. A. (1979) Regulation and metamorphosis of the abdominal histoblasts of *Drosophila melanogaster*. *Roux's Arch. Dev. Biol.* **186,** 235–265.
11. Madhavan, M. M. and Madhavan, K. (1982) Pattern regulation in tergite of *Drosophila*: a model. *J. Theor. Biol.* **95,** 731–748.
12. Snodgrass, R. E. (1935) *Principles of Insect Morphology*, McGraw-Hill, New York.
13. Madhavan, M. M. and Madhavan, K. (1984) Do larval epidermal cells possess the blueprint for adult pattern in Drosophila? *J. Embryol. Exp. Morphol.* **82,** 1–8.
14. Madhavan, K. (1973) Morphogenetic effects of juvenile hormone and juvenile hormone mimics on adult development of *Drosophila*. *J. Insect Physiol.* **19,** 441–453.
15. Postlethwait, J. H. (1974) Juvenile hormone and the adult development of *Drosophila*. *Biol. Bull.* **147,** 119–135.
16. Riddiford, L. M. and Ashburner, M. (1991) Role of juvenile hormone in larval development and metamorphosis in *Drosophila melanogaster*. *Gen. Comp. Endocrinol.* **82,** 172–183.
17. Riddiford, L. M. (1993) Hormones and *Drosophila* development, in *The Development of Drosophila melanogaster* (Bate, M. and Martinez Arias, A., eds.), Cold Spring Harbor Laboratory Press, Plainview, NY, Vol. 2, pp. 899–939.
18. Merriam, J. R. (1978) Estimating primordial cell numbers in *Drosophila* imaginal discs and histoblasts, in *Genetic Mosaics and Cell Differentiation* (Gehring, W. J., ed.) Springer-Verlag, New York, pp. 71–96.
19. Shirras, A. D. and Cusso, J. P. (1996) Cell fates in the adult abdomen of *Drosophila* are determined by *wingless* during pupal development. *Dev. Biol.* **175,** 24–36.

20. Kopp, A., Blackman, R., and Duncan, I. (1999) Wingless, Decapentaplegic and EGF receptor signaling pathways interact to specify dorso-ventral pattern in the adult abdomen of *Drosophila*. *Development* **126,** 3495–3507.
21. Kornberg, T. (1981) Compartments in the abdomen of *Drosophila* and the role of the engrailed locus. *Dev. Biol.* **86,** 363–372.
22. Struhl, G., Barbash, D. A. ,and Lawrence, P. A. (1997a) Hedgehog organizes the pattern and polarity of epidermal cells in the *Drosophila* abdomen. *Development* **124,** 2143–2154.
23. Struhl, G., Barbash, D. A., and Lawrence, P. A. (1997b) Hedgehog acts by distinct gradient and signal relay mechanisms to organize cell type and cell polarity in the *Drosophila* abdomen. *Development* **124,** 2155–2165.
24. Kopp, A., Muskavitch, M. A. T., and Duncan, I. (1997) The roles of *hedgehog* and *engrailed* in patterning adult abdominal segments of *Drosophila*. *Development* **124,** 3703–3714.
25. Lawrence, P. A., Casal, J., and Struhl, G. (1999) *hedgehog* and *engrailed*: pattern formation and polarity in the *Drosophila* abdomen. *Development* **126,** 2431–2439.
26. Lawrence, P. A. (2001) Morphogens: how big is the big picture? *Nature Cell Biol.* **3,** E151–154.
27. Ephrussi, B. and Beadle, G. W. (1936) A technique of transplantation for *Drosophila*. *Amer. Naturalist* **70,** 218–225.
28. Pearse, E, A. G. (1968) *Histochemistry: Theoretical and Applied*, 3rd ed., Churchill Livingston, London, Vol. 1.
29. Ashburner, M. (1989) Drosophila: *A Laboratory Handbook*. Cold Spring Harbor Laboratory Press, Cold Spring Harbor, New York.

24

Visualizing Apoptosis

**Kimberly McCall, Jason S. Baum,
Kristen Cullen, and Jeanne S. Peterson**

1. Introduction

Cells undergoing apoptosis display a number of morphological changes, including chromatin condensation, cytoplasmic shrinkage, membrane blebbing, and the formation of apoptotic bodies ***(1)***. These morphological changes are accompanied by structural changes within the cell, such as the reorganization of actin, nuclear lamin cleavage, fragmentation of DNA, and "flipping" of the phospholipid phosphatidylserine from the interior leaflet of the plasma membrane to the exterior of the cell ***(2–5)***.

Many of the morphological and structural changes that occur in apoptotic cells are a result of caspase-mediated cleavage of cellular targets ***(6–8)***. Caspases are a class of cysteine proteases that function in the immune system and during apoptosis. In mammals, caspase activity is regulated by upstream signaling pathways, which induce either the oligomerization of caspases or the release of cytochrome-*c* from the mitochondria into the cytosol ***(7,9,10)***. Cytoplasmic cytochrome-*c* then activates the apoptosome, a multiprotein complex including pro-caspases. The genome sequence of *Drosophila* has revealed fly homologs for most components of the mammalian cell death machinery. In addition, genetic studies have uncovered three novel cell death activators: *reaper*, *hid,* and *grim* ***(11–13)***.

Cell death occurs normally in diverse developmental processes in *Drosophila*, including the formation of the embryonic nervous system, the destruction of larval tissues during metamorphosis, the morphogenesis of the eye, and the generation of eggs in the ovary ***(14–17)***. Additionally, cells die ectopically in response to developmental abnormalities and environmental stimuli, such as X-rays ***(15)***. Expression of cell death genes in *Drosophila* can be visualized in

From: *Methods in Molecular Biology, vol. 247:* Drosophila *Cytogenetics Protocols*
Edited by: D. S. Henderson © Humana Press Inc., Totowa, NJ

many tissues by whole-mount RNA *in situ* hybridization or immunocytochemistry. In particular, the expression pattern of *reaper* closely reflects the pattern of cell death during development and can be detected by *in situ* hybridization or expression of a *reaper–lacZ* transgene ***(11,17–23)***. Antibodies have been described for some of the cell death proteins, including Hid, Thread, cytochrome-*c*, and nuclear lamins, which are caspase substrates ***(16,24–28)***. The antibody CM1, which recognizes mammalian caspases-3 and -7, has also been shown to label dying cells in *Drosophila* ***(29,30)***. The detection of macrophages is correlated with the amount of cell death, and macrophages can be visualized by antibodies such as those against Peroxidasin and Croquemort ***(15,31–34)***. In addition to studying cell death in the intact fly, several *Drosophila* cell lines exist that can be subjected to the same analysis as mammalian cell lines ***(34,35)***.

Apoptosis can be visualized in *Drosophila* using a number of standard cell biological techniques, such as staining with propidium iodide or 4',6-diamidino-2-phenylindole (DAPI), which label condensed apoptotic nuclei more intensely than healthy nuclei. Condensed chromatin and other morphological changes of apoptotic cells can also be seen with transmission electron microscopy ***(15,34,36)***. In this chapter, we describe three methods specifically used for the detection of apoptosis in a variety of tissues. The TUNEL (terminal deoxynucleotidyl transferase-mediated dUTP nick end labeling) technique labels cells with fragmented DNA by the incorporation of labeled nucleotides into 3'OH DNA ends ***(37)***. Acridine orange is one of several vital dyes that stain apoptotic cells selectively ***(15)***. Annexin V binds tightly to phosphatidylserine, and in unfixed cells, it will only bind to phosphatidylserine that has been flipped to the cell surface ***(38,39)***. This property allows Annexin V to function as a specific label for apoptotic cells, and it is often the earliest detectable change in cells undergoing apoptosis.

2. Materials

2.1. General Supplies and Reagents

1. Baskets with 80 µm Nitex mesh (Sefar America, Kansas City, MO) for dechorionating embryos. To make a basket, cut a 1-in. length of a 15- or 50-ml Falcon tube at the cap end. Use the cap to hold a small piece of mesh in place. Place the basket in a small beaker to hold solutions.
2. Fine forceps, tungsten needles, and glass plates or depression slides for dissection.
3. Apple juice/agar plates: Mix 90 g of Difco agar with 3 L of water, autoclave for 50 min and cool in a 60°C water bath. Mix 1 L of apple juice with 100 g of sugar and heat to 60°C to dissolve. Combine agar/water and juice/sugar mixtures, stir, add 60 mL of a 10% solution of p-Hydroxy benzoic acid methyl ester (Sigma) in ethanol and pour the plates. The tops of 35 × 10-mm plates (Falcon) will fit fly food bottles from Applied Scientific.

4. Egg-laying chambers. To make chambers, cut a hole in the side of a dry fly food bottle and stuff it with a cotton ball. The apple juice/agar plate will fit on the mouth of the bottle.
5. Yeast paste: Mix granular yeast (Sci-Mart, Inc., St. Louis, MO) and water into a smooth paste.
6. *Drosophila* Ringer's, 1X (DR): 130 m*M* NaCl, 4.7 m*M* KCl, 1.9 m*M* $CaCl_2$, 10 m*M* HEPES, pH 6.9. Make up as a 10X solution and store at 4°C.
7. Phosphate-buffered saline, 1X (PBS): 137 m*M* NaCl, 2.7 m*M* KCl, 10 m*M* Na_2HPO_4, 2 m*M* KH_2PO_4, pH 7.4. Make up as a 10X solution and store at room temperature.
8. Fix: 4% Paraformaldehyde (Sigma-Aldrich) in PBS. Heat to dissolve. Store at 4°C for up to 1 wk.
9. Microcentrifuge tube rotator (e.g., Labquake/Thermolyne no. 400-110, available from VWR).
10. Fluorescence microscope equipped with fluorescein, rhodamine, and ultraviolet (UV) filters, bright field/differential interference-contrast (DIC), and a camera.

2.2. TUNEL Materials

1. PBT: PBS with 0.1% Tween-20.
2. Heptane.
3. Triton X-100.
4. Proteinase K (Fisher) stock solution, 20 mg/mL in distilled water (dH_2O), stored frozen in 10-µL aliquots.
5. Bovine serum albumin (BSA) (Fisher).
6. Normal goat serum (Gibco-BRL).
7. pH 9 Buffer: 0.1 *M* Tris-HCl, pH 9.5, 50 m*M* $MgCl_2$, 0.1% Tween-20.
8. 70% Glycerol in PBS.
9. Methanol.
10. Household bleach (e.g., Clorox).
11. ApopTag reagents (Serologicals Corp., Norcross, GA): Equilibration buffer (EB), reaction buffer containing nucleotides labeled with digoxigenin (RXB), terminal deoxyribonucleotidyl transferase (TdT), and Stop-wash buffer (SWB).
12. Roche reagents (Indianapolis, IN): Antidigoxigenin antibody complexed to alkaline phosphatase (anti-DIG-AP), nitroblue tetrazolium salt (NBT) and 5-bromo-4-chloro-3-indolyl phosphate toluidinium salt (X-Phos).

2.3. Acridine Orange Materials

1. Stock solution acridine orange (AO) (Sigma, A 6014) dissolved in dH_2O at 1 mg/mL, stored in dark at 4°C.
2. 0.1 *M* Phosphate buffer, pH approx 7.0.
3. Heptane.
4. Halocarbon oil (series 700; Halocarbon Products Corporation, River Edge, NJ).

2.4. Annexin V Materials

1. Annexin-binding buffer (ABB) (Molecular Probes), diluted from 5X to 1X.
2. Alexa Fluor 488 Annexin V (Molecular Probes).
3. Vectashield mounting medium for fluorescence with DAPI, 1.5 µg/mL (Vector Laboratories).

3. Methods

3.1. Sample Preparation

For well-developed ovaries or good embryo production, start with equal numbers of 2- to 7-d-old male and female flies kept together in uncrowded conditions, transferring them to new food vials supplemented with wet yeast paste once or twice daily for two or more days before collecting samples.

3.1.1. Ovary Dissection

1. Anesthetize flies under CO_2 or on ice.
2. Dissect females in depression plates or slides in a drop of DR. Grasp fly between thorax and abdomen with forceps and pull at the terminal part of the abdomen with another pair of forceps to release the ovaries and other organs from the cavity.
3. Tease ovaries away from debris and separate ovarioles from each other with tungsten needles.
4. Transfer tissue in DR to microcentrifuge tubes (*see* **Notes 1** and **2**). Hold tissues on ice until all samples have been collected. Proceed to **Subheading 3.2.** for TUNEL, **Subheading 3.3.** for AO staining, or **Subheading 3.4.** for Annexin V staining.

3.1.2. Embryo Collection

1. Apply a dab of fresh yeast paste to an apple juice/agar plate. Attach the apple juice/agar plate to the mouth of the egg-laying chamber. Transfer flies to the chamber and allow flies to lay eggs for the desired time (*see* **Note 3**).
2. Use water and a fine brush to dislodge the embryos from the surface of the plate and collect them with a large (1000-µL) pipet tip (*see* **Note 2**). Alternatively, pour embryos into the baskets with a gentle stream of water.
3. Transfer the embryos to baskets and remove the water. Dechorionate embryos in baskets using 50% bleach for 2–5 min and wash several times with water. Proceed to **Subheading 3.2.2.** for TUNEL or **Subheading 3.3.** for AO staining.

3.1.3. Imaginal Disc Dissection

1. Select larvae from the food or the side of the vial using forceps.
2. Dissect larvae in depression plates or slides in DR. Hold the larval head close to the mouth hooks with one set of forceps while using a second set to grasp the middle of the larva. Slowly separate the head from the body. The brain, salivary

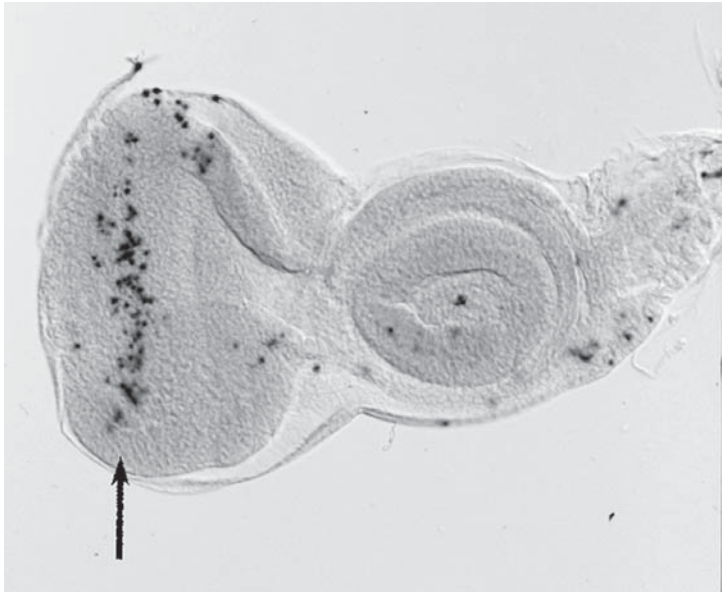

Fig. 1. Eye-antennal imaginal disc from a third instar larva labeled with the TUNEL method. Significant labeling is seen in the posterior region of the eye disc (arrow).

glands, and imaginal discs will remain attached to the head and will pull apart from the rest of the larval body.
3. Peel away the remaining cuticle and mouth hooks and remove desired imaginal discs (*see* **Note 4**).
4. Transfer tissue in DR to microcentrifuge tubes (*see* **Notes 1** and **2**). Hold tissues on ice until all samples have been collected. Proceed to **Subheading 3.2.3.** for TUNEL staining. *See* **ref.** ***34*** for AO staining of imaginal discs.

3.2. TUNEL Staining

The TUNEL technique is used to detect dying cells with fragmented DNA (**Fig. 1**). For TUNEL staining, ovaries or embryos are treated as for *in situ* hybridization and antibody staining. The following protocol was derived from the description of ovarian tissue preparation by Verheyen and Cooley ***(40)***, from descriptions of embryo staining in protocols 54 and 95 in **ref.** ***41*** and from the description of TUNEL staining by White et al. ***(11,42)***.

3.2.1. Ovary Fixation

1. Remove DR from ovaries (*see* **Note 5**), add 100 µL fix and 500 µL heptane, and rotate gently for 30 min at room temperature (RT).
2. Remove heptane/fix and wash twice with excess PBT, taking care to remove all heptane droplets. Proceed to **Subheading 3.2.4.**

3.2.2. Embryo Fixation

1. Mix 500 µL heptane and 500 µL fix.
2. Transfer the embryos to the fixing solution (*see* **Note 6**), shake well, and rotate for 20 min at RT.
3. Remove the fix (bottom layer) first and then remove the heptane. Add fresh heptane and shake.
4. Add a double quantity of methanol and shake hard (vortex) for 2 min to remove the vitelline membrane.
5. Discard embryos at the interface, remove the heptane and then the methanol, and wash twice with methanol.
6. Rehydrate through a series of 75%, 50%, and 25% methanol in PBT. Proceed to **Subheading 3.2.4.**

3.2.3. Imaginal Disc Fixation

1. Remove DR, replace with 500 µL fix/500 µL heptane, and rotate for 30 min.
2. Remove the fix and rinse twice with PBT for 5 min while rotating.
3. Remove the PBT and rinse with methanol. Wash again with methanol for 30 min while rotating. Tissue may be stored indefinitely in methanol at –20°C following the first methanol wash.
4. Rehydrate through a series of 75%, 50%, and 25% methanol in PBT. Proceed to **Subheading 3.2.4.**

3.2.4. General TUNEL Staining Protocol

1. Treat fixed tissue with Proteinase K, 10 µg/mL in PBT (50–250 µL, 5 min for ovaries and imaginal discs, 3 min for embryos), and wash twice with PBT.
2. Postfix for 20 min in a solution of 4% paraformaldehyde in PBS, then wash five times, 5 min each, in PBT.
3. Equilibrate for 1 h at RT in EB.
4. Incubate overnight at 37°C in a reaction mix consisting of RXB and TdT in a 2 : 1 ratio, with 0.3% Triton X-100 (total volume 50–100 µL).
5. Preabsorb anti-DIG-AP, diluted 1 : 2000 in PBT, with fixed tissue at RT for 2 h or at 4°C overnight.
6. Remove the RXB and TdT from tissue and incubate in SWB diluted to 1 : 34 in water at 37°C for 3–4 h, first with three quick washes and then once every 30 min. Remove SWB and wash three times, 5 min each, in PBT.
7. Block in a solution of 2 mg/mL BSA and 5% normal goat serum in PBT for 1 h at RT.
8. Incubate tissue in preabsorbed antibody for 2 h at RT or overnight at 4°C.
9. Wash four times for 20 min each in PBT and wash twice, 20 min each, in pH 9.0 buffer.
10. Add 3.5 µL of NBT and 4.5 µL of X-Phos to 1 mL of pH 9.0 buffer and incubate tissues, watching carefully for the color reaction.
11. Stop the reaction with two PBT washes and mount in 70% glycerol.

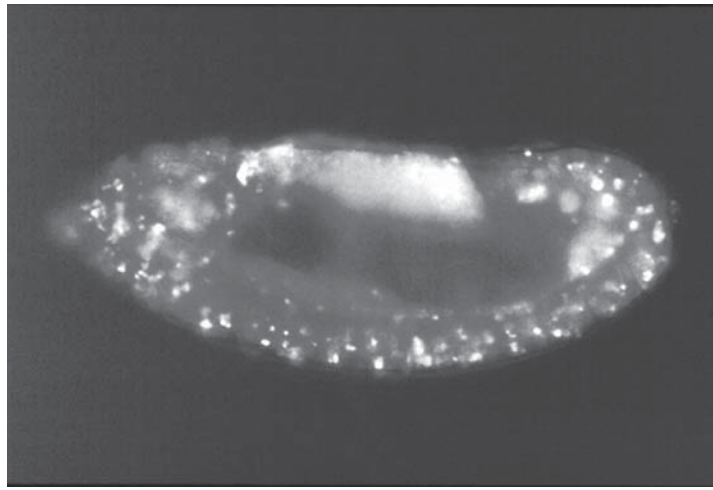

Fig. 2. A 10-h embryo stained with acridine orange. Most of the staining is in the head and central nervous system. The dorsal staining is due to autofluorescence of the yolk.

3.3. Acridine Orange Staining

Acridine orange is a vital dye that differentially stains living and dying cells (**Fig. 2**). The advantage of acridine orange is that it is performed quickly on live tissue. However, this also means that the tissue must be examined and photographed immediately after staining. These protocols are derived from protocols described in **refs. *15*** and ***43***.

3.3.1. Embryo Protocol

1. Dilute AO stock solution to 5 µg/mL in 0.1 *M* phosphate buffer.
2. Collect embryos in mesh baskets as described and wash only in water (*see* **Note 7**). Using a fine-tipped paintbrush, transfer embryos from the mesh to tubes containing an equal volume of heptane and the 5 µg/mL AO solution. Microcentrifuge tubes or glass tubes with tight-fitting caps may be used.
3. Shake tubes vigorously by hand for 3–5 min. Shaking by hand improves the permeability of the embryos (*see* **Note 8**).
4. Pipet off the liquid and replace with heptane.
5. Pipet the embryos in heptane onto glass slides. Try to keep the embryos separated and soak up the heptane using a Kimwipe twisted into a point (*see* **Note 9**). Quickly cover the embryos with halocarbon oil and a cover slip.
6. View the slide immediately under epifluorescence. AO staining is visible under both rhodamine and fluorescein filters. The rhodamine filter often looks

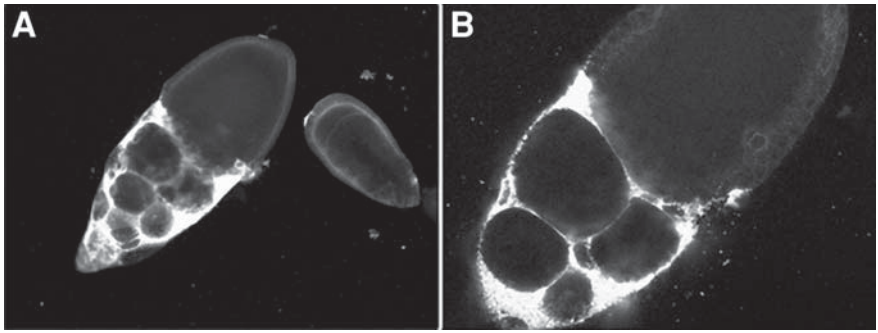

Fig. 3. Annexin V labeling of egg chambers. **(A)** Intense staining is seen on nurse cell membranes at stage 10, but not in the smaller stage 8 egg chamber. **(B)** Higher magnification (400×) reveals punctate staining on the membrane (reduced from original magnification).

better, as the fluorescein filter shows more background and smearing from residual heptane.

3.3.2. Ovary Protocol

1. Dilute AO stock solution to 10 µg/mL in phosphate buffer.
2. Transfer dissected ovaries to an Eppendorf tube containing 15 µL of heptane and 15 µL of 10-µg/mL AO solution.
3. Flick the tube gently to mix and allow to rotate for 5 min.
4. Transfer ovaries to slides and spread out the ovary tissue into individual egg chambers if possible. Pipet off the AO/heptane mixture or use a Kimwipe twisted into a point (*see* **Note 9**). Cover with halocarbon oil and a cover slip.
5. View the slide immediately under epifluorescence, using the fluorescein, rhodamine, or UV filter. Under UV, the apoptotic nuclei stain yellow or red ***(43)***.

3.4. Annexin V Staining

Annexin V has previously been reported to stain dying cells when injected into *Drosophila* pupae ***(44)***. Here, we describe a method we have developed to stain ovary tissue, modifying the cell culture protocol from Molecular Probes. We find that significant Annexin V labeling of nurse cells is first detected during stage 9, several hours before other apoptotic changes are apparent (**Fig. 3**).

1. Dissect ovaries into ovarioles as described in **Subheading 3.1.1.** Remove egg chambers from the muscle sheath surrounding each ovariole by gently sliding forceps back and forth along ovarioles and/or lightly squeezing out egg chambers (*see* **Note 10**).
2. Transfer the egg chambers to microcentrifuge tubes (*see* **Notes 1** and **2**) and keep on ice.

3. Remove DR and wash egg chambers with 500 µL of 1X ABB.
4. Mix 200 µL of 1X ABB with 20 µL of Annexin V conjugate. Remove wash from egg chambers and add Annexin/ABB solution. Incubate for 15 min at RT while gently rotating.
5. Remove annexin/buffer and wash with 500 µL of 1X ABB.
6. Remove wash, add 100 µL fix and 600 µL heptane and rotate for 10 min at RT.
7. Remove heptane/fix and wash twice with excess PBT.
8. Remove fix, add 100 µL of Vectashield mounting medium with DAPI, and mount on slides.
9. Observe egg chambers under the fluorescein filter of a fluorescent microscope. Those undergoing apoptosis should display strong green staining by Annexin V on the surface. DAPI staining can help to identify stages of development by viewing UV filter.

4. Notes

1. Use no-stick microcentrifuge tubes (USA Scientific, Inc., Ocala, FL) to minimize the amount of tissue adhering to the side of the tube.
2. To move embryos or dissected tissue from plates to staining tubes and from staining tubes to slides, use plastic pipet tips from which 3/16-in. of the end has been removed with a razor. Rinse the tip in PBT just before using, hold the pipet vertically at all times and pipet very slowly. Glass Pasteur pipets may also be used, but tissue must only be held in the tip portion of the pipet, otherwise tissue may adhere to the inside of the pipet.
3. Cell death occurs from stage 11 until the end of embryogenesis. The pattern of cell death is dynamic and it is often useful to compare embryos that are approximately the same age. Embryos can be collected for a short period of time (0–3 h) and then aged to the desired stage. Embryos can be allowed to develop at 18°C overnight, which takes approximately twice as long as development at 25°C.
4. To maintain the integrity of imaginal discs and avoid tissue loss, it is helpful to leave all discs as one piece of tissue with any connections that remain following dissection. Individual discs can be separated upon completion of the procedure.
5. To change solutions in which embryos or tissues are incubating, use glass pipets drawn out to a fine tip. Remove most of the liquid from the samples and then carefully touch the tip to the meniscus, moving it slowly toward the sample.
6. Embryos may be transferred directly from the mesh to the fix with a fine paintbrush. Alternatively, embryos may be washed in the baskets with 0.1% Triton-X in water. The embryos are then pipetted to an empty tube and allowed to settle to the bottom of the tube. Remove the 0.1% Triton-X solution and replace with heptane/fix.
7. For acridine orange staining, it is critical that there is no trace of detergent (such as Triton-X) present when embryos are washed. Detergent will completely abolish AO staining.
8. It is essential that the tubes containing embryos be shaken very hard by hand. Standard rotation of the tubes is not sufficient for the heptane/AO to permeabilize the vitelline membrane.

9. Do not allow embryos or ovary tissues to dry out when the heptane is removed, as they will shrivel up quickly. Heptane evaporates rapidly; blowing gently on the slide will speed up its evaporation.
10. It is critical that the muscle sheath be removed from egg chambers because the Annexin V is not able to penetrate the unfixed muscle sheath. Furthermore, Annexin V stains the muscle sheath, which can affect the interpretation of results.

Acknowledgments

We thank John Tullai for advice on Annexin V staining and Margaret Barkett and Bonni Laundrie for helpful comments. KM is supported by grants from the Clare Boothe Luce Foundation, the American Cancer Society, the March of Dimes, and the NIH.

References

1. Kerr, J. F. R., Wyllie, A. H., and Currie, A. R. (1972) Apoptosis, a basic biological phenomenon with wide-ranging implications in tissue kinetics. *Br. J. Cancer* **26,** 239–257.
2. Wyllie, A. H., Morris, R. G., Smith, A. L., and Dunlop, D. (1984) Chromatin cleavage in apoptosis: association with condensed chromatin morphology and dependence on macromolecular synthesis. *J. Pathol.* **142,** 67–77.
3. Fadok, V. A., Voelker, D. R., Campbell, P. A., Cohen, J. J., Bratton, D. L., and Henson, P. M. (1992) Exposure of phosphatidylserine on the surface of apoptotic lymphocytes triggers specific recognition and removal by macrophages. *J. Immunol.* **148,** 2207–2216.
4. Oberhammer, F. A., Hochegger, K., Fröschl, G., Tiefenbacher, R., and Pavelka, M. (1994) Chromatin condensation during apoptosis is accompanied by degradation of lamin A + B, without enhanced activation of cdc2 kinase. *J. Cell Biol.* **126,** 827–837.
5. Mills, J. C., Stone, N. L., and Pittman, R. N. (1999) Extranuclear apoptosis. The role of the cytoplasm in the execution phase. *J. Cell Biol.* **146,** 703–708.
6. Cryns, V. and Yuan, J. (1998) Proteases to die for. *Genes Dev.* **12,** 1551–1570.
7. Earnshaw, W. C., Martins, L. M., and Kaufmann, S. H. (1999) Mammalian caspases: structure, activation, substrates, and functions during apoptosis. *Annu. Rev. Biochem.* **68,** 383–424.
8. Nicholson, D. W. (1999) Caspase structure, proteolytic substrates, and function during apoptotic cell death. *Cell Death Differ.* **6,** 1028–1042.
9. Hengartner, M. O. (2000) The biochemistry of apoptosis. *Science* **407,** 770–776.
10. Adrain, C. and Martin, S. J. (2001) The mitochondrial apoptosome: a killer unleashed by the cytochrome seas. *Trends Biochem. Sci.* **26,** 390–397.
11. White, K., Grether, M. E., Abrams, J. M., Young, L., Farrell, K., and Steller., H. (1994) Genetic control of programmed cell death in *Drosophila*. *Science* **264,** 677–683.
12. Grether, M. E., Abrams, J. M., Agapite, J., White, K., and Steller, H. (1995) The *head involution defective* gene of *Drosophila melanogaster* functions in programmed cell death. *Genes Dev.* **9,** 1694–1708.

13. Chen, P., Nordstrom, W., Gish, B., and Abrams, J. M. (1996) *grim*, a novel cell death gene in *Drosophila*. *Genes Dev.* **10,** 1773–1782.
14. Wolff, T. and Ready, D. F. (1991) Cell death in normal and rough eye mutants of *Drosophila*. *Development*. **113,** 825–839.
15. Abrams, J. M., White, K., Fessler, L. I., and Steller, H. (1993) Programmed cell death during *Drosophila* embryogenesis. *Development* **117,** 29–43.
16. McCall, K. and Steller, H. (1998) Requirement for DCP-1 caspase during *Drosophila* oogenesis. *Science* **279,** 230–234.
17. Jiang, C., Lamblin, A. F., Steller, H., and Thummel, C. S. (2000) A steroid-triggered transcriptional hierarchy controls salivary gland cell death during *Drosophila* metamorphosis. *Mol. Cell.* **5,** 445–455.
18. Frank, L. H. and Rushlow, C. (1996) A group of genes required for maintenance of the amnioserosa tissue in *Drosophila*. *Development* **122,** 1343–1352.
19. Nordstrom, W., Chen, P., Steller, H., and Abrams, J. M. (1996) Activation of the *reaper* gene during ectopic cell killing in *Drosophila*. *Dev. Biol.* **180,** 213–226.
20. Robinow, S., Draizen, T. A., and Truman, J. W. (1997) Genes that induce apoptosis: transcriptional regulation in identified, doomed neurons of the *Drosophila* CNS. *Dev. Biol.* **190,** 206–213.
21. Nassif, C., Daniel, A., Lengyel, J. A , and Hartenstein, V. (1998) The role of morphogenetic cell death during *Drosophila* embryonic head development. *Dev. Biol.* **197,** 170–186.
22. Pazdera, T. M., Janardhan, P., and Minden, J. S. (1998) Patterned epidermal cell death in wild-type and segment polarity mutant *Drosophila* embryos. *Development* **125,** 3427–3436.
23. Myat, M. M. and Andrew, D. J. (2000) Forkhead prevents apoptosis and promotes cell shape change during formation of the *Drosophila* salivary glands. *Development* **127,** 4217–4226.
24. Smith, D. E. and Fisher, P. A. (1989) Interconversion of *Drosophila* nuclear lamin isoforms during oogenesis, early embryogenesis, and upon entry of cultured cells into mitosis. *J. Cell Biol.* **108,** 255–265.
25. Riemer, D., Stuurman, N., Berrios, M., Hunter, C., Fisher, P. A., and Weber, K. (1995) Expression of *Drosophila* lamin C is developmentally regulated: analogies with vertebrate A-type lamins. *J. Cell Sci.* **108,** 3189–3198.
26. Haining, W. N., Carboy-Newcomb, C., Wei, C. L., and Steller, H. (1999) The proapoptotic function of *Drosophila* Hid is conserved in mammalian cells. *Proc. Natl. Acad. Sci. USA* **96,** 4936–4941.
27. Varkey, J., Chen, P., Jemmerson, R., and Abrams, J. M. (1999) Altered cytochrome c display precedes apoptotic cell death in *Drosophila*. *J. Cell Biol.* **144,** 701–710.
28. Lisi, S., Mazzon, I., and White, K. (2000) Diverse domains of THREAD/DIAP1 are required to inhibit apoptosis induced by REAPER and HID in *Drosophila*. *Genetics* **154,** 669–678.
29. Srinivasan, A., Roth, K. A., Sayers, R. O., et al. (1998) *In situ* immunodetection of activated caspase-3 in apoptotic neurons in the developing nervous system. *Cell Death Differ.* **5,** 1004–1016.

30. Baker, N. E. and Yu, S. Y. (2001) The EGF receptor defines domains of cell cycle progression and survival to regulate cell number in the developing *Drosophila* eye. *Cell* **104,** 699–708.
31. Nelson, R. E., Fessler, L. I., Takagi, Y., et al. (1994) Peroxidasin: a novel enzyme-matrix protein of *Drosophila* development. *EMBO J.* **13,** 3438–3447.
32. Franc, N. C., Dimarcq, J. L., Lagueux, M., Hoffmann, J., and Ezekowitz, R. A. (1996) Croquemort, a novel *Drosophila* hemocyte/macrophage receptor that recognizes apoptotic cells. *Immunity* **4,** 431–443.
33. Franc, N. C., Heitzler, P., Ezekowitz, R. A., and White, K. (1999) Requirement for *croquemort* in phagocytosis of apoptotic cells in *Drosophila*. *Science* **284,** 1991–1994.
34. White, K., Lisi, S., Kurada, P., Franc, N., and Bangs, P. (2001) Methods for studying apoptosis and phagocytosis of apoptotic cells in *Drosophila* tissues and cell lines. *Methods Cell Biol.* **66,** 321–338.
35. Cherbas, L. and Cherbas, P. (2000) *Drosophila* cell culture and transformation, in Drosophila *Protocols* (Sullivan, W., Ashburner, M., and Hawley, R. S., eds.), Cold Spring Harbor Laboratory Press, Plainview, NY, pp. 373–387.
36. McDonald, K. L., Sharp, D. J., and Rickoll, W. (2000) Preparation of thin sections of *Drosophila* for examination by transmission electron microscopy, in Drosophila *Protocols* (Sullivan, W., Ashburner, M., and Hawley, R. S., eds.), Cold Spring Harbor Laboratory Press, Plainview, NY, pp. 245–271.
37. Gavrieli, Y., Sherman, Y., and Ben-Sasson, S. A. (1992) Identification of programmed cell death *in situ* via specific labeling of nuclear DNA fragmentation. *J. Cell Biol.* **119,** 493–501.
38. Martin, S. J., Reutelingsperger, C. P., McGahon, A. J., et al. (1995) Early redistribution of plasma membrane phosphatidylserine is a general feature of apoptosis regardless of the initiating stimulus: inhibition by overexpression of Bcl-2 and Abl. *J. Exp. Med.* **182,** 1545–1556.
39. Williamson, P., van den Eijnde, S., and Schlegel, R. A. (2001) Phosphatidylserine exposure and phagocytosis of apoptotic cells. *Methods Cell Biol.* **66,** 339–364.
40. Verheyen, E. and Cooley, L. (1994) Looking at oogenesis, in *Methods in Cell Biology* (Goldstein, B, L. S. and Fyrberg, E. A., eds.), Academic, New York, pp. 545–561.
41. Ashburner, M. (1989) Drosophila: *A Laboratory Handbook*. Cold Spring Harbor Laboratory Press, Cold Spring Harbor, NY.
42. White, K., Tahaoglu, E., and Steller., H. (1996) Cell killing by the *Drosophila* gene *reaper*. *Science* **271,** 805–807.
43. Foley, K. and Cooley, L. (1998) Apoptosis in late stage *Drosophila* nurse cells does not require genes within the H99 deficiency. *Development* **125,** 1075–1082.
44. van den Eijnde, S. M., Boshart, L., Baehrecke, E. H., De Zeeuw, C. I., Reutelingsperger, C. P. M., and Vermeij-Keers, C. (1998) Cell surface exposure of phosphatidylserine during apoptosis is phylogenetically conserved. *Apoptosis* **3,** 9–16.

25

RNAi in Cultured *Drosophila* Cells

Ling-Rong Kao and Timothy L. Megraw

1. Introduction

Double-stranded RNA (dsRNA)-mediated interference, or RNAi, has emerged as an effective technique to phenocopy the loss of function of a given gene product. With this tool researchers can study the functions of individual molecules in living cells and elucidate the mechanisms that regulate cell division. For example, many molecules that are important for regulating mitosis and for controlling the assembly of the mitotic spindle are mutated in different cancer cell types (for a review, *see* **ref.** ***1***). Functional analysis in vivo of molecules that play a role in mitosis is best implemented by a genetic analysis. For this, genetically malleable organisms such as *Drosophila*, *Caenorhabditis elegans*, yeast, and other micro-organisms have been extremely useful. Whereas genetic analysis usually requires a long-term effort, RNAi provides a rapid method for the reverse genetic analysis of gene product function and can be exploited to great advantage. In the era of sequenced genomes, this technique provides a valuable tool for functional genomics. Here, a detailed procedure for RNAi in *Drosophila* cells in culture is presented.

RNA interference was first described using *C. elegans* ***(2)***, although the phenomenon has been described in plants as posttranscriptional gene silencing (PTGS) ***(3)*** and as "quelling" in *Neurospora* ***(4)***. Furthermore, RNAi has been demonstrated on a number of organisms ***(2–9)***. For *Drosophila*, RNAi has been accomplished by injection of dsRNA into early syncytial cleavage stage embryos ***(6)***. Subsequently, heritable RNAi has been achieved in *C. elegans* and *Drosophila* using transgenic dsRNA "hairpin"-generating constructs ***(10–13)***. An important advance came when RNAi was demonstrated with cultured *Drosophila* cells ***(7)***.

From: *Methods in Molecular Biology, vol. 247:* Drosophila *Cytogenetics Protocols*
Edited by: D. S. Henderson © Humana Press Inc., Totowa, NJ

More recently, RNAi has been applied successfully to vertebrate cells in culture using short interfering RNAs (siRNAs) ***(14,15)***. For this, the first step in the cellular response mechanism to dsRNA (*see* below) has to be bypassed, because full-length dsRNAs produce nonspecific effects in vertebrate cells ***(16–19)***.

RNAi-mediated interference occurs by a posttranscriptional mechanism that targets mRNA homologous to the dsRNA that is introduced for destruction (for reviews, *see* **refs. *20–22***). Using *Drosophila* embryo and S2 cell extracts, the mechanisms for RNAi are being elucidated ***(16,23)***. In these extracts, dsRNA is cleaved into 21- to 25-bp siRNAs with 5' phosphates, 3' hydroxyl groups, and contain two to three nucleotide 3' overhangs. dsRNA cleavage is mediated by Dicer, an ATP-dependent RNaseIII family RNase ***(24)***. siRNAs assemble into an approx 360-kDa complex called RNA-induced silencing complex (RISC) in *Drosophila* extracts ***(25)***. The siRNAs then unwind in an ATP-dependent manner ***(23,25)***. The single-stranded siRNAs in the RISC complex provide the homologous targeting to mRNA ***(23,26)***, enabling degradation by the RNase associated with RISC. Furthermore, Argonaute proteins are components of RISC ***(27)*** with homologs in plants, fungi, and *C. elegans* that are required for RNAi in those organisms ***(28–30)***. The degraded target mRNA appears to then be cycled into new siRNAs that repeat the process in an RNA polymerase-dependent cycle of mRNA degradation and siRNA production ***(31)***. The complete mechanism for RNAi has not been elucidated.

A teleological explanation for the existence of a mechanism to destroy mRNAs in response to homologous dsRNA has been proposed ***(32)***. It has been suggested that RNAi evolved as a mechanism to combat invading dsRNA viruses or to inhibit the activity of retrotransposons. Moreover, there is at least one gene in *Drosophila*, *Stellate*, that is regulated by dsRNA-mediated gene silencing in the testis ***(33)***.

This chapter describes the application of RNAi to cultured *Drosophila* cells, with a particular emphasis on the imaging of the cytoskeleton and chromosomes in affected cells. Materials and methods are provided to enable the researcher to implement the design and production of dsRNA from polymerase chain reaction (PCR) templates, the culture of *Drosophila* cells and their treatment by RNAi, the analysis of target protein depletion by Western blotting, and the fixation and treatment of cells for microscopic imaging. The depletion of centrosomin (Cnn) a centrosomal protein that is required for mitotic centrosome assembly and function ***(34–37)*** from S2 cells is presented for example, but the technique is widely applicable to different targets and cell lines ***(7,17,38)***. Importantly, *Drosophila* cells in culture readily take up exogenous dsRNA, and there is no need to use carriers or transfection methods like those required with mammalian cell culture ***(7)***. Thus, RNAi holds great promise for the analysis of protein function in living cells.

2. Materials

2.1. DNA Templates for Making dsRNA

1. Oligonucleotide primers for PCR.
2. Thermostable DNA polymerase (e.g., Clontech Advantage2 PCR reagent).
3. 10X buffer for PCR.
4. 10X Deoxyribonucleotide triphosphate (dNTP) mixture (solution containing 2 m*M* each of dATP, dGTP, dCTP, and dTTP).
5. PCR purification kit (Qiagen).
6. RNase-free water.
7. Thermal cycler.

2.2. Synthesis of dsRNA

1. T7 PCR template in water at approx 0.1 µg/µL.
2. Ambion MEGAscript T7 kit (cat no. 1334), or Promega Ribomax large-scale RNA Production System–T7 (cat. no. P1300).
3. RNase-free water.

2.3. Culture and Treatment of Cells

1. Live culture of *Drosophila* S2 cells (ATCC CRL-1963).
2. 100 × 20-mm cell culture dishes.
3. Sterile 15- or 50-mL conical centrifuge tubes.
4. Fetal bovine serum (FBS) (Hyclone or GIBCO). Heat treat at 65°C for 30 min prior to use (*see* **Note 1**).
5. Culture medium: M3 + BPYE (Bacto-peptone, yeast extract). Per liter: Mix 39.4 g Shields and Sang M3 powder (Sigma-Adrich) and 0.5 g $KHCO_3$ into 800 mL deionized water. Mix until dissolved, then bring pH to 6.6 with HCl. Add 1 g Yeastolate (yeast extract, cell culture grade; Sigma-Aldrich), 2.5 g Bacto-peptone and deionized water to a final volume of 1 L. Filter sterilize; store at 4°C (*see* **Note 2**).
6. M3 + BPYE + 10% FBS
7. Multiple well flat-bottomed Cluster-6 plates, or 60-mm culture dishes.

2.4. Western Blotting

1. 30:0.8 Acrylamide : bisacrylamide.
2. 1.5 *M* Tris-HCl, pH 8.8.
3. 0.5 *M* Tris-HCl, pH 6.8.
4. 10% (w/v) Sodium dodecyl sulfate (SDS).
5. 25% Ammonium persulfate (APS) (store at 4°C for up to 1 mo).
6. TEMED.
7. Protein minigel apparatus (e.g., Bio-Rad Protean system).
8. Gel transfer apparatus (e.g., Bio-Rad minigel transfer system).
9. SDS-polyacrylamide gel electrophoresis (SDS-PAGE) electrophoresis buffer: 25 m*M* Tris base, 192 m*M* glycine, 0.1% SDS.

10. 5X SDS-PAGE loading buffer: 350 m*M* Tris-HCl, pH 6.8, 25% glycerol, 2% SDS, 5% 2-mercaptoethanol, 0.01% bromophenol blue.
11. Gel transfer buffer: 25 m*M* Tris base, 192 m*M* glycine, 20% methanol.
12. TBS-T: 50 m*M* Tris-HCl, pH 7.2, 120 m*M* NaCl, 0.1% Tween-20, autoclaved.
13. Blocking Solution: 5% Nonfat dry milk in TBS-T.
14. Horseradish peroxidase (HRP)-conjugated secondary antibody (Jackson IRL).
15. Chemiluminescence detection reagent (ECL, Amersham, or Supersignal West Pico, Pierce).

2.5. Cell Fixation and Staining

1. Glass slides (untreated) with approx 10-mm-diameter wells (e.g., Fisher cat. no. 12-568-20, or PGC Scientifics cat. no. 60-5453-24).
2. Coplin jars.
3. Humid chamber for slides.
4. Poly-L-lysine solution (MW > 300,000, Sigma-Aldrich P1524), 1 mg/mL.
5. 10X Phosphate-buffered saline (PBS): 18.6 m*M* NaH_2PO_4, 84.1 m*M* Na_2HPO_4, 1.75 *M* NaCl, pH 7.4.
6. PBS: Dilute 10X PBS stock to 1X with water.
7. 10% Solution of saponin (Sigma-Aldrich). Store aliquots at –20°C.
8. 100 mg/mL bovine serum albumin (BSA, fraction V) in PBS + 0.02% solium azide. Store at 4°C.
9. Methanol at –20°C.
10. Primary antibodies (e.g., anti-α-tubulin mouse monoclonal DM1A [Sigma-Aldrich]).
11. DAPI (4', 6-diamidine-2'-phenylindole) or TOTO-3 DNA dye (Molecular Probes).
12. Fluorescent secondary antibodies (e.g., fluorescein isothiocyanate [FITC]-conjugated donkey anti-mouse [Jackson ImmunoResearch Laboratories]).
13. Clear nail polish.

2.6. Imaging

1. Mountant: 0.05% *p*-Phenylenediamine, 0.1 *M* Tris, pH 8.8 in 90% glycerol. Store at –20°C shielded from light. Solution will turn brown over time. Make fresh every 6 mo.
2. Microscope with 600–1000× magnification (confocal microscope is preferred).
3. Filter sets for FITC, tetramethylrhodamine (TRITC) (or Cy3 or Texas Red), and Cy5 (for TOTO-3) (*see* **Note 3**).

3. Methods

3.1. Preparation of Templates by PCR To Be Used for In Vitro Transcription

1. Design oligo. Oligonucleotides should be designed against cDNA or exon sequences of the gene of choice, preceded by the T7 promoter sequence: TAATACGACTCACTATAGGGA (the underlined G is the transcription start site for T7 polymerase) (**Fig. 1A**). Design primers to produce templates of 700–1000 bp in length, although shorter dsRNAs also appear to work ***(17)***. In general, the target sequence of the primer should be 18–24 nucleotides in length. Programs

such as Oligo (Molecular Biology Insights), MacVector (Oxford Molecular Group), or Primer3 (free on the WWW) ***(39)*** can be used to design primers that fit guidelines for PCR effectiveness such as GC content and predicted Tm.

2. Amplify template by PCR. Mix: In a 0.5 mL tube mix 10 µL Advantage 2 PCR reagent (Clontech), 10 µL of 2 m*M* dNTP mix, 0.2 µ*M* each primer, 50 ng cDNA or 1 µg of genomic DNA, and water to a final volume of 100 µL (*see* **Note 4**). Amplify in a thermal cycler for 30 cycles: 94°C for 30 s, 55°C for 30 s, 72°C for 1 min.
3. Analyze 5 µL of the reaction by agarose gel electrophoresis. The PCR product should appear as a single band of the expected size on the gel (*see* **Note 5** and **Fig. 1B**).
4. Purify the PCR product using a PCR purification kit (Qiagen). Collect the DNA in RNase-free water (included in Ambion MEGAscript kit) (*see* **Note 6**).
5. Quantify the PCR product using a spectrophotometer or by using the ethidium bromide spot method ***(40)***.
6. Adjust the concentration of PCR DNA to 0.1 µg/µL with RNase-free water.

3.2. Production of dsRNA (Briefly, from the Ambion MEGAscript Kit Protocol)

1. Mix 10 µL PCR DNA (1–2 µg), 16 µL nucleotide triphosphate mix, 6 µL RNase-free water, 4 µL of 10X reaction buffer, and 4 µL enzyme mix in a 0.5- or 1.5-mL tube to a final volume of 40 µL.
2. Incubate at 37°C for 5 h.
3. Add 1 µL DNase; incubate at 37°C for 15 min.
4. Precipitate RNA: add 50 µL RNase-free water, 10 µL 3.0 *M* sodium acetate pH 5.2, 250 µL 95% ethanol, and place at –20°C for >15 min.
5. Centrifuge for 15 min in microfuge at 4°C. Discard the supernatant.
6. Wash the pellet with 1 mL ice-cold 70% ethanol, centrifuge for 5 min.
7. Remove as much of the wash solution as possible and suspend the pellet in 100 µL RNase-free water. Perform this and subsequent handling of the dsRNA in a sterile hood. Repeated vortexing may be necessary to dissolve the RNA pellet.
8. Quantify the RNA concentration by ultraviolet (UV) absorbance with a spectrophotometer. Begin by diluting your samples 1:100–1:200 to obtain a reading in the linear range. To calculate yield, assume 1 A_{260} unit corresponds to 40 µg/mL [$A_{260} \times$ dilution factor $\times$ 40 = µg/mL dsRNA].
9. Analyze the integrity of dsRNA by agarose gel electrophoresis of the sample (3–5 µg).
10. Store the dsRNA solution at –20°C.

3.3. RNAi Treatment of Cells (see Note 7)

1. Culture S2 cells to a density of 0.5–1.0 $\times$ 10^6 cells/mL in 100-mm dishes, 6–7 mL of culture per dish.
2. Suspend the cells by gently pipetting with a 10-mL pipet and transfer to a 15-mL conical tube. If using serum-free medium, suspend cells and skip to **step 8**.
3. Centrifuge for 2 min at 2000 rpm in a clinical centrifuge.

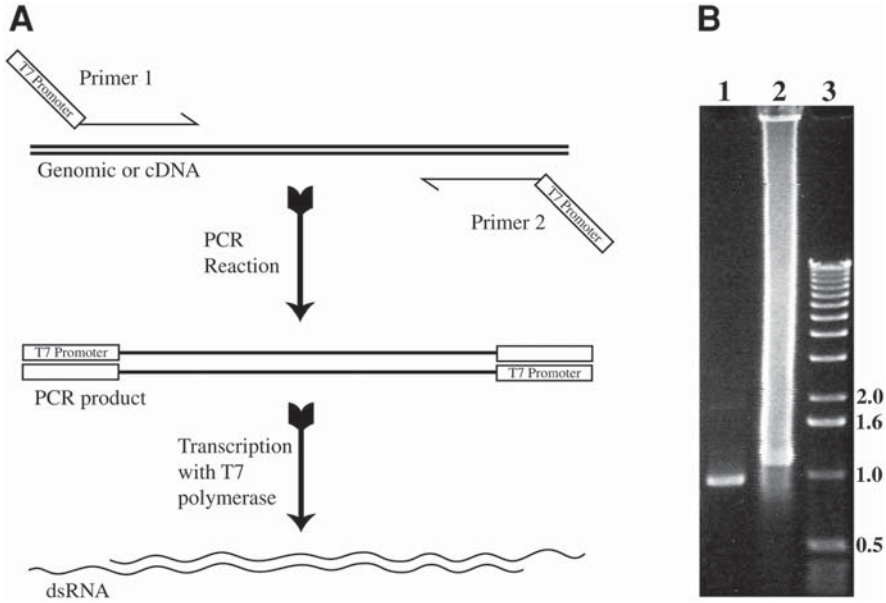

Fig. 1. Polymerase chain reaction (PCR) template DNA and dsRNA. **(A)** Diagram illustrating the scheme for producing T7 promoter-flanked templates by PCR. In *panel 1,* primers, designed with T7 promoter sequences at their 5' ends, are used to amplify a DNA fragment from genomic or cDNA sources. *Panel 2* shows the PCR product, with the T7 promoter flanks, to be used for transcription of dsRNA by T7 RNA polymerase. *Panel 3* illustrates the dsRNA product that is produced from the transcription of both strands of the template drawn in *panel 2*. **(B)** PCR amplification of a 938-bp segment of *cnn* cDNA with T7 flanking sequences (*lane 1*). Transcription from the PCR fragment with T7 polymerase yields a double-stranded RNA product that migrates slower on a gel than the double-stranded DNA template (*lane 2*). The sample in *lane 2* was treated with DNase I prior to loading. dsRNA samples typically produce a smear on an agarose gel like that shown in *lane 2*. DNA size markers (1-kb ladder) are shown in *lane 3*.

4. Suspend the cells in 10 mL of serum-free medium (M3+BPYE).
5. Centrifuge for 2 min at 650*g* in a clinical centrifuge.
6. Repeat **steps 4** and **5**.
7. Suspend the cells in 10 mL of serum-free medium.
8. Add 1 mL of cells into each well of a six-well cluster dish, or into a 60-mm culture dish (*see* **Note 8**). Alternatively, use 12-well dishes with 0.5 mL culture per well.
9. Add dsRNA to a final concentration of 40 nM (*see* **Note 9**) and mix well by swirling.
10. Incubate the cells and dsRNA for 1 h at room temperature.

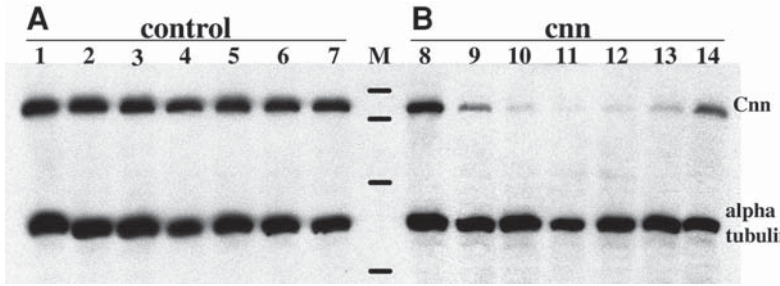

Fig. 2. Time-course of Cnn protein levels following RNAi treatment. Protein samples were collected from control RNAi **(A)** and Cnn RNAi **(B)** S2 cells at 24-h time-points: d 0, *lanes 1 and 8*; d 1, *lanes 2 and 9*; d 2, *lanes 3 and 10*; d 3, *lanes 4 and 11*; d 4, *lanes 5 and 12*; d 5, *lanes 6 and 13*; d 7, *lanes 7 and 14*. No sample was collected on d 6. Prestained protein size markers (Bio-Rad Kaleidoscope) were loaded in the lane labeled M and are (from the top) 200 kDa, 120 kDa, 85 kDa, and 45 kDa. Lysate from approx 2.5×10^5 cells were loaded into each lane. Samples were electrophoresed on a single 7% sodium dodecyl sulfate–polyacrylamide gel electrophoresis (SDS-PAGE) minigel using the Bio-Rad Protean II system and a 15-well comb. The blot was probed with anti-Cnn and anti-α-tubulin antibodies (as a loading control). Cnn levels dropped perceptibly in the first 24 h and continued to drop until d 5, when the levels appear to rise again. By d 7, Cnn levels still had not returned to normal.

11. Add 2 mL of medium with serum (M3 + BPYE + 10% FBS). Skip this step if using serum-free medium.
12. Examine cells daily. Passage as needed to maintain 30–80% confluence until d 4–9.
13. Wait an appropriate amount of time to examine the cells, which should be determined empirically in a time-course assay for each protein to be targeted (*see* **Note 10** and **Fig. 2**).

3.4. Western Blot Analysis of RNAi-Treated Cells

Western blotting, like that shown for Cnn in **Fig. 2**, is recommended to assay the efficiency and time-course of decay for each target protein.

1. Remove aliquots of S2 cells at different time points and place in 1.5-mL tubes. Remove an aliquot of the cells at time zero (500 µL; *see* **Note 11**), before dsRNA addition, and remove aliquots every day (or other time increments thereafter), for several days.
2. Pellet cells by centrifugation in a microfuge. Discard the supernatant and suspend in 50 µL 1X SDS-PAGE loading dye. Load 10 µL of the sample onto SDS-PAGE gel following heating to 95–100°C for 5 min. Samples can be stored at –20°C or –70°C.

3. Pour an SDS-PAGE minigel (*see* **Note 12**). For the resolving gel, mix acrylamide (7–15% final, depending on the size of your protein), 375 m*M* Tris-HCl, pH 8.8, 0.1% SDS, 1/1000 volume of 25% APS, 1/1000 volume TEMED. Pour gel immediately after the addition of TEMED, leaving about a 3-cm space for the stacking gel. Overlay with approx 100 µL water. Let polymerize for 1 h. For the stacking gel, mix acrylamide (4%), 125 m*M* Tris-HCl, pH 6.8, 0.1% SDS, 1/1000 volume of 25% APS, 1/1000 volume TEMED. Remove the overlay solution, then pour immediately and insert the comb. Let polymerize at least 30 min.
4. Separate the proteins by electrophoresis on an SDS-PAGE minigel.
5. Transfer to nitrocellulose membrane in gel transfer buffer using a cooled transfer chamber at 100 V for 1 h.
6. Place the membrane in 20 mL of blocking solution in a 9 × 9 cm square Petri dish or similar chamber. Incubate for 1 h at room temperature with gentle shaking.
7. Remove the blocking solution. Add primary antibody in 10 mL TBS-T and incubate for 1 h at room temperature (or overnight at 4°C).
8. Remove the antibody solution and wash the blot three times with 20 mL TBS-T for 5 min each.
9. Incubate with HRP-conjugated secondary antibody (1 : 10,000) in 10 mL TBS-T for 30 min.
10. Repeat **step 8**.
11. Treat the blot with chemiluminescence substrate reagent and expose to X-ray film for various times.

3.5. Staining of Cells

1. Treat the slides with poly-L-lysine as follows: Wash glass slides in water and wipe dry with a Kimwipe. Apply 50 µL of 1 mg/mL poly-L-lysine into each well on the slide and let sit for 45 min. Wash slides with water three times in Coplin jars. Let slides dry (*see* **Note 13**).
2. Apply 50 µL of cells to each well and let sit for 30 min.
3. Rinse cells briefly (2 s) in PBS and then place directly into –20°C methanol. For this, dip the slides into a Coplin jar containing PBS and place them into a Coplin jar with methanol that has been kept in the freezer. Incubate the slides in –20°C methanol for 10 min.
4. Remove the slides from –20°C and place into a Coplin jar with PBS. Rinse once with fresh PBS. The cells should appear as a film in the well. The cells should not be permitted to dry in any of the subsequent procedures.
5. Using a Kimwipe twisted into the shape of a probe, or using a cotton swab, blot the PBS from the region of the slide surrounding the well dry. This will prevent the antibody solution from spreading out from the well in subsequent procedures.
6. Apply the primary antibodies, diluted in PBS + 0.1% saponin + 5 mg/mL BSA, 50 µL per well. If DNA dyes such as propidium iodide or TOTO-3 are to be used, RNase A can be added at this step at a concentration of 50 µg/mL (*see* **Note 14**). We recommend using one combination of antibodies for all the samples on the

same slide to prevent cross-contamination. For different antibody mixtures, use additional slides.
7. Incubate slides in a humid chamber for 1 h at room temperature, or overnight at 4°C. A simple humid chamber can be made by taking an empty pipet tip box, adding water into the box, and placing the slides onto the slotted tip holder.
8. Wash slides in a Coplin jar with three changes of PBS, 5 min each.
9. Apply secondary antibodies to the slides (*see* **Note 15**). First, blot the area around the wells dry as described in **step 5**. Add 50 µL of secondary antibodies, diluted in PBS + 0.1% saponin + 5 mg/mL BSA, into the wells. Incubate for 1 h at room temperature in the dark.
10. Wash as in **step 8**; then, blot the slides dry as in **step 5**.
11. Apply 4 µL of Mountant to each well. Overlay a cover slip slowly and at an angle to prevent the inclusion of air bubbles under the cover slip (*see* **Note 16**). Fix coverslip to the slide with clear nail polish.

3.6. Imaging Cells by Confocal Microscopy

1. High magnification with a 60× or higher objective is required to image S2 cells effectively. These objectives require immersion in oil or water (*see* **Note 17**).
2. For confocal microscopy, use multiple excitation lasers to image multiple fluorophors. There are a variety of configurations available; some include lasers that produce lines typically at 488, 568, and 647 nm (argon–krypton), or 488, 568, and 633 nm (argon, krypton, and helium–neon (RedHeNe), or 488, 543, and 633 nm (argon, GreenHeNe, RedHeNe). These should all be compatible with three-color imaging like that shown in **Figs. 3** and **4**, where the (excitation peak wavelength/emission peak wavelength [in nm]) for FITC (490/520), TRITC (541/572), and TOTO-3 (642/660) allowed separation of all three emission signals.
3. S2 cells are small, approx 10 µm thick. Therefore, when a z-series is collected, a large stack of images will not need to be produced. Steps of 0.5–1.0 µm may be adequate for most purposes.
4. If bleaching becomes a problem, one method is to set up the imaging using only one of the fluorescent signals (the more robust) to view the cell. Then, turn on the other lasers when the images are being captured. This strategy reduces the bleaching of weaker signals or sensitive fluorophors.

4. Notes

1. Fetal bovine serum is of the highest quality (mycoplasma, virus, bacteriophage, and endotoxin tested). Store serum at –20°C before heat treatment and at 4°C after heat treatment unless it will be stored for a long period, and in that case, store it at –20°C. We have used Hyclone and GIBCO brands of FBS.
2. S2 cells can also be cultured in commercially available Schneider's *Drosophila* medium (GIBCO) supplemented with 10% FBS, or adapted to CCM3, a synthetic medium supplied by Hyclone.

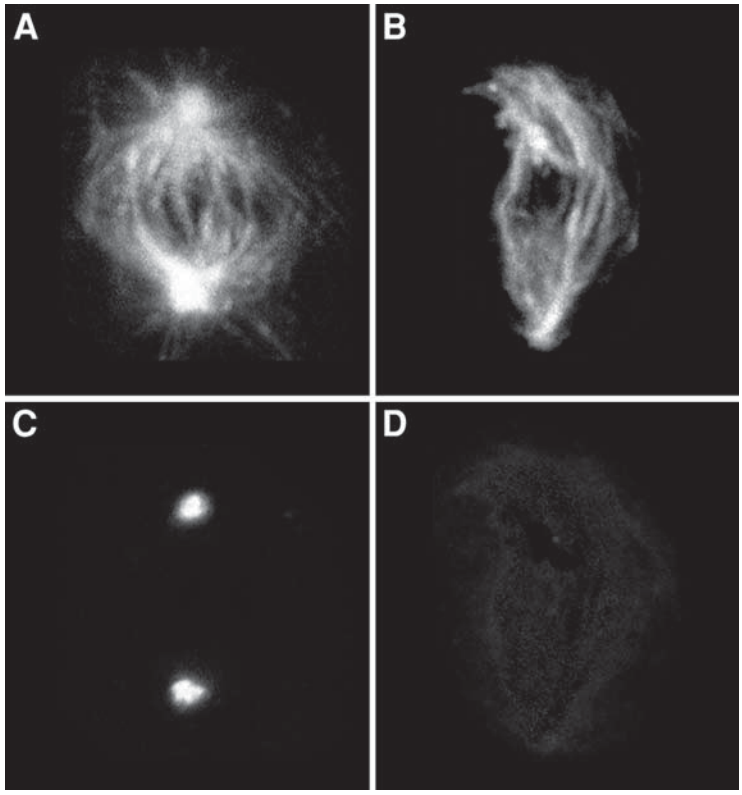

Fig. 3. Spindle assembly in cells depleted of Cnn by RNAi. S2 cells treated with control dsRNA (**A** and **C**) and *cnn* dsRNA (**B** and **D**) were fixed and stained for microtubules (anti-α-tubulin) (**A** and **B**) and Cnn (**C** and **D**). The cells were also stained for DNA, and the merged three-color images are shown in Fig 4. Note that in the cell depleted of Cnn by RNAi, there is no signal for Cnn detected at the spindle poles, which are consequently deficient in astral microtubules. Cells at different stages of the cell cycle are deficient in astral microtubules in Cnn RNAi cells (not shown). In these cells, the mitotic spindle is assembled via an alternate pathway that does not utilize centrosomes ***(34)***. The images shown were captured on a Leica TCS SP confocal microscope equipped with argon, krypton and He–Ne Red lasers. The images were collected as a Z-series about 6 μm thick, and the maximum projection through the stack is shown.

3. A variety of fluorophore conjugates are available commercially. Molecular Probes sells a set of secondary antibodies conjugated to a variety of "Alexa" fluorophores, which are more resistant to bleaching.
4. For PCR, substitute any thermostable DNA polymerase and reaction conditions with which you are familiar. We have found that the Clontech Advantage2 PCR enzyme/buffer mixture gives a high yield of product.

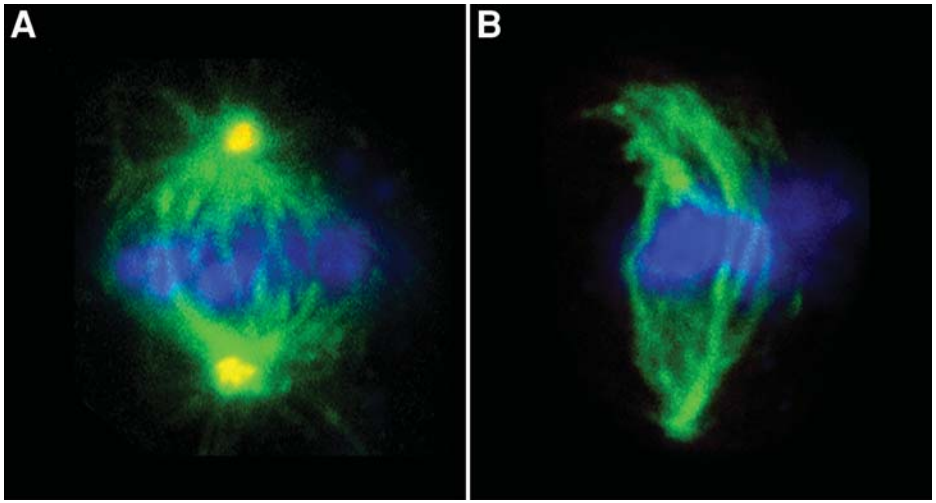

Fig. 4. Three-color merged image of cells depleted of Cnn by RNAi. Shown are S2 cells treated with control dsRNA **(A)** and *cnn* dsRNA **(B)** that were fixed and stained for microtubules (anti-α-tubulin) (green), Cnn (red), and DNA (TOTO-3, blue). For more details, *see* legend to **Fig. 3**. (*See* color plate 7 in the insert following p. 242.)

5. If the PCR produces multiple bands, the reaction conditions need to be optimized. *See* **ref. *41***, or the *Promega Protocols and Applications Guide* (free from Promega) for guidelines. If the yield is low, multiple reactions can be combined.
6. As an alternative, satisfactory results were obtained from PCR templates that were cleaned up by phenol/$CHCl_3$ and $CHCl_3$ extraction followed by ethanol precipitation and a wash with ice-cold 70% ethanol.
7. The methods for the preparation of culture media and the culture of *Drosophila* cells were all from **ref. *42***.
8. It is necessary to always include a control dsRNA in these experiments. Use something that should have no effect (like lacZ, green fluorescent protein [GFP], or bacterial plasmid vector sequences).
9. For a dsRNA of approx 700 bp in length, 40 n*M* corresponds to approx 15 µg of dsRNA in 1 mL of medium. If 15 µg of dsRNA does not effectively reduce the target mRNA, consider increasing the amount to 30 µg, as this increased amount appears to have no side effects on control cells.
10. When Cnn levels were measured following RNAi, the protein fell to low levels by d 3 and 4 and then began to rise again by d 7 (*see* **Fig. 2**). In one experiment, Cnn was knocked down four consecutive times (not shown). Following the initial RNAi, the procedure was repeated three more times on the culture every 4 d. This experiment was possible in this case, because Cnn is not required for cell viability. One can also add dsRNA to the culture every day to achieve depletion of the target protein ***(43)***. Half-lives vary widely among proteins. Wei et al. ***(38)*** showed

that one protein (HSF) with a known half-life of 8–10 h was reduced dramatically 2 d following treatment, whereas the more stable β-tubulin protein was relatively less diminished in the same time period upon RNAi targeting. Thus, for more stable proteins, it might be necessary to implement a second dose of RNAi on d 4.

11. Five hundred microliters of the cell pellet from the culture at d 0 gives ample protein for one or two gel loadings. S2 cells double approx once every 24 h, so on d 2, take 250 µL of the culture, on d 3 take 125 µL, and so on. It may be necessary to supply fresh medium to the cells on d 3, and this dilution should be accounted for when taking the next aliquot.
12. Precast gels are commercially available from Invitrogen, Bio-Rad, and others. Make sure the company's gels will fit your system.
13. Slides can be prepared in advance and stored dry for at least 2 wk.
14. For triple labeling cells *in situ*, like those in **Figs. 3** and **4**, we generally use a combination of secondary antibodies that include FITC, TRITC, and Cy5. For DNA staining we use TOTO-3. Texas Red emission overlaps too much with Cy5 and TOTO-3. For microtubule staining, Sigma sells a FITC-conjugated version of the DM1A monoclonal that gives a robust signal.
15. When the secondary antibodies are applied, other dyes can also be incubated in the same mixture (TOTO-3, Rhodamine-Phalloidin, etc.). Thus, a third incubation step is not required following the application of secondary antibodies.
16. Slides can be stored at –20°C for 2 wk, and possibly longer, with retention of the fluorescent signals.
17. Because the cells need to be imaged under an immersion lens, it is important that there is not too much solution under the cover slip. Otherwise, the surface tension from the immersion fluid will cause the cover slip to move in the Z direction, distorting the image. Alternatively, the cover slip can be anchored to the slide with clear nail polish applied to the edges of the cover slip.

Acknowledgments

Special thanks to all the students of the 2002 and 2003 physiology course at the Marine Biological Laboratories who used and tested this as a teaching manual for part of the course. We are grateful to Jack Dixon and Carolyn Worby for sharing their RNAi protocol and discussion prior to publication. We also thank Lucy and Peter Cherbas for their guidance in the use of *Drosophila* cell culture. We thank Jeana Stubbert who provided valuable help with the manuscript.

References

1. Jordan, M. A. and Wilson, L. (1998) Microtubules and actin filaments: dynamic targets for cancer chemotherapy. *Curr. Opin. Cell. Biol.* **10,** 123–130.
2. Fire, A., Xu, S., Montgomery, M. K., Kostas, S. A., Driver, S. E., and Mello, C. C. (1998) Potent and specific genetic interference by double-stranded RNA in Caenorhabditis elegans. *Nature* **391,** 806–811.

3. Vaucheret, H., Beclin, C., and Fagard, M. (2001) Post-transcriptional gene silencing in plants. *J. Cell Sci.* **114,** 3083–3091.
4. Cogoni, C. (2001) Homology-dependent gene silencing mechanisms in fungi. *Annu. Rev. Microbiol.* **55,** 381–406.
5. Cogoni, C. and Macino, G. (2000) Post-transcriptional gene silencing across kingdoms. *Curr. Opin. Genet. Dev.* **10,** 638–643.
6. Kennerdell, J. R. and Carthew, R. W. (1998) Use of dsRNA-mediated genetic interference to demonstrate that frizzled and frizzled 2 act in the wingless pathway. *Cell* **95,** 1017–1026.
7. Clemens, J. C., Worby, C. A., Simonson-Leff, N., et al. (2000) Use of double-stranded RNA interference in *Drosophila* cell lines to dissect signal transduction pathways. *Proc. Natl. Acad. Sci. USA* **97,** 6499–6503.
8. Brown, S. J., Mahaffey, J. P., Lorenzen, M. D., Denell, R. E., and Mahaffey, J. W. (1999) Using RNAi to investigate orthologous homeotic gene function during development of distantly related insects. *Evol. Dev.* **1,** 11–15.
9. Hughes, C. L. and Kaufman, T. C. (2000) RNAi analysis of *Deformed*, *proboscipedia* and *Sex combs reduced* in the milkweed bug *Oncopeltus fasciatus*: novel roles for *Hox* genes in the hemipteran head. *Development* **127,** 3683–3694.
10. Tavernarakis, N., Wang, S. L., Dorovkov, M., Ryazanov, A., and Driscoll, M. (2000) Heritable and inducible genetic interference by double-stranded RNA encoded by transgenes. *Nature Genet.* **24,** 180–183.
11. Kennerdell, J. R. and Carthew, R. W. (2000) Heritable gene silencing in *Drosophila* using double-stranded RNA. *Nature Biotechnol.* **18,** 896–898.
12. Piccin, A., Salameh, A., Benna, C., et al. (2001) Efficient and heritable functional knock-out of an adult phenotype in *Drosophila* using a GAL4-driven hairpin RNA incorporating a heterologous spacer. *Nucleic Acids Res.* **29,** E55–5.
13. Kalidas, S. and Smith, D. P. (2002) Novel genomic cDNA hybrids produce effective RNA interference in adult Drosophilia. *Neuron* **33,** 177–184.
14. Elbashir, S. M., Harborth, J., Lendeckel, W., Yalcin, A., Weber, K., and Tuschl, T. (2001) Duplexes of 21-nucleotide RNAs mediate RNA interference in cultured mammalian cells. *Nature* **411,** 494–498.
15. Caplen, N. J., Parrish, S., Imani, F., Fire, A., and Morgan, R. A. (2001) Specific inhibition of gene expression by small double-stranded RNAs in invertebrate and vertebrate systems. *Proc. Natl. Acad. Sci. USA* **98,** 9742–9747.
16. Tuschl, T., Zamore, P. D., Lehmann, R., Bartel, D. P., and Sharp, P. A. (1999) Targeted mRNA degradation by double-stranded RNA in vitro. *Genes Dev.* **13,** 3191–3197.
17. Caplen, N. J., Fleenor, J., Fire, A., and Morgan, R. A. (2000) dsRNA-mediated gene silencing in cultured *Drosophila* cells: a tissue culture model for the analysis of RNA interference. *Gene* **252,** 95–105.
18. Oates, A. C., Bruce, A. E., and Ho, R. K. (2000) Too much interference: injection of double-stranded RNA has nonspecific effects in the zebrafish embryo. *Dev. Biol.* **224,** 20–28.
19. Zhao, Z., Cao, Y., Li, M., and Meng, A. (2001) Double-stranded RNA injection produces nonspecific defects in zebrafish. *Dev. Biol.* **229,** 215–223.

20. Hammond, S. M., Caudy, A. A., and Hannon, G. J. (2001) Post-transcriptional gene silencing by double-stranded RNA. *Nat. Rev. Genet.* **2,** 110–119.
21. Carthew, R. W. (2001) Gene silencing by double-stranded RNA. *Curr. Opin. Cell Biol.* **13,** 244–248.
22. Zamore, P. D. (2001) RNA interference: listening to the sound of silence. *Nature Struct. Biol.* **8,** 746–750.
23. Hammond, S. M., Bernstein, E., Beach, D., and Hannon, G. J. (2000) An RNA-directed nuclease mediates post-transcriptional gene silencing in *Drosophila* cells. *Nature* **404,** 293–296.
24. Bernstein, E., Caudy, A. A., Hammond, S. M., and Hannon, G. J. (2001). Role for a bidentate ribonuclease in the initiation step of RNA interference. *Nature* **409,** 363–366.
25. Nykanen, A., Haley, B., and Zamore, P. D. (2001) ATP requirements and small interfering RNA structure in the RNA interference pathway. *Cell* **107,** 309–321.
26. Zamore, P. D., Tuschl, T., Sharp, P. A., and Bartel, D. P. (2002) RNAi: double-stranded RNA directs the ATP-dependent cleavage of mRNA at 21 to 23 nucleotide intervals. *Cell* **101,** 25–33.
27. Hammond, S. M., Boettcher, S., Caudy, A. A., Kobayashi, R., and Hannon, G. J. (2001) Argonaute2, a link between genetic and biochemical analyses of RNAi. *Science* **293,** 1146–1150.
28. Fagard, M., Boutet, S., Morel, J. B., Bellini, C., and Vaucheret, H. (2000) AGO1, QDE-2, and RDE-1 are related proteins required for post-transcriptional gene silencing in plants, quelling in fungi, and RNA interference in animals. *Proc. Natl. Acad. Sci. USA* **97,** 11,650–11,654.
29. Catalanotto, C., Azzalin, G., Macino, G., and Cogoni, C. (2000) Gene silencing in worms and fungi. *Nature* **404,** 245.
30. Tabara, H., Sarkissian, M., Kelly, W. G., et al. (1999) The *rde-1* gene, RNA interference, and transposon silencing in *C. elegans*. *Cell* **99,** 123–132.
31. Lipardi, C., Wei, Q., and Paterson, B. M. (2001) RNAi as random degradative PCR: siRNA primers convert mRNA into dsRNAs that are degraded to generate new siRNAs. *Cell* **107,** 297–307.
32. Waterhouse, P. M., Wang, M. B., and Lough, T. (2001) Gene silencing as an adaptive defence against viruses. *Nature* **411,** 834–842.
33. Aravin, A. A., Naumova, N. M., Tulin, A. V., Vagin, V. V., Rozovsky, Y. M., and Gvozdev, V. A. (2001) Double-stranded RNA-mediated silencing of genomic tandem repeats and transposable elements in the *D. melanogaster* germline. *Curr. Biol.* **11,** 1017–1027.
34. Megraw, T. L., Kao, L. R., and Kaufman, T. C. (2001) Zygotic development without functional mitotic centrosomes. *Curr. Biol.* **11,** 116–120.
35. Raff, J. W. (2001). Centrosomes: central no more? *Curr. Biol.* **11,** R159–R161.
36. Megraw, T. L., Li, K., Kao, L. R., and Kaufman, T. C. (1999) The centrosomin protein is required for centrosome assembly and function during cleavage in *Drosophila*. *Development* **126,** 2829–2839.

37. Vaizel-Ohayon, D. and Schejter, E. D. (1999) Mutations in centrosomin reveal requirements for centrosomal function during early *Drosophila* embryogenesis. *Curr. Biol.* **9,** 889–898.
38. Wei, Q., Marchler, G., Edington, K., Karsch-Mizrachi, I., and Paterson, B. M. (2000) RNA interference demonstrates a role for nautilus in the myogenic conversion of Schneider cells by daughterless. *Dev. Biol.* **228,** 239–255.
39. Rozen, S and Skaletsky, H. J. (2002) Primer3 on the WWW for general users and for biologist programmers. In *Bioinformatics Methods and Protocols: Methods in Molecular Biology*. (Krawetz, S. and Misener, S., eds.), Humana Press, Totowa, NJ, pp. 365–386.
40. Ausubel, F. M. (1987) *Current Protocols in Molecular Biology*, Greene Publishing, Brooklyn, NY.
41. Roux, K. H. (1995) Optimization and troubleshooting in PCR. *PCR Methods Appl.* **4,** S185–S194.
42. Cherbas, C. and Cherbas, P. (1998) Cell Culture, in Drosophila: *A Practical Approach,* 2nd ed. (Roberts, D. B., ed.), IRL/Oxford University Press, Oxford, pp. 319–338.
43. Bruick, R. K. and McKnight, S. L. (2001) A conserved family of prolyl-4-hydroxylases that modify HIF. *Science* **294,** 1337–1340.